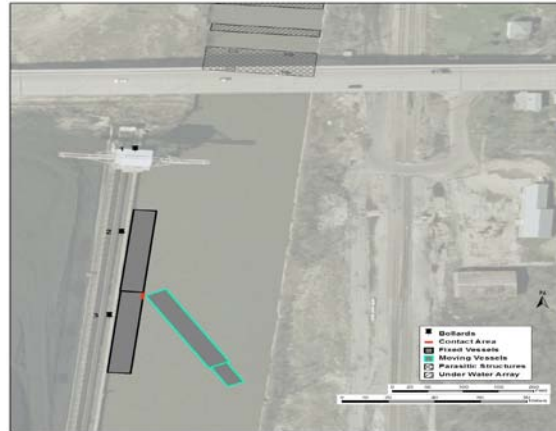


# Dispersal Barrier Efficacy Study

Efficacy Study Interim Report IIA, Chicago Sanitary and Ship Canal Dispersal Barriers – Optimal Operating Parameters Laboratory Research and Safety Tests



September 2011



US Army Corps  
of Engineers®  
Chicago District

## SECTION 1– Study Background

### 1.1 – Dispersal Barrier Efficacy Study Purpose

The U.S. Army Corps of Engineers (USACE) was authorized in Section 3061(b)(1)(D) of the Water Resources Development Act of 2007 (WRDA 2007) to conduct a study of a range of options or technologies for reducing impacts of hazards that may reduce the efficacy of the Electrical Dispersal Barrier located on the Chicago Sanitary and Ship Canal (CSSC), hereafter referred to as the Efficacy Study. The Electrical Dispersal Barrier was designed to prevent inter-basin transfer of fish between the Mississippi River and Great Lakes drainage basins via the CSSC, and it has been partially completed. The Barrier consists of three separate barriers. Although all three barriers are operational, USACE intends to upgrade the first barrier constructed in the future.

The first dispersal barrier was authorized as a demonstration project under section 1202(i)(3) of the Aquatic Nuisance Prevention and Control Act P.L. 101-646, and Barrier I has been in operation since April 2002. The second dispersal barrier was initially implemented by Section 1135 of WRDA 1986, P.L. 99-662, as further authorized by section 345 of the District of Columbia Appropriations Act of 2005, P.L. 108-335. Barrier II is a set of two barriers, Barrier IIA and Barrier IIB. Barrier IIA has been in operation since April 2009, Barrier IIB has been operational since April 2011. The combination of these three barriers is designed to function together to prevent inter-basin transfer of fish between the Mississippi River and Great Lakes drainage basins, particularly the northerly movement of two species of Asian carp.

Although the Electric Dispersal Barrier system is designed to prevent the movement of any fish species through the CSSC, the current species of concern are the Asian carp (Cypriniformes: Cyprinidae). Asian carp have the potential to damage the Great Lakes and confluent large riverine ecosystems. Two species of Asian carp, bighead carp (*Hypophthalmichthys nobilis*) and silver carp (*H. molitrix*), have become well established in the Mississippi and Illinois Rivers exhibiting exponential population growth in recent years. Certain life history traits have enabled bighead and silver carp to achieve massive population numbers soon after establishing a presence in these areas.

The USACE is implementing a four-pronged strategy to address threat posed by Asian carp. The strategy is consistent with the *Asian Carp Control Strategy Framework*, developed by the Asian Carp Regional Coordinating Committee (ACRCC), which includes the United States Environmental Protection Agency (USEPA), the United States Fish and Wildlife Service (USFWS), the United States Coast Guard (USCG), the Illinois Department of Natural Resources (IDNR), the City of Chicago, the Metropolitan Water Reclamation District of Greater Chicago (MWRD), the White House Council on Environmental Quality (CEQ), the United States Geological Survey (USGS), the Great Lakes Fishery Commission (GLFC), USACE and the Great Lakes states. Operating within this framework, the USACE four-pronged strategy consists of:

- (1) design, construction, operation, maintenance, and improvement of the Electrical Dispersal Barriers;
- (2) monitoring, working with agency partners, for the potential presence of Asian carp;

- (3) leveraging the Efficacy Study process to recommend additional measures to reduce the risk of Asian carp entering Lake Michigan; and,
- (4) using the Great Lakes and Mississippi River Inter-Basin Study to develop long term solutions to prevent the transfer of invasive species between basins.

The Efficacy Study is being conducted and documented in a series of interim studies and associated reports:

- Interim I, *Dispersal Barrier Bypass Risk Reduction Study and Integrated Environmental Assessment* – This interim report was approved by the Assistant Secretary of the Army for Civil Works (ASA(CW)) on 12 January 2010 to construct measures to prevent Asian carp from bypassing the electrical barrier system during flood events on the Des Plaines River and through culverts in the Illinois and Michigan (I&M) Canal. Construction of the bypass barrier and I&M Canal blockage was completed in October 2010.
- Interim IIA, *Electrical Barrier Optimal Operating Parameters: Phase A, Laboratory Research and Safety Tests* – This interim report is presented in this document, and provides an evaluation of tests conducted to determine the optimal operating parameters. Although there is sufficient information currently available to serve as a basis for a decision on operating parameters, a follow on report, Interim IIB, is expected to be released after additional tests and evaluation of risk factors have been completed. Interim IIB will be used primarily to further inform barrier operations and verify the recommendation provided in Interim IIA.
- Interim III, *Modified Structures and Operations, Chicago Area Waterways Risk Reduction Study and Integrated Environmental Assessment* – This interim report presented an evaluation of the potential for risk reduction that might be achieved through potential changes in the operation of the CAWS structures, such as locks, sluice gates, and pumping stations in consultation with the multi-agency working group. The report included an assessment of operational changes that could be implemented as needed by agencies that are responsible for fish population management efforts such as electro-fishing, spot piscicide application, or intensive commercial fishing efforts by the U.S. Fish and Wildlife (USFWS) and Illinois Department of Natural Resources (IDNR). This report was approved by the ASA (CW) on 13 July 2010. Installation of the sluice gate screens at the T.J. O'Brien L&D was completed in January 2011.
- Interim IIIA, *Fish Deterrent Barriers, Illinois and Chicago Area Waterways Risk Reduction Study and Integrated Environmental Assessment* – This interim report investigated and evaluated additional deterrent measures within USACE authority that could be quickly employed to potentially reduce the risk of the Asian carp dispersing into the Great Lakes. This report focuses on evaluating measures that apply readily available fish deterrent and guidance technologies at key locations in the CAWS and downstream in the Illinois Waterway (IWW). This analysis was initially included in the scope of Interim III, but was cycled out to consider fielding a developing technology that was initially thought to be

quickly deployable and relatively inexpensive. This report was approved by the ASA (CW) on 13 July 2010.

- *Comprehensive Efficacy Report* - This report will provide a summary of all interim reports and recommend a multi-agency comprehensive strategy for improving the efficacy of the dispersal barriers and reducing the population effects of Asian carp within the area waterways. The report will include a discussion of those improvements to the Barriers Project that have been completed by the Corps of Engineers since the enactment of WRDA 2007. The report will also contain an evaluation of additional risk reduction measures to specifically address the open pathways to Lake Michigan: the Grand Calumet River which outlets at the Indiana Harbor and Canal; and the Little Calumet River, which outlets at Burns Ditch. Addenda to this report will address potential bypasses in the Des Plaines watershed through old structures that were erected in the past century including the McCook Levee, the Summit Conduit and the Lyons Levee (historic Chicago Portage).

The study will also provide updates on behavioral barriers, monitoring and response actions and other modes of transit including ballast water and bait buckets. Finally, the report will include a summary of other agency efforts as part the collaborative Asian Carp Control Strategy Framework, including detailed discussions of the efforts of the multi-agency Monitoring and Rapid Response Work Group (MRRWG). In all cases, permanent solutions to the inter-basin transfer of aquatic nuisance species will be evaluated in the longer term Great Lakes and Mississippi River Inter-Basin Study, (GLMRIS).

In this dynamic process, USACE and federal, state and local agencies are evaluating many options and cycling out concepts as they are ready for evaluation and potential implementation based on thorough analyses, review, approval and any necessary authorization. These options have independent utility, potentially each providing ways to impede Asian carp migration, and can be considered in separate decision-making processes. Ultimately, any implemented measures are expected to complement each other to provide a comprehensive solution, pending further assessment of a possible permanent solution.

This report presents the results of the operational protocols research for the electric barriers and certain tests designed to determine whether USACE is capable of operating barriers safely at the recommended parameters.

## **1.2 – Study & Implementation Authority**

Authorization for the Efficacy Study is provided in Section 3061(b)(1)(D) of the Water Resources Development Act of 2007 (P.L. 110-114), quoted below. Recommendations provided in this report may also be implemented under this authority, which directs the Secretary to operate and maintain the electric barriers.



**WRDA 2007 SEC. 3061. CHICAGO SANITARY AND SHIP CANAL DISPERSAL BARRIERS PROJECT, ILLINOIS.**

(a) TREATMENT AS SINGLE PROJECT.—The Chicago Sanitary and Ship Canal Dispersal Barrier Project (in this section referred to as “Barrier I”), as in existence on the date of enactment of this Act and constructed as a demonstration project under section 1202(i)(3) of the Nonindigenous Aquatic Nuisance Prevention and Control Act of 1990 (16 U.S.C. 4722(i)(3)), and the project relating to the Chicago Sanitary and Ship Canal Dispersal Barrier, authorized by section 345 of the District of Columbia Appropriations Act, 2005 (Public Law 108–335; 118 Stat. 1352) (in this section referred to as “Barrier II”) shall be considered to constitute a single project.

(b) AUTHORIZATION.—

(1) IN GENERAL.—The Secretary, at Federal expense, shall—

(A) upgrade and make permanent Barrier I;

(B) construct Barrier II, notwithstanding the project cooperation agreement with the State of Illinois dated June 14, 2005;

(C) operate and maintain Barrier I and Barrier II as a system to optimize effectiveness;

(D) conduct, in consultation with appropriate Federal, State, local, and nongovernmental entities, a study of a range of options and technologies for reducing impacts of hazards that may reduce the efficacy of the Barriers; and

(E) provide to each State a credit in an amount equal to the amount of funds contributed by the State toward Barrier II.

### 1.3 – General Study Area

The regional study area for the fish dispersal system includes the Mississippi River and Great Lakes Basins, the IWW and the CAWS. The general vicinity of the study area includes reaches of the CSSC, lower Des Plaines River, I&M Canal, Cal-Sag Channel, Calumet River, Little Calumet River, Grand Calumet River, Chicago River, South Branch Chicago River, North Branch Chicago River and North Shore Channel. The study area is in all or part of Cook, Du Page, Lake and Will Counties in the metropolitan Chicago area in Illinois, and in Lake County, Indiana. The electric Dispersal Barriers Project is located at river mile 296.25, roughly 0.2 miles or 1300-foot upstream of the 135th Street Bridge in Romeoville, IL, Lockport Township, in Will County (Figures 1 and 2).

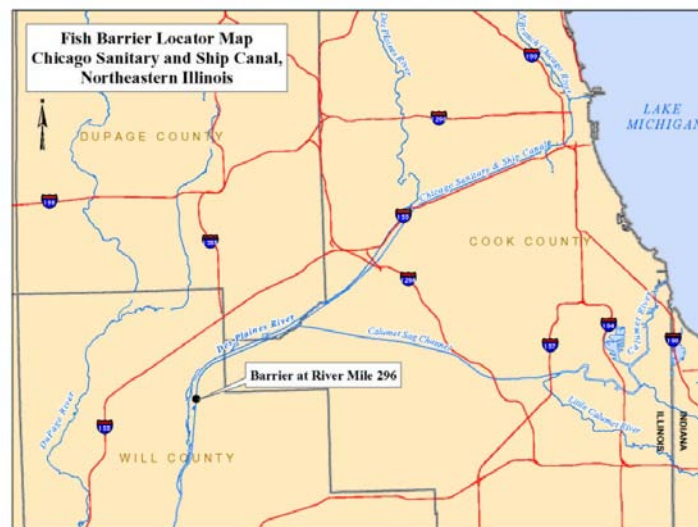


**Figure 1 - Electric Dispersal Barriers Project Location Map**

## SECTION 2 – Barrier Operations

The electric barriers operate by creating a waterborne pulsed direct current electric field in the Chicago Sanitary and Ship Canal. Fish penetrating the electric field are exposed to electrical stimuli which act as a deterrent. As fish swim into the field they feel increasingly uncomfortable. When the sensation is too intense, the fish is either immobilized or is deterred from progressing further into the field. The barrier electric field can be characterized by the equipment parameters of field strength or amplitude (voltage), pulse frequency (Hertz), and pulse length (duration) of the direct current pulses. The effectiveness of the barrier is influenced by these equipment parameters and by environmental parameters such as water conductivity, water temperature, and water flow velocity. The current barrier operating parameters are provided in Table 1.

Barrier	Date of Activation	Voltage (volts/inch)	Frequency (Hz)	Pulse Duration (ms)
Demo	2002	1.0	5	4
IIA*	2009	2.0	15	6.5
IIB	2011	2.0	15	6.5

\* Barrier IIA is currently in standby mode.

**Table 1 - Electric Dispersal Barriers Operating Parameters**

### 2.1 - Chicago Sanitary & Ship Canal, Dispersal Barrier I

The CSSC's first dispersal barrier (Barrier I or the Demonstration Barrier) was implemented as a demonstration project under authority granted by the Nonindigenous Aquatic Nuisance Prevention and Control Act of 1990, P.L. 101-646, 16 U.S.C. § 4722(i)(3) as amended. Barrier I was activated in April 2002, and was rehabilitated in 2008.

The demonstration barrier consists of twelve steel cables secured just above the canal bottom. The upstream-to-downstream length of the barrier is 54 feet (see Figure 2). A rapidly pulsed DC current is sent through the cables creating an electric field in the water that extends to the water surface. The cables, known as electrodes, are arranged in benthic and full water-column pairs. The three northern-most electrodes are the benthic electrodes. They target bottom-dwelling fish while the other electrodes target fish higher in the water column. The equipment for controlling the electric pulses is housed in a building on the east side of the canal.

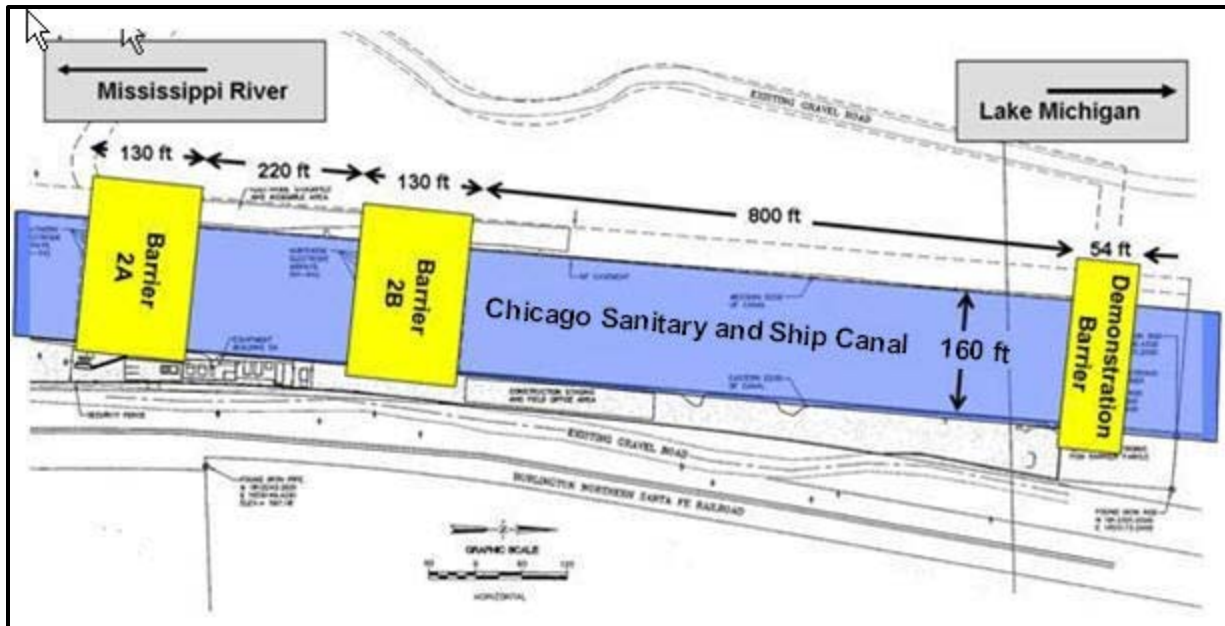


Figure 2 - Schematic of Electric Dispersal Barriers Project

## 2.2 - Chicago Sanitary & Ship Canal, Dispersal Barrier II

The second dispersal barrier (Barrier II) on the CSSC was initially implemented by the Corps under the Section 1135 program of the Water Resources Development Act of 1986, P.L. 99-662, as further authorized in Section 345 of the District of Columbia Appropriations Act, 2005, P.L. 108-335 and Section 3061(b)(1)(B) of WRDA 2007, P.L. 110-114. Barrier II is also an electrical field barrier, but includes design improvements identified during monitoring and testing of the demonstration barrier. Barrier II consists of two independently operated barriers, IIA and IIB.

Barrier IIA and Barrier IIB each consist of two sets of electrified arrays of 4" x 6" steel bars ("electrodes") that rest on the bottom and run across the width of the canal. Jacketed copper cables are fastened to the ends of the submerged electrodes that travel up individual bore-holes to copper buss bars located inside the barrier buildings. The buss bars connect to electrically operated Polarity Switches and then to the output of electronic pulse generators ("Pulsers"). A large capacitor array stores electrical charge that the electronic switch sends in short repetitive pulses of DC voltage, to the electrodes. These capacitor arrays receive DC power from the electronic chargers. There are three such chargers, one for each of the three Pulsers. Two Pulsers are needed to energize each of the two electrode arrays, while the third Pulser is a spare that can be pressed into service by operation of the appropriate polarity switch.

Barrier IIA was activated in April 2009 at the same settings as the demonstration barrier. These settings were increased to the current settings in August 2009 in response to monitoring results that suggested Asian carp were closer to the barriers than earlier believed.

Barrier IIB was activated in April 2011 at Barrier IIA's settings, and Barrier IIA was placed into warm standby mode.

## **SECTION 3 – Research Efforts**

### **3.1 – Operational Protocols for Electric Barriers**

The Operating Protocols Report reviews laboratory research efforts related to the impacts on very small Asian carp of various operating parameters and environmental stimuli at the Electrical Dispersal Barrier system in the Chicago and Sanitary Ship Canal (CSSC). The research included five different laboratory experiments which focused on how very small fish were affected by various electrical parameters, water conductivity, volitional challenge of electric fields, and water velocity. The experiments were conducted in a controlled environment in the research laboratories at the U.S Army Engineer Research and Development Center (ERDC), in a collaborative effort with the Corps' barrier contractor, Smith-Root, Inc. (SRI). Most of the experiments discussed in the Operating Protocols Report focus on defining the electric barrier operating parameters necessary to deter the movement of very small Asian carp, two to three inch fish, of a size that would have been spawned that year. Longer fish are more readily deterred than shorter fish, because the longer the fish, the greater the electrical gradient that develops across the fish. As a result of the inverse relationship between fish size and immobilization caused by the electric field, research on optimal operating parameters can be completed on shorter fish with confidence that operating parameters that deter the shorter fish will also be effective on longer fish. This report is included as Appendix A.

a. Pilot Study Tank Tests on Juvenile Asian Carp. In April 2009, laboratory tank tests were conducted by ERDC and SRI on wild caught juvenile (although not the smaller young of the year) silver carp between 5.4 to 11 inches long. In these tests, it was determined that operating parameters of 15 pulses per second with each pulse 6.5 milliseconds long and a maximum in water field strength at the water surface of 2 Volts per inch immobilized all of the juvenile Asian carp used in the research. These are the parameters currently in effect at Barrier IIB.

b. Initial Environmental DNA Results. As a result of collaboration with the University of Notre Dame to apply its emerging technology of environmental DNA to the CSSC to determine if Asian carp DNA could be detected in the waterway, in July 2009, Notre Dame scientists reported to the Corps that Asian carp DNA was detected approximately 6 miles south of the Barrier. In response, the Corps increased Barrier IIA's operating parameters to 15 pulses per second with each pulse 6.5 milliseconds long and a maximum in water field strength at the water surface of 2 Volts per inch in August 2009, following close coordination with the Coast Guard on additional safety testing.

c. Tank Testing on Very Small Bighead Carp. The Corps focused its next phase of laboratory research on very small Asian carp approximately 2 to 3 inches in length which were spawned that year. From September to December 2009, a second phase of tank testing using bighead carp 2 to 3 inches in length was conducted. Because it is difficult to obtain wild-caught Asian carp of this small size, the experiments used pond cultured bighead carp. Results from the second phase of tank testing indicated that the current settings at Barrier IIA may not immobilize the smallest fish tested, although all of the exposed fish did exhibit behavior that appeared to be avoidance responses. Additional flume testing was scheduled to further study the avoidance responses of the fish.

d. Volitional Flume Tests on Very Small Bighead Carp. In April 2010, flume tests were completed which evaluated the behavior of 2 to 3 inch bighead carp in a shallow oval flume with flowing water and a small-scale, modeled barrier electric field. The purpose of this test was to determine whether Asian carp voluntarily avoided or challenged an electrical field in the water. During the tests, some fish challenged the barrier repeatedly, even shortly after recovering from being immobilized in a previous attempt, and some fish were able to pass through the electrified area. The tests results do not necessarily indicate that very small fish will pass through the barriers because the modeled electrical field in the flume was only approximately 1/10 the length of the electric field at the barriers. In addition, a small viewing window in the experiment may have allowed the fish a respite from the electric current and water velocity, and thus assisted in their passage through the modeled field. Additional research on the status of the canal walls near the electric barriers is recommended to see if a similar issue exists in the field. However, the preliminary indication of this research is that the barriers as currently operated may not immobilize very small sizes of fish.

e. Water Conductivity and Water Velocity Impact Research. Other tests have also been completed on bighead carp 2 to 3 inches in length to evaluate the effect of variations in water conductivity and water velocity on barrier effectiveness. In general, higher water conductivities make an electric barrier less effective and higher water currents make the barrier more effective against fish swimming upstream into the electric field. Barrier II's power output is automatically adjusted to maintain the desired voltage at the water surface as a result of the conductivity tests in order to lessen any potential risk during times when the conductivity in the canal is high.

f. Summary. The combined results of the aforementioned studies indicate operation of the barrier at 30 pulses per second with each pulse 2.5 milliseconds long and a maximum in water field strength at the water surface of 2.3 Volts per inch may be necessary to maximize the barrier's effectiveness in deterring very small Asian carp.

### **3.2 – In-Water Safety Testing with Increased Voltage and Frequency Operating Parameters**

The In-Water Testing report, included as Appendix B, documents the results of tests conducted within the canal in February and June 2011 by ERDC's Construction Engineering Research Laboratory (CERL) to determine how operation of the barriers at different configurations impacts public safety. Testing protocols were coordinated with the United States Coast Guard (USCG). The target test configurations are listed in Table 2.

The tests, conducted in February and June 2011, were designed to accomplish the same objectives as the tests conducted prior to operating Barrier IIA, as follows:

- a. Meet regulatory requirements established by Illinois Department of Natural Resources permit NE2004099
- b. Field strength mapping
- c. Sparking potential during fleeting operations
- d. Sparking potential in the event of a collision in the fleeting area
- e. Voltage potential between barges traversing the canal over the barriers
- f. Personnel shock potential at the bollards at the fleeting area

- g. Corrosion potential
- h. Optimal settings for the parasitic system

	<b>Barrier IIA</b>	<b>Barrier IIB</b>	<b>Barrier I</b>
A (Alpha)*	2.0 V/in., 15 Hz, 6.5 ms	2.3 V/in., 30 Hz, 2.5 ms	1 V/in., 5 Hz, 4 ms
B (Bravo)*	2.3 V/in., 30 Hz, 2.5 ms	2.3 V/in., 30 Hz, 2.5 ms	1 V/in., 5 Hz, 4 ms
C (Charlie)*	2.0 V/in., 15 Hz, 6.5 ms	2.0 V/in., 15 Hz, 6.5 ms	1 V/in., 5 Hz, 4 ms
D (Delta)*	2.3 V/in., 30 Hz, 2.5 ms	OFF	1 V/in., 5 Hz, 4 ms
E (Echo)*	OFF	2.3 V/in., 15 Hz, 6.5 ms	1 V/in., 5 Hz, 4 ms
F (Foxtrot)*	OFF	2.0 V/in., 30 Hz, 2.5 ms	1 V/in., 5 Hz, 4 ms

\* Actual test field strengths approximate

**Table 2 – Target In-Water Test Operational Scenarios**

a. Field Strength Mapping. Field mapping to determine the extent of the electrical field within the canal was performed for each of the operational scenarios (see Figures 3 through 8) using a 22-foot fiberglass hulled boat. Measurements of voltage (1) between horizontal electrodes spaced 1 – 6 ft apart were used to map the horizontal electric field, and (2) between two vertical electrodes spaced 5 ft apart were used to map the vertical field. Measurements of current (1) through a 100-ohm ( $\Omega$ ) resistor between two horizontal electrodes spaced 1 ft apart was used to simulate current flow through the chest, (2) through a 500  $\Omega$  resistor between two horizontal electrodes spaced 6 ft apart was used to simulate current flow through a body floating prone in the canal, and (3) through a 500  $\Omega$  resistor between two vertical electrodes spaced 5 ft apart was used to simulate current flow through an upright body. Figures 3 through 8 depict the relative locations of the areas of likely harmful effects for the operational scenarios tested. The results show the electrical field is longer when both barriers are operational, which indicates greater area of likely harmful effects to a person in the water.





Figure 3 - Operational Scenario ALPHA



Figure 4 - Operational Scenario BRAVO



Figure 5 - Operational Scenario CHARLIE

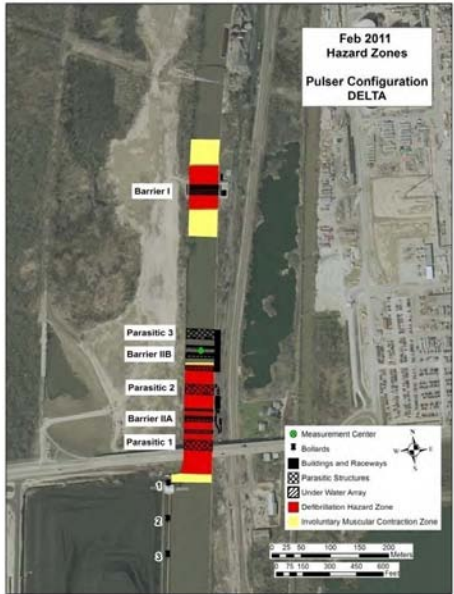


Figure 6 - Operational Scenario DELTA

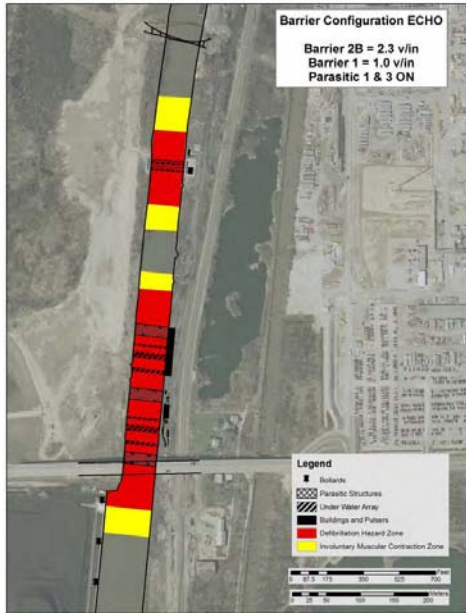


Figure 7 - Operational Scenario ECHO

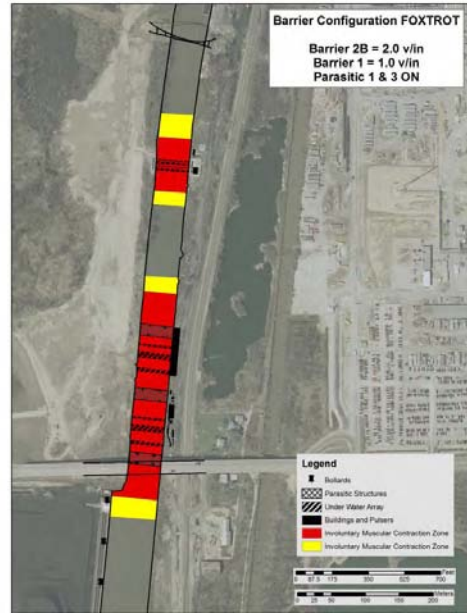


Figure 8 - Operational Scenario FOXTROT

b. Sparking potential during fleeing operations and in the event of a collision in the fleeing area. Sparking potential testing was completed for each of four operational scenarios. Three configurations for assembling a tow were utilized for testing sparking potential during fleeing operations: assembling a tow with the barges in *series*, in *parallel*, and *insertion* (see Figures 9 through 11) of a single barge into a tow. A fourth test simulated the collision of a tow consisting of five barges in series with two towboats (one on each end of the tow) spanning both Barriers IIA and IIB with two parallel barges moored in the fleeing area. The tow passed over the electrode arrays of Barrier IIA and Barrier IIB while approaching the fleeing area. Test results show that there is greater risk of sparking during the insertion fleeing operation than during series or parallel tow operations. The results also show that the operation of both barriers at the same time increases the potential for sparking during fleeing operations. For coal-handling operations in the barge loading and fleeing area, and in the open storage area, the pertinent literature does not support concern for electrical sparking to create an explosion hazard. Further, there is no appreciable increase in sparking risk when operating one barrier at 2.3 volts per inch, 30 Hz and 2.5 ms pulses when compared to operation at 2.0 volts per inch, 15 Hz and 6.5 ms pulses.





Figure 9 – Barges in series

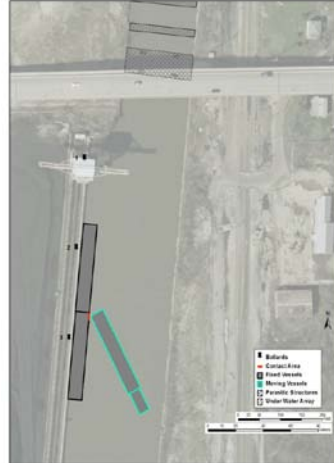


Figure 10 – Barges in parallel

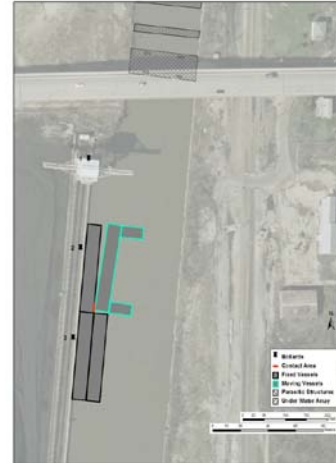


Figure 11 – Barges in insertion

c. Voltage potential between barges traversing the canal over the barriers. Long tow testing was completed for each of the barrier operational scenarios. In these tests a tow of five fully loaded barges in a single line made a minimum of three trips traversing from the fleeting area to above the aerial pipeline arch. There were two towboats, one at each end of the five-barge tow. The boats are designated 0 and 6, the barges 1 – 5, which resulted in six measurement channels (see Figure 12). All components of the tow were connected using wire rope, as is typical for transit on the canal. The test was not adequately completed due to an equipment failure, but based on completed tests there is a low probability for sparking between barges in a tow while traversing the barriers. Previous testing indicated there is no significant risk associated with these tests, which are designed to identify the potential for sparking between barges traveling in a long-tow formation using wire rope to connect the barges.

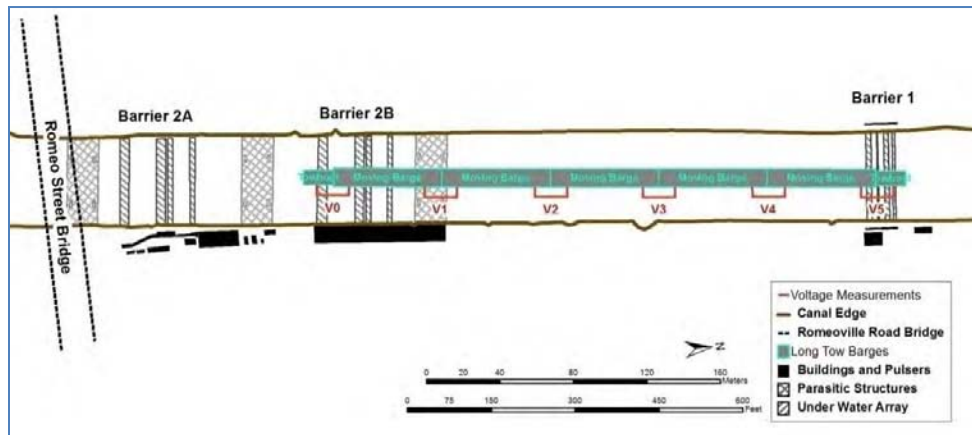


Figure 12 – Long tow test arrangement

d. Personnel shock potential at the bollards at the fleeting area. Voltage and current measurements at the fleeting area south of the dispersal barriers were recorded for each of the six barrier operational scenarios. This test measured the voltages and currents between fixed barges in the fleeting area and the dock. Tests were conducted at the number 2 and number 3 tee-moorings using a 500 Ω resistor, as this resistance simulates the impedance of the human body from hand to foot. The results of this test indicated no personnel shock hazard at the fleeting area due to operation of the barriers.

e. Corrosion potential. In order to determine if barrier operations accelerated the corrosion rate of in-water steel structures in the fleeting area, corrosion potential measurements were made on moored barges assembled in series while the sparking potential tests were conducted. Hull voltage potentials were measured between a copper/copper sulfate reference electrode immersed in canal water at the stern corner on the starboard side of the moored barge and the steel hull, as diagrammed. The barge was fully loaded to achieve maximum hull exposure underwater. The results of this testing event, in addition to previous results, indicate long term corrosion effects would not be an issue provided the tow is electrically connected while entering, passing through, and continuing beyond the barrier by at least several hundred feet at a relatively uniform rate.

f. Optimal settings for the parasitic system. As part of Barrier IIB construction steel grids, referred to as parasitics, were mounted on concrete curbs that rest on the bottom of the canal to control the spread of electric current within the water. These grids were placed above Barrier IIB, between Barrier IIB and IIA, and below Barrier IIA. The parasitics are controlled by switches that connect them to an electrical bus onshore, which also provides a low-impedance path for those currents to return to other side of barrier. In an effort to determine the optimal configuration of these structures, the connections between the parasitics were varied throughout the other tests conducted as part of this research effort. To achieve the optimal parasitic configuration, the tests show it is only necessary to operate the two structures directly adjacent to the active barrier arrays.

g. Summary. The results of the in-water safety tests indicate existing risks of sparking, corrosion, and personnel shock hazard are not appreciably increased by operating one barrier at 2.3 volts per inch, 30 hertz, and 2.5 millisecond pulse length versus 2.0 volts per inch, 15 hertz and 6.5 millisecond pulse length.

### **3.3 – Ground Current Investigation**

In February 2010, USACE began an investigation of impacts of barrier operations on canal and earth surface potential (voltage) gradients. During the following months data was collected in the areas surrounding the barriers, which was used to establish the extent and influence of ground current under various barrier operational scenarios and parasitic configurations. Over 40 test points were monitored by driving metal rods into the soil in a right triangle configuration near a grounded conductive structure of interest. Measurements were taken in accordance with industry standard to represent situations where a human could come into contact with ground currents near the barrier. The results of the investigation show no appreciable change to existing safety risks by operating the barrier at 2.3 volts per inch versus 2.0 volts per inch. Measures to mitigate the effects of ground current have been implemented as necessary, and have found to be effective in reducing the risk of electrical shock.

## **SECTION 4 – Asian Carp Location in Relation to the Electric Barriers**

In March 2011, scientists representing agencies of the ACRCC with expertise in Asian carp demographics prepared a summary of the documented current range of both adult and juvenile bighead and silver carp in the IWW.

### ACRCC Statement from March 2011:

“It is highly unlikely that small Asian carp are present in Lockport or Brandon Road pools of the IWW. Currently, the best estimate of the closest location of a potentially reproducing population of Asian carp is in the Marseilles Pool, approximately 25 miles and three locks downstream of the electric barriers.

The sustainable population front of an established adult population is in Dresden Island Pool and has remained there since 2007; we have not observed any upstream progression of a sustained Asian carp population above RM 286. Since we do not have evidence of spawning in the Dresden Island Pool, and only the potential for reproduction in Marseilles, we can conclude that the risk of small Asian carp presence in the Brandon Road and Lockport Pools is unlikely. This known spatial extent of Asian carp, coupled with the driving factor of poor habitat quality, are reasons why we also do not expect this risk to change significantly in the near future.

Additionally, USGS has documented that larval Asian carp require a drift period, totaling well over a hundred hours of drift, before moving into nursery habitat to grow and thrive. This means that juvenile Asian carp, to reach the barrier, would have to swim back upstream that drift distance PLUS the distance from the spawning site to the barrier. This distance likely exceeds the ability for a small (5 inches and smaller) Asian carp to travel in their first year of life.

Additional systematic surveys and assessments by USFWS and other cooperating partners will be conducted to monitor for the presence of very small Asian carp on an ongoing basis. However, the absence of an established adult population coupled with the lack of suitable habitat in the lock pools nearest the fish barrier reduces the likelihood that very small Asian carp are present in either of these pools.”

In April 2011, Illinois Department of Natural Resources (IDNR) confirmed that the most upstream location of verified spawning (presence of young-of-year, YOY, fish) was at river mile (RM) 181 near Chillicothe, Illinois, over 150 miles from Lake Michigan and 115 miles downstream from the barriers. This information facilitated the characterization of the risk that very small Asian carp might be in the Peoria Pool. Asian carp monitoring efforts indicate the location of spawning adults is limited to below Dresden Island Lock and Dam, which is located at RM 271 (62 miles from Lake Michigan and 25 miles below the Barrier), yet no juvenile or YOY have been captured in pools with the adults. Further, the population of either species has not expanded beyond RM 278 (around the I-55 bridge near Channahon, Illinois) since 2006 with two exceptions - a single bighead carp captured in Lockport pool during the December 2009 rotenone event and a single bighead carp captured in Lake Calumet in June 2010. It is unknown how the Lake Calumet might have arrived at that location, whether by human transport, prior to barrier construction, or other means.

An interagency team (USACE, IDNR, and USFWS) is preparing a white paper to specifically document the occurrences of all life stages of bighead and silver carp, characterize the existing information and better define data gaps. This white paper will take into account the documented evidence, as well as expert opinion of state, Federal, and academic biologists, and aim to develop a predictive theory to allow continued vigilance on the presence of small Asian carp in the IWW. The white paper will also outline a plan of action to continue assessing this risk over time.

In direct response to the results of the Operating Protocols research, USACE engaged in a field test of small fish response to the barriers using the existing ultrasonic telemetry current. Small receivers were surgically implanted into 14 non-Asian carp species in June 2011. Fish ranged in size from 2.1 to 7.5 inches; species included white sucker, sunfish spp, bullhead, largemouth bass, and crappie. Species for tagging were selected based on body type, total length, swimming characteristics (speed, position in water column), and availability of catch. Fish were captured using mini-fyke nets and DC electrofishing. Six fish were released immediately upstream of Barrier IIB; the remaining 8 fish were released immediately downstream of Barrier IIB. Fish movements were continuously tracked by stationary receivers that triangulate the position of the fish to give precise location and movement data.

Results indicate that from 20 June 2011 through 11 August 2011, none of the fish released below the barrier moved upstream; they all remained below the barrier. Two of the six fish released upstream of the barrier passed downstream through both arrays of Barrier IIB; two moved down into the array of IIB and remained there; and the last two moved upstream away from the barriers. Nearly 300,000 detections from the small fish study support the preliminary conclusion that the barriers at the current operating parameters effectively prevent all upstream passage of tagged fish down to 2.1 inches in length.

## **SECTION 5 – Conclusions and Recommendations**

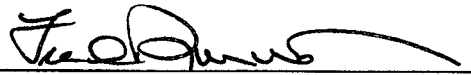
I have considered all relevant aspects of the problems and opportunities as they relate to the safe operation of the Electric Dispersal Barriers and the risk of bighead and silver carp in the Illinois Waterway and the Chicago Area Waterways.

Existing laboratory research indicates the barrier at its current settings is effective for deterring fish greater than 5.4 inches in length, but may not be as effective in deterring very small fish. In addition, monitoring efforts indicate there is no present threat of juvenile Asian carp smaller than 6 inches being present in the vicinity of the barrier, as the closest location of a potentially reproducing population of Asian carp is in the Marseilles pool, approximately 25 miles downstream of the barriers. Furthermore, the closest location of verified Asian carp spawning is in the Peoria pool, approximately 116 miles downstream of the barriers.

Field testing and investigations show that there is no appreciable change to existing risks to the safety of people or structures by increasing operating parameters to the slightly elevated protocols indicated by the Operational Protocols Laboratory Research report.

I recommend continued operation of the demonstration barrier at its current settings and operation of only one of the Barrier II facilities at a time, either Barrier IIA or Barrier IIB, as conditions warrant. I further recommend increasing the operating parameters from 2.0 volts per inch, 15 hertz and 6.5 millisecond pulse length to 2.3 volts per inch, 30 hertz, and 2.5 millisecond pulse length upon completion of necessary coordination with the United States Coast Guard and the navigation community. In order to take the most conservative approach possible, I make this recommendation despite the current state of knowledge regarding the likely location of small Asian carp and the effectiveness of current barrier settings.

I also recommend continuing research efforts underway to ensure the safe operation and to assess the effectiveness of the barriers.



Frederic A. Drummond, Jr.  
Colonel, U.S. Army  
District Commander  
Chicago District

## **Appendix A**

### **Operational Protocols Research Report**



**DEPARTMENT OF THE ARMY**  
U.S. ARMY ENGINEER DIVISION, GREAT LAKES AND OHIO RIVER  
CORPS OF ENGINEERS  
550 MAIN STREET  
CINCINNATI, OH 45202

CELRD-DE

24 MAR 2011

**SUBJECT:** "Operational Protocols for Electric Barriers on the Chicago Sanitary and Ship Canal: Influence of Electrical Characteristics, Water Conductivity, Fish Behavior, and Water Velocity on Risk for Breach by Small Silver and Bighead Carp"

1. **PURPOSE:** This memorandum summarizes the research and conclusions of the report titled "Operational Protocols for Electric Barriers on the Chicago Sanitary and Ship Canal: Influence of Electrical Characteristics, Water Conductivity, Fish Behavior, and Water Velocity on Risk for Breach by Small Silver and Bighead Carp" (Operating Protocols Report). This memorandum also describes how the Operating Protocols Report fits into the larger context of the Interim II Study and other ongoing efforts by the Corps related to the fish barrier, as well as other ongoing and planned research efforts by the US Fish and Wildlife Service (USFWS) and the US Geological Survey (USGS) related to the location of Asian carp in the upper Illinois waterway system. The Operating Protocols Report describes specific research commissioned by the Corps and conducted through a collaborative effort between the Corps' Engineer Research & Development Center (ERDC) and the Corps' barrier contractor, Smith-Root, Inc. (SRI). This Operating Protocols Report was conducted as part of the Congressionally authorized "Efficacy Study", and as such is a component of one of the reports related to that study, called Interim Report II, which will be released later in 2011.

2. **OPERATING PROTOCOLS REPORT SUMMARY.** The Operating Protocols Report reviews laboratory research efforts related to the impact of the fish barrier and various other conditions likely to be encountered at the Electrical Dispersal Barrier system in the Chicago and Sanitary Ship Canal (CSSC), which could affect the behavior of small Asian carp, applying conservative hypothetical "worst case" scenarios. The research included five different laboratory experiments, which focused on how very small fish were affected by various electrical parameters, water conductivity, volitional challenge of electric fields, and water velocity. The experiments were conducted in a controlled environment in the research laboratories at ERDC. Most of the experiments discussed in the Operating Protocols Report focus on defining the electric barrier operating parameters necessary to deter the movement of very small Asian carp, two to three inch fish, of a size that would have been spawned that year. For any fish that are at a given spot within the electrified water created by a barrier, the longer a fish is, the greater the electrical gradient that develops across the fish. Therefore, longer fish are more readily deterred than shorter fish, and research on optimal operating parameters can be completed on shorter fish with confidence that operating parameters that deter the shorter fish will also be effective on longer fish.

3. **DESCRIPTION OF ELECTRICAL BARRIER SYSTEM.** The electric barriers operate by creating a waterborne-pulsed direct current electric field in the Chicago Sanitary and Ship Canal. Fish penetrating the electric field are exposed to electrical stimuli, which act as a deterrent. The

CELRD-DE

SUBJECT: "Operational Protocols for Electric Barriers on the Chicago Sanitary and Ship Canal: Influence of Electrical Characteristics, Water Conductivity, Fish Behavior, and Water Velocity on Risk for Breach by Small Silver and Bighead Carp"

barrier electric field can be characterized by the equipment parameters of field strength or amplitude (voltage), pulse frequency (Hertz), and pulse length (duration) of the direct current pulses. The effectiveness of the barrier is influenced by these equipment parameters and by environmental parameters such as water conductivity, water temperature, and water flow velocity.

4. PREVIOUS RESEARCH. Prior to the experiments discussed in the Operating Protocols Report, the Corps and other entities had already engaged in several other studies. The first electric barrier (Barrier I), completed in 2002, had its initial operating settings based on the prior experience of the designer of the barrier system. From 2003 to 2008, the University of Illinois and the Illinois Natural History Survey conducted a field research program in the area of the Chicago Sanitary and Ship Canal near the electric dispersal barrier in which 145 radio-tagged common carp were placed downstream of Barrier I. Of those 145 tagged fish, only one radio transmitter crossed from downstream to upstream of Barrier I, in 2003, but that fish did not appear to have survived the crossing because the transmitter remained stationary shortly after transiting the barrier. It appears that this fish may have been carried across the barrier in the wake of a transiting barge. This incident resulted in additional studies and the decision to change the operating parameters of Barrier I to 5 pulses per second with each pulse 4 milliseconds long and maximum in-water field strength at the water surface of 1 Volt per inch. The Corps made changes to the design of Barrier II with regard to the number and spacing of the electrodes to counteract the potential impact of passing barges that may have led to this incident.

a. The Corps designed and constructed Barriers IIA and IIB to operate over a wider range of pulse parameters and voltages than Barrier I as a result of additional research published by other scientists. No radio-tagged fish crossed Barrier I after the operating parameters were changed in 2003. The Corps believes that the operating parameters of Barrier I are effective against adult Asian carp.

b. Between 2007 and 2009, the Corps and other agencies implemented the use of acoustic telemetry to tag and track Asian carp in the upper pools of the Illinois Waterway from the Starved Rock, Marseilles, and Dresden Island pools approximately 52 miles below the electric barriers. Telemetry stationary and mobile receivers detect movement of the tagged carp. To date, none of the tagged carp have ventured upstream of the Dresden Island pool.

#### 5. OPERATING PROTOCOL RESEARCH.

a. Pilot Study Tank Tests on Juvenile Asian Carp. In April 2009, laboratory tank tests were conducted by ERDC and SRI on wild caught juvenile (although not the smaller young of the year) silver carp between 5.4 to 11 inches long. In these tests, it was determined that operating parameters of 15 pulses per second with each pulse 6.5 milliseconds long and a maximum in water field strength at the water surface of 2 Volts per inch immobilized all of the juvenile Asian carp used in the research. These are the current settings used at Barrier IIA.



CELRD-DE

SUBJECT: "Operational Protocols for Electric Barriers on the Chicago Sanitary and Ship Canal: Influence of Electrical Characteristics, Water Conductivity, Fish Behavior, and Water Velocity on Risk for Breach by Small Silver and Bighead Carp"

b. Tank and Swim Tunnel Testing on Very Small Bighead Carp. The Corps focused its next phase of laboratory research on very small Asian carp approximately 2 to 3 inches in length. Asian carp of this size are within the first year after spawning. From September to December 2009, tank and swim tunnel testing using Bighead carp 1.7 to 3.2 inches in length was conducted. Because it is difficult to obtain wild-caught Asian carp of this small size, the experiments used pond cultured Bighead carp. Results from the second phase of tank testing indicated that the current settings at Barrier IIA might not immobilize the smallest fish tested, although all of the exposed fish did exhibit behavior that is typical of avoidance responses. Additional flume testing was scheduled to further study the avoidance responses of the fish.

c. Volitional Flume Tests on Very Small Bighead Carp. In April 2010, flume tests were completed which evaluated the behavior of approximately 2 to 3 inch long bighead carp in a shallow oval flume with flowing water and a small-scale, modeled barrier electric field. The purpose of this test was to determine whether Asian carp voluntarily avoided or challenged an electrical field in the water. During the tests, some fish challenged the barrier repeatedly, even shortly after recovering from being immobilized in a previous attempt, and some fish were able to pass through the electrified area. The tests results do not necessarily indicate that very small fish will pass through the barriers because the modeled electrical field in the flume was only approximately 1/10 the length of the electric field at the barriers. In addition, a small viewing window in the experiment may have allowed the fish a respite from the electric current and water velocity, and thus assisted in their passage through the modeled field. Additional research on the status of the canal walls near the electric barriers is recommended to see if a similar issue exists in the field. However, the preliminary indication of this research is that the barriers as currently operated may not immobilize very small sizes of fish. If very small fish are potentially in the vicinity of the fish barrier, this would imply a change to the current operating parameters is warranted. However, as explained further below, all evidence indicates that the closest population of very small bighead and silver carp is in the Marseilles Pool, approximately 25 miles downstream from the electrical barriers, and not in a position to challenge the barriers at this time.

d. Water Conductivity and Water Velocity Impact Research. Other tests have also been completed on bighead carp 2 to 3 inches in length to evaluate the effect of other relevant environmental factors, especially variations in water conductivity and water velocity, on barrier effectiveness. In general, higher water conductivities make an electric barrier less effective and higher water currents make the barrier more effective against fish swimming upstream into the electric field. As a result of the conductivity tests, the Corps instituted changes to Barrier IIA's operational protocols in order to lessen any potential risk during times when the conductivity in the canal is high. Spikes in conductivity can occur during winter months when salt runoff from roads is high.

6. INTERIM II STUDY. The Interim II Study will evaluate all of the research information from the Operating Protocols Report, along with potential safety and operational impacts on the

CELRD-DE

SUBJECT: "Operational Protocols for Electric Barriers on the Chicago Sanitary and Ship Canal: Influence of Electrical Characteristics, Water Conductivity, Fish Behavior, and Water Velocity on Risk for Breach by Small Silver and Bighead Carp"

barrier system of altering the parameters, as well as additional evaluation of information on the location of very small Asian carp in the upper Illinois River. This comprehensive evaluation is designed to leverage all currently available information in making the best-informed decision possible related to the barrier system's operating parameters. It is undesirable to operate the barriers at higher operating parameters than necessary because of the increased safety hazards associated with higher parameters, and the increased wear and tear on the equipment resulting in more frequent maintenance needs.

a. Location and Threat of Very Small Asian Carp. The Interim II Study will also include an assessment of the current knowledge on the location of very small 2 to 3 inch Asian carp and their proximity to electric barriers. Currently, the best estimate of the closest location of a potentially reproducing population of Asian carp, which is necessary to produce the very small fish of the size tested in this research, is in the Marseilles Pool, located between the Marseilles Lock and Dam (RM 246) and the Dresden Island Lock and Dam (RM 271). The upstream limit of the Marseilles Pool is approximately 25 miles and 3 locks downstream from the electrical barriers. Reproduction has not been confirmed in this pool, but is possible. The furthest upstream location of a verified reproducing population in the Illinois Waterway is in the Peoria Pool, below Starved Rock Lock and Dam, 5 locks and over 65 miles downstream of the Barrier. Because of the lack of an established adult population in the lock pools nearest the fish barrier (Lockport and Brandon Road Pools), and the unsuitable habitat to support young of the year Asian carp near the barrier, current conclusions are that it is unlikely that very small Asian carp are present in either of these pools.

b. Larval Asian Carp Drift. Additionally, USGS has documented that larval Asian carp require a drift period, totaling well over a hundred hours of drift, before moving into nursery habitat to grow and thrive. This means that juvenile Asian carp, to reach the barrier, would have to swim back upstream that drift distance plus the distance from the spawning site to the barrier. This distance likely exceeds the ability for a small (5 inches and smaller) Asian carp to travel in their first year of life.

c. Future Research on the Threat of Small Asian Carp. Additional systematic surveys and assessments by USFWS and other cooperating partners will be conducted to monitor for the presence of very small Asian carp in the upper Illinois waterway on an ongoing basis. However, the absence of an established adult population coupled with the lack of suitable habitat in the lock pools nearest the fish barrier reduces the likelihood that very small Asian carp are present in either of these pools.

d. Safety Considerations. A significant factor in any decision to alter the operating parameters at the barriers is safety. The Interim II Study will evaluate the results of recent safety tests. In February of 2011, the Corps conducted safety testing of Barrier IIA and IIB at the current operating parameters as well as at the increased operating parameters that would immobilize 2 to 3 inch fish as indicated by the Operating Protocols Report. The results of those

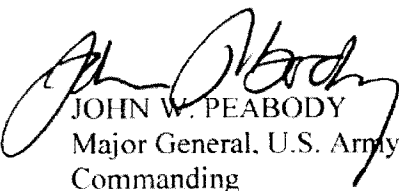
CELRD-DE


SUBJECT: "Operational Protocols for Electric Barriers on the Chicago Sanitary and Ship Canal: Influence of Electrical Characteristics, Water Conductivity, Fish Behavior, and Water Velocity on Risk for Breach by Small Silver and Bighead Carp"

tests are being compiled and analyzed. Further safety testing may be required. The Corps is coordinating with the US Coast Guard with regard to the safety aspects of the operation of the electric barriers.

7. FIELD RESEARCH. In addition to the Interim II Study, the Corps, in coordination with assistance from members of the Asian Carp Regional Coordinating Committee (ACRCC), is conducting a variety of research efforts in the field near the fish barrier system to evaluate the actual efficacy of the electric barriers in the CSSC. The Corps is using ultrasonic telemetry to track 81 tagged fish in the Chicago Area Waterway System and near the barrier. To date, 61 of those fish have been detected a total of over 620,000 times, but none of the tagged fish have crossed the electric barrier. An additional 24 fish have been tagged but not yet monitored. This spring and summer the Corps will tag 95 more fish (fathead minnow, golden shiner, creek chub, and common carp), including 30 small fish, which will be released between and below the barriers, and their movement will be monitored. The Corps and the ACRCC will also use dual frequency sonar (DIDSON) camera to evaluate real-time fish response to the electrical field to monitor and further validate the efficacy of the barriers in field conditions. In 2011, the U.S. Fish and Wildlife Service have already begun to conduct tests with caged fish using surrogate species other than Asian carp. Specifically, fish are briefly acclimated to the caged environment, and then passed through Barriers I and IIA while being observed through the DIDSON camera. The initial results from the caged fish tests showed all fish tested becoming completely incapacitated at the same point in Barrier IIA.

8. CONCLUSION. The Corps will continue to evaluate and refine the operation of the electric dispersal barrier system to ensure its efficacy. In particular, the Corps intends to adjust the operating parameters if evidence indicates that very small Silver or Bighead carp migrate closer to the electric barrier, once a full understanding of safety and maintenance implications is achieved. Any questions about this Operating Protocols Report should be directed to the Chicago District Public Affairs Office at 312-846-5330.

  
JOHN W. PEABODY  
Major General, U.S. Army  
Commanding

  
VINCENT V. QUARLES  
Colonel, U.S. Army  
District Commander



**Smith-Root, Inc.**  
14014 NE Salmon Creek Avenue  
Vancouver, Washington 98686

**Final Report**  
Submitted: July 2010  
Final Revision: March 2011

---

**Operational Protocols for Electric Barriers on the  
Chicago Sanitary and Ship Canal: Influence of Electrical  
Characteristics, Water Conductivity, Fish Behavior, and  
Water Velocity on Risk for Breach by Small Silver and  
Bighead Carp**

**Final Report**

Principal Investigator  
F. Michael Holliman, PhD

## Table of Contents

Figures.....	iii
Tables.....	iv
Units and Conversion of SI (Metric) to Non-SI Units of Measurement.....	iv
Executive Summary.....	1
Acknowledgements.....	6
1 – Pilot Study on Operational Protocols for Induction of Passage-Preventing Behaviors in Small Silver Carp.....	7
Introduction .....	7
Methods.....	10
Results.....	12
Discussion.....	17
Work cited.....	20
2 – Evaluation of Operational Protocols for Induction of Passage-Preventing Behaviors in Small Bighead Carp.....	22
Introduction .....	23
Methods.....	27
Results.....	34
<i>Screening trial</i> .....	34
<i>Experiment for predictive modeling</i> .....	37
Discussion.....	48
Work cited.....	54
3 – Evaluation of Effects of Water Conductivity on Barrier Effectiveness.....	57
Summary .....	57
Introduction .....	57
Methods.....	59
Results.....	63
Discussion.....	75
Work cited.....	79
4 – Evaluation of Volitional Challenge of Electric Fields by Small Bighead Carp .....	81
Summary .....	81
Introduction .....	82
Methods.....	84
Results.....	89
Discussion.....	94
Work cited.....	97
5 – Effects of Water Velocity on Risk for Breach of Barrier Electric Fields by Small Bighead Carp .....	98
Summary .....	98
Introduction .....	99
Methods.....	101
Results.....	105
Discussion.....	111
Work cited.....	115
6 – Conclusions and Directions for Future Research .....	116
Work cited.....	119

## Figures

Figure 1 – 1. Closed water-recirculating systems .....	11
Figure 1 – 2. Exposure tank.....	11
Figure 1 – 3. Protective netting, frame, and cover for the exposure tank .....	13
Figure 1 – 4. Power supply for the exposure tank .....	13
Figure 1 – 5. Barrier IIA output capabilities .....	14
Table 1 – 1. Operational protocols tested in the pilot study on silver carp .....	15
Figure 1 – 6. Length-frequency histogram.....	15
Figure 1 – 7. Cumulative percent of silver carp immobilized .....	16
Figure 2 – 1. Simulation of the electric field of Barrier IIA. A. Representation of .....	25
Figure 2 – 2. Barrier output capabilities .....	28
Figure 2 – 3. Exposure tank for the experiments in the screening trial.....	29
Figure 2 – 4. Brett swim tunnel.....	30
Figure 2 – 5. Electric fields applied in the simulations.....	32
Figure 2 – 6. Proportions of fish immobilized in the screening experiments .....	36
Figure 2 – 7 A. Thresholds of targeted responses in the simulations.....	39
Figure 2 – 7 B. Thresholds of targeted responses in the simulations.....	40
Figure 2 – 8. Proportions of fish immobilized in the simulations for predictive modeling .....	43
Figure 2 – 9. Relative risk of fish not being immobilized .....	44
Figure 2 – 10. Occurrence and predicted probability of immobilization in 46 – 72 mm bighead carp .....	47
Figure 3 – 1. Closed water recirculating systems.....	61
Figure 3 – 2. Electric field in the simulations .....	62
Figure 3 – 3. Water conductivity on the CSSC.....	64
Figure 3 – 4. Water temperature and ambient conductivity at Lockport Lock and Dam. ....	66
Table 3 – 1. Mean ambient conductivity. Mean .....	66
Figure 3 – 5. Plots of behavioral threshold power density versus water conductivity.....	67
Figure 3 – 6. Threshold field strength for behavioral responses .....	68
Figure 3 – 7. Plot of threshold power density for flight versus water conductivity .....	70
Figure 3 – 8. Cumulative exposure thresholds .....	71
Figure 3 – 9. Plot of threshold cumulative exposure for immobilization .....	72
Figure 3 – 10. Multiplier for constant power in relation to water conductivity.....	73
Figure 4 – 1. The apparatus employed in the experiment on volitional challenge of electric fields.....	85
Figure 4 – 2. Profile of field strength (E, voltage gradient, V/cm) .....	86
Figure 4 – 3. Field strength (V/cm) along the apparatus in the trials.....	86
Figure 4 – 4. Proportions of small bighead carp traversing the field.....	90
Figure 4 – 6. Proportion of successful challenges.....	93
Figure 4 – 7. Relative risk for successful challenge of the electric field by small bighead carp .....	93
Figure 5 – 1. Brett swim tunnel.....	102
Figure 5 – 2. Electric field in the simulations .....	104
Figure 5 – 3. Proportion of small bighead carp not impinged in simulations.....	107
Figure 5 – 4. Relative risk for fish to maintain position .....	108
Figure 5 – 5. Water velocity as a function of discharge on the Canal.....	109
Figure 5 – 6. Boxplots and point estimates of daily mean water velocity on the Canal.....	109
Figure 5 – 7. Risk for daily mean water velocity to be less than 15 and 22 cm/s.....	110

## Tables

Table 1 – 1. Operational protocols tested in the pilot study on silver carp .....	15
Table 2 – 1. Mean threshold field strength .....	41
Table 2 – 2. Model selection .....	45
Table 3 – 1. Mean ambient conductivity. Mean .....	66
Table 3 – 2. Table of multiplier for constant power (MCP). .....	74
Table 4 – 1. Average field strength of the operational protocols.....	88

## Units and Conversion for SI (metric) to Non-SI Units of Measurement

Units	Divide By	To Obtain
Centimeter	2.54	Inches (in)
Millimeter	25.40	Inches (in)
Meters	0.3048	Feet (12 in)
Meters/second (m/s)	0.3048	Feet/second (fps)
Centimeters/second (cm/s)	30.48	Feet/second (fps)
Cubic centimeter (cm <sup>3</sup> )	16.387	Cubic inches (in <sup>3</sup> )
Grams	28.3495	Ounces (mass) (oz)

## Executive Summary

Bighead carp *Hypophthalmichthys nobilis* and silver carp *Hypophthalmichthys molitrix* are nuisance invaders of the Mississippi River System and potential invaders of the Great Lakes. Electric barriers, developed by Smith-Root, Inc. (Vancouver, Washington) and operated by the US Army Corps of Engineers, are employed in the Chicago Sanitary and Ship Canal (CSSC) to deter dispersal of aquatic nuisance species through the waterway.

Herein, research on operational protocols and risk for breach of the barriers is described. A Conceptual Risk Model for Breach of the Electric Barriers (based on technical, biological, and environmental factors hypothesized to influence risk for breach),

<u>Technical factors</u>	<u>Biological factors</u>	<u>Environmental factors</u>
Pulsed DC field strength	Fish species	Water conductivity
Pulsed DC pulse-frequency	Fish size	Water velocity
Pulsed DC pulse-duration	Behavior	Water depth
Field orientation (direction of electric current flow)	Swimming speed (duration of exposure)	Habitat,
Field size		
Field distribution (shape)		

was devised to facilitate understanding of the electric barriers, to aid development of hypotheses for testing, and to provide a conceptual framework for the research. Five experiments related to the operation and efficiency of the electric barriers in the CSSC (a pilot experiment and experiments on electrical parameters, water conductivity, volitional challenge of electric fields, and water velocity) were conducted in a controlled environment. The influence of individual factors (in the model) on risk for breach of the barriers was directly tested in the experiments, was addressed in the approach used in the experiments, or their influence was apparent in the outcomes of the experiments.

The pilot study was conducted with small [137 to 280 (mean  $\pm$  standard deviation;  $195 \pm 35$ ) mm total length; 5.4 to 11.0 ( $7.7 \pm 1.4$ ) inches] silver carp. The remaining experiments were conducted on small bighead carp [42 – 93 ( $57 \pm 6$ ) mm total length; 1.7 – 3.7 ( $2.2 \pm 0.2$ ) inches]. In the experiments on effects of electrical parameters, water conductivity, and water velocity, fish were subjected to electrical exposures in a fashion that mimicked exposure that would be received by fish penetrating the electric field of Barrier IIA in the CSSC (simulations of encroachment). The immobilization of encroaching fish (i.e., fish rendered incapable of swimming motions), first response to electrical stimulation, and flight behaviors were the primary outcomes of interest. The simulations were based on a hypothesized worst-case scenario for preventing passage of the targeted fish through the barrier field: (1) encroaching fish were small, (2) encroaching fish were swimming at the surface of the CSSC, (3) fish penetrating the electric barrier continued upstream despite receiving electrical stimulus, (4) fish traversed the barrier at maximum swimming speeds, and (5) water velocity was zero or minimal. In the experiment on effects of water conductivity, the simulations were conducted at various levels of water conductivity (100  $\mu\text{S}/\text{cm}$  to 4,000  $\mu\text{S}/\text{cm}$ ). In the experiment on water velocity, condition 5 was changed, as the simulations were conducted at three levels of water flow.

The effectiveness of various combinations of pulsed DC field strength (FS; V/cm), pulse-frequency (PF; Hz), pulse-duration (PL; ms), and the electrical parameters characterizing of the waterborne electric field of Barrier IIA (referred to as operational protocols for brevity) for preventing passage of smaller carp were evaluated in two experiments. Outcomes showed that risk for failing to immobilize encroaching



fish was strongly influenced by the operational protocol applied in the simulations. The operational protocol FS: 0.79 V/cm, PF: 15 Hz, PL: 6.5 ms was demonstrated effective in the pilot study on small silver carp (137 to 280 mm total length). This protocol is presently being applied at Barrier IIA. Risk for failing to immobilize encroaching small bighead carp (51 – 76 mm total length) was significantly reduced by the operational protocol FS: 0.91 V/cm, PF: 30 Hz, PL: 2.5 ms, compared to the operational protocol presently being employed. Similarly, this protocol significantly reduced the risk for fish to successfully challenge and traverse the electric field in the experiment on volitional challenge of electric fields by small bighead carp. The outcomes on small bighead carp were achieved in water of 2,000  $\mu\text{S}/\text{cm}$  ambient conductivity.

The orientation of the field (direction of electric current flow) employed by the electric barriers can strongly influence the risk for failing to immobilize fish penetrating the field. Electrical exposure (and the likelihood of immobilization) is maximized when fish are oriented parallel with the direction of electric current flow and minimized when fish are perpendicular. The electric barriers in the CSSC employ cross-channel electrodes, ensuring maximum exposure to fish swimming upstream, into the flow (water and electric current). Thus, the simulations of encroachment were conducted under a condition of no (or minimal) water current flow, allowing fish opportunities to minimize electrical exposure by turning perpendicular to the direction of current flow, to provide conservative estimates of risk for failing to immobilize fish.

The size and distribution (shape) of the waterborne electric field generated by Barrier IIA is determined by the characteristics and placement of the electrodes and the electric energy applied. Measurements taken from the surface of the CSSC show the distribution of field strength of the Barrier IIA field as characterized by two lobes: a low-field (wider, downstream) and a high-field (narrower, upstream). The field strength applied in the simulations varied over time to mimic the field strength that a fish swimming through the electric field of Barrier IIA would experience, while swimming at the surface of the CSSC (fish would swim through a stationary field on the CSSC; the field was moved over the fish in the simulations). The patterns of field strength applied in the simulations reflected the size and shape of the in-water electrical signal generated by Barrier IIA, with rates of change (over time) in the field determined by fish swimming speed. Observations of fish behaviors and outcomes from the simulations indicate that even when operational protocols demonstrated effective in the experiment are applied (e.g., ultimate field strength: 0.91 V/cm; pulse-frequency: 30 Hz; pulse-duration: 2.5 ms) penetration of the low field of Barrier IIA by small bighead carp is likely. The sharply increasing voltage gradients on the rising side of the high field are expected to serve as the boundary for upstream penetration.

Species differences in vulnerability to electrical stimulation were not experimentally evaluated in the present study. Significant differences in vulnerability to electrical stimulation, which in extreme cases can be manifested as electrical stimulus leading to immobilization in one species but flight in another, has been demonstrated between dissimilar fishes. Morphological and taxonomic differences between bighead carp and silver carp are relatively subtle. Thus, differences in response to electrical stimulation between these species are also expected to be subtle. Field study of electric barrier effectiveness on the CSSC has relied upon various fishes as surrogates for invasive Asian carp. Whether the vulnerability to electrical stimulation of these surrogates is similar to that of bighead carp or silver carp is not known. Determination of suitable surrogate fishes for invasive carps, followed by field study of electric barrier efficacy, using suitable surrogates or suite of surrogates, is strongly recommended.

It is well established (in the context of capturing wild fish with electricity) that the reactions of fish to electrical exposure are often size dependent. The phenomenon of larger fish having lower thresholds of response to a given electric field than smaller fish is significant and attributed to bigger fish intercepting

a greater difference in electrical potential than smaller fish. Size-dependent response to electric stimulation was demonstrated in the present study despite the relatively small size and narrow range in sizes tested (bighead carp 51 – 76 mm total length were targeted). Risk for failing to immobilize fish encroaching upon the barrier field is dependent upon fish size. There is flexibility in operational protocol selection, based on minimum size of fish targeted. Operational protocols and electrical settings effective on small fish can be expected to be even more effective on larger fish.

Fish behavior, as a risk factor, was addressed in the simulations of encroachment and in the experiment on volitional challenge of waterborne electric fields by small bighead carp (48 – 82 mm total length). Fish behavior was addressed in the simulations of encroachment by conducting the simulations with no (or minimal) water flow velocity. In the simulations, fish often utilized body-voltage minimizing behaviors. In the experiment on volitional challenge of waterborne electric fields, fish were able to avoid the electric field altogether. Fish were clearly able to discern the downstream-most margin of the field in the tests on volitional challenge, yet fish repeatedly swam into the field. In many instances, fish followed, or attempted to follow, others into the electric field. It was common for fish immobilized (stunned) during incursions into the field to again challenge the electric field upon righting (after being immobilized/stunned and washed out of the electric field by water current flow). In the experiment on volitional challenge of electric field, fish clearly did not avoid the electric field, but instead challenged the electric field repeatedly and after penetrating the field continued to swim upstream despite apparent distress. The behavior of the small bighead carp in the experiment support the condition in the simulations of fish continuing to swim into the barrier field despite electrical stimulation and indicate it prudent to maintain the barrier field in the CSSC at levels capable of immobilizing encroaching fish of the targeted size.

The effects of swimming speed on risk for breach of the Barriers was not directly tested in the present study but was a consideration in the simulations of encroachment. The minimum duration of electrical exposure of fish swimming through the waterborne electric fields in the CSSC will be determined by how quickly (or slowly) fish swim through the field. Thus, the minimum duration of electrical exposures experienced by fish swimming through barrier field is determined by fish swimming speed coupled with size of the electric field, most simply under conditions of no flow. The scenario applied in the simulations was that fish encroached upon and swam through the electric field at maximum swimming speed. A swimming speed of 50 cm/s was assumed in the simulations of encroachment, which provided an exposure of 88 seconds. The 50 cm/s swim speed was assumed to be a worst case scenario, as the 50 cm/s swimming speed is at the high-end in terms of swim speed estimates for 51 – 76 mm bighead carp. Milling behaviors and deceleration (fatigue) which might increase duration of exposure were not addressed in the simulations. Hence, cumulative electrical exposures in the simulations and estimates of risk for failing to immobilize encroaching fish may be conservative.

The electrical conductivity of water in the CSSC (the ability of the water to conduct electricity) is important to barrier operation and efficiency through power demand on the systems and mismatch in conductivity between water and fish; when conductivity of water in the CSSC increases power demand increases and the efficiency of electric energy transfer from waterborne field to flesh of fish decreases. Water electrical conductivity (the inverse of electrical resistivity) is a measure of the net motion of the charged ions present. Measures of water conductivity are temperature dependent. Specific conductivity (conductivity adjusted to a temperature of 25°C), which reflects the ion content of water as thermal effects on the measure are removed, is typically reported. Ambient water conductivity (the water conductivity at the ambient temperature) more closely reflects electrical conductivity. Analysis of MWRDGC measures of specific water conductivity collected near the barriers October 1998 – April 2010,

provided mean specific conductivity of  $981 (\pm 402) \mu\text{S}/\text{cm}$  and maximum values occurring December through March ( $3049 - 4697 \mu\text{S}/\text{cm}$ ) demonstrating a seasonal fluctuation in ion concentration in the water of the CSSC. Estimates of water ambient conductivity collected at Lockport Lock and Dam (5 miles downstream of the barriers) ranged between 388 and 2551 ( $852 \pm 261$ ; 95% CI 843 – 862)  $\mu\text{S}/\text{cm}$ . Mean ambient conductivity varied significantly among months of the year. The seasonal fluctuation evident in measures of specific conductivity collected near the barriers was also evident in the estimates of ambient conductivity, but the extremes were greatly reduced. Fish effective conductivity ( $c_f$ ) was estimated to be  $90 \mu\text{S}/\text{cm}$  via threshold power-density methodology, providing the means to estimate power requirements necessary to maintain barrier field efficiency, as water conductivity changes, after a standard for operation has been established. In simulations of encroachment (described above) conducted in water having ambient conductivity from 100 to 4,000  $\mu\text{S}/\text{cm}$ , 80 – 100% of fish were immobilized with the operational protocol FS: 0.79 – 0.91 V/cm, PF: 30 Hz, PL: 2 ms.

The effects that water flow has on risk for small bighead carp to successfully traverse barriers depend on the velocity of the flow. The motivation for fish to challenge the barrier field under conditions of no or very low water flow is uncertain, but this is a worst-case scenario for preventing breach, as fish penetrating the field can orient perpendicular to the direction of electric current flow (to reduce body-voltage) without being swept back downstream by water currents. Positive rheotaxis (motivation for swimming upstream into water current flow) was absent in small bighead carp (51 – 76 mm total length) in water flowing at 3 cm/s, but was present at a velocity of 6 – 7 cm/s (48 – 82 mm fish) in the experiment on volitional behavior and at 7, 15, and 22 cm/s in the experiment on effects of water velocity. Thus, risk for small bighead carp to challenge the barrier field may be increased when water current velocity on the CSSC is  $\geq \sim 7$  cm/s. However, water velocity may reduce risk for fish penetrating the barrier field to breach of the barrier by forcing increased periods of alignment with the direction of electric current flow, through magnification of electroshock-induced reductions in swimming capability, and by effects associated with increased duration of electrical exposure. The influence that water velocity may have on risk for breach of Barrier IIA by small bighead carp (44 – 93 mm total length) was evaluated experimentally. The outcome of interest was whether fish maintained their position in the field during electrical exposures (indicating fish would not be swept back by water current flow during incursions into a barrier field in the CSSC). Risk for fish to maintain their position in the field (not be swept back) was inversely related to water velocity. Based on outcomes of the simulations, risk for breach of Barrier IIA is significantly reduced under conditions of flow velocity  $\geq 15$  cm/s compared when flow is  $\leq 7$  cm/s and was reduced further with water velocity  $\geq 22$  cm/s. Outcomes indicate that under conditions of increased flow, some parameters within the operational protocols could be reduced (e.g., pulse frequency, field strength) without loss of barrier efficiency, but additional research to develop and test relations between flow velocity and risk for breach of the barrier is necessary.

The direction of water flow may be a concern on the CSSC, as there are occurrences of reverse flow and high velocity reverse flow could sweep fish into or through the barrier field. Examination of USGS discharge data for the CSSC (near Lamont, IL; daily values for a period of 5.5 years) provided an average daily water current velocity of  $\sim 22$  cm/s, flow velocity exceeded 50 cm/s on 4% of the days, was  $\geq 22$  cm/s on 37% of the days,  $\geq 15$  cm/s on 72% of the days, and  $\geq 7$  cm/s on 99% of the days. Examination of water current velocity measures (readings every minute, 3/1/2010 – 6/29/2010) showed there to be very little risk for fish to be swept into, or through, the barrier field by reversals of water flow on the CSSC; the incidence of reverse flow was rare ( $< 0.1\%$ ), with even lower incidence of reverse flow sufficient to induce positive rheotaxis (6 – 7 cm/s) or to influence the ability of fish to maintain position within the electric field.

Effects of water depth at the electric barriers were not directly tested in the present study. The significant influence of ultimate field strength on probability of immobilization demonstrated in the tests with operational protocols provides indirect evidence that barrier effectiveness will be influenced by changes in depth of the CSSC. The electric barriers in the CSSC employ bottom-mounted electrodes. The intensity of the field (field strength) increases with proximity to the electrodes, decreases with increasing distance. As water depth increases, the intensity of the barrier field at the surface of the CSSC will be reduced, requiring compensation of barrier output to maintain effectiveness.

The effects of habitat were not directly tested in the present study. However, the outcomes and behaviors of small bighead carp during the experiment on volitional challenge of electric fields indicate that habitat, in the form of breaks, cracks, and crevices in the walls of the CSSC, could increase risk for fish to traverse the barrier field. Specifically, breaks, cracks, and crevices in the canal wall at the location of the high-field (of Barrier IIA) could provide fish penetrating the barrier field respite from water flow and exposure to electric current, providing opportunity for recovery. Evaluation of the suitability of breaks and crevices in the walls of the CSSC (in the barrier fields) to serve as refuges for small fish is recommended.

The outcomes of the experiments, simulations, and analyses in this study provide the best information presently available regarding relative effectiveness of the various operational protocols for the electric barriers in the Chicago Sanitary and Ship Canal and the likelihood of immobilizing small bighead carp penetrating the field of Barrier IIA. The prognostic model (FS, PF, PL, L, PL\*L) demonstrates the influence of the operational protocol (field strength, pulse-frequency, pulse-duration) being applied and the size (length) of fish encroaching upon the barrier field on the likelihood of immobilization. Water conductivity may influence barrier effectiveness at inducing passage-preventing behaviors in encroaching fish. However, risk for breach of the barriers was assessed in water of  $\sim 2,000 \mu\text{S}/\text{cm}$  ambient conductivity (the exception was the experiment on effects of water conductivity) a level exceeded in the CSSC only in winter months. A water flow velocity of 22 cm/s was shown to reduce risk significantly for small bighead carp to maintain position during exposure to barrier fields: the average daily water flow velocity of the CSSC. The operational protocol FS: 0.91 V/cm, PF: 30 Hz, PL: 2.5 ms was demonstrated effective in the simulations under conditions of  $2,000 \mu\text{S}/\text{cm}$  and minimal flow. Experimentation in the CSSC is difficult, but is necessary for confirmation and verification of the outcomes of this study. Experimentation on the CSSC, in the barrier fields, using appropriate surrogate fishes, is recommended.

## Acknowledgements

This project was a collaborative effort between the U.S. Army Corps of Engineers (USACE), Chicago District, Chicago, Illinois; the USACE, Environmental Laboratory – Engineer Research Development Center (EL-ERDC), Vicksburg, Mississippi; and Smith-Root, Inc. (SRI), Vancouver, Washington. Dr. F. Michael Holliman (SRI) conducted the research and wrote this report. Dr. F. Michael Holliman and Dr. Jack Killgore (EL-ERDC) were the Principal Investigators for the project. Mr. Scott Kozak and Mr. Charles Shea (USACE, Chicago District), Project Managers and liaisons, Mr. Lee Carstensen and Mr. Doug Malone (SRI), Electrical Engineers, were critical to the concept, design, development, and success of the project. This work was sponsored by the USACE, Chicago District and appreciation is made to the individuals within the USACE, Chicago District, that facilitated this project for their guidance, support, and patience.

Appreciation is made to the Fish Ecology Team, EL-ERDC (Mrs. Krista Boysen, Mr. Jay Collins, Mrs. Audrey Harrison, Dr. Jan Hoover, Dr. Jack Killgore, Dr. Todd Slack, and Mr. Larry Southern) for assistance in obtaining and maintaining fish, in conducting experiments, and in experimental design. Thanks go out to the EL-ERDC for providing technical support during the project and to the ERDC Institutional Animal Care and Use Committee for their patience and oversight during the permitting phases of the experiments.

The ERDC's Aquatic Nuisance Species Research Program (<http://el.erdcl.usace.army.mil/programs.cfm?Topic=ansrp&Option=Program>) provided funding for the swimming speed studies conducted by the EL-ERDC that were used to calibrate exposure time in the various experiments and that allowed ERDC to respond to the project's expedited schedule.

Thanks go out to the SRI Team (Mr. Carl Burger, Mr. Brad Carstensen, Mr. Jason Crump, Mr. Rick Crump, Mrs. Dixie Fuller, Mrs. Lisa Harlin, Mrs. Kathryn Harper, Mr. Jeff Smith) for providing invaluable guidance and assistance throughout the project, especially to the SRI Project Management Team (Mr. Matthew Brinkman, Mr. Brandon Byrne, and Mrs. Barbara Stern) for their support and assistance throughout the project.

This report was reviewed by Mrs. Kelly Baerwaldt and Mr. Mark Cornish (USACE, Rock Island District, Rock Island, Illinois), Dr. Jan Hoover and Dr. Jack Killgore (EL-ERDC), and Mr. Matthew Shanks (USACE, Chicago District).

## 1 – Pilot Study on Operational Protocols for Induction of Passage-Preventing Behaviors in Small Silver Carp

---

Summary.—A pilot study evaluating the effectiveness of various operational protocols [combinations of in-water field strength (V/cm), pulse-frequency (Hz), and pulse-duration (ms)] for electric barriers (specifically, Barrier IIA) operating on the Chicago Sanitary and Ship Canal was conducted in April 2009. A controlled experiment was conducted, where captured, wild small silver carp [137 to 280 mm (5.4 – 11.0 inches) total length] were individually exposed to electrical treatments in a completely randomized experimental design. Fish were exposed to eight levels of field strength, each level greater than the last, exposure at each level lasting a period of 3 seconds. This approach provided “snapshots” of fish behavior at discrete points of the field of Barrier IIA. Immobilization of fish during the 24-second cumulative exposure was the primary outcome of interest. The effects of 10 operational protocols were evaluated. The operational protocol field strength: 0.79 V/cm, pulse-frequency: 15 Hz, pulse-duration: 6.5 ms, was demonstrated the most effective of those operational protocols tested. The electric barriers on the Chicago Sanitary and Ship Canal are presently applying this operational protocol.

---

### Introduction

Constructed for wastewater management and shipping access between the Great Lakes and the Mississippi River System, the Chicago Sanitary Ship Canal (CSSC) is a potential conduit for exchange of invasive aquatic species between the systems. Colonizing aquatic invaders have been discovered in the CSSC (e.g., round goby *Neogobius melanostomus*, zebra mussel *Dreissena polymorpha*), following introduction to the Great Lakes (Charlebois et al. 1997). Invasive Asian carp, bighead carp *Hypophthalmichthys nobilis* and silver carp *H. molitrix*, have established reproducing populations in the Mississippi River System. The life cycle of these fishes includes prespawn upstream migrations. There is a potential threat of invasion of the Great Lakes by bighead carp and silver carp with the CSSC serving as a pathway. Asian carp have been reported in the Illinois River, downstream from the CSSC, since 2005 (Stainbrook et al. 2005). A bighead carp was recently collected from the CSSC approximately five river miles downstream from the electric barriers deployed on the CSSC to serve as an invasive species deterrence system (Illinois Department of Natural Resources 2009).

A series of electric barriers, which are operated by the US Army Corps of Engineers (USACE), have been deployed to prevent the transfer of aquatic nuisance species through the CSSC. The most upstream electric barrier, designated Barrier I, designed and developed by Smith-Root, Inc. (SRI; Vancouver, Washington) as a demonstration project, has been in operation since April 2002. The second barrier, designated Barrier IIA, also designed and developed by SRI, covers more area than Barrier I [the electric field covers the CSSC from side-to-side and about 44 meters (m) in the upstream-downstream direction] and is capable of generating electric fields of significantly greater intensity, began operation in 2009. Construction of a third barrier, designated Barrier IIB, designed and developed cooperatively by SRI and the USACE, is nearing completion, planned to become operational in the spring of 2011.

The primary systems in electric barriers are the physical structure, the electrodes, and the power supply (Sternin et al. 1976). As power supplies have become more powerful and sophisticated, a monitoring-control system has also become necessary in modern electric barriers. The physical structure typically

houses the electrical power systems, backup power supplies, and includes structures anchoring the electrodes. A collection of electrodes (an electrode array) provides the interface between the onshore electrical power system and the environmental water. Early electric barriers typically applied single- or three-phase alternating current (AC) to guide or block passage of fish. In the 1950s, pulsed direct current (pulsed DC) was found to be effective (Halsband 1967) and replaced or augmented the use of AC, sometimes to prevent or reduce fish mortality (McLain 1957; Hunn and Youngs 1980). Most early electric barriers employed vertical, hanging electrodes, but bottom-mounted cable-like electrodes have become more common (Hunn and Youngs 1980; Swink 1999). Positioning the cable-like electrodes cross-channel ensures maximum exposure to fish swimming upstream. The electric barriers operating on the CSSC employ pulsed DC and cross-channel, bottom-mounted electrode systems.

Electric barriers function by incorporating environmental water into an electrical circuit composed of conductors (the submersed electrodes) and a source of electrical energy (the onshore power supply). In this circuit, environmental water (and local environment) acts as a path for electrical current flow and the “load” (resistance) for the circuit. When the circuit is closed and a difference in electrical potential [voltage (V)] is applied to the submersed electrodes, an electric field is created in the water by the flow of electric current. The quantity of electric current flowing through the circuit is determined by the voltage applied to the electrodes and the resistance experienced by the circuit, which is directly related to the ability of the environmental water to conduct electricity (that is, the conductivity of the water). The conductivity of the water is determined by ion concentration (the charge carriers) and temperature. Electromagnetic forces of attraction and repulsion, the local environment, and characteristics of the electrode array (electrode orientation, size, spacing) determine the distribution of electric current (the electric field) in the water. In general, the strength of the electric field increases with proximity to the electrodes in both the vertical and horizontal aspects.

The voltage (amplitude), frequency, and duration of the DC pulses applied to the submersed electrodes can characterize the electric energy output by the onshore power supplies of the electric barriers on the CSSC. The characteristics of the pulsed DC applied to the electrodes, by the on-shore power supply, are directly reflected in the waterborne electric field. The strength of the waterborne electric field (i.e., field strength), measured as the voltage per unit distance [i.e., voltage gradient, volts/centimeter (V/cm)], is directly proportional to the voltage applied to the electrodes. The rate at which the waterborne electric field pulses [measured in cycles per second (Hz)] and the duration of each pulse [the pulse duration, measured in milliseconds (ms)], matches the pulses of the DC applied to the electrodes. The ratio of the pulse-duration to the period of the pulse (the period is the time required for one complete pulse cycle) is referred to as the duty cycle and is typically reported in percentage (%). The characteristics of the waterborne DC pulses are referred to as operational protocols in this report.

Electric barriers are regarded as behavioral technologies that function by inducing avoidance and immobilization responses in fish to block passage or direct movement. There is a long history of electric barriers and electric screens usage in fisheries management (e.g., McMillan 1928), but relatively few published evaluations on the effectiveness of these systems. There are even fewer published accounts of comparative tests of the electrical parameters employed by the systems. The design and operation of electric barriers are often site, species, and circumstance specific (Stewart 1990a). The individuality of the systems and their operations may render available information inapplicable to other facilities (Johnson et al. 1990), driving the need for research specific to the barriers operating on the CSSC.

Initial evaluations of the effectiveness of Barrier I often employed adult common carp *Cyprinus carpio*. An Asian carp was only recently collected near the electric barriers; a single Asian carp was collected five

river miles downstream of the electric barriers during a rotenone event (Illinois Department of Natural Resources 2009). There are anecdotal observations from July 2002 of the upstream passage of adult common carp being thwarted, as numerous fish were observed maintaining position immediately downstream of the barrier (Sparks et al. 2004). Field evaluations on Barrier I effectiveness were conducted in 2002, 2003, and 2004, where the movement of acoustic- and radio-tagged common carp (Dettmers and Creque 2004; Sparks et al. 2004) released below the barrier were monitored. Of 115 fish implanted with transmitters, fixed receivers at the dispersal barrier located 97, while mobile tracking accounted for 111 fish. There was one known breach of the barrier by a tagged carp. On 3 April 2003, fixed radio receivers indicated a tagged fish traveled upstream through Barrier I. Barrier I was operating normally before, during, and immediately after the breach (Sparks et al. 2004). Investigation of the incident revealed the fish might have been entrained by a commercial vessel traveling upstream and pulled through the electric field. The fish was later located 1.5 miles upstream of the barrier, believed dead. The incident demonstrated that commercial traffic in the CSSC may influence barrier efficiency and led to the development of corrective measures (Dettmers et al. 2005).

In response to the breach by a tagged fish, the operational protocol (i.e., the electrical parameters characterizing the electric field) for Barrier 1 was changed; the pulse rate and duty cycle were increased from 2 Hz, 0.4% duty cycle (2 ms pulse duration) to 3 Hz, 1.5% duty cycle (5 ms pulse duration). Later in 2003, Barrier I operational protocol was changed again, pulse-frequency was increased to 5 Hz and duty cycle was increased to 2% (4 ms pulse duration). The maximum field strength was maintained at 0.4 V/cm. There have been no further reports of tagged fish crossing the electric barriers.

The relative effectiveness of various electrical parameters, in combination with acoustic-bubble barriers in some tests, at preventing passage of adult bighead carp and juvenile silver carp through an electric field was evaluated in a raceway experiment, initiated in 2001. In the study, passage of adult bighead carp was prevented by an electric field characterized by 3 Hz, 1.5% duty cycle (5.0 millisecond pulse duration)]; 100% (59/59) of attempts, by adult bighead carp, to traverse the field were thwarted. Large bighead carp were reported as very sensitive to electric fields (Dettmers and Pegg 2003). Juvenile silver carp, however, successfully breached the electric fields in the tests. Subsequent testing succeeded in preventing the passage of juvenile silver carp through the electric field, but the electrical parameters were reported as not within practical limits for use on the CSSC (Pegg and Chick 2003; Pegg and Chick 2004).

The difference in rate of passage through the electric field between the bighead carp and silver carp in the raceway experiments of Pegg and Chick (2004) was likely driven by the difference in size between the groups of fish used in the tests. The bighead carp used in the experiment were  $\geq 600$  mm in length (adults), while the silver carp were  $\leq 150$  mm (juveniles). It is well established (in the context of capturing wild fish with electricity) that the reactions of fish to electrical exposure are often size- and species-dependent (Taylor et al. 1957; Biwas and Karmarker 1979; Edwards and Higgins 1973; Seidel and Klima 1974; Bird and Cowx 1993). The phenomenon of larger fish having lower thresholds of response to a given electric field than smaller fish is significant and has been attributed to bigger fish intercepting a greater potential difference than smaller fish (Halsband 1967). Maximum susceptibility to an electric field may occur at different pulse-frequencies, among fish species (Edwards and Higgins 1973; Bird and Cowx 1993). Differences in vulnerability among dissimilar species can be manifested as electrical stimulus leading to immobilization in one species but flight in another (Seidel and Klima 1974; Holliman 1998). Bighead carp and silver carp are morphologically and taxonomically similar enough to hybridize (Kolar et al. 2005). Differences in response to electrical stimulation between bighead carp and silver carp are expected to be subtle, but this hypothesis has not been tested. The breach of the electric field by



smaller silver carp in the raceway experiment of Pegg and Chick (2004), demonstrates the need for additional research on the effectiveness of the electric barriers on the CSSC specific to preventing passage of small fish.

The present study is the first step in a comprehensive evaluation of operating protocols for the electric barriers on the CSSC for deterrence of small invasive carp. Specific objectives for this initial work were to search for and review relevant scientific literature to aid development of experimental approaches and to conduct a pilot experiment on small invasive carp. The electric field and operational capabilities of Barrier IIA, the larger and more powerful of the two electric barriers, was the focus of the research.

## Methods

A pilot study exploring the effectiveness of various electrical parameter combinations for preventing dispersal of small invasive carp through the electric barriers in the CSSC was conducted at the USACE, Environmental Laboratory, Aquatic Ecosystem Research Development Center, Environmental Laboratory Engineer Research Development Center (EL-ERDC), Vicksburg, Mississippi, 20-24 April 2009. Wild silver carp, captured with nets by the EL-ERDC Fish Ecology Team, were used in the experiment. Fish were transported to the host facilities via hatchery vehicle, immediately after capture and prior to the outset of the experiment. Fish were held in closed, water-recirculating aquaculture systems (Figure 1 – 1) prior to use in the experiment. The EL-ERDC supplied fish, facilities, equipment and other critical logistic support for the study.

Estimations of output capabilities of Barrier IIA [in-water field strength (V/cm), pulse-duration [milliseconds (ms)], and pulse-frequency (Hz)] were needed to ensure that operational protocols evaluated in the experiment were feasible. A software application was developed in the Microsoft EXCEL (2007) spreadsheet program to estimate the maximum pulse-duration the electric barrier power system could sustain when generating in-water field strengths from 0.2 to 1.5 volts/cm (in increments of 0.04 V/cm) at pulse frequencies from 0.1 to 40 Hz (in increments of 0.1 Hz). Constraints included a maximum acceptable voltage “droop” on the pulses, a maximum peak electrical output of 1.5 megawatts, and maintenance of appropriate levels of electrical current and charging times for system capacitor banks. The estimates were developed using the electrical load equivalent to that on the CSSC when water conductivity is 2000  $\mu\text{S}/\text{cm}$ . Operational protocols evaluated in the experiment were selected from the simulation outcome. Barrier output to achieve field strengths greater than 1.5 V/(cm) exceeds the theoretical capabilities of various electrical components in the system; 1.5 V/cm ultimate field strength was regarded as the upper limit for Barrier IIA.

Fish were exposed to electrical treatments in a 213 cm x 61 cm x 56 cm fiberglass tank outfitted with identical stainless steel plate electrodes. The electrodes were positioned parallel, separated by 150 cm, extended above the water surface, and covered the entire cross-sectional area of the tank (Figure 1 – 2), thus, generating a homogeneous electric field (Holliman and Reynolds 2002).



Figure 1 – 1. Closed water-recirculating systems. Captured small silver carp were held in closed water-recirculating systems during the pilot study on operating protocols for electric barriers on the Chicago Sanitary Ship Canal. The pilot study was conducted at the USACE, Aquatic Ecosystem Research Development Center, Environmental Laboratory, Engineer Research Development Center (EL-ERDC), Vicksburg, Mississippi. The experiment was conducted 20-24 April 2009.



Figure 1 – 2. Exposure tank. Small silver carp were exposed to electrical treatments in a 530 liter (l) dielectric tank in the pilot study on operational protocols for electric barriers on the Chicago Sanitary and Ship Canal. Flat, perforated, stainless steel electrodes (insert) were positioned parallel to one another in the tank, covered the entire cross-section of the tank, and extended above the surface of the water, creating a homogeneous electric field. The experiment was conducted at the USACE, ERDC-EL, Vicksburg, Mississippi 20-24 April 2009.

Cloth netting stretched tautly over a rectangular frame of PVC pipe, fitted to the internal dimensions of the tank and inserted into the tank, prevented fish from incurring physical injury through contact with the tank walls and electrodes during the electrical exposures. Sheets of clear Plexiglass affixed to the top of the PVC pipe frame prevented fish from leaping from the tank during the electrical exposures, while allowing visual observation of fish behavioral responses (Figure 1 – 3).

A customized Model BP-1.5 Programmable Output Waveform (POW) Fish Barrier Pulsator (Smith-Root, Inc., Vancouver, Washington) served as the power supply for the exposure tank (Figure 1 – 4). The BP-1.5 POW was customized with a discrete eight-step transformer and an analog variable transformer to allow gross and fine adjustment of the amplitude of the electrical output. The duration and frequency of the DC pulses applied to the tank electrodes, which were directly reflected in the waterborne electric field, and the duration of the exposures (3 seconds), were programmed into the BP-1.5 POW with customized Fish Barrier Technology Control Software (Smith-Root, Inc., Vancouver, Washington). A calibrated, digital oscilloscope, electrically connected to the electrodes, was used to confirm the parameters defining the experimental treatments (Figure 1 – 4).

Electrical treatments were administered to fish individually (one at a time). The treatments were applied as a series of eight exposures to pulsed DC, each lasting 3 seconds, characterized by combinations of voltage, pulse-frequency, and pulse-duration. Voltage increased with each exposure. The 3 s electrical exposures were interrupted by 2 – 3 s of no electrical exposure, the time required to adjust (increase) the applied voltage. The cumulative electrical exposure period was 24 seconds. In some cases, field strengths were applied that exceeded the output capabilities of Barrier IIA to provide valuable data should output within the capabilities of the system have proven ineffective for immobilizing small silver carp.

Fish behavior was monitored during and after each electrical exposure. The series of electrical exposures comprising a treatment were terminated if the fish being tested became incapacitated (i.e., immobilized; indicated by tetany, loss of equilibrium, cessation of swimming movements). Ambient water conductivity in the test tank was 687 to 765  $\mu\text{S}/\text{cm}$  during the tests. Water temperature was 21.1 – 23.3 ( $21.4 \pm 0.7$ ) °C. Fish response was reported as cumulative percentage (%) of fish within each experimental group incapacitated (immobilized) at each of the levels of field strength applied in the treatments.

## Results

Electrical treatment selection was based on the simulation of Barrier IIA output capabilities (Figure 1 – 5). In general, inverse relations were demonstrated between the maximums of pulse-duration, pulse-frequency, and field strength that can be sustained by the Barrier IIA power system. Hence, the range of field strengths applied in each treatment was determined by the pulse-duration and frequency combination. Barrier IIA was operating at a field strength of 0.4 V/cm, pulse-frequency of 5 Hz, and pulse-duration of 4 ms at the time of the experiment. The pulse-frequencies applied in the electrical treatments equaled or exceeded the 5 Hz pulse rate being output by Barrier IIA at the time of the experiment (Table 1 – 1).



Figure 1 – 3. Protective netting, frame, and cover for the exposure tank. A frame constructed from PVC pipe was covered with a double layer of cloth netting and inserted into the exposure tank to prevent silver carp from making contact with the sides of the tank and electrodes. A clear Plexiglass cover prevented silver carp from leaping from the exposure tank during the electrical treatments, while allowing visual observation of fish responses. The pilot study was conducted at the USACE, ERDC-EL, Vicksburg, Mississippi 20-24 April 2009.

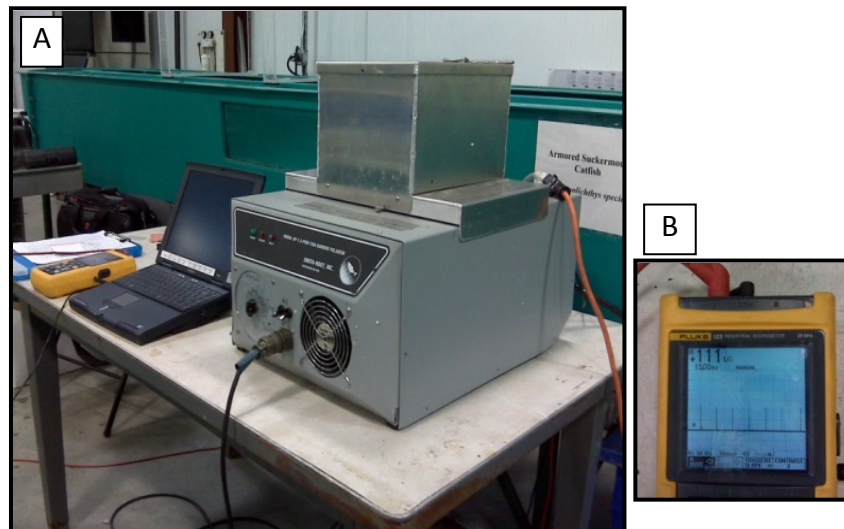


Figure 1 – 4. Power supply for the exposure tank. A. A customized Barrier Pulsator (BP-1.5 POW; Smith-Root, Inc.) was used as the power supply for the exposure tank. B. A digital oscilloscope was used to measure the electrical output of the system. The DC pulse-duration and frequency and the exposure period were programmed into the BP-1.5 POW using custom Fish Barrier Technology Control Software.

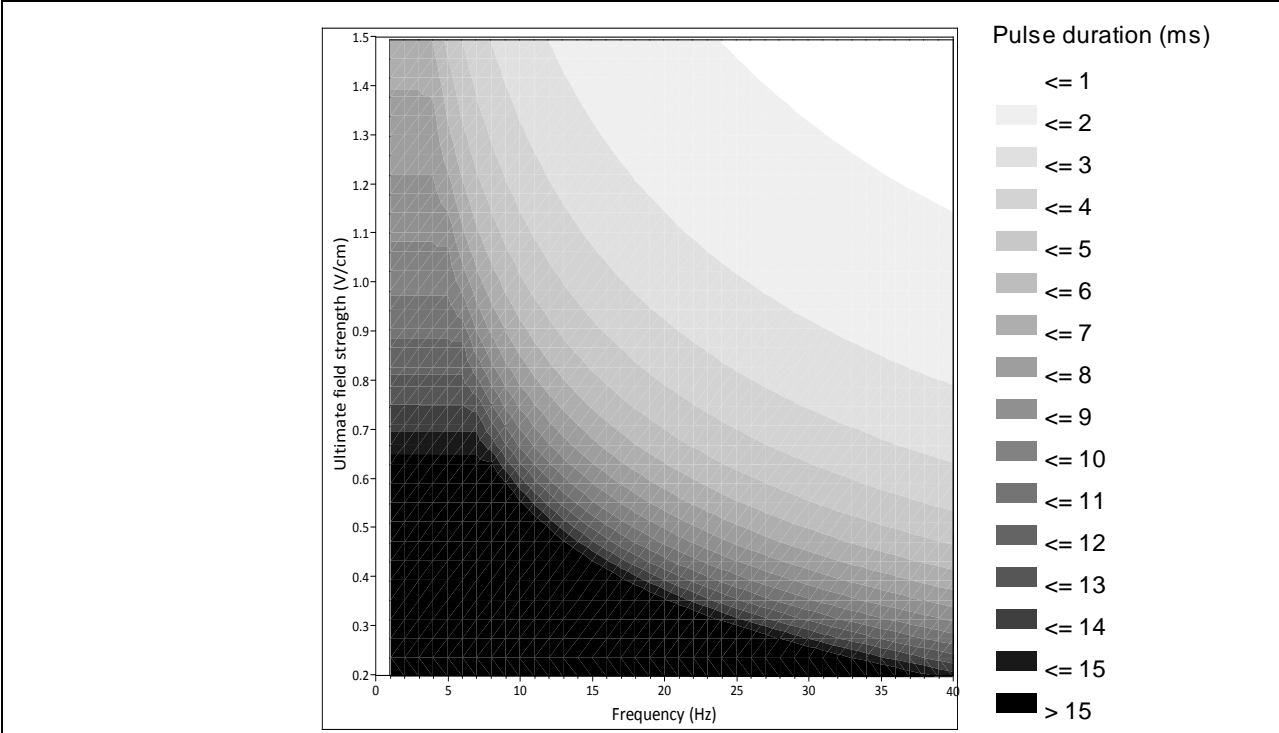


Figure 1 – 5. Barrier IIA output capabilities. Contours of estimated maximum pulse duration (ms) and field strength (volts/cm) that can be sustained by Electric Barrier IIA, as a function of the pulse frequency (Hz), is shown . The estimated output capabilities of Barrier IIA were used to guide selection of electrical treatments applied in the pilot experiment on small silver carp conducted at the USACE, ERDC-EL, Vicksburg, Mississippi 20-24 April 2009.

The response of silver carp to electrical exposure was evaluated in 80 fish (eight fish per treatment). Considerably more fish had been captured and were available for use. However, fish response to the electrical exposures changed significantly after the second day of the experiment (second day of captivity). The change was likely a result of cumulative stress from capture, transport, and new environment. Thus, data collection ceased to prevent bias of previously collected information.

Fish used in the experiment were 137 to 280 (average  $\pm$  SD;  $195 \pm 35$ ) mm total length and weighed from 20.3 to 469 ( $73 \pm 63$ ) grams (Figure 1 – 6). Cumulative percentage of fish stunned during the electrical exposures varied markedly among the treatments (Figure 1 – 7).

Electrical treatments employing DC pulses of 4.8 milliseconds, 8.9 milliseconds, and 13.8 milliseconds duration at a frequency of 5 Hz and field strengths of 0.4 – 1.9 V/cm, 0.3-1.4 V/cm, 0.2-0.9 V/cm (respectively) stunned 38%, 63%, and 25% of fish exposed, respectively. Of the four electrical treatments utilizing 10-Hz pulses of DC (2.4 milliseconds duration, 0.4 – 1.9 V/cm; 4.3 milliseconds duration, 0.3 – 1.4 V/cm; 9.8 milliseconds duration, 0.2 – 0.9 V/cm; and, 24 milliseconds duration, 0.2 – 0.5 V/cm), only the 2.4 millisecond pulses at a frequency of 10 Hz treatment stunned all fish in the treatment. The field strength required for 100% effectiveness with 2.4 ms pulse-lengths and 10 Hz exceeded the theoretical upper limit for field strength for the electric barrier (Figures 1 – 5 and 1 – 7). All of the fish (100%) in each of the treatments utilizing DC pulses of 15 Hz (1.6 milliseconds duration, 0.4 – 1.9 V/cm;

Table 1 – 1. Operational protocols tested in the pilot study on silver carp. The operational protocols [combinations of DC pulse-duration (ms), pulse-frequency (Hz), and in-water field strength (volts/cm)] evaluated in the pilot study on small silver carp. Individual fish were exposed to incrementally increasing pulsed DC electric fields at eight levels of field strength. Each exposure lasted 3 seconds, for a cumulative exposure of 24 seconds. The tests were conducted at the USACE, Environmental Laboratory, Engineer Research Development Center, Vicksburg, Mississippi April 20 – 24, 2009.

Electrical treatments [Pulse frequency, pulse width, in-water field strength (V/cm)]									
Voltage gradient (volts/cm)									
5 Hz			10 Hz				15 Hz		
4.8 ms	8.9 ms	13.8 ms	2.4 ms	4.3 ms	9.8 ms	24 ms	1.6 ms	2.9 ms	6.5 ms
0.39	0.28	0.16	0.39	0.28	0.16	0.12	0.39	0.28	0.16
0.59	0.43	0.28	0.59	0.43	0.28	0.16	0.59	0.43	0.28
0.79	0.55	0.35	0.79	0.55	0.35	0.24	0.79	0.55	0.35
0.98	0.71	0.43	0.98	0.71	0.43	0.28	0.98	0.71	0.43
1.18	0.87	0.55	1.18	0.87	0.55	0.31	1.18	0.87	0.55
1.34	0.98	0.63	1.34	0.98	0.63	0.39	1.34	0.98	0.63
1.57	1.14	0.71	1.57	1.14	0.71	0.43	1.57	1.14	0.71
1.93	1.42	0.87	1.93	1.41	0.87	0.51	1.93	1.42	0.87

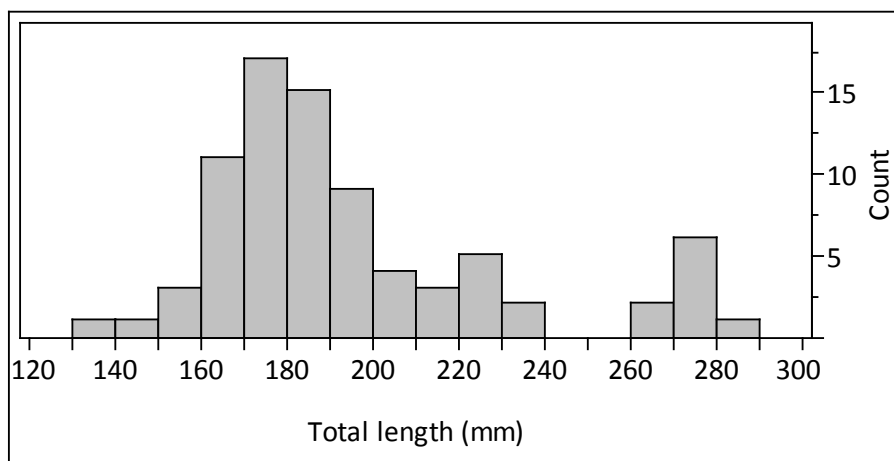


Figure 1 – 6. Length-frequency histogram. Histogram of total length (mm) of silver carp used in the pilot study evaluating operational protocols for electric barriers operating on the Chicago Sanitary and Ship Canal. The tests were conducted at the USACE, EL-ERDC, Vicksburg, Mississippi April 20 – 24, 2009.

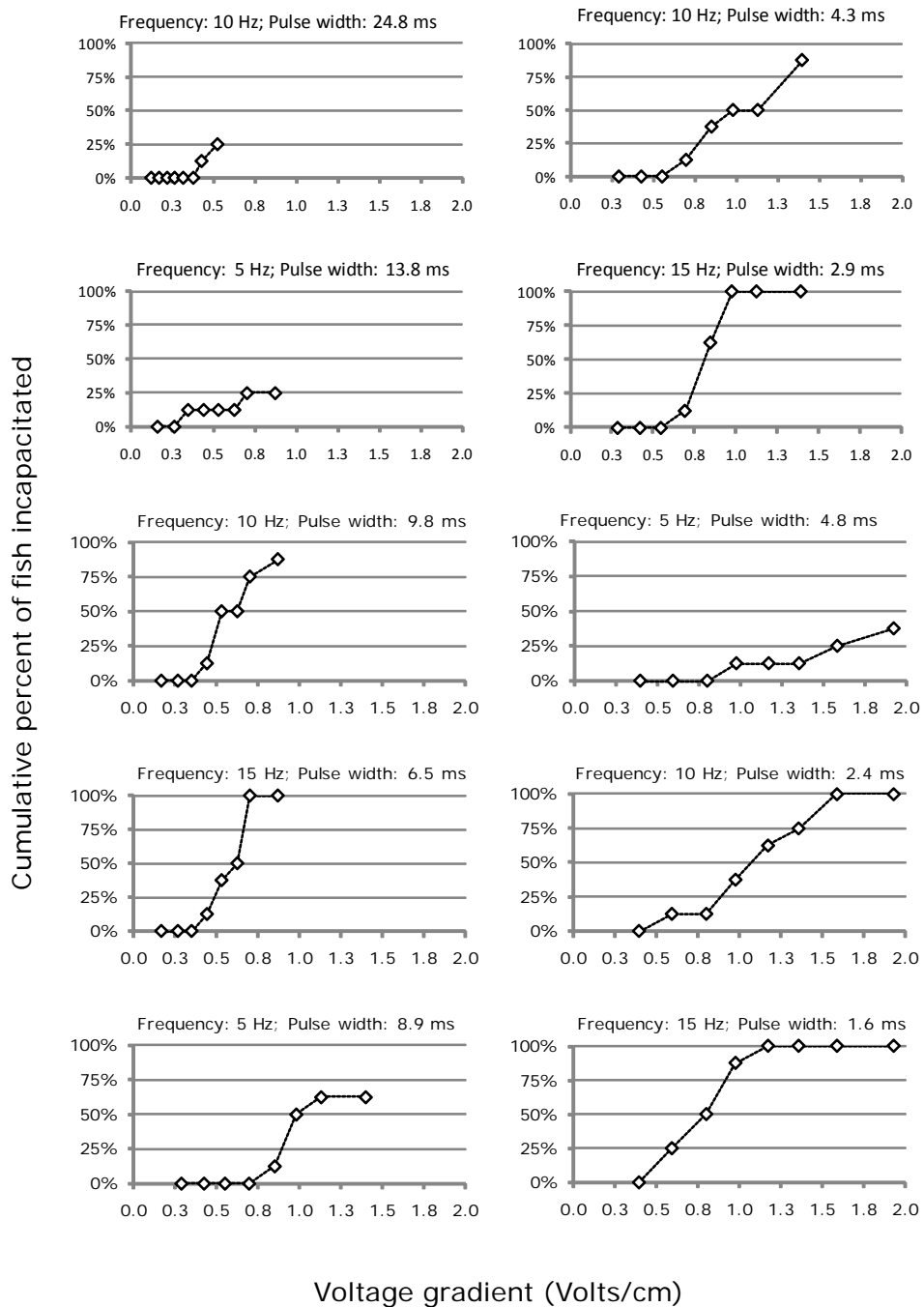


Figure 1 – 7. Cumulative percent of silver carp immobilized. The cumulative percent (%) of silver carp immobilized during electrical exposures, as a function of field strength (V/cm), during the pilot experiment conducted at the ERDC-EL 20-24 April 2009. Data from 80 fish are represented, eight fish per treatment group. Fish were exposed to treatments individually in a completely randomized experimental design.

2.9 milliseconds duration, 0.3-1.4 V/cm; 6.5 milliseconds duration, 0.2 – 0.9 V/cm) were stunned at field strengths within the output capabilities of Barrier IIA (Figures 1 – 5 and 1 – 7). All fish exposed to 24 ms pulse-duration at a 10 Hz frequency (the treatment applying the lowest field strengths of those tested) exhibited escape or avoidance behaviors when exposed at 0.15 V/cm, but no response or twitch was induced in 63% of those exposed to 0.12 V/cm (the lowest level applied). This could indicate a field strength threshold for an escape/avoidance response. Vigorous flight behaviors were demonstrated by all fish exposed to the lowest levels of field strengths applied at the other pulse-duration and frequency combinations, including the most effective treatments.

## Discussion

Published studies directly testing the effectiveness of various electrical parameters for preventing fish passage are sparse. Considerable effort and resources have, however, been expended in scientific investigations to delineate relations between electrical exposures and behaviors induced in fish, in the context of electrofishing. This electrofishing-oriented work indicates that the effectiveness of electric fields at producing targeted behaviors in fish is dependent upon biological (e.g., fish species and size), technical (e.g., characteristics of the electric field), and environmental factors (e.g., water conductivity; Zalewski and Cowx 1990). These principles may prove applicable to the use of electric barriers to block passage of invasive fishes through the CSSC. The duration of the electrical exposure may also prove influential in preventing passage of invasive fishes, as it may influence the types and depths of behaviors induced in fish (Sternin et al. 1976).

Knowledge of the breadth of output capabilities of Electric Barrier IIA was needed to ensure that the electrical conditions simulated in the experiment were applicable to operations on the CSSC. Concerns for human and equipment safety prevent field study to establish the upper limits for barrier electrical output. Hence, output capabilities of Barrier IIA were estimated using mathematical simulations based on specifications and limits of various electronic components in the Barrier IIA Pulsator systems. The electrical treatments applied in the experiment typically employed combinations of pulse-duration, pulse-frequency, and field strength estimated to be within the output capabilities of Barriers IIA. In some treatments, however, the maximum field strength of the system was exceeded to provide valuable information should the electrical parameter combinations falling within the estimated system capabilities prove ineffective at immobilizing small silver carp.

In the present study, captured wild silver carp were exposed to homogeneous fields of pulsed DC in a controlled environment. This approach allowed simulation of fish response to electrical conditions on the CSSC while controlling sources of variation common to field studies with waterborne electric fields. Fish were individually exposed to controlled, precise electrical treatments, where electric treatments were eight 3-second exposures to pulsed DC characterized by combinations of pulse-duration, pulse-frequency, and field strength. Field strength was incrementally increased for each exposure in the treatments, with the 3-second exposures interrupted by 2 – 3 seconds of no electrical exposure. The application of increasing field strength in the sequence of exposures characterizing a treatment and the cessation of the electrical exposure to adjust output were constraints imposed by the power supply used in the electrical exposures. This approach was state of the art. In the treatments, the increasing field strengths applied can be related to the extent of penetration into the electrified zone by a fish swimming upstream at the surface of the CSSC. The various pulse-durations and frequencies represent the electric barriers operating under differing protocols. Field strength increased with each of the electrical exposures, and the exposures were terminated after exposure to the maximum field strength. The exposures simulate penetration into the aspects of the barrier field that is increasing in relative field



strength. Because electrical exposure was not continuous in the treatments, the responses of fish at each exposure are best interpreted as “snap-shots” of behavior at various points of intensity within the electric field of Barrier IIA, with the last exposure occurring at the maximum field strength (33 meters into the field).

The maximum cumulative period of electrical exposure was 24 seconds in the treatments. The estimated maximum economic swim speed for silver carp reported by Konagaya and Cai (1987) was < 200 cm/s. The maximum field strength in the electric field of Barrier IIA occurs approximately 33 m into the field (electric field simulations are presented in Figure 2 – 1). Calibration of the 24 second exposure period with penetration of the electric field to 33 meters, the maximum field intensity, provides a swimming speed of ~ 138 cm/s. Tests on swimming capabilities of fish from the cohort used in the present study, conducted after completion of the pilot study, provided maximum swim speeds of fish from the cohort ~ 140 cm/s (personal communication, Dr. Jan Hoover, USACE, Environmental Laboratory, Engineer Research Development Center, Vicksburg, Mississippi). Unlike the exposure to fish penetrating the barrier field on the CSSC, the electrical exposures in the experiment were interrupted. Because the interruptions provided fish opportunities to recover, it is hypothesized that the estimates of effectiveness are conservative.

Stewart (1990a) reported that fish penetrating an electric field might be unable to discern directions of increasing intensity and continue into the field when receiving electrical stimulation. Hence, the ultimate field strength in barriers (like those operating on the CSSC) should be capable of stopping progress of the smallest fish targeted. According to Stewart (1990b), the appearance of the electric barrier may be critical. For example, a physical marker could be useful when applying electric fields to block fish movement, as fish encountering novel stimuli may approach the stimuli slowly providing the opportunity to encounter the field slowly and to learn to avoid the electric field.

Inclusion of some novel stimuli in the electrified zones of the barriers on the CSSC, as aids to fish learning to avoid electric stimulation, and in some cases doubling as deterrents, may be worthy of investigation. Because raceway and field study indicates the electric barriers are effective for large fish (Dettmers and Pegg 2003; Pegg and Chick 2003; Pegg and Chick 2004; Dettmers and Creque 2004; Sparks et al. 2004), the additional stimuli should target small fish. Stewart (1990b) found that a submersed rope provided the opportunity for fish to learn to avoid an adjacent electric field. Physical markers are not practical for use on the CSSC, however, being an obstruction to commercial traffic. Other stimuli for consideration include light, sound, bubbles, water currents, scents, and imitations of predators. An important consideration is the graduation of the electric field, where fish of differing sizes would encounter noxious electrical stimulation at differing depths of penetration within the electrified zone, influencing positioning of alternate stimuli. In a test of a composite BioAcoustic Fish Fence (BAFF) and electric barrier, Pegg and Chick (2004) found effectiveness decreased when the technologies were combined, compared to the function of each individually. This result could be an artifact of the experimental design and configuration of the experimental apparatus (the BAFF was located in the center of the electrical array/field), but illustrates the need for research into hybrid barriers to prevent unexpected outcomes.

In the present study, fish exposed to the 6.5 ms-15 Hz treatment exhibited flight-escape responses at 0.16 V/cm. Simulations of the electric field of Barrier IIA demonstrate this level of field strength occurs at the CSSCI surface approximately 6.1 meters downstream of the most downstream “low-field” electrode array when 600 V were applied (as operated Spring 2009). Results from the present study indicate silver carp of 185 mm total length and above penetrating the electrified zone to this point

would experience electrical stimulation of a magnitude capable of inducing a behavioral response. Whether this stimulation would induce avoidance (flight) behaviors with fish fleeing the field is not known. Based on outcomes in the experiment, if Barrier IIA was generating DC pulses of 6.5 ms duration at 15 Hz, the field strength in the “high-field” would be inadequate to stun 185 mm silver carp were they to pass through the “low-field” and continue upstream, unless the voltage applied to the “high-field” electrode arrays was increased significantly. (Electric field simulations are presented in Figure 2 – 1).

In August 2009, the USACE increased the electrical output of Barrier IIA to achieve a field strength of 0.79 V/cm in the high-field, a pulse-frequency of 15 Hz, and a pulse-duration of 6.5 ms, an operational protocol demonstrated effective for inducing passage-preventing behaviors in small silver carp, in the present study. The increase in operational parameters was necessary as the results of the present study indicated that silver carp within the size range tested [137 to 280 (average  $\pm$  SD; 195  $\pm$  35) mm total length] could have successfully traversed the width of the electrified zone of Barrier IIA, as operated in the spring of 2009 (0.4 V/cm ultimate field strength-5 Hz pulse-frequency-4 ms pulse-duration). Pulse frequencies of 15 Hz were shown necessary to stun small silver carp, within the ranges of pulse-duration and field strength tested in the present study. Outcomes of the experiment demonstrate there is some latitude in the selection of operational protocols, as several combinations of electrical parameters were shown capable of blocking the passage of small silver carp through the electric barriers. In the treatments applying pulses of DC at 15 Hz, the field strength required to incapacitate all fish in the treatments was influenced by the duration of the pulses; an inverse relation was demonstrated between the effective field strength and pulse duration, where greater field strength was required to incapacitate fish when using pulses of shorter duration (0.71 V/cm, 6.5 ms versus 0.98 V/cm, 2.9 ms versus 1.18 V/cm, 1.6 ms) at 15 Hz. The operational protocol of 0.79 V/cm ultimate field strength, 15 Hz pulse-frequency, and 6.5 ms pulse-duration is presently employed at Barrier IIA.

## Work cited

- Bird D. J. and I. G. Cowx. 1993. The selection of suitable pulsed currents for electric fishing in freshwater. *Fisheries Research*, 18: 363-376.
- Biwas, K. P. and S. P. Karmarkar. 1979. Effect of electric stimulation on heart beat and body muscle in fish. *Fisheries Technology*, 16: 91-99.
- Charlebois, P. M., Marsden, J. E., Goettel, R. G., Wolfe, R. K., Jude, D. J. and S. Rudnicka. 1997. The round goby, *Neogobius melanostomus* (Palles), a review of European and North American literature. INHS Special Publication No. 20, Indiana Sea Grant Program and Illinois Natural History Survey.
- Dettmers, J. and M. A. Pegg. 2003. Evaluating the Effectiveness of an Electric Barrier. Illinois Natural History Survey, Report 377: 1-2.
- Dettmers, J. M. and S.M. Creque. 2004. Field assessment of an electric dispersal barrier to protect sport fishes from invasive exotic fishes. Annual Report to the Division of Fisheries, Illinois Department of Natural Resources, Illinois Natural History Survey, Center for Aquatic Ecology and Conservation.
- Dettmers, J. M., B.A. Boisvert, T. Barkley, and R.E. Sparks. 2005. Potential impact of steel-hulled barges on movement of fish across an electric barrier to prevent the entry of invasive carp into Lake Michigan. October 2003 – September 2005. Completion Report for US FWS; INT FWS 301812J227.
- Edwards, J. L. and J.D. Higgins. 1973. The effects of electric currents on fish. Engineering Experiment Station, Georgia Institute of Technology, Atlanta. Rep. B-397, B-400, and E-200-301.
- Halsband E. 1967. Basic principles of electrofishing. Pages 57–64 in R. Vibert, editor. *Fishing with Electricity - Its Applications to Biology and Management*. Fishing News Books, Blackwell Scientific Publications Ltd., Oxford, England.
- Holliman, F. M. 1998. A field and laboratory investigation of the effectiveness of electrical parameter combinations for capturing cichlids. Master's thesis. North Carolina State University, Raleigh.
- Holliman, F. M. and J. B. Reynolds. 2002. Electroshock-induced injury in juvenile white sturgeon. *North American Journal of Fisheries Management*, 22: 494-499.
- Hunn, J. B. and W. D. Youngs. 1980. Role of physical barriers in the control of sea lamprey (*Petromyzon marinus*). *Canadian Journal of Fisheries and Aquatic Sciences*, 37: 2118-2122.
- Illinois Department of Natural Resources. "Bighead Asian Carp Found in Chicago Sanitary and Ship Canal". 2009. <<http://www.asiancarp.org/rapidresponse/documents/AsiancarpfoundinCSSC.pdf>>
- Johnson, I. K., W. R. C. Beaumont and J.S. Welton. 1990. The use of electric fish screens in the Hampshire Test and Itchen, England. Pages 256 – 265 in I.G. Cowx , editor. *Developments in Electric Fishing*. London, England: Fishing News Books.
- Kolar, C. S., D. C. Chapman, W. R. Courtenay, C. M. Housel, J. D. Williams, and D. P. Jennings. 2005. Asian carps of the genus *Hypophthalmichthys* (Pisces, Cyprinidae) – A biological synopsis and environmental risk assessment. Report to U.S. Fish and Wildlife Service 94400-3-012, LaCrosse, Wisconsin.

- Konagaya, T. and Q. H. Cai. 1987. Telemetry of the swimming movements of silver carp and bighead. *Nippon Suisan Gakkaishi*, 53: 705 – 709.
- McLain, A. L. 1957. The Control of the Upstream Movement of Fish with Pulsated Direct Current. *Transactions of the American Fisheries Society*, 86: 269-284.
- McMillan, F. O. 1928. Electric fish screen. *Bureau of Fisheries Bulletin*, 44: 97-128.
- Pegg M. A. and J. H. Chick. 2003. Aquatic nuisance species: an evaluation of barriers for preventing the spread of bighead and silver carp to the Great Lakes. Annual Report, Illinois-Indiana Sea Grant.
- Pegg M. A. and J. H. Chick. 2004. Aquatic nuisance species: an evaluation of barriers for preventing the spread of bighead and silver carp to the Great Lakes. Final Report, Illinois-Indiana Sea Grant.
- Seidel W. R. and E. F. Klima. 1974. In situ experiments with coastal pelagic fishes to establish design criterion for electrical fish harvesting systems. *NOAA Fish Bulletin* 72: 657-669.
- Sparks, R., Dettmers, J. and T. Barkley. 2004. Assessment of an electric barrier to prevent dispersal of aquatic nuisance fishes. Final Report to the Great Lakes Protection Fund.
- Stainbrook, K., S. Creque and J. Dettmers. 2005. Field assessment of an electric dispersal barrier to protect sport fishes from invasive exotic fishes. Annual Report to the Division of Fisheries, Illinois Department of Natural Resources, Illinois Natural History Survey, Center for Aquatic Ecology and Conservation.
- Sternin, V. G., I. V. Bikonrov and Y. K. Bumeister. 1976. *Electrical Fishing: Theory and Practice*. (E. Viliam, Trans.) Jerusalem: Keter Publishing House. Israel Program for Scientific Translations.
- Stewart, P. A. M. 1990a. Electric screens and guides. In I.G. Cowx and P. Lamarque. *Fishing with Electricity – Applications in Freshwater Fisheries Management*. London, England: Fishing News Books.
- Stewart, P. A. M. 1990b. Electric barriers for marine fish. In I.G. Cowx (Ed.), *Developments in Electric Fishing* (pp. 243-255). London, England: Fishing News Books.
- Swink, W. D. 1999. Effectiveness of an electrical barrier in blocking a sea lamprey spawning migration on the Jordan River, Michigan. *North American Journal of Fisheries Management* 19: 397-405.
- Taylor, G. N., L. S. Cole, and W. F. Sigler. 1957. Galvanotaxic response of fish to pulsating direct current. *Journal of Wildlife Management*, 21: 201-213.
- Zalewski, M. and I. G. Cowx. 1990. Factors affecting the efficiency of electric fishing. Pages 89-111 in I.G. Cowx and P. Lamarque, editors. *Fishing with Electricity, Applications in Freshwater Fisheries Management*. Fishing News Books, Oxford, England.

## 2 – Evaluation of Operational Protocols for Induction of Passage-Preventing Behaviors in Small Bighead Carp

---

Summary.—The effectiveness of various operational protocols [combinations of pulsed DC field strength (V/cm), pulse-frequency (Hz), pulse-duration (ms)] to immobilize encroaching small [51 – 76 mm (2.0 – 3.0 inches) total length] bighead carp *Hypophthalmichthys nobilis* was evaluated in a controlled experiment conducted September – December 2009. Simulations of encroachment into the field of Barrier IIA on the Chicago Sanitary and Ship Canal (CSSC) developed for the experiment employed the hypothesized worst case scenario for preventing passage of the targeted fish: (1) encroaching fish were small, (2) encroaching fish were swimming at the surface of the CSSC, (3) fish penetrating the electric barrier continued upstream despite receiving electrical stimulus, (4) very low or no water current, and, (5) fish traversed the barrier at maximum swimming speeds. The field strength applied in the electrical treatments varied over time to mimic that experienced by fish swimming through the electric field of Barrier IIA at a constant rate of 50 cm/s, at the surface of the CSSC. Small bighead carp were individually exposed to electrical treatments in completely randomized experimental designs, 20 fish per experimental cell. A total of 500 fish were used in the screening trial used to determine a set of promising operational protocols. A total of 400 fish were used in an experiment focusing on promising operational protocols and prognostic modeling of probability of immobilization. Outcomes in the present study support the hypothesis that the characteristics of the waterborne electric field influence probability of immobilization of encroaching small bighead carp, supporting facets of the conceptual risk model for barrier effectiveness. A multivariable relationship was demonstrated (between field strength, pulse-frequency, pulse-duration, fish length, and the interaction between pulse-duration and fish length, and the probability of immobilization) in the prognostic model. Outcomes of the present study provide the best information available regarding the likelihood of immobilizing small bighead carp encroaching upon Electric Barrier IIA and the relative effectiveness of various operational protocols. Several of the operational protocols tested reduced risk for failing to immobilize encroaching small bighead carp compared to the protocol presently used by the barriers on the CSSC. Risk was significantly reduced with pulse-frequency of 30 Hz when applied at ultimate field strength of 0.91 V/cm and pulse-durations of 2.5 ms. Outcomes and observations indicate the extent to which fish penetrate barrier fields on the CSSC will be inversely related to fish length, with large (adult) fish deterred from penetration at the downstream edge. Penetration of the low field of Barrier IIA by small bighead carp challenging the barrier is likely, regardless of the operational protocol employed (of those tested). The sharply increasing gradients of the rising side of the high field of Barrier IIA will serve as the boundary for upstream penetration by small fish, when operational protocols demonstrated effective in the experiment (e.g., ultimate field strength: 0.91 V/cm; pulse-frequency: 30 Hz; pulse-duration: 2.5 ms) are applied. The prognostic model (FS, PF, PL, L, PL\*L) developed from the simulations provides the best information available regarding the likelihood of immobilizing 51 – 76 mm bighead carp encroaching upon Electric Barrier IIA. It must be emphasized, however, that the outcomes are based on electrical exposures conducted under controlled conditions (simulations) and should be verified through field study.

---

## Introduction

Bighead carp *Hypophthalmichthys nobilis* and silver carp *H. molitrix* are nuisance invaders of the Mississippi River System and potential invaders of the Great Lakes. Bighead carp and silver have established reproducing populations in the Mississippi River System and their lifecycle includes prespawn upstream migrations (Kolar et al. 2005). Large populations of bighead carp are present in the Illinois River, downstream from the CSSC (Stainbrook et al. 2005). A 21 7/8" bighead carp was recently collected from the Chicago Sanitary and Ship Canal (CSSC), approximately five river miles downstream of the electric barriers, during a rotenone event (Illinois Department of Natural Resources 2009) confirming the presence of invasive carp in the CSSC.

The US Army Corps of Engineers (USACE), Chicago District operates a series of electric barriers (designated Barrier I, Barrier IIA, Barrier IIB is nearing completion) on the CSSC to thwart upstream dispersal of invasive carp through the waterway. Barriers I and IIA (and soon Barrier IIB) generate localized waterborne electric fields to act as barriers, to prevent passage of invasive fishes through the CSSC. The electric barriers were designed and developed by Smith-Root, Inc. (Vancouver, Washington). The waterborne electric fields are generated when an electric circuit composed of an electrical power supply (on-shore), submersed conductors (electrodes), and environmental water, is closed. The characteristics of the pulsed direct current (pulsed DC) generated by the on-shore power supply, which is applied to the electrodes, is directly reflected in the waterborne electric field. Electromagnetic forces of attraction and repulsion, the local environment, and electrode orientation, size, and spacing determine the distribution of electric current (the electric field) within the water column. In general, the strength of the electric field increases with proximity to the electrodes in both the vertical and horizontal aspects. The electric barriers operating in the CSSC employ cross-channel, bottom-mounted electrode systems to ensure that fish swimming upstream are exposed to maximum field strengths.

Electric barriers are regarded as behavioral technologies that function by inducing avoidance and/or immobilization responses in fish to block passage or direct movement. Although there is a long history of electric barriers and electric screen usage in fisheries management (e.g., McMillan 1928), there are relatively few published evaluations on the efficiency of these systems at blocking fish passage. The individuality of the systems and their operations often render available information inapplicable to other facilities (Johnson et al. 1990). There are few accounts of comparative tests of electrical parameters for electric barriers and fish guidance systems. The effects of electricity on fish, in the context of capture of wild fish, have been topics of scientific interest over the past century, however.

Fishing with electric current in surface waters (electrofishing) has proven an effective method for scientific sampling of freshwater fish populations (Reynolds 1996). It is well established, in the context of electrofishing, that the reactions of fish to electrical exposure is species- and size-dependent (Taylor et al. 1957; Biwas and Karmarker 1979; Edwards and Higgins 1973; Seidel and Klima 1974; Bird and Cowx 1993; Holliman 1998). Maximum susceptibility to electrical exposure often occurs at different frequencies of pulsed DC, among species (Edwards and Higgins 1973; Bird and Cowx 1993). These differences in vulnerability among species can be manifested in extreme cases as electrical stimulus leading to immobilization in one species, but flight in another (Seidel and Klima 1974; Holliman 1998). Fish of different sizes (of the same species) also appear to exhibit their greatest susceptibility at different pulse frequencies (Edwards and Higgins 1972). The phenomenon of larger fish having lower threshold values than smaller fish is significant, as more intense electric fields may be necessary when targeting smaller fish. This size selectivity has been attributed to bigger fish intercepting a greater

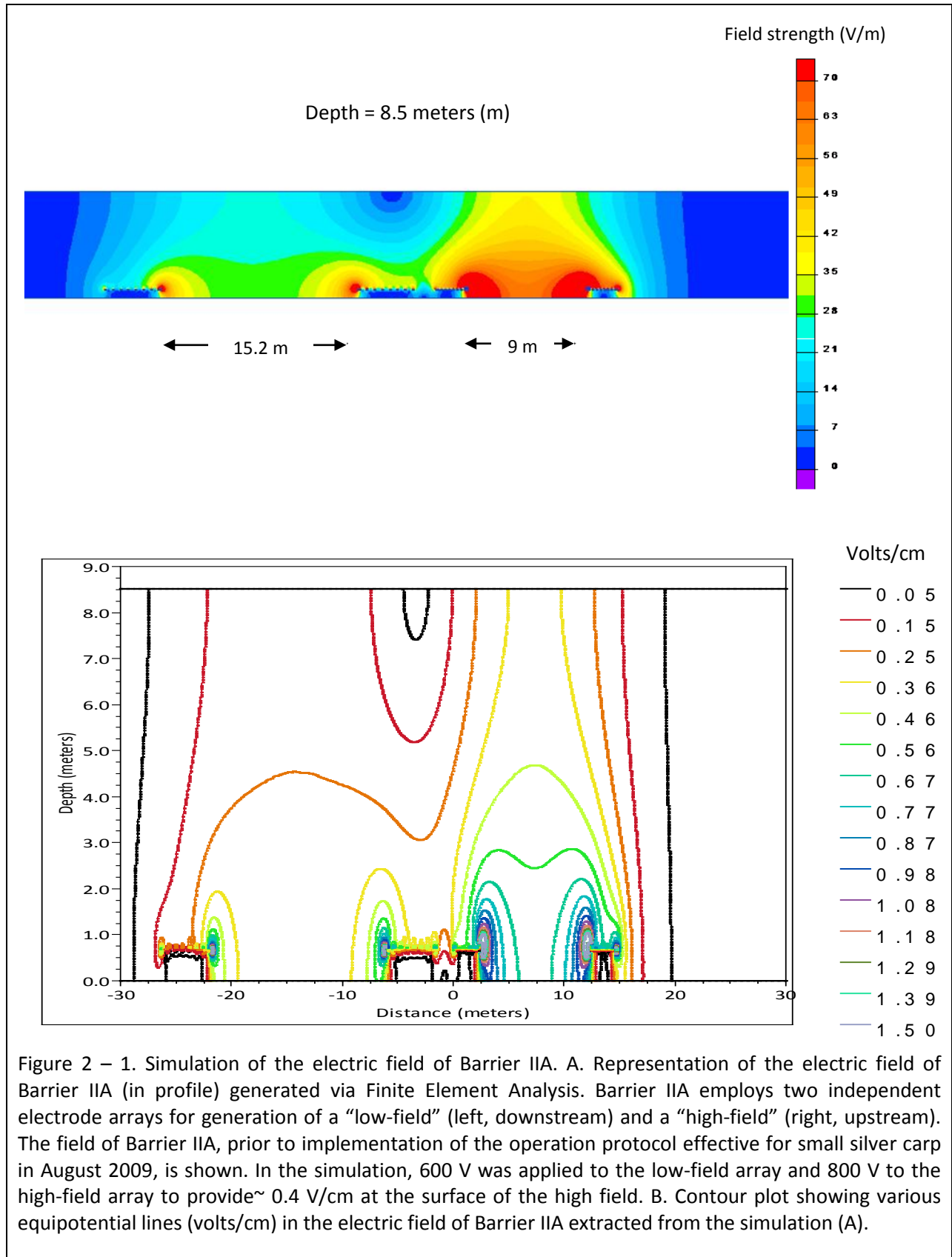
potential difference than smaller fish. According to Lamarque (1967) and Halsband (1967), fish reactions are dependent upon voltage drop per unit length of fish. Preliminary experimentation with small silver carp demonstrated that field strength, pulse-frequency, and pulse-duration influences effectiveness at inducing passage-preventing behaviors in these fish (Holliman, this report).

Hartley and Simpson (1967) and Stewart (1990a) provide general guidance for successful barrier design and operation. Hartley and Simpson (1967) suggest that graduated electric fields are necessary for electric barriers to be successful. With a graduated barrier field, fish challenging the field are exposed to increasingly unpleasant stimuli as they penetrate further and can learn to avoid it. The extent (width) of the field is critical (the width is measured in the direction that fish swim), where the width of the field must prevent fast swimming fish from passing through the electrified zone under their own power. The width of the field necessary for success is influenced by the frequency of the DC pulses. The DC pulse rate must ensure that fast swimming fish cannot pass through the field, or penetrate too deeply, between pulses. Furthermore, a graduated electric field allows fish to penetrate to the extent that they are able, with larger fish stopping at an earlier stage than smaller fish (i.e., size selection). The ultimate field strength should be adequate to stop the smallest fish targeted (Hartley and Simpson 1967).

Stewart (1990a) and Zhong (1990) suggest that knowledge of the behavior of the fish species being managed is vital for successful application of electric barriers, in a given circumstance. The motivation for fish movement is an important consideration. An example is the drive to reproduce in salmon, where these fish are often not deterred by extreme hazards, making repeated attempts to pass barriers. Stewart (1990b) relays that the appearance of the electric barrier is critical, that a physical marker may be necessary for electric fields to block fish movement effectively. In his evaluation of electric barriers for marine fish, Stewart (1990b) found that fish swimming into unmarked electric fields swam vigorously upon electrical stimulation, either back or through the field. The field was ineffective in his tests because fish were unable to identify and avoid the electrified zone. Further, when the field distribution was non-uniform, fish may not have been able to discern the direction of increasing intensity, swimming into rather than out of the electrified zone. When a novel stimulus was coupled with the margin of the electric field, fish slowed their approach and learned to avoid the electric field (Stewart 1990b).

Simulations of the Barrier IIA electric field, prior to implementation of the operational protocol effective for small silver carp (Figure 2 – 1), indicate that it meets the criterion for a successful barrier outlined by Hartley and Simpson (1967), having a graduated electric field. The field changes gradually, without abrupt changes in field strength over short distances, the exception being in proximity to the electrodes. Anecdotal observations and studies of fish movement indicated Barrier I to block upstream movement of large fish (e.g., common carp *Cyprinus carpio*) effectively (Sparks et al. 2004, Dettmers and Creque 2004). Barrier IIA has a larger electric field and greater output capabilities than Barrier I; it is expected that Barrier IIA will be at least as effective as Barrier I.

There is little published information on the effects of electrical exposure on silver carp or bighead carp. Liu (1990) demonstrated that when using 3-phase alternating current, the electric field intensity required to induce the flight response of 18.3 cm bighead carp and 29.4 cm silver carp to be relatively stable in water 30 to 1000  $\mu\text{S}/\text{cm}$ . Miranda and Dolan (2003) report the relationship between threshold field strength and water conductivity reported by Liu (1990) to be in accord with power transfer theory. Lui et al. (1990) found that using a seine net outfitted with irregular pulsed DC (irregular half-wave rectified alternating current) improved catch of silver carp and bighead carp over a traditional seine. The work of Pegg and Chick (2004) on silver and bighead carp indicated size-dependent effectiveness of electrical fields for preventing passage through an electric field. The recently completed pilot study on





effective operational protocols for electric barriers on the CSSC demonstrated several operational protocols effective for immobilizing small silver carp, but 0.79 V/cm, pulse-frequency of 15 Hz and pulse-duration of 6.5 ms was most effective of those tested (Holliman, this report).

To my knowledge, there are no other accounts describing of effects of various electrical parameters on smaller silver carp or bighead carp.

The objective in this phase of the project was to determine the characteristics of waterborne pulsed DC barrier fields, for electric barriers on the CSSC, effective for inducing passage-preventing behaviors in small bighead carp. As with most pioneering research, the protocols in the present study integrated components of accepted scientific methods, with experimental treatment selection guided by initial and subsequent findings. This work was accomplished in a controlled environment, where in-water electrical conditions associated with the electrified zones on the CSSC were simulated in tanks and sources of variation commonly associated with electrically oriented field studies controlled. Because of the large number of electrical parameter combinations available for use on the CSSC, screening trials were necessary to identify a range of promising electrical parameters for more focused evaluation.

The basic experimental protocols employed in the pilot study were sufficient. The simulations of the electric fields (electrical exposures) in the pilot experiment were “state of the art”, but relatively crude. Refinement of the simulation of the barrier fields was desired to improve translation of observations and inference of results from the laboratory environment to the Canal. Hence, a more sophisticated electric field simulation system was developed in the interval between pilot study and the present study. The new electric field simulation system provided a continuous pulsed DC signal that could be varied (increased or decreased) in intensity and was programmable to ensure repeatability. The experimental approach coupled with the electric field simulations applied in the present study represent significant progress in the “state of the art” for research on electroshock-induced effects in fish, improving data quality and the inference of experimental results.

Based on the outcomes of the pilot study, the tenets associated with the use of waterborne electric fields for capture of fish (e.g., Zalewski and Cowx 1990), and prior work on electric barriers, a Conceptual Risk Model for Breach of the Electric Barriers was devised. The Model, which is based on technical, biological, and environmental factors hypothesized to influence risk for breach,

<u>Technical factors</u>	<u>Biological factors</u>	<u>Environmental factors</u>
Pulsed DC field strength	Fish species	Water conductivity
Pulsed DC pulse-frequency	Fish size	Water velocity
Pulsed DC pulse-duration	Behavior	Water depth
Field orientation	Swimming speed	Habitat,
(direction of electric current flow)	(duration of exposure)	
Field size		
Field distribution (shape)		

was devised to facilitate understanding of the electric barriers, to aid development of hypotheses for testing, and to provide a conceptual framework for the research. Simulations of encroachment into the barrier field of Barrier IIA were developed, which were based on the hypothesized worst-case scenario for preventing passage of the targeted fish through the barrier field: (1) encroaching fish were small, (2) encroaching fish were swimming at the surface of the Canal, (3) fish penetrating the electric barrier continued upstream despite receiving electrical stimulus, (4) fish traversed the barrier at maximum swimming speeds, and (5) water velocity was zero or minimal.

A reliable source of fish was critical for study success, as availability of wild silver carp and bighead carp in the size range targeted would be unpredictable. Pond-culture of bighead carp was arranged by the USACE, Environmental Laboratory, Engineer Research Development Center (EL-ERDC), Fish Ecology Team to insure sufficient quantities of small bighead carp were available for experimentation. This study was a continuation of collaborative efforts between the USACE, Chicago District, the EL-ERDC, Vicksburg, Mississippi, and Smith-Root, Inc. (SRI), Vancouver, Washington.

## Methods

A series of experiments evaluating operational protocols for the electric barriers on the Chicago Sanitary and Ship Canal were conducted from 3 September to 30 December 2009. The electric barriers on the Canal are capable of generating an enormous number of combinations of field strength, pulse-frequency, and pulse-duration (Figure 2 – 2). The ultimate field strength (V/cm), pulse-frequency (Hz), and pulse-duration (ms) tested (in combination) were selected from the simulation of barrier output capabilities using a hierarchy of pulse-frequency (Hz), ultimate field strength (V/cm), and pulse-duration (ms). The pulse-duration used with a pulse-frequency and ultimate field strength combination was the estimated maximum for that combination (Figure 2 – 2). The field strength, pulse-frequency, and pulse-duration tested in combination are referred to as an operational protocol for brevity.

A screening trial consisting of five experiments was conducted to establish operation and performance of the electric field simulation system and ranges of electrical parameter combinations potentially effective for inducing passage-preventing behaviors in small bighead carp. Operational protocols employing pulse-frequencies of 10, 15, 20, 25, and 30 Hz were evaluated in each of the screening experiments. The ultimate field strength applied in the operational protocols was varied among the five experiments (0.79, 0.91, 1.02, 1.14, 1.5 V/cm), but was constant within each experiment. Percent (%) duty cycle, calculated as  $\% \text{ duty cycle} = 100\% \times (\text{pulse duration}/T)$ , where T was the period of one cycle of the pulse (ms), was also constant within each experiment, but varied among the experiments. The pulse-duration (ms) applied in the operational protocols was varied to attain the appropriate % duty cycle. There was an inverse relation in the pairings of ultimate field strength with % duty cycle applied in the operational protocols, applied in the experiments (0.79 V/cm – 8% duty cycle; 0.91 V/cm – 6.0% duty cycle; 1.02 V/cm – 5% duty cycle; 1.14 V/cm – 4% duty cycle; 1.5 V/cm – 2% duty cycle).

Based on observations and outcomes in the screening trial, eighteen promising operational protocols were selected for evaluation and predictive modeling. A 3 x 3 x 2 factorial design [ultimate field strength, 0.79 V/cm, 0.91 V/cm, 1.02 V/cm; pulse-frequency, 20 Hz, 25 Hz, 30 Hz; pulse-duration, 2.0 ms, 2.5 ms (% duty cycles of 4%, 5%, 6%, or 8%)] was employed in the experiment. A null treatment, where fish were subjected to experiment protocols and procedures with the exception of electrical exposure, was also included in the experiment.

At the conclusion of data collection in the factorial experiment, an additional four simulations were conducted applying the operational protocol shown effective for immobilizing silver carp in the pilot study (ultimate field strength of 0.79 V/cm and pulse-frequency of 15 Hz and pulse-duration of 6.5 ms). These last four simulations served as a precursor for experimentation on effects of water velocity on risk for breach of the barriers and as a baseline for comparison with outcomes from the factorial experiment. These simulations were conducted using groups of fish (five fish). Water velocity was maintained at 3 cm/s (N = 1), 5 cm/s (N = 1), or 10 cm/s (N = 2). The outcomes of these simulations were

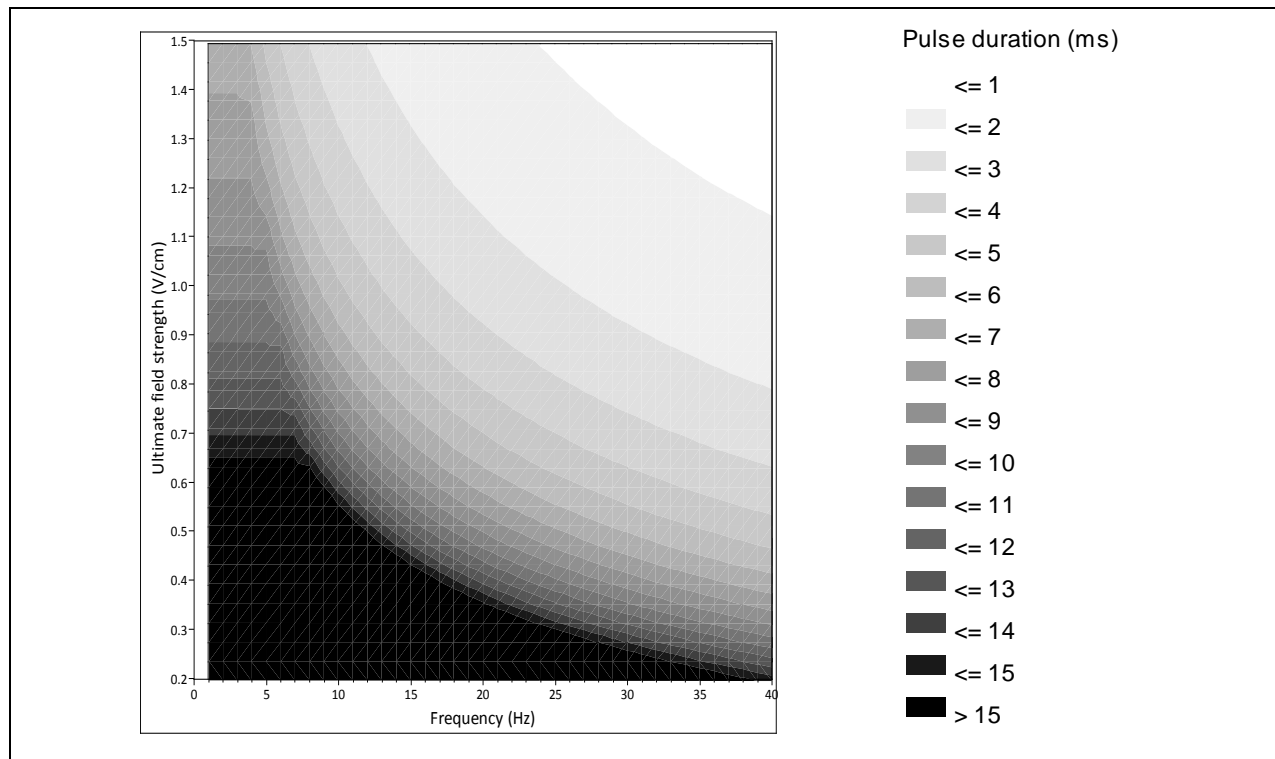


Figure 2 – 2. Barrier output capabilities. A contour plot demonstrating the estimated maximum pulse-length (ms) and ultimate field strength (volts/cm) that can be sustained in the high-field by Electric Barrier IIA, as a function of the pulse frequency (Hz). The estimations of the output capabilities guided selection of electrical parameter combinations applied in the experiments on small bighead carp conducted at the ERDC-EL, Vicksburg, Mississippi September – December 2009.

pooled and employed post hoc as a baseline for statistical comparisons of risk with outcomes from the factorial experiment.

All simulations were conducted with naïve fish. The simulations were conducted on individual fish; the exception was simulations serving as the baseline for statistical comparison of risk, where fish were tested in groups of five fish. The screening experiments and the experiment with promising operational protocols were conducted using completely randomized experimental designs, the exception being the four simulations at the conclusion of the experiment on promising operational protocols, described above. Fish were randomly assigned to operational protocols. The sequence in which the operational protocols were tested was randomized within each experiment. Twenty fish were assigned to each experimental cell. A total of 100 fish were used in each of the five experiments in the screening trial, a total of 500 fish. A total of 400 fish were used in the experiment focused on promising operational protocols, as there was total of 20 experimental groups in this experiment, 18 in the factorial experiment, one control group and one group designated as the baseline for statistical reference. Of those fish used in the experiment on promising operational protocols, the first 190 were monitored for acute mortality and the last 190 were evaluated for injury. Those fish evaluated for acute mortality were transferred to a holding tank, segregated by treatment and monitored for a minimum of 12 hours. Injury was evaluated via inspection of exposed flesh and the vertebral column (for hemorrhage) after bilateral filleting of fish. Measures of total length (mm) and weight (g) were collected

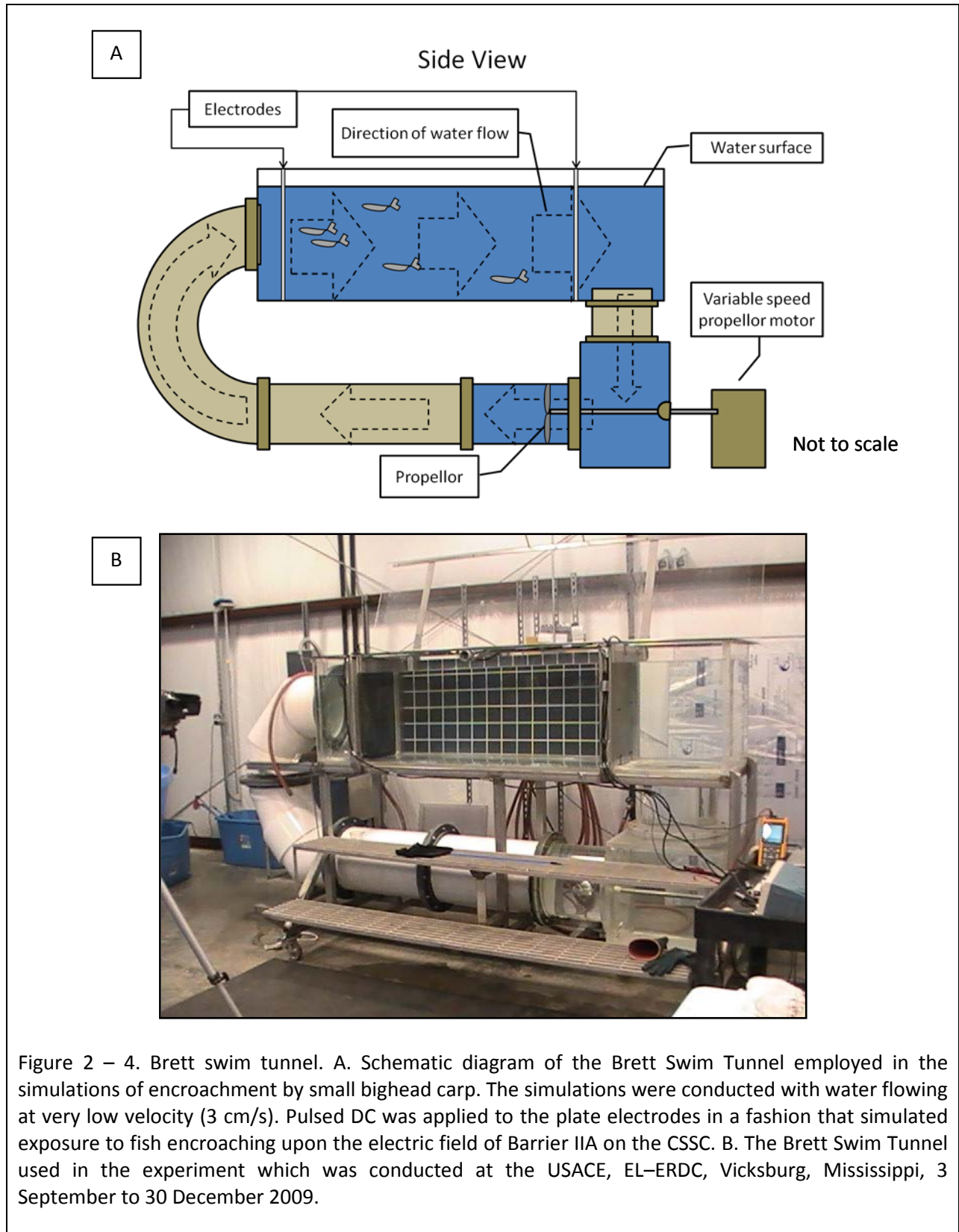


Figure 2 – 3. Exposure tank for the experiments in the screening trial. Experiments in the screening trial were conducted in a 168 cm x 42 cm rectangular fiberglass tank (water depth was 40 cm). Plate electrodes were used to create a homogeneous electric field in the tank. Each simulation was video recorded. The screening experiments were part of a more comprehensive study of operational protocols for the electric barriers on the CSSC, conducted at the USACE, EL-ERDC, Vicksburg, MS, 3 September to 30 December 2009.

on all fish. All fish were killed by immersion in an overdose solution of MS-222 immediately after completion of the experimental treatment or period of monitoring.

The experiments in the screening trial were conducted in a 168 cm x 42 cm rectangular fiberglass tank filled with water to a depth of 40 cm (Figure 2 – 3). The tank was outfitted with two perforated stainless steel, plate electrodes that were positioned parallel, covered the cross-sectional area of the tank, and extended above the water surface. Electrode spacing was 63 cm. A linear change in voltage (i.e., a constant voltage gradient) was produced in the tank (Holliman and Reynolds 2002). The ambient conductivity of water in the tank was between 980 and 1050 ( $1016 \pm 22$ )  $\mu\text{S}/\text{cm}$  at 19.9 to 22.1 ( $20.4 \pm 0.5$ ) °C. There was no water current flow in the tank during the screening experiments. Two video recorders were mounted above the tank to record fish responses during the electrical exposures.

Simulations with the set of promising operational protocols were conducted in the rectangular section of a Brett Swim Tunnel (Figure 2 – 4) to improve visual observation of fish responses and the quality of video recordings over that with the opaque fiberglass tank used in the screening experiment. Two video cameras were directed at the side of the tank to record fish response during the simulations of encroachment into the barrier field. The rectangular section of the swim tunnel was outfitted with two perforated stainless steel plate electrodes, that were positioned parallel, extended above the water surface, and were separated by 152.4 cm (Figure 2 – 4). The rectangular section of the swim tunnel was



57.5 cm wide and filled with water to a depth of 52.1 cm. The ambient conductivity of water in the swim tunnel was maintained between 1913 and 2040 ( $1996 \pm 36$ )  $\mu\text{S}/\text{cm}$ . Water temperature was between 19.0 and 20.8° C. The swim tunnel allowed fine control of water flow velocity (through a variable speed motor connected to a propeller) and velocity was maintained at 3 cm/s to aid in detection of immobilization in fish (through drift). The 3 cm/s rate of flow was below the threshold for positive rheotaxis. Intuitively, in a confined space, any flow velocity would increase time spent by fish being more aligned with the direction of water flow (and electric current flow), compared to a flow rate of 0 cm/s. However, fish were not motivated to swim consistently into the flow and body-voltage minimizing behaviors were possible for extended periods. No differences are expected in the outcomes of the experiment compared to if the simulations had been conducted with water velocity at 0 cm/s.

The field strength applied in the simulations of encroachment into the barrier field was based on in-water voltage measurements taken from the surface of the Chicago Sanitary and Ship Canal at Barrier IIA by the USACE, Engineer Research and Development Center, Construction Engineering Research Laboratory, Champaign, Illinois. In the simulations, the strength of the electric field was varied over time to mimic the electrical exposure that fish traversing the electrified zone of Electric Barrier IIA would experience, when swimming at the surface of the Canal (Figure 2 – 5). The two distinct lobes characterizing the electric field of Barrier IIA, the “low field” (downstream) and the “high field” upstream were represented in the exposures. The maximum field strength of the high field, referred to as the “ultimate field strength”, was varied depending on the treatment and experiment. The range of field strengths associated with the low-field was consistent across all the simulations with a maximum of  $\sim 0.2$  V/cm.

The duration of the simulations, which determined rates of change in field strength, was calibrated to the minimum estimate of time required for 51 – 76 mm bighead carp to traverse the  $\sim 44$  meter electric barrier under the conditions of no water current flow. Maximum sustained swimming speeds of small bighead carp of the targeted size was 20 cm/s in swim tests on individuals and 40 cm/s in swim tests on groups of 3 or 5 fish. Bighead carp from this cohort typically swam 50 cm/s for less than 1 minute, although some high performers in groups did swim longer periods (personal communication, Dr. Jack Killgore, Dr. Jan Hoover, USACE, Environmental Laboratory – Engineer Research Development Center, Vicksburg, Mississippi). The exposure period was calibrated to a swimming speed of 50 cm/s, simulations of 88 seconds duration. An exposure thought to be the worst-case, as duration of electrical exposure was minimized.

Electrical energy was supplied to the test tanks by a custom, programmable-pulsed DC electric field simulation system. The simulation system allowed independent control of the duration of the exposures, field strength, pulse-frequency, and pulse-duration. The patterns of field strength applied in the simulations (Figure 2 – 5) were programmed into the system as sequences of 1024 individual points. The characteristics of the electrical parameters characterizing the operational protocols applied in the simulations were measured with a calibrated, digital oscilloscope.

Fish behavior was monitored during each of the simulations. An external timer was used to estimate exposure time at the onset of first response, flight, and immobilization, and righting. First response was categorized as the initial reaction to the presence of the electric field, which typically included rapid starts, distinctive twitches of the head or tail, or brushing against the side or bottom of the tank. Flight was characterized by the onset of rapid (frantic) non-directed swimming. Flight often transitioned to

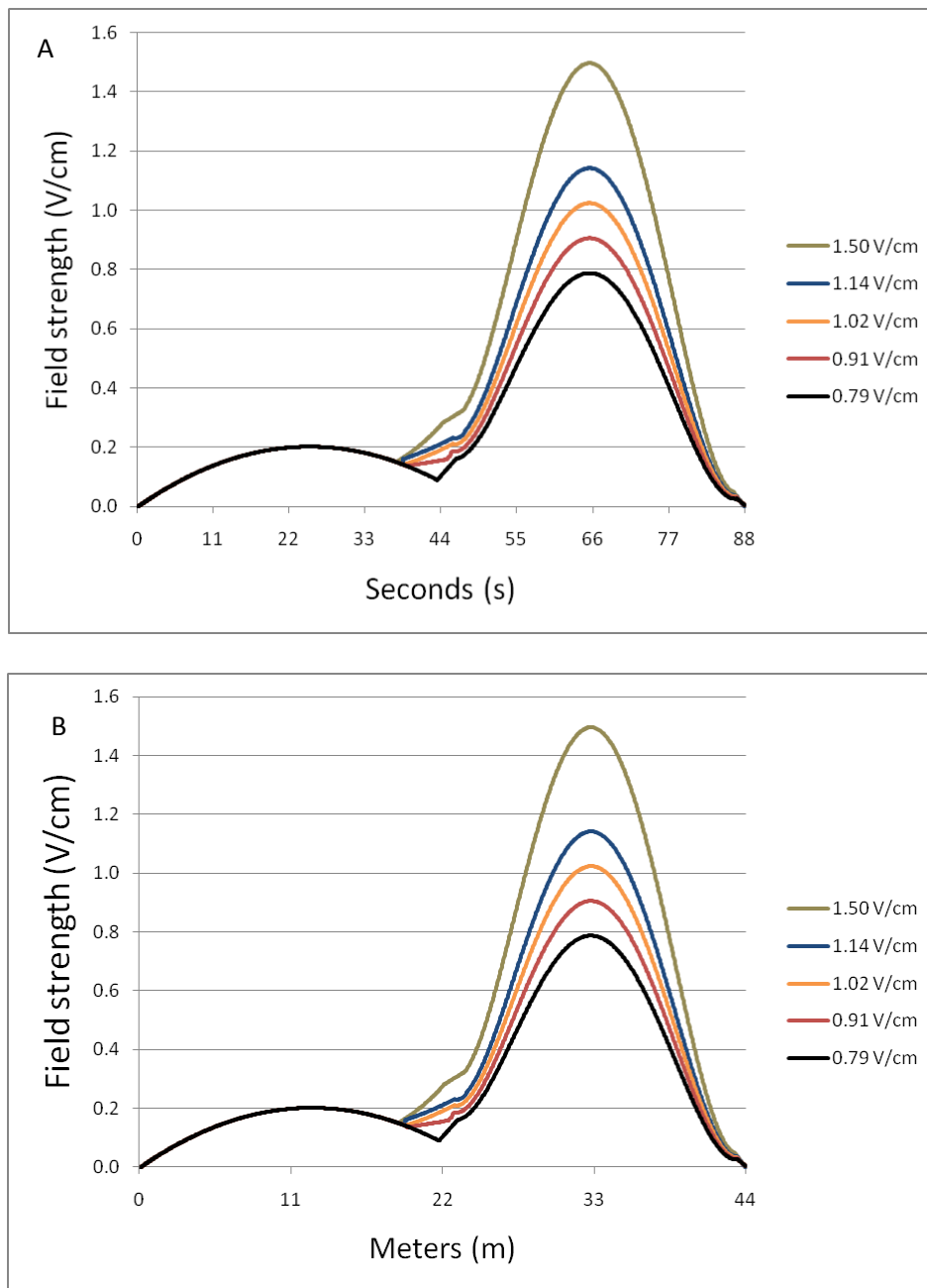


Figure 2 – 5. Electric fields applied in the simulations. (A) Electric field strength was varied with time (seconds) in the simulations of encroachment into the field of Barrier IIA by small bighead carp, in the screening trial and the experiment for predictive modeling. (B) The strength of the electric field applied in the simulations in relation to distance (meters) on the Canal. The simulations of encroachment mimicked exposure to fish swimming through the electric field of Barrier IIA at a constant rate of 50 cm/s, at the surface of the Chicago Sanitary Ship Canal. Patterns of field strength associated with the low-field (downstream, left) was constant among the operational protocols. The ultimate field strength applied [peak of the high field (upstream, right)] varied according to the operational protocol.

swimming from side-to-side in the tank (body-voltage minimizing behaviors), forced swimming while righted and forced swimming with loss-of-equilibrium. Immobilization was characterized by the complete cessation of swimming motions and was typically accompanied by loss-of-equilibrium. Righting was recorded as the resumption of upright orientation by fish previously losing equilibrium while immobilized.

Estimates of threshold voltage gradient ( $E$ , V/cm), threshold power density ( $\mu\text{W}/\text{cm}^3$ ), and threshold cumulative exposure ( $\mu\text{W}/\text{cm}^3\cdot\text{s}$ ) for the targeted responses were based on the estimated time at threshold response (rounded to the nearest second) and were extracted from the patterns of field strength applied in the simulations (Figure 2 – 5). Threshold power density ( $D_a$ ) was estimated with  $D_a = E^2 \times c_w$ , where  $E$  was the threshold voltage gradient (V/cm) and  $c_w$  was the ambient conductivity of tank water ( $\mu\text{S}/\text{cm}$ ; Kolz 1989). Threshold cumulative exposure for the targeted responses was estimated as the sum of ( $D_a$ ) from the start of the exposure to the onset of the response of interest.

*Data analysis.*—The distributions of fish size and measures associated with thresholds of targeted behaviors were examined with box-and-whisker plots. The box-and-whisker plots demonstrated the 25<sup>th</sup> and 75<sup>th</sup> quartiles (ends of the boxes), the interquartile range (IQR; the distance between the box ends), the median (line across the interior of the box), and the outer-most data points falling within 1.5 x IQR (the whiskers extending outward from the ends of the boxes). Means and the 95% confidence intervals on the mean were represented in the plots with a split diamond (Sall et al. 2007).

Fish size and measures associated with thresholds of targeted responses in the experiment for prognostic modeling were summarized with means, standard deviations (SD), and 95% confidence intervals. Data were rank (average rank) transformed if the distribution was non-normal, skewed, or contained extreme values. Analysis of Variance (ANOVA) was used to test for differences in means among groups of interest. The Brown-Forsythe test was used to test statistical hypotheses of homogeneity of variance (Brown and Forsythe 1974; SAS 2008). Welch's ANOVA was employed when there was statistical evidence that the variance differed among the groups of interest. Tukey's Honestly Significant Difference test was used in post hoc pair-wise comparisons when evidence of unequal means was provided by ANOVA (SAS 2008).

Counts, proportions, and percentages were used to summarize the relationships between the independent variables and the occurrence of targeted behavioral responses. The occurrence of immobilization, a binary response, was the outcome of primary interest in the simulations. The hypothesis of equality of proportions in contingency table margins, among levels of field strength, pulse-frequency, and pulse-duration, was evaluated using the Pearson Chi-Square Test.

In the experiment for predictive modeling, the relative risk (RR), the ratio of the proportions being compared, was used to estimate risk (probability) for failing to immobilize fish with the various operational protocols compared to the operational protocol designated as the baseline. In the event of a zero cell in the tables, a constant (a value of 1) was added to each cell of the table to allow estimation of relative risk (Agresti 1990). An RR exceeding 1.0 indicated a increase in risk of failing to immobilize fish (an undesired effect in this case). An RR less than 1.0 indicated a reduction in the risk for failing to immobilize fish. If  $RR = 1.0$  or if 1.0 was within the bounds of the confidence interval, there was no difference in risk of failing to immobilize fish between the operational protocols being compared.

Field strength ( $FS$ ), pulse-frequency ( $PF$ ), pulse-duration [abbreviated as  $PL$ , (pulse-length) to prevent any confusion with power density (PD)], and fish total length ( $L$ ) were treated as candidate predictors of



immobilization in small bighead carp. Logistic regression was employed to evaluate candidate predictive models developed from the potentially predictive factors. Univariate models (*FS*; *PF*; *L*) and the *FS*, *PF* model were applied to the data from the screening trial (*PL* was confounded with *FS* in the screening trial and not evaluated independently). The candidate set of models applied to data from the factorial experiment (with promising operational protocols) included univariate and multivariable models (*FS*; *PF*; *PL*; *L*; *FS*, *PF*, *PL*; *FS*, *PF*, *PL*, *L*; *FS*, *PF*, *PL*, *FS\*PF*; *FS*, *PF*, *PL*, *FS\*PL*; *FS*, *PF*, *PL*, *PF\*PL*; *FS*, *PF*, *PL*, *L*, *FS\*PF*; *FS*, *PF*, *PL*, *L*, *FS\*PL*; *FS*, *PF*, *PL*, *L*, *FS\*L*; *FS*, *PF*, *PL*, *L*, *PF\*L*; *FS*, *PF*, *PL*, *L*, *PL\*L*; *FS*, *PF*, *PL*, *L*, *L\*L*; *FS*, *PF*, *PL*, *L*, *L\*L\*L*). The models in the candidate set addressed assumptions of additivity between the experiment factors, additivity of the covariate fish total length, and linearity of the covariate fish total length. Field strength, pulse-frequency, and pulse-duration were treated as ordinal categorical variables and fish length as a continuous variable. Factors failing tests that the estimated parameter equaled zero in univariate models were dropped from further consideration, in the analysis.

Akaike's information criterion (AIC), which includes a penalty for number of model parameters, approximates information lost in the conversion from data to model. Smaller AIC values indicate smaller losses of information (Buckland et al. 1997; Burnham and Anderson 1998; Franklin et al. 2001). The differences in corrected Akaike information criterion (AICc) values between each model and the model with the smallest AICc value ( $\Delta_i = AIC_i - \min[AIC]$ ) and normalized Aikaike weights  $\omega_i = \exp(-\Delta_i/2) / \sum_{r=1}^R \exp(-\Delta_r/2)$  were calculated for each model in the candidate set of *R* models. The differences in AICc indicated the level of empirical support for the model, where there was substantial support for the model as best when  $0 \leq \Delta_i \leq 2$ , less when  $4 \leq \Delta_i \leq 7$ , and little support when 10. Normalized Aikaike weights allowed comparison of model plausibility (Burnham and Anderson 1998; Franklin et al. 2001). Model calibration was evaluated with Goodness-of-Fit tests (GOF) based on the negative log-likelihood and the Pearson Chi-square test (SAS 2008). Model discrimination was evaluated with the area under the receiver-operating characteristic curve (ROC; SAS 2008). The area under the ROC curve was a measure of the model's overall predictive capability (defined in this case as the ability to separate those fish likely to be immobilized from those likely not). An area under the ROC = 0.5 suggested no discrimination (random), an area of  $0.7 \leq \text{ROC} \leq 0.8$  was regarded as acceptable discrimination, an area of  $0.8 \leq \text{ROC} \leq 0.9$  was considered excellent discrimination, and an area under the ROC  $\geq 0.90$  was considered outstanding discrimination (Hosmer and Lemeshow 2000). Models with ROC areas above 0.80 have been endorsed for individual predictions (Johnston et al. 2000). Null hypotheses regarding the effects of individual levels of the independent variables were evaluated with Wald Chi-square tests, in the model determined to represent the empirical data best (SAS 2008). Statistical significance in all tests was assessed using  $\alpha = 0.05$ . Statistical analyses were accomplished using JMP Statistical software, Version 8 (SAS 2009).

## Results

### *Screening trial*

Fish used in the screening trial were 43 to 72 (mean  $\pm$  SD;  $56 \pm 6$ ) mm total length, weighing 0.5 to 3.1 ( $1.4 \pm 0.5$ ) grams. Distinct first responses to the electric field were detected in 83% of the simulations, occurring from 5 to 49 ( $15 \pm 8$ ; 95% CI 14 – 16) seconds into the exposure, at field strengths from 0.07 to 0.32 ( $0.15 \pm 0.04$ ; 95% CI 0.146 – 0.154) V/cm. In the majority of cases, fish reacted to the presence of an electric field at times and field strengths associated with encroachment upon the "low-field" of Barrier IIA.

Fish demonstrated flight responses in 98% of the simulations in the screening trial. The onset of rapid non-directed swimming occurred from 37 to 60 ( $52 \pm 3$ ; 95% CI 51.5 – 52) seconds into the exposures, at field strengths from 0.15 to 1.0 ( $0.44 \pm 0.13$ ; 95% CI 0.04 – 0.47) V/cm. In simulations employing 20 Hz, 25 Hz, or 30 Hz pulsed DC, flight responses often transitioned into forced-swimming with or without loss-of-equilibrium. The threshold for flight was relatively consistent across the simulations, occurring during exposure to the rising side of the high-field (Figure 2 – 5), where there was relatively rapid increase in field strength.

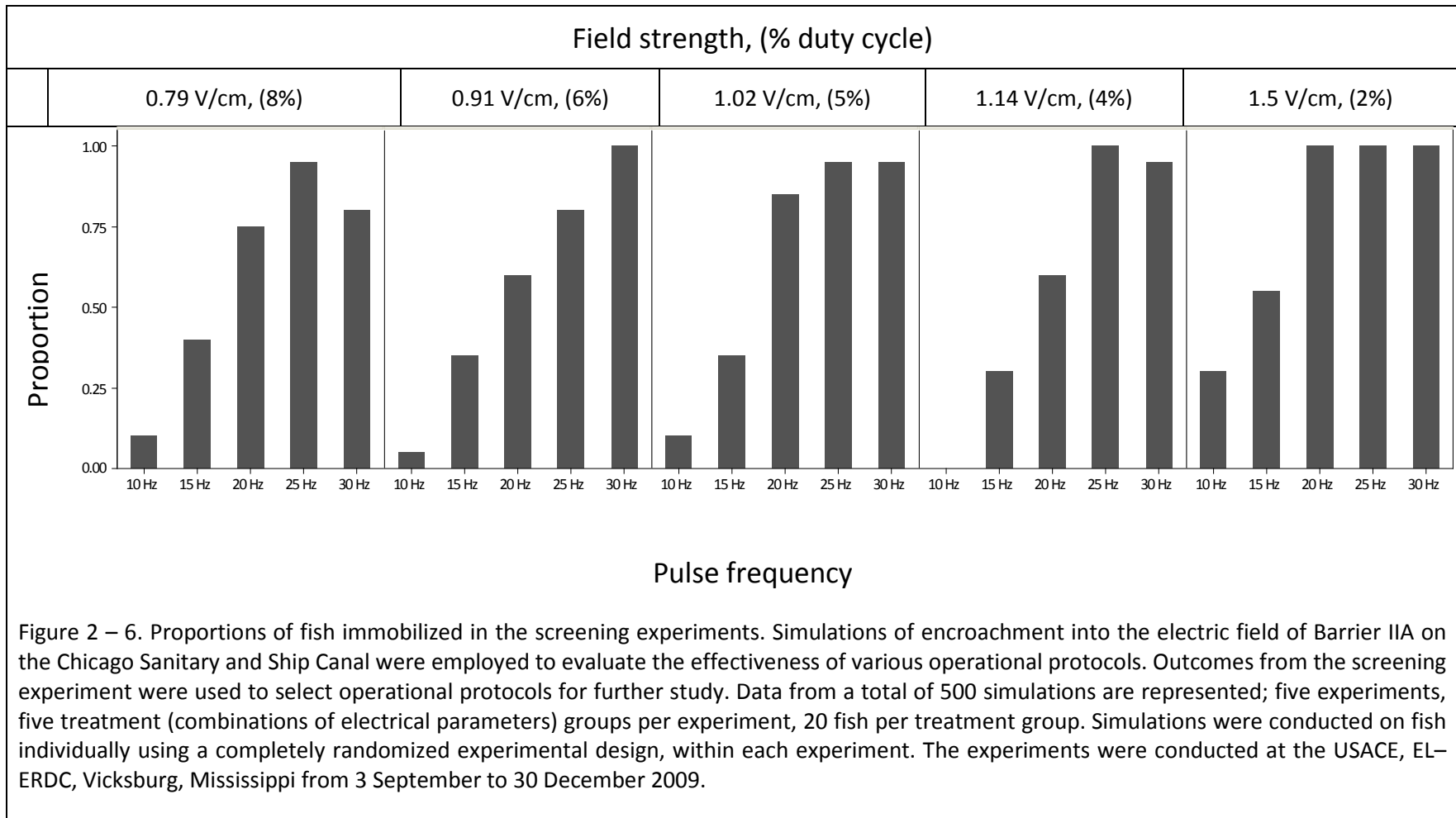
Fish were immobilized during 63% of the simulations of encroachment in the screening trial. Proportions of fish immobilized, in the margins of the contingency tables, differed significantly among the levels of ultimate field strength:

0.79 V/cm, 0.60,  
 0.91 V/cm, 0.56,  
 1.02 V/cm, 0.64,  
 1.14 V/cm, 0.57,  
 1.50 V/cm, 0.77,

( $\chi^2 = 12.448$ ,  $P = 0.0143$ ) and among the pulse-frequencies:

10 Hz, 0.11,  
 15 Hz, 0.39,  
 20 Hz, 0.76,  
 25 Hz, 0.94,  
 30 Hz, 0.94,

( $\chi^2 = 38.557$ ,  $P = 0.0001$ ; Figure 2 – 6). Field strength (FS) and pulse-frequency (PF) were significant single predictors of immobilization in the screening trial, as indicated by logistic regression. Hypotheses that the estimated parameter was zero was rejected in the Likelihood-Ratio Chi-square test in each of these univariate models ( $\chi^2 = 13 - 255$ ;  $DF = 4$ ;  $P \leq 0.0001-0.0112$ ). The GOF tests supported the hypotheses that each of these univariate models adequately fit the data ( $\chi^2 = 500$ ;  $DF = 495$ ;  $P = 0.4288$ ). Fish length (L), however, failed to improve model performance over the constant response probability ( $\chi^2 = 0.6010$ ;  $DF = 1$ ;  $P = 0.4382$ ). The estimated coefficients in the multivariable FS, PF model were not zero ( $\chi^2 = 280$ ,  $DF = 8$ ,  $P < 0.0001$ ), as indicated by the Likelihood Ratio test. The GOF test indicated the FS, PF model adequately fit data from the screening trial ( $\chi^2 = 457$ ,  $DF = 491$ ,  $P = 0.8622$ ). Pulse-frequency ( $\chi^2 = 267$ ,  $DF = 4$ ,  $P < 0.0001$ ) and field strength ( $\chi^2 = 24$ ,  $DF = 4$ ,  $P < 0.0001$ ) were also significant predictors of the probability of immobilization, as indicated by the Effect Likelihood Ratio Tests. Pair-wise tests of pulse-frequency effects demonstrated significant differences between 10 Hz and the remaining pulse-frequencies ( $\chi^2 = 24 - 87$ ,  $DF = 1$ ,  $P < 0.0001$ ), between 15 Hz and the remaining protocols ( $\chi^2 = 31 - 50$ ,  $DF = 1$ ,  $P < 0.0001$ ), and between 20 Hz and 25 Hz and 30 Hz ( $\chi^2 = 11 - 14$ ,  $DF = 1$ ,  $P = 0.0002 - 0.0007$ ), but the difference between 25 Hz and 30 Hz was not statistically significant ( $\chi^2 = < 0.0001$ ,  $DF = 1$ ,  $P = 1.0$ ). Pair-wise hypothesis tests between the levels of field strength in the simulations demonstrated



significant differences between 1.5 V/cm and each of other levels of field strength ( $\chi^2 = 7.6 - 19$ ,  $DF = 1$ ,  $P \leq 0.0001 - 0.006$ ), but no statistically significant differences between remaining levels of field strength ( $\chi^2 = 0.04 - 2.63$ ,  $DF = 1$ ,  $P \leq 0.1048 - 0.8414$ ) in the pair-wise hypothesis tests. The area under the ROC curve (0.89) indicated the model to have very good discriminatory ability.

### *Experiment for predictive modeling*

Fish used in the simulations with the set of promising operational protocols, for predictive modeling of immobilization, were 46 to 72 ( $56 \pm 5$ ) mm total length, weighing 0.7 to 3.2 ( $1.6 \pm 0.5$ ) grams. A total of four fish died during the post-exposure monitoring period. There was no evidence of injury in any of the fish evaluated; no injury was detected via bilateral filleting and visual inspection of the vertebral column and exposed musculature.

There was statistical evidence that fish size differed among the experimental groups. Mean fish length differed significantly among the experimental groups, as indicated ANOVA ( $F_{18/361} = 1.9282$ ,  $P = 0.0131$ ). Post hoc pair-wise comparisons showed mean fish length differed significantly between the 0.91 V/cm-25 Hz-2.5 ms ( $59 \pm 5$  mm) and 0.79 V/cm-20 Hz-2.0 ms ( $54 \pm 6$  mm;  $P < 0.05$ ) experimental groups. There was also statistical evidence that mean weight differed among the experimental groups ( $F_{18/361} = 1.9416$ ,  $P = 0.0123$ ). Post hoc pair-wise comparisons indicated mean weight differed significantly between the 0.79 V/cm-25 Hz-2.0 ms ( $1.35 \pm 0.28$  grams) and the 1.02 V/cm-25 Hz-2.5 ms ( $1.88 \pm 0.50$  grams;  $P < 0.05$ ) experimental groups.

The distinctive twitches, jerks, starts, brushing motions characterizing first responses to electrical stimulation was observed in 83% of the simulations. Mean time to first response was 9 ( $\pm 6$ ) seconds, least in simulations applying the 0.91 V/cm-30 Hz-2.5 ms operational protocol (mean, 7; 95% CI, 5 – 8 seconds) and greatest in those applying 0.79 V/inch-20 Hz-2 ms operational protocol (mean, 12; 95% CI 4 – 20 seconds). There was no statistically significant differences in mean time to first response among the treatment groups ( $F_{17/288} = 1.0428$ ,  $P = 0.4114$ ). First responses were observed at field strengths from 0.01 to 0.33 ( $0.10 \pm 0.40$ ) V/cm (Figure 2 – 7). There was no statistical evidence that the mean threshold field strength for first response differed among the operational protocols ( $F_{17/288} = 0.9009446$ ,  $P = 0.5741$ ). Threshold cumulative exposure for first response was from 0.12 to 2853 ( $152 \pm 348$ )  $\mu\text{W}/\text{cm}^3 \cdot \text{s}$ . There was no statistical evidence that threshold cumulative exposure for first response differed significantly among the treatment groups, as indicated by ANOVA ( $F_{17/288} = 1.0997$ ,  $P = 0.3532$ ).

Flight responses were observed in 99% of fish in the simulations, occurring between 45 and 59 ( $52 \pm 2$ ) seconds into the exposures (Figure 2 – 7). There was strong statistical evidence that mean time to the onset of flight responses differed among the treatment groups ( $F_{17/126} = 2.840$ ,  $P < 0.0001$ ). Post hoc pair-wise comparisons demonstrated statistically significant differences in the mean time to onset of flight between fish in simulations applying

1.02 V/cm-30 Hz-2.5 ms ( $51 \pm 2$  seconds,  $P = 0.0005$ ) versus 0.79 V/cm-25 Hz-2.0 ms ( $52 \pm 3$  seconds),  
1.14 V/cm-30 Hz-2.0 ms ( $51 \pm 2$  seconds,  $P = 0.0106$ ) “  
1.14 V/cm-25 Hz-2.5 ms ( $51 \pm 2$  seconds,  $P = 0.0106$ ) “  
1.14 V/cm-20 Hz-2.0 ms ( $51 \pm 2$  seconds,  $P = 0.0336$ ) “

and between simulations applying 1.14 V/cm-30 Hz-2.5 ms versus 0.79 V/cm-30 Hz-2.5 ms ( $52 \pm 2$  seconds;  $P < 0.05$ ). The flight response occurred at field strengths of 0.16 to 0.76 ( $0.38 \pm 0.09$ ) volts/cm. There was no statistical evidence that the mean threshold field strength for flight differed among the

operational protocols ( $F_{17/338} = 1.3720$ ,  $P = 0.1476$ ). The threshold cumulative exposure for the flight response was 2156 to 6489 ( $2977 \pm 551$ )  $\mu\text{W}/\text{cm}^3\cdot\text{s}$ . There was strong statistical evidence of significant differences in the mean cumulative exposure threshold for flight among the operational protocols ( $F_{17/338} = 2.5909$ ,  $P = 0.0006$ ). Post hoc pair-wise comparisons indicated significant differences in mean cumulative exposure threshold for flight between fish exposed to the 0.79 V/cm-25 Hz-2.5 ms ( $2910 \pm 496$   $\mu\text{W}/\text{cm}^3\cdot\text{s}$ ) protocols compared to those exposed to the 1.02 V/cm-30 Hz-2.5 ms ( $2696 \pm 372$   $\mu\text{W}/\text{cm}^3\cdot\text{s}$ ,  $P = 0.0075$ ), the 1.02 V/cm-30 Hz-2.0 ms ( $2747 \pm 331$   $\mu\text{W}/\text{cm}^3\cdot\text{s}$ ,  $P = 0.0025$ ), the 1.02 V/cm-25 Hz-2.5 ms ( $2760 \pm 349$   $\mu\text{W}/\text{cm}^3\cdot\text{s}$ ,  $P = 0.0292$ ), and the 1.02 V/cm-20 Hz-2.0 ms ( $2774 \pm 310$   $\mu\text{W}/\text{cm}^3\cdot\text{s}$ ,  $P = 0.0391$ ) protocols.

Immobilization of fish was achieved in 74% of the simulations, occurring 49 to 78 ( $63 \pm 5$ ) seconds into the exposure (Figure 2 – 7). Fish immobilized in the simulations typically sank instead of floating. There was strong statistical evidence that mean time to immobilization differed among the treatment groups ( $F_{17/248} = 2.7182$ ,  $P = 0.0004$ ). Post hoc pair-wise comparisons showed significant differences in the mean time to immobilization of fish between simulations applying

1.02 V/cm-30 Hz-2.5 ms ( $60 \pm 1$  seconds;  $P = 0.0174$ ) versus 0.91 V/cm-20 Hz-2.5 ms ( $66 \pm 1$  seconds),  
1.02 V/cm-30 Hz-2.0 ms ( $59 \pm 1$  seconds;  $P = 0.0381$ ) versus “

and between simulations applying 0.79 V/cm-20 Hz-2.5 ms ( $66 \pm 2$  seconds) versus the 1.02 V/cm-30 Hz-2.5 ms protocol ( $P = 0.0253$ ). Immobilization occurred at field strengths from 0.28 to 1.02 ( $0.81 \pm 0.14$ ) volts/cm. In many cases, immobilization was induced on the falling (upstream) side of the high field (Figure 2 – 7). There was strong statistical evidence that the mean threshold field strength for immobilization differed among the operational protocols ( $F_{17/247} = 7.9845$ ,  $P < 0.0001$ ). Post hoc pair-wise comparisons of mean threshold field strength for immobilization indicated significant differences between numerous operational protocols (Table 2 – 1). Immobilization occurred at cumulative exposures between 2,398 and 24,005 ( $11,195 \pm 5,250$ )  $\mu\text{W}/\text{cm}^3\cdot\text{s}$ . There was strong statistical evidence that mean threshold cumulative exposure for immobilization differed among the operational protocols ( $F_{17/247} = 2.9059$ ,  $P = 0.0002$ ). Post hoc pair-wise comparisons demonstrated significant differences in mean threshold cumulative exposure for immobilization between simulations applying 0.79 V/cm-20 Hz-2.5 ms ( $14927 \pm 1567$   $\mu\text{W}/\text{cm}^3\cdot\text{s}$ ) compared to those applying 1.02 V/cm-30 Hz-2.0 ms ( $7622 \pm 1137$   $\mu\text{W}/\text{cm}^3\cdot\text{s}$ ;  $P = 0.0224$ ) and 1.02 V/cm-30 Hz-2.5 ms ( $7888 \pm 1108$   $\mu\text{W}/\text{cm}^3\cdot\text{s}$ ;  $P = 0.0319$ ) and between simulations applying 0.91 V/cm-20 Hz-2.5 ms ( $14487 \pm 1374$   $\mu\text{W}/\text{cm}^3\cdot\text{s}$ ) compared to those applying 1.02 V/cm-30 Hz-2.0 ms ( $P = 0.0173$ ) and 1.14 V/cm-30 Hz-2.5 ms ( $P = 0.0252$ ) protocols.

Righting occurred from 1 to 113 seconds after immobilization. The mean period of incapacitation was greatest in fish exposed to 1.02 V/cm-30 Hz-2.0 ms (47 seconds) and least in those exposed to 0.79 V/cm-20 Hz-2.0 ms (7 s), and differed significantly among the experimental groups:

1.02 V/cm-30 Hz-2.0 ms, 47 seconds,	1.02 V/cm-30 Hz -2.5 ms, 33 seconds,
1.02 V/cm-25 Hz-2.5 ms, 27 seconds,	0.91 V/cm-30 Hz-2.5 ms, 21 seconds,
0.79 V/cm-30 Hz-2.0 ms, 21 seconds,	0.91 V/cm-30 Hz-2.0 ms, 18 seconds,
1.02 V/cm-25 Hz-2.0 ms, 16 seconds,	0.91 V/cm-25 Hz-2.5 ms, 16 seconds,
1.02 V/cm-20 Hz-2.5 ms, 14 seconds,	0.91 V/cm-20 Hz-2.0 ms, 14 seconds,
0.79 V/cm-30 Hz-2.5 ms, 13 seconds,	0.91 V/cm-20 Hz-2.5 ms, 12 seconds,
0.79 V/cm-25 Hz-2.5 ms, 12 seconds,	0.91 V/cm-25 Hz-2.0 ms, 11 seconds,
1.02 V/cm-20 Hz-2.0 ms, 10 seconds,	0.79 V/cm-20 Hz-2.5 ms, 9 seconds,
0.79 V/cm-25 Hz-2.0 ms, 8 seconds,	0.79 V/cm-20 Hz-2.0 ms, 7 seconds,

as indicated by Welch’s ANOVA ( $F_{17/81} = 4.0852$ ,  $P < 0.0001$ ).

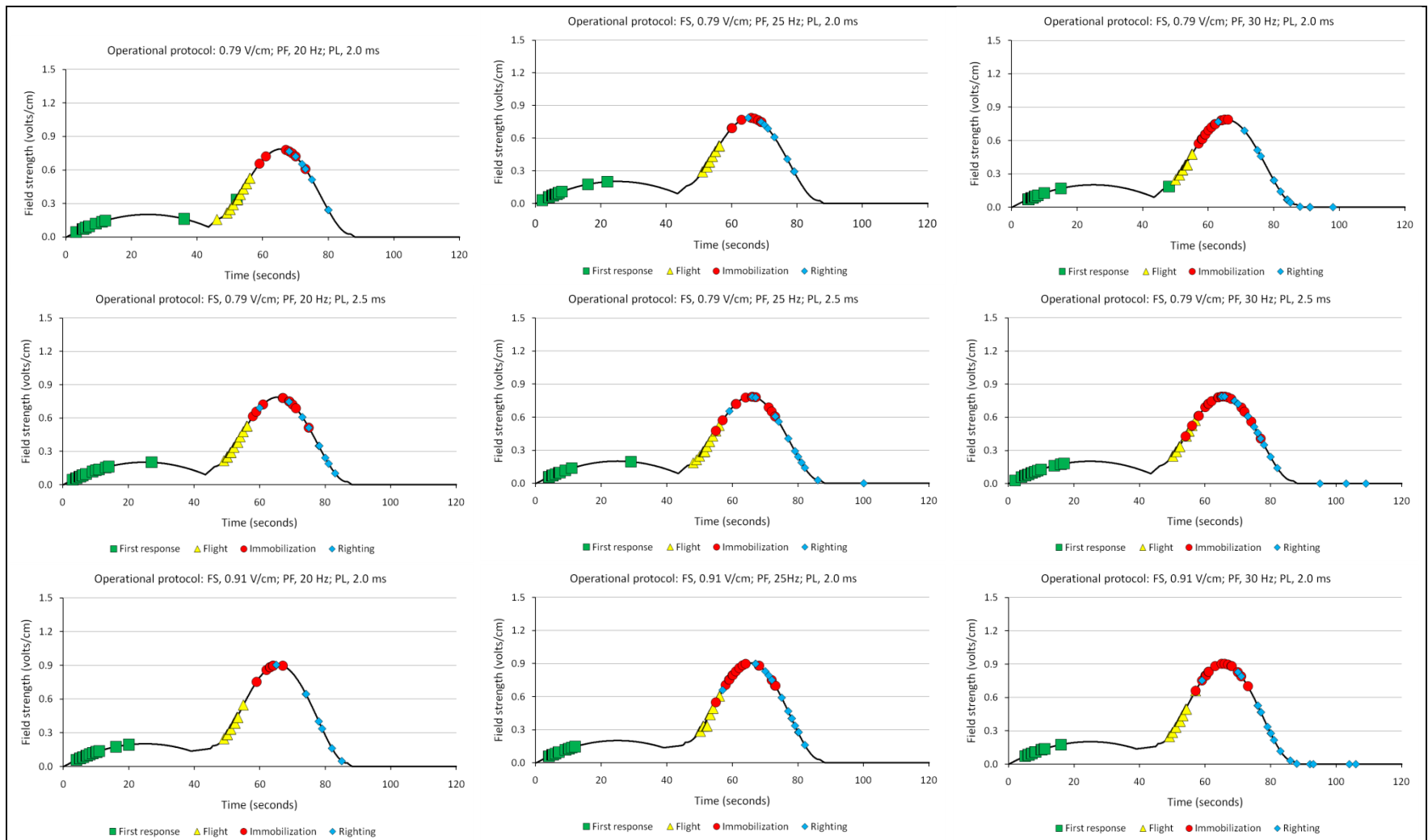


Figure 2 – 7 A. Thresholds of targeted responses in the simulations. Thresholds field strength (volts/inch) for the first response, flight, immobilization, and righting in the simulations of encroachment upon electric barrier IIA on the Chicago Sanitary and Ship Canal by small bighead carp. Data from a total of 360 simulations are represented in Figure 2 – 7 (A and B); 18 treatments (combinations of electrical parameters), 20 fish per treatment group. Simulations were conducted on fish individually using a completely randomized experimental design.

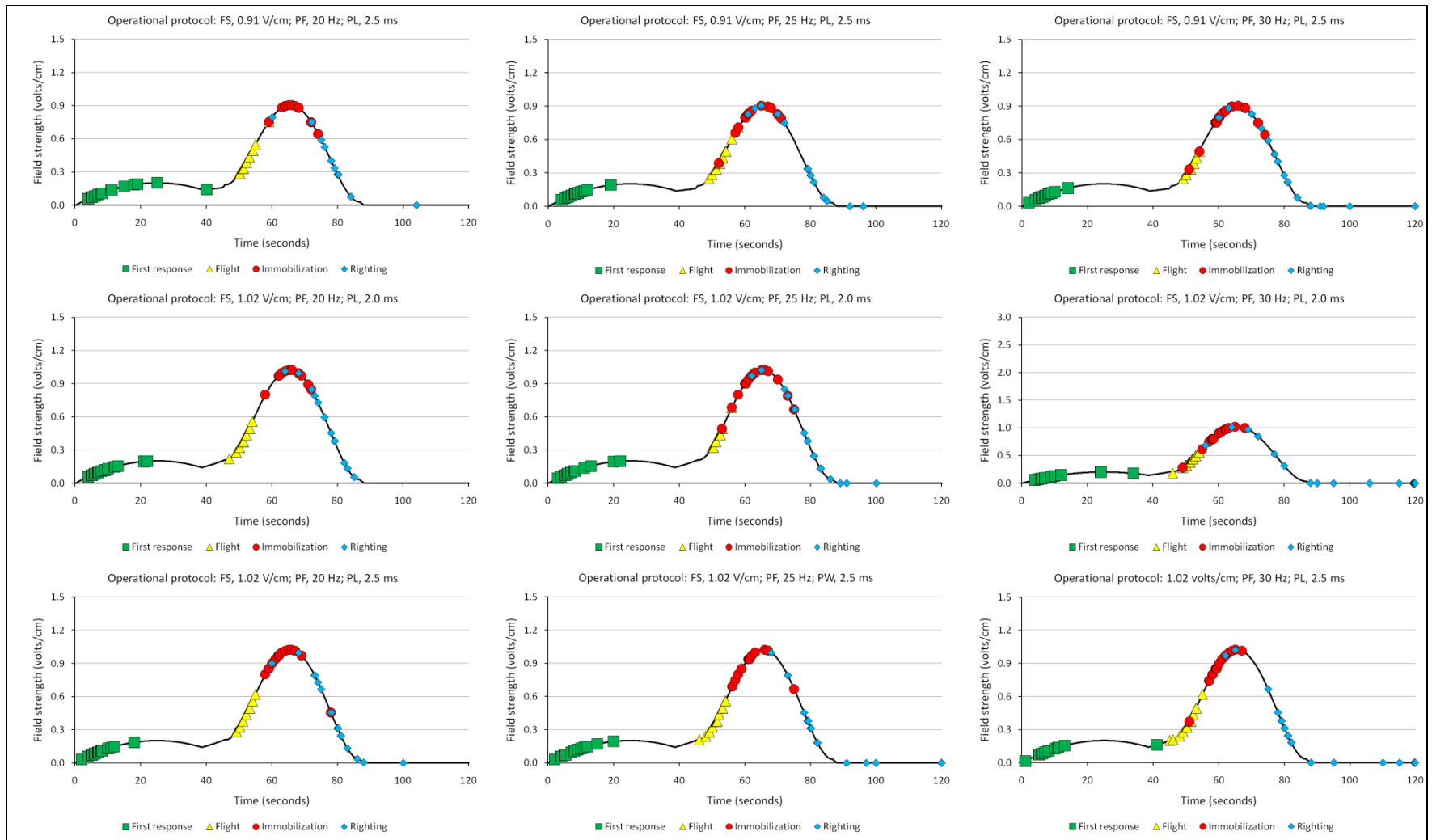


Figure 2 – 7 B. Thresholds of targeted responses in the simulations. Threshold field strength (volts/cm) for the first response, flight, immobilization, and righting in the simulations of encroachment upon electric barrier IIA on the CSSC by small bighead carp. Data from a total of 360 simulations are represented in Figure 2 – 7 (A and B); 18 treatment (combinations of electrical parameters), 20 fish per treatment group. Simulations were conducted on fish individually within a completely randomized experimental design.

Table 2 – 1. Mean threshold field strength (standard deviation in parentheses) for immobilization among the various operational protocols [ultimate field strength (V/cm), pulse-frequency (Hz), pulse-duration (ms)]. Statistically significant differences in pair-wise comparisons are indicated by levels not connected by same letter (P = 0.0002 – 0.0326).

Operational protocol			Mean (SD) threshold field strength for immobilization  (V/cm)	Levels not connected by the same letter indicates statistically significant difference in pairwise comparisons					
Ultimate field strength  (V/cm)	Pulse-frequency  (Hz)	Pulse-duration  (ms)							
1.02	20	2.0	0.96 (0.06)	A					
1.02	20	2.5	0.93 (0.08)	A	B				
1.02	25	2.5	0.88 (0.03)	A	B	C			
1.02	25	2.0	0.88 (0.10)	A	B	C			
0.91	20	2.0	0.86 (0.07)	A	B	C	D		
1.02	30	2.5	0.86 (0.12)	A	B	C			
0.91	20	2.5	0.85 (0.05)	A	B	C	D		
1.02	30	2.0	0.83 (0.08)	A	B	C	D		
0.91	30	2.0	0.81 (0.09)		B	C	D	E	
0.91	25	2.0	0.78 (0.12)			C	D	E	
0.91	25	2.5	0.77 (0.07)			C	D	E	
0.91	30	2.5	0.75 (0.14)			C	D	E	
0.79	25	2.0	0.74 (0.07)			C	D	E	
0.79	20	2.0	0.71 (0.13)			C	D	E	
0.79	30	2.0	0.70 (0.14)				D	E	
0.79	20	2.5	0.70 (0.12)				D	E	
0.79	25	2.5	0.70 (0.17)				D	E	
0.79	30	2.5	0.67 (0.14)					E	



Post hoc pair-wise comparisons indicated the mean period of incapacitation was significantly greater in fish immobilized in the simulations applying the 1.02 V/cm-30 Hz-2.0 ms protocol (47 s) versus simulations with the other protocols ( $P > 0.05$ ); the exception was simulations with the 1.02 V/cm-30 Hz -2.5 ms protocol (33 s) where there was no statistically significant difference ( $P > 0.05$ ).

Proportions of the experimental groups of fish that were immobilized in the simulations, in the margins of the contingency table, varied from 0.35 to 1.00 (Figure 2 – 8), differed significantly among levels of field strength:

0.79 V/cm, 0.59,  
0.91 V/cm, 0.74,  
1.02 V/cm, 0.88,

$\chi^2 = 26.463$ ,  $P = 0.0001$ ), among the pulse-rates:

20 Hz, 0.58,  
25 Hz, 0.72,  
30 Hz, 0.93,

$\chi^2 = 38.557$ ,  $P = 0.0001$ ), and between the two pulse-durations (2.0 ms, 0.67; 2.5 ms, 0.81;  $\chi^2 = 8.293$ ,  $P = 0.0040$ ).

Risk for failing to immobilize fish was significantly reduced by several of the operational protocols tested compared to the protocol effective for immobilizing small silver carp in the pilot study (Figure 2 – 9). Compared to the 0.79 V/cm-15 Hz-6.5 ms protocol shown effective for immobilizing small silver carp in the pilot study, relative risk for failing to immobilize small bighead carp was reduced in simulations applying:

0.79 V/cm-30 Hz-2.0 ms (RR, 0.42; 95% CI, 0.18 – 0.96),  
0.91 V/cm-25 Hz-2.0 ms (RR, 0.42; 95% CI, 0.18 – 0.96),  
0.91 V/cm-30 Hz-2.0 ms (RR, 0.17; 95% CI, 0.04 – 0.65),  
1.02 V/cm-25 Hz-2.0 ms (RR, 0.17; 95% CI, 0.04 – 0.65),  
1.02 V/cm-30 Hz-2.0 ms (RR, 0.08; 95% CI, 0.01 – 0.58),  
0.79 V/cm-30 Hz-2.5 ms (RR, 0.08; 95% CI, 0.01 – 0.58),  
0.91 V/cm-25 Hz-2.5 ms (RR, 0.33; 95% CI, 0.13 – 0.86),  
0.91 V/cm-30 Hz-2.5 ms (RR, 0.07, all fish immobilized),  
1.02 V/cm-20 Hz-2.5 ms (RR, 0.17; 95% CI 0.04 – 0.65),  
1.02 V/cm-25 Hz-2.5 ms (RR, 0.25; 95% CI 0.08 – 0.75),  
1.02 V/cm-30 Hz-2.5 ms (RR, 0.07, all fish immobilized)

(Figure 2 – 9).

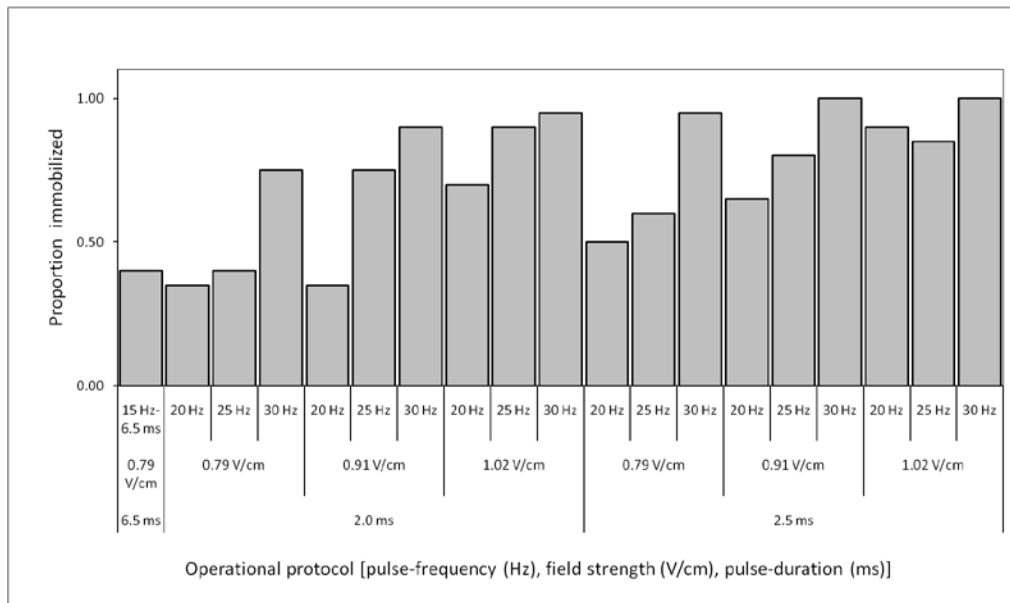


Figure 2 – 8. Proportions of fish immobilized in the simulations for predictive modeling. Proportions of fish in the immobilized during simulations of encroachment into Barrier IIA, on the Chicago Sanitary and Ship Canal, by small bighead carp, with various operational protocols. Operational protocols were characterized by ultimate field strength (V/cm), pulse-frequency (Hz) and pulse-duration (ms). Outcomes from simulations on 380 fish are represented, 20 fish per experimental group. The simulations of were conducted at the USACE, EL–ERDC, Vicksburg, MS.

Field strength (FS;  $P \leq 0.0001$ ), pulse-frequency (PF;  $P \leq 0.0001$ ), pulse-length (PL;  $P \leq 0.0001$ ), and fish length (L;  $P = 0.0043$ ) were each significant single predictors of immobilization in small bighead carp. Logistic regression demonstrated a multivariable relationship between field strength (FS), pulse-frequency (PF), pulse-length (PL), fish length (L), the pulse-length  $\times$  fish length (PL\*L) interaction, and probability of immobilization of small bighead carp. Goodness-of-Fit tests indicated that each model in the candidate set fit the data ( $\chi^2 = 308 - 343$ ; DF = 350 – 354;  $P = 0.60 - 0.95$ ). All models in the candidate set had excellent discrimination, as indicated by the area under the ROC curve (0.80 – 0.83). Nonetheless, there was strong support for the FS, PF, PL, L, PL\*L model as the best model presented by the  $\Delta_i$  and  $\omega_i$  (Table 2 – 2). Normalized Akaike weights ( $\omega_i$ ) indicated the FS, PF, PL, L, PL\*L model was about 3 times as likely as the next best (FS, PF, PL, L, PF\*PL) and about 5 times as likely as the third best model (FS, PF, PL, L; Table 2 – 2). Hence, the FS, PF, PL, L, PL\*L model was selected as the best of the candidate set. The model had an area under the ROC curve of 0.83, indicating excellent discriminatory ability.

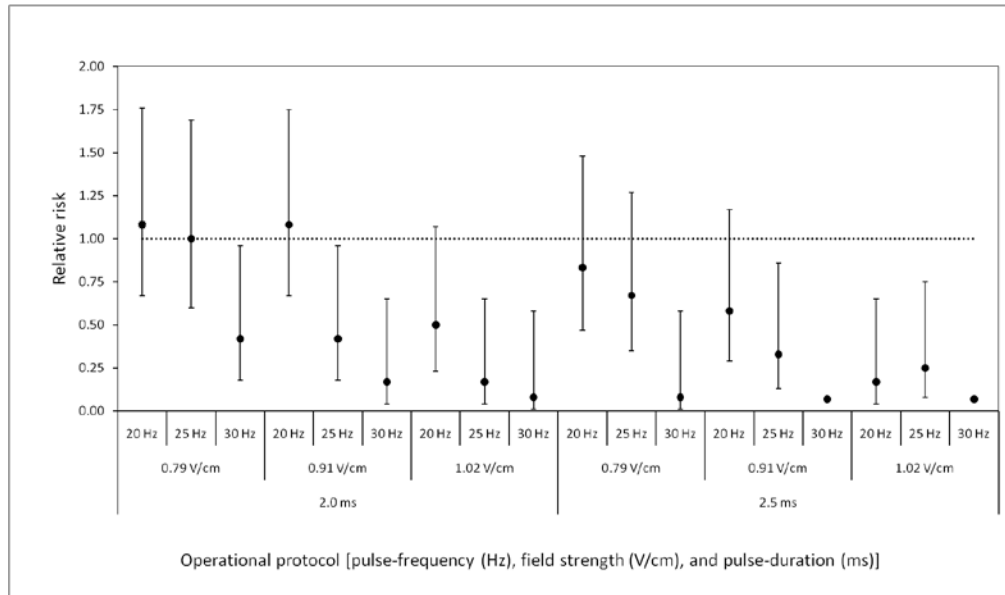


Figure 2 – 9. Relative risk of fish not being immobilized. Relative risk of small bighead not being immobilized during the simulations by various operational protocols compared to the operational protocol presently in use by Barriers on the Canal (FS: 0.79 V/cm; PF: 15 Hz; PL: 6.5 ms). Outcomes from simulations with 380 fish are represented, 20 fish per experimental group. The simulations were conducted at the USACE, EL-ERDC, Vicksburg, MS.

Field strength ( $\chi^2 = 27.02$ ; DF = 2;  $P < 0.0001$ ), pulse-frequency ( $\chi^2 = 54.35$ ; DF = 2;  $P < 0.0001$ ), pulse-length ( $\chi^2 = 9.46$ ; DF = 1;  $P = 0.0021$ ), and pulse-length\*fish length ( $\chi^2 = 5.40$ ; DF = 1;  $P = 0.0202$ ) were significant factors in the FS, PF, PL, L, PL\*L model. Statistical differences in levels of field strength were demonstrated in hypothesis tests. Specifically,

$$H_0: 0.79 \text{ volts/cm} = 0.91 \text{ volts/cm} (\chi^2 = 3.79; \text{DF} = 1; P = 0.0516),$$

$$H_0: 0.79 \text{ volts/cm} = 1.02 \text{ volts/cm} (\chi^2 = 26.81; \text{DF} = 1; P < 0.0001),$$

$$H_0: 0.91 \text{ volts/cm} = 1.02 \text{ volts/cm} (\chi^2 = 10.45; \text{DF} = 1; P = 0.0012).$$

Hypothesis tests demonstrated statistical differences between levels of pulse-frequency and pulse-length. Specifically,

$$H_0: 20 \text{ Hz} = 25 \text{ Hz} (\chi^2 = 6.54; \text{DF} = 1; P = 0.0106),$$

$$H_0: 20 \text{ Hz} = 30 \text{ Hz} (\chi^2 = 53.55; \text{DF} = 1; P < 0.0001),$$

$$H_0: 25 \text{ Hz} = 30 \text{ Hz} (\chi^2 = 23.72; \text{DF} = 1; P < 0.0001),$$

$$H_0: 2.0 \text{ ms} = 2.5 \text{ ms} (\chi^2 = 9.46; \text{DF} = 1; P = 0.0021).$$

The main effect of fish length was not statistically significant ( $\chi^2 = 1.92$ ; DF = 1;  $P = 0.1614$ ), but the PL\*L interaction was significant ( $\chi^2 = 5.40$ ; DF = 1;  $P = 0.0202$ ).

Table 2 – 2. Model selection. Akaike information criterion (AICc) values ( $\Delta_i$ ), normalized Akaike weights ( $\omega_i$ ), goodness-of-fit (GOF) P-values, and the area under the receiver operating characteristic (ROC) curve for prognostic models of electroshock-induced immobilization of small bighead carp, where FS = field strength, PF = pulse-frequency, PL = pulse-length, and L = total length.

Rank	Candidate models	$\Delta_i$	$\omega_i$	GOF ( <i>P</i> -value)	Area under ROC curve
1	FS, PF, PL, L, PL*L	0	0.54	0.88	0.83
2	FS, PF, PL, L, PF*PL	3	0.15	0.95	0.83
3	FS, PF, PL, L	3	0.10	0.92	0.83
4	FS, PF, PL, L, PF, L*L	4	0.09	0.91	0.83
5	FS, PF, PL, L, PF, L*L*L	5	0.04	0.92	0.83
6	FS, PF, PL, L, PF*L	6	0.03	0.95	0.83
7	FS, PF, PL, L, FS*L	7	0.02	0.92	0.83
8	FS, PF, PL, L, FS*PL	7	0.01	0.90	0.83
9	FS, PF, PL, L, FS*PF	9	0.01	0.89	0.83
10	FS, PF, PL	16	0.00	0.64	0.80
11	FS, PF, PL, PF*PL	16	0.00	0.72	0.80
12	FS, PF, PL, FS*PL	20	0.00	0.63	0.80
13	FS, PF, PL, FS*PF	22	0.00	0.60	0.80

Probability of immobilization predicted by the FS, PF, PL, L, PL\*L model varied widely among the operational protocols (Figure 2 – 10),

0.79 V/cm-20 Hz-2.0 ms (0.14 – 0.46),	0.79 V/cm-25 Hz-2.0 ms (0.34 – 0.52),
0.79 V/cm-30 Hz-2.0 ms (0.82 – 0.90),	0.91 V/cm-20 Hz-2.0 ms (0.33 – 0.54),
0.91 V/cm-25 Hz-2.0 ms (0.55 – 0.73),	0.91 V/cm-30 Hz-2.0 ms (0.83 – 0.93),
1.02 V/cm-20 Hz-2.0 ms (0.64 – 0.83),	1.02 V/cm-25 Hz-2.0 ms (0.78 – 0.87),
1.02 V/cm-30 Hz-2.0 ms (0.96 – 0.98),	0.79 V/cm-20 Hz-2.5 ms (0.23 – 0.95),
0.79 V/cm-25 Hz-2.5 ms (0.26 – 0.95),	0.79 V/cm-30 Hz-2.5 ms (0.74 – 1.00),
0.91 V/cm-20 Hz-2.5 ms (0.32 – 0.93),	0.91 V/cm-25 Hz-2.5 ms (0.50 – 0.99),
0.91 V/cm-30 Hz-2.5 ms (0.74 – 1.00),	1.02 V/cm-20 Hz-2.5 ms (0.73 – 0.94),
1.02 V/cm-25 Hz-2.5 ms (0.82 – 0.97),	1.02 V/cm-30 Hz -2.5 ms (0.97 – 0.99).

The combination of field strength, pulse-frequency, pulse-duration and the length of the bighead carp strongly influenced the probability of immobilization predicted by the model, meeting or exceeding 0.90 in fish having lengths:

- ≥ 71 mm (0.79 V/cm-30 Hz-2.0 ms),
- ≥ 53 mm (0.91 V/cm-30 Hz-2.0 ms),
- ≥ 51 mm (1.02 V/cm-30 Hz-2.0 ms),
- ≥ 69 mm (0.79 V/cm-20 Hz-2.5 ms),
- ≥ 64 mm (0.79 V/cm-25 Hz-2.5 ms),
- ≥ 56 mm (0.79 V/cm-30 Hz-2.5 ms),
- ≥ 64 mm (0.91 V/cm-20 Hz-2.5 ms),
- ≥ 61 mm (0.91 V/cm-25 Hz-2.5 ms),
- ≥ 51 mm (0.91 V/cm-30 Hz-2.5 ms),
- ≥ 61 mm (1.02 V/cm-20 Hz-2.5 ms),
- ≥ 53 mm (1.02 V/cm-25 Hz-2.5 ms),
- ≥ 51 mm (1.02 V/cm-30 Hz -2.5 ms; Figure 2 – 10).

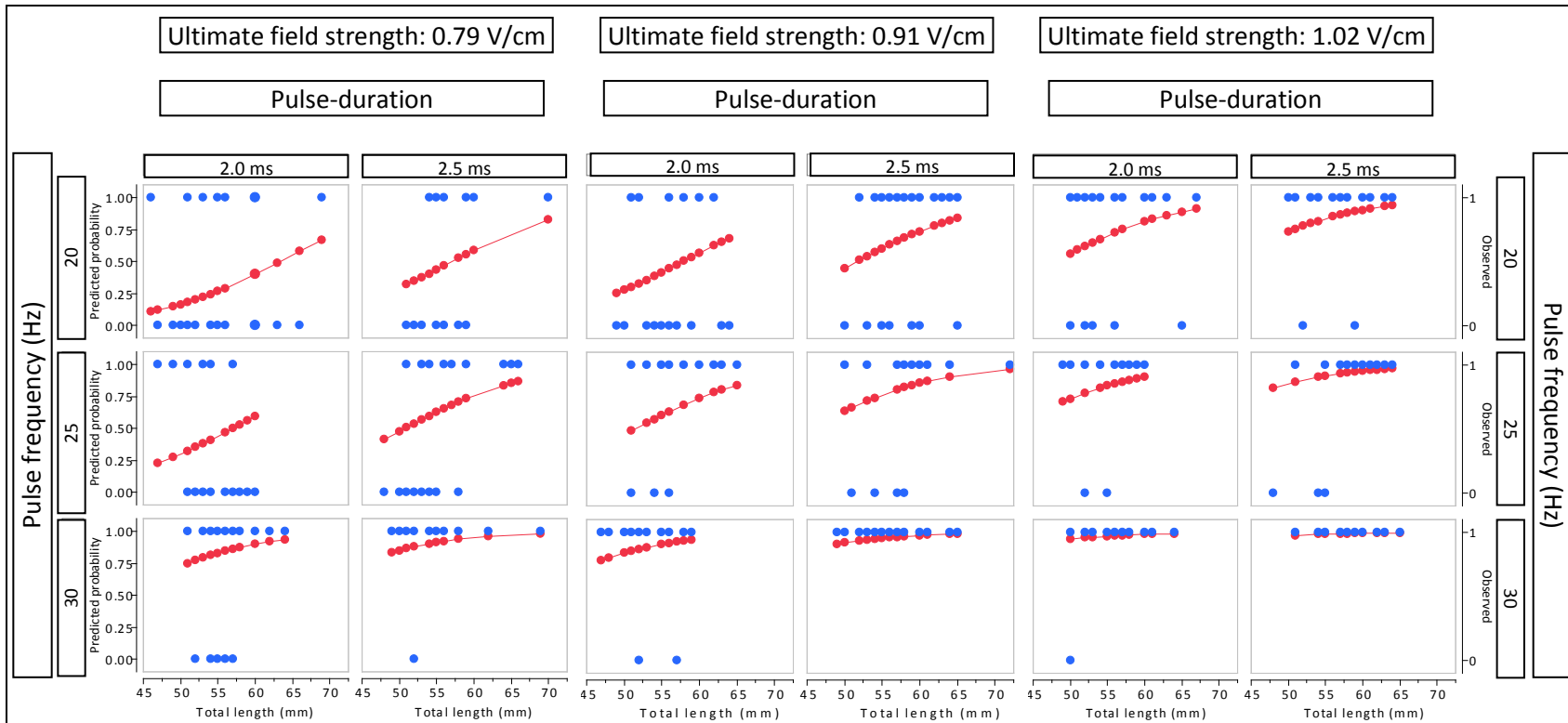


Figure 2 – 10. Occurrence and predicted probability of immobilization in 46 – 72 mm bighead carp. Probability of immobilization predicted by the FS, PF, PL, L, PL\*L prognostic model, which was developed from simulations of encroachment in the field of Barrier IIA by small bighead carp, are plotted in red, on the left axis. The occurrence of immobilization observed in the simulations (1 = immobilized, 0 = not immobilized) is plotted in blue, on the right axis. Data from a total of 360 simulations are represented; 18 treatments (combinations of electrical parameters; operational protocols) were evaluated using 20 fish per treatment group. Simulations were conducted on fish individually using a completely randomized experimental design. Outcomes are plotted as a function of fish length.

## Discussion

Simulations of encroachment into the field of electric Barrier IIA (on the Chicago Sanitary and Ship Canal) by small bighead carp were used to evaluate the effectiveness of various combinations of electrical parameters for inducing passage-preventing behaviors. The simulations were conducted under controlled conditions. Electrical stimulation in the simulations, which was based on measurements taken from the surface of the barrier fields on the CSSC, was continuous but varied in intensity over time to mimic the exposure fish swimming through the barrier field would experience. The simulations in the pilot study provided “snapshots” of expected fish behavior at discrete points in field of Barrier IIA. The simulations in the present study more closely resembled conditions in the barrier fields of the CSSC. The approach applied in the present study was a significant improvement over the pilot study and in the “state of the art” for research related to electrical exposure of fish. Subsequently, the quality of data collected and the inference of the experimental results improved. The scenario in the simulations employed various aspects of the conceptual risk model developed for barrier effectiveness. The simulations in the present study employed what was considered the worst-case scenario for preventing passage of invasive bighead carp and silver carp through the electric barriers, as (1) the fish encroaching upon the barrier were small, (2) the fish encroaching upon the electric barrier were swimming at the surface of the Canal, (3) fish penetrating the electric barrier continued upstream despite receiving electrical stimulus, (4) there was no water current flow or marginal flow, and, (5) fish swam through the electric barrier as quickly as possible (maximum swimming speed of 50 cm/s). The conditions in the scenario are directly or indirectly associated with components of the conceptual Risk Model of Barrier Effectiveness.

The present study targeted small fish. Although not directly tested, there was evidence to support the hypothesis that small fish represent the worst-case for inducing passage-preventing behaviors on the Canal. In the context of inducing capture-prone behaviors, fish reactions are dependent upon voltage drop per unit length of fish (Lamarque 1967; Halsband 1967). Higher field strengths may be required to induce paralysis in smaller fish. Lower frequencies may be less effective (than higher frequencies), requiring higher field strengths to induce paralysis (Edwards and Higgins 1973). Outcomes in the raceway experiments of Pegg and Chick (2004) demonstrated species or size dependent induction of passage-preventing behaviors when silver carp breached the electric field in the tests and bighead carp did not. The silver carp, in the study (by Pegg and Chick 2004), however, were only  $\frac{1}{4}$  the length of the bighead carp. Dolan and Miranda (2003) found, in a tank study, the effect of body size to overwhelm potential differences in species response to a given electrical stimulus. The differential effectiveness of the electric field for preventing passage between silver carp and bighead carp demonstrated in the work of Pegg and Chick (2004) was likely driven by differences in size between groups of fish rather than species differences. There is significant evidence that Barrier I (on the Canal) was effective on large common carp (Sparks et al. 2004; Dettmers and Creque 2004) when applying operational protocols having pulse-frequencies of 2 Hz, 3 Hz, and 5 Hz. In comparison, substantially greater field strength, pulse-frequency, and pulse-duration were necessary to immobilize 137 to 280 mm silver carp in the pilot study (Holliman, this report). The size range of silver carp in the pilot study encompassed the size of silver carp in the study of Pegg and Chick (2004). The present study targeted even smaller fish [bighead carp (51 – 76 mm)] as a worst-case, as effects are expected to be more pronounced in larger fish.

The patterns of field strength applied in the simulations were calibrated to fish swimming at the surface, which was assumed to represent a worst-case scenario for preventing fish passage. Fish swimming upstream at some depth will penetrate the barrier field to the extent possible. Models and in-water measurements of the electric barriers on the Canal demonstrate the strength of the field increases with

proximity to the electrodes; field strength is lowest at the surface. The extent of the upstream penetration of the field by fish swimming at depth will be determined by some threshold of *in vivo* electrical stimulation. If *in vivo* electrical stimulation is insufficient to induce a passage-preventing behavior, fish will breach the barrier. If of sufficient magnitude, *in vivo* electrical stimulation will induce a passage-preventing behavior and/or will lead fish to the surface.

It is hypothesized that the shape of the barrier field, demonstrated in the analysis and simulations of the electric field, will tend to guide fish toward the surface. *In vivo* thresholds for evoked behaviors correspond spatially to an equipotential boundary within the field (a boundary of field strength) extending across the Canal. It is hypothesized that fish motivated to swim upstream and similarly motivated to not to exceed some electrical threshold for *in vivo* stimulation will follow this equipotential boundary to the water surface. This expectation is based on anecdotal observation and experience, but no data is available to support it. The relation between field strength and fish size is the basis for expectations of differential penetration of the graduated electric barriers on the Chicago Sanitary and Ship Canal, by fish of different sizes. Fish swimming at the surface may penetrate more deeply into the field, as the strength of the electric barrier is least at the surface. Thus, fish swimming at or near the water surface is expected and is regarded as the worst case.

In the simulations, fish were assumed to continue upstream despite increasing electrical stimulation. With a graduated field, fish challenging the barrier will be exposed to increasingly unpleasant stimuli gradually and learn to avoid the stimuli (Hartley and Simpson 1967). However, fish excited by the electrical stimulation may continue into fields of higher intensity (Barwick and Miller 1996). The outcome reported by Barwick and Miller (1996) may have been an unintentional consequence of abrupt changes in field strength (based on descriptions of the electrode array), where fish unintentionally crossed boundaries in field strength and became excited by high levels of electrical stimulation that would have otherwise been avoided. Stewart (1990b) reported similar outcomes in tests with a marine barrier. Bullen and Carlson (2004) report that electric fields have limited potential as a deterrent to fish behavior as fish do not have the ability to detect the direction of an electric field source and will often swim into stronger fields, even to their death. Thus, it was prudent to assume, in the simulations, that fish would continue to swim upstream into the barrier despite noxious stimuli.

Volitional avoidance of the electric field was not addressed in the present study. If bighead carp and silver carp will avoid the increasingly unpleasant electrical stimuli associated with continued penetration of the electric barrier on the CSSC is not known. Further, if learning to avoid the electric field does occur, the threshold for noxious electrical stimulation associated with the learning is also not known. The threshold electrical exposure for avoidance would be below that for rendering fish physically incapable of progressing upstream, the desired outcome in the present study. If avoidance should prove a reliable passage-preventing response to electrical stimulation and the threshold is below that for incapacitation, Barrier electrical output could be reduced. The reduction in output could substantially reduce required electrical energy and equipment wear and increase the margin for human safety. Study of volitional avoidance of waterborne electric fields by the targeted species is warranted.

The simulations assumed the condition of no, or minimal, water current flow as worst-case scenarios. The electric barriers on the Canal utilize cross-channel electrodes. The direction of electric current flow is, therefore, parallel with the direction of water current flow. Fish oriented in the upstream-downstream direction experience the greatest electrical exposure (greatest body-voltage), being aligned parallel with the direction of electrical current flow. The scenario of no water flow in the simulations represents the worst-case scenario, as fish could minimize body-voltage (by turning perpendicular to the



direction of electric current flow, perpendicular to the upstream-downstream direction) during the exposures. This circumstance can occur on the Canal, where under conditions of no flow (or very low flow) fish penetrating the electric field to the extent of receiving unpleasant stimulation may turn perpendicular to the direction of electric current flow, along an equipotential line (Vibert 1967), without being swept downstream. Fish turning near perpendicular to the direction of electric current flow, but still directed slightly upstream, could continue to swim forward and breach the barrier if the electrical stimulus were insufficient to render fish incapable of forward progress. No water current flow or minimal flow velocity was used in the simulations to mimic this circumstance, where fish orientation to the direction of electric current flow was uncontrolled and fish could minimize body-voltage. Thus, the operational protocols effective in the simulations were proven so under the worst-case environmental scenario of no (very low) water current flow.

A minimum duration of exposure was assumed the worst-case scenario in the simulations. A direct relation between duration of exposure and probability of immobilization was hypothesized, where longer exposure periods would increase probability of immobilization and, conversely, shorter exposure periods would decrease probability of immobilization. The duration of the simulations (88 seconds), which influences cumulative exposure and rates of change in the field strength, were calibrated to the estimated maximum swimming speeds for 51 – 76 mm bighead carp and represent the estimated minimum duration of exposure on the Canal under the condition of no water current flow. A direct relation has been demonstrated between duration of exposure to pulsed DC and mortality in bluegill *Lepomis macrochirus* (90 to 170 mm length), fantail darters *Etheostoma flabellare* (25 mm to 75 mm length; Whaley et al. 1978) and Cape Fear shiners *Notropis mekistocholas* (25 – 65 mm length; Holliman et al. 2003), in the context of electrofishing. Sternin et al. (1976) notes that the reaction of an organism depends not only on the intensity of an action at an instant, but also on the overall volume of the stimulant. The cumulative effect of an electrical exposure may lead to changes in fish reaction or even gradual depression of the central nervous system. When the intensity of direct current is increased slowly, immobilization can be induced by the simultaneous effects of low gradient and cumulative exposure [e.g., narcosis sans the typical progression of fish reaction (i.e., perception/first response, taxis, pseudo-forced swimming, immobilization; Sheminsky 1924 in Sternin et al. 1976)]. Prel (1991) reported that the phenomenon of accommodation and cumulative effect strongly influences threshold values of fish response, with gradient for response decreasing with the total volume of stimulus. Although fish did react (first response) to the field strengths associated with the low-field (in the simulations), the relatively weak stimulus did not appear unpleasant, as fish did not appear to be in distress and swimming was unimpaired. Living organisms often adapt to weak stimuli (irritants), low gradients (Prel 1991).

Flight responses were consistently induced on the rising side of the high-field in the simulations. This region of the exposure is associated with rapidly increasing gradient. Given that fish showed little response to the low-field, the rising side of the high field, the region of rapidly increasing gradient may serve as equipotential boundaries to upstream penetration by small fish. If small fish penetrating the electric field tend to maintain position below this equipotential boundary, as has been reported in large fish at the barriers on the Canal, they will be continually exposed to weak (relative to gradients in the high-field) electrical stimuli. Based on the work of Prel (1991), exposure to the low field may increase susceptibility to electrical stimulus in the fish, increasing probability of immobilization when challenging the high field. According to Sternin et al. (1976), the cumulative effect of an electrical exposure may lead to changes in fish reaction or even gradual depression of the central nervous system. Thus, exposure to the low-field may predispose these smaller fish to immobilization by the high-field.

It is hypothesized that probability of immobilization increases with duration of exposure to low gradients. Additional study to test this hypothesis is warranted. The effects of cumulative exposure to low levels of electrical stimulation on the physiology and immobilization thresholds of fish are largely unknown. Investigation into the effects of low gradient exposure to electric fields is warranted. It is hypothesized that long term exposure to low gradient will act on the physiology of fish to increase susceptibility to increased electrical gradients. Similarly, investigation of effects on swim speed, in the context of increasing or decreasing durations of exposure, on immobilization thresholds is warranted.

In the experiment for predictive modeling, comparisons of threshold cumulative exposure (and time to onset) for flight demonstrated significant differences among the operational protocols. In general, threshold cumulative exposure for the flight responses were least when ultimate field strength was greatest (1.02 V/cm). Because ultimate field strength was reached at the same time in the patterns of the exposures regardless of ultimate field strength, the gradients were greater for the 1.02 V/cm exposures as compared to the patterns with lower ultimate field strengths. The reduction in cumulative exposure thresholds are believed to have resulted from the greater rates of increase, as the threshold for flight (based on time) was also least in protocols applying 1.02 V/cm, which is in accordance with the results of Prel (1991).

Measures of cumulative exposure may be more appropriate than field strength for comparisons of threshold response given the relatively long exposure times and heterogeneous nature of the patterns of exposure in the tests. Comparisons of thresholds for immobilization among the operational protocols demonstrated significant differences in time, field strength, and cumulative exposure. In general, time to threshold response and cumulative exposure for immobilization were least in protocols applying 1.02 V/cm ultimate field strength and pulse-frequency of 30 Hz. Comparisons of mean threshold field strength demonstrated protocols applying 0.79 V/cm often had significantly lower threshold for immobilization compared to protocols applying 1.02 V/cm. This outcome is misleading as immobilization was significantly less frequent with these protocols and often occurred on the falling size of the high field.

Outcomes in the present study support hypotheses that characteristics of waterborne electric fields influence probability of induction of passage-preventing behaviors in small bighead carp, supporting facets of the Conceptual Risk Model for Barrier Effectiveness. Pulse-frequency and field strength were demonstrated to be significant individual predictors of immobilization in the screening experiments. Similarly, field strength, pulse-frequency, and pulse-duration were significant individual predictors in the experiment for predictive modeling but the outcomes were best represented by the multivariable FS, PF, PL, L PL\*PL model. Based on the outcomes of the experiment, efficiency of the electric barriers on the Canal will be strongly influenced by the operational protocol employed (technical factors in the conceptual model).

Statistical significance was apparent among the levels of field-strength, pulse-frequency and pulse-duration in the prognostic FS, PF, PL, L, PL\*L model. There were direct relations between the proportions of fish immobilized and field strength, pulse-frequency, and pulse-duration. A strong dependence between probability of immobilization and fish length was also demonstrated. The size range was relatively small, fish were between 46 and 72 mm in length, but a statistically significant positive relation was evident between probability of immobilization and fish length. Holliman et al. (2003) found a similar relation between mortality and fish length in Cape Fear shiners of a similar size range (42 – 83 mm). The probability of immobilization of bighead 51 to 71 mm, predicted by the FS, PF, PL, L, PL\*L mode, was  $\geq 0.90$  depending upon the operational protocol applied.

The FS, PF, PL, L, PL\*L prognostic model was statistically superior to the other models evaluated and provides the best information available regarding the likelihood of immobilizing 46 – 72 ( $56 \pm 5$ ) mm bighead carp encroaching upon the field of Barrier IIA on the Chicago Sanitary and Ship Canal. It must be emphasized, however, that the model is based on simulations and relatively small sample sizes. The FS, PF, PL, L, PL\*L model was based on 20 fish per experimental cell (combination of experimental factors), a relatively small number of fish. This is especially important with regard to confidence intervals for point estimates of probability for immobilization. For example, in experimental cells where 100% of fish (20/20) were immobilized [FS: 1.02 V/cm; PF: 30 Hz, PL: 2.5 ms; FS: 0.91 V/cm, PF: 30 Hz, PL: 2.5 ms], the long term average percent of fish immobilized could be as low as 86% (this is the lower 95% confidence interval for a binary response, for the point estimate of 100% with  $N = 20$ ). Even though all of the fish were immobilized in some treatments larger sample sizes are needed to reduce the confidence interval about the point estimate. How large a sample size is determined by the level of confidence desired.

The sample size estimate is complicated by the objective of desiring immobilization in all fish (no failure to induce immobilization), which leads to non-events and a zero cell in the tables. Events can be rare or zero cells introduced into the analysis when goals for treatment effectiveness are reached. Application of the rule of three to the scenario of no failure to induce immobilization in the simulations indicates that when 100% of fish in an experimental cell are immobilized, the lower limit of the 95% CI would be 90% of fish immobilized with 30 fish/cell, 95% of fish immobilized with 60 fish/cell, 97% of fish immobilized with 100 fish/cell, and 99% of fish immobilized with 300 fish/cell (van Belle 2002). The experiment for predictive modeling was conducted with 20 fish per group x 20 groups = 400 fish. If a confidence interval of stopping 99/100 fish is desired, according to the rule three, 300 fish would have been needed per experimental group (6,000 fish total with 20 treatments evaluated). The number of fish required for full factorial experiment can become impractical when near certainty of an event is desired (in this case no failure to immobilize fish in the simulations). Extensive testing for reduction of confidence intervals can be conducted with the few treatments shown effective in the experiment conducted for predictive modeling. Field experimentation on the CSSC to confirm outcomes and model predictions is recommended.

Silver carp, bighead carp and common carp share the behavioral characteristics of swimming against the flow (Zhong 1990). There are numerous anecdotal reports of large fish at the water surface, apparently motivated to swim upstream, interacting with the low-field of electric barrier IIA, repeatedly penetrating the field and falling back. The pilot study completed April 2009 demonstrated an ultimate field strength of 0.79 V/cm, pulse-frequency of 15 Hz, 6.5 ms pulse-duration effective for immobilizing silver carp 137 to 279 ( $196 \pm 36$ ) mm total length. The operational protocol is presently used by Barrier IIA on the Canal. If the single bighead carp discovered in the Canal (3 December 2009, ~ 556 mm bighead carp collected during a rotenone event; Illinois Department of Natural Resources) interacted with the electric barrier is not known. Based on the outcomes from the pilot study, it is expected that passage of the fish would have been deterred by Barrier IIA, as the fish collected from the Canal was 2 to 4 times the length of fish used in the pilot experiment. Additional study is warranted for verification of the FS, PF, PL, L, PL\*L model and refinement of predictions.

Several of the operational protocols applied in the simulations reduced the risk for failure to immobilize small bighead carp compared to the protocol presently in use on the Canal,

0.79 V/cm-30 Hz-2.0 ms (RR, 0.42; 95% CI, 0.18 – 0.96),  
0.91 V/cm-25 Hz-2.0 ms (RR, 0.42; 95% CI, 0.18 – 0.96),  
0.91 V/cm-30 Hz-2.0 ms (RR, 0.17; 95% CI, 0.04 – 0.65),  
1.02 V/cm-25 Hz-2.0 ms (RR, 0.17; 95% CI, 0.04 – 0.65),

1.02 V/cm-30 Hz-2.0 ms (RR, 0.08; 95% CI, 0.01 – 0.58),  
0.79 V/cm-30 Hz-2.5 ms (RR, 0.08; 95% CI, 0.01 – 0.58),  
0.91 V/cm-25 Hz-2.5 ms (RR, 0.33; 95% CI, 0.13 – 0.86),  
0.91 V/cm-30 Hz-2.5 ms (RR, 0.07, all fish immobilized),  
1.02 V/cm-20 Hz-2.5 ms (RR, 0.17; 95% CI 0.04 – 0.65),  
1.02 V/cm-25 Hz-2.5 ms (RR, 0.25; 95% CI 0.08 – 0.75),  
1.02 V/cm-30 Hz-2.5 ms (RR, 0.07, all fish immobilized).

In general, risk for failing to incapacitate bighead carp in the simulations was reduced with operational protocols employing pulse-frequencies of 25 or 30 Hz. Overall, operational protocols applying DC pulsed at 15 Hz (or less) were relatively unsuccessful in immobilizing small bighead carp. Rates of immobilization ranged from 0.30 to 0.55 in simulations applying 15 Hz pulsed DC; in the screening experiment, (0.55 was achieved at an ultimate field strength of 1.5 V/cm). Rates of immobilization with operational protocols applying 10 Hz pulse-frequency were even lower. Thus, operational protocols applying 10 and 15 Hz were excluded from the experiment for predictive modeling, as they were demonstrated ineffective.

The simulations serving as the baseline in the post hoc comparisons of risk, from the experiment for predictive modeling, were conducted as precursors to later research on the effects of water current flow on the efficiency of the electric barriers. The combined rate of immobilization was 0.40 in these simulations with the operational protocol presently in use on the Canal (FS: 0.79 V/cm, PF: 15 Hz: PL: 6.5 ms). Because three of these simulations were conducted with water flow rates of 5 cm/s or 10 cm/s, which were greater the rate used in the other simulations (3 cm/s), immobilization rates in these simulations may be greater than if the simulations had been conducted at 3 cm/s. Thus, post hoc estimates of RR may be underestimated. Further, the experiment for predictive modeling was conducted on individual fish and the simulations serving as the baseline was conducted on groups of fish. Thus, there is potential for behavioral differences between fish exposed in groups versus those exposed as individuals. If these behavioral differences influence rates of immobilization is unknown, but the combined rate of immobilization in the baseline groups was very similar to the rates of immobilization associated with 15 Hz operational protocols in the screening experiments (which were conducted with flow at 0 cm/s).

Outcomes in the present study provide support for inclusion of fish size as a biological factor in the conceptual Risk Model for Barrier Effectiveness. Similarly, support for inclusion of field strength, pulse-frequency, and pulse-duration as technical factors in the model was shown. An inverse relation was demonstrated between risk for failing to immobilize encroaching fish and fish size and a multivariable relation was demonstrated between the factors defining the waterborne field and risk for breaching the barrier.

Verification of FS, PF, PL, L, PL\*L model, as individual factors if necessary, and other components of the conceptual Risk Model for Barrier Effectiveness, on the Canal, is recommended. Development of a widely available, innocuous, surrogate species, or suite of species, though comparative testing under controlled conditions, for evaluation, calibration, and verification of Barrier performance on the Canal would be prudent.

## Work cited

- Agresti, A. 1990. *Categorical Data Analysis*. A Wiley-Interscience Publication, John Wiley & Sons, New York.
- Barwick, D. H, and L. E. Miller. 1996. Effectiveness of an electric barrier in blocking fish movement. *Proceedings of the Annual Conference of the SouthEastern Association of Fish and Wildlife Agencies*, 50: 139-147.
- Bird D. J. and I.G. Cowx. 1993. The selection of suitable pulsed currents for electric fishing in freshwater. *Fisheries Research*, 18: 363-376.
- Biwas, K. P. and S. P. Karmarkar. 1979. Effect of electric stimulation on heart beat and body muscle in fish. *Fisheries Technology*, 16: 91-99.
- Brown, M. B. and A. B. Forsythe. 1974. The small sample behavior of some statistics which test the equality of several means. *Technometrics*, 16: 129-132.
- Buckland, S. T., K. P. Burnham and N. H. Augustin. 1997. Model selection: an integral part of inference. *Biometrics*, 53:602-618.
- Bullen, C.R. and T.J. Carlson. 2004. Non-physical fish barrier systems: their development and potential applications to marine ranching. *Reviews in Fish Biology and Fisheries*, 13: 201 -211.
- Burnham, K. P. and D. R. Anderson. 1998. *Model Selection and Inference: A Practical Information-Theoretic Approach*. Springer-Verlag, New York.
- Dettmers, J. M. and S. M. Creque. 2004. Field assessment of an electric dispersal barrier to protect sport fishes from invasive exotic fishes. *Annual Report to the Division of Fisheries, Illinois Department of Natural Resources, Illinois Natural History Survey, Center for Aquatic Ecology and Conservation*.
- Dolan C. R. and L. E. Miranda. 2003. Immobilization thresholds of electrofishing relative to fish size. *Transactions of the American Fisheries Society*, 132: 969-976.
- Edwards J. L. and J. D. Higgins. 1973. The effects of electric currents on fish. *Engineering Experiment Station, Georgia Institute of Technology, Atlanta*. Rep. B-397, B-400, and E-200-301.
- Franklin, A. B., T. M. Shenk, D. R. Anderson and K. P. Burnham. 2001. Statistical model selection: an alternative to null hypothesis testing. Pages 75 – 90 in T.M. Shenk and A.B. Franklin, editors. *Modeling in natural resources management: development, interpretation and application*. Island Press, Washington D.C.
- Halsband E. 1967. Basic principles of electrofishing. Pages 57–64 in R. Vibert, editor. *Fishing with Electricity - Its Applications to Biology and Management*. Fishing News Books, Blackwell Scientific Publications Ltd., Oxford, England.
- Hartley, W. G. and D. Simpson. 1967. Electric fish screens in the United Kingdom. Pages 183-201 in R. Vibert, editor. *Fishing with Electricity - Its Applications to Biology and Management*. London, England: Fishing News Books.

- Hosmer, D. W. and S. Lemeshow. 2000. Applied Logistic Regression. A Wiley-Interscience Publication, John Wiley & Sons, Inc. New York.
- Holliman, F. M. 1998. A field and laboratory investigation of the effectiveness of electrical parameter combinations for capturing cichlids. Master's thesis. North Carolina State University, Raleigh.
- Holliman, F. M. and J. B. Reynolds. 2002. Electroshock-induced injury in juvenile white sturgeon. North American Journal of Fisheries Management, 22: 494-499.
- Holliman, F. M., J. B. Reynolds and T. J. Kwak. 2003. A predictive risk model for electroshock-induced mortality of the endangered Cape Fear shiner. North American Journal of Fisheries Management, 23: 905-912.
- Illinois Department of Natural Resources. "Bighead Asian Carp Found in Chicago Sanitary and Ship Canal". 2009. <<http://www.asiancarp.org/rapidresponse/documents/AsiancarpfoundinCSSC.pdf>
- Johnson, I. K., W. R. C. Beaumont and J. S. Welton. 1990. The use of electric fish screens in the Hampshire Test and Itchen, England. Pages 256 – 265 in I.G. Cowx , editor. Developments in Electric Fishing. London, England: Fishing News Books.
- Johnston, K. C., A. F. Conners, Jr., D. P. Wagner, W. A. Knaus, X. Q. Wang, and E. C. Haley, Jr. 2000. A predictive risk model for outcomes of ischemic stroke. Stroke, 31: 448-455.
- Kolar, C. S., D. C. Chapman, W. R. Courtenay, C. M. Housel, J. D. Williams, and D. P. Jennings. 2005. Asian carps of the genus *Hypophthalmichthys* (Pisces, Cyprinidae) – A biological synopsis and environmental risk assessment. Report to U.S. Fish and Wildlife Service 94400-3-012 LaCrosse, Wisconsin.
- Kolz A. L. 1989. A power transfer theory for electrofishing. U.S. Fish and Wildlife Service Fish and Wildlife Technical Report, 22: 1-11.
- Lamarque P. 1967. Electrophysiology of fish subject to the action of an electric field. Pages 65-92 in R. Vibert, editor. Fishing with Electricity - Its Applications to Biology and Management. Fishing News Books, Blackwell Scientific Publications Ltd., Oxford, England.
- Liu, Q.. 1990 Development of the Model SC-3 Alternating Current Scan Fish Driving Device. Pages 46-50 in I.G. Cowx, editor. Developments in Electric Fishing. Fishing News Books, London.
- Lui, Q., Wu D., Xu R. and J. Li. 1990. A method of improving fish efficiency in lakes by using a seine net with pulsed current. Pages 41-45 in I. G. Cowx, editor. Developments in Electric Fishing. FishingNews Books, London.
- McMillan, F. O. 1928. Electric fish screen. Bureau of Fisheries Bulletin, 44: 97-128.
- Miranda, L. E. and C. R. Dolan. 2003. Test of a power transfer model for standardized electrofishing. Transactions of the American Fisheries Society, 132: 1179-1185.
- Pegg M. A. and J. H. Chick. 2004. Aquatic nuisance species: an evaluation of barriers for preventing the spread of bighead and silver carp to the Great Lakes. Final Report, Illinois-Indiana Sea Grant.
- Prel, E. T. 1991. Effect of voltage gradient in an electrical field on threshold indices of fish response. Acta Ichthyologica et Piscatoria, 21: 37 – 44.

- Reynolds, J. B. 1996. Electrofishing. Pages 221-253 in B. R. Murphy and D. W. Willis, editors. Fisheries techniques, 2nd edition. American Fisheries Society, Bethesda, Maryland.
- Sall, J., Lee C. and A. Lehman. 2007. JMP® Start Statistics: A guide to statistics and data analysis using JMP®, fourth edition. Cary NC; SAS Institute Inc.
- SAS 2008. JMP® Statistics and graphics guide, Volumes 1 and 2. Cary, NC: SAS Institute Inc.
- SAS 2009. JMP, Version 8. SAS Institute Inc., Cary, NC, 1989-2009.
- Seidel W. R. and E. F. Klima. 1974. In situ experiments with coastal pelagic fishes to establish design criterion for electrical fish harvesting systems. NOAA Fish Bulletin, 72: 657-669.
- Sparks R., J. Dettmers and T. Barkley. 2004. Assessment of an electric barrier to prevent the dispersal of aquatic nuisance fishes. Final Report to the Great Lakes Protection Fund.
- Stewart, P. A. M. 1990a. Electric screens and guides. In I. G. Cowx and P. Lamaque, editors, Fishing with Electricity – Applications in Freshwater Fisheries Management. London, England: Fishing News Books.
- Stewart, P. A. M. 1990b. Electric barriers for marine fish. In I. G. Cowx, editors, Developments in Electric Fishing (pp. 243-255). London, England: Fishing News Books.
- Stainbrook, K., S. Creque and J. Dettmers. 2005. Field assessment of an electric dispersal barrier to protect sport fishes from invasive exotic fishes. Annual Report to the Division of Fisheries, Illinois Department of Natural Resources, Illinois Natural History Survey, Center for Aquatic Ecology and Conservation.
- Taylor, G. N., L. S. Cole, and W. F. Sigler. 1957. Galvanotaxic response of fish to pulsating direct current. Journal of Wildlife Management, 21: 201-213.
- van Belle, G. 2002. Statistical Rules of Thumb. A Wiley-Interscience Publication, John Wiley & Sons, New York.
- Vibert, R. 1967. General report of the working party on the applications of electricity to inland fishery biology and management. Pages 3 – 51 in R. Vibert, editor. Fishing with Electricity: Its Application to Biology and Management. Fishing News Books, Ltd., London.
- Whaley, R. A., O. E. Maughan and P. H. Wiley. 1978. Lethality of electroshock to two freshwater fishes. The Progressive Fish-Culturist, 40: 161-163.
- Zalewski ,M. and I. G. Cowx. 1990. Factors affecting the efficiency of electric fishing. Pages 89-111 in IG Cowx and P Lamarque, editors. Fishing with Electricity, Applications in Freshwater Fisheries Management. Fishing News Books, Oxford, England.
- Zhong, W. G. 1990. Model LD-1 electric fishing screen in reservoir fisheries in China. Pages 297 – 305 in I.G. Cowx, editor. Developments in Electric Fishing. Fishing News Books, Blackwell Scientific Publications Ltd., Oxford, England.

### 3 – Evaluation of Effects of Water Conductivity on Barrier Effectiveness

---

Summary.—Water electrical conductivity (the inverse of electrical resistivity) is a measure of the net motion of charged ions present. Measures of water conductivity are temperature dependent. Specific conductivity reflects ion content of water as thermal effects on the measure are removed. Ambient water conductivity, the water conductivity at the ambient temperature, more closely reflects electrical conductivity. The electrical conductivity of water (the ability of the water to conduct electricity) in the Chicago Sanitary and Ship Canal influences electrical power output by the electric barriers and transfer of electrical energy from water to fish; when conductivity of water in the Canal increases power demand increases and the efficiency of electric energy transfer from waterborne field to flesh of fish decreases. Analysis of specific water conductivity measures collected near the barriers October 1998 – April 2010, showed specific conductivity of water in the CSSC was 489 to 4697  $\mu\text{S}/\text{cm}$  over the period. Variation in specific conductivity was seasonal, ranging between 3049 and 4697  $\mu\text{S}/\text{cm}$  from December to March and from 489 to 1940  $\mu\text{S}/\text{cm}$  the rest of the year. Estimates of water ambient conductivity (via conversion of specific measures at Lockport Lock and Dam) ranged between 388 and 2551 ( $852 \pm 261$ ; 95% CI 843 – 862)  $\mu\text{S}/\text{cm}$ . Mean ambient conductivity varied significantly among months of the year, with a seasonal fluctuation evident. Mean ambient conductivity was greatest in February and least in September. The FS, PF, PL, L, PL\*PL model (described previously) was developed from simulations (electrical exposures) to fish in water of 2,000  $\mu\text{S}/\text{cm}$ . An experiment evaluating effects of water conductivity on the effectiveness of the barrier for immobilizing small bighead carp [42 – 72 mm (1.7 – 2.8 inches) total length] was conducted October – November 2009. Fish effective conductivity ( $c_f$ ) was estimated to be 90  $\mu\text{S}/\text{cm}$  via threshold power-density methodology. Simulations of encroachment, conducted on individual fish (20 fish per experimental group), in water of 100, 150, 500, 1000, 2000, and 4,000  $\mu\text{S}/\text{cm}$  ambient conductivity, targeted first response, flight, and immobilization. From 80 to 100% of fish in the experimental groups were immobilized during exposure to an operational protocol of FS: 0.79 – 0.91 V/cm, PF: 30 Hz, PL: 2 ms, in the simulations. The operational protocol employed in the simulations, in water of various conductivity, was shown effective in the screening experiment, which was conducted in water of 1,000  $\mu\text{S}/\text{cm}$ , and was shown relatively effective in the experiment for prognostic modeling (described earlier), which was conducted with water of 2,000  $\mu\text{S}/\text{cm}$ . Outcomes of electrical exposures (simulations) indicate that effectiveness of Barrier IIA will be relatively constant with operational protocols applying 0.79 – 0.91 V/cm ultimate field strength, pulse-frequency of 30 Hz, and pulse-duration of 2 ms in water of conductivity from 100 to 4000  $\mu\text{S}/\text{cm}$ . Verification of the experiment outcomes on the Canal, under field conditions is recommended.

---

#### Introduction

Simulations of outcomes of encroachment upon the electric barriers by small bighead carp demonstrate the likelihood of immobilizing small bighead carp is strongly influenced by the characteristics and magnitude of the waterborne electric field (Holliman, this report). Ultimately, it is the characteristics and magnitude of electric current that is introduced into the flesh of fish, however, that determines whether passage-preventing behaviors are induced. The efficiency of this transfer of electrical energy from the water transmitting the electric field to the flesh of fish immersed within the waterborne electric field is determined by the mismatch in abilities to conduct electricity between the two mediums.



Water electrical conductivity (the inverse of electrical resistivity) is a measure of the net motion of the charged ions present. Measures of water conductivity are temperature dependent. Specific conductivity, conductivity adjusted to a temperature of 25°C, which reflects the ion content of water as thermal effects on the measure are removed, is typically reported. Ambient water conductivity, the water conductivity at the ambient temperature, reflects electrical conductivity and determines the electrical “load” experienced by the Barrier power systems.

The fluctuations in the conductivity of water in the Canal are important to the operation of the barrier in the context of the electrical load experienced by the power system (i.e., power demand) and in the mismatch in conductivity between water and fish. The power system for the barrier is a constant voltage system. As such, the system automatically compensates for the changes in electrical load (water conductivity) by changing the electrical current output to maintain output voltage, within the power limits of the system. Whether additional compensation in the electrical output of the barrier, beyond the automatic compensation by the power system, will be necessary to overcome mismatches in conductivity between water and fish and maintain the effectiveness electric barrier at inducing passage-preventing behaviors in the targeted fishes is a concern.

The Power Transfer Theorem shows that transfer of electrical signals is maximized under conditions of matched resistance (inverse of conductance) between electrical source and load. Kolz (1989) applied the Power Transfer Theorem to electrofishing (i.e., the use of electricity for capture of wild fish), developing a mathematical model for calculating electrical energy transfer from waterborne electric field to fish. Instrumentation to quantify the conductivity of water ( $c_w$ ) is widely available. The determination of conductivity of live fish during an electrical exposure is, however, problematic (Kolz 2006). The estimation of the “effective” conductivity of fish ( $c_f$ ), which is based on patterns of thresholds for behavioral responses to electrical exposures, is more tractable.

Behavioral response of fish to electrical exposure can be employed as an indirect measure of *in vivo* power achieved in a fish (Kolz 1989, Kolz 2006). The energy levels in waterborne electric fields associated with thresholds for behavioral responses of fish have been shown to vary in accordance with the concepts of Power Transfer Theory (Kolz 1989, Kolz and Reynolds 1989, Miranda and Dolan 2003, Bearlin et al. 2008). Because fish behavioral responses reflect levels of *in vivo* power, similar responses can be expected from fish though the aquatic environment may vary. Hence, the threshold-response relationship is useful for inference of laboratory results for field operations.

Effective conductivity has been estimated for a few sizes and species of fish. Based on thresholds for immediate induction of immobilization, fish effective conductivity point estimates for 60 – 90 mm goldfish *Carassius auratus* varied with the characteristics of the electric current (DC, 83  $\mu\text{S}/\text{cm}$ ; AC, 156  $\mu\text{S}/\text{cm}$ ; 50 Hz pulsed DC of 2, 5 and 10 ms pulse-duration, 145  $\mu\text{S}/\text{cm}$ , 160  $\mu\text{S}/\text{cm}$ , and 137  $\mu\text{S}/\text{cm}$ ; Kolz and Reynolds 1989). Estimates of fish effective conductivity of 270 – 350 mm channel catfish *Ictalurus punctatus* immobilized by 3-second exposures to DC or 1 ms pulses of DC at 15, 20, 30, 60 or 110 Hz, ranged from 89 to 138  $\mu\text{S}/\text{cm}$  (Miranda and Dolan 2003). Effective conductivity estimates for Murray cod *Maccullochella peelii peelii* exposed to 4 ms pulses of DC at 60 Hz for 3 seconds varied with targeted response (escape, 65  $\mu\text{S}/\text{cm}$ ; forced swimming, 78  $\mu\text{S}/\text{cm}$ ; immobilization, 80  $\mu\text{S}/\text{cm}$ ; narcosis, 46  $\mu\text{S}/\text{cm}$ ). Threshold voltage gradients for flight in bighead carp and silver carp exposed to 50 Hz AC, in water of various conductivity (Liu 1990), conformed to power transfer theory, resulting in point estimates for fish effective conductivity of 56  $\mu\text{S}/\text{cm}$  and 96  $\mu\text{S}/\text{cm}$  (Dolan and Miranda 2003). Threshold voltage gradients for forced swimming in 30 cm eels, reported by Lamarque (1967), and for first response in trout, reported by Sternin et al. (1976) conform to power transfer theory. Analysis of this

data for this report provides an effective conductivity estimate of 76  $\mu\text{S}/\text{cm}$  for eels and 100  $\mu\text{S}/\text{cm}$  for trout.

Comparison of previous estimates of fish effective conductivity, for various species, with measures of water conductivity in the Canal indicate that a significant mismatch in the conductivity between the two mediums is likely; the effective conductivity of fish encroaching upon the electric barrier will be considerably less than the conductivity of the water transmitting the electric field. The goal of this phase of the study was to determine operational protocols for the electric barriers to maintain efficiency at inducing passage-preventing behaviors in small bighead carp in water having various levels of conductivity. Specific objectives were to (1) evaluate water conductivity levels in the CSSC, (2) estimate fish effective conductivity  $c_f$  and threshold levels of transferred power density ( $D_m$ ) for small bighead carp, (3) estimate fish effective conductivity ( $c_f$ ) and threshold levels of transferred electrical energy in small bighead carp based on cumulative exposure ( $D_m \cdot s$ ), and (4) relate these factors to operation of the barriers on the Chicago Sanitary and Ship Canal.

## Methods

Water specific conductivity and temperature measures from the Chicago Sanitary and Ship Canal were evaluated. The electric barriers are located at river mile 296.1 on the Chicago Sanitary and Ship Canal. Data from water quality monitoring stations on the CSSC, upstream of the barriers at Romeoville Road and Route 83 (river miles 296.2 and 304.7) and downstream at Lockport Lock and Dam (river mile 291.0), taken periodically from October 1998 to April 2010, by the Metropolitan Water Reclamation District, were analyzed. Because ambient water conductivity more closely reflects electrical conductivity and electrical “load” experienced by the power systems of the electric barriers on the Canal, estimates of ambient conductivity were desired. A dataset of water temperature collected at Lockport Lock and Dam was combined with specific conductivity measures from the same location to estimate ambient conductivity. Hourly measures of specific conductivity were converted to a daily mean, providing a total of 3,108 daily values of water conductivity and temperature (from August 1998 through March 2008) in the dataset. Daily measures of water temperature were converted from Fahrenheit ( $^{\circ}\text{F}$ ) to Celsius ( $^{\circ}\text{C}$ ) with  $(^{\circ}\text{F} - 32) \times 5/9 = ^{\circ}\text{C}$ . Ambient conductivity ( $c_a$ ) was estimated as  $c_a = c_s[1 + 0.0191(T - 25)]$  where  $c_s$  is specific conductivity ( $\mu\text{S}/\text{cm}$ ) corrected to 25 $^{\circ}\text{C}$  (provided by most metering systems) and  $T$  is water temperature ( $^{\circ}\text{C}$ ; APHA et al. 1985).

The distributions of conductivity and temperature measures were examined, by month, with box-and-whisker plots. The box-and-whisker plots demonstrated the 25<sup>th</sup> and 75<sup>th</sup> quartiles (ends of the boxes), the interquartile range (IQR; the distance between the box ends), the median (line across the interior of the box), and the outer-most data points falling within 1.5 x IQR (the whiskers extending outward from the ends of the boxes; Sall et al. 2007). Means, standard deviations, and maximum and minimum measures were reported for each location. Analysis of Variance (ANOVA) was used to test for differences in mean specific conductivity among the locations and for differences in mean ambient conductivity and temperature at the Lockport Lock and Dam among months. The Brown-Forsythe test was used to test statistical hypotheses of homogeneity of variance (Brown and Forsythe 1974; SAS 2008). Welch’s ANOVA was employed if there was statistical evidence that the variance differed among the groups of interest. Tukey’s Honestly Significant Difference test was used in post hoc pair-wise comparisons when evidence of unequal means was provided by ANOVA (SAS 2008).

Two independent experiments were conducted at the Army Corp of Engineers (USACE), Aquatic and Ecosystem Research and Development Center, Environmental Laboratory, Engineer Research and

Development Center (EL-ERDC), Vicksburg, Mississippi from 6 October 2010 to 9 November 2009. Pond-cultured bighead carp were used in the study. Fish were transported to the host facility via hatchery vehicle and held in closed, water re-circulating systems (Figure 3 – 1) for a minimum of one week after transport, prior to being used in the experiment.

Electrical exposures were applied in one of two non-conductive tanks, depending on the experiment. Threshold power density levels for targeted responses were determined with exposures applied in a 61 cm x 22 cm x 32 cm glass tank. Cumulative exposure thresholds were determined with exposures applied in a 170 cm x 45 cm x 51 cm fiberglass tank. Electric fields uniform in the cross-section with linear changes in voltage gradient (E) along their lengths (Holliman and Reynolds 2002) were generated by applying electrical energy to stainless steel, plate electrodes, fitted to the inner dimensions of the exposure tanks and positioned parallel. The electrodes were covered with a non-conductive plastic mesh to protect from fish from contact with the electrodes. Pulsed DC electric fields were generated within the tanks using the electric field simulation system or a programmable power supply. A calibrated digital oscilloscope connected to the electrodes was used to confirm and monitor the electrical characteristics of the treatments.

All of the electrical exposures were applied to naïve bighead carp individually. Fish were exposed to 2 ms pulses of DC, cycling at 30 Hz, a pulse frequency-pulse duration combination shown effective for inducing passage-preventing behaviors in prior simulations of encroachment into the field of Electric Barrier IIA by small bighead carp (Holliman, this report). The exposures were applied in well water (ambient conductivity ~ 250  $\mu\text{S}/\text{cm}$ ) after de-ionization or application of Instant Ocean® to achieve levels of ambient conductivity of approximately 20, 40, 100, 150, 500, 1000, 2000, and 4000  $\mu\text{S}/\text{cm}$ . The order in which the levels of conductivity were tested was random. Appropriate numbers of fish were acclimated to water of each targeted level of conductivity for a minimum of 3 days prior to use in the experiment. Each fish was immersed in an overdose solution of MS-222 immediately after completion of the electrical exposures. Measures of total length (mm) and weight were collected on each fish.

The behaviors of the fish during the electrical exposures were monitored. Targeted responses in the power-density-threshold-response experiment were first response, forced swimming with loss of equilibrium, and immobilization. Targeted responses in the cumulative exposure experiment were first response, flight, and immobilization. First response (the initial reaction to the presence of an electric field) typically included startle, rapid start, distinctive twitches of the head or tail, or brushing the body against the side or bottom of the tank. Forced swimming with loss of equilibrium was characterized by short-stroke, rapid tail-beat, ineffectual swimming accompanied by loss-of-equilibrium. Flight was characterized as the onset of rapid (frantic) non-directed swimming, and often included fish swimming from side-to-side in the tank (minimizing “body-voltage”). The flight response often transitioned into forced swimming while righted or forced-swimming accompanied by loss-of-equilibrium. Immobilization (tetany) was characterized by a complete cessation of swimming motions and was typically accompanied by loss-of-equilibrium.

Power density thresholds for first response, forced swimming, and immobilization were determined with electrical exposures lasting only long enough to ascertain fish response. The temperature of water



Figure 3 – 1. Closed water recirculating systems. Pond cultured small bighead carp were held closed, water-recirculating systems at the US Army Corp of Engineers, Aquatic Ecosystem Research Development Center, Environmental Laboratory, Engineer Research Development Center (EL-ERDC), Vicksburg, Mississippi prior to being used in the study. The experiments evaluating effects of water conductivity variation on electric barrier operation on the Chicago Sanitary Ship Canal was conducted 6 October to 9 November 2009.

in the tank was between 20.0 and 22.4 ( $21.6 \pm 1.4$ ) °C. An incremental process was employed to determine the onset (threshold) of the targeted responses, where fish were incrementally exposed to various levels of field strength to discover the threshold of the targeted responses. The number of exposures was limited to avoid fatigue in the exposed fishes. The strength of the electric field [(voltage gradient, E, (volts/cm)] associated with the onset of first response and forced swimming with loss-of-equilibrium or first response and immobilization were determined for each fish. A total of 50 fish were used at each of the levels of water conductivity in the power density threshold tests.

Simulations of encroachment upon electric Barrier IIA were employed to establish cumulative exposure thresholds for first response, flight, and immobilization. The temperature of water in the tank was 19.4 to 20.6 ( $19.8 \pm 0.5$ ) C. The strength of the electric field was varied over time to simulate the electrical exposure experienced by fish traversing the field of Electric Barrier IIA, at the surface of the canal (Figure 3 – 2). The range of field strength associated with the “low-field” was consistent among the treatments. The ultimate field strength, the peak of the high-field, was varied between 0.79 V/cm and 1.5 V/cm, depending on water conductivity.

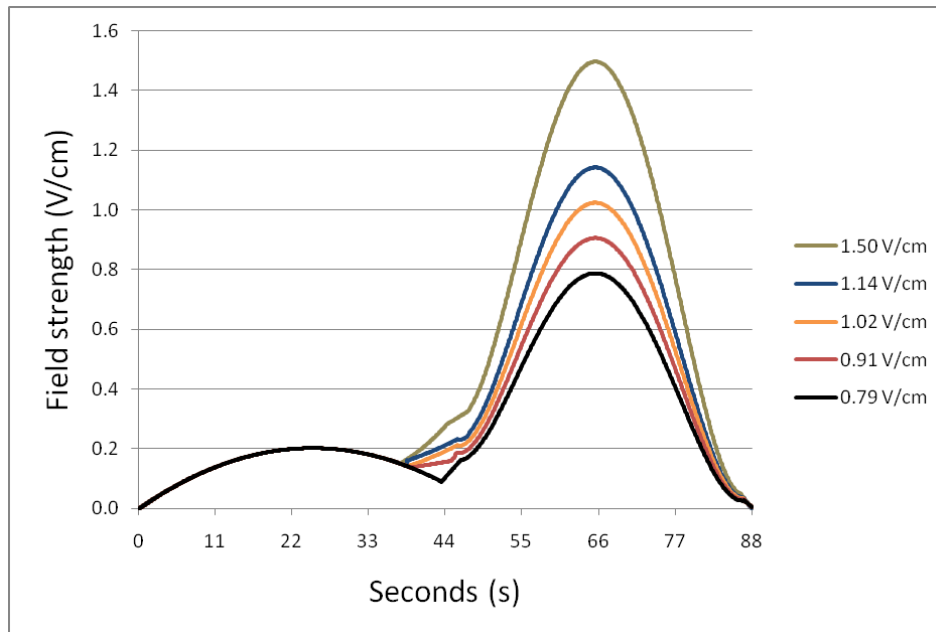


Figure 3 – 2. Electric field in the simulations. The electric field strength varied with time in the simulations of encroachment into Barrier IIA under various conditions of water conductivity in the Canal. The exposures simulated the electrical signal of Barrier IIA, at the surface of the Chicago Sanitary Ship Canal. Patterns of electric field strength associated with simulations applying ultimate field strengths of 0.79, 0.91, 1.02, 1.14, and 1.50 V/cm are shown. The strength of the electric field in the simulations varied with time (seconds). The exposures were 88 seconds in duration, an exposure period calibrated to encroachment upon the electric field at a constant rate of 50 cm/s.

Maximum sustained swimming speeds of bighead carp was 20 cm/s in swim tests on individuals and 40 cm/s in swim tests on groups of 3 or 5 fish. Bighead carp from the cohort typically swam 50 cm/s for less than 1 minute, although some high performers in groups did swim longer periods (personal communication, Dr. Jack Killgore, Dr. Jan Hoover, USACE, Environmental Laboratory –Engineer Research Development Center, Vicksburg, Mississippi). The exposure period was calibrated to a swimming speed of 50 cm/s, simulations of 88 seconds duration, an exposure thought to be the worst-case, as duration of exposure was minimized. An external timer was used to estimate exposure time at the onset of targeted behaviors, which was then used to estimate threshold voltage gradient (V/cm), threshold power density ( $\mu\text{W}/\text{cm}^3$ ) and threshold cumulative electrical energy ( $\mu\text{W}/\text{cm}^3 \cdot \text{s}$ ).

A total of 20 fish were used at each of the water conductivity levels in the simulations. Previous testing had been conducted with the 30 Hz, 2 ms operational protocol in water with conductivity of 1000  $\mu\text{S}/\text{cm}$  (Holliman, this report), these data were included in this analysis, and the trial was not repeated.

Applied power density ( $D_a$ ,  $\mu\text{W}/\text{cm}^3$ ) associated with the onset of targeted behaviors was estimated for each fish using,  $D_a = E^2 \cdot c_w$ , where  $E$  was the threshold voltage gradient (V/cm) and  $c_w$  was the ambient conductivity of the water in the test tank. Threshold cumulative exposure for the targeted behaviors ( $D_a \cdot s$ ,  $\mu\text{W}/\text{cm}^3 \cdot \text{s}$ ) in the simulations was estimated by summing the products of discrete

power density ( $D_a$ ,  $\mu\text{W}/\text{cm}^3$ ) levels and time intervals from the beginning of the exposure to the onset of the targeted behavior. The exposures were divided into 1024 discrete intervals of time and field strength for the calculations.

Threshold values of applied power density  $D_a$  were fitted by the non-linear least-squares method against the theoretical curves for maximum power transfer:  $D_a = D_m[1/2 + 1/4(c_f/c_w + c_w/c_f)]$ , where  $D_m$  was the threshold *in vivo* power density and  $c_f$  = fish effective conductivity (Kolz and Reynolds 1990). The equation was solved iteratively to achieve the best fit for estimation of parameters for  $D_a$  and  $c_f$  (with 95% or 90% confidence intervals). Similarly, threshold cumulative exposures ( $D_a \cdot s$ ) for targeted responses in the simulations were fit to the theoretical curve for maximum power transfer to estimate  $D_m \cdot s$ , the *in vivo* cumulative exposure for the flight response and  $c_f$ . Theoretical curves for maximum power transfer were also fit to threshold  $D_a \cdot s$  values for immobilization (from the simulations of encroachment) using values of  $c_f$  estimated in the power-density-threshold-response experiment, to estimate  $D_m \cdot s$  and to evaluate model fit with the various  $c_f$ . Model goodness-of-fit was quantified with the  $R^2$  statistic (Kvålseth 1985), calculated as:  $R^2 = 1 - \sum_i (y_i - \hat{y}) / (y_i - \bar{y})$ , where  $y_i$  was the logarithm of threshold electrical energy,  $\hat{y}$  was the predicted electrical energy, and  $\bar{y}$  was the arithmetic mean of all  $y_i$ .

The multiplier for constant power (MCP; Kolz 1989) was calculated with  $MCP = (1 + c_f/c_w) / (4 c_w/c_f)$ , using estimates of  $c_f$  for forced-swimming (with loss of equilibrium) and immobilization from the power-density-threshold-response experiment. The intersection of the MCP distributions for the two values of  $c_f$  was used to estimate the  $c_f$  roughly splitting the difference between the curves (Miranda and Dolan 2003). The MCP was provided for specific water conductivity between 400 and 4,000  $\mu\text{S}/\text{cm}$  and water temperatures from 5 to 35 °C. Statistical analyses and model fitting were accomplished using JMP statistical software, Version 8 (SAS 2009).

## Results

There were a total of 220,719 measures of specific conductivity in the dataset, taken at the three locations August 1998 through April 2010. Measures taken at river mile 296.2 (Romeoville Road) were limited to August 1998 to April 2004 and April 2008 to November 2008. The overall mean specific conductivity was 1,026  $\mu\text{S}/\text{cm}$ . Mean specific conductivity varied significantly among the three sites, as indicated by Welch's ANOVA ( $F_{2/220717} = 396$ ,  $P \leq 0.0001$ ). The differences in mean conductivity were statistically significant between each of the sites (Lockport Lock and Dam, 1056  $\mu\text{S}/\text{cm}$  > Romeoville Road, 1010  $\mu\text{S}/\text{cm}$  > Route 83, 1000  $\mu\text{S}/\text{cm}$ ;  $P \leq 0.05$ ). Marked monthly variation was apparent in the distributions of specific water conductivity at each of the locations (Figure 3 – 3). Water specific conductivity was 380 to 3697  $\mu\text{S}/\text{cm}$  at Lockport Lock and Dam monitoring station, 424 to 3588 at the Romeoville Road station, and 388 to 4697 at the Route 83 station. Examination of distributions of specific water conductivity measures by month demonstrates marked seasonal variation, with extreme (outlier) measures of conductivity occurring December, January, February, and March, at each of the locations.

Water temperature at the Lockport Lock and Dam ranged from 0.5 to 31.1 °C ( $17.5 \pm 6.9$ ; 95% CI 17.2 – 17.7) °C [33 to 88 ( $63 \pm 12$ ; 95% CI 63.02 – 63.9 °F)]. Mean temperature varied significantly among the months, as indicated by Welch's ANOVA ( $F_{11/1334} = 1769$ ,  $P \leq 0.0001$ ). Seasonal variation was apparent in the water temperatures, with higher temperatures occurring June through September (Figure 3 – 4). Pairwise comparisons of mean temperature between months demonstrated mean temperature was

greatest in August and July ( $P < 0.05$ ), and least in February and January ( $P < 0.05$ ), compared to each of the other months:

August 26.4 °C,	June 22.9 °C,	November 16.8 °C,	March 10.5 °C,
July 25.8 °C,	October 20.7 °C,	April 14.8 °C,	February 9.0 °C,
September 24.8 °C,	May 18.3 °C,	December 11.9 °C,	January 9.0 °C.

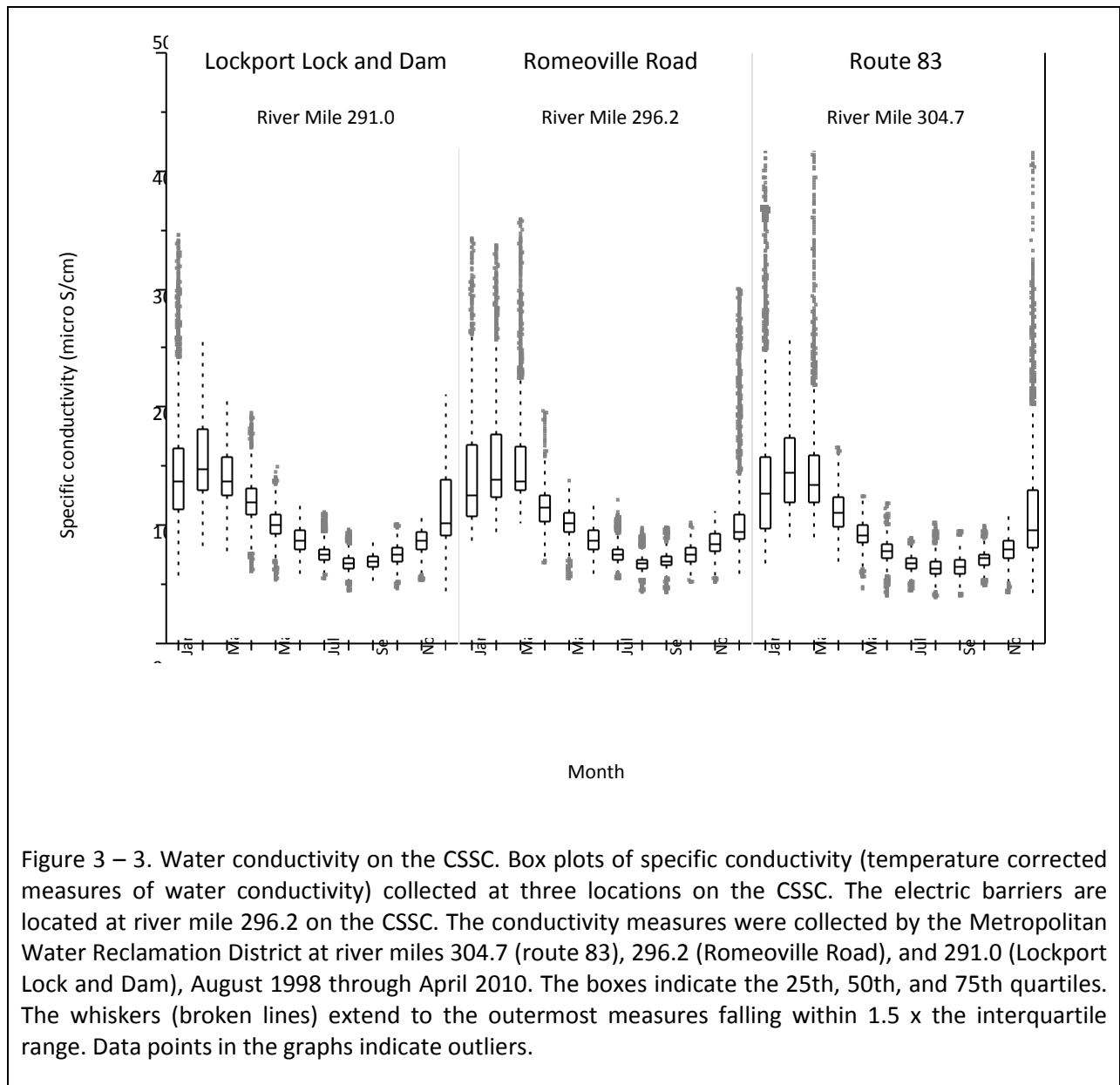


Figure 3 – 3. Water conductivity on the CSSC. Box plots of specific conductivity (temperature corrected measures of water conductivity) collected at three locations on the CSSC. The electric barriers are located at river mile 296.2 on the CSSC. The conductivity measures were collected by the Metropolitan Water Reclamation District at river miles 304.7 (route 83), 296.2 (Romeoville Road), and 291.0 (Lockport Lock and Dam), August 1998 through April 2010. The boxes indicate the 25th, 50th, and 75th quartiles. The whiskers (broken lines) extend to the outermost measures falling within 1.5 x the interquartile range. Data points in the graphs indicate outliers.

Estimates of water ambient conductivity at Lockport Lock and Dam ranged between 388 and 2551 ( $852 \pm 261$ ; 95% CI 843 – 862)  $\mu\text{S}/\text{cm}$ . Mean ambient conductivity varied significantly among the months, as indicated by Welch's ANOVA ( $F_{11/1206} = 196$ ,  $P \leq 0.0001$ ). The seasonal fluctuation evident in measures of specific conductivity were evident in the estimates of ambient conductivity, but the extremes were greatly reduced (Figure 3 – 4). Pairwise comparisons revealed that mean ambient conductivity differed significantly between most months, but was greatest in February and least in September (Table 3 – 1).

Threshold power density estimates for the various responses were collected on a total of 400 bighead carp. The fish were 42 to 71 (mean  $\pm$  standard deviation;  $53 \pm 5$ ) mm total length, weighing 0.3 to 2.9 ( $1.2 \pm 0.4$ ) grams. Thresholds for the behavioral responses varied in accordance with power transfer theory. Estimates of bighead carp effective conductivity and transferred power density varied with behavioral response. Based on the threshold power density for first response,  $c_f$  was estimated to be 39 (95% CI, -7 – 69; 90% CI 3 - 64)  $\mu\text{S}/\text{cm}$  and  $D_m$  was estimated to be 0.68 (95% CI -0.13 – 1.18; 90% CI, 0.05 – 1.11)  $\mu\text{W}/\text{cm}^3$ . Based on the estimates of threshold power density for forced swimming with loss of equilibrium,  $c_f$  was estimated to be 95 (95% CI, 60 – 135)  $\mu\text{S}/\text{cm}$  with  $D_m$  estimated to be 112 (95% CI, 87 – 112)  $\mu\text{W}/\text{cm}^3$ . Based on estimates of threshold power density for immobilization,  $c_f$  of small bighead carp was estimated to be 84 (95% CI, 66 – 100)  $\mu\text{S}/\text{cm}$  and  $D_m$  was estimated to be 166 (95% CI, 133-195)  $\mu\text{W}/\text{cm}^3$  (Figure 3 – 5). The  $R^2$  statistics for the models fit to the threshold power density data were 0.84 for first response, 0.88 for pseudo-forced swimming, and 0.90 for immobilization.

In all, 160 fish were used in simulations of fish challenging the electric barrier under various conditions of water conductivity. Fish in these simulations were 42 to 72 ( $54 \pm 5$ ) mm total length, weighing from 0.6 to 2.9 ( $1.3 \pm 0.4$ ) grams. First response was recorded for 83% of fish used in the simulations. Flight responses were recorded in 95% of fish used in the simulations. Immobilization was induced in 66% of fish used in the simulations (Figure 3 – 6). The incidence of immobilization varied from 0.00 to 1.00, among the water conductivity levels (23  $\mu\text{S}/\text{cm}$ , 0.00; 43  $\mu\text{S}/\text{cm}$ , 0.00; 97  $\mu\text{S}/\text{cm}$ , 0.90; 151  $\mu\text{S}/\text{cm}$ , 0.90; 530  $\mu\text{S}/\text{cm}$ , 0.85; 986  $\mu\text{S}/\text{cm}$ , 1.00; 1965  $\mu\text{S}/\text{cm}$ , 0.90; 4049  $\mu\text{S}/\text{cm}$ , 0.80).

The threshold for first responses varied markedly in the simulations, occurring from one to 54 seconds leading to outliers in the data distributions (Figure 3 – 6). The variability in the threshold power density and cumulative exposure for first response (in the simulations) strongly influenced the fit of model. The model fit to threshold power density estimates failed to converge, preventing estimation of model parameters, until outliers from the 4000  $\mu\text{S}/\text{cm}$  exposures were removed. The fit of the power transfer curve to the threshold cumulative exposure data was very poor ( $R^2 = 0.27$ ), as reflected in the confidence intervals of estimated  $c_f$  (90% CI, -126 – 108)  $\mu\text{S}/\text{cm}$  and transferred power  $D_m \cdot s = 27.6$  (90% CI -110 – 80)  $\mu\text{W}/\text{cm}^3 \cdot \text{s}$ .



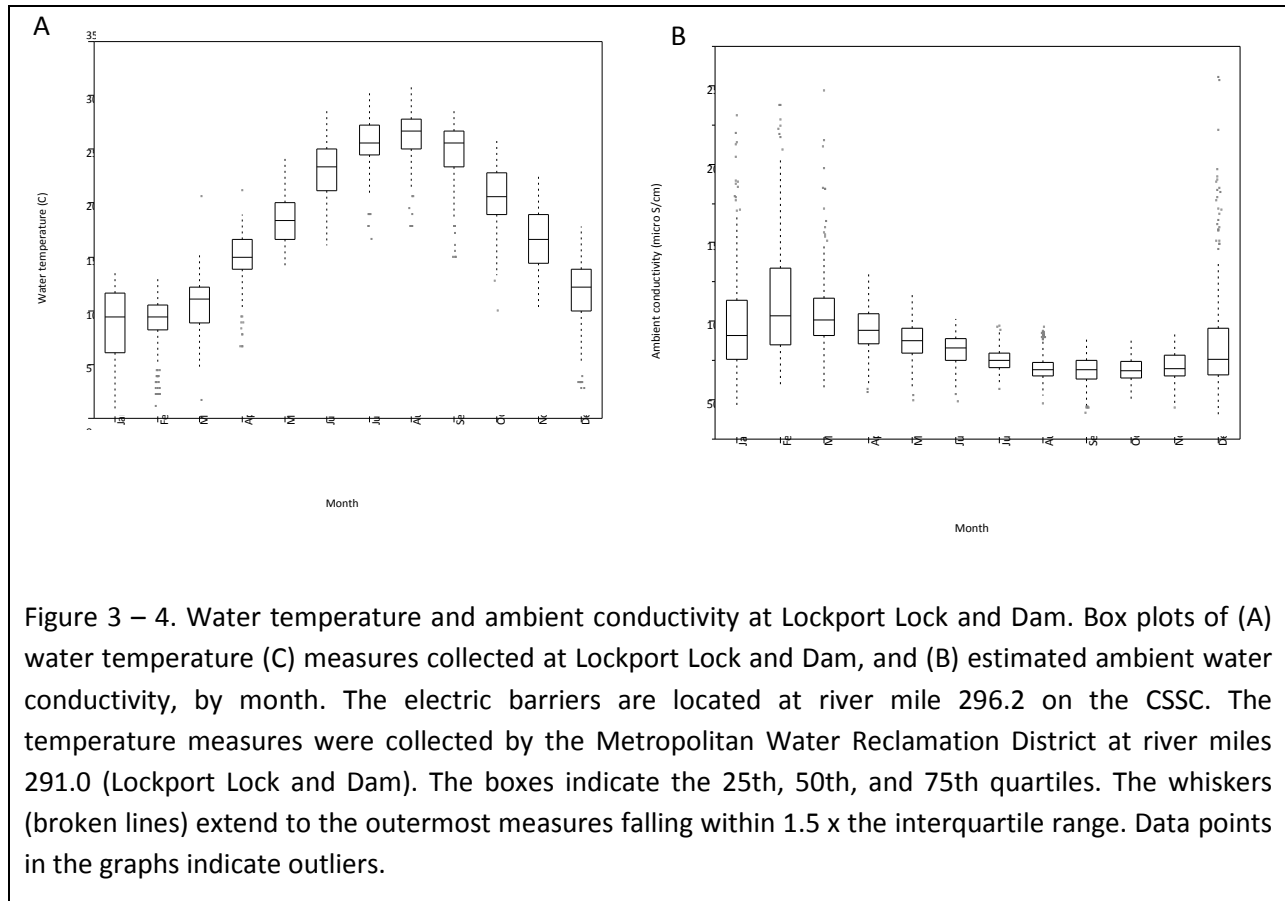


Table 3 – 1. Mean ambient conductivity. Mean ambient conductivity (standard deviation in parentheses), by month, estimated from temperature and specific conductivity data collected at Lockport Lock and Dam. Statistically significant differences ( $P < 0.05$ ) in pair-wise comparisons are indicated by levels not connected by same letter.

Month	Ambient conductivity ( $\mu\text{S}/\text{cm}$ )	Levels not connected by the same letter indicates statistically significant difference in pairwise comparisons of the means
February	1139 ( $\pm 377$ )	A
March	1058 ( $\pm 258$ )	B
January	992 ( $\pm 339$ )	C
April	947 ( $\pm 139$ )	C
May	879 ( $\pm 116$ )	D
December	872 ( $\pm 359$ )	D E
June	813 ( $\pm 106$ )	E F
July	754 ( $\pm 69$ )	F G
November	713 ( $\pm 92$ )	G H
August	695 ( $\pm 85$ )	G H
October	686 ( $\pm 81$ )	H
September	684 ( $\pm 88$ )	H

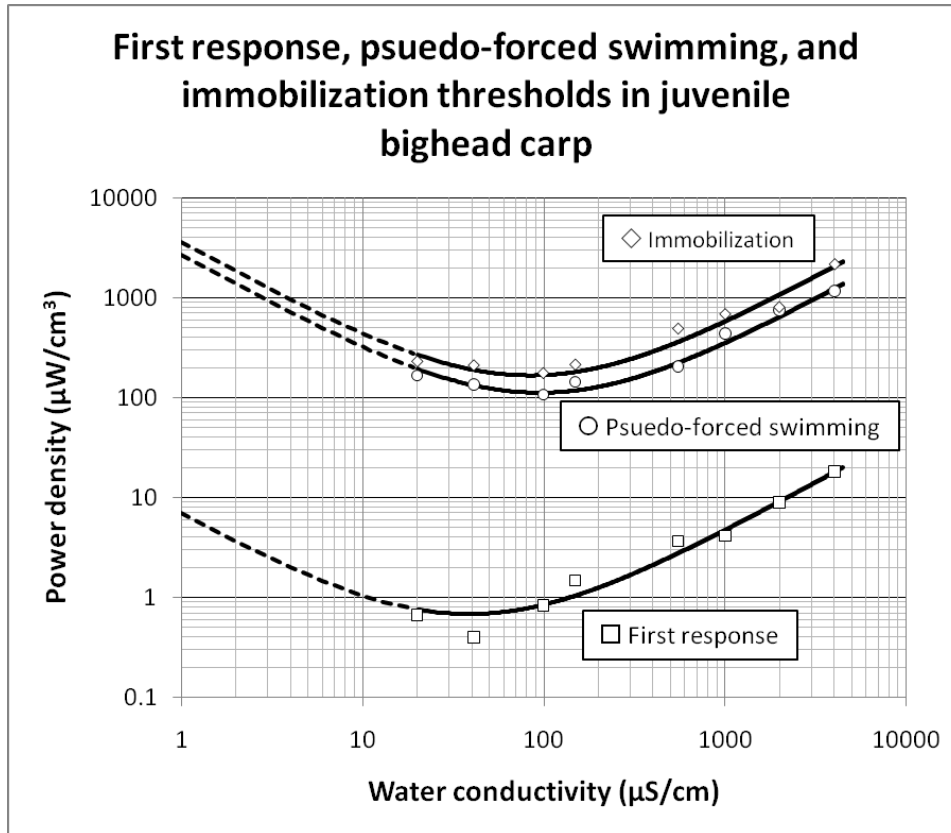


Figure 3 – 5. Plots of behavioral threshold power density versus water conductivity. Log-log plot of power density versus water conductivity for predicting power to elicit first response, forced swimming, and immobilization in small bighead carp. Mean values of the response threshold-power-density and the fitted theoretical curves for maximum power transfer are plotted as functions of water conductivity. Effective conductivity for bighead carp was estimated to be 39 (90% CI, 3 - 64)  $\mu\text{S}/\text{cm}$  based on thresholds for first response, 95 (95% CI, 60-135)  $\mu\text{S}/\text{cm}$  based on thresholds for pseudo-forced swimming, and 84 (95% CI, 41-121)  $\mu\text{S}/\text{cm}$  based on thresholds for immobilization. *In vivo* threshold power density was estimated to be 0.68  $\mu\text{W}/\text{cm}^3$  for the first response, 112 (95% CI, 87-112)  $\mu\text{W}/\text{cm}^3$  for pseudo-forced swimming, and 172 (95% CI, 119-199)  $\mu\text{W}/\text{cm}^3$  for immobilization. A total of 400 fish were used in the threshold-power density experiment, 50 fish at each level of water conductivity. A power density threshold for first response was targeted in all fish. The immobilization and pseudo-forced swimming responses were each targeted in 25 fish. The order in which the levels of water conductivity were tested was random.

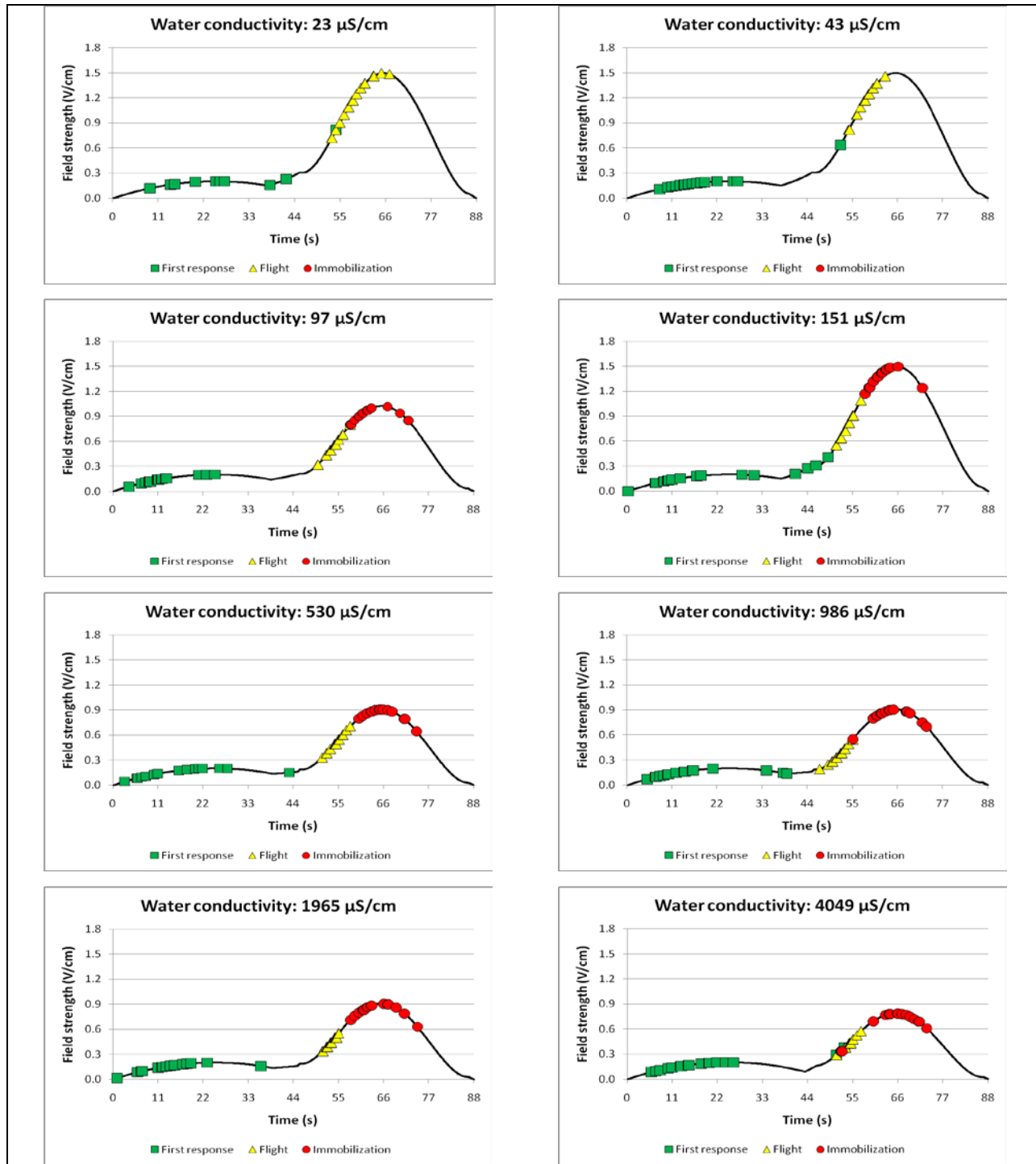


Figure 3 – 6. Threshold field strength for behavioral responses. Thresholds of field strength for targeted behavioral responses in simulations of encroachment upon electric barrier IIA on the CSSC on small bighead carp, under various conditions of water conductivity. In the simulations, a protocol of 2 ms pulse-duration and 30 Hz pulse-frequency was applied at various levels of ultimate field strength. Outcomes from a total of 160 simulations are represented, with simulations conducted with 20 fish at each of the levels of water conductivity. The simulations were conducted on individual fish.

In all cases, flight responses were induced on the rising (downstream) side of the “high-field” (Figure 3 – 6). Thresholds of power density and cumulative exposure for the flight response varied in accordance with power transfer theory. Using threshold power density for the flight response,  $c_f$  was estimated to be 64 (95% CI 33 – 89)  $\mu\text{S}/\text{cm}$  and  $D_m$  to be 43 (95% CI 23 – 59)  $\mu\text{W}/\text{cm}^3$  (Figure 3 – 7), with an  $R^2$  statistic of 0.77. Based on estimates of threshold cumulative exposure for the flight response,  $c_f$  was estimated to be 42 (95% CI 25 – 57)  $\mu\text{S}/\text{cm}$  and  $D_m \cdot s$  to be 278 (95% CI 65 – 373)  $\mu\text{W}/\text{cm}^3 \cdot \text{s}$  (Figure 3 – 7), with an  $R^2$  statistic of 0.90.

Immobilization responses were often induced on the falling (upstream) side of the “high-field” in the simulations (Figure 3 – 6). In this instance, thresholds of cumulative exposure (Figure 3 – 8) are more appropriate than threshold power density for estimation of  $c_f$ , as like levels of power density occurred on each side of the high-field. No fish were immobilized in the simulations conducted in water of 23  $\mu\text{S}/\text{cm}$  and 43  $\mu\text{S}/\text{cm}$  conductivity, but 0.90 of fish in the simulations conducted in 97  $\mu\text{S}/\text{cm}$  water were immobilized. The lack of response in the lowest conductivity levels prevented adequate fit of the power transfer model to threshold cumulative exposure data to estimate  $c_f$  and  $D_a \cdot s$  for immobilization.

There were inverse relations between values of  $c_f$  and the  $R^2$  statistics for the models, and estimates of  $D_a \cdot s$

39 $\mu\text{S}/\text{cm}$ ,	$R^2 = 0.85$ ,	1175 (95% CI 1106 – 1243),
42 $\mu\text{S}/\text{cm}$ ,	$R^2 = 0.85$ ,	1262 (95% CI 1188 – 1336),
64 $\mu\text{S}/\text{cm}$ ,	$R^2 = 0.80$ ,	1889 (95 % CI 1777 – 2000),
84 $\mu\text{S}/\text{cm}$ ,	$R^2 = 0.74$ ,	2437 (95% CI 2292 – 2582),
95 $\mu\text{S}/\text{cm}$ ,	$R^2 = 0.71$ ,	2702 (95% CI 2565 – 2892),

when the power transfer model was fit to threshold cumulative exposure data for immobilization, with  $c_f$  estimated from other targeted responses. Examination of the threshold cumulative exposure data and the fitted model indicate the outcomes from simulations conducted in water of 97  $\mu\text{S}/\text{cm}$  were primarily responsible for the reduction in fit of the model to the data (Figure 3 – 9).

The cumulative electrical exposure in the simulations conducted in water of 43  $\mu\text{S}/\text{cm}$  conductivity was similar to that in simulations conducted in water of 97  $\mu\text{S}/\text{cm}$ ; there was extensive overlap in levels of cumulative exposure between the simulations conducted in water of 43  $\mu\text{S}/\text{cm}$  and 97  $\mu\text{S}/\text{cm}$ . No fish were immobilized in simulations conducted in water of 43  $\mu\text{S}/\text{cm}$  conductivity and the estimated fish effective conductivity of 42  $\mu\text{S}/\text{cm}$  provided the best fit of the power transfer model to threshold cumulative exposure for immobilization data. In contrast to the simulations conducted in water of 43  $\mu\text{S}/\text{cm}$  conductivity, 90% of fish in the simulations conducted in water of 97  $\mu\text{S}/\text{cm}$  conductivity were immobilized. The contrast in incidence of immobilization between the two levels of water conductivity is

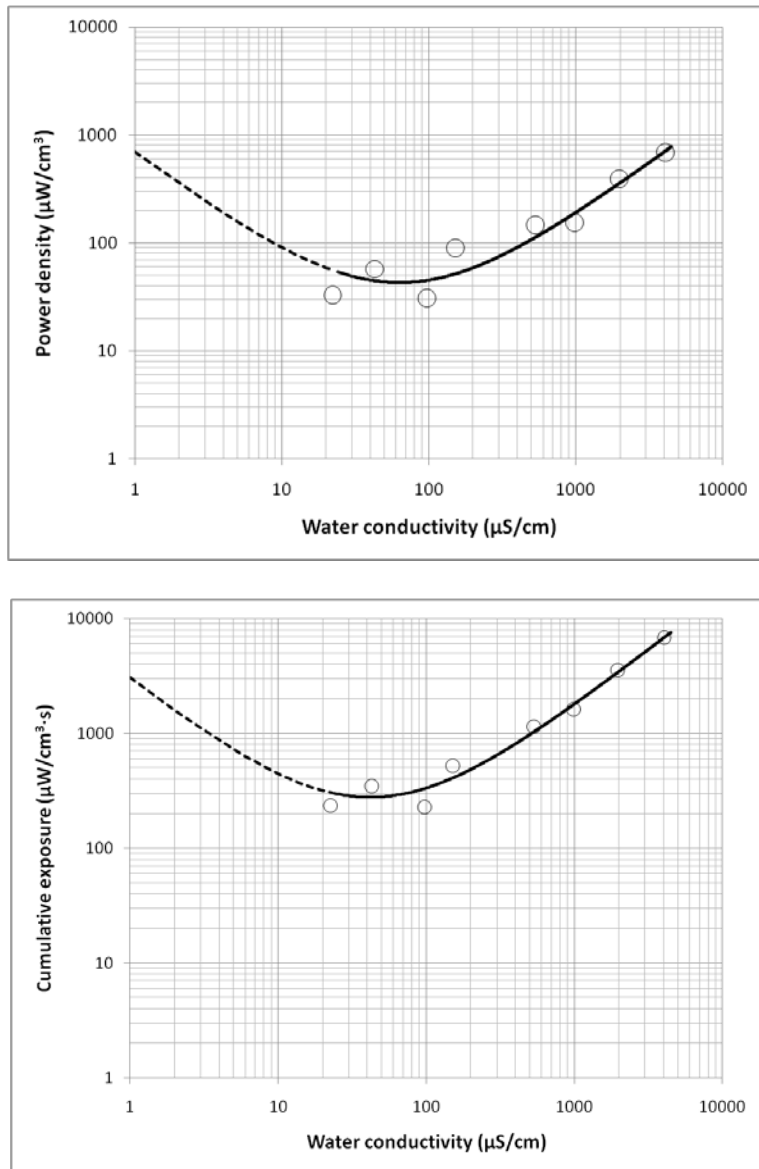


Figure 3 – 7. Plot of threshold power density for flight versus water conductivity. (A) Log-log plot of power density ( $\mu\text{W}/\text{cm}^3$ ) (B) log-log plot of cumulative exposure ( $\mu\text{W}/\text{cm}^3 \cdot \text{s}$ ) versus water conductivity for predicting power thresholds for flight responses in small bighead carp. Mean values of the response threshold power density and cumulative exposure and the fitted theoretical curves for maximum power transfer are plotted as functions of water conductivity. Using the threshold power density for the flight response,  $c_f$  was estimated to be 64 (95% CI 33 – 89)  $\mu\text{S}/\text{cm}$  and  $D_m$  to be 43 (95% CI 23 – 59)  $\mu\text{W}/\text{cm}^3$ . The  $R^2$  statistic for the model was 0.77. Using threshold cumulative exposure for the flight response,  $c_f$  was estimated to be 42 (95% CI 25 – 57)  $\mu\text{S}/\text{cm}$  and *in vivo* cumulative exposure to be 278 (95% CI 65 – 373)  $\mu\text{W}/\text{cm}^3 \cdot \text{s}$ . The model  $R^2$  statistic was 0.90. A total of 160 fish were used in the simulations, 1 fish per simulation, 20 fish per level of water conductivity.

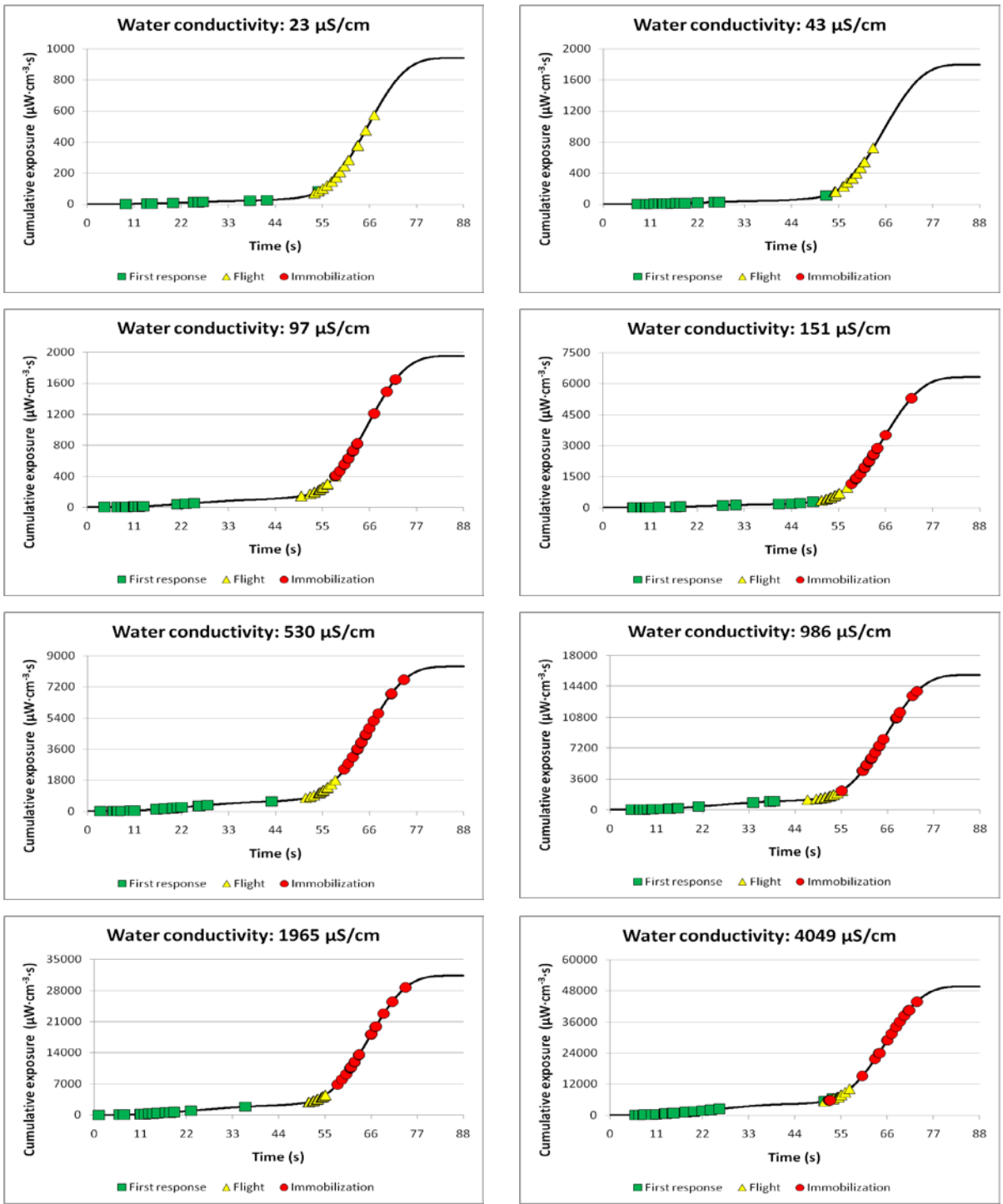


Figure 3 – 8. Cumulative exposure thresholds. Cumulative exposure thresholds for targeted behavioral responses in simulations of encroachment into the Barrier IIA field by 51 – 76 mm bighead carp, in water of varying conductivity. The electric fields were characterized by pulses of DC of 2 ms duration and 30 Hz at various levels of ultimate field strength. The vertical scale changes markedly in the plots. Data from a total of 160 fish are represented, 1 fish per simulation, 20 fish per level of water conductivity.

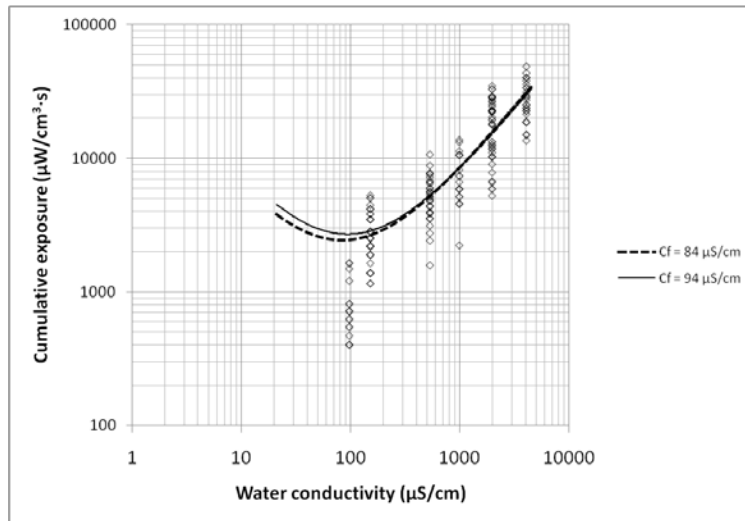


Figure 3 – 9. Plot of threshold cumulative exposure for immobilization. Log-log plot of cumulative exposure ( $\mu\text{W}/\text{cm}^3 \cdot \text{s}$ ) thresholds for immobilization in simulations of encroachment on electric barrier IIA by small bighead carp. Models were fit using  $c_f$  estimated from power density thresholds for immobilization ( $84 \mu\text{S}/\text{cm}$ ;  $R^2 = 0.74$ ) and pseudo-forced swimming ( $95 \mu\text{S}/\text{cm}$ ;  $R^2 = 0.71$ ). Data from 160 simulations are represented, 1 fish per simulation, 20 fish per level of water conductivity.

interpreted as evidence that  $97 \mu\text{S}/\text{cm}$  is a closer match to the effective conductivity of bighead carp than  $43 \mu\text{S}/\text{cm}$ .

The multiplier for constant power (MCP), in relation to  $c_w$  was calculated with estimates of effective conductivity estimated from the power-density-threshold-response experiment, from thresholds of forced swimming with loss of equilibrium ( $c_f = 95 \mu\text{S}/\text{cm}$ ) and immobilization ( $c_f = 84 \mu\text{S}/\text{cm}$ ; Figure 3 – 10). The MCP minima (1) reflected the matched condition between fish effective conductivity and water and water conductivity, where  $c_w = c_f$ . The MCP curves for  $c_f = 95 \mu\text{S}/\text{cm}$  and  $c_f = 84 \mu\text{S}/\text{cm}$  intersect at  $c_f = 90 \mu\text{S}/\text{cm}$ , a value approximately splitting the difference between the curves. The condition of  $c_w > c_f$  is anticipated as typical on the Canal. The MCP for Barrier output on the Canal ranged from 1.32 (specific water conductivity,  $400 \mu\text{S}/\text{cm}$ ; temperature,  $5^\circ\text{C}$ ) to 14.7 (specific water conductivity,  $4000 \mu\text{S}/\text{cm}$ ; temperature,  $35^\circ\text{C}$ ; Table 3 – 2).

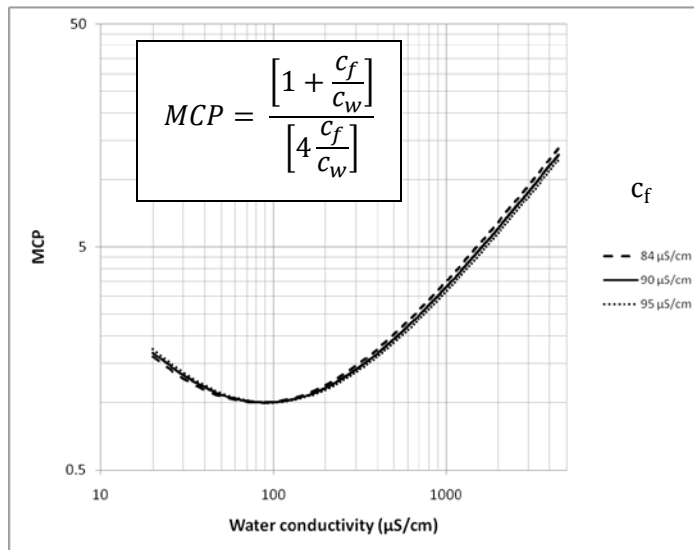


Figure 3 – 10. Multiplier for constant power in relation to water conductivity. The relation of the multiplier for constant power (MCP) and conductivity of water ( $c_w$ ) for small bighead carp developed from threshold-power-density techniques. The MCP was calculated for fish effective conductivities ( $c_f$  of 95 and 84  $\mu\text{S/cm}$  estimated from thresholds of forced swimming (with loss of equilibrium) and immobilization. The distance between the curves was evenly split with  $c_f = 90 \mu\text{S/cm}$ .



Table 3 – 2. Table of multiplier for constant power (MCP). Multiplier for constant power (MCP), based on power transfer theory, calculated for various levels of water temperature (°C) and specific conductivity (μS/cm), with fish effective conductivity ( $c_f$ ) = 90 μS/cm. The MCP can be used to estimate power output requirements for the electric barriers on the CSSC required to maintain efficiency across various levels of water conductivity and temperature.

Specific conductivity (μS/cm)	Water temperature (°C)						
	5	10	15	20	25	30	35
400	1.320666	1.422986	1.527990	1.634829	1.742976	1.852090	1.961938
500	1.487604	1.620621	1.755785	1.892417	2.030095	2.168547	2.307586
600	1.660206	1.823161	1.987906	2.153874	2.320714	2.488199	2.656173
700	1.836044	2.028505	2.222499	2.417542	2.613333	2.809676	3.006439
800	2.013904	2.235600	2.458638	2.682593	2.907202	3.132295	3.357755
900	2.193113	2.443863	2.695806	2.948565	3.201905	3.455674	3.709770
1000	2.373266	2.652944	2.933696	3.215182	3.497190	3.779586	4.062275
1100	2.554106	2.862620	3.172110	3.482267	3.792900	4.103885	4.415136
1200	2.735460	3.072741	3.410917	3.749705	4.088929	4.428474	4.768265
1300	2.917210	3.283206	3.650027	4.017413	4.385201	4.753287	5.121599
1400	3.099272	3.493940	3.889375	4.285334	4.681667	5.078276	5.475094
1500	3.281582	3.704889	4.128912	4.553425	4.978286	5.403405	5.828719
1600	3.464095	3.916014	4.368605	4.821654	5.275030	5.728647	6.182449
1700	3.646774	4.127283	4.608424	5.089996	5.571877	6.053984	6.536265
1800	3.829592	4.338673	4.848350	5.358434	5.868810	6.379400	6.890153
1900	4.012527	4.550163	5.088364	5.626952	6.165815	6.704881	7.244102
2000	4.195562	4.761740	5.328455	5.895537	6.462881	7.030418	7.598102
2100	4.378681	4.973390	5.568611	6.164181	6.760000	7.356003	7.952146
2200	4.561874	5.185105	5.808823	6.432875	7.057165	7.681630	8.306229
2300	4.745131	5.396874	6.049084	6.701612	7.354369	8.007293	8.660345
2400	4.928444	5.608692	6.289387	6.970388	7.651607	8.332987	9.014490
2500	5.111807	5.820553	6.529728	7.239198	7.948876	8.658709	9.368660
2600	5.295212	6.032451	6.770103	7.508037	8.246172	8.984456	9.722853
2700	5.478657	6.244383	7.010507	7.776903	8.543492	9.310225	10.07707
2800	5.662136	6.456345	7.250937	8.045792	8.840833	9.636013	10.43130
2900	5.845646	6.668334	7.491392	8.314702	9.138194	9.961818	10.78554
3000	6.029184	6.880347	7.731867	8.583632	9.435571	10.28764	11.13981
3100	6.212747	7.092381	7.972362	8.852579	9.732965	10.61348	11.49408
3200	6.396333	7.304436	8.212874	9.121541	10.03037	10.93932	11.84837
3300	6.579940	7.516508	8.453402	9.390518	10.32779	11.26518	12.20266
3400	6.763566	7.728597	8.693944	9.659507	10.62522	11.59105	12.55697
3500	6.947209	7.940701	8.9345	9.928508	10.92267	11.91694	12.91129
3600	7.130868	8.152819	9.175068	10.19752	11.22012	12.24282	13.26561
3700	7.314541	8.364949	9.415647	10.46654	11.51758	12.56872	13.61994
3800	7.498228	8.577091	9.656236	10.73557	11.81505	12.89463	13.97428
3900	7.681927	8.789243	9.896834	11.00461	12.11253	13.22054	14.32863
4000	7.865638	9.001406	10.13744	11.27366	12.41001	13.54646	14.68298

## Discussion

The relation between the conductivity of water transmitting the electric field and the conductivity of fish determines quantities of power transferred from water to fish. Subsequently, the conductivity of water influences fish behaviors evoked by electrical energy (Vibert 1967, Lamarque 1967, Halsband 1967, Biwas and Karmarker 1979, Kolz 1989, Kolz and Reynolds 1989, Miranda and Dolan 2003, Bearlin et al. 2008). The conductivity of water in the Canal varies markedly, potentially influencing effectiveness of the electric barriers for evoking passage-preventing reactions from encroaching fishes. The present study evaluated effects that variation in water conductivity may have on the effectiveness of Barrier IIA for inducing passage-preventing behaviors in small invasive carp.

Conductivity is a measure of the ability of a material to conduct electric current and is a measure of the net motion of the charged ions present. The conductivity of water is strongly dependent upon the quantity of dissolved ions. Because temperature strongly influences conductivity, conductivity measures are often temperature corrected (specific conductivity) to allow direct comparison ion content, as thermal effects are removed. Water conductivity measures in the experiments and simulations, and all calculations, are ambient measures, conductivity at ambient temperature, which more closely reflects electrical conductivity. Most meters provide temperature corrected measures of water conductivity (i.e., specific conductivity). Ambient conductivity ( $c_a$ ) is calculated as  $c_a = c_s[1 + 0.0191(T - 25)]$ , where  $c_s$  is specific conductance ( $\mu\text{S}/\text{cm}$ ) corrected to 25°C (provided by most metering systems) and  $T$  is water temperature (°C; APHA et al. 1985).

Estimates of fish effective conductivity for small bighead carp and *in vivo* power density under matched conditions ( $D_m$ ), were acquired via power density technique employing an approach similar to those applied by Kolz and Reynolds (1989), Miranda and Dolan (2003) and Bearlin et al. (2008). The estimates of  $c_f$  for small bighead carp differed among the targeted responses. A  $c_f$  of 39  $\mu\text{S}/\text{cm}$  was estimated from thresholds for first response, a  $c_f$  of 95  $\mu\text{S}/\text{cm}$  from thresholds of forced swimming, and a  $c_f$  of 84  $\mu\text{S}/\text{cm}$  from thresholds of immobilization. The  $c_f$  estimated for small bighead carp from first response thresholds was lower than the estimates acquired from the other responses targeted. Reports by Kolz and Reynolds (1989) and Bearlin et al. (2008) show similar patterns in exposures to pulsed DC, where the least severe behavioral response targeted provided the lowest estimated values for  $c_f$ . Thresholds for twitch provided estimates of  $c_f$  of 83 to 99  $\mu\text{S}/\text{cm}$  compared to estimates of 137 to 160  $\mu\text{S}/\text{cm}$  for immobilization in goldfish exposed to 50 Hz pulsed DC (Kolz and Reynolds 1989). Thresholds for escape provided an estimate of  $c_f$  of 65  $\mu\text{S}/\text{cm}$  while thresholds for immobilization provided a  $c_f$  estimate of 80  $\mu\text{S}/\text{cm}$  in Murray cod exposed to 60 Hz pulsed DC (Bearlin et al. 2008). Similar to the increased variance in threshold power density estimates for the escape response, relative to the other targeted responses, reported by Bearlin et al. (2008), variation associated with thresholds of first response was greater than for the other responses in the present study. Kolz and Reynolds (1989) did not indicate the variability associated with their estimates. The hypothesis presented by Bearlin et al. (2008), that the increased variation associated with escape was a reflection of the actions and signs associated with the response being less distinguishable than those associated with more extreme responses, also applies to the outcomes in the present study.

The first response to the presence of the electric field by fish in the experiment often included movements that appeared as attempts to physically brush against surfaces in the exposure tank, a response reminiscent of fish reactions to low grade irritation (e.g., external parasite). The hypothesis that the low gradient electrical exposures associated with the first response stimulated different neural

structures (than those associated with the other responses) is offered as an explanation for the shift in  $c_f$  observed among the targeted behaviors. The low electrical gradients associated with first response stimulated somatic sensory nerves as opposed to direct stimulation of the CNS and motoneurons that resulted in pseudo-forced swimming and immobilization response is proposed as an explanation for the shift in  $c_f$  observed between the targeted responses. Model fit improved as fish responses to electrical exposure became more pronounced, as indicated by the  $R^2$  statistic, likely resulting from the actions and signals associated with the behaviors becoming more distinguishable.

The estimates of  $c_f$  for bighead carp based on forced swimming (95  $\mu\text{S}/\text{cm}$ ) and immobilization (84  $\mu\text{S}/\text{cm}$ ) thresholds in the present study are consistent with previous estimates of fish effective conductivity. Exposures of goldfish to 50 Hz pulsed DC of 2, 5 and 10 ms provided point estimates of effective conductivity, based on immobilization, from 137  $\mu\text{S}/\text{cm}$  to 160  $\mu\text{S}/\text{cm}$  (Kolz and Reynolds 1989). Estimates of effective conductivity of channel catfish immobilized by 3-second exposures to DC or 1 ms pulses of DC at 15, 20, 30, 60 or 110 Hz, ranged from 89 to 138  $\mu\text{S}/\text{cm}$  (Miranda and Dolan 2003). Effective conductivity estimates for Murray cod *Maccullochella peelii peelii* exposed to  $\sim 4$  ms pulses of DC at 60 Hz for 3 seconds varied with targeted response (escape, 65  $\mu\text{S}/\text{cm}$ ; forced swimming, 78  $\mu\text{S}/\text{cm}$ ; immobilization, 80  $\mu\text{S}/\text{cm}$ ; narcosis, 46  $\mu\text{S}/\text{cm}$ ). Application of the power transfer curve to previously published threshold response data and water conductivities increases the number of estimates of fish effective conductivity for comparison. Fit of the theoretical power transfer curve to threshold power density for forced swimming in 30 cm eels, calculated here from data reported by Lamarque (1967), and for first response in trout, estimated here from data reported by Sternin et al. (1976), provides  $c_f$  values of 76  $\mu\text{S}/\text{cm}$  ( $R^2 = 0.85$ ) for eels and 100  $\mu\text{S}/\text{cm}$  ( $R^2 = 0.92$ ) for trout. Fit of power transfer curves to previously published thresholds for flight response, from exposures to 50 Hz AC (Liu 1990; Miranda and Dolan 2003), provides estimates for  $c_f$  of 56  $\mu\text{S}/\text{cm}$  for bighead carp and 96  $\mu\text{S}/\text{cm}$  for silver carp. Thus, the estimates of bighead carp effective conductivity in the present study are consistent with those on a variety of species.

The scenario in the simulations used to estimate thresholds of cumulative exposure for the targeted responses was similar to that employed in the screening trial and the experiment for prognostic modeling (Holliman, this report). The scenario was assumed to be the worst case for preventing passage of invasive bighead carp and silver carp through the electric barriers, as (1) the fish encroaching upon the barrier were small, (2) the fish encroaching upon the electric barrier were swimming at the surface of the Canal, (3) fish penetrating the electric barrier continued upstream despite receiving electrical stimulus, (4) there was no or minimal water current flow, and, (5) fish swam straight through the electric barrier, as quickly as possible. In the present study, an additional component was added to the scenario, (6) the conductivity of water in the Canal varied. The circumstance in the simulations is expected to worsen as levels of water conductivity deviate from the matched condition with fish effective conductivity ( $\sim 90 \mu\text{S}/\text{cm}$ ). The simulations conducted for prognostic modeling were conducted in water of 2000  $\mu\text{S}/\text{cm}$  conductivity.

The duration of an electrical exposure can significantly influence the behavioral response evoked in fish (Sternin et al. 1976, Prel 1991). Possible physiological mechanisms for the immobilization response in the simulations include strong stimulation of the central nervous system leading to summation of signals and muscular cramp (Halsband 1967), synaptic exhaustion due prolonged exposure (Lamarque 1967), and depression of the central nervous system (Sternin et al. 1976). Intuitively, the duration of the electrical exposures employed (as long as they are consistent) should have no bearing on estimates of fish effective conductivity, unless the thresholds of response in the neural-muscular structures stimulated differ over differing durations of exposure or different neural-muscular structures are

stimulated as exposure period changes. It is expected that duration of exposure would influence power density minima (quantity of energy required for a response), but not the location of the minima along the conductivity spectrum (which would influence estimates of fish effective conductivity). However, duration of exposure dependent thresholds in neural-muscular structures stimulated and period of exposure dependent stimulation of different neural structures that influence estimates of fish effective conductivity cannot be discounted.

To my knowledge, this is the first application of power transfer theory to thresholds of fish behaviors based on cumulative electrical exposure. Application of the power transfer model to threshold data from the simulation provided  $c_f = 64 \mu\text{S}/\text{cm}$  for flight when based on power density and  $c_f = 42 \mu\text{S}/\text{cm}$  when applied to cumulative exposure. The estimate of  $c_f = 64 \mu\text{S}/\text{cm}$  is similar to that estimated from thresholds for the escape response in Murray cod ( $c_f = 65 \mu\text{S}/\text{cm}$ ) and the relative shift in  $c_f$  from the estimates based on thresholds of forced swimming and immobilization are similar to that reported by Bearlin et al. (2008). The estimate of  $c_f = 42 \mu\text{S}/\text{cm}$  from thresholds of cumulative exposure for flight is a marked shift from the estimates based on thresholds of forced swimming  $c_f = 95 \mu\text{S}/\text{cm}$  and immobilization  $c_f = 84 \mu\text{S}/\text{cm}$ . Bearlin et al. (2008) reported a similar shift in the  $c_f$  estimates based on immobilization (pulsed DC exposure) and narcosis (DC exposure). The mechanisms associated with narcosis and immobilization involves different neural structures (Sternin et al. 1976), which may account for the shift in  $c_f$  reported by Bearlin et al. (2008). The shift in  $c_f$  between models fit to power density data and cumulative exposure data is more likely an artifact of the modeling procedure, as the models were fit to data acquired in the same exposures. Additional model terms may be needed to account for duration of exposure, but are beyond the scope of the present study. Additional investigation into the effects that duration of exposure may have on induced response and estimates of fish effective conductivity is warranted.

Comparisons of models of power transfer applied cumulative exposure for immobilization employing estimates of  $c_f$  acquired via power transfer technique showed an inverse relation between model fit and effective conductivity estimates:  $c_f = 39 \mu\text{S}/\text{cm}$ ,  $R^2 = 0.85$ ;  $c_f = 42 \mu\text{S}/\text{cm}$ ,  $R^2 = 0.85$ ;  $c_f = 64 \mu\text{S}/\text{cm}$ ,  $R^2 = 0.80$ ;  $c_f = 84 \mu\text{S}/\text{cm}$ ,  $R^2 = 0.74$ , and  $c_f = 95 \mu\text{S}/\text{cm}$ ,  $R^2 = 0.71$ . The models applying  $c_f = 39$  and  $c_f = 42$  accounted for the most variation in the data among those tested, provided the best fit, as indicated by a slightly greater  $R^2$  statistic. Though  $c_f = 42 \mu\text{S}/\text{cm}$  gave the best model fit to the data, the numbers of fish immobilized in the simulations (conducted in water of conductivity similar to these estimates of effective conductivity) suggests an effective conductivity closer to  $97 \mu\text{S}/\text{cm}$ .

No fish were immobilized in the simulations conducted in water of  $22 \mu\text{S}/\text{cm}$  or  $43 \mu\text{S}/\text{cm}$  conductivity. Based on power transfer theory, the cumulative exposure minima should occur at the water conductivity providing a matched condition with fish effective conductivity. No fish were immobilized in water of conductivity similar to the  $c_f$  estimate best fitting the threshold cumulative exposure for immobilization data, the expected location of the cumulative exposure minima. Comparison of cumulative exposure between the simulations in water of  $43 \mu\text{S}/\text{cm}$  conductivity and those in water of  $97 \mu\text{S}/\text{cm}$  conductivity demonstrate extensive overlap. The outcomes in these two exposures differed markedly, 90% of fish in the the simulations conducted in  $97 \mu\text{S}/\text{cm}$  conductivity water were immobilized compared to no fish (0%) immobilized in water of  $43 \mu\text{S}/\text{cm}$ . The power transfer model fit the threshold cumulative exposure for flight data well ( $R^2 = 0.90$ ). It is concluded that the lack of data in the two lowest levels of conductivity prevented adequate fit of the theoretical power transfer model to the threshold cumulative exposure for immobilization data.

Field study to determine effective levels of operation for the electric barriers is recommended. Once effective levels of operation has been determined, the results of the threshold power density experiment provides fundamental information to determine power output necessary for the electric barriers to maintain effectiveness (on fish) under various conditions of water conductivity. Power transferable from water to fish can be calculated with  $P_t = P_a/MCP$ , where  $P_a$  is the power level determined to provide acceptable operation. Power output goals  $P_g$  for the Barrier under different conditions of water conductivity can be calculated by substituting  $P_t$  for  $P_a$  in the equation, providing  $P_g = P_t \times MCP$  (Burkhardt and Gutreuter 1995). Fish effective conductivity information can also be used to improve electrofishing-based monitoring of bighead carp. Because conductivity of water in the Canal varies widely, standardizing electrical power applied during electrofishing is warranted (Burkhardt and Gutreuter 1995). Comparing the MCP based on  $c_f$  estimates of 90  $\mu\text{S}/\text{cm}$  for bighead carp with that based on the generalized  $c_f$  of 115  $\mu\text{S}/\text{cm}$  (Miranda and Dolan 2003), estimates of MCP (and subsequently estimates of applied power) was consistently greater with  $c_f = 90 \mu\text{S}/\text{cm}$ , underestimated by the generalized  $c_f = 115 \mu\text{S}/\text{cm}$  by 15% in 400  $\mu\text{S}/\text{cm}$  water, 22% in 1,000  $\mu\text{S}/\text{cm}$  water, 25% in 2,000  $\mu\text{S}/\text{cm}$  water, and 26% in 3,000 and 4,000  $\mu\text{S}/\text{cm}$  water.

The estimates of  $c_f$  were based on electrical exposures to DC pulsed at 30 Hz, pulses of 2 ms. Application of other combinations of pulse-frequency and pulse-duration may raise or reduce the quantity of electrical energy necessary to induce targeted responses, but  $c_f$  would be unaffected. The simulations of fish encroachment in water of ambient conductivity similar to that occurring in the Canal were conducted with ultimate field strength of 0.91 V/cm; the exceptions were simulations at 4049  $\mu\text{S}/\text{cm}$ , which were conducted with ultimate field strength of 0.79 V/cm. The proportions of fish immobilized in the simulations in water of conductivity similar to that in the Canal (0.80 – 1.0) was relatively constant. The operational protocol employed in the simulations, in water of various conductivity, was shown effective in the screening experiment (described earlier), which was conducted in water of 1,000  $\mu\text{S}/\text{cm}$ , and was shown relatively effective in the experiment for prognostic modeling (described earlier), which was conducted with water of 2,000  $\mu\text{S}/\text{cm}$ . Outcomes of electrical exposures (simulations) indicate that effectiveness of Barrier IIA will be relatively constant with operational protocols applying 0.79 – 0.91 V/cm ultimate field strength, pulse-frequency of 30 Hz, and pulse-duration of 2 ms in water of conductivity from 100 to 4000  $\mu\text{S}/\text{cm}$ . Verification of the experiment outcomes on the Canal, under field conditions is recommended.

## Work cited

- APHA (American Public Health Association). American Water Works Association, and Water Pollution Control Federation. 1985. Standard methods for examination of water and wastewater. 16<sup>th</sup> edition. APHA, Washington, D.C.
- Bearlin A. R., S. J. Nicol and T. Glenane. 2008. Behavioral responses of Murray cod *Macculloshella peelii* to pulse frequency and pulse width from electric fishing machines. Transactions of the American Fisheries Society, 137: 107-113.
- Burkhardt, R. W. and S. Gutreuter. 1995. Improving electrofishing catch consistency by standardizing power. North American Journal of Fisheries Management, 15: 375-311.
- Dolan, C. R. and L. E. Miranda. 2003. Immobilization thresholds of electrofishing relative to fish size. Transactions of the American Fisheries Society, 132: 969-976.
- Halsband, E. 1967. Basic principles of electrofishing. Pages 57–64 in R. Vibert, editor. Fishing with Electricity - Its Applications to Biology and Management. Fishing News Books, Blackwell Scientific Publications Ltd., Oxford, England.
- Kvålseth, T. O. 1989. Cautionary note about R2. American Statistician, 39: 279 – 285.
- Kolz A. L. 1989. A power transfer theory for electrofishing. U.S. Fish and Wildlife Service Fish and Wildlife Technical Report 22: 1-11.
- Kolz A. L. and J.B. Reynolds. 1989. Determination of power threshold response curves. U.S. Fish and Wildlife Service, Fish and Wildlife Technical Report, 22:15-24.
- Kolz, A. L.. 2006. Electrical conductivity as applied to electrofishing. Transactions of the American Fisheries Society, 135: 509 – 518.
- Lamarque, P. 1967. Electrophysiology of fish subject to the action of an electric field. Pages 65-92 in R. Vibert, editor. Fishing with Electricity - Its Applications to Biology and Management. Fishing News Books, Blackwell Scientific Publications Ltd., Oxford, England.
- Miranda, L. E. and C. R. Dolan. 2003. Test of a power transfer model for standardized electrofishing. Transactions of the American Fisheries Society, 132:1179-1185.
- Prel, E. T. 1991. Effect of voltage gradient in an electrical field on threshold indices of fish response. Acta Ichthyological et Piscatoria, 21: 37 – 44.
- Sternin, V. G., I. V. Nikonorov and Y. K. Bumeister. 1972. Electrical fishing: Theory and Practice. Pishchevaya Promyshlennost', Moskva. Translated by E. Vilim, Israel Program for Scientific Translations, 1976. Keter Publishing House Jerusalem Ltd., Jerusalem.
- Lamarque, P. 1967. Electrophysiology of fish subject to the action of an electric field. Pages 65-92 in R. Vibert, editor. Fishing with Electricity - Its Applications to Biology and Management. Fishing News Books, Blackwell Scientific Publications Ltd., Oxford, England.

Liu, Qi-Wen. 1990 Development of the Model SC-3 Alternating Current Scan Fish Driving Device. Pages 46-50 in I. G. Cowx and P. Lamarque, editors. Developments in Electric Fishing. Fishing News Books, London.

Sall, J., Lee C. and A. Lehman. 2007. JMP® Start Statistics: A guide to statistics and data analysis using JMP®, fourth edition. Cary NC; SAS Institute Inc.

SAS 2008. JMP® Statistics and graphics guide, Volumes 1 and 2. Cary, NC: SAS Institute Inc.

SAS 2009. JMP, Version 8. SAS Institute Inc., Cary, NC, 1989-2009.

Vibert, R. 1967. General report of the working party on the applications of electricity to inland fishery biology and management. Pages 3 – 51 in R. Vibert, editor. Fishing with Electricity: Its Application to Biology and Management. Fishing News Books, Ltd., London.

## 4 – Evaluation of Volitional Challenge of Electric Fields by Small Bighead Carp

---

Summary.— The objective in this experiment was to evaluate volitional challenge of barrier fields, electric fields characterized by potential operational protocols for the barriers on the Chicago Sanitary and Ship Canal by small bighead carp [48 – 82 mm (1.9 – 3.2 inches) total length]. If small bighead carp avoid increasingly intense waterborne electric fields it may not be necessary to maintain the electric barriers at field strengths capable of immobilization, potentially a significant reduction in electrical power requirements, equipment wear, and hazards to humans. Our approach was to evaluate the incidence and outcomes of challenges to the electric fields under controlled conditions, in a relatively shallow circular flume. The electric fields in the tests were approximately 1/10 the width (upstream-downstream dimension) of electric Barrier IIA on the Canal and had markedly greater gradients of field strength compared to those present in the barriers at the Canal surface; the proportions of fish breaching the field in this experiment do not estimate passage rate of the electric Barriers on the Canal, the differences in scale and the distributions of electric energy between the electric fields in the flume and the barrier fields on the Canal is too great for direct inference of outcomes. However, the experiment provides invaluable insight into the relative effectiveness of the operational protocols applied and the likelihood of volitional challenge and avoidance of waterborne electric fields by small bighead carp. A total of 400 fish were used in the experiment, 20 fish per experimental cell. Fish exhibited positive rheotaxis, typically swimming upstream into the flow of water. Fish in the present study had opportunity to avoid the field and to exit the field after swimming into it. Fish actions and behaviors indicate they were able to detect the edge of the field and, therefore, could avoid entering the field and avoid further interaction with the field. However, in many cases, fish challenged the field repeatedly. Further, fish often continued to challenge the field despite being immobilized (incapacitated) during incursions into the field only moments earlier, re-challenging the field immediately upon recovery of an upright orientation. Risk for fish to breach the field varied among the operational protocols. Risk of successful challenge of the field and risk for successful passage through the field was significantly reduced with several of the operational protocols (0.91 V/cm-25 Hz-2.0; 0.91 V/cm-30 Hz-2.0 ms; 1.02 V/cm-30 Hz-2.0 ms; 0.91 V/cm-30 Hz-2.5 ms; 1.02 V/cm-20 Hz-2.5 ms; 1.02 V/cm-25 Hz-2.5 ms; 1.02 V/cm-30 Hz-2.5 ms) compared to the protocol shown effective for small silver carp in the pilot study (0.79 V/cm, 15 Hz, 6.5 ms). The ultimate field strength and pulse-frequency were greater in the operational protocols that reduced risk for successful challenge and passage compared to the baseline protocol, but average field strength was reduced (as the pulse-duration was only 31% or 38% (2.0 ms and 2.5 ms versus 6.5 ms). In the simulations of encroachment (described previously), there was little indication of distress in during exposure to field strengths associated with the low-field of Barrier IIA. Responses similar to flight responses evoked in the simulations (upon exposure to the rising side of the high-field) were often observed in fish penetrating the field in the present study; fish penetrating the field typically appeared distressed, swam rapidly and abnormally, and utilized body-voltage minimizing actions. Unless immobilized by the electrical field, fish exhibiting these “flight” responses continued to swim upstream. Based on the outcomes of the experiment, the rheotaxis response to water flow, the repeated challenges to the barrier fields, and the upstream progression of fish penetrating the field despite apparent distress, it is recommended that electric barriers on the Canal utilize protocols capable of inducing immobilization in targeted sizes of bighead carp.

---



## Introduction

Bighead carp *Hypophthalmichthys nobilis* and silver carp *H. molitrix* are nuisance invaders of the Mississippi River System and potential invaders of the Great Lakes. B carp and silver have established reproducing populations in the Mississippi River System and their lifecycle includes prespawn upstream migrations (Kolar et al. 2005). The US Army Corps of Engineers (USACE) Chicago District employs a series of localized waterborne electric fields in the Chicago Sanitary and Ship Canal (CSSC) to act as barriers to dispersal of aquatic nuisance species through the waterway.

Electric barriers, electric screens, and electrical guidance systems, are regarded as behavioral technologies that function by inducing fright and avoidance responses in fish to block passage or direct movement. Hartley and Simpson (1967) indicate that graduated electric fields are necessary for electric barriers to be successful, as fish challenging the barrier are gradually exposed to increasingly unpleasant stimuli and can learn to avoid the stimuli. The extent of the field is critical; the field must be wide enough to prevent fast swimming fish from breaching the field under their own power. The width necessary is influenced by the characteristics of the field. For example, the pulse rate in a pulsed DC field must ensure that fast swimming fish cannot pass through or penetrate too deeply into the electrified zone between pulses. Barriers of graduated electric fields allow penetration by fish to the extent that they can, with larger fish stopping at an earlier stage than smaller fish. The ultimate field strength in the barrier should be adequate to stop the smallest fish (Hartley and Simpson 1967).

Bullen and Carlson (2004), however, report that electric fields have limited potential as a deterrent to fish behavior as fish do not have the ability to detect the direction of an electric field source and will often swim into stronger fields, even to their death. Stewart (1990b) reported similar outcomes in tests with a marine barrier. If bighead carp and silver carp will learn to avoid the increasingly unpleasant electrical stimuli associated with continued penetration of the electric barrier on the CSSC is not known. If passage-prevention will be based on fish learning to avoid noxious stimuli, the threshold for noxious electrical stimulation associated with the avoidance learning is also not known.

Silver carp, bighead carp and common carp share the behavioral characteristics of swimming against the flow and attraction to slow water currents, behaviors that are more pronounced during the breeding season (Zhong 1990). Thus, it is expected that fish motivated to swim upstream in the Chicago Sanitary and Ship Canal will penetrate the electric barrier to the extent they can. The simulations in the prior experiments (Holliman, this report) were conducted under a scenario of no or minimal flow and fish continuing upstream into the Barrier despite electrical stimulation. Although fish did react (first response) to the presence of pulsed DC during exposure to field strengths associated with the low-field, there was little indication of distress. The onset of behaviors associated with the flight response, however, could indicate the threshold for aversive responses, perhaps a behavioral threshold associated with maximum depth of penetration of the barrier. Upon reaching this level of penetration fish may retreat downstream or maintain their position within the field. There are anecdotal observations of this behavior in large fish (undetermined species) in the electric barriers on the Chicago Sanitary and Ship Canal, of large fish maintaining position at some boundary within the field (personal communication, Doug Malone, Smith-Root, Inc., Vancouver, Washington). Whether these fish had penetrated the field further, prior to observation is not known.

In tests of a pulsed DC graduated electric barrier using gizzard shad *Dorosoma cepedianum* (150 – 250 mm), golden shiner *Notemigonus crysoleucas* (40 – 80 mm), rainbow trout *Oncorhynchus mykiss* (160 – 220 mm), brown trout *Salmo trutta* (170 – 200 mm), and largemouth bass *Micropterus salmoides* (250 –

310 mm) many fish receiving electrical stimulation continued into fields of higher intensity (Barwick and Miller 1996). First responses were observed at field strengths of 0.5 – 1.0 V/cm and fish were usually repelled at the edge of the field. The barrier blocked passage of 83 – 94% of fish, but those penetrating into the electric field beyond 1 V/cm often became excited by the electrical stimulation and darted forward, continuing into the barrier [the width of the barrier was 4.5 meters]. The excitement during stimulation, which was accompanied by fish darting into fields of increasing intensity, suggests the threshold for flight responses may not necessarily indicate a boundary of field strength beyond which 51 – 76 mm bighead carp will not penetrate, but the boundary for onset of rapid swimming and body-voltage minimizing behaviors, possibly with continued upstream progress.

Pegg and Chick (2004) reported successful deterrence of bighead carp in their experiment, but silver carp successfully traversed the electric fields. The differences in susceptibility to electric fields demonstrated by the bighead carp and silver carp in the work by Pegg and Chick (2004) was most likely a product of the size difference between fish (by species) used in the tests. The bighead carp employed in the study were adults  $\geq 600$  mm. Whereas, the silver carp used in the study, which were not deterred by the electric field, were  $\leq 150$  mm. The phenomenon of larger fish having lower thresholds of response to a given electric field than smaller fish is significant. This size dependence in effect has been attributed to big fish intercepting a greater potential difference (in a given electric field) than smaller fish (Halsband 1967). The breach of the electric field in the experiment by smaller silver carp illustrates the need for research on the effectiveness of the electric barriers on smaller fish.

Fish behavior is hypothesized to be a risk factor for Barrier effectiveness and is included as biological factor in the conceptual Risk Model for Barrier Effectiveness. The nature of the simulations of encroachment described previously (Holliman, this report) prevented collection of information on volitional challenge of electric fields by the small bighead carp targeted in the experiments. The simulations included the assumption that fish would continue into increasingly intense electric fields unless rendered incapable of forward progress (i.e., immobilized). If small bighead carp avoid increasingly intense waterborne electric fields it may not be necessary to maintain the electric barriers at field strengths capable of immobilization, a significant reduction in electrical power requirements and equipment wear.

The objective in this phase of the study was to evaluate volitional challenge of electric fields by small bighead carp, electric fields characterized by potential operational protocols for the barriers on the Canal. Our approach was to evaluate the incidence and outcomes of challenges to the electric fields under controlled conditions, in a relatively shallow circular flume. The electric fields in the tests were approximately 1/10 the width (upstream-downstream dimension) of electric Barrier IIA on the Canal and had markedly greater gradients of field strength compared to those present in the barriers at the Canal surface. Thus, the proportions of fish breaching the field in this experiment do not estimate passage rate of the electric Barriers on the Canal, the differences in scale and the distributions of electric energy between the electric fields in the flume and the electric Barriers on the Canal is too great to allow direct inference of outcomes. The experiment does provide invaluable insight into the relative effectiveness of the operational protocols applied and the likelihood of volitional challenge and avoidance of waterborne electric fields by small bighead carp. This study was a continuation of cooperative efforts between the USACE, Chicago District, the USACE, Environmental Laboratory, ERDC (EL-ERDC), Vicksburg, Mississippi and Smith-Root, Inc. (SRI), Vancouver, Washington

## Methods

Volitional challenge of waterborne electric fields by small bighead carp was evaluated in a non-conductive, oval shaped (straight sides, rounded ends), continuous raceway (Figure 4 – 1). The channel of the raceway was 30.5 cm x 30.5 cm in the cross-section. The straight sections of the raceway were 503 cm long with 120 cm viewing windows recessed into the outermost side (recessed approximately 1 cm). The raceway was filled with water to a depth of 27.5 cm. Water in the raceway was 20.4 to 21.8 ( $21.4 \pm 0.4$ ) °C with an ambient conductivity of 1967 to 2287 ( $2137 \pm 106$ )  $\mu\text{S}/\text{cm}$  during the tests.

An apparatus consisting of five electrodes, a pulsed DC power supply, video cameras, and a device to restrict access of fish to the lower water column was installed in one of the two straight sections of the raceway (Figure 4 – 1). The five stainless steel electrodes were spaced over a distance of 500 cm along the length of the raceway. Electrodes two (E2), three (E3), four (E4), and five (E5) were positioned 120 cm, 260 cm, 410 cm, and 500 cm upstream from the downstream most electrode (E1). The electrodes were 0.74 mm thick, flat, stainless steel, bent into an “L” shape. The vertical aspect of the electrodes was electrically insulated. The electrodes rested on the raceway bottom, fitted snugly to the sides of the channel. The electrodes were 2.5, 10, or 20 cm wide (E1 and E5, 2.5 cm; E2 and E4, 10 cm; E3, 20 cm). The three innermost electrodes were connected to a programmable pulsed DC power supply, with electrodes E2 and E4 connected to one polarity (-/+) and E3 to the other. The primary electric field was constrained between electrodes E2 and E4. The two outermost electrodes were electrically floating, connected together. Electrical connections to all of the electrodes were made above the water surface.

Non-conductive fiberglass mesh stretched the length of the apparatus restricted fish to the upper 15 cm of the water column. The mesh was tautly stretched along the length of the channel, sealed to the sides with silicon, and supported in the middle by sections of PVC pipe (1/2 inch diameter). A sheet of perforated, non-conductive, plastic positioned immediately upstream of E1 served as a ramp to transition fish onto the apparatus (Figure 4 – 1). Flow within the raceway was provided the return of water from the external, gravity-fed filtration system. Water was returned to the raceway by two submersible pumps located in the filtration system, plumbed to return water in two perforated, cross-channel pipes (figure 4 – 1). Water current velocity was 6 – 7 cm/s.

A profile of the electric field generated in the raceway was established via in-water voltage measurements. Voltage gradients (E, V/cm) were measured along three transects running the length of the apparatus, which were equally spaced across the width of the channel, at 10 cm increments, at various depths, using a calibrated digital oscilloscope and a 1 cm probe. The arithmetic means of the measurements taken at the points along the apparatus were used to create a base profile of field strength (Figure 4 – 2). The intensity of the waterborne electric field decayed rapidly with distance from electrodes E2 and E4, as expected. Measurement of the field ceased 60 cm upstream from E1 and 40 cm downstream of E5, where field intensity declined to levels indistinguishable from ambient electrical noise. Applied voltage was manipulated during the measurement procedures to achieve an ultimate field strength of  $\sim 0.91$  V/cm in the base profile.

A total of 20 operational protocols, defined by ultimate field strength (V/cm), pulse-frequency (Hz) and pulse-duration (ms) were evaluated in the experiment. The operational protocols included the 18 identified as potentially effective for immobilizing 51 – 76 mm bighead carp in the previous experiments [ultimate field strength: 0.79 V/cm, 0.91 V/cm, 1.02 V/cm; pulse-frequency: 20 Hz, 25 Hz, 30 Hz; pulse-duration: 2.0 ms, 2.5 ms] and the protocol identified to be effective for immobilizing 137 to 280 mm

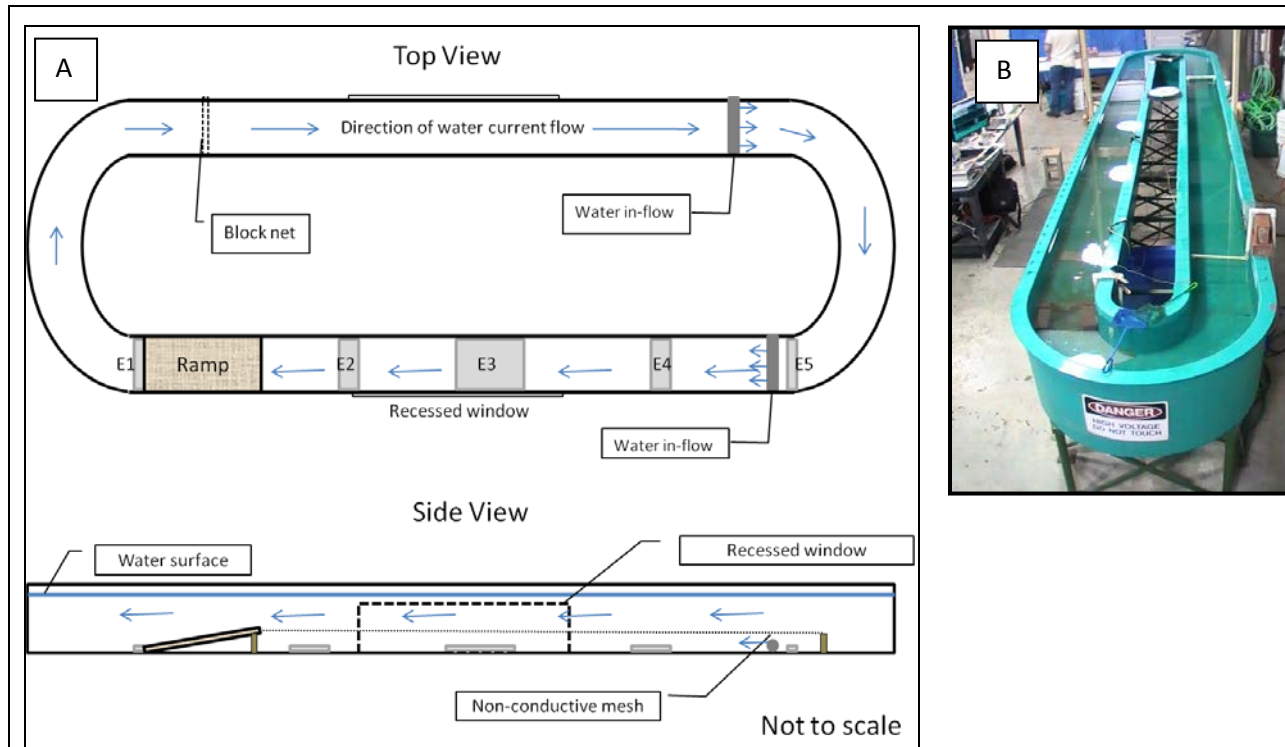


Figure 4 – 1. The apparatus employed in the experiment on volitional challenge of electric fields. A. Schematic diagram of the apparatus developed for testing volitional challenge of waterborne electric fields by small bighead carp. Five electrodes (E1 – E5) were mounted along the bottom of the channel. Non-conductive mesh prevented fish from getting close to the electrodes. B. The continuous raceway housing the apparatus for testing volitional challenge of waterborne electric fields in the experiment. C. The tests were video-recorded from a vantage point above the electrode system. The primary camera is indicated by the circle, the second camera was positioned near E5 (not shown). D. A flow-through ramp transitioned fish onto the apparatus. E. The non-conductive mesh stretched along the length of the apparatus protected fish from intense electric fields in the immediate vicinity of the electrodes. The experiment was conducted at the USACE, EL-ERDC, Vicksburg, Mississippi March – April 2010.

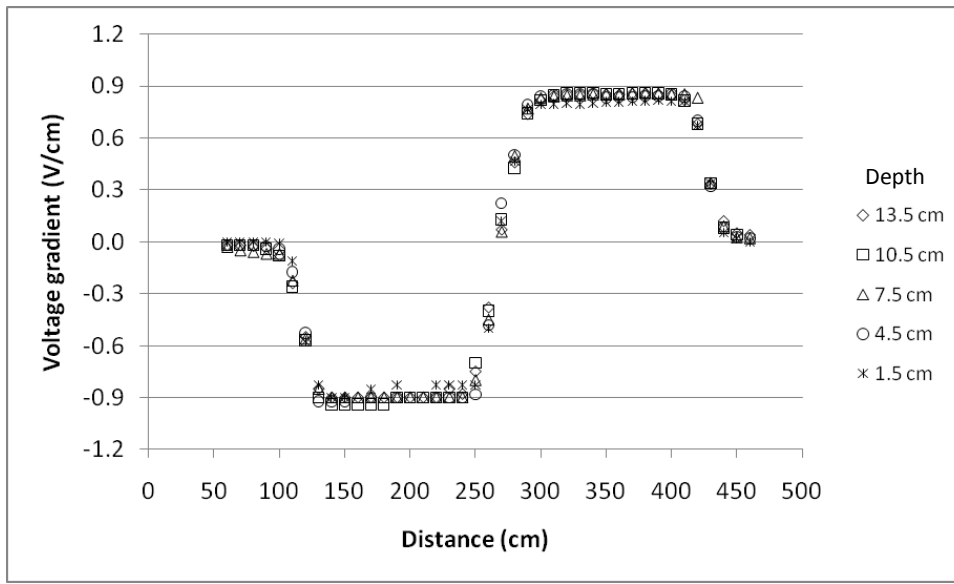


Figure 4 – 2. Profile of field strength (E, voltage gradient, V/cm) along the apparatus. Field strength (V/cm) at various water depths as a function of location along the experimental apparatus. Tests on small bighead carp volitional interaction with electric fields were conducted March – April 2010.

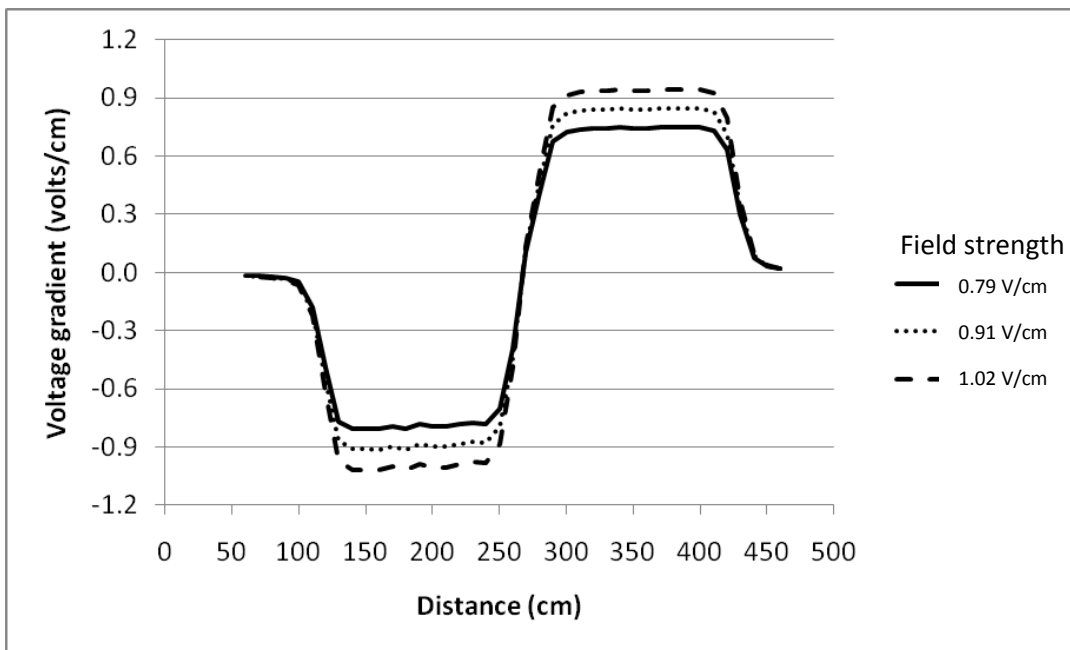


Figure 4 – 3. Field strength (V/cm) along the apparatus in the trials. Applied voltage was manipulated to achieve low 0.79 V/cm, 0.91 V/cm, and 1.02 V/cm levels of ultimate field strength in the tests on small bighead carp volitional interaction with electric fields conducted March – April 2010.

silver carp [ultimate field strength: 0.79 V/cm; pulse-frequency: 15 Hz; pulse-duration: 6.5 ms] in the pilot study. The operational protocol demonstrated effective in the pilot study was designated the baseline protocol for statistical comparisons. Another protocol in the tests was similar to that from the pilot study, but employed greater ultimate field strength: 0.91 V/cm, pulse-frequency: 15 Hz, pulse-duration: 6.5 ms. The voltage applied to the electrodes was manipulated, using the base electric field profile as a starting point, to achieve low (0.79 V/cm), medium (0.91 V/cm), and high (1.02 V/cm) levels of ultimate field strengths during the trials (Figure 4 – 3). The average field strength of the operational protocols tested were 50% to 115% of that of the protocol shown effective for immobilizing small silver carp in the pilot study (Table 4 – 1).

The trials were conducted on groups of fish, five fish per group. Individual fish were randomly assigned to groups; groups were randomly assigned to the operational protocols. The 20 operational protocols were treated as a replicate in the randomization scheme, with the sequence in which the protocols were tested randomized within each replicate. A single group of fish was assigned to each operational protocol, within each replicate. There were four replicates, a total of 20 fish per treatment. Fish were introduced into the raceway as a group.

Each of the trials began with a 5-minute period to allow fish to become familiar with the raceway and experimental apparatus prior to initiating the electrical test. Preliminary observations showed this 5-minute period adequate for the groups of fish to begin to swim freely in the raceway. Fish typically exhibited positive rheotaxis to the water current flow, swimming continuously into the water current.

The groups of fish were introduced into a section of the raceway previously blocked off with removable nets; fish were constrained to a section of the raceway upon introduction to maintain cohesion of the group. After a brief period, the upstream most net was removed. After fish had moved out of the immediate area, the remaining block net was removed to provide a continuous raceway. During this pre-exposure period, individuals losing association with the group were herded back to the group. In many cases, the groups of fish swam the entire raceway several times during the pre-exposure period, crossing the apparatus numerous times. Occasionally, individuals or groups swimming upstream stopped or hesitated at the ramp, these fish were gently herded up the ramp onto the apparatus. A single block net was placed in the raceway arm opposite the experimental apparatus, at the conclusion of the pre-exposure period, trapping fish downstream. Fish could only enter the apparatus from the downstream direction. Electrical testing was not initiated until all fish within a group crossed the experimental apparatus at least once during the pre-exposure period.

In the trials, the experimental apparatus was energized by the appropriate operational protocol for a period of 15 minutes. Care was taken to ensure that no fish were on the apparatus when it was initially energized; fish were not in the electric field as it was generated, but approached the field after it had been established. Behaviors of the fish and interactions with the electric field were observed and cataloged from a vantage point above the raceway. Two video cameras were mounted above the raceway; one was trained on the length of the apparatus, the other on the upstream-most edge. Video was reviewed to confirm counts of fish breaching the field and to estimate counts of challenges to the field. Fish successfully traversing the apparatus were netted on the upstream side of the apparatus, when possible, to prevent multiple crossings.

Fish were removed from the raceway after completion of the trial and the apparatus was de-energized. To minimize stress and handling, fish were individually transferred to a clear plastic bag and total length

Table 4 – 1. Average field strength of the operational protocols. The average of the ultimate field strength (FS) in the operational protocols applied in the evaluation of volitional challenge of electric fields by 51 – 76 mm bighead carp. Percent duty cycle was calculated with  $\% \text{ duty cycle} = 100\% \times (\text{pulse duration}/T)$ , where  $T$  (the period of the pulse) was calculated with  $T = 1/\text{pulse frequency}$ . Average field strength was calculated with  $FS_{\text{average}} = FS(\% \text{ duty cycle})$ .

Ultimate field strength (V/cm)	Pulse-frequency (Hz)	Pulse-duration (ms)	% Duty cycle	Ultimate field strength (V/cm) <sub>average</sub>
0.79	15	6.5	9.8	0.08
0.91	15	6.5	9.8	0.09
0.79	20	2.0	4.0	0.03
0.79	25	2.0	5.0	0.04
0.79	30	2.0	6.0	0.05
0.91	20	2.0	4.0	0.04
0.91	25	2.0	5.0	0.05
0.91	30	2.0	6.0	0.05
1.02	20	2.0	4.0	0.04
1.02	25	2.0	5.0	0.05
1.02	30	2.0	6.0	0.06
0.79	20	2.5	5.0	0.04
0.79	25	2.5	6.3	0.05
0.79	30	2.5	7.5	0.06
0.91	20	2.5	5.0	0.05
0.91	25	2.5	6.3	0.06
0.91	30	2.5	7.5	0.07
1.02	20	2.5	5.0	0.05
1.02	25	2.5	6.3	0.06
1.02	30	2.5	7.5	0.08

estimated for each fish through the bag, with fish remaining submersed in water. Afterward, fish were segregated in flow-through cages within a holding tank (described previously), which was treated with appropriate quantities of Stress Coat®. Survival was monitored for 24 hours and fish were then released into the holding tank.

*Data analysis.*— Data were pooled across replicate for analysis. The outcomes of interest were the proportion of fish successfully traversing the primary electric field and the proportion of successful challenges of the electric field between and among the experimental groups. Outcomes were summarized via analysis of contingency table margins measures of relative risk, and with descriptive statistics. Differences in proportions in the contingency table margins were evaluated with the Pearson

Chi-square test (Sall et al. 2007). Counts of fish penetrating the lower aspect of the electric field (E2 – E3) and the upper aspect of the field (E3 – E4) and percentage immobilized were reported.

The relative risk (RR), the ratio of the proportions being compared, was used to estimate risk (probability) of successful challenge of the electric fields among the various levels of ultimate field strength, pulse-frequency, and pulse-duration defining the operational protocols. Relative risk was also used to compare risk for passage and risk for successful challenge of fields generated by the various operational protocols compared to the field characterized by the baseline operational protocol. In the event of a zero cell in the tables, a constant (value of 1) was added to each cell of the table to allow estimation of relative risk (Agresti 1990). An RR exceeding 1.0 indicates an increase in risk of fish passing through the field (an undesired effect in this case). An RR less than 1.0 indicates a reduction in risk for fish to traverse the field. If RR = 1.0 or if 1.0 is within the bounds of the confidence interval, there is no indication of a difference in risk for passage between the operational protocols. Statistical analyses were accomplished using JMP statistical software, Version 8 (SAS 2009).

## Results

No mortality occurred during the 24 hour post-trial period of monitoring. Estimates of total length for fish in the experiment ranged from 48 – 82 (mean  $\pm$  standard deviation;  $60 \pm 6$ ) mm.

Fish exhibited positive rheotaxis, usually consistently swimming upstream into the flow of water. After the initial crossing of the apparatus during the pre-test phase of the trials, fish usually did not react to the presence of the apparatus (specifically the ramp) in the raceway. The fish typically swam in close association, as a group. Individuals separated from the group often retreated from the field and sought cover. In many cases, however, fish did challenge and interact with the electric field as individuals, often attempting to rejoin with individuals or the group as it penetrated the field. It was more common for fish to approach and challenge the field in pairs or as a group.

In many instances, fish followed, or attempted to follow, others into the electric field. As expected, smaller fish were less susceptible to the electric field relative to larger fish. Smaller fish appeared to penetrate more deeply into the field and to traverse the field more easily than larger fish. Larger fish often became immobilized during attempts to follow smaller fish through the field. It was common for fish immobilized (stunned) during encroachment upon the field to again challenge the electric field upon righting (after being immobilized/stunned and washed out of the electric field by water current flow). There were also cases where fish that were in the electric field followed other fish back downstream and exited the field.

During some tests, fish repeatedly challenged the downstream edge of the field, challenging and re-challenging the field upon deterrence. Often fish penetrating the field became immobilized repeatedly, repeatedly challenging and re-challenging the electric field after becoming tetanized in prior attempts. Individuals and groups of fish challenging the edge of the field often swam side-to-side in the channel, darting into and out of the field repeatedly. In some cases, groups of fish appeared to charge the field after having retreated downstream. In some groups of fish, challenges of the downstream edge of the field appeared to be instigated by one or two fish. Fish penetrating the field appeared distressed, usually swimming rapidly, with large undulations of the body, progressing upstream in a zigzag fashion; the exception was relatively small fish. Depending on the electrical treatment and the size of the fish, swimming ability was often interrupted in fish penetrating the field. There were several instances where



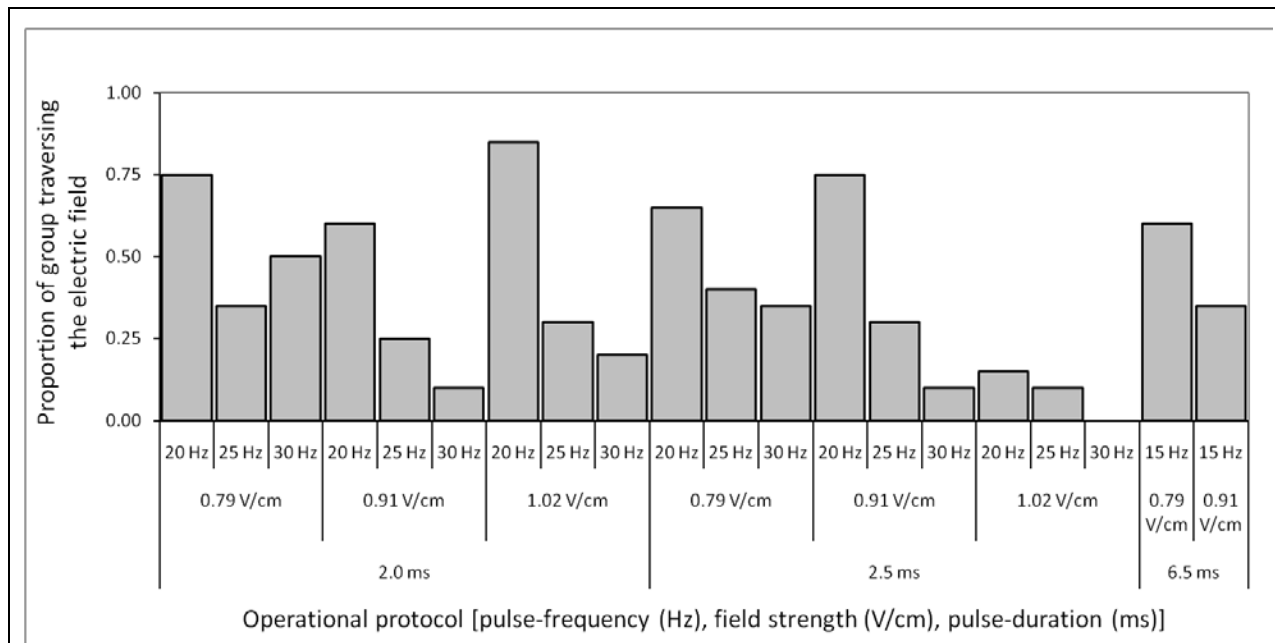


Figure 4 – 4. Proportions of small bighead carp traversing the field. Proportions of small bighead carp successfully traversing the field in the evaluation of volitional challenge of electric fields characterized by various operational protocols for electric barriers on the CSSC. Outcomes of tests on a total of 400 fish are represented. A randomized block design was employed in the experiment, where tests were conducted on groups (five fish), with four replicates, (replicates were treated as blocks). Outcomes were pooled across replicate; the proportion of groups of 20 fish successfully traversing the electric fields in the tests is shown.

fish that were maintaining position immediately downstream of the field margin immediately swimming upstream through the apparatus when the field was de-energized.

Overall, 153 (38%) fish in the trials traversed the length of the electric field. The proportions of fish within the experimental groups (replicates pooled) successfully traversing the electric field varied from 0.00 to 0.85 (Figure 4 – 4). Risk for successful passage through the field differed significantly among the levels of ultimate field strength (0.79 V/cm, 0.51; 0.91 V/cm, 0.35; 1.02 V/cm, 0.27;  $\chi^2 = 17.737$ ,  $P < 0.0001$ ), pulse-frequency (15 Hz, 0.48; 20 Hz, 0.63; 25 Hz, 0.28; 30 Hz, 0.21;  $\chi^2 = 52.734$ ,  $P < 0.0001$ ), and pulse-duration (2.0 ms, 0.43; 2.5 ms, 0.31; 6.5 ms, 0.48;  $\chi^2 = 7.302$ ,  $P = 0.0260$ ) defining the operational protocols.

Risk for fish to traverse the electric field was significantly reduced with operational protocols employing 0.91 V/cm (RR, 0.68; 95% CI 0.52 – 0.90) or 1.02 V/cm (RR, 95% CI 0.52 – 0.73) compared to those applying 0.79 V/cm, but did not differ significantly between those employing ultimate field strengths of 0.91 V/cm and 1.02 V/cm (RR, 0.76; 95% CI 0.53 – 1.11). Risk for fish to traverse the electric field with protocols applying 15 Hz did not differ significantly from those applying 20 Hz (RR, 1.31; 95% CI 0.92 – 1.87), but was significantly greater compared to protocols applying 25 Hz (RR, 0.60; 95% CI 0.39 – 0.92) or 30 Hz (RR, 0.44; 95% CI 0.27 – 0.71; Figure 4 – 5). Similarly, risk for fish to traverse the electric field was reduced with protocols applying 25 Hz (RR, 0.45; 95% CI 0.33 – 0.62) or 30 Hz (RR, 0.33; 95% CI 0.23 –

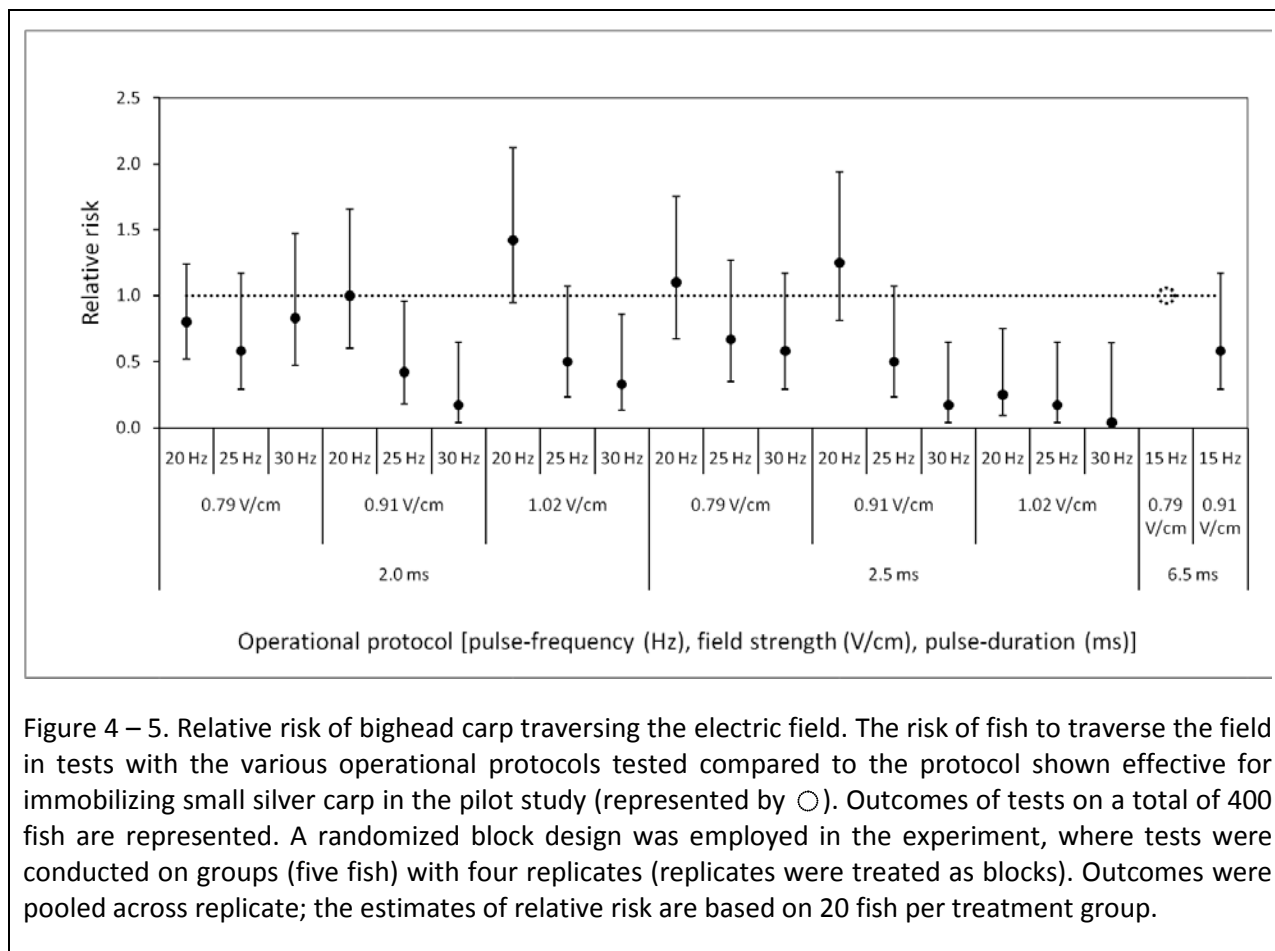


Figure 4 – 5. Relative risk of bighead carp traversing the electric field. The risk of fish to traverse the field in tests with the various operational protocols tested compared to the protocol shown effective for immobilizing small silver carp in the pilot study (represented by ○). Outcomes of tests on a total of 400 fish are represented. A randomized block design was employed in the experiment, where tests were conducted on groups (five fish) with four replicates (replicates were treated as blocks). Outcomes were pooled across replicate; the estimates of relative risk are based on 20 fish per treatment group.

0.49) compared to protocols applying 20 Hz. Risk for successful passage through the electric field did not differ significantly between protocols applying 25 Hz and 30 Hz (RR, 0.74; 95% CI 0.45 – 1.15). Risk for passage did not differ significantly between protocols applying pulse-durations of 2.0 ms and 6.5 ms (RR, 0.91; 95% CI 0.63 – 1.32), but was reduced with protocols applying pulse-durations of 2.5 ms when compared those applying 6.5 ms (RR, 0.65; 95% CI 0.44 – 0.97) and those applying 2.0 ms (RR, 0.72; 95% CI 0.55 – 0.94). Risk for small bighead carp to traverse the electric field was significantly reduced with 0.91 V/cm-2.0 ms-25 Hz, 0.91 V/cm-2.0 ms-30 Hz, 0.1.02 V/cm-2.0 ms-30 Hz, 0.91 V/cm-2.5 ms-30 Hz, and 1.02 V/cm-2.5 ms-20 Hz, 1.02 V/cm-2.5 ms-25 Hz, and 1.02 V/cm-2.5 ms-30 Hz protocols, compared to the protocol serving as the baseline (the protocol effective for silver carp in the pilot study; Figure 4 – 5).

There were 548 occurrences of fish encroaching upon the lower aspect of the field (the E2 – E3 zone), 18% of these incursions resulted in fish becoming immobilized. There were 234 instances of fish penetrating the upper aspect of the field (the E3 – E4 zone), with fish becoming immobilized in 27% of these incursions. There were 98 instances of fish using the recessed (window) area in the side of the raceway. The recessed area may have acted as a refuge, providing fish some protection from the electric field and water current flow. There were instances of fish entering the recessed area in the lower half of the field, exiting in the upper half of the field, and immediately continuing through the field. Although the recessed area may have provided some protection from water current flow and the electric field,

there was flow in the recessed area and the field did penetrate the recessed area, as there were also instances of fish becoming immobilized while in the recessed area and being washed out.

Fish challenged the electric field a total of 1551 times over the course of the experiment. Of these, 90% of the challenges failed, where fish interacted with the field but failed to traverse the field successfully [failed to penetrate the field or failed to traverse the field after penetration (immobilized and washed out downstream, immobilized and remained in the field or trapped in the field at the conclusion of the trial)]. The number of individual challenges varied among the operational protocols, from 30 to 171 ( $78 \pm 39$ ). The proportion of challenges resulting in successful passage through the electric field varied among the operational protocols, from 0.00 to 0.50 (Figure 4 – 6). Evidence of statistically significant differences in risk for successful challenges of the electric field was present in the analysis of the margins of the contingency tables; risk for successful challenge of the electric fields differed among the levels of ultimate field strength (0.79 V/cm, 0.17; 0.91 V/cm, 0.09; 1.02 V/cm, 0.05;  $\chi^2 = 36.395$ ,  $P < 0.0001$ ), pulse-frequency (15 Hz, 0.16; 20 Hz, 0.22; 25 Hz, 0.07; 30 Hz, 0.04;  $\chi^2 = 81.536$ ,  $P < 0.0001$ ), and pulse-duration (2.0 ms, 0.13; 2.5 ms, 0.06; 6.5 ms, 0.15;  $\chi^2 = 24.473$ ,  $P < 0.0001$ ; Figure 4 – 6).

Risk for successful challenge of the electric field was significantly reduced by operational protocols applying ultimate field strength of 0.91 V/cm (RR, 0.54; 95% CI 0.38 – 0.76) and 1.02 V/cm (RR, 0.32; 95% CI 0.22 – 0.48) compared to 0.79 V/cm (Figure 4 – 7). Similarly, risk for successful challenge of the field was significantly reduced in protocols applying 1.02 V/cm (RR, 0.60; 95% CI 0.39 – 0.92) compared to those applying 0.91 V/cm. Risk for successful challenge of the electric field with operational protocols applying 15 Hz did not differ significantly from those using 20 Hz (RR, 1.42; 95% CI 0.90 – 2.25), but was significantly greater compared to those applying 25 Hz (RR, 0.45; 95% CI 0.26 – 0.76) and 30 Hz (RR, 0.25; 95% CI 0.14 – 0.45). Risk for successful challenge of the electric field was significantly reduced with operational protocols applying 25 Hz (RR, 0.32; 95% CI 0.22 – 0.46) and 30 Hz (RR, 0.18; 95% CI 0.11 – 0.28) compared to those applying 20 Hz as well as for protocols applying 30 Hz (RR, 0.56; 95% CI 0.33 – 0.94) compared to those applying 25 Hz. Risk for successful challenge of the electric field did not differ between protocols utilizing 2.0 ms and 6.5 ms pulse-durations (RR, 0.87; 95% CI 0.55 – 1.39), but was significantly reduced when protocols utilized pulses of 2.5 ms duration compared to those using pulses of 6.5 ms (RR, 0.25; 95% CI 0.25 – 0.67) and those using pulses of 2.0 ms duration (RR, 0.47; 95% CI 0.34 – 0.66). Risk for successful challenge of the electric fields by small bighead carp was significantly reduced with several of the operational protocols tested, compared to the operational protocol effective for 137 to 280 mm (5.4 to 11 inch) silver carp (Figure 4 – 7).

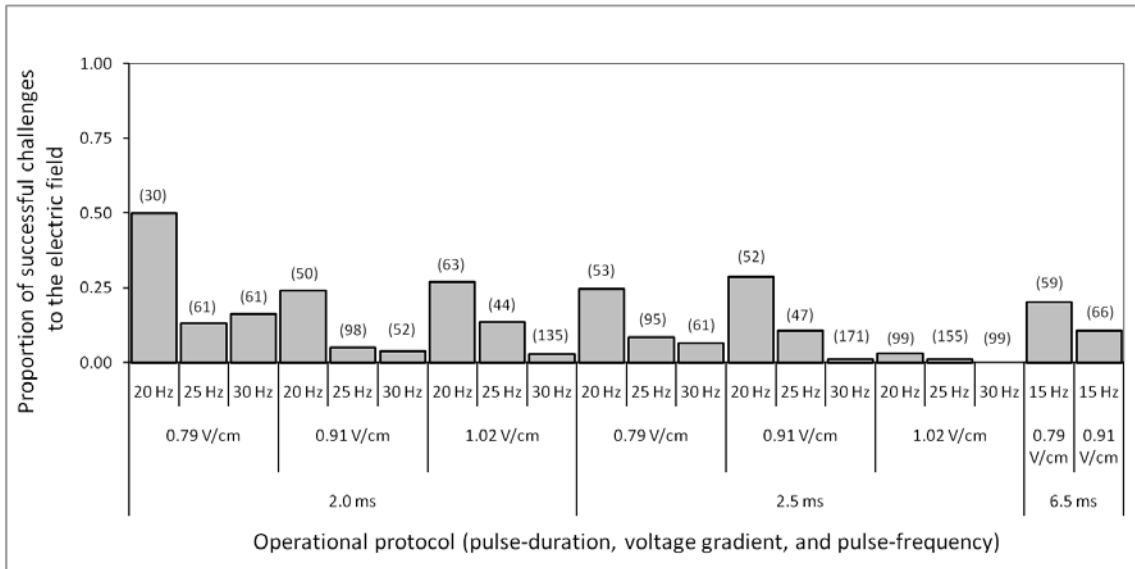


Figure 4 – 6. Proportion of successful challenges. Proportion of challenges by small bighead carp that led to fish successfully traversing the electric field in tests with various barrier operational protocols. Outcomes of tests on a total of 400 fish are represented. A randomized block design was employed, with tests conducted on groups (five fish) with four replicates. Outcomes were pooled across replicate (20 fish per experimental cell). Numbers above the columns (in parentheses) are counts of challenges to the electric field by fish in the experimental groups.

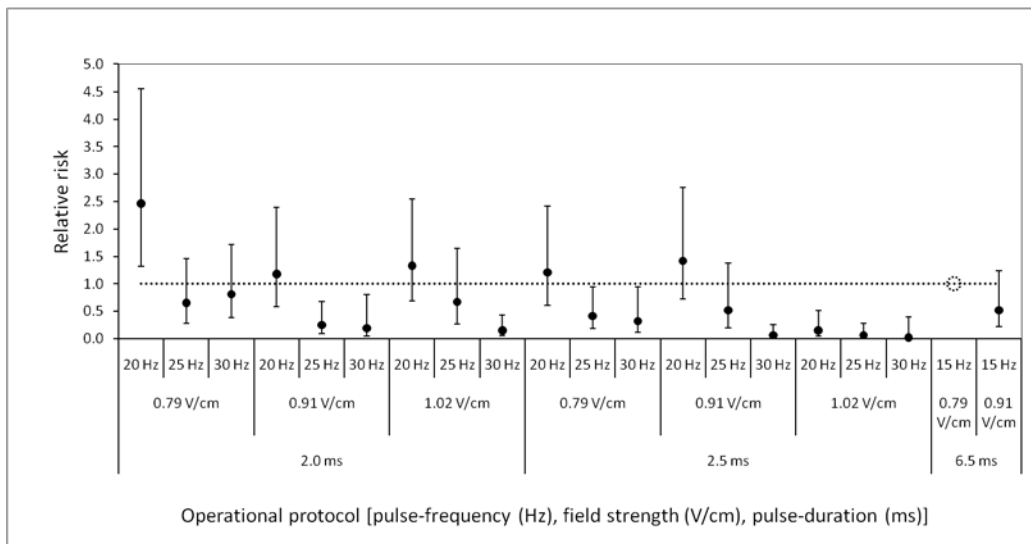


Figure 4 – 7. Relative risk for successful challenge of the electric field by small bighead carp. Risk relative to that with the operational protocol shown effective for immobilizing small silver carp in the pilot study (0.79 V/cm, 15 Hz, 6.5 ms). Outcomes of test with a total of 400 fish are represented. A randomized block design was employed, with tests were conducted on groups (five fish), with four replicates. Outcomes were pooled across replicate; the estimates are based on 20 fish per group.

## Discussion

The 6 – 7 cm/s water current flow in the flume, though relatively low, was adequate induce positive rheotaxis in small bighead carp, providing motivation to swim upstream. Thus, supporting the behavioral characteristic (tendency to swim upstream) reported by Zhong (1990).

Fish interacting with the electric field were clearly able to discern the downstream-most margin of the field. The behaviors at the edge of the field were largely dependent upon the characteristics of the operational protocol in the test. For example, in tests with protocols applying 0.91 V/cm or 1.02 V/cm ultimate field strengths and pulses at 30 Hz, fish often swam side-to-side and darted into and out of the field, repeatedly challenging the field. In tests with protocols applying 0.79 V/cm and pulses at 20 Hz, fish crossing the downstream most boundary sometimes exited the field briefly, then challenged the field again and despite apparent distress, progressed upstream in a zig-zag fashion via rapid, large undulations of the body (abnormal pattern of swimming). There were numerous occurrences of avoidance, where fish encroached upon the lower aspect of the field and immediately retreated downstream. There were also numerous occurrences of fish again encroaching upon the field after initial interactions and upon recovery from immobilization (tetany, incapacitation) incurred in previous incursions into the field.

The actions of the fish at the downstream margin of the field parallel the anecdotal descriptions of the actions of large fish maintaining position in the Canal at the downstream most margins of the low field of Barrier IIA. Fish near the water surface have been observed to swim upstream to a point within the field then drift downstream, repeatedly (personal communication, Doug Malone, Smith-Root, Inc., Vancouver, Washington). The equipotential boundary for penetration of the field, by these large fish, occurred near the downstream margin of the low field.

In the present study, whether field strengths associated with the downstream margin of the field served as equipotential boundaries for penetration by fish depended upon the operational protocol applied. In many instances, fish maintaining position at the origin of the field swam upstream through the apparatus immediately when the field was de-energized. Similar responses may occur on the Canal when the barriers are de-energized on purpose or accidentally; fish holding position in the field, or at the margin of the field, can be expected to resume upstream progress immediately upon de-energizing of the field. Thus, Barrier shutdown presents a significant threat. Development of protocols and procedures to prevent fish from progressing upstream in the event of accidental or scheduled shutdown of the Barriers is recommended.

The actions and behaviors of fish upon interacting with the sharply increasing gradients in electrical energy associated with the rising side of the high-field, in the screening experiments and the experiment with promising protocols previously described (Holliman, this report), indicate this region of the field could serve as the equipotential boundaries for incursion by small bighead carp on the Canal. In the simulations, flight responses were consistently evoked from fish in this region of the exposure, regardless of the operational protocol being tested. Similar responses were often observed in fish penetrating the field in the present study; fish penetrating the field appeared distressed, swam rapidly and abnormally, and utilized body-voltage minimizing actions. These fish continued upstream, despite significant distress, unless immobilized by the actions of the electric field. The rising side of the high-field may represent the equipotential boundaries for flight, rapid swimming and body-voltage minimizing behaviors, and recovery in fish immobilized during incursions into the high-field.

Fish continuing into the field despite electrical stimulation was the scenario applied in the simulations of encroachment described previously (Holliman, this report). In contrast, fish in the present study had opportunity to avoid the field and to exit the field after swimming into it. Fish actions and behaviors indicate they were able to detect the edge of the field and, therefore, could avoid entering or further interaction with the field. In many cases, however, fish challenged the field repeatedly. Further, fish often continued to challenge the field despite being immobilized (incapacitated) only moments earlier, re-challenging the field immediately upon recovery of an upright orientation. Outcomes in the present study are in accord with those reported by Barwick and Miller (1996) and support the observations of Stewart (1990) that fish receiving electrical stimulation may continue into fields of higher intensity.

Examination of data from the experiment revealed evidence of overdispersion as well as possible interactions in the experimental factors. Dispersion is a measure of the spread of data. Overdispersion indicated the variance (spread) of the data was greater than expected from a binomial distribution (Ramsey and Schafer 2002). Treatments were applied to fish in groups (5 fish per group). The experiment was designed for observations to be treated as independent, based on the expectation that fish receiving electrical stimulation would act independent of others in the group. The evidence of overdispersion indicates that the fish did not act independently, that there was a schooling effect. Thus, it may be necessary in future experiments with groups of fish to treat the group as the experimental unit, greatly increasing numbers of fish required. For example, the present experiment was conducted with 20 treatments and 20 experimental units (one fish per unit); if groups had been the experimental unit in this experiment 20 treatments x 20 experimental units (five fish per unit) then 2,000 fish would have been required for the experiment. Because there was evidence of overdispersion in the data, the p-values and confidence intervals should be regarded as optimistic. Nonetheless, the outcomes of the experiment provide clear evidence of differences in relative effectiveness of the operational protocols tested and the observations on fish behavior are invaluable to the project.

Risk for fish to breach the field varied among the operational protocols. Risk for fish to pass through the field was significantly reduced with protocols applying ultimate field strengths of 0.91 V/cm or 1.02 V/cm when compared to those applying 0.79 V/cm. There was no statistical difference in risk for passage between the two highest levels of field strength tested, indicating a possible threshold in effectiveness at 0.91 V/cm. There was no difference in risk for fish to breach the barrier between protocols applying 15 Hz and 20 Hz, but risk was reduced significantly with protocols applying 25 Hz or 30 Hz. Risk for fish to breach the barrier was not significantly different between protocols applying 25 Hz and 30 Hz, possibly indicating a threshold at 25 Hz in effectiveness. Risk for passage was reduced significantly when a pulse-duration of 2.5 ms was employed compared to 2.0 ms.

Risk of successful challenge of the field and risk for successful passage through the field was reduced significantly with several of the operational protocols (0.91 V/cm, 25 Hz and 30 Hz, 2.0 ms; 1.02 V/cm, 30 Hz, 2.0 ms; 0.91 V/cm, 30 Hz, 2.5 ms; and, 1.02 V/cm, 20 Hz and 25 Hz and 30 Hz, 2.5 ms) as compared to the protocol shown effective for small silver carp in the pilot study (0.79 V/cm, 15 Hz, 6.5 ms), the baseline. The ultimate field strength and pulse-frequency were greater in the operational protocols that reduced risk for successful challenge and passage compared to the baseline protocol. However, the pulse-duration was only 31% or 38% of that in the baseline protocol (2.0 ms and 2.5 ms versus 6.5 ms). Comparison of average field strength between the operational protocols reducing risk of passage with that of the baseline demonstrates as much as 41% reduction in average field strength.

Outcomes in the simulations in the screening and model development experiments indicate that penetration of the low field of Barrier IIA is likely, regardless of the operational protocol employed. The

actions and behaviors of fish in the present study, with consideration of actions and behaviors in the simulations of encroachment previously described (Holliman, this report), indicate the sharply increasing gradients on rising side of the high field may serve as equipotential boundaries for the onset of flight in 51 – 76 mm fish, but not avoidance. The continued challenge of the downstream margin of the electric field in the present study indicate it prudent to assume that fish will not avoid the high-field of Barrier IIA but will likely penetrate the high-field to the extent that they can. The operational protocol for the Barrier should be adequate to stun the smallest fish of interest. The outcomes of the present study indicates the behavior of 51 – 76 mm bighead carp to increase risk for breach of the Barrier, providing support for inclusion of behavior as a risk factor in the conceptual Risk Model for Barrier Effectiveness. The motivation for repeatedly challenging the electric field, with the exception of water current flow and apparent desire to follow others in the cohort, is not known. The trials in the experiment were only 15 minutes in duration. Additional study to evaluate volitional challenge of electric fields under various conditions of flow over longer periods of time is warranted.

The use of the recessed windows in the raceway provides indirect support for inclusion of habitat as a risk factor in the conceptual Model for Barrier Effectiveness. In the experiment, the recessed area in the raceway provided fish some protection from water flow and the electric field. Although observations of refuge use was not quantified and were anecdotal, use of the refuge by fish in the experiment appeared to increase risk for breach of the electric field. A similar circumstance could occur on the Canal, where cracks and crevices in the walls of the CSSC at the barrier field could afford small fish protection from water current flow and the electric field, allowing fish to recover from electrical exposure negating any cumulative effects of low gradient electrical exposure. Evaluation of cracks and crevices in the walls of the CSSC, within the barrier fields, as potential refuges is warranted.

## Work cited

- Agresti, A. 1990. Categorical data analysis. Wiley-Interscience Publication, New York, New York.
- Barwick, D. H, and L. E. Miller. 1996. Effectiveness of an electric barrier in blocking fish movement. Proceedings of the Annual Conference of the SouthEastern Association of Fish and Wildlife Agencies, 50: 139-147.
- Bullen, C. R. and T. J. Carlson. 2004. Non-physical fish barrier systems: their development and potential applications to marine ranching. Reviews in Fish Biology and Fisheries, 13: 201-211.
- Hartley, W. G. and D. Simpson. 1967. Electric fish screens in the United Kingdom. Pages 183-201 in R. Vibert, editor. Fishing with Electricity - Its Applications to Biology and Management. London, England: Fishing News Books.
- Kolar, C. S., D. C. Chapman, W. R. Courtenay, C. M. Housel, J. D. Williams, and D. P. Jennings. 2005. Asian carps of the genus *Hypophthalmichthys* (Pisces, Cyprinidae) – A biological synopsis and environmental risk assessment. Report to U.S. Fish and Wildlife Service 94400-3-012 LaCrosse, Wisconsin.
- Pegg M. A. and J. H. Chick. 2004. Aquatic nuisance species: an evaluation of barriers for preventing the spread of bighead and silver carp to the Great Lakes. Final Report, Illinois-Indiana Sea Grant.
- Ramsey, F. L. and D. W. Schafer. 2002. The Statistical Sleuth: A Course in Methods of Data Analysis, Second Edition. Belmont, California: Brooks/Cole Cengage Learning.
- Sall, J., Lee C. and A. Lehman. 2007. JMP® Start Statistics: a guide to statistics and data analysis using JMP®, fourth edition. Cary NC; SAS Institute Inc.
- SAS 2009. JMP, Version 8. SAS Institute Inc., Cary, NC, 1989-2009.
- Stewart, P. A. M. 1990b. Electric barriers for marine fish. In I. G. Cowx (Ed.), Developments in Electric Fishing (pp. 243-255). London, England: Fishing News Books.
- Zhong, W. G. 1990. Model LD-1 electric fishing screen in reservoir fisheries in China. Pages 297 – 305 in I.G. Cowx, editor. Developments in Electric Fishing. Fishing News Books, Blackwell Scientific Publications Ltd., Oxford, England.



## 5 – Effects of Water Velocity on Risk for Breach of Barrier Electric Fields by Small Bighead Carp

---

Summary.—Water velocity influences risk for breach of the barrier fields by invasive fishes. In experiments described previously, positive rheotaxis (swimming against the flow) was observed in 51 – 76 mm bighead carp in water flowing at 7 cm/s, but was absent with water flowing at 3 cm/s. Increases in the velocity of water flow may reduce risk for breach of the barrier field by encroaching fish by: (1) sweeping fish that attempt to minimize body-voltage back downstream, (2) forcing increased periods of alignment with the direction of electric current flow, (3) by magnification of deleterious effects of electroshock on swimming capabilities, and (4) through effects of electroshock associated with increased exposure duration. The effects of operational protocol and water velocity on risk for fish to maintain position during exposure to barrier field was evaluated in a controlled experiment. Small bighead carp [44 to 93 mm (1.7 – 3.7 inches) total length] were exposed to simulated barrier fields characterized by various operational protocols (ultimate field strength: 0.79 or 0.91 V/cm; pulse-frequency: 15, 20, or 25 Hz; pulse-duration: 2.0 or 6.0 ms) in water flowing at 7, 15, or 22 cm/s. Fish were exposed to homogeneous electric fields that changed in field strength over time to mimic the exposure of fish swimming through the Barrier IIA field, at the surface of the Canal. A total of 440 bighead carp, 20 fish per treatment group were used in the experiment. In comparisons among operational protocols applying pulses of 2.0 ms duration, risk for fish to maintain position in the field was significantly reduced by ultimate field strength of 0.91 V/cm as compared to 0.79 V/cm (0.36 versus 0.68; RR, 0.53, 95% CI 0.43 – 0.66), and pulse-frequency of 20 (RR, 0.80; 95% CI 0.65 – 0.98) or 25 Hz (RR, 0.40; 95% CI 0.29 – 0.55) as compared to 15 Hz (0.69) and 25 Hz (RR, 0.50; 95% CI 0.36 – 0.70) when compared to 20 Hz. Risk for fish to maintain position during the exposures was significantly reduced when water velocity was 22 cm/s (RR, 0.39; 95% CI 0.29 – 0.51) or 15 cm/s (RR, 0.54; 95% CI 0.42 – 0.68) compared to when it was 7 cm/s. There were no significant differences in risk for fish to maintain position between the various protocols and the protocol found effective for immobilization of small silver carp in the pilot study. Evaluation of water velocity and discharge data (retrieved from the USGS real-time monitoring site 05536890 CHICAGO SANITARY AND SHIP CANAL NR LEMONT, IL showed mean stream velocity, from January 2005 through June 2010 (~2000 readings), was 21.6 ( $\pm$  SD,  $\pm$  13) cm/s, daily mean velocity during this period exceeded 50 cm/s on 4% of the days, 22 cm/s on 37% of the days, 15 cm/s on 72% of the days, and 7 cm/s on 97% of the days. Risk for estimated daily mean water velocity to fall below 15 cm/s (the threshold for reducing risk in the experiment) was greatest in the month of November and least in the month of August. There was no indication of flow reversal in the estimates of daily mean velocity. Examination of finer scale discharge data, readings each minute from 3/1/2010 through 6/29/10, showed as incidence of reverse flow of 0.09% (159/169,478 minutes). Velocity of reverse flow was from -0.03 to -21 ( $-2.4 \pm 3$ ) cm/s, with 11 instances of flow exceeding -7 cm/s, with a single reading that exceeded 15 cm/s (the maximum of -21 cm/s). In the present study, exposure to field strengths associated with the low field sometimes interrupted normal swimming, but there was no significant effect on fish swimming capability as all fish maintained position during the exposure. The onset of flight, however, was accompanied by fish being swept downstream. Thus, the high gradients of the rising side of the high field may indicate equipotential boundaries for penetration of the barrier field by small bighead carp, in flowing water. The outcomes in the present experiment indicate risk for breach of the barrier is reduced when water current velocity is  $\geq$  15 cm/s.

---

## Introduction

Water current velocity is hypothesized to influence risk for breach of the barrier by invasive fishes and is included as a risk factor in the Conceptual Risk Model for Barrier Effectiveness (Holliman, this report). Prior research demonstrated that risk for breach of the electric barriers on the CSSC by nuisance invasive fishes is influenced by technical, biological, and environmental factors (Holliman, this report). The operational protocol (ultimate field strength, pulse-frequency, pulse-duration), a technical factor, strongly influenced risk for failing to immobilize small bighead carp, in simulations of encroachment. An inverse relation was demonstrated between fish size, a biological factor, and risk for breach of the barrier, where risk for breach of the barrier was reduced as fish size increased. Fish behavior, a biological factor, was demonstrated to influence risk for breach of the barrier, as fish repeatedly failed to avoid electric fields. The actions of the waterborne electric field on encroaching fish ultimately depend on the transfer of adequate quantities of electric energy from field to fish. The efficiency of this transfer decreases as the conductivity of water in the Canal increases (within the range of conductivity of water in the Canal). Thus, water conductivity, an environmental factor, influences risk for breach of the barrier by invasive fishes. It is hypothesized that water current flow velocity, another environmental factor, influences risk for breach of the barrier by invasive fishes, where risk for breach of the barrier is hypothesized to be inversely related to water current velocity.

The simulations of encroachment employed in the prior studies assumed no or very low water current flow as a worst-case scenario. The electric barriers on the Canal utilize cross-channel electrodes; the direction of electric current flow within the field parallels the direction of water current flow on the Canal. Fish encroaching upon the electric barrier experience the greatest electrical exposure (greatest body-voltage) when oriented parallel with the direction of electrical current flow (upstream-downstream direction). The intensity of the the electrical exposure, for fish encroaching upon the electric barrier, decreases as fish alignment deviates from parallel; body-voltage (electrical exposure) is minimum when fish are aligned perpendicular to electric current flow.

Silver carp, bighead carp and common carp share the behavioral characteristics of swimming against the flow (Zhong 1990). In experiments described previously, positive rheotaxis was observed in 51 – 76 mm bighead carp in water flowing at 7 cm/s, but was absent with water flowing at 3 cm/s, (Holliman, this report). Thus, when water current flow on the Chicago Ship Canal is  $\geq 7$  cm/s conditions may be favorable for water current flow to induce swimming against the flow in small bighead carp leading to challenge of barrier fields. However, if flow velocity exceeds the swimming capabilities of these small fish, they will be unable to progress upstream to challenge the barrier field. Under conditions of little or no water flow in the Canal, where positive rheotaxis (swimming against the flow) is not induced, the motivation for fish to challenge the electrical barrier is uncertain, but it is prudent to consider invasive fishes attempting to cross the barrier under this worst-case scenario. It is conceivable that under conditions of reverse flow on the Canal, if the flow is of sufficient magnitude to induce positive rheotaxis, invasive fish could swim into the flow away from the electric barriers.

Increases in the velocity of water flow may reduce risk for breach of the barrier by encroaching fish through sweeping fish that attempt to minimize body-voltage back downstream, forcing increased periods of alignment with the direction of electric current flow, by magnification of impacts of electroshock-induced reductions on fish swimming capabilities, and through effects associated with increased exposure duration. As the velocity of water flow increases, fish must align parallel with the direction of water flow to progress forward or hold position in the flow. The need to align with the

direction of water current flow, which simultaneously results in maximum electrical exposure, will compete with the need to minimize body-voltage by turning to the side, and being swept downstream.

Flight responses [rapid non-directed swimming and body-voltage minimizing behaviors] that often progressed into forced swimming and immobilization, were consistently induced in fish during simulations of encroachment into the electric field of Barrier IIA, upon exposure to the rising side of the high-field (Holliman, this report). The threshold field strengths for flight responses (in the simulations) likely represents the point in the electric field where small fish will dart either forward into the increasing field, or turn to the side to minimize body-voltage and progress along an equipotential line (Vibert 1967) or retreat downstream. Fish penetrating the electric barrier to the extent of receiving unpleasant stimulation (e.g., flight response) would experience reduced electrical exposure (body-voltage) upon turning perpendicular or near perpendicular to the direction of electric current flow, providing motivation for fish to maintain the orientation. Under conditions of no water current flow, fish turning near perpendicular to the direction of electric current flow, but still slightly upstream, could breach the barrier if the electrical stimulus is insufficient to render fish incapable of forward progress. Under conditions of flow, fish reducing body-voltage by turning to the side simultaneously orient perpendicular to the direction of water current flow and are swept downstream.

Risk to breach the barrier may be inversely related to water velocity though electroshock-induced reductions in swimming performance, through interference with normal neuro-muscular function. Fish swimming is a complex neuromuscular activity characterized by a rostral-caudal pattern of muscle activity resulting in undulatory motions that project fish forward (Wardle et al. 1995; Altringham and Ellerby 1999). If of sufficient magnitude, electric current introduced into the flesh of fish will override normal neuro-muscular transmissions. The induction of forced-swimming during the simulations, where flight often progressed into forced swimming behaviors, indicates interruption of the normal function of the neuro-muscular system and potential impairment of fish swimming ability. Depending on the magnitude and characteristics of electric current introduced, normal functioning of the nervous system may be interrupted and muscles involuntarily contracted (immobilization, tetanus). The threshold for interruption of volitional muscle activation (demonstrated by forced-swimming) was below that for complete immobilization. Thus, the threshold for electric current-induced impairment of swimming ability can be expected to be below the threshold for immobilization. If the interruption of normal muscle function will be sufficient to prevent upstream progress by fish encroaching upon the electric barrier is not known.

Swimming into the flow reduces the maximum forward progress possible by fish with the maximum forward progress inversely related to water flow velocity. Thus, as water flow velocity increases the minimum time for fish to traverse the field also increases. Risk to breach the barrier may be inversely related to water velocity through increased duration of exposure and manifested physiologically. A minimum duration of exposure was assumed the worst-case scenario in the simulations of encroachment described previously (Holliman, this report). It is hypothesized that longer exposure periods would increase probability of immobilization and shorter exposure periods would decrease probability of immobilization. The 88 second duration in the simulations (88 seconds) was calibrated to the estimated maximum sustainable swimming speed for 51 – 76 mm bighead carp and represented the minimum duration of exposure on the Canal (based on no water current flow). A direct relation has been demonstrated between duration of exposure to pulsed DC and mortality in bluegill *Lepomis macrochirus* (90 to 170 mm length), fantail darters *Etheostoma flabellare* (25 mm to 75 mm length; Whaley et al. 1978) and Cape Fear shiners *Notropis mekistocholas* (25 – 65 mm length; Holliman et al. 2003), in the context of electrofishing. Sternin et al. (1976) noted that the reaction of an organism

depends not only on the intensity of an action at an instant, but on the overall volume of the stimulant also. The cumulative effect of an electrical exposure may lead to changes in fish reaction or even gradual depression of the central nervous system. When the intensity of direct current is increased slowly, immobilization can be induced by the simultaneous effects of low gradient and cumulative exposure, narcosis sans the typical progression of fish reaction (i.e., perception/first response, taxis, pseudo-forced swimming, immobilization; Sheminsky 1924, *in* Sternin et al. 1976). Thus, increases in water velocity are expected to increase the time necessary for fish to traverse the electric field, increasing the duration of exposure, decreasing risk for breach of the barrier.

The objective in this phase of the study was to evaluate the relation between water current velocity on the Chicago Sanitary and Ship Canal and risk for breach of the electric barrier by 51 – 76 mm bighead carp. The objective was achieved by evaluating the outcomes of simulations of encroachment upon electric barrier IIA by 51 – 76 mm bighead carp under various conditions of flow (water velocity). In the simulations, an electric field was generated in a variable flow swim tunnel (Brett Swim tunnel). The intensity of the electric field was varied over the course of the trials to simulate the electrical exposures to fish traversing barrier IIA at the surface of the Canal would experience. Various operational protocols [(ultimate field strength (V/cm), pulse-frequency (Hz), pulse-duration (ms))] were evaluated at various rates of water velocity. The operational protocols evaluated were within the estimated output capabilities of Barrier IIA with water conductivity in the Canal at 2000  $\mu\text{S}/\text{cm}$ . The duration of the electrical exposures were calibrated to the maximum estimated net swimming speed, the difference between the estimated maximum sustainable swimming speed and water current flow velocity. The primary outcome of interest in the experiment was the proportion of fish maintaining position (not impinged upon the swim tunnel posterior screen) during electrical exposures.

The need to evaluate effects of water current flow on risk for breach of the electric barriers on the Canal was critical. Unfortunately, prior experimentation exhausted stores of available fish. Rather than forgo the experiment, fish from the experiment on volitional challenge of electric fields (Holliman, this report) were reused in the present study. Electrical exposure to individual fish in the volitional challenge experiment varied markedly. The effects that the previous electrical exposures may have on outcomes in the present study are unknown.

## Methods

The ability of small bighead carp encroaching upon the field of Barrier IIA to maintain position in the barrier field under various conditions of water current flow was simulated under controlled conditions. The experiment was conducted at the USACE, Aquatic Ecosystem Research and Development Center, Environmental Laboratory, Engineer Research and Development Center, Vicksburg, Mississippi from 23 March 2010 to 8 April 2010. Pond cultured bighead carp previously used in the experiment on volitional challenge of electric field previously described (Holliman, this report) were used in the study.

Simulations of encroachment into the field of Barrier IIA by small bighead carp, under various conditions of water current flow, were conducted in the rectangular portion (57.5 cm x 52.1 cm, with 152.4 cm electrode spacing) of a Brett Swim Tunnel (Figure 5 – 1). The swim tunnel was a closed, recirculating system, with water flow generated by a spinning propeller, which was controlled by a variable speed, electric motor. Rates of water velocity in the test tank were established with measurements taken at locations equally spaced along the length and across the width of the chamber,

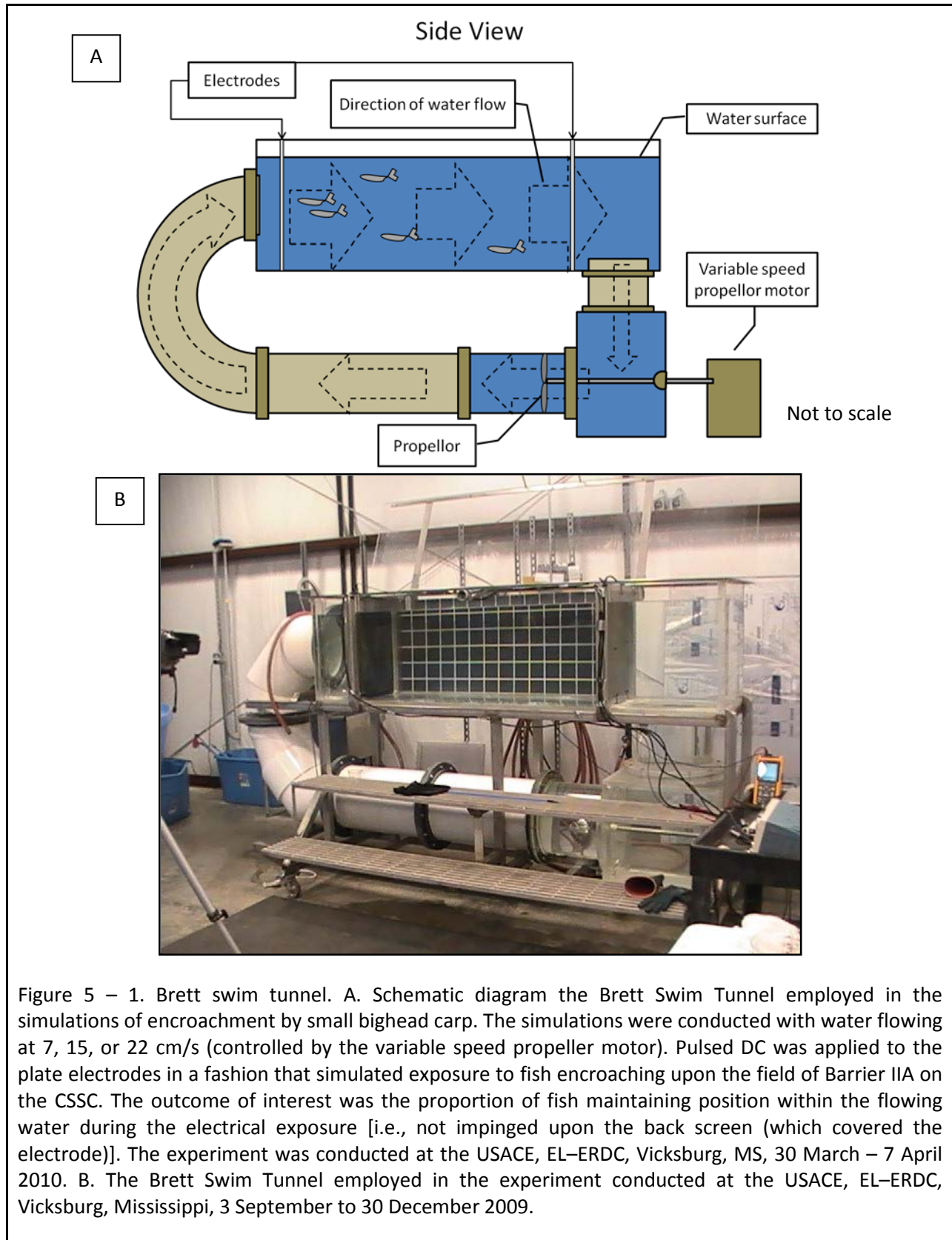


Figure 5 – 1. Brett swim tunnel. A. Schematic diagram the Brett Swim Tunnel employed in the simulations of encroachment by small bighead carp. The simulations were conducted with water flowing at 7, 15, or 22 cm/s (controlled by the variable speed propeller motor). Pulsed DC was applied to the plate electrodes in a fashion that simulated exposure to fish encroaching upon the field of Barrier IIA on the CSSC. The outcome of interest was the proportion of fish maintaining position within the flowing water during the electrical exposure [i.e., not impinged upon the back screen (which covered the electrode)]. The experiment was conducted at the USACE, EL–ERDC, Vicksburg, MS, 30 March – 7 April 2010. B. The Brett Swim Tunnel employed in the experiment conducted at the USACE, EL–ERDC, Vicksburg, Mississippi, 3 September to 30 December 2009.

at depths 8 cm, 25 cm, and 43 cm off the bottom, replicated three times, using a digital, rod-suspended water current meter.

The strength of the electric field in the swim tunnel varied over the course of the electrical exposures to simulate that experienced by fish traversing the field of Barrier IIA at the surface of the Canal (Figure 5 – 2). Water in the swim tunnel was between 19.4 and 20.7 ( $20.11 \pm 0.43$ ) °C with ambient conductivity from 1961 to 2084 ( $2027 \pm 42$ )  $\mu\text{S}/\text{cm}$ . Experimental protocols and procedures were similar to those in the screening and directed experiments.

A total of 21 operational protocols, including a null treatment, were evaluated in the trial. The barrier operational protocols applied in the simulations were characterized by a DC pulse-duration of 2 ms, a pulse-frequency of 15 Hz, 20 Hz, or 25 Hz, and ultimate field strengths of 0.79 V/cm or 0.91 V/cm (Figure 5 – 2). Additionally, a protocol similar to that shown effective for immobilizing 137 to 280 mm silver carp was included in the experiment [ultimate field strength, 0.79 V/cm; pulse-frequency, 15 Hz; pulse-duration, 6.0 ms]. The operational protocols were applied with water flowing at 7 ( $\pm 1$ ) cm/s, 15 ( $\pm 4$ ) cm/s, and 22 ( $\pm 4$ ) cm/s. Fish were monitored during the simulations to determine whether fish maintained position or were swept back and pinned on the posterior screen of the swim tunnel (impinged on the back screen). Two video cameras were trained on the test tank, recording actions and behaviors of fish during the treatments. Video was reviewed to confirm and refine outcomes of the simulations.

Fish challenging the electric field of Barrier IIA would be traveling upstream, against the direction of water current flow. The duration of the simulations, which determined rates of change in field strength, was calibrated to estimated time for required for small bighead carp to traverse the ~ 44 meter electric barrier under various conditions of water current flow. Maximum sustained swimming speeds of bighead carp was 20 cm/s in swim tests on individuals and 40 cm/s in swim tests on groups of 3 or 5 fish. Bighead carp from the cohort typically swam 50 cm/s for less than 1 minute, although some high performers in groups did swim longer periods (personal communication, Dr. Jack Killgore, Dr. Jan Hoover, USACE, Environmental Laboratory – Engineer Research Development Center, Vicksburg, Mississippi). The exposure periods in the simulations were based on a swimming speed of 50 cm/s, exposures of 88 seconds under conditions of no flow.

Any water current flow in the Canal reduces the rate of forward progress of fish challenging the electric field, increasing the amount of time fish would be in the electric field. The duration of the simulations was calibrated to the “net swimming speed”, the difference between a swimming speed of 50 cm/s and the water current velocity in the test. The simulations were 103, 123, or 154 seconds duration, conducted with water velocity at 7 cm/s, 15 cm/s or 22 cm/s (Figure 5 – 2).

The simulations of encroachment were conducted with groups of fish, five fish per group. Individual fish were randomly assigned to groups; groups were randomly assigned to the operational protocol being tested. There were 21 experimental treatments (20 combinations of operational protocol and water current flow and a null treatment group) evaluated. The operational protocols applied ultimate field strength of 0.79 V/cm or 0.91 V/cm, pulse frequencies of 15, 20, or 25 Hz, at a pulse-duration of 2 ms. Simulations of encroachment applying the operational protocol similar to that effective for immobilizing small silver carp in the pilot study (ultimate field strength: 0.79 V/cm; pulse-frequency: 15 Hz; pulse-duration: 6.0 ms) were conducted at each of the water velocities to provide a baseline for comparison. The sets of operational protocols were treated as replicates in the randomization scheme, with the

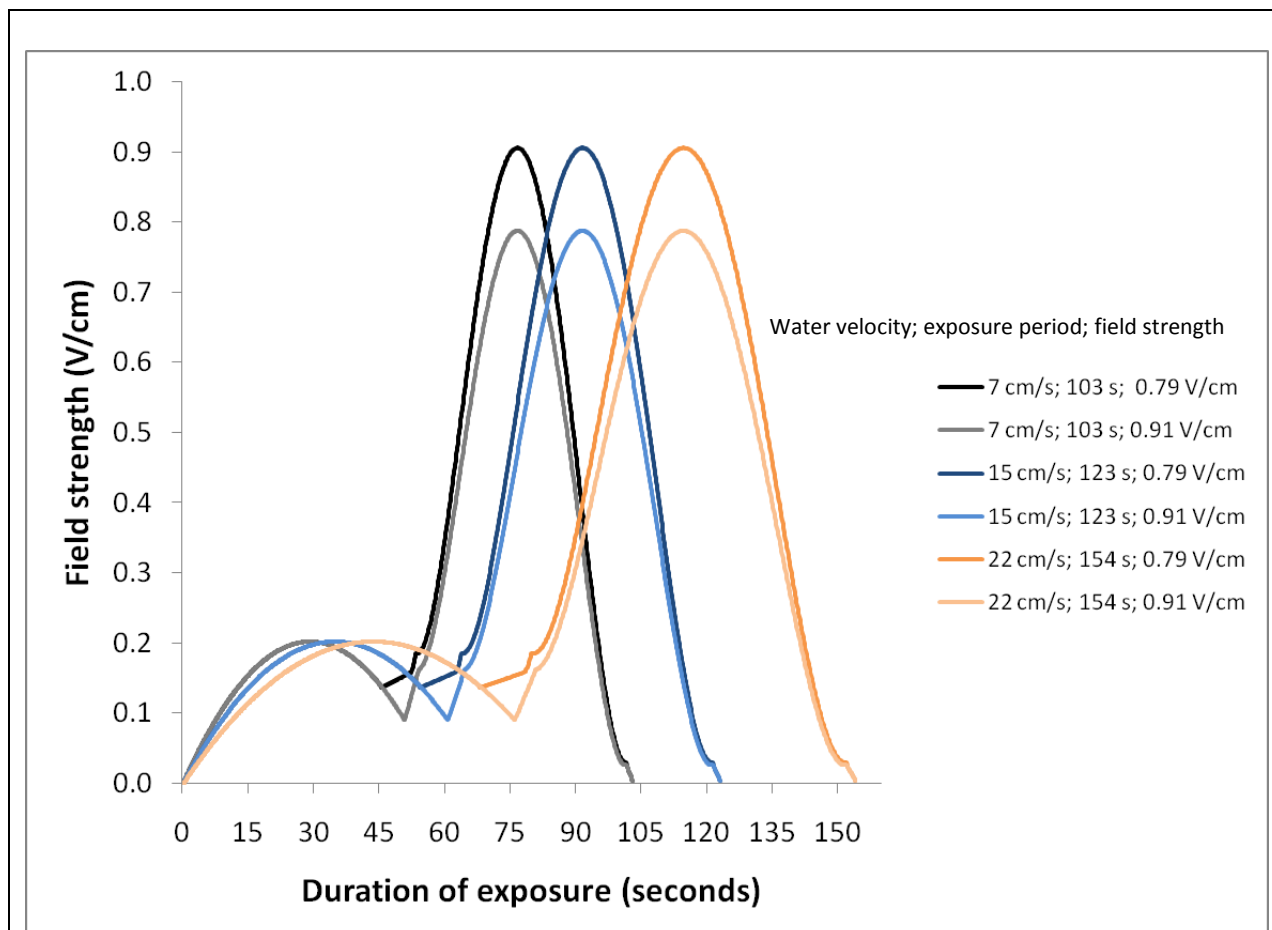


Figure 5 – 2. Electric field in the simulations. The electric field strength varied with time in the simulations of encroachment into Barrier IIA under various conditions of water current flow in the Canal. The simulations were applied at ultimate field strengths of 0.79 V/cm and 0.91 V/cm. The durations of the exposures (103 s, 123 s, 154 s) were calibrated to a swimming speed of 50 cm/s, matched with water flow velocity (7 cm/s, 15 cm/s, 22 cm/s), and simulated the time required for small bighead carp to traverse the 44 m field of Barrier IIA. The experiment was conducted at the USACE, EL-ERDC, Vicksburg, Mississippi, 30 March – 7 April 2010.

sequence in which the protocols were tested randomized within each replicate. The goal for the experiment was four replicates, a total of 20 fish per operational protocol.

It was necessary to reuse bighead carp from the volitional behavior experiment because of limited fish availability, (Holliman, this report). Because the effects that the prior electrical exposure may have had on the fish were unknown, it was necessary to establish fitness of the experimental animals prior to use in this experiment. Prior to the electrical simulation, fish were transferred to the swim tunnel as a group and left undisturbed for a period of 15 minutes with water velocity at 0 cm/s. Water velocity in the swim tunnel was then increased to 7 cm/s for 5 minutes, then to 15 cm/s for 5 minutes, and then to 22 cm/s for 5 minutes. Water velocity was then reduced to 0 cm/s for 5 minutes (a 5-minute recovery period) prior initiation of the electrical tests. The group was replaced if fish struggled or failed to hold position

during this “fitness test”. The simulations of encroachment were conducted immediately following the completion of the 35-minute cycle of recovery-swim-recovery. The ability of fish to maintain position in the tank in the absence of electrical exposure was established with a total of 20 fish (4 groups of five), randomly designated as controls (null treatment). In the null treatment, instead of electrical exposure after the “fitness test” water velocity was increased to 22 cm/s, the maximum velocity employed in the simulations, for a period of 154 seconds (the maximum period of the simulations).

*Data analysis.*— Data were pooled across replicate for analysis. The outcomes of interest were proportions of fish maintaining position (not impinged upon the posterior screen of the swim tunnel) during the simulations. Outcomes were summarized via analysis of contingency table margins, including measures of relative risk and descriptive statistics. Statistical significance was evaluated with the Pearson chi-square test (Sall 2007). The relative risk (RR), the ratio of the proportions being compared, was used to estimate risk (probability) for failing to impinge fish during the simulation (i.e., fish maintained position in the field) between the various levels of the factors defining the operational protocols. The operational protocol similar to that effective for immobilizing 137 to 280 mm silver carp [ultimate field strength: 0.79 V/cm; pulse-frequency: 15 Hz; pulse-duration: 6.0 ms] was designated a baseline for comparisons of risk for failing to impinge fish during the simulation. The RR was used to estimate risk of fish not being impinged between the operational protocols under consideration and the baseline protocol, within each of the levels of water velocity, and to compare risk between levels of water velocity when the baseline protocol was applied. In the event of a zero cell in the tables, a constant (value of 1) was added to each cell of the table to allow estimation of relative risk (Agresti 1990). An RR exceeding 1.0 indicates an increase in risk of failing to impinge fish (an undesired outcome). An RR less than 1.0 indicates a reduction in risk for failing to impinge fish during the simulation. If RR = 1.0 or if 1.0 is within the bounds of the confidence interval, there is no indication of a difference between the operational protocols in risk for failing to impinge fish.

Water velocity and discharge data were retrieved from the USGS real-time monitoring site 05536890 CHICAGO SANITARY AND SHIP CANAL NR LEMONT, IL ([http://waterdata.usgs.gov/il/nwis/uv/?site\\_no=05536890&PARAMeter\\_cd=00065,00060](http://waterdata.usgs.gov/il/nwis/uv/?site_no=05536890&PARAMeter_cd=00065,00060)). Linear regression of discharge (cubic feet per second) on water velocity (feet per second), acquired every minute from 3/1/2010 – 6/29/2010, was employed to establish the relation between the two variables. The resulting regression equation was applied to mean daily discharge data from 1/1/2005 – 6/27/2010 to estimate mean daily water velocity (feet per second) over the period, which were converted to cm/s. The distribution of estimated daily mean velocities were summarized via outlier boxplots, where the lower edge of the box represented the lower quartile, the upper edge the upper quartile [the distance between the upper and lower edges is the interquartile range (IQR)], and the middle of the box represented the median. The tails of the box extend to farthest point falling within 1.5 x IQR (Sall et al. 2007). Percentages were used to summarize counts of daily mean velocity exceeding 7 cm/s, 15 cm/s, 22 cm/s, and 50 cm/s. The proportion of days per month with daily mean velocity less than 7 cm/s, 15 cm/s, 22 cm/s, and 50 cm/s, over this period, was used to quantify risk associated with water velocity by month. Statistical analyses were accomplished using JMP statistical software, Version 8 (SAS 2009).

## Results

A total of 440 bighead carp, from 44 to 93 ( $61 \pm 7$ ) mm total length and weighing from 0.7 to 7.2 ( $2.1 \pm 0.8$ ) grams, were used in the experiment. No fish were impinged upon the swim tunnel posterior screen during the recovery-swim-recovery fitness tests conducted prior to the simulations. No fish designated as controls were impinged on the back screen during the experimental treatments.



All fish maintained position within the field during the simulations of encroachment during exposures to field strengths associated with the low-field. There were behavioral manifestations of electrical exposure to field strengths associated with the low-field, as normal swimming patterns were interrupted, by starts, jerks, vibrations, and increased rates of tail-beats. Flight responses, forced-swimming, and immobilization were induced upon exposure to the high-field. Fish demonstrated a tendency to collect near the upstream-most screen prior to exposure to the rising-side of the high field, indicating water current velocity was less than the maximum swimming speed and that swimming performance was not severely impeded. In most cases, exposure to the rising-side of the high field resulted in rapid, non-directed swimming and fish being swept or drifting back in the swim tunnel toward the downstream most screen, regardless of whether or not impingement eventually occurred. Anecdotal observation of fish response during exposure to field strengths associated with the low field indicate fish reacted more strongly to the cathode than the anode.

A total of 212 (50%) fish were maintained position in the electric fields (were not impinged) during the simulations of encroachment. Proportions of fish not impinged ranged between 1.00 and 0.05 (Figure 5 – 3). Analysis of contingency table margins demonstrated that the proportions of fish not impinged during the simulations differed significantly among the three levels of water velocity (7 cm/s, 0.76; 15 cm/s, 0.44; 22 cm/s, 0.30;  $\chi^2 = 56$ ;  $P < 0.0001$ ). Risk for failing to impinge fish during the electrical exposures was significantly reduced when water current velocity was 22 cm/s (RR, 0.39; 95% CI 0.30 – 0.52) or 15 cm/s (RR, 0.57; 95% CI, 0.45 – 0.72) compared to when it was 7 cm/s. Similarly, risk for failing to impinge fish during the simulations of encroachment was significantly reduced when water current velocity was 22 cm/s compared to when it was 15 cm/s (RR, 0.69; 95% CI 0.49 – 0.94).

In comparisons among operational protocols applying pulses of 2.0 ms duration, risk for failing to impinge fish during the simulations was significantly reduced with operational protocols applying an ultimate field strength of 0.91 V/cm compared to those applying 0.79 V/cm (0.36 versus 0.68; RR, 0.53, 95% CI 0.43 – 0.66). Proportions of fish not impinged during the simulations differed significantly among the pulse frequencies characterizing the operational protocols (15 Hz, 0.69; 20 Hz, 0.55; 25 Hz, 0.28;  $\chi^2 = 42$ ;  $P < 0.0001$ ). Risk for failing to impinge fish was significantly reduced when 20 Hz (RR, 0.80; 95% CI 0.65 – 0.98) or 25 Hz (RR, 0.40; 95% CI 0.29 – 0.55) was applied in the operational protocols compared to when 15 Hz (0.69) was applied. Similarly, risk for failing to impinge fish was significantly reduced when operational protocols employed a pulse-frequency of 25 Hz (RR, 0.50; 95% CI 0.36 – 0.70) compared to when 20 Hz was applied. Proportions of fish not impinged differed significantly among the three rates of water velocity (7 cm/s, 0.78; 15 cm/s, 0.42; 22 cm/s, 0.31;  $\chi^2 = 61$ ;  $P < 0.0001$ ). Risk for fish to not be impinged during the simulations was significantly reduced when water velocity was 22 cm/s (RR, 0.39; 95% CI 0.29 – 0.51) or 15 cm/s (RR, 0.54; 95% CI 0.42 – 0.68) compared to when it was 7 cm/s, but not when water velocity was 22 cm/s (RR, 0.73; 95% CI 0.52 – 1.03) compared to 15 cm/s (Figure 5 – 4).

Risk for failing to impinge fish in simulations applying the baseline protocol (field strength, 0.79 V/cm; frequency, 15 Hz; pulse-duration, 6.0 ms) was significantly reduced when water velocity was 22 cm/s (RR, 0.21; 95% CI 0.09 – 0.51) or 15 cm/s (RR, 0.42; 95% CI 0.24 – 0.73) compared to when water velocity was 7 cm/s, but was not significantly different between water velocities of 22 cm/s (RR, 0.5; 95% CI 0.18– 1.40) and 15 cm/s. No obvious patterns were apparent among simulations with the various

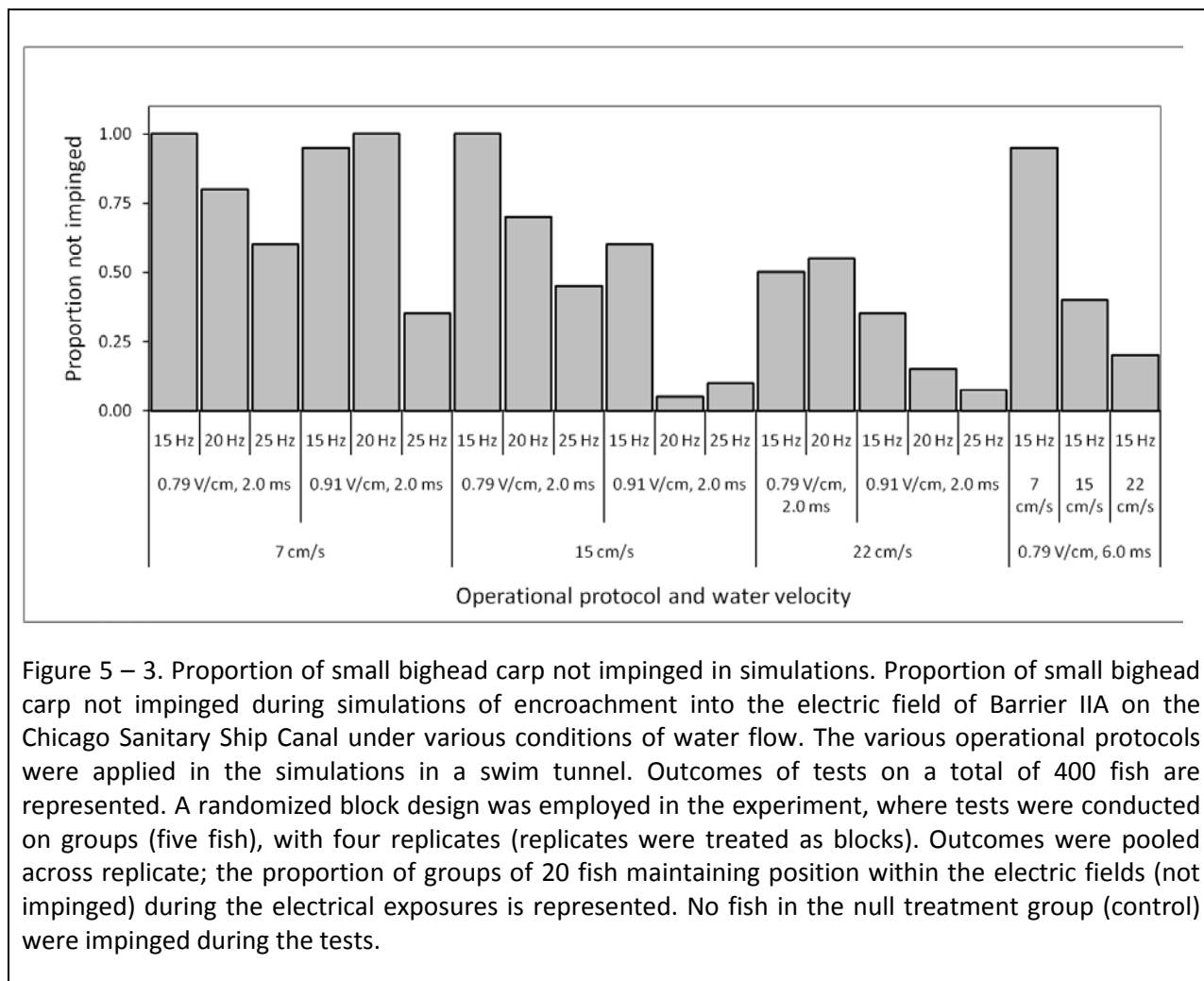


Figure 5 – 3. Proportion of small bighead carp not impinged in simulations. Proportion of small bighead carp not impinged during simulations of encroachment into the electric field of Barrier IIA on the Chicago Sanitary Ship Canal under various conditions of water flow. The various operational protocols were applied in the simulations in a swim tunnel. Outcomes of tests on a total of 400 fish are represented. A randomized block design was employed in the experiment, where tests were conducted on groups (five fish), with four replicates (replicates were treated as blocks). Outcomes were pooled across replicate; the proportion of groups of 20 fish maintaining position within the electric fields (not impinged) during the electrical exposures is represented. No fish in the null treatment group (control) were impinged during the tests.

operational protocols in the risk for failing to impinge fish relative to those simulations applying the baseline protocol. In most cases, the 95% confidence intervals about the point estimates of RR included 1.0, indicating no significant difference in risk for failing to impinge fish in the simulations with the various operational protocols relative to the protocol employed as a baseline (Figure 5 – 4).

A strong relation was apparent between discharge [cubic feet per second (fps)] and stream velocity (fps; Figure 5 -5). The simple linear regression of stream velocity on discharge data collected from 3/1/2010 through 6/29/2010 was significant ( $P < 0.00001$ ) and provided  $R^2 = 0.998$  and the equation  $stream\ velocity, fps = -0.02813 + 0.000251(discharge, cubic\ fps)$ . Application of the regression equation to daily mean discharge data from 1/1/2005 – 6/27/2010 provided estimates of stream velocity from 5 to 129 cm/s (Figure 5 – 6). The estimated mean stream velocity from January 2005 through June 2010 was 21.6 ( $\pm SD, \pm 13$ ) cm/s.

From January 2005 through June 2010, estimated daily mean velocity was  $\geq 50$  cm/s for 4% of the days,  $\geq 22$  cm/s for 37% of the days,  $\geq 15$  cm/s for 72% of the days, and  $\geq 7$  cm/s for 97% of the days (Figure 5 – 7). Risk for estimated daily mean water velocity to fall below 15 cm/s was greatest in the month of

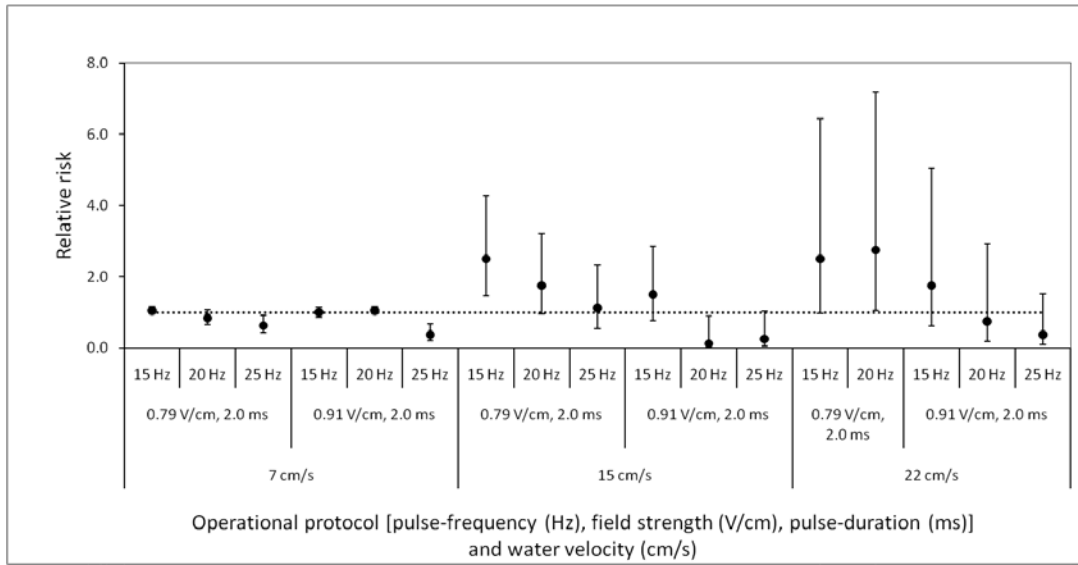


Figure 5 – 4. Relative risk for fish to maintain position. Relative risk of small bighead carp not being impinged (to maintain position) during simulations of encroachment into the electric field of Barrier IIA, on the Chicago Sanitary and Ship Canal, with various operational protocols, at various rates of water flow velocity. Risk for fish to not be impinged during simulations with each protocol was compared with risk from simulations applying an operational protocol similar to that effective for immobilizing small silver carp in the pilot study [ultimate field strength: 0.79 V/cm; pulse-frequency: 15 Hz; pulse-duration: 6.0 ms] conducted at the same water velocity. That is, risk comparisons were made within levels of water velocity. Outcomes of tests on a total of 420 fish are represented. A randomized block design was employed in the experiment, where tests were conducted on groups of fish (five fish per group), with four replicates (replicates were treated as blocks). Outcomes were pooled across replicate; the estimates of relative risk are based on 20 fish per treatment group. No fish in the null treatment group (control) were impinged during the tests.

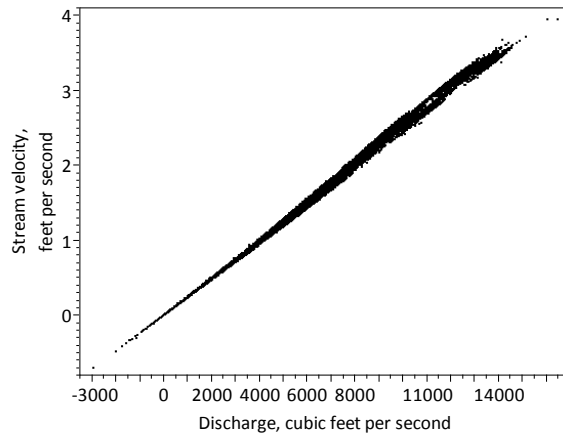


Figure 5 – 5. Water velocity as a function of discharge on the Canal. Discharge and stream velocity data for the Chicago Sanitary Ship Canal from 3/1/2010 – 6/29/2010 retrieved from station USGS 05536890 located near Lemont, IL.

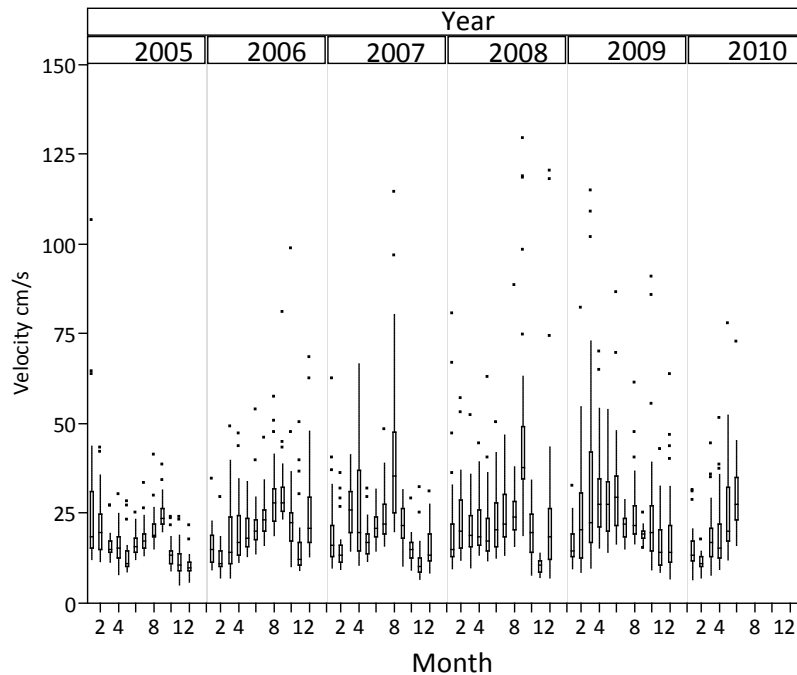


Figure 5 – 6. Boxplots and point estimates of daily mean water velocity on the Canal. Daily mean velocity (cm/s) for the Chicago Sanitary Ship Canal, by month (1 – 12) and year from 1/2005 to 6/2010, was estimated from daily mean discharge data collected at the USGS monitoring station (05536890) located near Lemont, IL. Mean water velocity was 21.6 ( $\pm$  13) cm/s for the period.

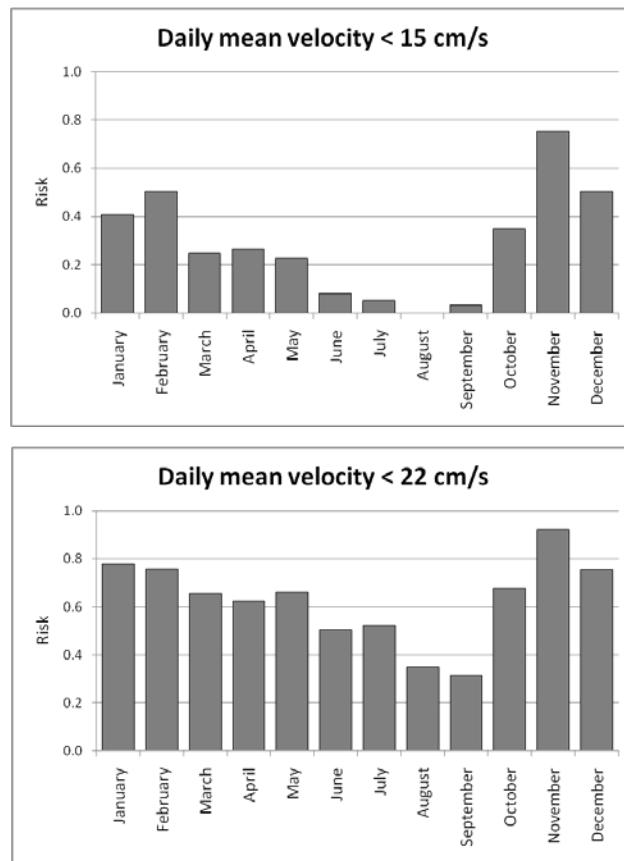


Figure 5 – 7. Risk for daily mean water velocity to be less than 15 and 22 cm/s. Risk for daily mean water velocity (cm/s) to be less than 15 or 22 cm/s on the Chicago Sanitary Ship Canal by month. Data were estimated from daily mean discharge data collected at the USGS monitoring station (05536890) located near Lemont, IL.

November and least in the month of August. Risk for estimated daily mean velocity to fall below 22 cm/s was greatest in November and least in September (Figure 5 – 7).

Examination of discharge data collected each minute from 3/1/2010 through 6/29/10 showed a 0.09% incidence of reverse flow (159/169,478) at the gage. Readings of reverse flow ranged from -0.03 to -21 cm/s ( $-2.4 \pm 3$  cm/s). During this 120 day period there were 11 instances (gage readings) of reverse flow exceeding -7 cm/s, with a single reading that exceeded 15 cm/s (the maximum of -21 cm/s). Gage height at the monitoring station varied between 6.7 and 7.8 ( $7.5 \pm 0.2$ ) meters over this period.

## Discussion

The outcomes in the present experiment indicate water velocity and the characteristics of the electric current defining the barrier field influence risk for fish to maintain position in electric fields in flowing water. These outcomes provide additional support for inclusion of ultimate field strength and pulse-frequency as technical factors in the conceptual Risk Model for Barrier Effectiveness. The outcomes also support inclusion of water current velocity as an environmental factor in the conceptual Risk Model for Barrier Effectiveness (Holliman, this report). An inverse relation was demonstrated between risk for breach of the electric barrier and water current velocity.

Silver carp, bighead carp, and common carp share the behavioral characteristics of swimming against the flow and attraction to slow water currents, which are more pronounced during the breeding season (Zhong 1990). It is expected that fish motivated to swim upstream in the Chicago Sanitary and Ship Canal will penetrate the electric barrier to the extent they can. Outcomes of the experiment on volitional challenge of the electric field indicate behavior to be a factor that increases risk for breach of the Barrier, as fish may repeatedly challenge the electric field (Holliman, this report). The simulations in the prior experiments (Holliman, this report) were conducted under a scenario of no flow and fish continuing upstream into the Barrier despite electrical stimulation. Although fish did react (first response) to the presence of pulsed DC during exposure to field strengths associated with the “low-field”, there was little indication of distress. The field strengths associated with the onset of behaviors associated with the flight response upon interaction with the “high-field”, however, could indicate the position in the field where fish dart forward into the increasingly intense field, retreat downstream, or attempt to maintain their position within the field. There are anecdotal observations of this behavior in large fish (undetermined species) in the electric barriers on the Chicago Sanitary and Ship Canal, of large fish maintaining position at a boundary within the field (personal communication, Doug Malone, Smith-Root, Inc., Vancouver, Washington).

The flight response was consistently evoked in fish in prior simulations and the threshold field strength for the response may indicate the boundary for the onset of aversion behaviors in small fish. In the present study, a tendency for fish to collect near the upstream-most screen, prior to exposure to the rising-side of the high field, was demonstrated. Exposure to field strengths associated with the low field had no significant effect on fish swimming capability, as no fish were impinged during exposure to the low field, though normal swimming was sometimes interrupted. Thus, penetration of the low-field of Barrier IIA by small bighead carp is likely. Similar to simulations of encroachment previously described, there was onset of rapid non-directed swimming upon exposure to high gradients associated with the rising-side of the high field in the present study. The onset of flight was accompanied by fish drifting back in the swim tunnel toward the downstream most screen. Interaction with the high gradients of the rising side of the high field could indicate locations of equipotential boundaries for penetration of the field by small bighead carp. Experimentation on volitional challenge of waterborne electric fields, however, demonstrated that aversion cannot be relied upon to prevent encroachment upon high gradients of electrical exposure.

The electric barriers on the Canal utilize cross-channel electrodes; the direction of electric current flow is parallel with the direction of water current flow on the Canal. Fish swimming upstream experience the greatest electrical exposure (greatest body-voltage) when oriented parallel with the direction of electrical current flow (the upstream-downstream direction). As the velocity of water flow increases, for fish to progress against the flow or maintain position the need for fish to be aligned parallel with the direction of flow increases compared to when flow is less. Thus, the need to align in the direction of water flow, which is the direction of maximum electrical current flow and electrical exposure, will

compete with the need to minimize body-voltage, which is accomplished by turning to the side. Fish turning to the side, away from alignment with the direction of flow will be swept downstream. Thus, it is expected that, in flowing water, these competing motivations will result in a repeated action where fish align parallel with the directions of water and electric current flow and swim upstream, where upon reaching some point of discomfort (some equipotential boundary) they will turn to the side in an attempt to minimize body-voltage and be swept back downstream, where in the less intense electric field they will re-align with the directions of water and current and swim back upstream. Based on outcomes in the present study, earlier simulations (described previously; Holliman, this report), and the experiment on volitional behavior (Holliman, this report), it is expected that these actions will occur in bighead carp of the size targeted in this study at the downstream margin of the high-field and in large fish at the edge of the low-field.

The scenario in the simulations was that of fish continuing upstream into increasing field strength despite electric stimulation. Swimming, which is a complex neuromuscular activity (Wardle et al. 1995; Altringham and Ellerby 1999) appeared to be impaired in tests with several of the operational protocols, resulting in fish being impinged upon the back screen. The risk for failing to impair swimming ability was significantly reduced as water velocity increased from 7 to 15 cm/s. A threshold may have been reached in the effects of water velocity, as there was no statistically significant difference between velocities of 15 and 22 cm /s.

Water current velocity may influence risk for breach of the Barrier though increasing challenges to the barrier, forcing fish alignment with electric current flow, though impacts of swimming ability and through increased duration of exposure. Silver carp, bighead carp and common carp share the behavioral characteristics of swimming against the flow (Zhong 1990). A water current velocity of 7 cm/s was adequate to induce positive rheotaxis in the experiment on volitional challenge of electric fields (Holliman, this report). It is likely that bighead carp and silver carp response to water current flow will be influenced by the magnitude and direction of water current flow. Under conditions of reverse flow on the Canal, if of sufficient magnitude to induce positive rheotaxis, fish would swim into the flow away from the electric barriers away from the Great Lakes. Under conditions of no water flow in the Canal, the motivation for fish to challenge the electrical barrier is uncertain, but it is prudent to consider the worst-case scenario of invasive fishes attempting to cross the barrier. It is likely that challenges to the Barrier, the incidence of fish swimming upstream into the field will be directly related to water velocity.

If water current velocity and discharge data collected near Lemont, IL are representative of that at the electric barriers, average daily water current velocity near the Barriers from 1/2005 through 6/2010 was ~22 cm/s. During this period, water flow velocity exceeded the estimated maximum sustainable swimming speed for 51 – 76 mm bighead carp of 50 cm/s, 4% of the time (60/2000 days). This can be interpreted to indicate that, based on daily mean velocity values, 51 – 76 mm bighead carp would have been able to progress upstream to challenge the Barrier on 96% of the days from 1/2005 to 6/2010. Water current velocity exceeded 15 cm/s, the threshold for reducing risk for fish to maintain position in the field on 72% of the days (1431/2000 days). Daily mean water current velocity was at a rate that reduced risk for fish to breach the Barrier 72% of the time, from 1/2005 to 6/2010. Daily mean velocity exceeded 7 cm/s > 99% of the days between 1/2005 and 6/2010. In the volitional challenge of electric fields experiment, a flow velocity of 7 cm/s was adequate for positive rheotaxis of fish in the test, provided motivation for fish to swim into the flow. A flow velocity of 3 cm/s failed to induce positive rheotaxis (Holliman, this report). There were no instances of reverse flow in the daily mean velocity data.

Gage readings at the Lemont, IL monitoring station accurately reflect reverse flow (personal communication, Kevin Johnson, USGS Field Station Manager, Urbana, Illinois). Examination of water velocity data collected from 3/1/2010 through 6/29/2010 demonstrated reverse flow occurred less than 0.01% of the time (based on readings taken every minute during this 120 day period). Instances of reverse flow attaining velocities that induced positive rheotaxis in fish (in the volitional challenge of electric fields by small bighead carp experiment described previously; Holliman, this report) were even rarer and there were no instances of the velocity of reverse flow exceeding 22 cm/s. Thus, there was no indication, during this period of monitoring, that during periods of reverse flow the water velocity would exceed the swimming capabilities of bighead carp of the size range targeted in the present studies, sweeping these fish into the barrier field. Risk for fish encroaching upon the barrier field to breach the field could be increased under conditions of reverse flow, even at very low velocities of flow because fish immobilized may be swept through the high-field. The average velocity during reverse flow, in the data set evaluated, was - 2.4 cm/s. Based on observed behaviors of 51 – 76 mm bighead carp in the simulations conducted at a flow velocity of 3 cm/s, positive rheotaxis would not be induced in fish by the average velocity during reverse flow (Holliman, this report). Should fish enter the high-field and become immobilized, at this rate of flow it would take immobilized fish ~ 400 seconds to drift 10 meters. Thus, immobilized fish would receive significant electrical exposure while drifting through the high-field during low velocity reverse flow. Throughout the studies, small bighead carp immobilized by electrical exposure sank. Electrical exposure would be dramatically increased in fish sinking upon immobilization in the Canal. Whether electrical exposures associated with drifting through the field, or sinking in the field, during periods of reverse flow would prove lethal to immobilized fish is not known. Research on effects of cumulative exposure to targeted fish is warranted.

Treatments applying pulse-frequencies of 30 Hz were not included in this experiment. The increased effectiveness of 30 Hz relative to other pulse rates were obvious in the pilot study, in the screening experiments, in the experiment conducted for predictive modeling, and in the experiment on volitional behavior. In each case, 30 Hz was more effective than lower pulse rates; the exception was 25 Hz where there was no statistically significant difference between 25 Hz and 30 Hz, in some instances. Based on the previous outcomes, significant pulse frequency effects were expected in the tests with water velocity, with 30 Hz being at least as effective as 25 Hz (if not more effective) and more effective than the lower pulse-rates. Thus, 30 Hz treatments were not applied in the present experiment and the range of pulse frequency applied in the experiment was shifted downward to include 15 Hz. Similar to the outcomes of the previous studies conducted in no flow or minimal water flow, where operational protocols applying 2.5 ms pulse duration were more effective at inducing passage-preventing behaviors in small bighead carp than those applying 2.0 ms pulse duration, operational protocols applying 2.5 ms pulse duration are also expected to be more effective in flowing water than those applying 2.0 ms pulse duration.

There were several complicating and confounding factors in the present experiment. The effects of water velocity were confounded with duration of exposure. The fish used in the present study had been used in a previous experiment, with unknown latent effects. Comparisons of outcomes with prior simulations are complicated by the use of naïve fish in prior experiments and fish previously exposed to electric fields in the present experiment. Comparisons are further complicated by the potential for a behavioral component in that simulations were conducted on fish in groups in the present experiment compared to simulations on individuals in the previous experiments. Limited fish availability prevented inclusion of additional controls to assess immobilization in the groups under conditions of no flow.

There was evidence of statistical overdispersion in the data as well as possible interactions in the experimental factors. Thus, the binomial based inferences may be biased; confidence intervals may



be too narrow and p-values too small. Overdispersion of the data could be evidence of group behavior in the simulations, indicating it necessary to treat group as the experimental unit in subsequent experiments greatly increasing numbers of fish required for experimentation.

There was evidence of overdispersion in the data as well as possible interactions in the experimental factors. Dispersion is a measure of the spread of data. Overdispersion indicated the variance (spread) of the data was greater than expected from a binomial distribution (Ramsey and Schafer 2002). Treatments were applied to fish in groups (5 fish per group). The experiment was designed for observations to be treated as independent, based on the expectation that fish receiving electrical stimulation would act independent of others in the group. The evidence overdispersion indicates that the fish did not act independently, there was a schooling effect. Thus, it may be necessary in future experiments with groups of fish to treat the group as the experimental unit, greatly increasing numbers of fish required. Because there was evidence of overdispersion in the data, the p-values and confidence intervals should be regarded as optimistic. Nonetheless, the outcomes of the experiment provide clear evidence that water velocity influences risk for breach of the barrier field by small bighead carp.

There was an obvious pattern of reduced risk of fish maintaining position in the field with increased water flow velocity, during the simulations of encroachment, supporting inclusion of flow velocity as a factor in the Risk Model for Barrier Effectiveness. Outcomes of the experiment indicate the forward progress of fish encroaching upon the barrier may be thwarted or the ability of fish to hold position reduced with water flow velocity of 15 and 22 cm/s compared to 7 cm/s. The effectiveness of the 0.91 V/cm ultimate field strength, 30 Hz pulse frequency, and 2.5 ms pulse duration operational protocol, shown to reduce risk of failing to immobilize encroaching small bighead carp under conditions on no or minimal flow, is expected to be enhanced in flowing water, further reducing risk for breach of the barrier field. Additional research is warranted to clarify relations between water velocity and operational protocols for the electric barriers on the CSSC and risk for breach of the barrier fields on the CSSC by small silver carp and bighead carp.

## Work cited

Agresti, A. 1990. Categorical data analysis. Wiley-Interscience Publication, New York, New York.

Altringham, J. D. and D. J. Ellerby. 1999. Fish swimming: patterns in muscle function. *The Journal of Experimental Biology* 202: 3397 – 3403.

Ramsey, F. L. and D. W. Schafer. 2002. *The Statistical Sleuth: A Course in Methods of Data Analysis*, Second Edition. Belmont, California: Brooks/Cole Cengage Learning.

Sall, J., C. Lee and A. Lehman. 2007. *JMP® Start Statistics: A guide to statistics and data analysis using JMP®*, fourth edition. Cary NC; SAS Institute Inc.

SAS 2009. *JMP, Version 8*. SAS Institute Inc., Cary, NC, 1989-2009.

Wardle, C.S., J. J. Videler and J. D. Altringham. 1995. Tuning in to fish swimming waves: body form, swimming mode and muscle function. *The Journal of Experimental Biology* 198: 1629 – 1636.

## 6 – Conclusions and Directions for Future Research

A conceptual Risk Model for Barrier Effectiveness was devised. Several factors in the Model,

<u>Technical factors</u>	<u>Biological factors</u>	<u>Environmental factors</u>
Pulsed DC field strength	Fish species	Water conductivity
Pulsed DC pulse-frequency	Fish size	Water velocity
Pulsed DC pulse-duration	Behavior	Water depth
Field orientation (direction of electric current flow)	Swimming speed (duration of exposure)	Habitat,
Field size		

were directly tested in the experiments.

Simulations of encroachment into the field of electric Barrier IIA were used to evaluate the effectiveness of various combinations of electrical parameters for inducing passage-preventing behaviors in 51 – 76 mm bighead carp. The simulations were conducted under controlled conditions using homogeneous electric fields. Electrical stimulation was pulsed DC during the simulations and varied in intensity over time to mimic the exposure fish swimming through the electric barrier would experience. The approach applied in the present study was a significant improvement over the pilot study and in the “state of the art” for research related to electrical exposure of fish. Subsequently, the quality of data collected and the inference of the experimental results improved. The scenario in the simulations employed various aspects of the conceptual risk model developed for barrier effectiveness.

Outcomes in the present study support the hypotheses that the characteristics of the waterborne electric field influence probability of immobilization of encroaching small bighead carp, supporting facets of the conceptual risk model for barrier effectiveness. A multivariable relationship was demonstrated (between field strength, pulse-frequency, pulse-duration, fish length, and the interaction between pulse-duration and fish length, and the probability of immobilization) in the prognostic model developed from promising operational protocols. Based on the outcomes of the experiment, efficiency of the electric barriers on the Canal is strongly influenced by technical factors. Specifically, the operational protocol employed.

The prognostic model (FS, PF, PL, L, PL\*L) developed from the simulations provides the best information available regarding the likelihood of immobilizing 51 – 76 mm bighead carp encroaching upon Electric Barrier IIA. It must be emphasized, however, that the model was based on simulations, relatively small sample sizes, and should be verified. The FS, PF, PL, L, PL\*L model was based on 20 fish per experimental cell (i.e., combination of experimental factors), a relatively small number of fish. This is especially important with regard to point estimates of probability for immobilization. For example, in experimental cells where 100% of fish (20/20) were immobilized [FS: 1.02 V/cm; PF: 30 Hz, PL: 2.5 ms; FS: 0.91 V/cm, PF: 30 Hz, PL: 2.5 ms], the long term average percent immobilized could be as low as 85% (this is the lower 95% confidence interval for the point estimate of 100%, for a binary response and N = 20). The confidence interval about the point estimates shrinks as the sample size in the experimental cells increases. According to the rule of threes when there has been no event, when employing a 95% confidence interval (95% CI) and 100% of fish in an experimental cell are immobilized, the lower limit of the 95% CI would be 90% with 30 fish/cell, 95% with 60 fish /cell, 97% with 100 fish/cell, and 99% with 300 fish/cell (van Belle 2002). The number of fish required in a full factorial experiment may become

prohibitive, depending on the desired level of confidence and the number of factors evaluated. Extensive testing for reduction of confidence intervals, for validation and refinement of the model, can be conducted on a select few experimental cells.

Statistical significance was apparent among the levels of field-strength, pulse-frequency and pulse-duration evaluated in the prognostic model. The FS PF, PL, L, PL\*L model demonstrates strong dependence between probability of immobilization and fish length. There were direct relations between the proportions of fish immobilized and field strength, pulse-frequency, and pulse-length. Comparisons between the operational protocols targeting small bighead carp and the protocol shown effective for immobilizing small silver carp demonstrated risk for failure to immobilize the targeted fish was significantly reduced with pulse-frequency of 30 Hz when applied at ultimate field strength of 0.91 V/cm and pulse-durations of 2.5 ms.

Small fish were targeted in the present study. A direct relation is evident between probability of immobilization and fish length. There is significant evidence that Barrier I (on the Canal) was effective on large common carp (Sparks et al. 2004; Dettmers and Creque 2004) when applying operational protocols having pulse-frequencies of 2 Hz, 3 Hz, and 5 Hz. In comparison, substantially greater field strength, pulse-frequency, and pulse-duration was necessary to immobilize small silver carp [0.79 V/cm, 15 Hz pulse frequency, and 6.5 ms pulse-duration]. This operational protocol is presently in use on the CSSC. The present study targeted 51 – 76 mm (2 to 3 inch) bighead carp as a worst case, as effects will be even more pronounced in even slightly larger fish.

The actions of the fish at the downstream margin of the field observed in the experiment on volitional behavior (conducted March – April 2010) parallel the anecdotal observations and descriptions of the actions of large fish maintaining position in the Canal at the downstream most margin of the low field of Barrier IIA. For example, on June 25, 2009, prior to the increase in operating parameters to those presently employed, a large common carp and a large gizzard shad were observed near the water surface at the downstream margin of the low-field of Barrier IIA, swimming upstream to some point within the field and then drifting down stream, repeatedly (personal communication, Mr. Doug Malone and Mr. David Mease, Smith-Root, Inc., Vancouver, Washington). The equipotential boundary for penetration of the field, by these large fish, occurs near the downstream margin of the low field.

In the experiment on volitional challenge, fish had opportunity to avoid an electric field and to exit the field after swimming into it. Fish actions and behaviors indicated they were able to detect the edge of the field and, therefore, could avoid entering or interacting with the field. However, fish challenged the field repeatedly. Further, fish often continued to challenge the field despite being immobilized (incapacitated) only moments earlier, re-challenging the field immediately upon recovery of an upright orientation. Outcomes in the present study are in accord with those reported by Barwick and Miller (1996) and support the observations of Stewart (1990) that fish receiving electrical stimulation may continue into fields of higher intensity.

Outcomes in the simulations indicate that penetration of the low field of Barrier IIA by small bighead carp (42 – 92 mm) is likely, regardless of the operational protocol employed (of those tested), no fish were immobilized, or were in significant distress, or had difficulty maintaining position within the electric field in flowing water. The actions and behaviors of fish in the experiment on volitional challenge, with consideration of actions and behaviors of fish in the simulations, indicate the sharply increasing gradients on rising side of the high field may serve as equipotential boundaries for the onset of flight in these small fish, but not avoidance. The continued challenge of the downstream margin of

the electric field in the volitional challenge study indicate it prudent to assume that fish will not avoid the high-field of Barrier IIA, that they will likely penetrate the high-field to the extent possible. The operational protocol for the Barrier should be adequate to stun the smallest fish of interest. The outcomes of the present study indicate the behavior of small bighead carp to increase increase risk for breach of the Barrier, providing support for inclusion of behavior as a risk factor in the conceptual Risk Model for Barrier Effectiveness.

The effects that water flow has on risk for small bighead carp to successfully traverse barriers depend on the velocity of the flow. Silver carp, bighead carp and common carp share the behavioral characteristics of swimming against the flow (Zhong 1990). Positive rheotaxis (motivation for swimming upstream into water current flow) was absent in small bighead carp (51 – 76 mm total length) in water flowing at 3 cm/s, but was present at a velocity of 6 – 7 cm/s (48 – 82 mm fish) in the experiment on volitional behavior and at 7, 15, and 22 cm/s in the experiment on effects of water velocity. Thus, risk for small bighead carp to challenge the barrier field may be increased when water current velocity on the CSSC is  $\geq 7$  cm/s. Risk for fish to maintain position in a barrier field was inversely related to water velocity. Risk for small bighead carp (44 to 93 mm) to breach the Barriers on the CSSC is expected to be reduced under conditions of flow velocity  $\geq 15$  cm/s compared to when flow is  $\leq 7$  cm/s. Average daily water current velocity was  $\sim 22$  cm/s near Lemont, IL, from 1/2005 through 6/2010. During this period, daily water flow velocity exceeded 50 cm/s on 4% of the days, velocity was  $\geq 15$  cm/s (a rate that reduced risk for fish to breach the Barrier) 72% of the days, velocity was  $\geq 7$  cm/s on 99% of the days (a flow adequate for motivation for small bighead carp to swim upstream in the experiments). Examination of water current velocity measures on the CSSC showed there to be very little risk for fish to be swept into, or through, the barrier field by reversals of water flow on the CSSC.

## Work cited

Barwick, D. H, and L. E. Miller. 1996. Effectiveness of an electric barrier in blocking fish movement. Proceedings of the Annual Conference of the SouthEastern Association of Fish and Wildlife Agencies, 50: 139-147.

Dettmers, J. M. and S. M. Creque. 2004. Field assessment of an electric dispersal barrier to protect sport fishes from invasive exotic fishes. Annual Report to the Division of Fisheries, Illinois Department of Natural Resources, Illinois Natural History Survey, Center for Aquatic Ecology and Conservation.

Sparks R., J. Dettmers and T. Barkley. 2004. Assessment of an electric barrier to prevent the dispersal of aquatic nuisance fishes. Final Report to the Great Lakes Protection Fund.

Stewart, P. A. M. 1990. Electric barriers for marine fish. In I. G. Cowx (Ed.), Developments in Electric Fishing (pp. 243-255). London, England: Fishing News Books.

van Belle, G. 2002. Statistical Rules of Thumb. A Wiley-Interscience Publication, John Wiley & Sons, New York.

Zhong, W. G. 1990. Model LD-1 electric fishing screen in reservoir fisheries in China. Pages 297 – 305 in I. G. Cowx, editor. Developments in Electric Fishing. Fishing News Books, Blackwell Scientific Publications Ltd., Oxford, England.

---

Considerable progress has been made in understanding mechanisms of electric barrier function on the Chicago Sanitary and Ship Canal and in identifying risk factors and directions of risk for breach of the barrier. Thus far, research has been conducted in a controlled environment. Extensive commercial traffic coupled with the dangers associated with the waterborne electric barrier fields adds to the challenges of research on the Canal. Research on the Canal will require innovation. It is imperative to verify outcomes of the present study on the Canal, where possible. Additional research within a comparable framework to that described herein is needed to address factors not yet tested and to refine and expand knowledge of factors previously tested and the inter-relationships among the biological, environmental, and technical factors in the conceptual Risk Model for Barrier Effectiveness. Because of the host of factors that may confound field experiments and the difficulty associated with experimenting directly on the Canal, refinement of the simulations employed in the present study is recommended. The simulations employed in the present study represent a significant improvement in the state of the art. Nonetheless, the simulations can be improved for even more representative exposures to account for changes in field strength and polarities, the summation of pulses within regions of the field and the response of fish in flowing water.

Potential directions for research and actions on the Canal (in no particular order):

- Based on outcomes in the present study, the penetration of the low-field of Barrier IIA by 51 – 76 mm bighead carp is likely and the sharply increasing gradients of the rising side of the high-field of Barrier IIA is expected to serve as the boundary for upstream penetration of the barrier by 51 – 76 mm fish. Research and monitoring to confirm or refute this expectation is **critical**. For example, DIDSON monitoring to establish reactions of small fish and experimentation on the Canal with proven surrogate species.
- The presence of boundary conditions near the walls of the Canal, both electrical and water current, increase risk for breach of the barrier. Small fish, especially, may tend to gather near the walls of the Canal, driven by commercial traffic and avoidance of open water. The presence of reduced currents, electrical and water flow, near the walls may provide an avenue for unimpeded progression upstream. The presence of boundary conditions next to the walls of the Canal should be evaluated. If boundary conditions exist, acoustic bubbles, bubble barriers or water jets could be employed near walls to drive small fish out from the walls, into open water and electric current. Recessed traps offering protection to fish (recessed to protect from commercial traffic) could be developed for monitoring and removal of fish.
- Periodic stocking of indigenous predatory fish could reduce numbers of small invasive carps available to challenge the barriers. Preliminary work should establish the propensity of the predatory fish to prey on bighead carp and silver carp fingerlings and juveniles. Stomach content analysis of predatory fish, whether stocked or naturally occurring, collected from the Canal, may provide insight into presence and relative abundance of small invasive fish.

- Because of the relation between water velocity and risk for breach of the barrier, the relationship between measurements of water conditions taken at the USGS station at Lemont, Illinois and conditions at the location of the barriers needs to be established or a water flow monitoring site established at the Barrier site.
- Relationships between onshore Barrier output metering and in-water field strength should be established. Protocols, locations, and equipment for in-water field measurements should be developed and standardized. Barrier output and physical in-water field strength measurements should be routinely cataloged. Additionally, a biological indicator of barrier effectiveness should be developed. For example, use of DIDSON to determine expected fish responses at various locations in the field and periodic confirmation of expected responses.
- Protocols for removal of fish maintaining position below or within the Barriers (depends on fish size) are warranted.
- The potential for commercial traffic to entrain small fish that are maintaining position within the barrier field, near the high field, and pull them upstream through the electric field, is a concern and should be evaluated.
- Evaluations of acoustic bubbles and bubble curtains as additional deterrents to the passage of small carp on the Canal are recommended. These additional deterrents may be most effective if located throughout the rising side of the high field.
- Verification of FS, PF, PL, L, PL\*L model, as individual factors if necessary, and other components of the conceptual Risk Model for Barrier Effectiveness, on the Canal, is recommended. Experimentation on the Canal is difficult, but necessary. The information gained in the present study must be augmented by experimentation with appropriate surrogate species on the Canal.
- Fish in the study had a tendency to sink upon immobilization. Morphological differences often account for differences in probability to sink versus float, between species. There has been very little research into factors causing individual fish within species to float versus sink upon electrical immobilization. Unless washed out of the field by water current, fish sinking within the Barrier will likely perish, as the field strength increases dramatically with depth. Unless fish break the surface of the Canal, interactions with the barrier will go undetected. Development of an underwater monitoring program is prudent. This may be most easily accomplished via DIDSON (Dual-frequency IDentification SONar).
- Exploration of development of flow regimes to reduce risk of breach of the barriers by small fish. Manage water flow rates on the Canal during peak seasons of challenge to the barrier to impede upstream progress of smallr fish.
- The potential for cracks and crevices in the walls of the CSSC, near the barrier fields, to serve as refuges (from water and electric current flow) for small bighead carp and silver carp should be evaluated.
- Continued development of the conceptual Risk Model for Barrier Effectiveness and development of operational rules for the barriers.



Directions for research under controlled conditions (in no particular order):

- Additional study into the effects of water velocity on risk for breach of the barrier is warranted. The study on effects of water velocity described in this report was conducted with fish used in a prior experiment. Reuse of experimental animals is generally avoided to prevent introduction of known and unknown bias and latent factors into the experiment. Because additional bighead carp within the targeted size range were not available, it was necessary to reuse experimental animals in this experiment. The study undoubtedly was worthwhile, providing useful information, but should be repeated with naïve fish (and potentially with larger sample sizes to account for group behaviors). Evaluation of the effects of water velocity should include the operational protocols used to develop the FS, PF, PL, L, PL\*L model and the operational protocol found effective on small silver carp and additional levels of velocity. This information may be used for development of operational rules for barriers on the Canal, based on water velocity.
- Research on additional barrier technologies is recommended.
- Outcomes in the present study indicated penetration of the low field of Barrier IIA by 51 – 76 mm bighead carp is likely, regardless of the operational protocol employed. The sharply increasing gradients of the rising side of the high field of Barrier IIA may serve as the spatial boundary for upstream penetration of the barrier by 51 – 76 mm fish. Investigation into fish behavior-physiology in the context of duration of low-level (relative) electrical exposure is warranted, as prolonged exposure to low gradients may influence induction of passage-preventing behaviors though increased or decreased susceptibility to higher gradient exposure, disturbance in physiological balances, and reduced swim performance. It is hypothesized that probability of immobilization increases with duration of exposure to low gradients, physiological balances will be disturbed by low gradient exposures, and swim performance inhibited. Additional research is warranted.
- Similar responses to electroshock are expected from silver carp and bighead carp of the same size, but should be confirmed. Species differences at the barrier are expected to be related to behavioral factors (e.g., preferred depth).
- Sources and facilities for bighead carp and silver carp should be developed to insure adequate numbers and sizes of fish for experimentation.
- Development of a widely available, innocuous, surrogate species, or suite of species, though comparative testing with bighead carp and silver carp under controlled conditions, for evaluation, calibration, and verification Barrier performance on the Canal and in the laboratory, would be prudent.
- There has been little research on the effects of water temperature on electrical exposure-induced behaviors in fish. Water conductivity fluctuations on the Canal have a strong seasonal component, with conductivity highest in the winter months when water temperature may be lowest. Power demands on the Barrier are greatest in these months. Depending on the effects of temperature, the Barrier may be operated at lower levels during periods of low water temperature leading to potentially enormous savings in electrical energy use and equipment wear, without loss of effectiveness at preventing passage of targeted species.

- Fish size was demonstrated a significant factor in determining risk for breach of the barrier. Additional study with larger fish would expand knowledge of relative effectiveness of parameters in the FS, PF, PL, L, PL\*L model. Operational protocols relatively ineffective for immobilization of 2 -3 inch fish are likely to be effective on even slightly larger fish. Experimentation with larger fish can provide estimates of effectiveness useful for decision making with regard to changes in operational protocols under various environmental conditions.
- Evaluate electroshock-induced mortality in bighead carp and silver carp.
- Explore effects of fish encroaching upon the electric barriers in groups versus individuals.

## **Appendix B**

### **In-Water Safety Testing**



US Army Corps  
of Engineers®  
Engineer Research and  
Development Center

## 2011 In-Water Testing of Aquatic Nuisance Species Dispersal Barriers IIA And IIB with Increased Voltage and Frequency Operating Parameters

Michael K. McNerney, Brianna S. Aubin,  
Jonathan C. Trovillion, Carey L. Baxter, Ethan T. Trovillion,  
Vincent F. Hock, Jr., and David M. Weir

August 2011





# **2011 In-Water Testing of Aquatic Nuisance Species Dispersal Barriers IIA and IIB with Increased Voltage and Frequency Operating Parameters**

Michael K. McInerney, Brianna S. Aubin, Jonathan C. Trovillion, Carey L. Baxter, Ethan T. Trovillion, and Vincent F. Hock, Jr.

*Construction Engineering Research Laboratory  
U.S. Army Engineer Research and Development Center  
2902 Newmark Drive  
Champaign, IL 61822*

David M. Weir

*US Army Engineer District Chicago  
111 North Canal Street  
Chicago, IL 60606-7206*

Final report

Approved for public release; distribution is unlimited.

Prepared for U.S. Army Corps of Engineers  
Washington, DC 20314-1000

Under Project 114532, "CSSC Dispersal Barrier II, ERDC-CERL Safety Studies"

**Abstract:** US Army Engineer District – Chicago operates an electric field-based aquatic nuisance species dispersal barrier system in the Chicago Sanitary and Ship Canal (CSSC), Romeoville, IL. The barriers were constructed to prevent the movement of invasive species, such as Asian big-head carp (*Hypophthalmichthys nobilis*) and silver carp (*Hypophthalmichthys molitrix*) between the Mississippi River and Great Lakes basins. The objective of this project was to perform a series of in-water tests on the barrier addressing field-strength mapping, sparking potential during barge fleeting and collision, voltage potentials between barges traversing the barriers, personnel in-water shock potential, stray-current corrosion potential, and optimal settings for the parasitic barrier system. Test results and analysis indicate there is no significant risk of personnel shock hazard in the fleeting area during barrier operations for any operating configuration. Also, while some operational scenarios were found to increase sparking risk if barges collide with each other or separate metal objects, analysis indicates that concerns about coal dust explosion hazard from sparking are not supported by the technical literature. A detailed set of data, analysis, conclusions, and recommendations is provided in the report text and four appendices.

## Executive Summary

In an ongoing effort to test and define the relative safety of the three invasive species dispersal barriers on the Chicago Sanitary and Ship Canal (CSSC) at Romeoville, IL, the Engineer Research and Development Center – Construction Engineering Research Laboratory (ERDC-CERL) and Chicago District performed in-water safety testing using various operational settings and configurations. The work was performed from 4 - 12 February and 12 - 16 June 2011. The seven objectives established for this testing effort: (1) map field strengths, (2) determine sparking potential during fleeting operations, (3) determine sparking potential in the event of a collision in the fleeting area, (4) measure voltage potential between barges traversing the canal over the barriers, (5) determine personnel shock potential at the bollards at the fleeting area, (6) determine corrosion potential, and (7) determine the optimal settings for the parasitic barrier system. Each objective was accomplished for six different target operational configurations: (A) IIA at 2.0 V/in., IIB at 2.3 V/in., (B) both IIA and IIB at 2.3 V/in., (C) both IIA and IIB at 2.0 V/in., (D) IIA alone at 2.3 V/in., (E) IIB alone at 2.0 V/in., and (F) IIB alone at 2.3 V/in. The measurements and observations recorded during these tests were compiled and analyzed to determine the in-water safety concerns associated with each of the various operational configurations.

The field strength testing and analysis indicated that larger areas of risk to a person-in-water are present when operating barriers IIA and IIB concurrently. However, only a small increase in the area of risk results with an increase of operational parameters from 2.0 V/in. to 2.3 V/in. Sparking was observed during fleeting operations, mainly during the insertion procedure when both barriers were in operation. No significant increase in risk of sparking was observed due to the increase in operations from 2.0 V/in. to 2.3 V/in. There is a significant increase in risk of sparking when a tow spanning both IIA and IIB with both operating (versus barrier IIA operating alone) collides with barge in fleeting area. The likelihood of sparking causing an explosion or fire at the coal-loading facility due to coal dust is negligible. Operation of the barriers does not adversely affect corrosion potential for in-water steel structures at Midwest Generation fleeting area. No risk of personal shock hazard was observed at the bollards in the fleeting area. Test results did not provide any clear evidence to refute that the



optimal parasitic electrode configuration is consistent with SRI recommendations that only two of the three parasitic structures are connected together such that they are the outermost structures adjacent to the active arrays.

# Table of Contents

<b>Executive Summary</b> .....	<b>iii</b>
<b>List of Figures and Tables</b> .....	<b>vii</b>
<b>Preface</b> .....	<b>ix</b>
<b>1 Introduction</b> .....	<b>1</b>
1.1 Background.....	1
1.2 Objective .....	3
1.3 Approach .....	4
<b>2 Experiments</b> .....	<b>5</b>
2.1 Field mapping (Objective 1).....	5
2.1.1 Procedure.....	5
2.1.2 Analysis.....	6
2.1.3 Results and observations .....	7
2.1.4 Conclusions .....	10
2.2 Sparking potential testing at fleeting area (Objectives 2 and 3).....	13
2.2.1 Procedure.....	13
2.2.2 Analysis.....	17
2.2.3 Results and observations .....	18
2.2.4 Conclusions .....	22
2.3 Long tow voltage potential test (Objective 4).....	23
2.3.1 Procedure.....	23
2.3.2 Analysis.....	25
2.3.3 Results and observations .....	25
2.3.4 Conclusions .....	26
2.4 Shock potential at fleeting dock bollards (Objective 5).....	27
2.4.1 Procedure.....	27
2.4.2 Analysis.....	27
2.4.3 Results and observations .....	27
2.4.4 Conclusions .....	28
2.5 Corrosion potential (Objective 6).....	28
2.5.1 Procedure.....	28
2.5.2 Analysis.....	29
2.5.3 Results and observations .....	29
2.5.4 Conclusions .....	29
2.6 Parasitic grid configuration testing (Objective 7).....	29
2.6.1 Procedure.....	29
2.6.2 Results and observations .....	30
2.6.3 Conclusions .....	30

---

<b>3</b>	<b>Conclusions and Recommendations .....</b>	<b>31</b>
	Conclusions .....	31
	Recommendations .....	31
<b>4</b>	<b>Unabridged Data Tables .....</b>	<b>33</b>
	<b>References .....</b>	<b>65</b>
	<b>Appendix A: Instrumentation and Data Reduction .....</b>	<b>A1</b>
	<b>Appendix B: Electric Hazard Analysis .....</b>	<b>B1</b>
	<b>Appendix C: V12 Electric Field Plots .....</b>	<b>C1</b>
	<b>Appendix D: V12 Electric Field Maps .....</b>	<b>D1</b>
	<b>Report Documentation Page</b>	

# List of Figures and Tables

## Figures

Figure 1. Relative locations of Barriers I, IIA, and IIB in the canal.....	1
Figure 2. Electrode array for voltage gradient and current mapping.....	6
Figure 3. Relative locations of areas of likely harmful effects for the four pulser configurations of Table 5 (continued to next page).....	10
Figure 4. Locations of likely harmful effects for the six pulser configurations in Table 5, Chapter 4.....	13
Figure 5. Sparking potential testing scenario for a tow with barges in series, 5 February 2011.....	14
Figure 6. Instrumentation for testing of a tow with barges in series.....	14
Figure 7. Sparking potential testing scenario for a tow with barges in parallel, 5 February 2011.....	14
Figure 8. Instrumentation for testing of assembling a tow with barges in parallel.....	14
Figure 9. Sparking potential testing scenario for inserting a barge into a tow on 5 February 2011.....	15
Figure 10. Instrumentation for testing of inserting a barge into a tow.....	15
Figure 11. A tow over Barriers IIA and IIB contacting a moored barge in the fleeting area on 7 February 2011.....	16
Figure 12. Electrical measurements between a tow over Barriers IIA and IIB and a barge moored in the fleeting area.....	16
Figure 13. Long tow consisting of five barges and two towboats traversing the barriers on 8 and 10 February when the pulsers were in configuration Bravo and Parasitic 2 was on.....	24
Figure 14. Diagram of five open-circuit voltage measurements ( $V_1$ - $V_5$ ) simultaneously captured for each barge in the long tow.....	24

## Summary Tables

Summary Table A. Target operational scenarios. ....	5
Summary Table B. Range of greatest extent of voltage gradients ( $\geq 0.05$ V/in.) sufficient to cause harmful physiological effects (see Table 3 and Table 4, Chapter 4). ....	9
Summary Table C. Summary of sparking observations based on test results for sparking potential during fleeing operations (see Table 6, Chapter 4). ....	19
Summary Table D. Summary of estimated energy based on results for sparking potential during fleeing operations (see Table 6, Chapter 4). ....	19
Summary Table E. Test results for sparking potential during collision simulations, conducted on 7 February 2011 (see Table 7, Chapter 4). ....	21
Summary Table F. Outline of test results for long tow traversing Barriers IIA, IIB, and I, conducted on 8 and 10 February 2011 (see Tables 8–10, Chapter 4). ....	25
Summary Table G. Voltage differences between outside barges and towboats. ....	26
Summary Table H. Concise results for bollard voltage potential and 500-ohm current tests at fleeing area, conducted on 7 February 2011 (see Table 11, Chapter 4). ....	27

## Tables

Table 1. Environmental conditions during testing. ....	34
Table 2. Pulser and parasitic configurations and approximate run times for field mapping, conducted on 11 and 12 February 2011, and 14 June 2011. ....	35
Table 3. Locations of Barriers IIA and IB voltage gradients sufficient to cause harmful physiological effects. ....	37
Table 4. Locations of Barrier I voltage gradients sufficient to cause harmful physiological effects. ....	44
Table 5. Pulser settings and target in-water field strengths for each test configuration. ....	48
Table 6. Test results for sparking potential during fleeing operations. ....	49
Table 7. Test results for sparking potential during collision simulations. ....	54
Table 8. Test results for long tow traversing Barrier IIA, conducted on 8 and 10 February 2011. ....	57
Table 9. Test results for long tow traversing Barrier IIB, conducted on 8 and 10 February 2011. ....	59
Table 10. Test results for long tow traversing Barrier I, conducted on 8 and 10 February 2011. ....	61
Table 11. Test results for bollard voltage potential and 500-ohm current tests at fleeing area. ....	63
Table 12. Barge corrosion potential measurements taken with Cu/CuSo <sub>4</sub> reference electrode, conducted on 5 February 2011. ....	64
Table 13. General corrosion rates for steel in fresh water. ....	64

## Preface

This study was conducted for the US Army Engineer District – Chicago under Project 114532, “CSSC Dispersal Barrier II, ERDC-CERL Safety Studies.” The technical monitor was Charles B. Shea, CELRC-PM-PM.

The work was performed by the Materials and Structures Branch (CF-M) of the Facilities Division (CF), US Army Engineer Research and Development Center – Construction Engineering Research Laboratory (ERDC-CERL). At the time of publication, Vicki L. Van Blaricum was Chief, CEERD-CF-M; L. Michael Golish was Chief, CEERD-CF; and Martin J. Savoie was the Technical Director for Installations. The Deputy Director of ERDC-CERL was Dr. Kirankumar Topudurti and the Director was Dr. Ilker Adiguzel.

COL Kevin J. Wilson was the Commander and Executive Director of ERDC, and Dr. Jeffery P. Holland was the Director.



# 1 Introduction

## 1.1 Background

US Army Engineer District – Chicago is safely operating an electric field-based aquatic nuisance species dispersal barrier system in the Chicago Sanitary and Ship Canal (CSSC), Romeoville, IL. The barriers were constructed by Smith-Root, Inc., sole licensees of US patent 4,750,451<sup>1</sup>, to prevent the movement of invasive species, such as Asian bighead carp (*Hypophthalmichthys nobilis*) and silver carp (*Hypophthalmichthys molitrix*) [12], between the Mississippi River and Great Lakes basins. The barrier project consists of two distinct parts: the demonstration barrier (Barrier I) and Barrier II. Barrier I, which consists of steel cables fastened to concrete supports that rest on the bottom of the canal, sends a low-voltage, pulsing direct current (DC) through the water in order to repel invasive fish. Barrier II, also a pulsed DC apparatus, is located 800 to 1,300 ft downstream of Barrier I. Barrier II is able to generate a more powerful electric field over a larger area. It consists of two sets of electrical arrays and control houses, known as Barriers IIA and IIB. Each control house and set of arrays can be operated independently. Barrier IIA is operated during maintenance activities or as otherwise needed, and Barrier IIB is fully operational. Figure 1 shows the relative locations of Barriers I, IIA, and IIB.

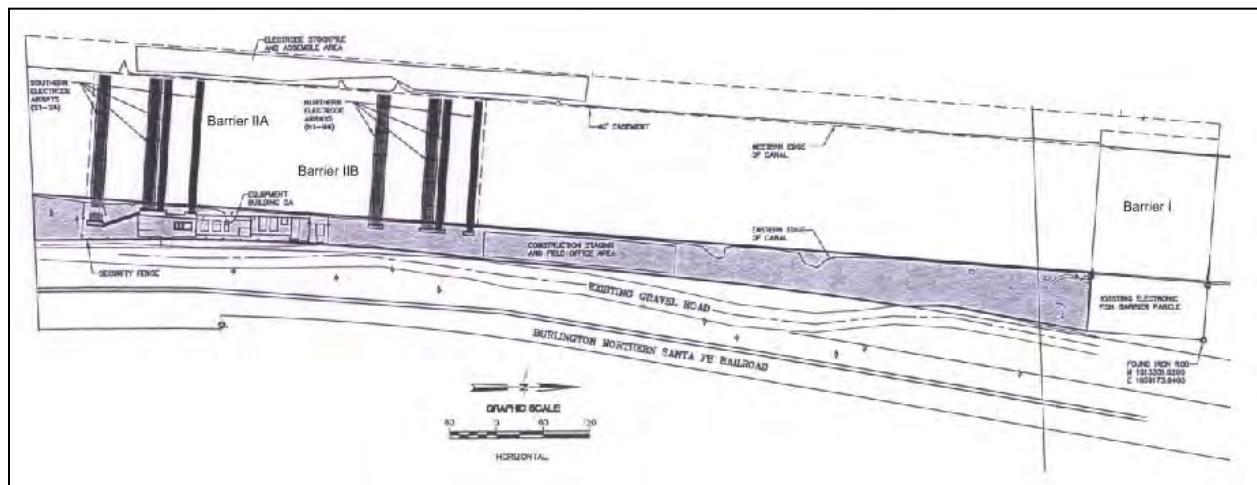


Figure 1. Relative locations of Barriers I, IIA, and IIB in the canal.

<sup>1</sup> Smith, David V. Fish repelling apparatus using a plurality of series connected pulse generators to produce an optimized electric field. United States Patent 4,750,451, issued 14 June 1988.



Before August 2009, Barriers I and IIA were operating at maximum in-water field strength at the water surface of 1 volt/inch (V/in.) with five pulses per second at a frequency of 5 hertz (Hz), and each pulse 4 milliseconds (ms) in duration. The US Army Corps of Engineers (USACE) and Smith-Root are engaged in an ongoing research program to identify the most effective combination of electric field strength, pulse frequency, and pulse duration for deterring all sizes of Asian carp. After environmental DNA (eDNA) monitoring indicated that Asian carp may have migrated closer to the barrier system than previously thought, the operating parameters at Barrier IIA were increased in August 2009 to levels recommended based on the research completed at that time: a maximum in-water field strength at the water surface of 2 V/in. with a pulse rate of 15 Hz and a pulse duration of 6.5 ms. The operating parameters at Barrier I were not changed because the equipment at Barrier I is not capable of operating at the higher recommended operating parameters.

Increasing the Barrier IIA operating parameters raised concerns about conducting barge and boat operations safely, and the potential hazards to a person who accidentally fell into the water while traversing the barriers. During preliminary discussions between ERDC-CERL<sup>2</sup>, the Ninth US Coast Guard (USCG) District and Captain of Port Lake Michigan, and Chicago District, it was emphasized that it is crucial to identify and understand the risks associated with the new operating parameters. Additional tests were completed in August and September 2009 by teams from ERDC-CERL and Coast Guard Office of Design and Engineering Standards (CG 521) with Barrier IIA operating at 2 V/in., 15 Hz, and 6.5 ms pulse width. Test results were shared with the USCG that resulted in changes in the rules of navigation to allow the safe passage of barges carrying combustible or flammable liquid in bulk (i.e., red-flag barges) and recreational boats across the barriers.

Research into the optimal operating parameters to deter all sizes of Asian carp has continued. The latest research indicates that operating at a pulse rate of 30 Hz, pulse duration of 2.5 ms, and a maximum in-water field strength at the water surface of 2.3 V/in. may be most effective for deterring even small Asian carp. USACE is considering changing the Barrier II operating parameters to the latter. Testing for safety concerns in the waterway along with ground currents and electromagnetic radiation (EMR)

---

<sup>2</sup> Engineer Research and Development Center - Construction Engineering Research Laboratory, Champaign, IL.

in the air were conducted in February 2011 to determine the effects of these new operational parameters. The results of the in-water testing are included in this report; safety testing results for ground currents and EMR will be documented in a separate report. The results of the safety testing will be a key element in recommendations about optimum operating parameters.

Barrier IIB has been operational since April 2011, and has undergone testing that verified it can perform at the specified parameters. Also, new parasitic structures have since been installed in the canal as part of Barrier IIB construction. These structures, typically referred to as “parasitics” in this report, are electrode arrays configured as steel grids and mounted to concrete curbs that rest on the bottom of the canal. These are located down-canal from Barrier IIA, up-canal from Barrier IIB, and between IIA and IIB. They collect the stray currents on one side of a barrier and, via an electrical bus on shore, provide a low-impedance path for those currents to return to other side of barrier.

The southernmost parasitic grid is designated as 1; the middle grid as 2; and the northernmost grid as 3. Each grid is connected to the electrical bus on the western shore by metal cables that are welded to the grid structure. There are several switches that allow each parasitic to be connected to and disconnected from the bus. By closing each switch (i.e., setting it to the *on* position), the parasitics are connected to each other via bus. By opening a switch (i.e., setting it to the *off* position), a parasitic may be disconnected from the bus. The positioning of these switches is presented throughout the report.

The in-water testing was undertaken to evaluate the effects of changing the barrier operating parameters, including operation of the parasitics on the safe operation of Barrier IIB.

## 1.2 Objective

The objective of this project was to support the Chicago District by performing a series of tests on the barrier to:

1. map and quantify the voltage gradient and current potential across Barrier I, Barrier IIA, and Barrier IIB in order to evaluate the voltages and currents a person would be subjected to while in the water in the barrier area

2. quantify and evaluate the potential for sparking during fleeting operations at the Midwest Generation, LLC, power facility fleeting area
3. quantify and evaluate the possibility of sparking between fixed barges at the fleeting area and a moving long tow that is traveling south over Barrier IIA and Barrier IIB while contacting a moored barge in the fleeting area
4. quantify the voltage potential between barges in a long tow while passing over Barrier I, Barrier IIB and Barrier IIA
5. assess the potential shock hazard between the fleeting area dock bollards and a fixed barge
6. assess the corrosion potential of in-water steel structures in the fleeting area
7. determine the most effective method for operating the parasitic system.

### **1.3 Approach**

Barrier IIA and IIB were adjusted to operate according to each of the testing objectives outlined above. The operational parameters were verified, and actual values were recorded during testing. Environmental data such as ambient temperature, humidity, and water conductivity were recorded throughout all testing.

The watercraft used for field mapping was a 22 ft fiberglass-hull Guardian Boston Whaler owned by USACE. The sparking potential, corrosion potential, and long-tow tests were performed with towboats and barges provided by commercial material-transfer companies.

The main text of this report includes summary tables, most of which are derived from the raw test data. The unabridged tables of raw data are presented separately, in Chapter 4, for more detailed examination.

Details on the instrumentation used for data collection and the data reduction procedures are presented in Appendix A.

## 2 Experiments

Tests were completed for the pulser target operational configurations listed in Summary Table A. Throughout all testing, environmental data such as ambient temperature, humidity, and water conductivity were recorded. The unabridged data are presented in Chapter 4, Table 1.

Summary Table A. Target operational scenarios.

	Barrier IIA	Barrier IIB	Barrier I
A (Alpha)*	2.0 V/in., 15 Hz, 6.5 ms	2.3 V/in., 30 Hz, 2.5 ms	1 V/in., 5 Hz, 4 ms
B (Bravo)*	2.3 V/in., 30 Hz, 2.5 ms	2.3 V/in., 30 Hz, 2.5 ms	1 V/in., 5 Hz, 4 ms
C (Charlie)*	2.0 V/in., 15 Hz, 6.5 ms	2.0 V/in., 15 Hz, 6.5 ms	1 V/in., 5 Hz, 4 ms
D (Delta)*	2.3 V/in., 30 Hz, 2.5 ms	OFF	1 V/in., 5 Hz, 4 ms
E (Echo)*	OFF	2.3 V/in., 30 Hz, 2.5 ms	1 V/in., 5 Hz, 4 ms
F (Foxtrot)*	OFF	2.0 V/in., 15 Hz, 6.5 ms	1 V/in., 5 Hz, 4 ms

\* Actual test field strengths approximate.

### 2.1 Field mapping (Objective 1)

#### 2.1.1 Procedure

Field mapping was conducted for each of the six operational scenarios. Measurements of voltage (1) between horizontal electrodes spaced 1 – 6 ft apart were used to map the horizontal electric field, and (2) between two vertical electrodes spaced 5 ft apart were used to map the vertical field. Measurements of current (1) through a 100-ohm ( $\Omega$ ) resistor between two horizontal electrodes spaced 1 ft apart was used to simulate current flow through the chest, (2) through a 500  $\Omega$  resistor between two horizontal electrodes spaced 6 ft apart was used to simulate current flow through a body floating prone in the canal, and (3) through a 500  $\Omega$  resistor between two vertical electrodes spaced 5 ft apart was used to simulate current flow through an upright body. A schematic of the testing apparatus is shown in Figure 2.

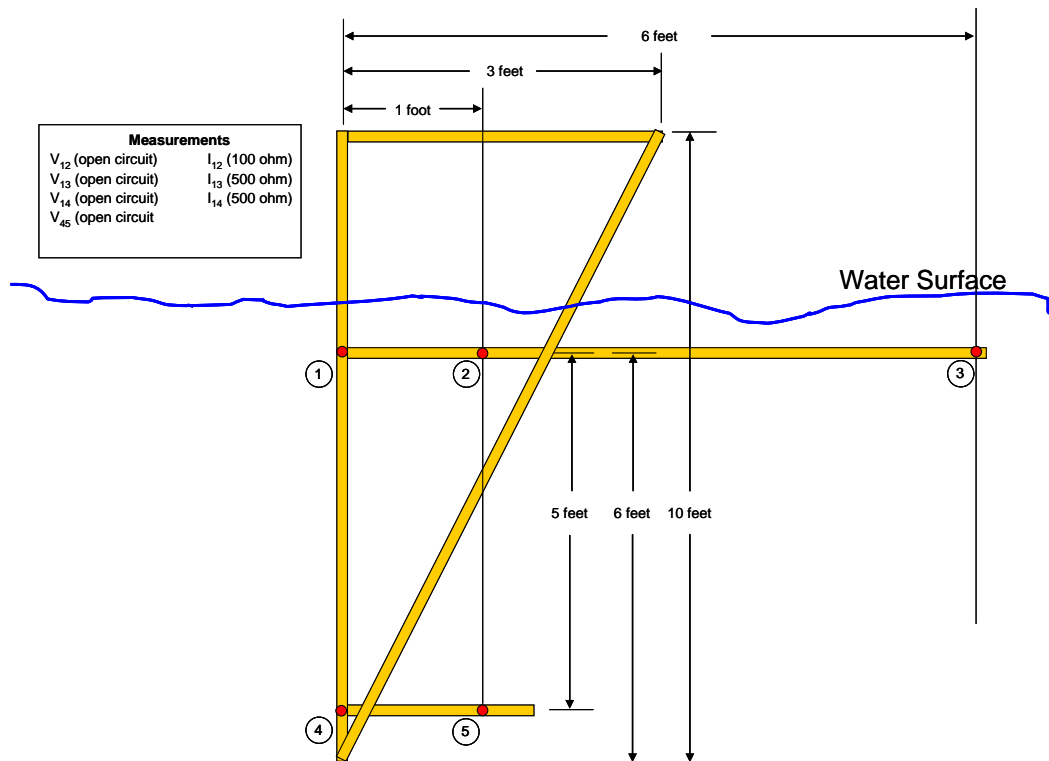


Figure 2. Electrode array for voltage gradient and current mapping.

Data were continuously collected as the boat traversed the barriers from south of the fleeting area to north of the pipeline arch. (See section 2.4.1 for layout illustrations.) This extends the data-collection region well beyond Barrier I to the north and Barrier IIA to the south.

Geopositional data were taken concurrently with the voltage and current measurements during field mapping to allow them to be georeferenced. A minimum of six passes — two along the center of the canal, two along the east wall, and two along the west wall — were taken at each of the pulser configurations shown in Summary Table A.

### 2.1.2 Analysis

Field mapping data were used to determine voltages and currents a person would be subjected to while in the water in the barrier area. The critical threshold voltage levels published in a Navy Experimental Diving Unit (NEDU) report [6] were used as the basis for computing the range of harmful physiological effects that would result from the measured values. The NEDU based its threshold voltage levels for harmful effects on International Electrotechnical Commission (IEC) Publication 60479-1, *Effects of Current on Human Beings and Livestock - Part 1: General Aspects* [11].

Table 13 in IEC Publication 60479-1, reproduced in Appendix B of this report as Table B1, defines four zones of physiological effects to the human body due to DC pulses. The zones are differentiated by duration of current pulse and body current. The most harmful effects occur in Zone DC-4; these include cardiac arrest, breathing arrest, and burns or other cellular damage.

The NEDU computation [6] is for the worst-case effect: current through the chest of a body upright over the barrier. For this scenario, the measurements of the open-circuit voltage with 1 ft electrode spacing at approximately 1 ft below the surface (referred to as V12) are used.<sup>3</sup> Minimum electric field strengths required to induce physiological effects were derived using the formulas and methods given in [6]. Details of the analysis are presented in Appendix B and summarized in Table B3. A worst-case value of 0.05 V/in. was determined to be the threshold for ventricular fibrillation. Worst-case values of 0.03 V/in. (for pulse width 2.5 ms) and 0.02 V/in. (for pulse width 6.5 ms) were determined to be the threshold for involuntary muscular contractions. The geographic limit values were obtained for each run by examining the electric field plots and estimating where the voltages crossed the threshold limit lines.

The actual field strength measured during this testing may be seen in the figures presented in Appendix C. Actual field strength sometimes exceeded the target operational configurations for these tests. In an effort to determine the impact of these higher values, sensitivity analysis was conducted (see Appendix B). Mapping runs which had at least one range of harmful effect values corresponding to one of the two greatest-extent values (one north of the barriers and one south) were selected from configuration Bravo. The entire dataset from these runs was scaled by +/- 20%. The change in the extent of the safety zones (+/- 0.05 V/in. man-overboard criteria) north and south of barriers IIA and IIB was then reevaluated using the scaled datasets.

### **2.1.3 Results and observations**

Pulser and parasitic configurations along with the approximate run times are listed in Table 2 (see Chapter 4). Electrical field strength data for V12

---

<sup>3</sup> Although five voltages and three currents were measured, only the V12 measurement is needed to perform the analysis in this report. The other voltage and current measurements were made for future analyses.

are presented in Appendices C and D. The zero point on the x-axis of these figures is centered on Barrier IIB's narrow array (see Figure C1). This is where the electric field strength of Barrier IIB is the strongest.

Peak voltage potential was measured. No filtering was applied to some of the images, such as run 16 on February 11 and run 4 on February 12, so background noise is evident in some cases. This noise is caused by radio interference from nearby transmitters and 60 Hz (and harmonic) stray electrical currents originating from the Midwest Generation electric power station. To improve graphical presentation, filtering was applied to some of the data in order to remove noise and clutter when it obscured the useful data. Peak voltages are not affected by the filtering.

No geo-tracking data were available for run 18 on February 11 and runs 17 and 18 on February 12 due to periodic changes in the GPS satellite constellation, which prevented adequate carrier phase lock to determine geopotential data through direct observation. Geo-referencing was accomplished by estimating the speed of the boat based on the travel time between IIA and IIB and between IIB and I. Because the geo tracks were interpolated, these runs were not used in the analysis of harmful effects.

The electric field dataset for run 16 on June 14 was incomplete. The data recorder stopped prematurely. Therefore, this run also was not used in the harmful-effects analysis.

The derivation of the hazardous electrical field levels and the procedure for finding the range of likely harmful effects are presented in Appendix B.

Table 3 and Table 4 (see Chapter 4) present the range of voltage gradients sufficient to cause harmful physiological effects for each run completed over each barrier. The greatest range of effect is shown in Summary Table B. The worst case (maximum extent) occurred, as expected, for pulser configuration B with all parasitics off. The best case (minimum extent) occurred, as expected, for pulser configuration D when Barrier IIB was not operating and parasitic 1 and 2 on. The best case with both Barrier IIA and IIB operating occurred for pulser configuration B with all parasitics on.

One would expect that the ranges of greatest extent for configurations E and F of Barriers IIA and IIB would be nearly the same as for configuration D. In all three cases, only one pulser is operating — pulser IIA for con-

figuration D and IIB for configurations E and F. It is thought that the parasitic settings affect the measured field strengths and, consequently, the ranges of physiological effects. In configuration D, parasitics 1 and 2 are on, both of which are directly adjacent to the Barrier IIA arrays. In configurations E and F, parasitics 1 and 3 are on. Parasitic 3 is directly adjacent to the Barrier IIB arrays, but parasitic 1 is not. Parasitic 1 is on the downstream side of Barrier IIA (as shown in Chapter 4, Figure 3) Pulser current from Barrier IIB is being directed from parasitic 3 to parasitic 1, raising the electrical field levels upstream from parasitic 1. Thus the field strength increases between parasitic 1 and 3, as reflected in configuration A, B, and C data. If parasitics 2 and 3 had been on in pulser configurations E and F, the range of greatest extent would be confined to the region immediately adjacent to Barrier IIB, as it is confined to the region immediately adjacent to Barrier IIA for configuration D with parasitics 1 and 2 on. In June, it was not possible to test with parasitics 2 and 3 on for configurations E and F due to electrical/mechanical problems with parasitic 2. Once parasitic 2 is repaired, mapping should be repeated with only parasitics 2 and 3 on.

The results of the sensitivity analysis (see Appendix B) show that the 20% increase or decrease in the voltage amplitude will result in a 10% increase or decrease in the extent of the safety zones associated with ventricular fibrillation north and south of barriers IIA and IIB. The 10% change equates to an increase or decrease of 120 ft (36 m) in the extent of the safety zone based on the 0.05 V/in. man-overboard criteria.

Summary Table B. Range of greatest extent of voltage gradients ( $\geq 0.05$  V/in.) sufficient to cause harmful physiological effects (see Table 3 and Table 4, Chapter 4).

Pulser Configuration	Parasitic Settings			Range of Greatest Extent					
	1	2	3	Barriers IIA and IIB, in ft (m)			Barrier I, in ft (m)		
				$\geq 0.05$ V/in (ventricular fibrillation)	$\geq 0.03$ V/in (involuntary muscular reactions)	$\geq 0.02$ V/in (involuntary muscular reactions)	$\geq 0.05$ V/in (ventricular fibrillation)	$\geq 0.03$ V/in (involuntary muscular reactions)	$\geq 0.02$ V/in (involuntary muscular reactions)
A (Feb 12)	On	Off	On	1,231 (375)	2,083 (635)*	1707 (520)	263 (80)	2149 (655)*	N/A
B (Feb 11)	Off	Off	Off	1,394 (425)	2,083 (635)*	N/A	296 (90)	2,083 (635)*	N/A
B (Feb 11)	On	Off	On	1,197 (365)	2,100 (640)*	N/A	296 (90)	2,100 (640)*	N/A
B (Feb 11)	On	On	On	1,131 (345)	1,411 (430)	N/A	263 (80)	607 (185)	N/A
C (Feb 12)	On	Off	On	1,165 (355)	N/A	1658 (505)	263 (80)	2149 (655)*	N/A



Pulser Configuration	Parasitic Settings			Range of Greatest Extent					
	1	2	3	Barriers IIA and IIB, in ft (m)			Barrier I, in ft (m)		
				≥ 0.05 V/in (ventricular fibrillation)	≥ 0.03 V/in (involuntary muscular reactions)	≥ 0.02 V/in (involuntary muscular reactions)	≥ 0.05 V/in (ventricular fibrillation)	≥ 0.03 V/in (involuntary muscular reactions)	≥ 0.02 V/in (involuntary muscular reactions)
D (Feb 12)	On	On	Off	607 (185)	804 (245)	N/A	247 (75)	542 (165)	N/A
E (June 14)	On	Off	On	1050 (320)	1181 (360)	N/A	295 (90)	492 (150)	N/A
F (June 14)	On	Off	On	1001 (305)	1132 (345)	1296 (395)	344 (105)	525 (160)	N/A

\* Range of harmful effects extends from south of Barrier IIA to north of Barrier I, there is no safe zone between barriers.

### 2.1.4 Conclusions

Figure 3 shows the areas of likely harmful effects for the six pulser configurations given in Chapter 4, Table 5. Areas associated with involuntary muscular contraction (yellow) are larger than those associated with ventricular fibrillation (red) due to lower threshold voltage values (Appendix B).

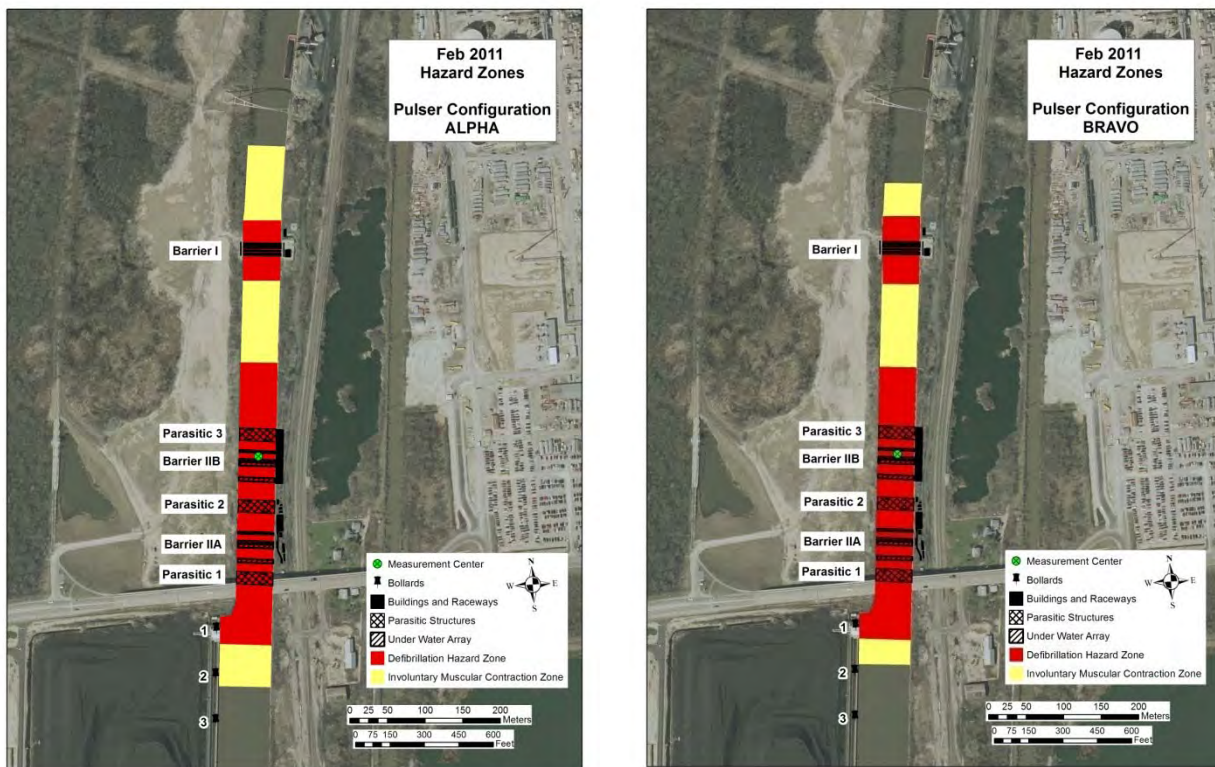


Figure 3. Relative locations of areas of likely harmful effects for the four pulser configurations of Table 5 (continued to next page).

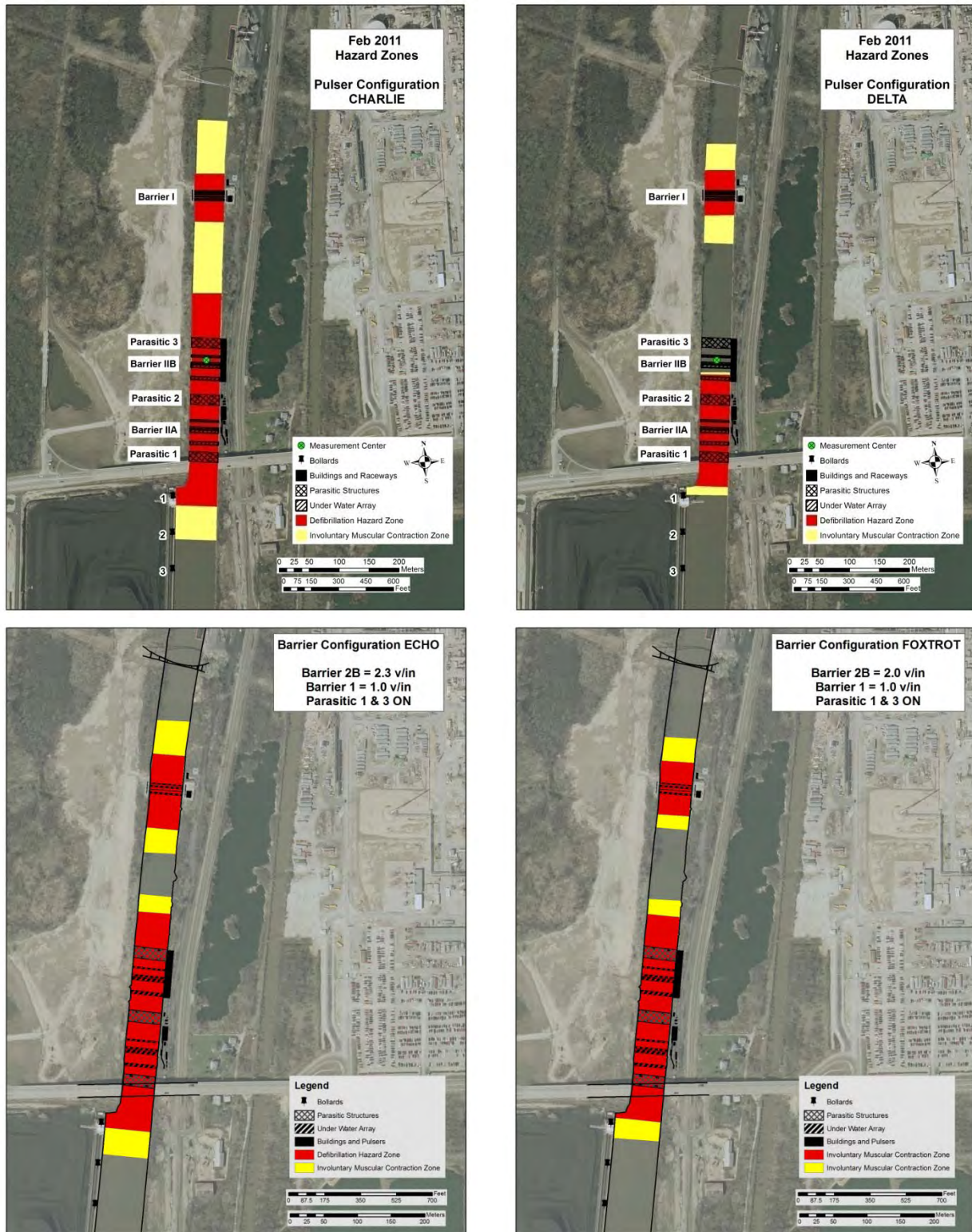


Figure 3 (concluded).

The six areas associated with ventricular fibrillation have been combined into Figure 4. The threshold values derived for pulser configurations Alpha,

Charlie, and Foxtrot are lower ( $\geq 0.02$  V/in.) than pulser configurations Bravo, Delta, and Echo ( $\geq 0.03$  V/in.) due to the longer pulse width as it was incorporated in the calculations. These six areas are shown with the harmful effect zone from 2009, when Barrier IIA was operating alone at 2.0 V/in. The results of the sensitivity analysis suggest that these areas represent worst-case estimates of the actual hazard zones.

For pulser configurations E and F, the harmful-effect zones are similar to configurations A, B, and C because field mapping was conducted with only parasitics 1 and 3 on. Electrical/mechanical problems with parasitic 2 prevented it from being used in the mapping. Once parasitic 2 is repaired, mapping should be repeated with only parasitics 2 and 3 on.

If the operating parameters of a barrier are changed, then the electric field strengths in the water must be mapped again to determine the areas of harmful effects. However, the approach laid out in Appendix B would still be applicable and can be used to evaluate the new field mapping results.



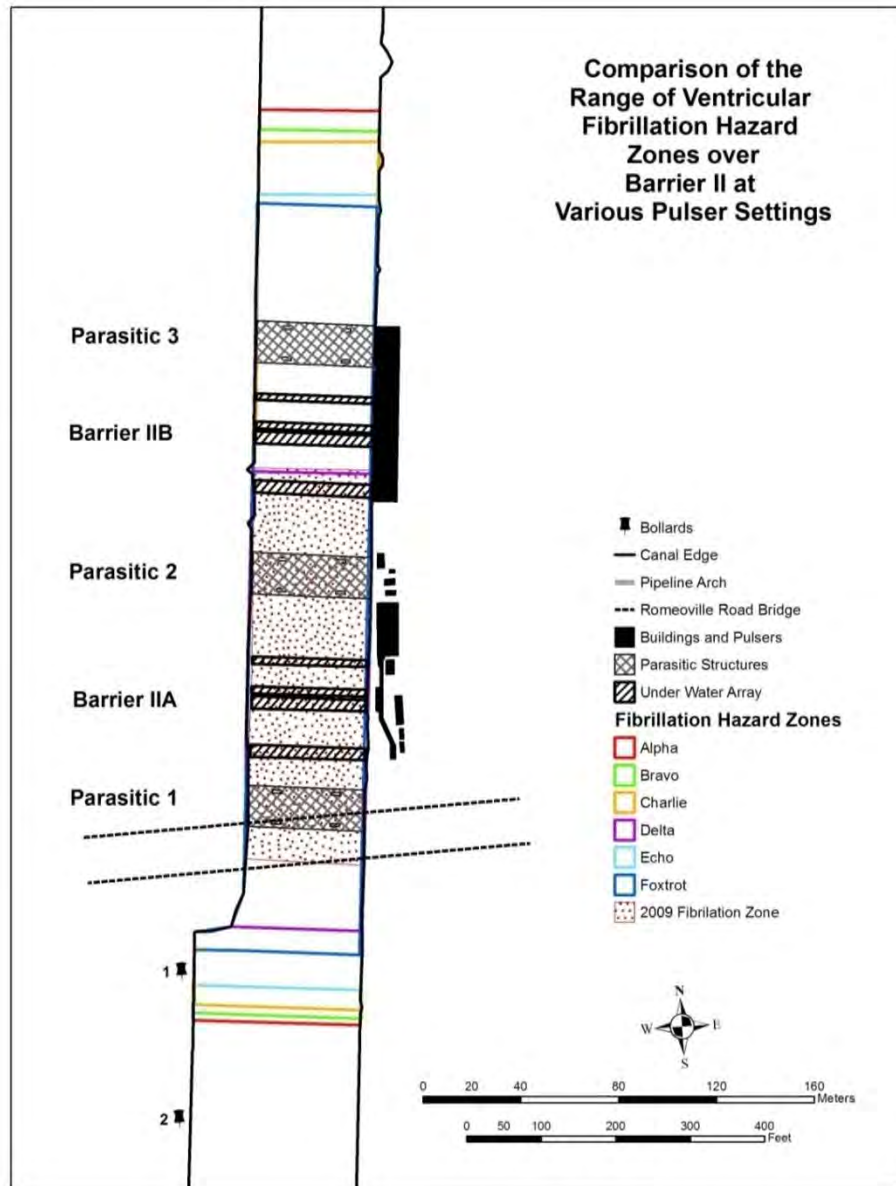


Figure 4. Locations of likely harmful effects for the six pulser configurations in Table 5, Chapter 4.

## 2.2 Sparking potential testing at fleeting area (Objectives 2 and 3)

### 2.2.1 Procedure

Sparking potential testing was completed for each of four operational scenarios. Three configurations for assembling a tow were utilized for testing sparking potential during fleeting operations: assembling a tow with the barges in *series* (Figure 5 and Figure 6), in *parallel* (Figure 7 and Figure 8), and *insertion* of a single barge into a tow (Figure 9 and Figure 10).

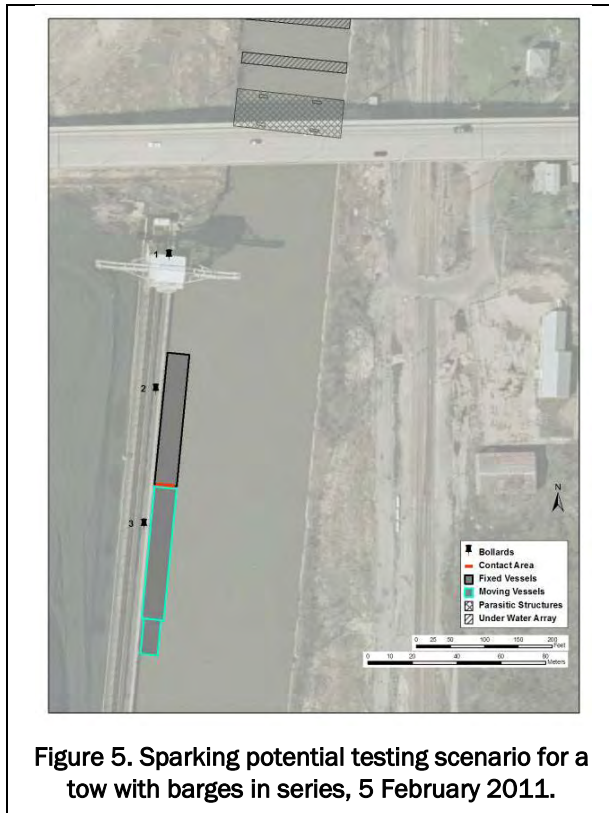


Figure 5. Sparking potential testing scenario for a tow with barges in series, 5 February 2011.

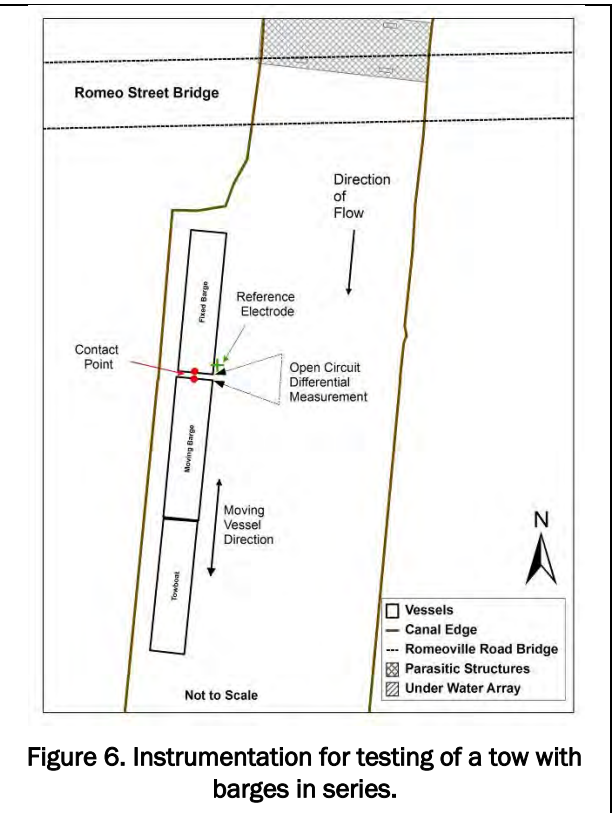


Figure 6. Instrumentation for testing of a tow with barges in series.

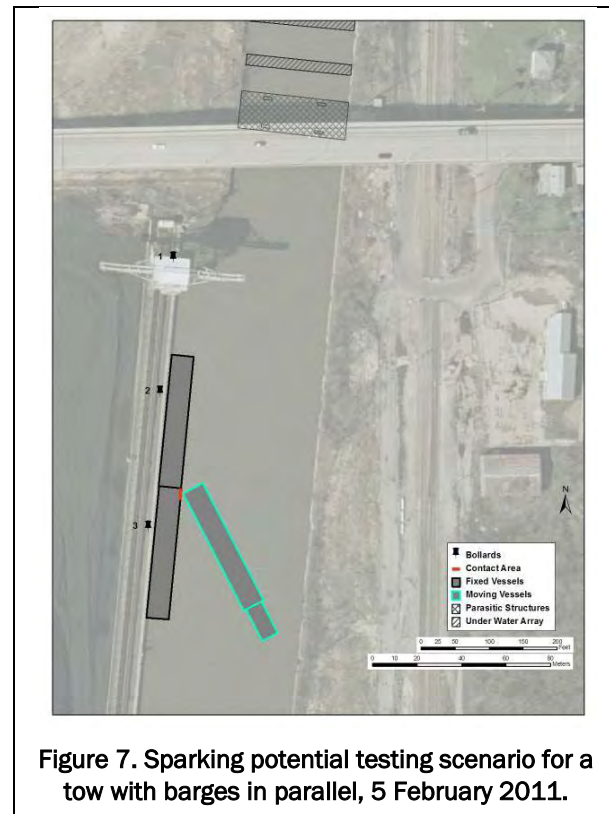


Figure 7. Sparking potential testing scenario for a tow with barges in parallel, 5 February 2011.

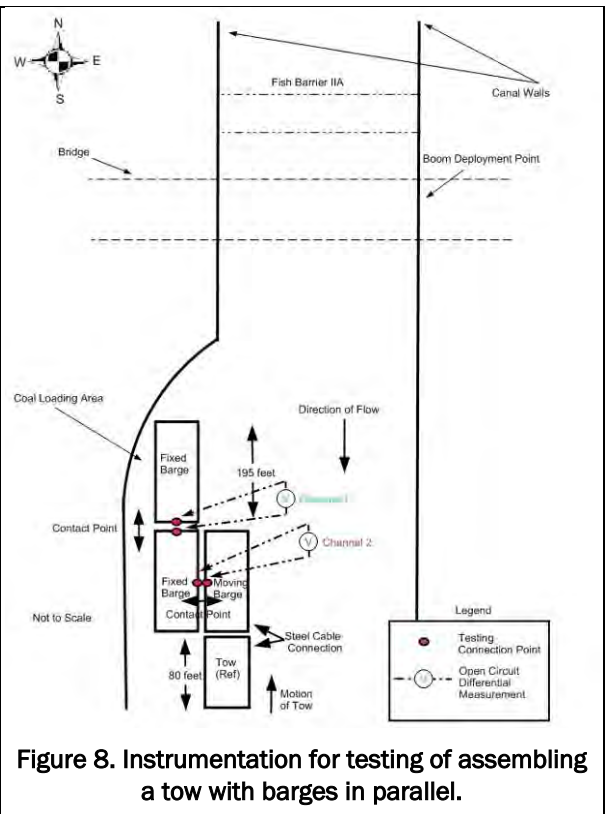


Figure 8. Instrumentation for testing of assembling a tow with barges in parallel.

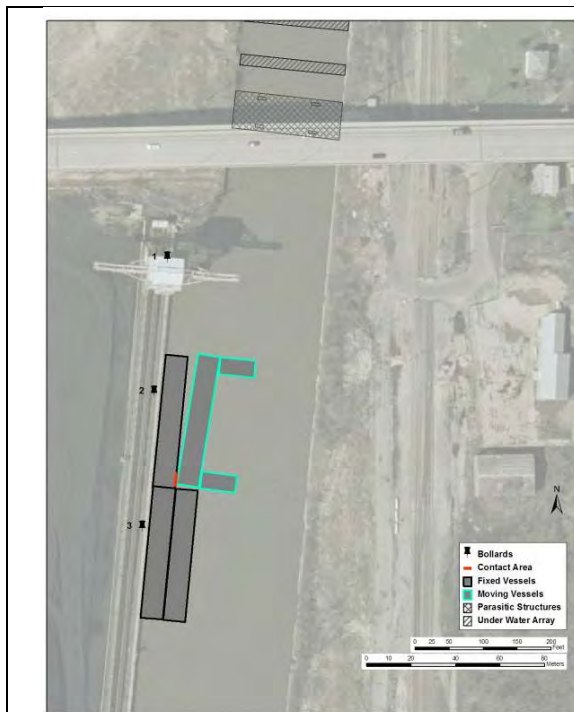


Figure 9. Sparking potential testing scenario for inserting a barge into a tow on 5 February 2011.

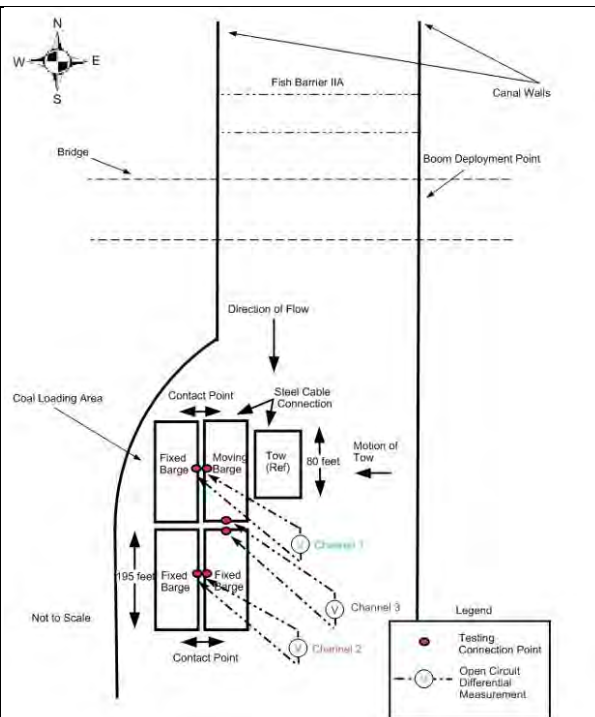


Figure 10. Instrumentation for testing of inserting a barge into a tow.

A fourth test simulated the collision of a tow consisting of five barges in series with two towboats (one on each end of the tow) spanning both Barriers IIA and IIB with two parallel barges moored in the fleeting area. The tow passed over the electrode arrays of Barrier IIA and Barrier IIB while approaching the fleeting area (Figure 11 and Figure 12).

In all cases, barge fleeting occurred at the Midwest Generation fleeting area at bollard 2 and southward. The following measurements and observations were recorded:

1. the open-circuit voltage potential between moored and moving barge as the tow approached and touched three times
2. the electric current flowing between moored and moving barges as the tow approached and touched three times.
3. observations of whether sparking occurred while the moving barge made and broke contact with the fixed barge three times.

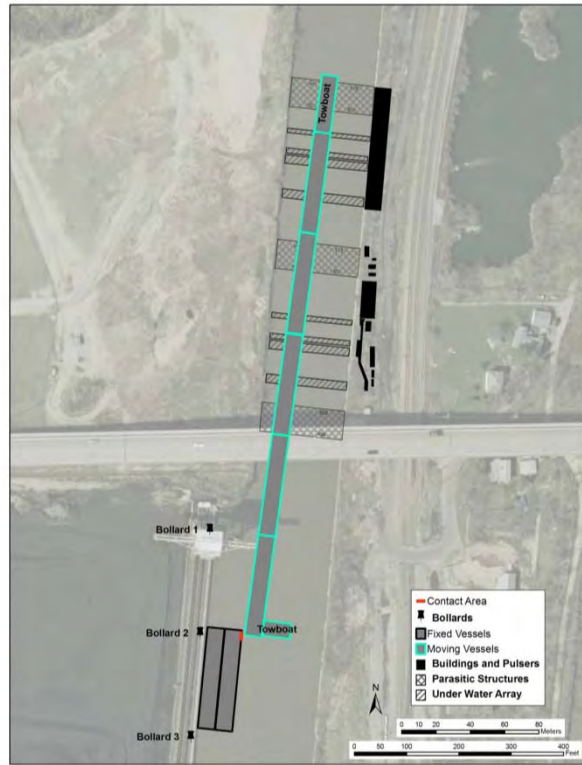


Figure 11. A tow over Barriers IIA and IIB contacting a moored barge in the fleeting area on 7 February 2011.

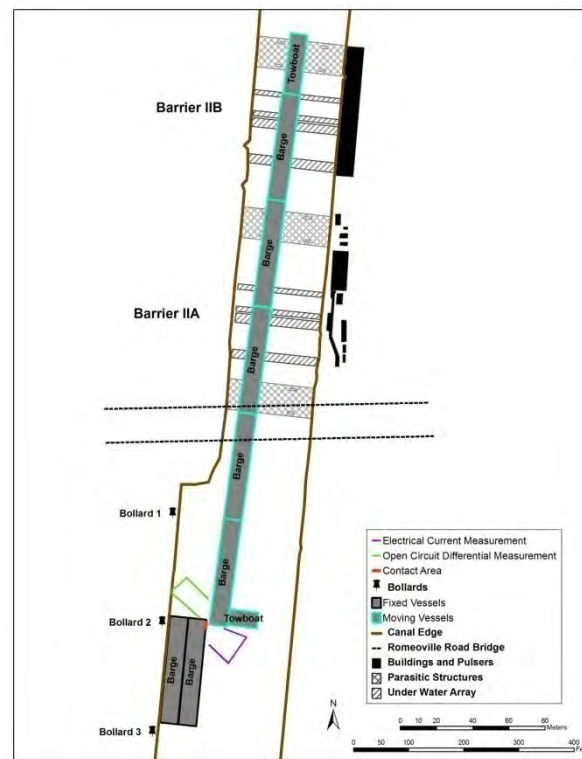


Figure 12. Electrical measurements between a tow over Barriers IIA and IIB and a barge moored in the fleeting area.

Sparking occurs when barges contact and separate. Therefore, for each tow configuration, the moving tow was positioned in close proximity to the moored barge that it made contact with. The contact points are shown on Figure 5, Figure 7, Figure 9, and Figure 11. The tow initially made contact with the moored barge and then slowly scraped the moored barge as it moved away. This was repeated at least three times. Key personnel were positioned to look for sparking during each contact and separation for each test. Voltages and currents between the fixed barges and the moving tow were alternately measured throughout this process. The measurement locations are shown on Figure 6, Figure 8, Figure 10 and Figure 12.

All barges used in the testing were fully loaded to achieve maximum underwater hull exposure. The moored barges for each sparking potential scenario were connected to the dock with soft line and to each other with wire rope. The steel barge-hulls were in contact with the wooden bumpers on the concrete dock walls providing a highly resistive ground path. The tow boat and moving barge were connected with wire rope. This mooring configuration—soft lines to shore and wire rope between barges and barges to tow boat—was consistent throughout testing.

### 2.2.2 Analysis

The percentage of sparking events for each pulser configuration was computed and peak voltages and currents at the time just before a bumping / collision event were visually estimated from plots of the data.

Rudimentary analyses of the electrical characteristics of a sparking event were performed using the voltage and current data. Voltage, or electric potential, is the amount of energy available to perform work on an individual charge. It is the energy per unit charge. The current is the rate at which the charges are moving. In the case of a steel barge hull, the charges are electrons.

From the voltage and current data, a rough estimate of the amount of energy in each pulse may be calculated using the formula

$$E = V \times I \times t_p$$

where

$E$  = energy (joules)



$V$  = voltage (volts)  
 $I$  = current (amps)  
 $t_p$  = time (pulse length in seconds).

This estimation method is analogous to the way energy use is recorded by a common residential electric meter. The value of  $t_p$  for each pulser configuration is listed in Table 5. Note that for the same voltage and current, longer pulses have more energy. The average voltage and current for each pulser configuration and parasitic setting were used for the energy computation.

### 2.2.3 Results and observations

Data for the sparking potential tests during fleeting operations are listed in Table 6, and data for the sparking potential tests during simulated collision are listed in Table 7. Sparking observers consisted of representatives from the test team at ERDC-CERL, one representative from Chicago District, one representative from the Coast Guard Marine Safety Unit, and barge crewmen.

During fleeting operations testing, an observer saw sparking on 1.9% (1/52) of the series (fore and aft) mooring tests, on 0% (0/49) of the parallel mooring tests, on 38% (18/48) of the insertion tests. During the collision tests, observers saw sparking on 100% (36/36) of the tests when barriers II A and II B were operating, on 100% (8/8) when only IIB was operating, and none 0% (0/6) when only Barrier IIA was operating. During the collision tests, significant voltages and currents were measured (see Table 7). In summary, sparking was observed during operational scenarios A, B, C, E, and F but never during D when only Barrier IIA was in operation.

Summary Table C compiles the basic sparking observation results during simulated fleeting operations in the fleeting area. There is little difference in the frequency of observed sparking between pulser configurations A, B, and C and the state of the parasitics; however configurations E and F had the lowest frequencies. Sparking was observed most frequently during the insertion process.

**Summary Table C. Summary of sparking observations based on test results for sparking potential during fleeting operations (see Table 6, Chapter 4).**

Pulser Configuration	Parasitic Settings			# Sparking Observations / # barge contacts		
	1	2	3	Series	Parallel	Insertion
A (Feb 5)	On	On	On	0/6	0/6	4/6
A (Feb 5)	On	Off	On	0/6	0/7	1/6
B (Feb 5)	On	On	On	0/6	0/6	4/6
B (Feb 5)	On	Off	On	0/6	0/6	2/6
C (Feb 5)	On	On	On	0/6	0/6	3/6
C (Feb 5)	On	Off	On	0/6	0/6	4/6
D (Feb 5)	On	On	Off	1/6	0/6	0/7
E (June 15)	On	Off	On	0/4	0/2	0/2
F (June 15)	On	Off	On	0/6	0/4	0/2

Voltage values where sparking was observed ranged from 4.7 – 10 volts, while the values where no sparking was observed ranged from 1.0 – 9.9 volts. Similarly, the current values during sparking were in the same range as values measured where no sparking was observed.

Summary Table D compiles the voltage, current and estimated energy results for the simulated fleeting operations, based on the data presented in Chapter 4, Table 6. Note the consistently lower energy, throughout all barge and pulser configurations, when parasitics 1, 2, 3 were all on. The average reduction was 46% and the maximum was 75%.

**Summary Table D. Summary of estimated energy based on results for sparking potential during fleeting operations (see Table 6, Chapter 4).**

Barge Configuration	Pulser Configuration	Parasitic Settings			Average Peak voltage (volts)	Average Peak Short Circuit Current (Amps)	Estimated Energy (mJoules)
		1	2	3			
Series	A (Feb 5)	On	On	On	6.5	1.1	44.8
Series	A (Feb 5)	On	Off	On	6.6	1.5	62.6
Series	B (Feb 5)	On	On	On	7.2	0.9	17.0
Series	B (Feb 5)	On	Off	On	8.4	1.6	33.5
Series	C (Feb 5)	On	On	On	6.0	0.8	29.5
Series	C (Feb 5)	On	Off	On	8.2	1.5	81.7

Barge Configuration	Pulser Configuration	Parasitic Settings			Average Peak voltage (volts)	Average Peak Short Circuit Current (Amps)	Estimated Energy (mJoules)
		1	2	3			
Series	D (Feb 5)	On	On	Off	4.4	0.3	2.9
Series	E (June 15)	On	Off	On	2.0	0.3	1.3
Series	F (June 15)	On	Off	On	1.2	0.2	1.6
Parallel	A (Feb 5)	On	On	On	2.3	0.3	4.7
Parallel	A (Feb 5)	On	Off	On	3.2	0.4	8.0
Parallel	B (Feb 5)	On	On	On	2.5	0.3	1.8
Parallel	B (Feb 5)	On	Off	On	2.5	0.4	2.6
Parallel	C (Feb 5)	On	On	On	2.6	0.4	6.6
Parallel	C (Feb 5)	On	Off	On	2.8	0.6	11.0
Parallel	D (Feb 5)	On	On	Off	1.6	0.2	0.7
Parallel	E (June 15)	On	Off	On	0.6	0.1	0.2
Parallel	F (June 15)	On	Off	On	0.5	0.1	0.3
Insertion	A (Feb 5)	On	On	On	6.7	1.0	43.3
Insertion	A (Feb 5)	On	Off	On	6.9	1.7	75.9
Insertion	B (Feb 5)	On	On	On	6.3	1.3	20.7
Insertion	B (Feb 5)	On	Off	On	8.6	1.7	35.5
Insertion	C (Feb 5)	On	On	On	5.5	1.0	34.4
Insertion	C (Feb 5)	On	Off	On	8.2	2.5	132.0
Insertion	D (Feb 5)	On	On	Off	1.6	0.2	0.9
Insertion	E (June 15)	On	Off	On	1.5	0.2	0.8
Insertion	F (June 15)	On	Off	On	1.3	0.2	1.7

The range of peak voltage measured for each operational configuration with all three parasitics in the on position was not significantly different than the ranges measured with only two of the parasitics connected. The estimated energy was consistently lower with all three parasitics in the on position in comparison to estimates with only two of the parasitic connected.

The collision tests (Table 7, with results compiled in Summary Table E) showed a range of peak voltages during sparking from 35.0 – 96.6 volts, in comparison to 15.3 – 19.2 volts when no sparking was observed. However, it should be noted that sparking was observed in every test of pulser configurations A, B, C, E, and F, but not during scenario D. No such range difference was observed in the electric current measurements.

Summary Table E. Test results for sparking potential during collision simulations, conducted on 7 February 2011 (see Table 7, Chapter 4).

Pulser Configuration	Parasitic Settings			Sparking Observations	Peak Voltage	Estimated Energy
	1	2	3			
A (Feb 7)	On	On	On	6/6	68.6 V - 78.4 V	5,667 mJ
A (Feb 7)	On	Off	On	6/6	60.3 V - 69.3 V	5,207 mJ
B (Feb 7)	On	On	On	6/6	67.4 V - 72.7 V	1,973 mJ
B (Feb 7)	On	Off	On	6/6	60.7 V - 72.6 V	1,941 mJ
C (Feb 7)	On	On	On	6/6	85.9 V - 96.3 V	12,033 mJ
C (Feb 7)	On	Off	On	6/6	19.8 V - 96.6 V	11,121 mJ
D (Feb 7)	On	On	Off	0/6	15.3 V - 19.2 V	727 mJ
E (June 15)	On	Off	On	4/4	35.0 - 62.0 V	2,774 mJ
F (June 15)	On	Off	On	4/4	68.0 - 72.0 V	2,581 mJ

During collision tests there was not a significant difference in the estimated energy between parasitic settings for each pulser configuration. This result was due to the tow spanning both barriers and all parasitics.

Sparking is caused by the separation of barges. When barges are positioned parallel with the stray current from the barriers, maximum potential difference between them may be observed. However, when barges are perpendicular to current, minimum potential difference and minimum current flow will be seen.

A limited literature review was conducted on the topic of electrical sparking. The US Occupational Safety and Health Administration (OSHA) has published several documents that discuss sparking, mostly related to machinery and protecting personnel from burns. OSHA has a web page about safety for the electric power generation, transmission, and distribution industry.<sup>4</sup> The review identified one document pertaining to explosion hazards in the coal industry, including coal-fired power plants [10]. This document suggests that the primary danger is from coal dust in a confined space. Concerning coal storage outside, the author states that

<sup>4</sup> <http://www.osha.gov/SLTC/powergeneration/index.html>

The raw coal for a pulverized fuel system is usually received from a variety of sources and the size is generally limited to approximately 2 inches or smaller. This raw coal is typically stored on an outside stockpile where it is moved around by frontend loaders. The fire and explosion hazards associated with this stockpile are usually limited to spontaneous combustion [10].

Further information on the potential ignition of coal dust from an electrical spark was provided through an examination of the Midwest Generation facility electrical safety provisions. Coordination with Midwest Generation environmental and electrical specialists provided information on the classification of various areas of the facility.

National Fire Protection Association (NFPA) Code 70, or the National Electric Code (NEC), is a US standard for the safe installation of electrical wiring and equipment. Chapter 5 of the code addresses electrical wiring in special occupancies and establishes various classifications. Of concern to the Midwest Generation facility are the classified areas defined by Class II (locations that are hazardous due to the presence of combustible dust), Division 1 (locations where hazardous concentrations are present in the air continuously, intermittently or periodically under normal operating conditions) and Group F (atmospheres containing carbon black, coal dust, or coke dust). These NEC provisions are related primarily to the use of proper enclosures, wiring trolleys, bronze hooks, stainless steel chain, or wire rope to provide the necessary spark resistance.

Electrical safety provisions of the plant were examined with respect to the above classification and it was determined that the coal stockpile did not require any special provisions. However, explosion-proof equipment has been installed in areas that contain enclosed rooms. This includes underground tunnels and the tripper room inside the plant. No area outside, including the stockpile and conveyors, is required to have explosion-proof equipment.

#### **2.2.4 Conclusions**

It is concluded that there is greater risk of sparking during the insertion fleeting operation than during series or parallel tow operations. It is also concluded that the operation of both barriers at the same time increases

the potential for sparking during fleeting operations. There is consistently lower energy per pulse when parasitics 1, 2, 3 are all on. For coal-handling operations in the barge loading and fleeting area, and in the open storage area, the pertinent literature does not support concern for electrical sparking to create an explosion hazard.

## **2.3 Long tow voltage potential test (Objective 4)**

### **2.3.1 Procedure**

Long tow testing was completed for each of the barrier operational scenarios. In these tests a tow of five fully loaded barges in a single line made a minimum of three trips traversing from the fleeting area to above the aerial pipeline arch (Figure 13 and Figure 14).

This testing was designed to measure the voltage potential between the barges and tow boats within a long tow during the operation of all three barrier systems. This was accomplished by recording six channels of barge open circuit voltage potentials as the long tow traverses the barrier region. The voltage potentials between adjacent components of the long tow ( $V_{01}$ ,  $V_{12}$ ,  $V_{23}$ ,  $V_{34}$ ,  $V_{45}$ , and  $V_{56}$ ) were measured as shown in Figure 14. Unlike previous testing, this time there were two towboats, one at each end of the five-barge tow. The boats are designated 0 and 6, the barges 1 – 5, which resulted in six measurement channels. All components of the tow were connected using wire rope, as is typical for transit on the canal.

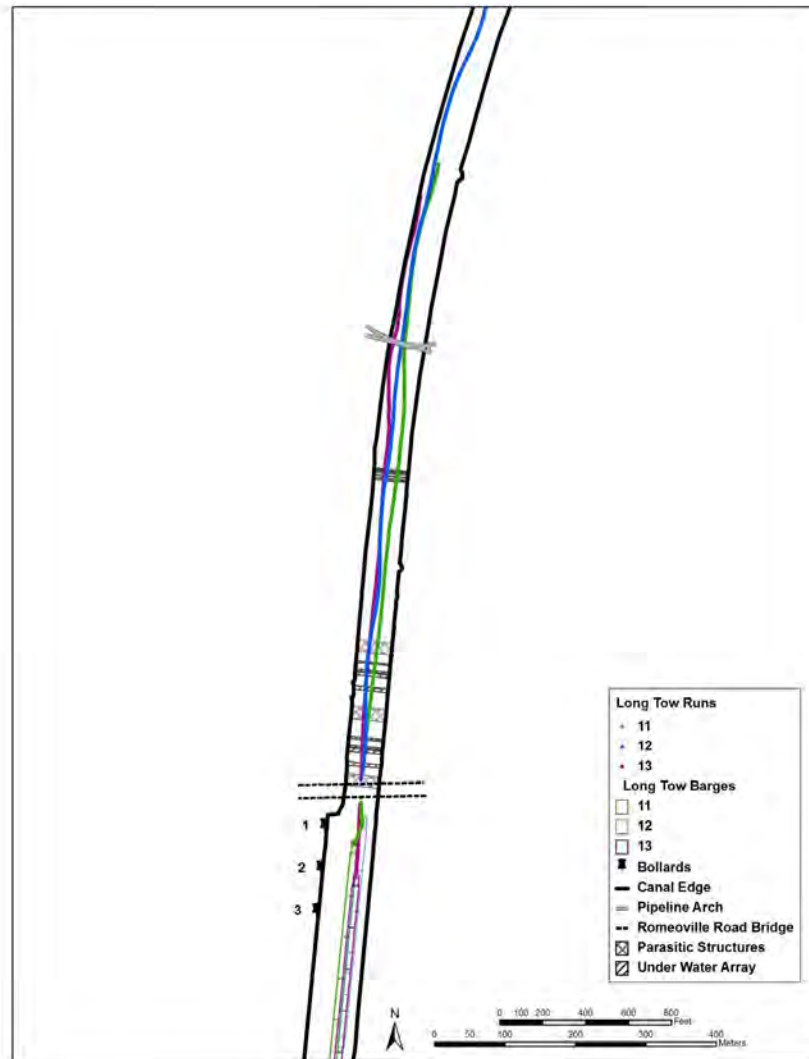


Figure 13. Long tow consisting of five barges and two towboats traversing the barriers on 8 and 10 February when the pulsers were in configuration Bravo and Parasitic 2 was on.

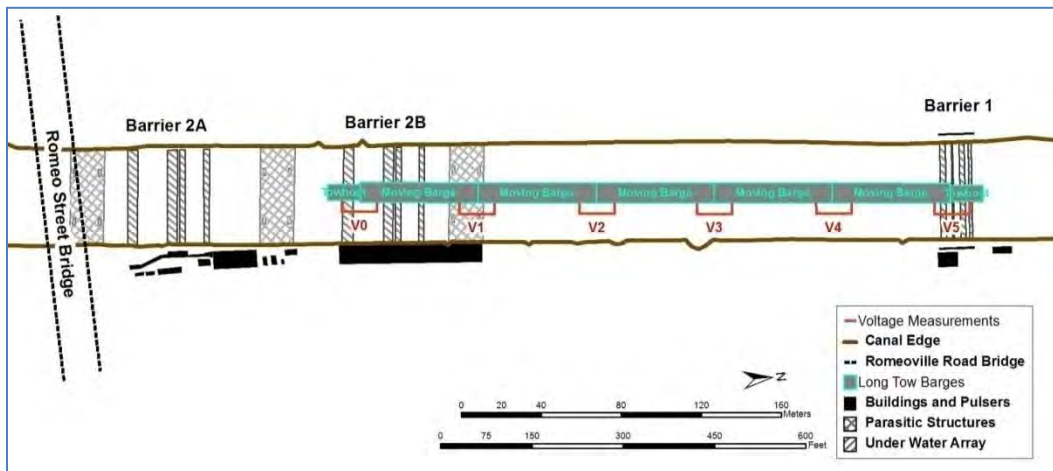


Figure 14. Diagram of five open-circuit voltage measurements ( $V_1$ – $V_5$ ) simultaneously captured for each barge in the long tow.

### 2.3.2 Analysis

The voltage plots were examined for each run, and the peak values when boats and barges passed over the barriers were noted.

### 2.3.3 Results and observations

Results of the long-tow voltage potential tests are listed in Chapter 4, Table 8, Table 9, and Table 10. The salient results are outlined below in Summary Table F.

Summary Table F. Outline of test results for long tow traversing Barriers IIA, IIB, and I, conducted on 8 and 10 February 2011 (see Tables 8–10, Chapter 4).

Pulser Configuration	Parasitic Settings			Range of voltage Differences between Barges		
	1	2	3	Over Barrier I	Over Barrier IIA	Over Barrier IIB
A	On	On	On	0.44V - 1.33V	1.60V - 3.23V	1.93V - 3.77V
A	On	Off	On	0.39V - 1.20V	1.26V - 3.45V	1.41V - 4.61V
B	On	On	On	0.55V - 1.15V	1.45V - 3.40V	1.37V - 5.99V
B	On	Off	On	0.36V - 1.70V	1.31V - 5.22V	1.86V - 4.56V
C	On	On	On	0.39V - 1.17V	1.09V - 2.93V	1.34V - 4.29V
C	On	Off	On	0.52V - 1.30V	1.22V - 4.36V	1.72V - 3.81V
D	On	On	Off	0.53V - 1.21V	1.47V - 4.64V	—

Long-tow voltage potential tests were not conducted for pulser configurations E and F. The primary data sampling and recording instrument failed, and the capabilities of the backup system were not sufficient (e.g., fewer recording channels) to adequately complete the long-tow tests. However, long-tow testing for pulser configurations E and F would be unlikely to show any new information. Previous testing indicated there is no significant risk associated with these tests, which are designed to identify the potential for sparking between barges traveling in a long-tow formation using wire rope to connect the barges.

The range of peak voltage differences measured over all three barriers in the B operational configuration does not appear to be significantly different than the range of peak voltage differences measured in the C configuration. The range of peak voltage differences when all three parasitics were



connected was not significantly different than the range of voltage differences when only two parasitics were connected.

The highest voltage difference between barges, for all pulser configurations, was about 5 volts while passing over Barrier IIA, about 6 volts over Barrier IIB, and 1.7 volts over Barrier I. These low voltage values between barges indicate good electrical contact between the barge pairs. The peak voltage between towboat and barge is greater than between barges because the towboat-barge connection can have higher electrical resistance. The towboat has rubber impact bumpers that serve to electrically isolate it from the barge, so the sole electrical connection between the two is the wire rope. The barges are electrically connected not only by the wire rope but also through contact of their steel hulls.

### 2.3.4 Conclusions

The long tow voltage measurements suggest that there is a low probability for sparking between barges in a tow while traversing the barriers. These voltage differences are very small when compared to the soft line connection values of about 250 volts previously measured for Barrier I (see [1]). All barge-to-barge potentials are consistent with previous measurements and are below the limit of concern. The higher voltages measured between the barge and tugboats (Summary Table G) are the result of a higher resistive path between the tow and barge due to the rubber bumpers and cable-to-winch connections. Even though the measured voltages between tugboat and barge are higher than between barges, there is still a low probability of sparking because the barge is winched very tightly to the towboat. Observations of sparking have shown that it occurs when electrical contact is broken between towboat and barge, which would be unlikely.

**Summary Table G. Voltage differences between outside barges and towboats.**

Pulser Configuration	Range of voltage Differences between TOWBOAT and BARGE					
	Over Barrier I		Over Barrier IIA		Over Barrier IIB	
	1*	2**	1*	2**	1*	2**
A	0.79V - 0.9V	7.4V - 8.27V	2.22V - 2.67V	18.1V - 21.5V	2.91V - 3.31V	26.9V - 29.1V
B	0.77V - 10.1V	7.38V - 9.91V	2.52V - 29.7V	21.5V - 25.3V	2.8V - 35.1V	26.5V - 32.9V
C	9.72V - 11.5V	7.28V - 8.04V	26.4V - 30.3V	18.3V - 21.5V	33.1V - 36.6V	24.2V - 28V
D	10.3V - 11.6V	7.76V - 7.98V	30.7V - 33.1V	21.8V - 23.6V	—	—

\*1: Potential between south towboat and Barge 1. \*\* 2: Potential between north towboat and Barge 5.

## 2.4 Shock potential at fleeting dock bollards (Objective 5)

### 2.4.1 Procedure

Voltage and current measurements at the Midwest Generation fleeting area were recorded for each of the six barrier operational scenarios. This test measured the voltages and currents between fixed barges in the fleeting area and the dock. Tests were conducted at the number 2 and 3 north tee-moorings.<sup>5</sup> A 500  $\Omega$  resistor was used for the current measurements.

### 2.4.2 Analysis

The voltage and current plots were examined for each record, and the peak values were noted.

### 2.4.3 Results and observations

Data for the shock potential tests are shown in Chapter 4, Table 11, and the results are presented in Summary Table H.

Summary Table H. Concise results for bollard voltage potential and 500-ohm current tests at fleeting area, conducted on 7 February 2011 (see Table 11, Chapter 4).

Pulser Configuration	Parasitic Settings			Peak voltage and Current at Bollards			
	1	2	3	Bollard 2		Bollard 3	
A (Feb 7)	On	On	On	6.3V	11.7 mA	3.0V	4.3 mA
A (Feb 7)	On	Off	On	7.9V	15.4 mA	3.8V	10.7 mA
B (Feb 7)	On	On	On	7.2V	11.3 mA	3.0V	4.3 mA
B (Feb 7)	On	Off	On	10.8V	17.0 mA	4.9V	7.4 mA
C (Feb 7)	On	On	On	6.9V	12.7 mA	4.3V	7.0 mA
C (Feb 7)	On	Off	On	11.2V	14.7 mA	7.9V	8.1 mA
D (Feb 7)	On	On	Off	3.0V	5.9 mA	1.6V	3.4 mA
E (June 15)	On	Off	On	3.3V	6.6mA	2.3V	5.6mA
F (June 15)	On	Off	On	3.5V	6.8mA	2.8V	5.2mA

<sup>5</sup> A tee-mooring is a large concrete-filled steel bollard with a steel crossbar that is used to tie barges and boats to the dock.

The 500  $\Omega$  resistance simulates the impedance of the human body from hand to foot. The hand to foot shock potential is referred to as the *touch potential*. Both peak voltage and current measurements were significantly lower at Bollard 3 than at Bollard 2, the latter being 200 ft (61 meters) closer to the barriers. There is no significant difference in either voltage potential or current between pulser configurations B and C. Having all three parasitics connected reduces the voltage and current for all pulser configurations at both bollard locations.

The maximum peak current was 17 mA and the maximum peak voltage was 11.2 volts. From Appendix B, Table B1 and Figure B1, these measurements are in the DC-2 range of IEC Publication 60479-1, where involuntary muscular contractions likely, especially when making, breaking or rapidly altering current flow, but usually without causing physiological harm.

#### **2.4.4 Conclusions**

There is no personnel shock hazard at the fleeting area due to barrier operation.

## **2.5 Corrosion potential (Objective 6)**

### **2.5.1 Procedure**

In order to evaluate the possibility of accelerated corrosion on in-water steel structures in the fleeting area due to barrier operation, corrosion potential measurements were made on a moored barge during the tow assembly scenarios shown in Figure 5. Hull voltage potentials were measured between a copper/copper sulfate reference electrode immersed in canal water at the stern corner on the starboard side of the moored barge and the steel hull, as diagrammed in Figure 6. The barge was fully loaded to achieve maximum hull exposure underwater.

These measurements were made at the time of the sparking potential tests. Because the barriers produce pulsing waveforms, an *IR-free measurement* was made. An IR-free measurement is one where the voltage drop ( $I$  is current,  $R$  is resistance) between the reference electrode and the structure (in this case, a barge hull) is eliminated. For a pulse, this is accomplished by taking the measurement at the instant the driving current goes to zero. This was done using an oscilloscope to view the potential waveform.

### **2.5.2 Analysis**

Previous analysis of the hull-to-electrode corrosion potentials show a near-perfect “net zero” value, which confirms that the pulsed fish barrier electrical field, in effect, induces an alternating current signal during the cycle of the tow entering, passing over, and leaving the barrier. Thus, so long as the tow is electrically connected while entering, passing through, and continuing beyond the barrier by at least several hundred feet at a relatively uniform rate, no long-term corrosion effects should be of concern for tows moored at the fleeting area.

### **2.5.3 Results and observations**

Results of the corrosion potential tests are listed in Chapter 4, Table 12. Anticipated corrosion activity for ferrous metal immersed in fresh water for several ranges of corrosion potentials are listed in Table 13, as derived from [9]. The measured corrosion potentials of 360 and 380 (-mV) indicate minimal corrosion activity.

### **2.5.4 Conclusions**

Based on the previous analyses of the barge corrosion potentials passing over the barriers and the recent stationary barge corrosion potentials measured at the fleeting area (Bollard 2), there is no indication of a long-term corrosion problem for barges moored at the fleeting area.

## **2.6 Parasitic grid configuration testing (Objective 7)**

### **2.6.1 Procedure**

In an effort to determine the optimal configuration of the parasitic structures shown in Figure 11, the connections between these structures were varied throughout the other tests documented in this report. As previously described, the parasitic structures consist of three steel grids placed on concrete supports on the bottom of waterway.

From southernmost to northernmost locations, the grids are numbered 1, 2, and 3, respectively. Each grid is connected by metal cables welded to the grid structure and connecting it to an electrical bus on the western shore of the canal. There are several switches that allow each parasitic grid to be connected and disconnected from the bus. By closing each switch (on posi-

tion), parasitics are connected to each other via the bus. By opening a switch (off position), a parasitic may be disconnected from the bus.

### **2.6.2 Results and observations**

Analysis of pulse energy during the fleeting area sparking tests shows higher energy at the fleeting area when only two parasitics are connected versus when all three are connected. No significant change in energy was observed in simulated collision as the tow spanned both barriers. The largest hazard area was noted when all three parasitic structures were not connected.

### **2.6.3 Conclusions**

These test results do not provide clear evidence to refute the barrier designer's recommendation that the optimal parasitic configuration is accomplished by connecting only two of the three parasitic structures: those directly adjacent to the active arrays.

## 3 Conclusions and Recommendations

### Conclusions

Summarized below are the principal conclusions drawn for each of the seven barrier-testing objectives:

1. Operating Barriers IIA and IIB concurrently creates a larger area of risk to a person in the water than operating them individually.
2. No significant increase in sparking risk was found when barrier operating parameters are set to 2.3 V/in. at 30 Hz with 2.5 ms pulses versus 2.0 V/in. at 15 Hz with 6.5 ms pulses.
3. For coal-handling operations in the barge loading and fleeting area, and in the open storage area, the pertinent literature does not support concern that electrical sparking creates an explosion hazard.
4. When a tow that spans Barriers IIA and IIB collides with a barge in the fleeting area, there is a higher risk of sparking when both barriers are operating than when only Barrier IIA is operating.
5. No significant increase in risk of sparking was found for a long tow spanning Barriers IIA and IIB when both are operating as long as the tow does not collide with other metal objects.
6. No significant risk of personnel shock hazard in the fleeting area was found during barrier operations for any operating configuration.
7. Operation of the barriers does not adversely affect corrosion potential for in-water steel structures at the Midwest Generation fleeting area.
8. The optimal parasitic grid configuration (i.e., best field pattern, least energy consumption, and least danger of sparking and shock in the fleeting area), utilizes connections between only the two parasitic structures directly adjacent to the active arrays.

### Recommendations

Regarding operation of the fish barrier, it is recommended that:

- When making rules for barge operations in the fleeting area, consideration be given to the finding that the pertinent literature does not support concern that electrical sparking creates an explosion hazard.

- When operating the pulsers, consideration be given to the finding that the optimal parasitic grid configuration utilizes connections between only the two parasitic structures directly adjacent to the active arrays.

It is further recommended that the U.S. Coast Guard consider the findings of this study when preparing Regulated Navigation Area (RNA) documents pertaining to navigation of the Chicago Sanitary and Ship Canal.

## **4 Unabridged Data Tables**

Editor's note: the tables presented in this chapter represent the raw data from which the summary tables, used in the main text, were derived.



Table 1. Environmental conditions during testing.

Date	Time	Mean Temperature (°F)	Average Humidity (%)	Precipitation (in)	Water Temperature (°F)	Water Conductivity (µS/cm)	Water Resistivity (ohm-cm)
4 Feb 2011	0910	17	73	None	39	1732	577
4 Feb 2011	1105	26	82	None			
4 Feb 2011	1400	29	88	None			
4 Feb 2011	1600	26	89	None			
5 Feb 2011	0800	17	73	None	37	1307	765
5 Feb 2011	1030	25	82	None			
5 Feb 2011	1400	32	89	None	41	1560	641
5 Feb 2011	1600	30	90	None			
7 Feb 2011	0845	27	91	None	39	1575	635
7 Feb 2011	1100	39	98	None			
7 Feb 2011	1450	35	54	None	41	1715	583
7 Feb 2011	1630	31	54	None			
8 Feb 2011	0850	12	48	None	41	1733	577
8 Feb 2011	1100	20	27	None			
8 Feb 2011	1400	21	25	None			
8 Feb 2011	1600	14	26	None			
10 Feb 2011	0800	-2	27	None	41	1733	577
10 Feb 2011	1030	12	27	None			
10 Feb 2011	1400	19	25	None			
10 Feb 2011	1600	18	30	None			
11 Feb 2011	1000	22	36	None	43	1575	577
11 Feb 2011	1130	28	32	None			
11 Feb 2011	1400	26	35	None			
11 Feb 2011	1600	27	38	None			
12 Feb 2011	0900	33	52	None	43	2242	446
12 Feb 2011	1100	39	35	None			
12 Feb 2011	1400	39	37	None			
12 Feb 2011	1600	38	40	None			

Table 2. Pulser and parasitic configurations and approximate run times for field mapping, conducted on 11 and 12 February 2011, and 14 June 2011.

Run Time	Run	Location	Pulser Configuration	Parasitic 1	Parasitic 2	Parasitic 3
<b>11 February 2011</b>						
08:40 – 09:00	1	East Wall	B	Off	Off	Off
09:00 – 09:20	2	West Wall	B	Off	Off	Off
09:20 – 09:40	3	Center	B	Off	Off	Off
Aborted	4	West Wall	B	Off	Off	Off
09:45 – 10:00	5	West Wall	B	Off	Off	Off
10:00 – 10:25	6	East Wall	B	Off	Off	Off
10:25 – 10:40	7	Center	B	Off	Off	Off
10:40 – 11:00	8	Center	B	On	Off	On
13:15 – 13:35	9	East Wall	B	On	Off	On
13:35 – 13:50	10	West Wall	B	On	Off	On
13:50 – 14:05	11	Center	B	On	Off	On
14:05 – 14:20	12	West Wall	B	On	Off	On
14:20 – 14:35	13	East Wall	B	On	Off	On
14:35 – 14:50	14	West Wall	B	On	On	On
14:50 – 15:05	15	East Wall	B	On	On	On
15:05 – 15:20	16	Center	B	On	On	On
15:20 – 15:35	17	East Wall	B	On	On	On
15:35 – 15:45	18	West Wall	B	On	On	On
15:45 – 16:00	19	Center	B	On	On	On
<b>12 February 2011</b>						
09:10 – 09:30	1	East Wall	D	On	On	Off
09:30 – 09:45	2	West Wall	D	On	On	Off
09:45 – 10:00	3	Center	D	On	On	Off
10:00 – 10:10	4	West Wall	D	On	On	Off
10:10 – 10:25	5	East Wall	D	On	On	Off
10:25 – 10:35	6	Center	D	On	On	Off
10:35 – 10:45	7	East Wall	A	On	Off	On
10:45 – 11:00	8	West Wall	A	On	Off	On

Run Time	Run	Location	Pulser Configuration	Parasitic 1	Parasitic 2	Parasitic 3
13:25 - 13:45	9	Center	A	On	Off	On
13:45 - 13:55	10	West Wall	A	On	Off	On
13:55 - 14:10	11	East Wall	A	On	Off	On
14:10 - 14:20	12	Center	A	On	Off	On
14:20 - 14:40	13	East Wall	C	On	Off	On
14:40 - 14:55	14	West Wall	C	On	Off	On
14:55 - 15:15	15	Center	C	On	Off	On
15:15 - 15:30	16	West Wall	C	On	Off	On
15:30 - 15:50	17	East Wall	C	On	Off	On
15:50 - 16:00	18	Center	C	On	Off	On
16:00 - 16:15	19	Center	C	On	On	On
<b>14 June 2011</b>						
08:59 - 09:19	8	East Wall	E	On	Off	On
09:20 - 09:31	9	West Wall	E	On	Off	On
09:31 - 09:46	10	Center	E	On	Off	On
09:46 - 09:56	11	West Wall	E	On	Off	On
09:58 - 10:07	12	East Wall	E	On	Off	On
10:08 - 10:23	13	Center	E	On	Off	On
13:03 - 13:23	14	East Wall	F	On	Off	On
13:23 - 13:35	15	West Wall	F	On	Off	On
13:35 - 13:51	16	Center	F	On	Off	On
13:51 - 14:05	17	West Wall	F	On	Off	On
14:06 - 14:19	18	East Wall	F	On	Off	On
14:19 - 14:36	19	Center	F	On	Off	On
16:08 - 16:25	26	East Wall	F	On	Off	On
16:26 - 16:34	27	West Wall	F	On	Off	On
16:35 - 16:45	28	Center	F	On	Off	On
16:45 - 16:51	29	West Wall	F	On	Off	On
16:52 - 17:02	30	East Wall	F	On	Off	On
17:02 - 17:15	31	Center	F	On	Off	On

**Table 3. Locations of Barriers IIA and IB voltage gradients sufficient to cause harmful physiological effects.**

Run Date	Pulser (Parasitic) Configuration	Location	Voltage Gradient	Range in ft (m)	Downstream Distance with respect to IIB in ft (m)*	Upstream Distance with respect to IIB in ft (m)*
1 (Feb 11th)	B (Off, Off, Off)	East Wall	≥0.05 V/in	1,361 (415)	-820 (-250)	541 (165)
2 (Feb 11th)	B (Off, Off, Off)	West Wall	≥0.05 V/in	1,361 (415)	-820 (-250)	541 (165)
3 (Feb 11th)	B (Off, Off, Off)	Center	≥0.05 V/in	1,345 (410)	-820 (-250)	525 (160)
4 (Feb 11th)**	B (Off, Off, Off)	West Wall	≥0.05 V/in	-	-	-
5 (Feb 11th)	B (Off, Off, Off)	West Wall	≥0.05 V/in	1,394 (425)	-853 (-260)	541 (165)
6 (Feb 11th)	B (Off, Off, Off)	East Wall	≥0.05 V/in	1,362 (415)	-837 (-255)	525 (160)
7 (Feb 11th)	B (Off, Off, Off)	Center	≥0.05 V/in	1,378 (420)	-837 (-255)	541 (165)
	<b>B (Off, Off, Off)</b>	<b>Greatest Extent</b>	≥0.05 V/in	<b>1,394 (425)</b>	<b>-853 (-260)</b>	<b>541 (165)</b>
8 (Feb 11th)	B (On, Off, On)	Center	≥0.05 V/in	1,181 (360)	-820 (-250)	361 (110)
9 (Feb 11th)	B (On, Off, On)	East Wall	≥0.05 V/in	1,116 (340)	-804 (-245)	312 (95)
10 (Feb 11th)	B (On, Off, On)	West Wall	≥0.05 V/in	1,115 (340)	-771 (-235)	344 (105)
11 (Feb 11th)	B (On, Off, On)	Center	≥0.05 V/in	1,115 (340)	-771 (-235)	344 (105)
12 (Feb 11th)	B (On, Off, On)	West Wall	≥0.05 V/in	1,164 (355)	-787 (-240)	377 (115)
13 (Feb 11th)	B (On, Off, On)	East Wall	≥0.05 V/in	1,116 (340)	-804 (-245)	312 (95)
	<b>B (On, Off, On)</b>	<b>Greatest Extent</b>	≥0.05 V/in	<b>1,197 (365)</b>	<b>-820 (-250)</b>	<b>377 (115)</b>
14 (Feb 11th)	B (On, On, On)	West Wall	≥0.05 V/in	1,099 (335)	-755 (-230)	344 (105)
15 (Feb 11th)	B (On, On, On)	East Wall	≥0.05 V/in	1,083 (330)	-771 (-235)	312 (95)
16 (Feb 11th)	B (On, On, On)	Center	≥0.05 V/in	1,099 (335)	-755 (-230)	344 (105)
17 (Feb 11th)	B (On, On, On)	East Wall	≥0.05 V/in	1,066 (325)	-787 (-240)	279 (85)
18 (Feb 11th)**	B (On, On, On)	West Wall	≥0.05 V/in	-	-	-
19 (Feb 11th)	B (On, On, On)	Center	≥0.05 V/in	1,083 (330)	-755 (-230)	328 (100)
	<b>B (On, On, On)</b>	<b>Greatest extent</b>	≥0.05 V/in	<b>1,131 (345)</b>	<b>-787 (-240)</b>	<b>344 (105)</b>
1 (Feb 12th)	D (On, On, Off)	East Wall	≥0.05 V/in	493 (150)	-591 (-180)	-98 (-30)
2 (Feb 12th)	D (On, On, Off)	West Wall	≥0.05 V/in	558 (170)	-640 (-195)	-82 (-25)
3 (Feb 12th)	D (On, On, Off)	Center	≥0.05 V/in	444 (135)	-542 (-165)	-98 (-30)
4 (Feb 12th)	D (On, On, Off)	West Wall	≥0.05 V/in	444 (135)	-542 (-165)	-98 (-30)
5 (Feb 12th)	D (On, On, Off)	East Wall	≥0.05 V/in	591 (180)	-689 (-210)	-98 (-30)
6 (Feb 12th)	D (On, On, Off)	Center	≥0.05 V/in	525 (160)	-607 (-185)	-98 (-30)

Run Date	Pulser (Parasitic) Configuration	Location	Voltage Gradient	Range in ft (m)	Downstream Distance with respect to IIB in ft (m)*	Upstream Distance with respect to IIB in ft (m)*
	<b>D (On, On, Off)</b>	<b>Greatest extent</b>	≥0.05 V/in	<b>607 (185)</b>	<b>-689 (-210)</b>	<b>-82 (-25)</b>
7 (Feb 12th)	A (On, Off, On)	East Wall	≥0.05 V/in	1,148 (350)	-804 (-245)	344 (105)
8 (Feb 12th)	A (On, Off, On)	West wall	≥0.05 V/in	1,182 (360)	-788 (-240)	394 (120)
9 (Feb 12th)	A (On, Off, On)	Center	≥0.05 V/in	1,198 (365)	-804 (-245)	394 (120)
10 (Feb 12th)	A (On, Off, On)	West Wall	≥0.05 V/in	1,198 (365)	-788 (-240)	410 (125)
11 (Feb 12th)	A (On, Off, On)	East Wall	≥0.05 V/in	1,133 (345)	-821 (-250)	312 (95)
12 (Feb 12th)	A (On, Off, On)	Center	≥0.05 V/in	1,198 (365)	-804 (-245)	394 (120)
	<b>A (On, Off, On)</b>	<b>Greatest extent</b>	≥0.05 V/in	<b>1,231 (375)</b>	<b>-821 (-250)</b>	<b>410 (125)</b>
13 (Feb 12th)	C (On, Off, On)	East Wall	≥0.05 V/in	1,083 (330)	-804 (-245)	279 (85)
14 (Feb 12th)	C (On, Off, On)	West Wall	≥0.05 V/in	1,132 (345)	-771 (-235)	361 (110)
15 (Feb 12th)	C (On, Off, On)	Center	≥0.05 V/in	1,148 (350)	-804 (-245)	344 (105)
16 (Feb 12th)	C (On, Off, On)	West Wall	≥0.05 V/in	1,149 (350)	-788 (-240)	361 (110)
17 (Feb 12th)	C (On, Off, On)	East Wall	≥0.05 V/in		-	-
18 (Feb 12th)	C (On, Off, On)	Center	≥0.05 V/in		-	-
	<b>C (On, Off, On)</b>	<b>Greatest extent</b>	≥0.05 V/in	<b>1,165 (355)</b>	<b>-804 (-245)</b>	<b>361 (110)</b>
19 (Feb 12th)	C (On, On, On)	Center	≥0.05 V/in	1,034 (315)	-706 (-215)	328 (100)
		<b>Greatest extent</b>	≥0.05 V/in	<b>1,034 (315)</b>	<b>-706 (-215)</b>	<b>328 (100)</b>
8 (June 14th)	E (On, Off, On)	East Wall	≥0.05 V/in	988 (301)	-712 (-217)	276 (84)
9 (June 14th)	E (On, Off, On)	West Wall	≥0.05 V/in	1033 (315)	-738 (-225)	295 (90)
10 (June 14th)	E (On, Off, On)	Center	≥0.05 V/in	1050 (320)	-755 (-230)	295 (90)
11 (June 14th)	E (On, Off, On)	West Wall	≥0.05 V/in	1017 (310)	-722 (-220)	295 (90)
12 (June 14th)	E (On, Off, On)	East Wall	≥0.05 V/in	1007 (307)	-738 (-225)	269 (82)
13 (June 14th)	E (On, Off, On)	Center	≥0.05 V/in	1033 (315)	-738 (-225)	295 (90)
	<b>E (On, Off, On)</b>	<b>Greatest Extent</b>	≥0.05 V/in	<b>1050 (320)</b>	<b>-755 (-230)</b>	<b>295 (90)</b>
14 (June 14th)	F (On, Off, On)	East Wall	≥0.05 V/in	984 (300)	-722 (-220)	262 (80)
15 (June 14th)	F (On, Off, On)	West Wall	≥0.05 V/in	1001 (305)	-722 (-220)	279 (85)
17 (June 14th)	F (On, Off, On)	West Wall	≥0.05 V/in	968 (295)	-722 (-220)	246 (75)
18 (June 14th)	F (On, Off, On)	East Wall	≥0.05 V/in	968 (295)	-705 (-215)	262 (80)
19 (June 14th)	F (On, Off, On)	Center	≥0.05 V/in	968 (295)	-689 (-210)	279 (85)

Run Date	Pulser (Parasitic) Configuration	Location	Voltage Gradient	Range in ft (m)	Downstream Distance with respect to IIB in ft (m)*	Upstream Distance with respect to IIB in ft (m)*
26 (June 14th)	F (On, Off, On)	East Wall	≥0.05 V/in	968 (295)	-705 (-215)	262 (80)
27 (June 14th)	F (On, Off, On)	West Wall	≥0.05 V/in	984 (300)	-705 (-215)	279 (85)
28 (June 14th)	F (On, Off, On)	Center	≥0.05 V/in	984 (300)	-738 (-225)	246 (75)
29 (June 14th)	F (On, Off, On)	West Wall	≥0.05 V/in	984 (300)	-705 (-215)	279 (85)
30 (June 14th)	F (On, Off, On)	East Wall	≥0.05 V/in	984 (300)	-722 (-220)	262 (80)
31 (June 14th)	F (On, Off, On)	Center	≥0.05 V/in	984 (300)	-705 (-215)	279 (85)
	<b>F (On, Off, On)</b>	<b>Greatest Extent</b>	≥0.05 V/in	<b>1001 (305)</b>	<b>-722 (-220)</b>	<b>279 (85)</b>
1 (Feb 11th)	B (Off, Off, Off)	East Wall	≥0.03 V/in	2,052 (625)***	-903 (-275)***	1,149 (350)***
2 (Feb 11th)	B (Off, Off, Off)	West Wall	≥0.03 V/in	2,052 (625)***	-903 (-275)***	1,149 (350)***
3 (Feb 11th)	B (Off, Off, Off)	Center	≥0.03 V/in	2,084 (635)***	-919 (-280)***	1,165 (355)***
4 (Feb 11th)**	B (Off, Off, Off)	West Wall	≥0.03 V/in	-	-	-
5 (Feb 11th)	B (Off, Off, Off)	West Wall	≥0.03 V/in	2,068 (630)***	-919 (-280)***	1,149 (350)***
6 (Feb 11th)	B (Off, Off, Off)	East Wall	≥0.03 V/in	2,019 (615)***	-919 (-280)***	1,100 (335)***
7 (Feb 11th)	B (Off, Off, Off)	Center	≥0.03 V/in	2,068 (630)***	-919 (-280)***	1,149 (350)***
	<b>B (Off, Off, Off)</b>	<b>Greatest Extent</b>	≥0.03 V/in	<b>2,084 (635)***</b>	<b>-919 (-280)***</b>	<b>1,165 (355)***</b>
8 (Feb 11th)	B (On, Off, On)	Center	≥0.03 V/in	1,412 (430)	-903 (-275)	509 (155)
9 (Feb 11th)	B (On, Off, On)	East Wall	≥0.03 V/in	1,445 (440)	-903 (-275)	542 (165)
10 (Feb 11th)	B (On, Off, On)	West Wall	≥0.03 V/in	1,461 (445)	-919 (-280)	542 (165)
11 (Feb 11th)	B (On, Off, On)	Center	≥0.03 V/in	2,018 (615)***	-886 (-270)***	1,132 (345)***
12 (Feb 11th)	B (On, Off, On)	West Wall	≥0.03 V/in	1,428 (435)	-886 (-270)	542 (165)
13 (Feb 11th)	B (On, Off, On)	East Wall	≥0.03 V/in	1,412 (430)	-903 (-275)	509 (155)
	<b>B (On, Off, On)</b>	<b>Greatest Extent</b>	≥0.03 V/in	<b>2,051 (625)***</b>	<b>-919 (-280)***</b>	<b>1,132 (345)***</b>
14 (Feb 11th)	B (On, On, On)	West Wall	≥0.03 V/in	1,346 (410)	-837 (-255)	509 (155)
15 (Feb 11th)	B (On, On, On)	East Wall	≥0.03 V/in	1,363 (415)	-903 (-275)	460 (140)
16 (Feb 11th)	B (On, On, On)	Center	≥0.03 V/in	1,379 (420)	-870 (-265)	509 (155)
17 (Feb 11th)	B (On, On, On)	East Wall	≥0.03 V/in	1,297 (395)	-854 (-260)	443 (135)
18 (Feb 11th)**	B (On, On, On)	West Wall	≥0.03 V/in	-	-	-
19 (Feb 11th)	B (On, On, On)	Center	≥0.03 V/in	1,347 (410)	-854 (-260)	493 (150)
	<b>B (On, On, On)</b>	<b>Greatest extent</b>	≥0.03 V/in	<b>1,412 (430)</b>	<b>-903 (-275)</b>	<b>509 (155)</b>

Run Date	Pulser (Parasitic) Configuration	Location	Voltage Gradient	Range in ft (m)	Downstream Distance with respect to IIB in ft (m)*	Upstream Distance with respect to IIB in ft (m)*
1 (Feb 12th)	D (On, On, Off)	East Wall	≥0.03 V/in	657 (200)	-722 (-220)	-65 (-20)
2 (Feb 12th)	D (On, On, Off)	West Wall	≥0.03 V/in	657 (200)	-722 (-220)	-65 (-20)
3 (Feb 12th)	D (On, On, Off)	Center	≥0.03 V/in	623 (190)	-706 (-215)	-83 (-25)
4 (Feb 12th)	D (On, On, Off)	West Wall	≥0.03 V/in	657 (200)	-740 (-225)	-83 (-25)
5 (Feb 12th)	D (On, On, Off)	East Wall	≥0.03 V/in	639 (195)	-722 (-220)	-83 (-25)
6 (Feb 12th)	D (On, On, Off)	Center	≥0.03 V/in	639 (195)	-722 (-220)	-83 (-25)
	<b>D (On, On, Off)</b>	<b>Greatest extent</b>	≥0.03 V/in	<b>657 (200)</b>	<b>-722 (-220)</b>	<b>-65 (-20)</b>
7 (Feb 12th)	A (On, Off, On)	East Wall	≥0.03 V/in	1,161 (445)	-903 (-275)	558 (170)
8 (Feb 12th)	A (On, Off, On)	West wall	≥0.03 V/in	1,444 (340)	-886 (-270)	558 (170)
9 (Feb 12th)	A (On, Off, On)	Center	≥0.03 V/in	2,035 (620)	-903 (-275)***	1,132 (345)***
10 (Feb 12th)	A (On, Off, On)	West Wall	≥0.03 V/in	1,444 (340)	-886 (-270)	558 (170)
11 (Feb 12th)	A (On, Off, On)	East Wall	≥0.03 V/in	1,478 (450)	-936 (-285)	542 (165)
12 (Feb 12th)	A (On, Off, On)	Center	≥0.03 V/in	2,052 (625)	-919 (-280)***	1,132 (345)***
	<b>A (On, Off, On)</b>	<b>Greatest extent</b>	≥0.03 V/in	<b>2,068 (630)</b>	<b>-936 (-285)</b>	<b>1,132 (345)***</b>
13 (Feb 12th)	C (On, Off, On)	East Wall	≥0.03 V/in	N/A	N/A	N/A
14 (Feb 12th)	C (On, Off, On)	West Wall	≥0.03 V/in	N/A	N/A	N/A
15 (Feb 12th)	C (On, Off, On)	Center	≥0.03 V/in	N/A	N/A	N/A
16 (Feb 12th)	C (On, Off, On)	West Wall	≥0.03 V/in	N/A	N/A	N/A
17 (Feb 12th)	C (On, Off, On)	East Wall	≥0.03 V/in	N/A	N/A	N/A
18 (Feb 12th)	C (On, Off, On)	Center	≥0.03 V/in	N/A	N/A	N/A
	<b>C (On, Off, On)</b>	<b>Greatest extent</b>	≥0.03 V/in	<b>N/A</b>	<b>N/A</b>	<b>N/A</b>
19 (Feb 12th)	C (On, On, On)	Center	≥0.03 V/in	N/A	N/A	N/A
		<b>Greatest extent</b>	≥0.03 V/in	<b>N/A</b>	<b>N/A</b>	<b>N/A</b>
8 (June 14th)	E (On, Off, On)	East Wall	≥0.03 V/in	1050 (320)	-771 (-235)	279 (85)
9 (June 14th)	E (On, Off, On)	West Wall	≥0.03 V/in	1148 (350)	-787 (-240)	361 (110)
10 (June 14th)	E (On, Off, On)	Center	≥0.03 V/in	1181 (360)	-820 (-250)	361 (110)
11 (June 14th)	E (On, Off, On)	West Wall	≥0.03 V/in	1165 (355)	-787 (-240)	377 (115)
12 (June 14th)	E (On, Off, On)	East Wall	≥0.03 V/in	1083 (330)	-804 (-245)	279 (85)
13 (June 14th)	E (On, Off, On)	Center	≥0.03 V/in	1165 (355)	-820 (-250)	344 (105)

Run Date	Pulser (Parasitic) Configuration	Location	Voltage Gradient	Range in ft (m)	Downstream Distance with respect to IIB in ft (m)*	Upstream Distance with respect to IIB in ft (m)*
	<b>E (On, Off, On)</b>	<b>Greatest Extent</b>	≥0.03 V/in	<b>1181 (360)</b>	<b>-820 (-250)</b>	<b>361 (110)</b>
14 (June 14th)	F (On, Off, On)	East Wall	≥0.03 V/in	1089 (332)	-820 (-250)	269 (82)
15 (June 14th)	F (On, Off, On)	West Wall	≥0.03 V/in	1132 (345)	-771 (-235)	361 (110)
17 (June 14th)	F (On, Off, On)	West Wall	≥0.03 V/in	1083 (330)	-771 (-235)	312 (95)
18 (June 14th)	F (On, Off, On)	East Wall	≥0.03 V/in	1066 (325)	-787 (-240)	279 (85)
19 (June 14th)	F (On, Off, On)	Center	≥0.03 V/in	1115 (340)	-787 (-240)	328 (100)
26 (June 14th)	F (On, Off, On)	East Wall	≥0.03 V/in	1050 (320)	-771 (-235)	279 (85)
27 (June 14th)	F (On, Off, On)	West Wall	≥0.03 V/in	1115 (340)	-755 (-230)	361 (110)
28 (June 14th)	F (On, Off, On)	Center	≥0.03 V/in	1083 (340)	-820 (-250)	262 (80)
29 (June 14th)	F (On, Off, On)	West Wall	≥0.03 V/in	1132 (345)	-771 (-235)	361 (110)
30 (June 14th)	F (On, Off, On)	East Wall	≥0.03 V/in	1066 (325)	-787 (-240)	279 (85)
31 (June 14th)	F (On, Off, On)	Center	≥0.03 V/in	1115 (340)	-787 (-240)	328 (100)
	<b>F (On, Off, On)</b>	<b>Greatest Extent</b>	≥0.03 V/in	<b>1132 (345)</b>	<b>-771 (-235)</b>	<b>361 (110)</b>
1 (Feb 11th)	B (Off, Off, Off)	East Wall	≥0.02 V/in	N/A	N/A	N/A
2 (Feb 11th)	B (Off, Off, Off)	West Wall	≥0.02 V/in	N/A	N/A	N/A
3 (Feb 11th)	B (Off, Off, Off)	Center	≥0.02 V/in	N/A	N/A	N/A
4 (Feb 11th)**	B (Off, Off, Off)	West Wall	≥0.02 V/in	N/A	N/A	N/A
5 (Feb 11th)	B (Off, Off, Off)	West Wall	≥0.02 V/in	N/A	N/A	N/A
6 (Feb 11th)	B (Off, Off, Off)	East Wall	≥0.02 V/in	N/A	N/A	N/A
7 (Feb 11th)	B (Off, Off, Off)	Center	≥0.02 V/in	N/A	N/A	N/A
	<b>B (Off, Off, Off)</b>	<b>Greatest Extent</b>	≥0.02 V/in	<b>N/A</b>	<b>N/A</b>	<b>N/A</b>
8 (Feb 11th)	B (On, Off, On)	Center	≥0.02 V/in	N/A	N/A	N/A
9 (Feb 11th)	B (On, Off, On)	East Wall	≥0.02 V/in	N/A	N/A	N/A
10 (Feb 11th)	B (On, Off, On)	West Wall	≥0.02 V/in	N/A	N/A	N/A
11 (Feb 11th)	B (On, Off, On)	Center	≥0.02 V/in	N/A	N/A	N/A
12 (Feb 11th)	B (On, Off, On)	West Wall	≥0.02 V/in	N/A	N/A	N/A
13 (Feb 11th)	B (On, Off, On)	East Wall	≥0.02 V/in	N/A	N/A	N/A
	<b>B (On, Off, On)</b>	<b>Greatest Extent</b>	≥0.02 V/in	<b>N/A</b>	<b>N/A</b>	<b>N/A</b>
14 (Feb 11th)	B (On, On, On)	West Wall	≥0.02 V/in	N/A	N/A	N/A



Run Date	Pulser (Parasitic) Configuration	Location	Voltage Gradient	Range in ft (m)	Downstream Distance with respect to IIB in ft (m)*	Upstream Distance with respect to IIB in ft (m)*
15 (Feb 11th)	B (On, On, On)	East Wall	≥0.02 V/in	N/A	N/A	N/A
16 (Feb 11th)	B (On, On, On)	Center	≥0.02 V/in	N/A	N/A	N/A
17 (Feb 11th)	B (On, On, On)	East Wall	≥0.02 V/in	N/A	N/A	N/A
18 (Feb 11th)**	B (On, On, On)	West Wall	≥0.02 V/in	N/A	N/A	N/A
19 (Feb 11th)	B (On, On, On)	Center	≥0.02 V/in	N/A	N/A	N/A
	<b>B (On, On, On)</b>	<b>Greatest extent</b>	≥0.02 V/in	<b>N/A</b>	<b>N/A</b>	<b>N/A</b>
1 (Feb 12th)	D (On, On, Off)	East Wall	≥0.02 V/in	N/A	N/A	N/A
2 (Feb 12th)	D (On, On, Off)	West Wall	≥0.02 V/in	N/A	N/A	N/A
3 (Feb 12th)	D (On, On, Off)	Center	≥0.02 V/in	N/A	N/A	N/A
4 (Feb 12th)	D (On, On, Off)	West Wall	≥0.02 V/in	N/A	N/A	N/A
5 (Feb 12th)	D (On, On, Off)	East Wall	≥0.02 V/in	N/A	N/A	N/A
6 (Feb 12th)	D (On, On, Off)	Center	≥0.02 V/in	N/A	N/A	N/A
	<b>D (On, On, Off)</b>	<b>Greatest extent</b>	≥0.02 V/in	<b>N/A</b>	<b>N/A</b>	<b>N/A</b>
7 (Feb 12th)	A (On, Off, On)	East Wall	≥0.02 V/in	1658 (505)	-985 (-300)	673 (205)
8 (Feb 12th)	A (On, Off, On)	West wall	≥0.02 V/in	1658 (505)	-952 (-290)	706 (215)
9 (Feb 12th)	A (On, Off, On)	Center	≥0.02 V/in	1674 (510)	-968 (-295)	706 (215)
10 (Feb 12th)	A (On, Off, On)	West Wall	≥0.02 V/in	1674 (510)	-968 (-295)	706 (215)
11 (Feb 12th)	A (On, Off, On)	East Wall	≥0.02 V/in	1674 (510)	-1001 (-305)	673 (205)
12 (Feb 12th)	A (On, Off, On)	Center	≥0.02 V/in	1707 (520)	-1001 (-305)	706 (215)
	<b>A (On, Off, On)</b>	<b>Greatest extent</b>	≥0.02 V/in	<b>1707 (520)</b>	<b>-1001 (-305)</b>	<b>706 (215)</b>
13 (Feb 12th)	C (On, Off, On)	East Wall	≥0.02 V/in	1641 (500)	-968 (-295)	673 (205)
14 (Feb 12th)	C (On, Off, On)	West Wall	≥0.02 V/in	1592 (485)	-968 (-295)	624 (190)
15 (Feb 12th)	C (On, Off, On)	Center	≥0.02 V/in	1576 (480)	-985 (-300)	608 (185)
16 (Feb 12th)	C (On, Off, On)	West Wall	≥0.02 V/in	1625 (495)	-968 (-295)	657 (200)
17 (Feb 12th)	C (On, Off, On)	East Wall	≥0.02 V/in	**	**	**
18 (Feb 12th)	C (On, Off, On)	Center	≥0.02 V/in	**	**	**
	<b>C (On, Off, On)</b>	<b>Greatest extent</b>	≥0.02 V/in	<b>1658 (505)</b>	<b>-985 (-300)</b>	<b>673 (205)</b>
19 (Feb 12th)	C (On, On, On)	Center	≥0.02 V/in	1477 (450)	-837 (-255)	640 (195)
		<b>Greatest extent</b>	≥0.02 V/in	<b>1477 (450)</b>	<b>-837 (-255)</b>	<b>640 (195)</b>

Run Date	Pulser (Parasitic) Configuration	Location	Voltage Gradient	Range in ft (m)	Downstream Distance with respect to IIB in ft (m)*	Upstream Distance with respect to IIB in ft (m)*
8 (June 14th)	E (On, Off, On)	East Wall	$\geq 0.02$ V/in	N/A	N/A	N/A
9 (June 14th)	E (On, Off, On)	West Wall	$\geq 0.02$ V/in	N/A	N/A	N/A
10 (June 14th)	E (On, Off, On)	Center	$\geq 0.02$ V/in	N/A	N/A	N/A
11 (June 14th)	E (On, Off, On)	West Wall	$\geq 0.02$ V/in	N/A	N/A	N/A
12 (June 14th)	E (On, Off, On)	East Wall	$\geq 0.02$ V/in	N/A	N/A	N/A
13 (June 14th)	E (On, Off, On)	Center	$\geq 0.02$ V/in	N/A	N/A	N/A
	<b>E (On, Off, On)</b>	<b>Greatest Extent</b>	$\geq 0.02$ V/in	<b>N/A</b>	<b>N/A</b>	<b>N/A</b>
14 (June 14th)	F (On, Off, On)	East Wall	$\geq 0.02$ V/in	1194 (364)	-919 (-280)	276 (84)
15 (June 14th)	F (On, Off, On)	West Wall	$\geq 0.02$ V/in	1247 (380)	-820 (-250)	427 (130)
17 (June 14th)	F (On, Off, On)	West Wall	$\geq 0.02$ V/in	1148 (350)	-787 (-240)	361 (110)
18 (June 14th)	F (On, Off, On)	East Wall	$\geq 0.02$ V/in	1181 (360)	-886 (-270)	295 (90)
19 (June 14th)	F (On, Off, On)	Center	$\geq 0.02$ V/in	1247 (380)	-853 (-260)	394 (120)
26 (June 14th)	F (On, Off, On)	East Wall	$\geq 0.02$ V/in	1165 (355)	-886 (-270)	279 (85)
27 (June 14th)	F (On, Off, On)	West Wall	$\geq 0.02$ V/in	1214 (370)	-837 (-240)	427 (130)
28 (June 14th)	F (On, Off, On)	Center	$\geq 0.02$ V/in	1214 (370)	-886 (-270)	328 (100)
29 (June 14th)	F (On, Off, On)	West Wall	$\geq 0.02$ V/in	1263 (385)	-837 (-255)	427 (130)
30 (June 14th)	F (On, Off, On)	East Wall	$\geq 0.02$ V/in	1165 (355)	-886 (-270)	279 (85)
31 (June 14th)	F (On, Off, On)	Center	$\geq 0.02$ V/in	1296 (395)	-886 (-270)	410 (125)
	<b>F (On, Off, On)</b>	<b>Greatest Extent</b>	$\geq 0.02$ V/in	<b>1296 (395)</b>	<b>-886 (-270)</b>	<b>410 (125)</b>

\* Distances are from a zero point at the center of Barrier IIB's narrow array. This point is shown on Figure 3.

\*\* Electric field measurements not included due to lack of GPS measurements.

\*\*\* Range of harmful effects extends from south of Barrier IIA to north of Barrier I, there is no safe zone between barriers.

Table 4. Locations of Barrier I voltage gradients sufficient to cause harmful physiological effects.

Run (Date)	Pulser (Parasitic) Configuration	Location	Voltage Gradient	Range in ft (m)	Downstream Distance with respect to IIB in ft (m)*	Upstream Distance with respect to IIB in ft (m)*
1 (Feb 11th)	B (Off, Off, Off)	East Wall	$\geq 0.05$ V/in	280 (85)	754 (230)	1,034 (315)
2 (Feb 11th)	B (Off, Off, Off)	West Wall	$\geq 0.05$ V/in	280 (85)	754 (230)	1,034 (315)
3 (Feb 11th)	B (Off, Off, Off)	Center	$\geq 0.05$ V/in	264 (80)	770 (235)	1,034 (315)
4 (Feb 11th)	B (Off, Off, Off)	West Wall	$\geq 0.05$ V/in	-	-	-
5 (Feb 11th)	B (Off, Off, Off)	West Wall	$\geq 0.05$ V/in	247 (75)	770 (235)	1,017 (310)
6 (Feb 11th)	B (Off, Off, Off)	East Wall	$\geq 0.05$ V/in	215 (65)	770 (235)	985 (300)
7 (Feb 11th)	B (Off, Off, Off)	Center	$\geq 0.05$ V/in	296 (90)	738 (225)	1,034 (315)
	<b>B (Off, Off, Off)</b>	<b>Greatest Extent</b>	$\geq 0.05$ V/in	<b>296 (90)</b>	<b>738 (225)</b>	<b>1034 (315)</b>
8 (Feb 11th)	B (On, Off, On)	Center	$\geq 0.05$ V/in	296 (90)	738 (225)	1,034 (315)
9 (Feb 11th)	B (On, Off, On)	East Wall	$\geq 0.05$ V/in	263 (80)	754 (230)	1,017 (310)
10 (Feb 11th)	B (On, Off, On)	West Wall	$\geq 0.05$ V/in	246 (75)	771 (235)	1,017 (310)
11 (Feb 11th)	B (On, Off, On)	Center	$\geq 0.05$ V/in	230 (70)	787 (240)	1,017 (310)
12 (Feb 11th)	B (On, Off, On)	West Wall	$\geq 0.05$ V/in	247 (75)	787 (240)	1,034 (315)
13 (Feb 11th)	B (On, Off, On)	East Wall	$\geq 0.05$ V/in	230 (70)	771 (235)	1,001 (305)
	<b>B (On, Off, On)</b>	<b>Greatest Extent</b>	$\geq 0.05$ V/in	<b>296 (90)</b>	<b>738 (225)</b>	<b>1,034 (315)</b>
14 (Feb 11th)	B (On, On, On)	West Wall	$\geq 0.05$ V/in	230 (70)	787 (240)	1,017 (310)
15 (Feb 11th)	B (On, On, On)	East Wall	$\geq 0.05$ V/in	246 (75)	771 (235)	1,017 (310)
16 (Feb 11th)	B (On, On, On)	Center	$\geq 0.05$ V/in	263 (80)	771 (235)	1,034 (315)
17 (Feb 11th)	B (On, On, On)	East Wall	$\geq 0.05$ V/in	246 (75)	771 (235)	1,017 (310)
18 (Feb 11th)**	B (On, On, On)	West Wall	$\geq 0.05$ V/in	-	-	-
19 (Feb 11th)	B (On, On, On)	Center	$\geq 0.05$ V/in	247 (75)	787 (240)	1,034 (315)
	<b>B (On, On, On)</b>	<b>Greatest extent</b>	$\geq 0.05$ V/in	<b>263 (80)</b>	<b>771 (235)</b>	<b>1,034 (315)</b>
1 (Feb 12th)	D (On, On, Off)	East Wall	$\geq 0.05$ V/in	230 (70)	787 (240)	1,017 (310)
2 (Feb 12th)	D (On, On, Off)	West Wall	$\geq 0.05$ V/in	214 (65)	803 (245)	1,017 (310)
3 (Feb 12th)	D (On, On, Off)	Center	$\geq 0.05$ V/in	247 (75)	787 (240)	1,034 (315)
4 (Feb 12th)	D (On, On, Off)	West Wall	$\geq 0.05$ V/in	214 (65)	803 (245)	1,017 (310)
5 (Feb 12th)	D (On, On, Off)	East Wall	$\geq 0.05$ V/in	230 (70)	787 (240)	1,017 (310)
6 (Feb 12th)	D (On, On, Off)	Center	$\geq 0.05$ V/in	214 (65)	803 (245)	1,017(310)

Run (Date)	Pulser (Parasitic) Configuration	Location	Voltage Gradient	Range in ft (m)	Downstream Distance with respect to IIB in ft (m)*	Upstream Distance with respect to IIB in ft (m)*
	<b>D (On, On, Off)</b>	<b>Greatest extent</b>	≥0.05 V/in	<b>247 (75)</b>	<b>787 (240)</b>	<b>1,034 (315)</b>
7 (Feb 12th)	A (On, Off, On)	East Wall	≥0.05 V/in	263 (80)	754 (230)	1,017 (310)
8 (Feb 12th)	A (On, Off, On)	West wall	≥0.05 V/in	214 (65)	803 (245)	1,017 (310)
9 (Feb 12th)	A (On, Off, On)	Center	≥0.05 V/in	214 (65)	803 (245)	1,017 (310)
10 (Feb 12th)	A (On, Off, On)	West Wall	≥0.05 V/in	230 (70)	787 (240)	1,017 (310)
11 (Feb 12th)	A (On, Off, On)	East Wall	≥0.05 V/in	198 (60)	787 (240)	985 (300)
12 (Feb 12th)	A (On, Off, On)	Center	≥0.05 V/in	214 (65)	787 (240)	1,001 (305)
	<b>A (On, Off, On)</b>	<b>Greatest extent</b>	≥0.05 V/in	<b>263 (80)</b>	<b>754 (230)</b>	<b>1017 (310)</b>
13 (Feb 12th)	C (On, Off, On)	East Wall	≥0.05 V/in	214 (65)	787 (240)	1,001 (305)
14 (Feb 12th)	C (On, Off, On)	West Wall	≥0.05 V/in	263 (80)	754 (230)	1,017 (310)
15 (Feb 12th)	C (On, Off, On)	Center	≥0.05 V/in	263 (80)	754 (230)	1,017 (310)
16 (Feb 12th)	C (On, Off, On)	West Wall	≥0.05 V/in	198 (60)	803 (245)	1,001 (305)
17 (Feb 12th)**	C (On, Off, On)	East Wall	≥0.05 V/in	-	-	-
18 (Feb 12th)**	C (On, Off, On)	Center	≥0.05 V/in	-	-	-
	<b>C (On, Off, On)</b>	<b>Greatest extent</b>	≥0.05 V/in	<b>263 (80)</b>	<b>754 (230)</b>	<b>1,017 (310)</b>
19 (Feb 12th)	C (On, On, On)	Center	≥0.05 V/in	197 (60)	804 (245)	1,001 (305)
		<b>Greatest extent</b>	≥0.05 V/in	<b>197 (60)</b>	<b>804 (245)</b>	<b>1,001 (305)</b>
8 (June 14th)	E (On, Off, On)	East Wall	≥0.05 V/in	295 (90)	738 (225)	1033 (315)
9 (June 14th)	E (On, Off, On)	West Wall	≥0.05 V/in	262 (80)	771 (235)	1033 (315)
10 (June 14th)	E (On, Off, On)	Center	≥0.05 V/in	279 (85)	755 (230)	1033 (315)
11 (June 14th)	E (On, Off, On)	West Wall	≥0.05 V/in	262 (80)	771 (235)	1033 (315)
12 (June 14th)	E (On, Off, On)	East Wall	≥0.05 V/in	279 (85)	755 (230)	1033 (315)
13 (June 14th)	E (On, Off, On)	Center	≥0.05 V/in	279 (85)	755 (230)	1033 (315)
	<b>E (On, Off, On)</b>	<b>Greatest Extent</b>	≥0.05 V/in	<b>295 (90)</b>	<b>738 (225)</b>	<b>1033 (315)</b>
14 (June 14th)	F (On, Off, On)	East Wall	≥0.05 V/in	312 (95)	722 (220)	1033 (315)
15 (June 14th)	F (On, Off, On)	West Wall	≥0.05 V/in	344 (105)	771 (235)	1115 (340)
17 (June 14th)	F (On, Off, On)	West Wall	≥0.05 V/in	262 (80)	771 (235)	1033 (315)
18 (June 14th)	F (On, Off, On)	East Wall	≥0.05 V/in	279 (85)	755 (230)	1033 (315)
19 (June 14th)	F (On, Off, On)	Center	≥0.05 V/in	262 (80)	771 (235)	1033 (315)

Run (Date)	Pulser (Parasitic) Configuration	Location	Voltage Gradient	Range in ft (m)	Downstream Distance with respect to IIB in ft (m)*	Upstream Distance with respect to IIB in ft (m)*
26 (June 14th)	F (On, Off, On)	East Wall	≥0.05 V/in	279 (85)	755 (230)	1033 (315)
27 (June 14th)	F (On, Off, On)	West Wall	≥0.05 V/in	246 (75)	771 (235)	1017 (310)
28 (June 14th)	F (On, Off, On)	Center	≥0.05 V/in	262 (80)	771 (235)	1033 (315)
29 (June 14th)	F (On, Off, On)	West Wall	≥0.05 V/in	262 (80)	771 (235)	1033 (315)
30 (June 14th)	F (On, Off, On)	East Wall	≥0.05 V/in	312 (95)	722 (220)	1033 (315)
31 (June 14th)	F (On, Off, On)	Center	≥0.05 V/in	262 (80)	771 (235)	1033 (315)
	<b>F (On, Off, On)</b>	<b>Greatest Extent</b>	≥0.05 V/in	<b>344 (105)</b>	<b>771 (235)</b>	<b>1115 (340)</b>
1 (Feb 11th)	B (Off, Off, Off)	East Wall	≥0.03 V/in	2052 (625)	-903 (-275)***	1149 (350)
2 (Feb 11th)	B (Off, Off, Off)	West Wall	≥0.03 V/in	2052 (625)	-903 (-275)***	1149 (350)
3 (Feb 11th)	B (Off, Off, Off)	Center	≥0.03 V/in	2084 (635)	-919 (-280)***	1165 (355)
4 (Feb 11th)**	B (Off, Off, Off)	West Wall	≥0.03 V/in	**	**	**
5 (Feb 11th)	B (Off, Off, Off)	West Wall	≥0.03 V/in	2068 (630)	-919 (-280)***	1149 (350)
6 (Feb 11th)	B (Off, Off, Off)	East Wall	≥0.03 V/in	2019 (615)	-919 (-280)***	1100 (335)
7 (Feb 11th)	B (Off, Off, Off)	Center	≥0.03 V/in	2068 (630)	-919 (-280)***	1149 (350)
	<b>B (Off, Off, Off)</b>	<b>Greatest Extent</b>	≥0.03 V/in	<b>2084 (635)</b>	<b>-919 (-280)***</b>	<b>1165 (355)</b>
8 (Feb 11th)	B (On, Off, On)	Center	≥0.03 V/in	542 (165)	640 (195)	1182 (360)
9 (Feb 11th)	B (On, Off, On)	East Wall	≥0.03 V/in	492 (150)	657 (200)	1149 (350)
10 (Feb 11th)	B (On, Off, On)	West Wall	≥0.03 V/in	476 (145)	689 (210)	1165 (355)
11 (Feb 11th)	B (On, Off, On)	Center	≥0.03 V/in	2017 (615)	-886 (-270)***	1131 (345)
12 (Feb 11th)	B (On, Off, On)	West Wall	≥0.03 V/in	442 (135)	689 (210)	1131 (345)
13 (Feb 11th)	B (On, Off, On)	East Wall	≥0.03 V/in	492 (150)	657 (200)	1149 (350)
	<b>B (On, Off, On)</b>	<b>Greatest Extent</b>	≥0.03 V/in	<b>2068 (630)</b>	<b>-886 (-270)***</b>	<b>1182 (360)</b>
14 (Feb 11th)	B (On, On, On)	West Wall	≥0.03 V/in	442 (135)	689 (210)	1131 (345)
15 (Feb 11th)	B (On, On, On)	East Wall	≥0.03 V/in	492 (150)	657 (200)	1149 (350)
16 (Feb 11th)	B (On, On, On)	Center	≥0.03 V/in	443 (135)	706 (215)	1149 (350)
17 (Feb 11th)	B (On, On, On)	East Wall	≥0.03 V/in	607 (185)	558 (170)	1165 (355)
18 (Feb 11th)**	B (On, On, On)	West Wall	≥0.03 V/in	**	**	**
19 (Feb 11th)	B (On, On, On)	Center	≥0.03 V/in	492 (150)	673 (205)	1165 (355)
	<b>B (On, On, On)</b>	<b>Greatest extent</b>	≥0.03 V/in	<b>607 (185)</b>	<b>558 (170)</b>	<b>1165 (355)</b>

Run (Date)	Pulser (Parasitic) Configuration	Location	Voltage Gradient	Range in ft (m)	Downstream Distance with respect to IIB in ft (m)*	Upstream Distance with respect to IIB in ft (m)*
1 (Feb 12th)	D (On, On, Off)	East Wall	≥0.03 V/in	443 (135)	706 (215)	1149 (350)
2 (Feb 12th)	D (On, On, Off)	West Wall	≥0.03 V/in	443 (135)	706 (215)	1149 (350)
3 (Feb 12th)	D (On, On, Off)	Center	≥0.03 V/in	509 (155)	673 (205)	1182 (360)
4 (Feb 12th)	D (On, On, Off)	West Wall	≥0.03 V/in	442 (135)	689 (210)	1131 (345)
5 (Feb 12th)	D (On, On, Off)	East Wall	≥0.03 V/in	542 (165)	640 (195)	1182 (360)
6 (Feb 12th)	D (On, On, Off)	Center	≥0.03 V/in	460 (140)	689 (210)	1149 (350)
	<b>D (On, On, Off)</b>	<b>Greatest extent</b>	≥0.03 V/in	<b>542 (165)</b>	<b>640 (195)</b>	<b>1182 (360)</b>
7 (Feb 12th)	A (On, Off, On)	East Wall	≥0.03 V/in	492 (150)	657 (200)	1149 (350)
8 (Feb 12th)	A (On, Off, On)	West wall	≥0.03 V/in	425 (130)	706 (215)	1131 (345)
9 (Feb 12th)	A (On, Off, On)	Center	≥0.03 V/in	556 (170)	575 (175)	1131 (345)
10 (Feb 12th)	A (On, Off, On)	West Wall	≥0.03 V/in	442 (135)	689 (210)	1131 (345)
11 (Feb 12th)	A (On, Off, On)	East Wall	≥0.03 V/in	491 (155)	640 (195)	1131 (345)
12 (Feb 12th)	A (On, Off, On)	Center	≥0.03 V/in	671 (205)	460 (140)	1131 (345)
	<b>A (On, Off, On)</b>	<b>Greatest extent</b>	≥0.03 V/in	<b>689 (210)</b>	<b>460 (140)</b>	<b>1149 (350)</b>
13 (Feb 12th)	C (On, Off, On)	East Wall	≥0.03 V/in	474 (145)	657 (200)	1131 (345)
14 (Feb 12th)	C (On, Off, On)	West Wall	≥0.03 V/in	574 (175)	591 (180)	1165 (355)
15 (Feb 12th)	C (On, Off, On)	Center	≥0.03 V/in	542 (165)	607 (185)	1149 (350)
16 (Feb 12th)	C (On, Off, On)	West Wall	≥0.03 V/in	427 (130)	689 (210)	1116 (340)
17 (Feb 12th)	C (On, Off, On)	East Wall	≥0.03 V/in	**	**	**
18 (Feb 12th)	C (On, Off, On)	Center	≥0.03 V/in	**	**	**
	<b>C (On, Off, On)</b>	<b>Greatest extent</b>	≥0.03 V/in	<b>574 (175)</b>	<b>591 (180)</b>	<b>1165 (355)</b>
19 (Feb 12th)	C (On, On, On)	Center	≥0.03 V/in	458 (140)	673 (205)	1131 (345)
		<b>Greatest extent</b>	≥0.03 V/in	<b>458 (140)</b>	<b>673 (205)</b>	<b>1131 (345)</b>
8 (June 14th)	E (On, Off, On)	East Wall	≥0.03 V/in	492 (150)	673 (205)	1165 (355)
9 (June 14th)	E (On, Off, On)	West Wall	≥0.03 V/in	443 (135)	689 (210)	1132 (345)
10 (June 14th)	E (On, Off, On)	Center	≥0.03 V/in	459 (140)	673 (205)	1132 (345)
11 (June 14th)	E (On, Off, On)	West Wall	≥0.03 V/in	459 (140)	689 (210)	1148 (350)
12 (June 14th)	E (On, Off, On)	East Wall	≥0.03 V/in	459 (140)	673 (205)	1132 (345)
13 (June 14th)	E (On, Off, On)	Center	≥0.03 V/in	476 (145)	656 (200)	1132 (345)

Run (Date)	Pulser (Parasitic) Configuration	Location	Voltage Gradient	Range in ft (m)	Downstream Distance with respect to IIB in ft (m)*	Upstream Distance with respect to IIB in ft (m)*
	<b>E (On, Off, On)</b>	<b>Greatest Extent</b>	≥0.03 V/in	<b>492 (150)</b>	<b>673 (205)</b>	<b>1165 (355)</b>
14 (June 14th)	F (On, Off, On)	East Wall	≥0.03 V/in	525 (160)	623 (190)	1148 (350)
15 (June 14th)	F (On, Off, On)	West Wall	≥0.03 V/in	427 (130)	705 (215)	1132 (345)
17 (June 14th)	F (On, Off, On)	West Wall	≥0.03 V/in	410 (125)	705 (215)	1115 (340)
18 (June 14th)	F (On, Off, On)	East Wall	≥0.03 V/in	492 (150)	656 (200)	1148 (350)
19 (June 14th)	F (On, Off, On)	Center	≥0.03 V/in	427 (130)	689 (210)	1115 (350)
26 (June 14th)	F (On, Off, On)	East Wall	≥0.03 V/in	492 (150)	656 (200)	1148 (350)
27 (June 14th)	F (On, Off, On)	West Wall	≥0.03 V/in	410 (125)	722 (220)	1132 (345)
28 (June 14th)	F (On, Off, On)	Center	≥0.03 V/in	443 (135)	689 (210)	1132 (345)
29 (June 14th)	F (On, Off, On)	West Wall	≥0.03 V/in	410 (125)	705 (215)	1115 (350)
30 (June 14th)	F (On, Off, On)	East Wall	≥0.03 V/in	459 (140)	656 (200)	1115 (350)
31 (June 14th)	F (On, Off, On)	Center	≥0.03 V/in	410 (125)	705 (215)	1115 (350)
	<b>F (On, Off, On)</b>	<b>Greatest Extent</b>	≥0.03 V/in	<b>525 (160)</b>	<b>623 (190)</b>	<b>1148 (350)</b>

\* Distances are from a zero point at the center of Barrier IIB’s narrow array. This point is shown on Figure 3.

\*\* Electric field measurements not included due to lack of GPS measurements.

\*\*\* Range of harmful effects extends from south of Barrier IIA to north of Barrier I, there is no safe zone between barriers.

**Table 5. Pulser settings and target in-water field strengths for each test configuration.**

Pulser Configuration	ϕ <sub>p</sub> (for energy calculation) ms	Barrier 2A Narrow			Barrier 2A Wide			Barrier 2B Narrow			Barrier 2B Wide			Barrier 1		
		V/in	ms	Hz	V/in	ms	Hz	V/in	ms	Hz	V/in	ms	Hz	V/in	ms	Hz
Alpha (A)	6.5	2.0	6.5	15	1.0	6.5	15	2.3	2.5	30	1.0	2.5	30	1.0	4.0	5
Bravo (B)	2.5	2.3	2.5	30	1.0	2.5	30	2.3	2.5	30	1.0	2.5	30	1.0	4.0	5
Charlie (C)	6.5	2.0	6.5	15	1.0	6.5	15	2.0	6.5	15	1.0	6.5	15	1.0	4.0	5
Delta (D)	2.5	2.3	2.5	30	1.0	2.5	30	OFF			OFF			1.0	4.0	5
Echo (E)	2.5	OFF			OFF			2.3	2.5	30	1.0	2.5	30	1.0	4.0	5
Foxtrot (F)	6.5	OFF			OFF			2.0	6.5	15	1.0	6.5	15	1.0	4.0	5

Table 6. Test results for sparking potential during fleeting operations.

Time	Barge Configuration	Pulser Configuration	Parasitic 1	Parasitic 2	Parasitic 3	Peak Voltage (Volts)	Peak Short Circuit Current (Amps)	Estimated Energy (mJoules)	Sparking Observed
08:10	Series	A	On	On	On	4.8			
08:12	Series	A	On	On	On	7.3			
08:13	Series	A	On	On	On	7.3		44.8	
08:15	Series	A	On	On	On		1.2		
08:17	Series	A	On	On	On		1.0		
08:18	Series	A	On	On	On		1.0		
08:20	Series	A	On	Off	On		1.5		
08:21	Series	A	On	Off	On		1.5		
08:23	Series	A	On	Off	On		1.4	62.6	
08:24	Series	A	On	Off	On	6.6			
08:25	Series	A	On	Off	On	7.4			
08:27	Series	A	On	Off	On	5.7			
08:35	Series	B	On	Off	On	8.7			
08:37	Series	B	On	Off	On	6.5			
08:38	Series	B	On	Off	On	9.9		33.5	
08:40	Series	B	On	Off	On		1.3		
08:42	Series	B	On	Off	On		1.8		
08:43	Series	B	On	Off	On		1.7		
08:47	Series	B	On	On	On		0.9		
08:48	Series	B	On	On	On		1.1		
08:50	Series	B	On	On	On		0.8	17.0	
08:52	Series	B	On	On	On	5.2			
08:53	Series	B	On	On	On	8.5			
08:56	Series	B	On	On	On	8.0			
09:06	Series	C	On	On	On	7.3			
09:07	Series	C	On	On	On	6.2			
09:09	Series	C	On	On	On	4.4		29.5	



Time	Barge Configuration	Pulser Configuration	Parasitic 1	Parasitic 2	Parasitic 3	Peak Voltage (Volts)	Peak Short Circuit Current (Amps)	Estimated Energy (mJoules)	Sparking Observed
09:12	Series	C	On	On	On		0.9		
09:14	Series	C	On	On	On		0.7		
09:16	Series	C	On	On	On		0.7		
09:22	Series	C	On	Off	On		1.5		
09:23	Series	C	On	Off	On		1.6		
09:25	Series	C	On	Off	On		1.5	81.7	
09:27	Series	C	On	Off	On	9.7			
09:29	Series	C	On	Off	On	7.7			
09:30	Series	C	On	Off	On	7.1			
09:37	Series	D	On	On	Off	4.4			
09:39	Series	D	On	On	Off	4.5			
09:40	Series	D	On	On	Off	4.3		2.9	
09:42	Series	D	On	On	Off		0.3		
09:43	Series	D	On	On	Off		0.3		YES
09:45	Series	D	On	On	Off		0.3		
09:56*	Series	E	On	Off	On		0.1		
10:00*	Series	E	On	Off	On	1.0		1.3	
15:34*	Series	E	On	Off	On	3.0			
15:39*	Series	E	On	Off	On		0.4		
09:43*	Series	F	On	Off	On	0.6			
09:45*	Series	F	On	Off	On	0.6			
09:48*	Series	F	On	Off	On		0.1	1.6	
09:52*	Series	F	On	Off	On		0.1		
15:21*	Series	F	On	Off	On		0.4		
15:28*	Series	F	On	Off	On	2.4			
10:25	Parallel	D	On	On	Off	1.6			
10:25	Parallel	D	On	On	Off	1.8			
10:27	Parallel	D	On	On	Off	1.5		0.7	

Time	Barge Configuration	Pulser Configuration	Parasitic 1	Parasitic 2	Parasitic 3	Peak Voltage (Volts)	Peak Short Circuit Current (Amps)	Estimated Energy (mJoules)	Sparking Observed
10:28	Parallel	D	On	On	Off		0.2		
10:29	Parallel	D	On	On	Off		0.2		
10:30	Parallel	D	On	On	Off		0.2		
10:36	Parallel	C	On	On	On		0.4		
10:38	Parallel	C	On	On	On		0.4		
10:39	Parallel	C	On	On	On		0.3	6.6	
10:40	Parallel	C	On	On	On	2.2			
10:41	Parallel	C	On	On	On	2.3			
10:42	Parallel	C	On	On	On	3.3			
10:48	Parallel	C	On	Off	On	2.4			
10:49	Parallel	C	On	Off	On	3.0			
10:51	Parallel	C	On	Off	On	2.9		11.0	
10:53	Parallel	C	On	Off	On		0.6		
10:53	Parallel	C	On	Off	On		0.7		
10:55	Parallel	C	On	Off	On		0.6		
13:19	Parallel	A	On	On	On	2.1			
13:20	Parallel	A	On	On	On	1.9			
13:21	Parallel	A	On	On	On	2.9		4.7	
13:25	Parallel	A	On	On	On		0.3		
13:26	Parallel	A	On	On	On		0.3		
13:27	Parallel	A	On	On	On		0.3		
13:29	Parallel	A	On	Off	On		0.4		
13:30	Parallel	A	On	Off	On		0.3		
13:31	Parallel	A	On	Off	On		0.4		
13:33	Parallel	A	On	Off	On		0.4	8.0	
13:34	Parallel	A	On	Off	On	2.7			
13:35	Parallel	A	On	Off	On	3.3			
13:37	Parallel	A	On	Off	On	3.6			

Time	Barge Configuration	Pulser Configuration	Parasitic 1	Parasitic 2	Parasitic 3	Peak Voltage (Volts)	Peak Short Circuit Current (Amps)	Estimated Energy (mJoules)	Sparking Observed
13:42	Parallel	B	On	Off	On	2.6			
13:43	Parallel	B	On	Off	On	2.5			
13:44	Parallel	B	On	Off	On	2.4		2.6	
13:46	Parallel	B	On	Off	On		0.4		
13:47	Parallel	B	On	Off	On		0.4		
13:49	Parallel	B	On	Off	On		0.4		
13:51	Parallel	B	On	On	On		0.3		
13:53	Parallel	B	On	On	On		0.3		
13:54	Parallel	B	On	On	On		0.3	1.8	
13:57	Parallel	B	On	On	On	2.6			
13:58	Parallel	B	On	On	On	2.6			
13:59	Parallel	B	On	On	On	2.2			
13:50*	Parallel	E	On	Off	On	0.6		0.2	
13:54*	Parallel	E	On	Off	On		0.1		
13:34*	Parallel	F	On	Off	On	0.5			
13:37*	Parallel	F	On	Off	On		0.1	0.3	
13:41*	Parallel	F	On	Off	On		0.1		
13:44*	Parallel	F	On	Off	On	0.4			
15:24	Insertion	D	On	On	Off	1.0			
15:25	Insertion	D	On	On	Off	1.8			
15:26	Insertion	D	On	On	Off	1.9		0.9	
15:28	Insertion	D	On	On	Off		0.2		
15:29	Insertion	D	On	On	Off		0.3		
15:37	Insertion	D	On	On	Off		0.2		
15:44	Insertion	C	On	On	On	7.1			YES
15:46	Insertion	C	On	On	On	4.7			YES
15:48	Insertion	C	On	On	On	4.7		34.4	YES
15:51	Insertion	C	On	On	On		1.1		

Time	Barge Configuration	Pulser Configuration	Parasitic 1	Parasitic 2	Parasitic 3	Peak Voltage (Volts)	Peak Short Circuit Current (Amps)	Estimated Energy (mJoules)	Sparking Observed
15:53	Insertion	C	On	On	On		1.0		
15:55	Insertion	C	On	On	On		0.9		
15:58	Insertion	C	On	Off	On		3.3		
16:10	Insertion	C	On	Off	On		2.3		
16:11	Insertion	C	On	Off	On		1.8	132.0	YES
16:13	Insertion	C	On	Off	On	7.2			YES
16:16	Insertion	C	On	Off	On	9.7			YES
16:18	Insertion	C	On	Off	On	7.8			YES
16:24	Insertion	B	On	Off	On	6.2			
16:26	Insertion	B	On	Off	On	9.7			YES
16:28	Insertion	B	On	Off	On	10.0		35.5	YES
16:31	Insertion	B	On	Off	On		1.5		
16:33	Insertion	B	On	Off	On		1.4		
16:34	Insertion	B	On	Off	On		2.1		
16:37	Insertion	B	On	On	On		1.5		YES
16:38	Insertion	B	On	On	On		1.4		
16:39	Insertion	B	On	On	On		1.0	20.7	YES
16:41	Insertion	B	On	On	On	5.7			YES
16:42	Insertion	B	On	On	On	6.4			
16:44	Insertion	B	On	On	On	6.9			YES
16:49	Insertion	A	On	Off	On	5.5			
16:50	Insertion	A	On	Off	On	7.0			
16:52	Insertion	A	On	Off	On	8.1		75.9	YES
16:55	Insertion	A	On	Off	On		1.6		YES
16:56	Insertion	A	On	Off	On		1.6		YES
16:57	Insertion	A	On	Off	On		1.9		YES
17:02	Insertion	A	On	On	On		1.6		
17:04	Insertion	A	On	On	On		0.6		

Time	Barge Configuration	Pulser Configuration	Parasitic 1	Parasitic 2	Parasitic 3	Peak Voltage (Volts)	Peak Short Circuit Current (Amps)	Estimated Energy (mJoules)	Sparking Observed
17:05	Insertion	A	On	On	On		0.8	43.3	
17:07	Insertion	A	On	On	On	5.8			
17:08	Insertion	A	On	On	On	7.7			
17:09	Insertion	A	On	On	On	6.7			YES
14:24*	Insertion	E	On	Off	On		0.2	0.8	
14:28*	Insertion	E	On	Off	On	1.5			
14:46*	Insertion	F	On	Off	On	1.3		1.7	
14:51*	Insertion	F	On	Off	On		0.2		

\*All data taken 5 February 2011 except rows denoted with an asterisk (\*), which were taken 15 June 2011.

Table 7. Test results for sparking potential during collision simulations.

Time	Pulser Configuration	Parasitic 1	Parasitic 2	Parasitic 3	Peak Voltage (Volts)	Peak Short Circuit Current (Amps)	Estimated Energy (mJoules)	Sparking Observed
09:06	A	On	On	On	68.6			YES
09:08	A	On	On	On	78.4			YES
09:09	A	On	On	On	72.8		5,667	YES
09:12	A	On	On	On		12.8		YES
09:13	A	On	On	On		11.9		YES
09:14	A	On	On	On		11.0		YES
09:16	A	On	Off	On		12.8		YES
09:17	A	On	Off	On		12.5		YES
09:18	A	On	Off	On		11.0	5,207	YES
09:20	A	On	Off	On	69.3			YES
09:21	A	On	Off	On	69.0			YES
09:23	A	On	Off	On	60.3			YES
09:29	B	On	Off	On	62.4			YES
09:30	B	On	Off	On	60.7			YES

Time	Pulser Configuration	Parasitic 1	Parasitic 2	Parasitic 3	Peak Voltage (Volts)	Peak Short Circuit Current (Amps)	Estimated Energy (mJoules)	Sparking Observed
09:31	B	On	Off	On	72.6		1,941	YES
09:33	B	On	Off	On		11.4		YES
09:35	B	On	Off	On		11.9		YES
09:36	B	On	Off	On		12.4		YES
09:40	B	On	On	On		11.4		YES
09:41	B	On	On	On		10.7		YES
09:43	B	On	On	On		11.4	1,973	YES
09:45	B	On	On	On	71.9			YES
09:46	B	On	On	On	72.7			YES
09:47	B	On	On	On	67.4			YES
09:53	C	On	On	On	85.9			YES
09:54	C	On	On	On	87.4			YES
09:55	C	On	On	On	96.3		12,033	YES
09:57	C	On	On	On		20.9		YES
09:58	C	On	On	On		20.3		YES
09:59	C	On	On	On		20.6		YES
10:03	C	On	Off	On		20.2		YES
10:05	C	On	Off	On		16.0		YES
10:06	C	On	Off	On		18.6	11,121	YES
10:08	C	On	Off	On	92.6			YES
10:10	C	On	Off	On	96.6			YES
10:11	C	On	Off	On	91.8			YES
10:30	D	On	On	Off	19.2			NO
10:33	D	On	On	Off	16.6			NO
10:34	D	On	On	Off	15.3		727	NO
10:40	D	On	On	Off		19.3		NO
10:42	D	On	On	Off		14.7		NO
10:44	D	On	On	Off		17.2		NO

Time	Pulser Configuration	Parasitic 1	Parasitic 2	Parasitic 3	Peak Voltage (Volts)	Peak Short Circuit Current (Amps)	Estimated Energy (mJoules)	Sparking Observed
N/A*	E	On	Off	On	62		2774	YES
N/A*	E	On	Off	On	35			YES
N/A*	E	On	Off	On		8.4		YES
N/A*	E	On	Off	On		9.2		YES
N/A*	F	On	Off	On	72		2581	YES
N/A*	F	On	Off	On	68			YES
N/A*	F	On	Off	On		13.5		YES
N/A*	F	On	Off	On		16		YES

\*All data taken 7 February 2011 except rows denoted with an asterisk (\*), which were taken 16 June 2011. Data acquisition times are not available for the 16 June data.

**Notes for Tables 8-10.**

V01 - Potential between south towboat and Barge 1  
 V12 - Potential between Barges 1 and 2  
 V23 - Potential between Barges 2 and 3  
 V34 - Potential between Barges 3 and 4  
 V45 - Potential between Barges 4 and 5  
 V56 - Potential between Barge 5 and north towboat  
 South Towboat on 8 Feb was the Joe Avery  
 North Towboat on 8 Feb was the Buster White  
 South Towboat on 10 Feb was the Jack Crowley  
 North Towboat on 10 Feb was the Buster White

**Table 8. Test results for long tow traversing Barrier IIA, conducted on 8 and 10 February 2011.**

Date Time	Pulser Configuration	Direction of Travel	Parasitic State			Barrier IIA Peak Potential Difference (volts)					
			1	2	3	V01	V12	V23	V34	V45	V56
8 Feb 09:50 - 10:10	A	Downstream	ON	ON	ON	2.23	2.11	2.06	2.09	1.60	18.66
8 Feb 10:26 - 10:51	A	Upstream	ON	ON	ON	2.22	2.07	2.77	2.41	1.65	18.67
8 Feb 13:40 - xxx	A	Aborted	ON	ON	ON	—	—	—	—	—	—
8 Feb 14:00 - 14:23	A	Upstream	ON	ON	ON	2.67	2.08	3.23	2.39	1.70	20.44
8 Feb 14:27 - 14:41	A	Downstream	ON	OFF	ON	2.47	1.98	1.75	3.04	2.10	21.50
8 Feb 14:43 - 15:00	A	Upstream	ON	OFF	ON	2.42	2.00	3.45	2.75	1.93	19.99
8 Feb 15:05 - 15:18	A	Downstream	ON	OFF	ON	2.38	2.44	2.40	2.49	1.26	18.08
8 Feb 15:23 - 15:41	B	Upstream	ON	OFF	ON	2.59	2.34	2.65	3.10	1.45	25.34



Date Time	Pulser Configuration	Direction of Travel	Parasitic State			Barrier IIA Peak Potential Difference (volts)					
			1	2	3	V01	V12	V23	V34	V45	V56
8 Feb 15:44 - 16:00	B	Downstream	ON	OFF	ON	2.65	2.28	3.40	2.22	2.18	22.97
8 Feb 16:01 - 16:17	B	Upstream	ON	OFF	ON	2.52	2.07	2.90	2.97	1.97	22.35
8 Feb 16:21 - 16:37	B	Downstream	ON	ON	ON	4.14	2.48	5.22	4.95	2.03	23.21
8 Feb 16:39 - 16:59	B	Upstream	ON	ON	ON	2.82	2.17	1.70	4.01	1.62	22.84
10 Feb 08:41 - 08:59	B	Downstream	ON	ON	ON	29.69	1.74	3.46	1.84	1.31	21.47
10 Feb 09:16 - 09:34	C	Upstream	ON	ON	ON	26.41	1.68	1.45	2.35	1.09	18.25
10 Feb 09:35 - 09:48	C	Downstream	ON	ON	ON	28.55	1.81	2.93	2.42	1.49	20.42
10 Feb 09:52 - 10:08	C	Upstream	ON	ON	ON	30.30	1.92	1.51	2.76	1.59	19.86
10 Feb 10:10 - 10:25	C	Downstream	ON	OFF	ON	27.85	2.57	1.78	2.48	1.22	19.40
10 Feb 10:26 - 10:42	C	Upstream	ON	OFF	ON	27.83	3.02	2.09	2.38	1.28	19.89
10 Feb 13:13 - 13:27	C	Downstream	ON	OFF	ON	28.34	1.68	4.36	2.62	1.46	21.49
10 Feb 13:30 - 13:48	D	Upstream	ON	ON	OFF	33.11	2.59	4.64	2.15	1.83	23.60
10 Feb 13:49 - 14:02	D	Downstream	ON	ON	OFF	30.73	2.07	3.38	2.08	1.68	21.81
10 Feb 14:02 - 14:16	D	Upstream	ON	ON	OFF	30.90	1.91	3.85	2.31	1.47	21.84

Table 9. Test results for long tow traversing Barrier IIB, conducted on 8 and 10 February 2011.

Date Time	Pulser Configuration	Direction of Travel	Parasitic State			Barrier IIB Peak Potential Difference (volts)					
			1	2	3	V01	V12	V23	V34	V45	V56
8 Feb 09:50 – 10:10	A	Downstream	ON	ON	ON	3.01	2.44	4.55	2.60	1.92	25.55
8 Feb 10:26 – 10:51	A	Upstream	ON	ON	ON	2.91	1.94	3.77	4.23	1.93	26.92
8 Feb 13:40 – xxx	A	Aborted	ON	ON	ON	–	–	–	–	–	–
8 Feb 14:00 – 14:23	A	Upstream	ON	ON	ON	3.31	3.16	3.70	3.65	1.96	27.16
8 Feb 14:27 – 14:41	A	Downstream	ON	OFF	ON	3.26	3.24	3.09	2.33	1.76	29.08
8 Feb 14:43 – 15:00	A	Upstream	ON	OFF	ON	3.24	2.65	4.61	2.90	1.71	28.70
8 Feb 15:05 – 15:18	A	Downstream	ON	OFF	ON	3.24	2.55	3.13	3.90	1.41	27.07
8 Feb 15:23 – 15:41	B	Upstream	ON	OFF	ON	2.89	2.17	4.56	2.58	2.26	26.47
8 Feb 15:44 – 16:00	B	Downstream	ON	OFF	ON	3.50	2.34	2.96	2.56	1.86	28.74
8 Feb 16:01 – 16:17	B	Upstream	ON	OFF	ON	2.92	2.35	4.40	2.81	2.49	29.08
8 Feb 16:21 – 16:37	B	Downstream	ON	ON	ON	4.94	2.97	5.99	3.34	2.76	32.90
8 Feb 16:39 – 16:59	B	Upstream	ON	ON	ON	2.80	2.53	4.76	4.70	2.17	26.56
10 Feb 08:41 – 08:59	B	Downstream	ON	ON	ON	35.14	2.02	2.82	4.96	1.37	26.95
10 Feb 09:16 – 09:34	C	Upstream	ON	ON	ON	34.63	1.90	4.29	2.71	1.34	24.17

Date Time	Pulser Configuration	Direction of Travel	Parasitic State			Barrier IIB Peak Potential Difference (volts)					
10 Feb 09:35 - 09:48	C	Downstream	ON	ON	ON	34.61	1.99	2.71	1.81	1.77	27.09
10 Feb 09:52 - 10:08	C	Upstream	ON	ON	ON	35.42	2.18	2.39	3.62	1.40	24.55
10 Feb 10:10 - 10:25	C	Downstream	ON	OFF	ON	33.93	3.09	3.50	3.00	2.20	27.98
10 Feb 10:26 - 10:42	C	Upstream	ON	OFF	ON	36.62	3.57	3.81	1.87	1.83	25.12
10 Feb 13:13 - 13:27	C	Downstream	ON	OFF	ON	33.06	2.03	2.01	2.16	1.72	25.55
10 Feb 13:30 - 13:48	D	Upstream	ON	ON	OFF	—	—	—	—	—	—
10 Feb 13:49 - 14:02	D	Downstream	ON	ON	OFF	—	—	—	—	—	—
10 Feb 14:02 - 14:16	D	Upstream	ON	ON	OFF	—	—	—	—	—	—

Table 10. Test results for long tow traversing Barrier I, conducted on 8 and 10 February 2011.

Date Time	Pulser Configuration	Direction of Travel	Parasitic State			Barrier I Peak Potential Difference (volts)					
			1	2	3	V01	V12	V23	V34	V45	V56
8 Feb 09:50 - 10:10	A	Downstream	ON	ON	ON	0.90	0.77	0.57	0.90	0.44	7.40
8 Feb 10:26 - 10:51	A	Upstream	ON	ON	ON	0.83	0.62	0.97	0.91	0.59	7.54
8 Feb 13:40 - xxx	A	Aborted	ON	ON	ON	—	—	—	—	—	—
8 Feb 14:00 - 14:23	A	Upstream	ON	ON	ON	0.82	0.64	1.04	1.33	0.90	7.80
8 Feb 14:27 - 14:41	A	Downstream	ON	OFF	ON	0.90	0.64	0.86	0.71	0.81	7.55
8 Feb 14:43 - 15:00	A	Upstream	ON	OFF	ON	0.79	0.56	1.20	0.80	0.83	8.27
8 Feb 15:05 - 15:18	A	Downstream	ON	OFF	ON	0.87	0.96	0.84	0.95	0.39	7.51
8 Feb 15:23 - 15:41	B	Upstream	ON	OFF	ON	0.85	0.64	1.37	0.62	0.36	7.52
8 Feb 15:44 - 16:00	B	Downstream	ON	OFF	ON	0.88	0.67	1.70	0.65	0.55	7.95
8 Feb 16:01 - 16:17	B	Upstream	ON	OFF	ON	0.79	0.61	0.67	0.67	0.61	7.38
8 Feb 16:21 - 16:37	B	Downstream	ON	ON	ON	1.24	0.65	0.70	0.99	0.79	9.91
8 Feb 16:39 - 16:59	B	Upstream	ON	ON	ON	0.77	0.62	1.11	0.93	0.57	7.60
10 Feb 08:41 - 08:59	B	Downstream	ON	ON	ON	10.14	0.55	1.14	0.72	0.79	7.43
10 Feb 09:16 - 09:34	C	Upstream	ON	ON	ON	11.46	1.04	1.55	0.69	0.44	7.76

Date Time	Pulser Configuration	Direction of Travel	Parasitic State			Barrier   Peak Potential Difference (volts)					
			1	2	3	V01	V12	V23	V34	V45	V56
10 Feb 09:35 - 09:48	C	Downstream	ON	ON	ON	11.48	0.60	0.76	0.82	0.39	8.04
10 Feb 09:52 - 10:08	C	Upstream	ON	ON	ON	9.82	0.59	1.17	0.82	0.56	7.35
10 Feb 10:10 - 10:25	C	Downstream	ON	OFF	ON	10.86	0.73	0.89	0.67	0.52	7.63
10 Feb 10:26 - 10:42	C	Upstream	ON	OFF	ON	9.72	0.67	0.80	0.79	0.53	7.31
10 Feb 13:13 - 13:27	C	Downstream	ON	OFF	ON	10.76	0.61	1.30	0.63	0.50	7.28
10 Feb 13:30 - 13:48	D	Upstream	ON	ON	OFF	10.25	1.19	1.21	0.67	0.53	7.76
10 Feb 13:49 - 14:02	D	Downstream	ON	ON	OFF	11.56	0.72	0.75	0.90	0.54	7.90
10 Feb 14:02 - 14:16	D	Upstream	ON	ON	OFF	10.70	0.73	0.54	0.78	0.61	7.98

Table 11. Test results for bollard voltage potential and 500-ohm current tests at fleeting area.

Time	Pulser Configuration	Parasitic 1	Parasitic 2	Parasitic 3	Bollard 2 Peak Voltage (Volts)	Bollard 3 Peak Voltage (Volts)	Bollard 2 Peak 500 $\Omega$ Current (mAmps)	Bollard 3 Peak 500 $\Omega$ Current (mAmps)
14:09 - 14:10	B	On	Off	On	10.8	4.9		
14:12 - 14:13	B	On	Off	On			16.0	6.7
14:16 - 14:18	B	On	Off	On			17.0	7.4
14:19 - 14:21	B	On	Off	On	9.2	4.7		
14:28 - 14:30	B	On	On	On	7.2	3.0		
14:31 - 14:33	B	On	On	On			11.3	5.1
14:51 - 14:54	A	On	On	On			11.7	4.3
14:55 - 14:57	A	On	On	On	6.3	3.0		
14:58 - 15:00	A	On	Off	On	7.9	3.8		
15:01 - 15:03	A	On	Off	On			15.4	10.7
15:06 - 15:08	C	On	Off	On			14.7	8.1
15:09 - 15:11	C	On	Off	On	11.2	7.9		
15:13 - 15:15	C	On	On	On	6.9	4.3		
15:16 - 15:18	C	On	On	On			12.7	7
15:21 - 15:23	D	On	On	Off			5.9	3.4
15:24 - 15:26	D	On	On	Off	3.0	1.6		
10:36 - 10:37*	F	On	Off	On	1.1	0.7		
10:38 - 10:39*	F	On	Off	On			2.0	1.4
15:59 - 16:00*	E	On	Off	On	3.3	2.3		
10:36 - 10:37*	F	On	Off	On	1.1	0.7		
10:38 - 10:39*	F	On	Off	On			2.0	1.4
15:59 - 16:00*	E	On	Off	On	3.3	2.3		

\*All data taken 7 February 2011 except rows denoted with an asterisk (\*), which were taken 15 June 2011.

**Table 12. Barge corrosion potential measurements taken with Cu/CuSO<sub>4</sub> reference electrode, conducted on 5 February 2011.**

Time	Measurement Location	Pulser Configuration	Potential (-mV)	Water Conductivity ( $\mu$ S/cm)
10:00	SE corner of north barge (just north of Bollard 3)	C	360	1590
14:00	SE corner of north barge (just north of Bollard 3)	B	380	1590

**Table 13. General corrosion rates for steel in fresh water.**

(Source: *Civil Engineering Corrosion Control, Volume 1 - Corrosion Control - General*, p 222.)

Potential between steel and Cu/CuSO <sub>4</sub> reference electrode (-mV)		Corrosivity
Min	Max	
550	and up-	Severe
450	550	Moderate
150	450	Mild
and below	150	Unlikely

Note: Fresh water is defined as having either greater than 300  $\Omega$ -cm resistivity or less than 3300  $\mu$ S/cm conductivity.

## References

- [1] US Army Corps of Engineers. May 2005. *Engineering Analyses of the Chicago Sanitary and Ship Canal Electric Fish Barrier: Electrical Effects on Barges and Tow Vessels*. Champaign, IL: US Engineer Research and Development Center, Construction Engineering Laboratory (ERDC-CERL).
- [2] U.S. Army Corps of Engineers. February 2006. *Engineering Analyses of the Chicago Sanitary and Ship Canal Electric Fish Barrier: Electrical Effects on Personnel in the Waster*. Champaign, IL: ERDC-CERL.
- [3] U.S. Army Corps of Engineers. 24 October 2006. *Dispersal Barrier IIA Electric Field Strength and Sparking Potential Testing*. Champaign, IL: ERDC-CERL.
- [4] U.S. Army Corps of Engineers. 11 June 2007. *Dispersal Barrier IIA Sparking Potential and Electric Field Strength Testing to Determine the Optimal Operating Configuration*. Champaign, IL: ERDC-CERL.
- [5] U.S. Army Corps of Engineers. 12 May 2008. *Demonstration Dispersal Barrier and Dispersal Barrier IIA Sparking Potential and Long Tow Testing to Determine Safety Considerations*. Champaign, IL: ERDC-CERL.
- [6] Navy Experimental Diving Unit. June 2008. *Evaluation of Risk Posed by Electric Fish Barriers to Human Immersion in the Chicago Sanitary and Ship Canal*. LT 07-05, NEDU TR 08-01.
- [7] U.S. Army Corps of Engineers. *September 2009 Electric Field Strength Analysis of the Chicago Sanitary and Ship Canal Electric Barrier System*. Champaign, IL: ERDC-CERL. January 2011
- [8] U.S. Army Corps of Engineers. In preparation. *Increased Voltage Safety Testing of the Aquatic Nuisance Species Dispersal Barrier IIA – Summary Compilation Report* (draft).
- [9] West, Lewis H. and Thomas F. Lewicki. January 1975. *Civil Engineering Corrosion Control, Volume 1 – Corrosion Control – General*. AFCEC-TR-74-6, Volume 1.
- [10] Clete, R. Stephan, P.E. *Coal Dust Explosion Hazards*. Pittsburgh, PA: Mine Safety and Health Administration.
- [11] International Electrotechnical Commission (IEC). 2005. *Effects of Current on Human Beings and Livestock - Part 1: General Aspects*. Publication 60479-1, 4th ed. IEC: Geneva, Switzerland.
- [12] Rasmussen, Jerry L. 1 January 2002. *The Cal-Sag and Chicago Sanitary and Ship Canal: A Perspective on the Spread and Control of Selected Aquatic Nuisance Fish Species*. Rock Island, IL: US Fish and Wildlife Service, Rock Island, IL.





# Appendix A: Instrumentation and Data Reduction

## Data acquisition equipment

A Pacific Instruments 6000 Series Data Acquisition System was used to continuously measure and record the voltage differentials. This system was chosen because of its multiple independent channel capabilities and its high sampling rate. The data acquisition system was connected to a laptop computer through a GPIB interface and the data was immediately transferred to the computer for storage. Because of the high sample rate and long scan times, barrier pulses were easily captured. When interpreting the Pacific data, the individual pulses and the 'envelope' (overall trend of the peak values) of the waveform may both be examined.

The Pacific Instruments 6000 Series Data Acquisition System is a high performance transducer signal conditioning, digitizing, and control system. The system is modular to accommodate applications of different size and transducer types. For this data collection, the Pacific Instruments Model 6033 8-channel strain gage transducer digitizing boards were used. These boards were configured for differential voltage measurements. The input to these boards has an impedance of 50 Megaohms shunted by 1000 picofarads. Measurements were taken using a sampling frequency of 8,000 samples/second for all testing. The unit has a 24-channel capability and the noise per channel is 200 microvolts ( $\mu\text{V}$ ) peak-to-peak.

Tektronix P5200 High voltage Differential Probes were used to attenuate the voltage signal level at the input and to isolate the Pacific Instruments 6000. The Tektronix Differential Probe has a 25 megahertz (MHz) bandwidth and an input impedance of 4 Megaohms with a common mode rejection ration of 80 dB at 60 Hz. The maximum voltage input at the 1/50 attenuation setting is 130 V. The maximum voltage input at the 1/500 setting is 1300 V.

## GPS data collection with Trimble GeoXH

Throughout the project all electrical measurements on moving vessels were referenced with geospatial coordinates to aid in mapping and determining the extent and nature of the electrical field. Global Positioning Sys-

tems (GPS) were used to record the data. A GPS was placed on the bow of the Boston Whaler and each towboat of the long tow. Maximum margins of error for GPS accuracy was +/- 0.1 meter. Data for testing runs that exceeded the minimal level accuracy were excluded from analysis.

The GPS recorded its position every two seconds. Because the data acquisition instruments recorded voltages at millisecond intervals, in order to georeference the electrical data a linear interpolation of the GPS data was required. The electrical measurements were georeferenced by using the barrier array as a marker. Because the maximum electrical measurement values occur over the barrier, the time values of the measurement files were georeferenced by synchronizing the time of the maximum values with the time of the location of the barrier arrays in the GPS files.

### **Data reduction**

In order to match the electrical data with the georeference data, the electrical data was downloaded into Matlab, along with the georeference data. The georeference data was broken down by run into separate files. The known GPS coordinates for the center of Barrier IIA were matched up with the largest absolute voltage value contained within each run for the electrical data, and the electrical data for each run matched up with the GPS data for that run via the time logs for each data set. Because the electrical data contained far more readings per minute than the georeference data, linear interpolation was used to infer the GPS coordinates for the voltage readings which occurred between GPS readings, thus providing an approximate GPS position for each reading contained within the electrical data. These newly combined files were then saved according to run number.

## Appendix B: Electric Hazard Analysis

### Computation of hazardous electric field levels

The analysis of the effects of the measured voltages and electric field gradients and the resultant body current on a human immersed in the CSSC near the barriers is complex. While many studies of the effects of electrical shock to animals and humans are published in the scientific literature, almost all investigate bodies in air, not immersed in water, and with single current burst shocks from 50 to 60 Hz alternating current (AC). The same is true for electrical safety standards and codes. In addition, many continuously changing environmental and physiological variables characterize the situation (NEDU TR 08-01).

The Navy Experimental Diving Unit (NEDU) reviewed electric shock studies as well as appropriate electrical safety specifications and codes in the scientific literature to determine conservative, relevant physiological effects likely to occur in humans exposed to electric shock while immersed in the water, with water conductivity and electric field strengths over the range found in the CSSC (NEDU TR 08-01).

Following conservative methods and assumption, NEDU used measured field strength data, together with generally accepted body resistance values, to evaluate the maximum electrical body currents likely to be experienced by a person immersed in the CSSC. The safety and possible physiological effects of derived maximum body currents were evaluated using research studies available in the open scientific literature as well as national and international electrical safety specifications and codes (NEDU TR 08-01).

Time-current zones of physiological effects of a DC current pulse on a human body are shown in Figure B1 (reproduced from the IEC Publication 60479-1). The zones, current boundaries, and physiological effects are listed in Table B1. They indicate that to remain below the threshold of causing patho-physiological effects, such as cardiac arrest, breathing arrest, and burns or other cellular damage, may occur the current through the body must be  $\leq 500$  milliamperes (mA) DC for pulse widths less than 10 ms..

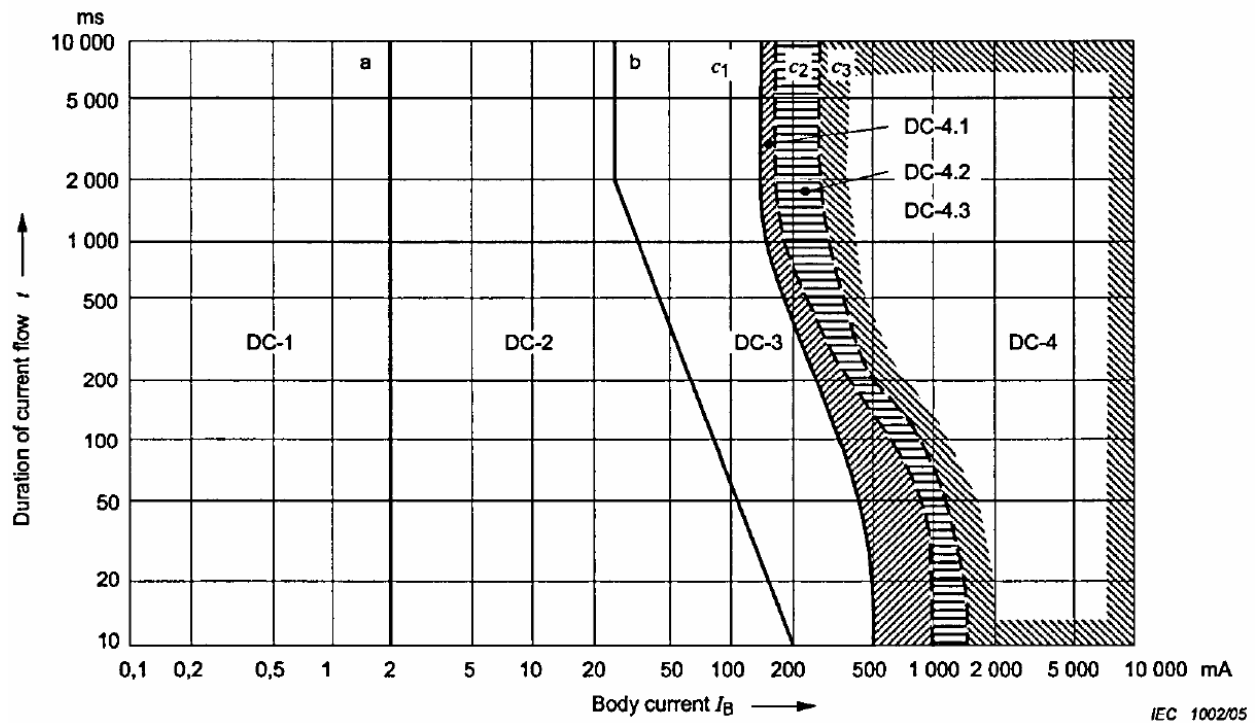


Figure B1. Time-Current Zones of Effects of DC Currents (figure 22 of IEC 60479-1).

Table B1. Time-current zones from Figure B1 for physiological effects of single-pulse DC Shock for hand-to-ft pathway. Source: IEC Publication 60479-1, Table 13.

Zones	Current Boundaries	Physiological Effects
DC-1	Up to 2.0 mA, Curve a	Slight pricking sensation possible when making, breaking or rapidly altering current flow.
DC-2	2.0 mA up to Curve b	Involuntary muscular contractions likely, especially when making, breaking or rapidly altering current flow but usually no harmful electrical physiological effects.
DC-3	Curve b & above	Strong involuntary muscular reactions and reversible disturbances of formation and conduction of impulses in the heart may occur, increasing with current magnitude and time. Usually no organic damage to be expected.
DC-4	Above Curve c1	Patho-physiological effects may occur such as cardiac arrest, breathing arrest, & burns or other cellular damage. Probability of ventricular fibrillation increasing with current magnitude and time.
	Between Curves c1 & c2	DC-4.1: Probability of ventricular fibrillation increasing up to about 5%
	Between Curves c2 & c3	DC-4.2: Probability of ventricular fibrillation increasing up to about 50%
	Beyond Curve c3	DC-4.3: Probability of ventricular fibrillation above 50%

The region where patho-physiological effects may occur is identified as region DC-4 in Figure B1. The minimum value of body current to pass into area DC-4 (the  $c_1$  curve in Figure B1) is 500 mA for durations of current flow less than 10 ms. The  $c_1$  curve appears to transition to vertical for pulse

duration less than 10 ms, so the 500 mA value is valid for both Barrier I's 4 ms and Barrier II's 2.5 and 6.5 ms pulse widths.

Figure B1 and Table B1 can also be used to evaluate the current bursts induced by repetitive pulse shocks. However, the threshold for ventricular fibrillation applicable to the second current burst can be as low as 65% of the threshold current applicable to the first burst. Each succeeding pulse reduces the threshold current appropriate for the preceding burst for ventricular fibrillation by another  $\approx 35\%$ , until a minimum threshold of  $\leq 10\%$  of the single-pulse threshold is reached for  $\geq 7$  bursts. Since a person immersed in the CSSC near a fish barrier will experience 5 or 6.5 pulses per second for an indefinite period, the value of the threshold current appropriate for evaluating the risk for ventricular fibrillation posed to such a person is  $\leq 10\%$  of the threshold current for a single-pulse DC shock.<sup>6</sup> Reducing the threshold to 10% of the single-pulse current value (as is appropriate for the continuously repeated fish barrier pulses) dramatically changes the fibrillation threshold to a  $< 50$  mA pulse for a  $< 5\%$  risk of fibrillation ( $c_1$  curve, Figure A-1 and Table A-1).<sup>7</sup>

Therefore, to identify the areas in the CSSC where it is likely harmful to be immersed in the water, it is necessary to be able to calculate the areas where an immersed person would develop a current through the body greater than 50 mA. This can be done using the demagnetizing factors technique.

In a swimmer not wearing an insulating garment, current can flow into the person through all areas of the body's surface. In addition, the field within the body can be significantly altered from that which was in the volume of water before the body was immersed. The degree of alteration is strongly influenced by the relative electric resistivity of the water compared with that of the immersed body. ERA Technology Limited, Stoner, and Osborn present a technique that represents the body as an ellipsoid and calculates the ratio of the current density in the body to that in the water before the body is immersed. It solves the problem by "analogy with a corresponding magnetic problem, namely that of determining the magnetic flux density inside a magnetic ellipsoid when introduced into a uniform magnetic field.

---

<sup>6</sup> Ibid, page 38.

<sup>7</sup> Ibid, page 38.

Solutions to this problem are well known and expressed in terms of ‘demagnetizing factors.’”<sup>8</sup>

The demagnetizing-factors technique reveals that the most severe physical orientation in low-resistivity (i.e., high-conductivity) water is that in which a person is upright, with the electric field oriented in the direction from chest to back (Case A). For high-resistivity (i.e., low-conductivity) water, the most severe exposure orientation occurs when a person’s body is parallel to the water surface, with the direction of the field oriented along the body length (Case S).<sup>9</sup>

In order to determine the worst-case electric field value (minimum electric field strength that might produce harmful physiological effects), four combinations of worst-case resistivities and body orientations were analyzed.

Water conductivity data collected by the Metropolitan Water Reclamation District of Greater Chicago at CSSC river miles 304.7 and 296.2 from October 1998 – April 2010 were used in the analysis. Resistivity is the inverse of conductivity. Resistivity ranged from a minimum of 2.13  $\Omega$ -m to a maximum of 20.45  $\Omega$ -m, with a median value of 10.19  $\Omega$ -m. The transition from low to high resistivity occurs around 10  $\Omega$ -m. Therefore, the median value of 10.19  $\Omega$ -m could be considered either low (Case A) or high (Case S) resistivity, and was evaluated for each case.

The computation of the minimum electric field strength likely to cause harmful effects can be done using equations from the NEDU report “Evaluation of Risk That Electric Fish Barriers Pose to Human Immersion in the Chicago Sanitary and Ship Canal.”

The variables used in the computations are:

- $k$  –(water resistivity)/(body resistivity)
- $I_b$  –current density in the body once it is immersed
- $I_o$  –current density in the water before the body is immersed
- $I_B$  –current produced through the chest area by body current density
- $I_b$
- $\rho$  –resistivity
- $E$  –electric field strength

<sup>8</sup> Ibid, pages 25-26.

<sup>9</sup> Ibid, page 26.

The assumptions used in the computations are:

1. Water resistivity (taken from October 1998 through April 2010 data)
  - a. minimum value of 2.13  $\Omega\text{-m}$
  - b. median value of 10.19  $\Omega\text{-m}$
  - c. maximum value of 20.45  $\Omega\text{-m}$
2. Body resistivity is 3.75  $\Omega\text{-m}$ <sup>10</sup>
3. Cross sectional area of chest is 0.08  $\text{m}^2$ <sup>11</sup>
4.  $I_B \leq 50 \text{ mA}$  (0.05 A) DC to avoid harmful effects (as explained above)

The computations for the four combinations of worst-case resistivities and body orientations for harmful physiological effects (zone DC-4 of Figure B1 and Table B1) are shown below. In these computations, references to equation numbers and pages refer to those items in the NEDU report. The results are summarized in Table B2. The lowest value where harmful effects are likely, and therefore the worst case, is approximately 0.05 V/in.

#### Low Resistivity Case A

$$k = 2.13 \Omega\text{-m} / 3.75 \Omega\text{-m} = 0.57 \quad (\text{Assumptions 1 and 2})$$

$$(I_b/I_o) = k/(1+[k-1] \times 0.566) \quad (\text{Equation for Case A, page 26})$$

$$(I_b/I_o) = 0.57/(1+[0.57-1] \times 0.566) = 0.75$$

$$I_b = 0.75 \times I_o$$

$$I_B = I_b \times 0.08 \text{ m}^2 = 0.75 \times I_o \times 0.08 \text{ m}^2 = 0.06 \text{ m}^2 \times I_o \quad (\text{Equation 2, page 27 and assumption 3})$$

$$I_o = I_B/0.06 \text{ m}^2$$

$$I_o \leq 0.05 \text{ A}/0.06 \text{ m}^2 \quad (\text{Assumption 4})$$

$$I_o \leq 0.833 \text{ A}/\text{m}^2$$

$$E = I_o \times \rho \quad (\text{Equation page 39})$$

---

<sup>10</sup>Ibid, page 26.

<sup>11</sup> Ibid, page 27.



$$E \leq 0.833 \text{ A/m}^2 \times 2.13 \text{ } \Omega\text{-m}$$

(Assumption 1)

$$**E \leq 1.77 \text{ V/m (0.54 V/ft)}**$$

Threshold for low resistivity  
Case A

#### Midrange Resistivity Case A

$$k = 10.19 \text{ } \Omega\text{-m} / 3.75 \text{ } \Omega\text{-m} = 2.72$$

(Assumptions 1 and 2)

$$(I_b/I_o) = k/(1+[k-1] \times 0.566)$$

(Equation for Case A, page  
26)

$$(I_b/I_o) = 2.72/(1+[2.72-1] \times 0.566) = 1.38$$

$$I_b = 1.38 \times I_o$$

$$I_B = I_b \times 0.08 \text{ m}^2 = 1.38 \times I_o \times 0.08 \text{ m}^2 = 0.11 \text{ m}^2 \times I_o$$

(Equation 2, page 27 and as-  
sumption 3)

$$I_o = I_B/0.11 \text{ m}^2$$

$$I_o \leq 0.05 \text{ A}/0.11 \text{ m}^2$$

(Assumption 4)

$$I_o \leq 0.455 \text{ A/m}^2$$

$$E = I_o \times \rho$$

(Equation page 39)

$$E \leq 0.455 \text{ A/m}^2 \times 10.19 \text{ } \Omega\text{-m}$$

(Assumption 1)

$$**E \leq 4.64 \text{ V/m (1.41 V/ft)}**$$

Threshold for midrange resis-  
tivity Case A

#### Midrange Resistivity Case S

$$k = 10.19 \text{ } \Omega\text{-m} / 3.75 \text{ } \Omega\text{-m} = 2.72$$

$$(I_b/I_o) = k/(1+[k-1] \times 0.034)$$

(Equation for Case S, page  
26)

$$(I_b/I_o) = 2.72/(1+[2.72-1] \times 0.034) = 2.57$$

$$I_b = 2.57 \times I_o$$

$$I_B = I_b \times 0.08 \text{ m}^2 = 2.57 \times I_o \times 0.08 \text{ m}^2 = 0.21 \text{ m}^2 \times I_o \quad (\text{Equation 2, page 27 and assumption 3})$$

$$I_o = I_B/0.21 \text{ m}^2$$

$$I_o \leq 0.05 \text{ A}/0.21 \text{ m}^2 \quad (\text{Assumption 4})$$

$$I_o \leq 0.238 \text{ A}/\text{m}^2$$

$$E = I_o \times \rho \quad (\text{Equation page 39})$$

$$E \leq 0.238 \text{ A}/\text{m}^2 \times 10.19 \text{ } \Omega\text{-m} \quad (\text{Assumption 1})$$

$$\mathbf{E \leq 2.43 \text{ V}/m (0.74 \text{ V}/ft)} \quad \text{Threshold for midrange resistivity Case S}$$

### High Resistivity Case S

$$k = 20.45 \text{ } \Omega\text{-m} / 3.75 \text{ } \Omega\text{-m} = 5.45$$

$$(I_b/I_o) = k/(1+[k-1] \times 0.034) \quad (\text{Equation for Case S, page 26})$$

$$(I_b/I_o) = 5.45/(1+[5.45-1] \times 0.034) = 4.73$$

$$I_b = 4.73 \times I_o$$

$$I_B = I_b \times 0.08 \text{ m}^2 = 4.73 \times I_o \times 0.08 \text{ m}^2 = 0.38 \text{ m}^2 \times I_o \quad (\text{Equation 2, page 27 and assumption 3})$$

$$I_o = I_B/0.38 \text{ m}^2$$

$$I_o \leq 0.05 \text{ A}/0.38 \text{ m}^2 \quad (\text{Assumption 4})$$

$$I_o \leq 0.132 \text{ A}/\text{m}^2$$

$$E = I_o \times \rho \quad (\text{Equation page 39})$$

$$E \leq 0.132 \text{ A/m}^2 \times 20.45 \text{ } \Omega\text{-m}$$

(Assumption 1)

$$E \leq \mathbf{2.70 \text{ V/m (0.82 V/ft)}}$$

Threshold for high resistivity  
Case S

Table B2. Minimum electric field strengths (voltage gradients) sufficient to cause harmful physiological effects.

Water Resistivity ( $\Omega\text{-m}$ )	Body Orientation*	Minimum Electric Field Strength (V/ft)	Minimum Electric Field Strength (V/in.)
2.16	A	0.54	0.05
11.34	A	1.41	0.12
11.34	S	0.74	0.06
26.32	S	0.82	0.07

\* A denotes low water resistivity, electrical field is oriented in direction from chest to back. S denotes high water resistivity, body is oriented horizontally to the water's surface with the direction of the field oriented along the body's length.

Computations similar to those above were performed for two other zones of physiological effects DC-3 in Table B1 (strong involuntary muscular reactions) and DC-1 in Table B1 (slight prickling sensation). The results are summarized in Table B3. The lowest value where effects are likely, and therefore the worst case, was always Low Resistivity Case A. Note that in the strong involuntary muscular reactions zone there are two values for minimum electric field strengths. This is because the maximum body current is dependent on the pulse width. The minimum electric field strengths used in the determination of the ranges of physiological effects in the report are highlighted in bold text.

Table B3. Time-current zones for physiological effects of single-pulse DC shock for hand-to-ft pathway\*.

Zones	Current Boundaries	2.5 ms Pulse Width**		4.0 ms Pulse Width**		6.5 ms Pulse Width**		Physiological Effects
		Maximum Body Current (mA)	Minimum Electric Field Strength (V/in.)	Maximum Body Current (mA)	Minimum Electric Field Strength (V/in.)	Maximum Body Current (mA)	Minimum Electric Field Strength (V/in.)	
DC-1	Up to 2.0 mA, Curve a	0.2	1.8E-4	0.2	1.8E-4	0.2	1.8E-4	Slight pricking sensation possible when making, breaking or rapidly altering current flow.
DC-2	2.0 mA up to Curve b	—	—	—	—	—	—	Involuntary muscular contractions likely, especially when making, breaking or rapidly altering current flow but usually no harmful electrical physiological effects.
DC-3	Curve b & above	34	<b>0.03</b>	29	<b>0.03</b>	24	<b>0.02</b>	Strong involuntary muscular reactions and reversible disturbances of formation and conduction of impulses in the heart may occur, increasing with current magnitude and time. Usually no organic damage to be expected.
DC-4	Above Curve c1	50	<b>0.05</b>	50	<b>0.05</b>	50	<b>0.05</b>	Patho-physiological effects may occur such as cardiac arrest, breathing arrest, & burns or other cellular damage. Probability of ventricular fibrillation increasing with current magnitude and time.
	Between Curves c1 & c2	—	—	—	—	—	—	DC-4.1: Probability of ventricular fibrillation increasing up to about 5%
	Between Curves c2 & c3	100	0.09	100	0.09	100	0.09	DC-4.2: Probability of ventricular fibrillation increasing up to about 50%
	Beyond Curve c3	138	0.12	138	0.12	138	0.12	DC-4.3: Probability of ventricular fibrillation above 50%

\* Information in this table is reproduced from Table 13 of IEC Publication 60479-1.

\*\* Since the minimum pulse width of Figure B1 (figure 22 of IEC 60479-1) is 10 ms, these maximum body current values were extrapolated from the curves.

### Determination of range of harmful effects

Figures B2 and B3 show the threshold for ventricular fibrillation, ±0.05 V/in., overlaid on top of the electric fields measured over Barrier IIA, IIB,

and I for run 1. These figures are representative as to how each run was analyzed to determine the range of harmful effects. The areas where the absolute peaks of the electric field are greater than  $\pm 0.05$  V/in. are potentially dangerous for a person to be in the water. The center of Barrier II B was established as the X-axis zero point on Figure B2 for distance measurements north and south of Barriers IIA and B.

Isolated spikes in the voltage gradient beyond the main “humps” of voltage gradient created by the barriers are due to random electrical noise and are not considered harmful. Previous testing has shown that these spikes due to electrical noise are detected in the canal even when the barriers are not operating. (See [1, 3, and 4].)

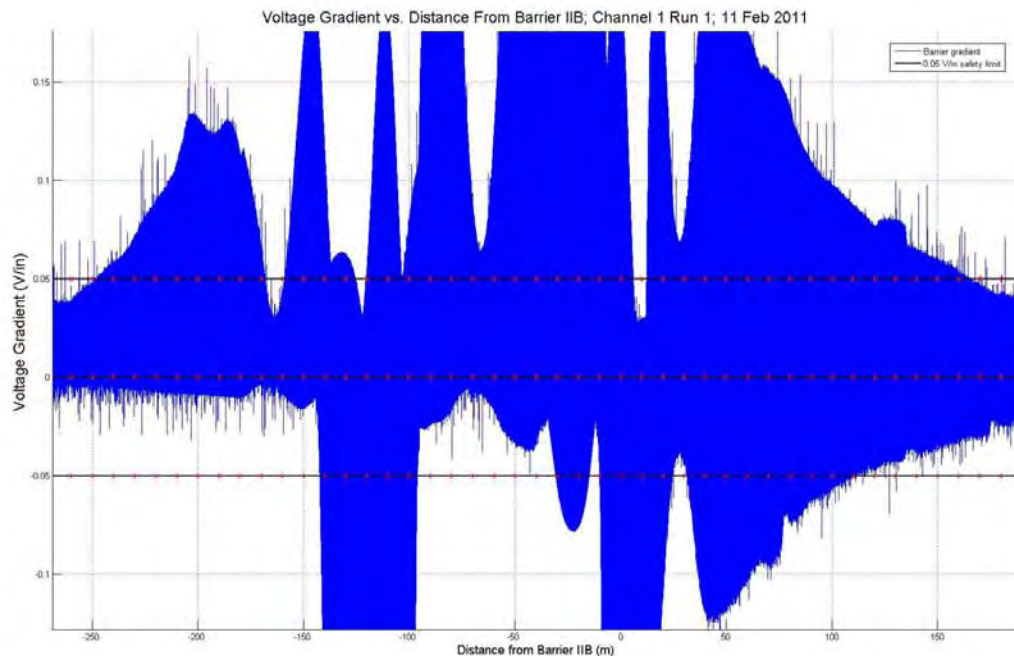


Figure B2. Example of minimum field strength shown on a plot of Barrier IIA and IIB field strength measurement run. Areas above or below the red lines are areas where the electric field strength from the barriers is sufficient to cause ventricular fibrillation (random isolated field spikes above these lines which occur outside the main area shown on the graph are noise and are not harmful).

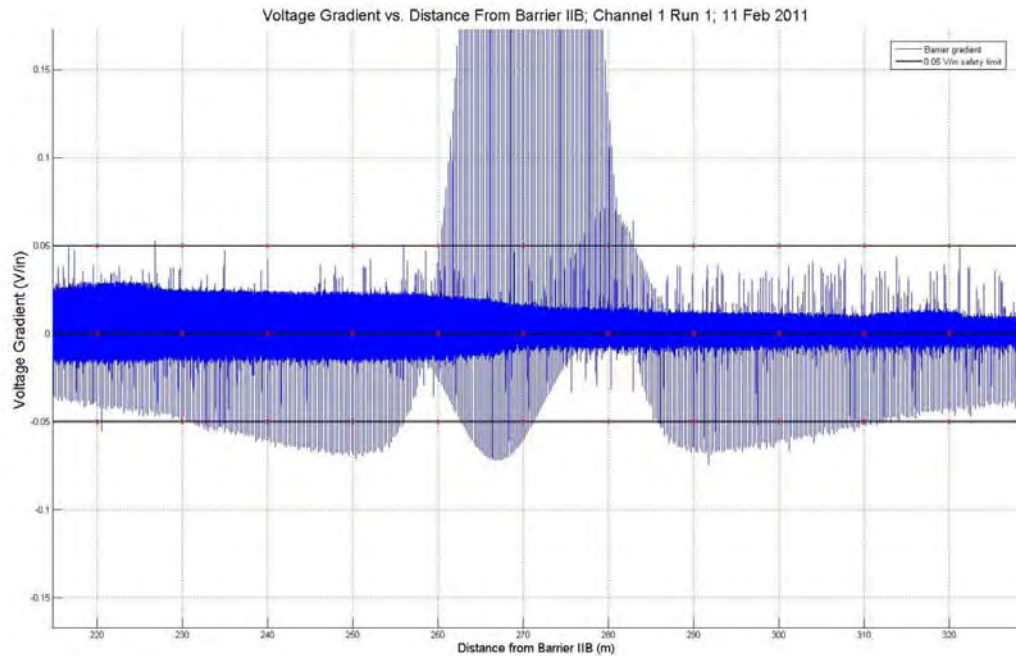


Figure B3. Example of minimum field strength shown on a plot of Barrier I field strength measurement run. Areas above or below the red lines are areas where the electric field strength from the barriers is sufficient to cause ventricular fibrillation (random isolated field spikes above these lines which occur outside the main area shown on the graph are noise and are not harmful).

## Sensitivity analysis

Actual electric field strength sometimes exceeded the target operational pulser configuration specifications. In an effort to determine the impact of these higher values, a sensitivity analysis was conducted by scaling the entire dataset (i.e., run) by +/- 20% and then reevaluating the range of harmful effects using the scaled dataset. As an example of the effect of scaling, the scaled data for V12, Run1 on 11 February 2011 (Configuration Bravo), is shown in Figures B4 –B9.

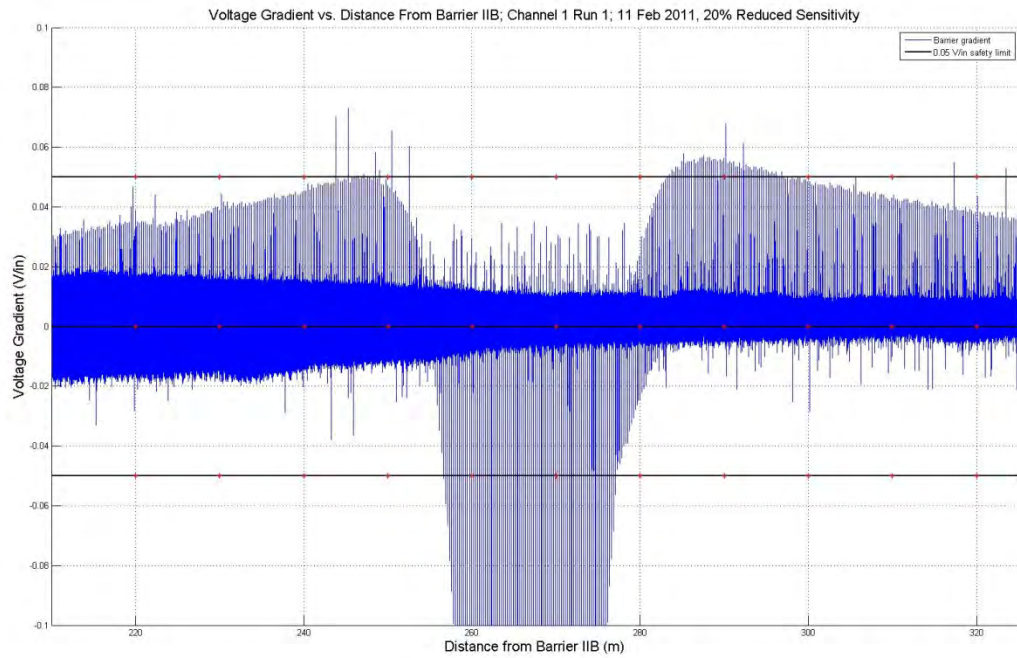


Figure B4. Sensitivity analysis at 20% reduced sensitivity 200 m away from Barrier IIB.

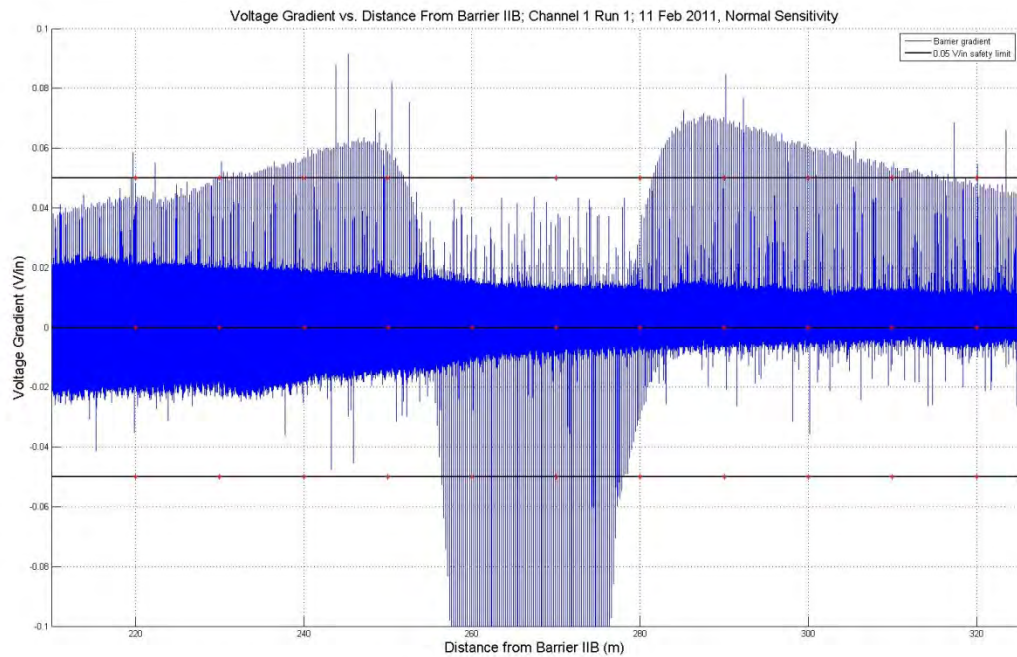


Figure B5. Sensitivity analysis at 20% normal sensitivity 200 m away from Barrier IIB.



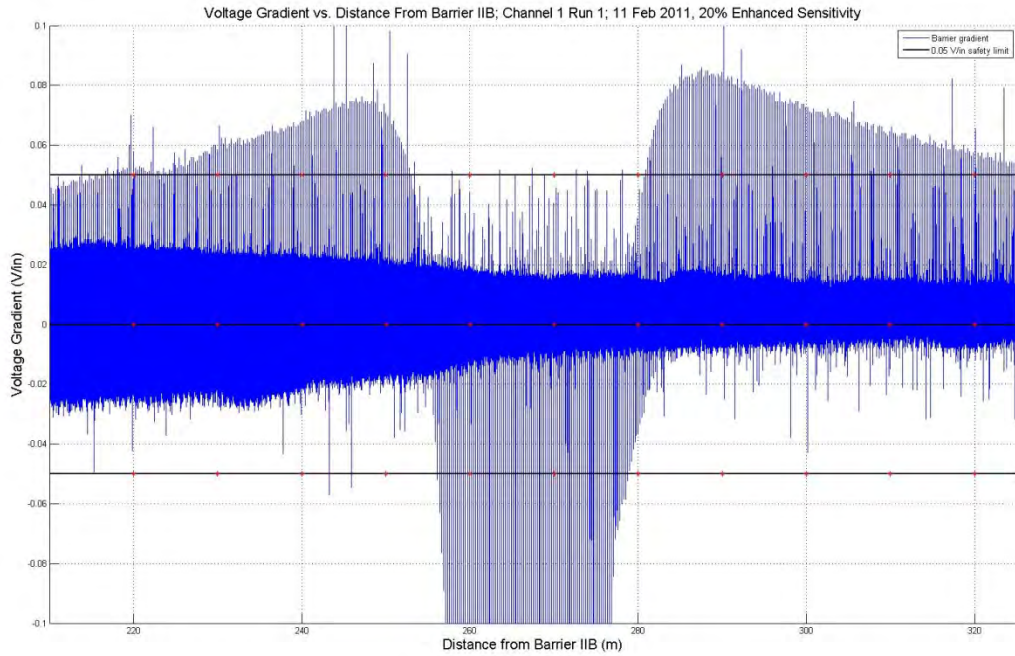


Figure B6. Sensitivity analysis at 20% enhanced sensitivity 200 m away from Barrier IIB.

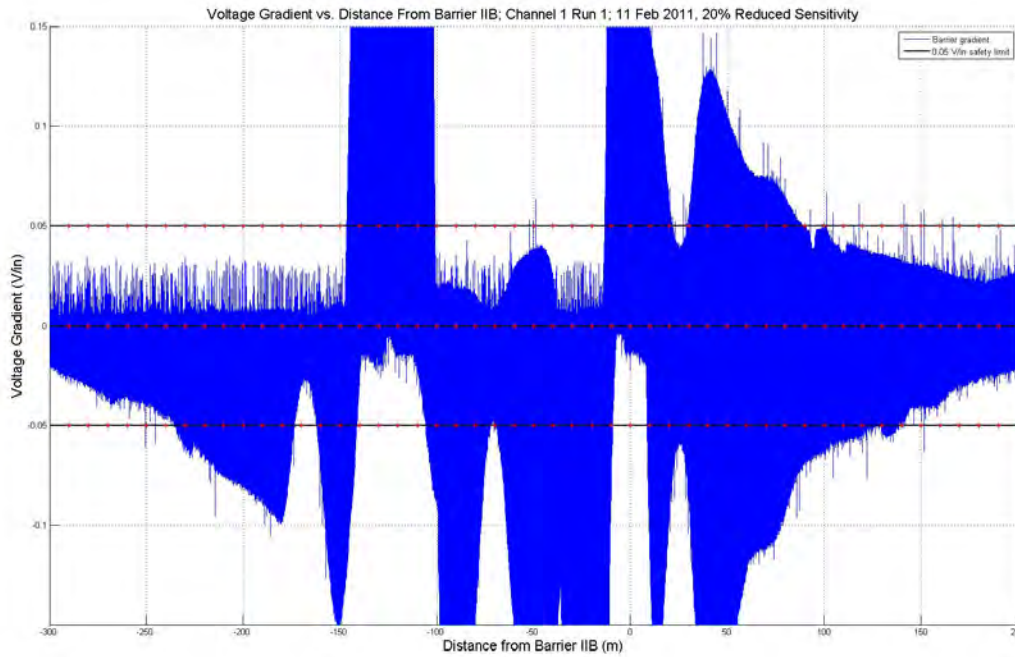


Figure B7. Sensitivity analysis at 20% reduced sensitivity at Barrier IIB.



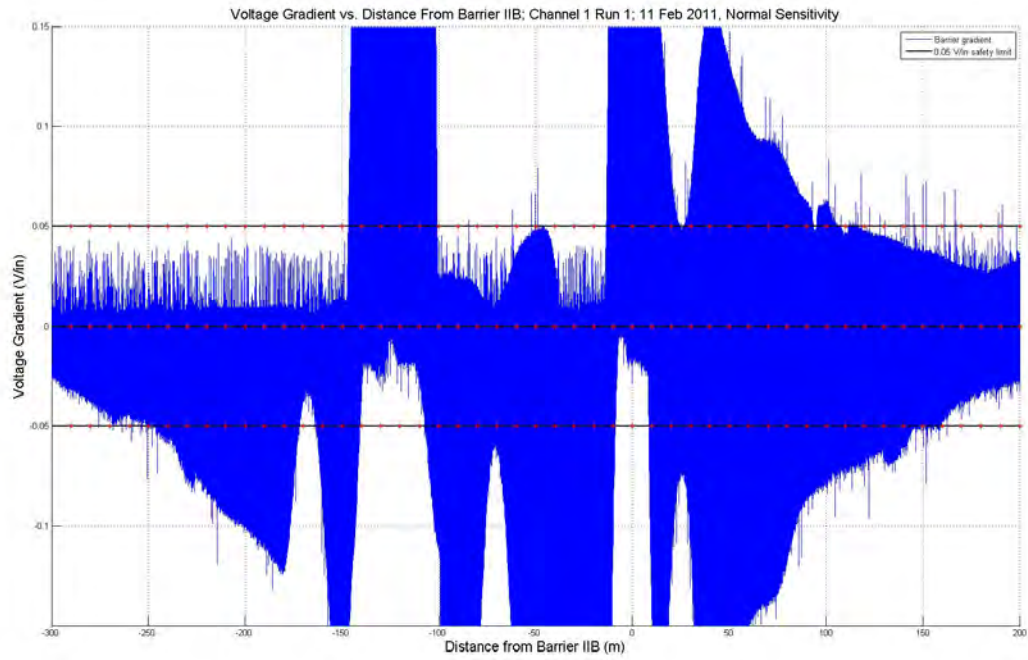


Figure B8. Sensitivity analysis at 20% normal sensitivity at Barrier IIB.

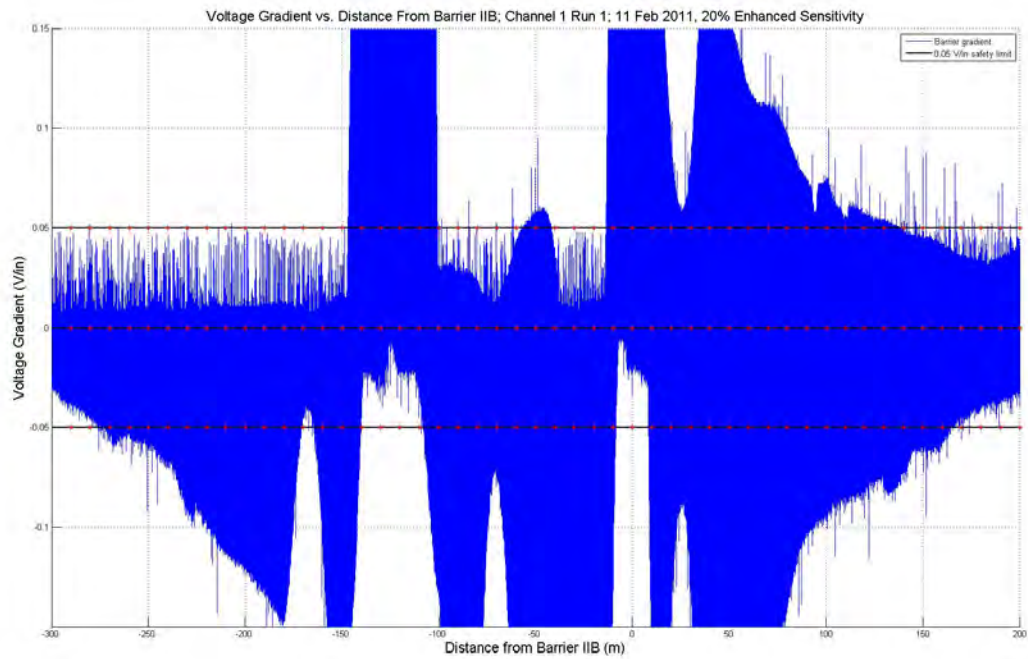


Figure B9. Sensitivity analysis at 20% enhanced sensitivity at Barrier IIB.

## Appendix C: V12 Electric Field Plots

This appendix contains plots for V12 (channel 1) of the electric field mapping activity conducted on 11 and 12 February 2011 and 14 June 2011. In these plots, the electric field strength data has been georeferenced with respect to the center of the narrow array of Barrier IIB. This point is labeled measurement center on Figure C1. Figure 2 in the body of the report shows the location of measurement V12. Chapter 4, Table 2 in the body of the report provides details of the approximate run times as well as pulser and parasitic configurations for these data. Included on these plots is the electric field limit (0.05 V/in), above which is sufficient to cause harmful physiological effects.

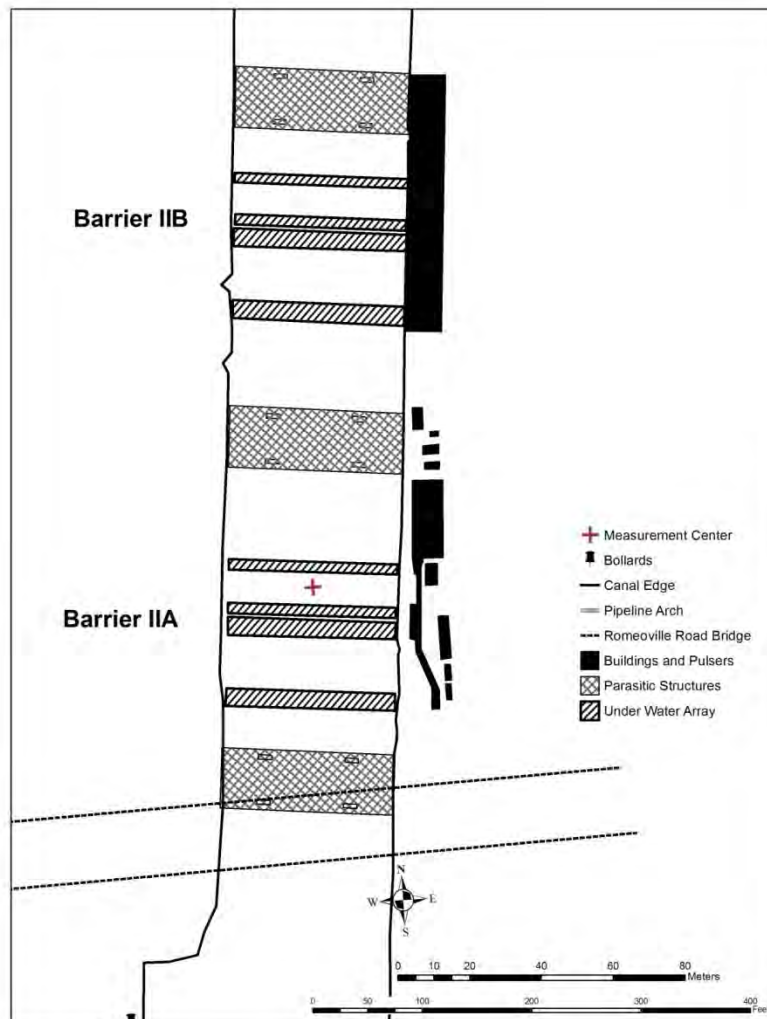


Figure C1. Location of reference point in canal for presentation of georeferenced data.

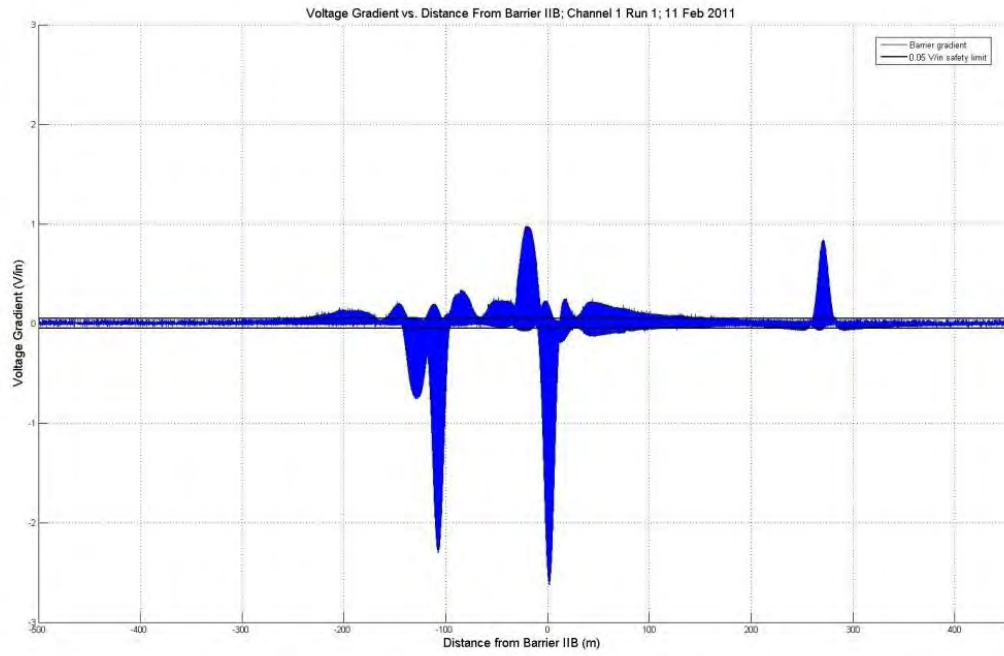


Figure C2. V12 for Run 1 on 11 February 2011 (Configuration B, Off, Off, Off, East Wall).

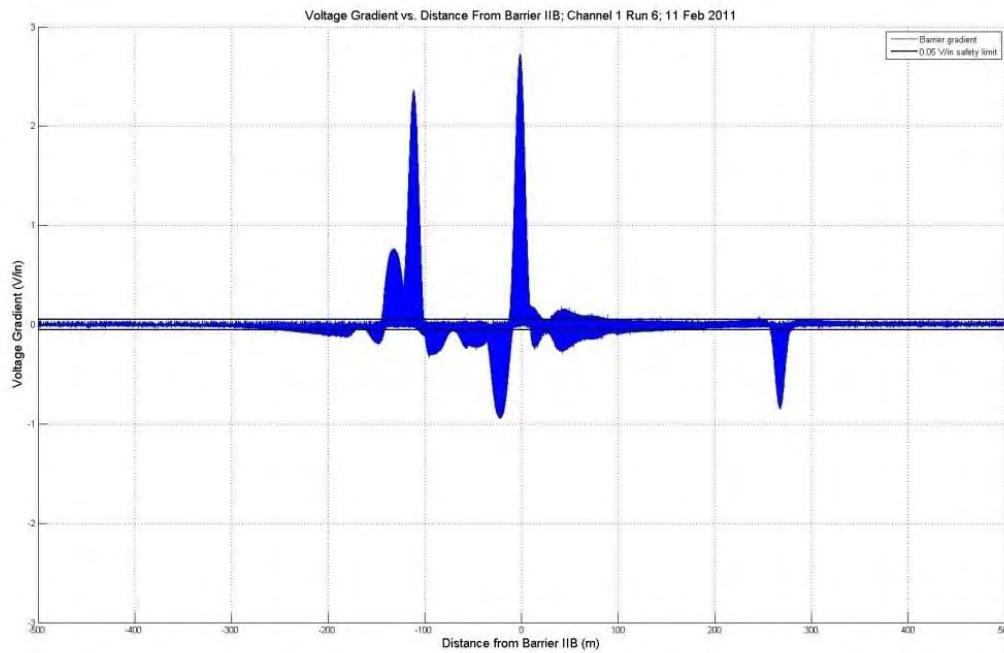


Figure C3. V12 for Run 6 on 11 February 2011 (Configuration B, Off, Off, Off, East Wall).

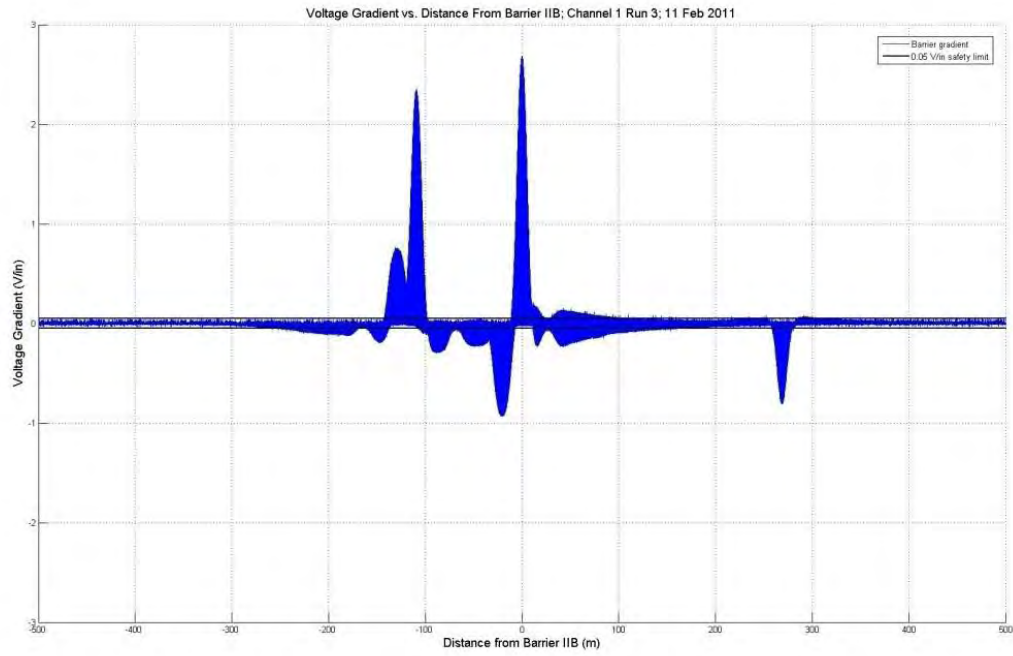


Figure C4. V12 for Run 3 on 11 February 2011 (Configuration B, Off, Off, Off, Center).

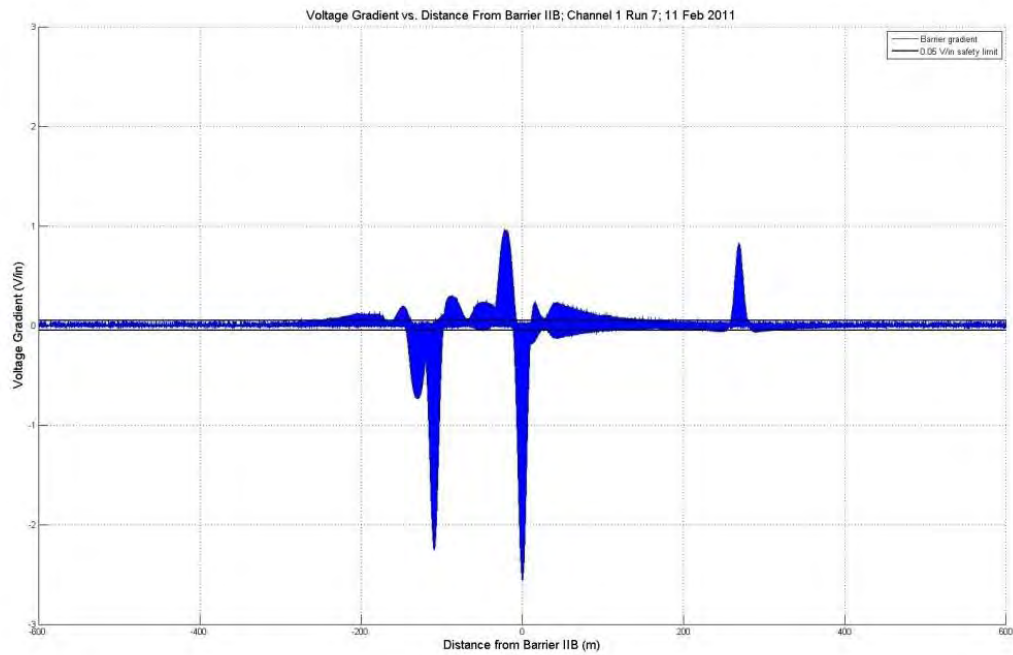


Figure C5. V12 for Run 7 on 11 February 2011 (Configuration B, Off, Off, Off, Center).

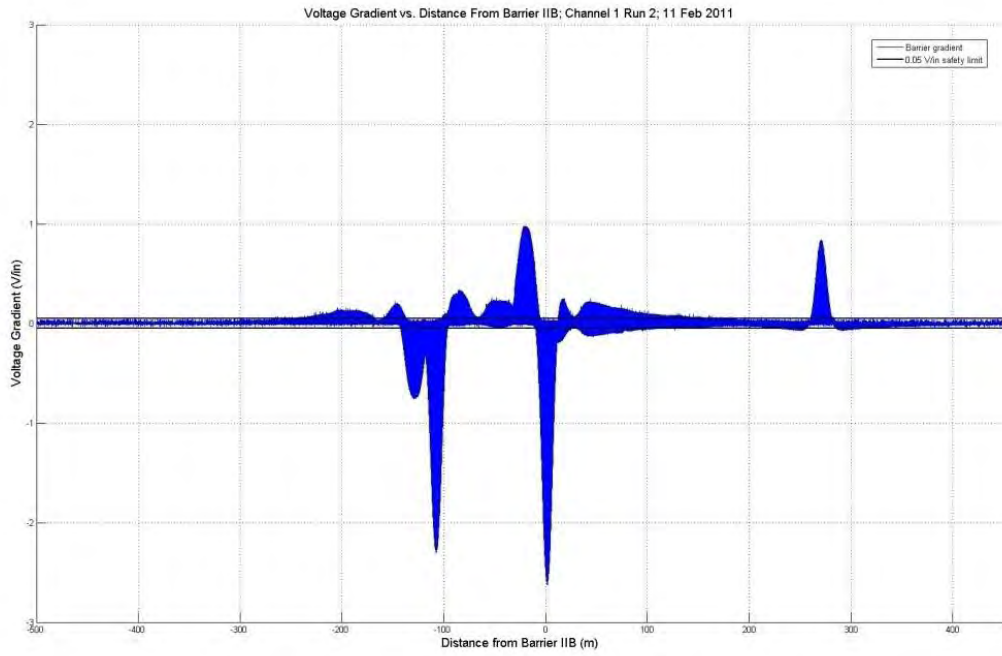


Figure C6. V12 for Run 2 on 11 February 2011 (Configuration B, Off, Off, Off, West Wall).

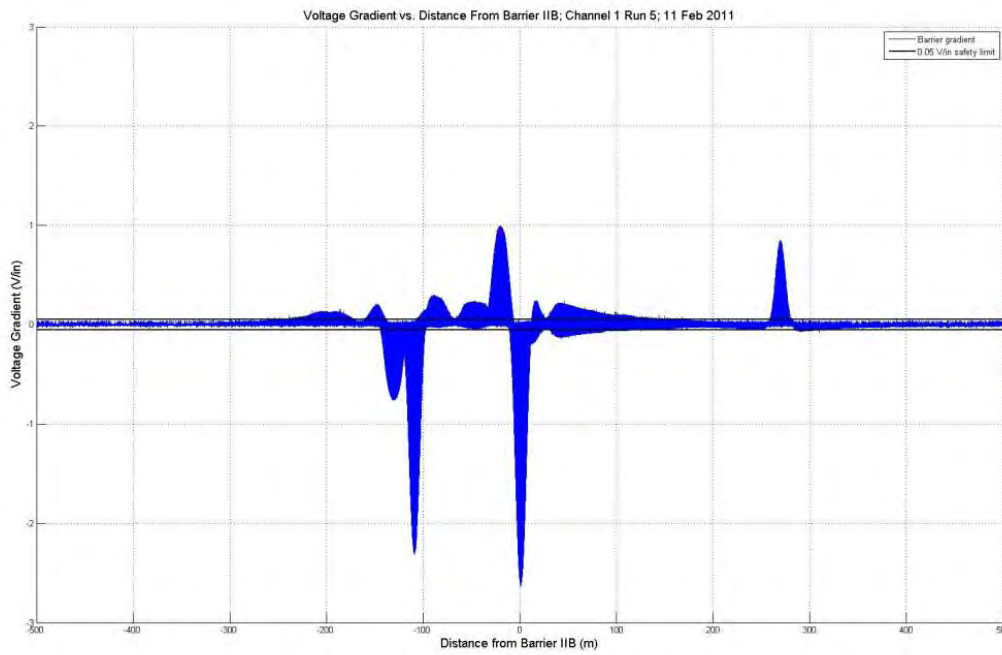


Figure C7. V12 for Run 5 on 11 February 2011 (Configuration B, Off, Off, Off, West Wall).



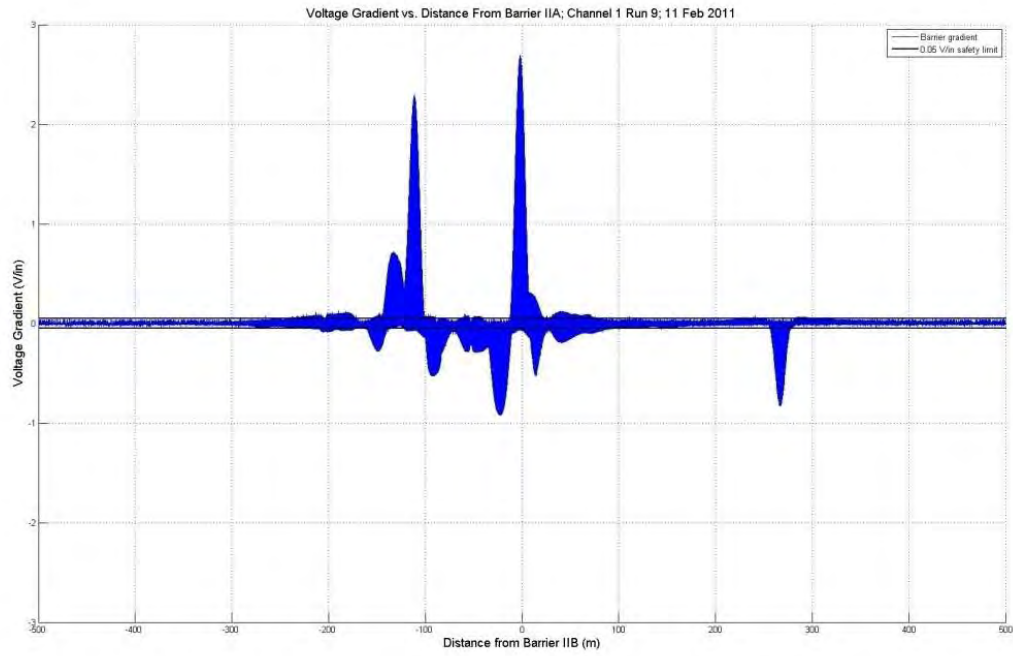


Figure C8. V12 for Run 9 on 11 February 2011 (Configuration B, On, Off, On, East Wall).

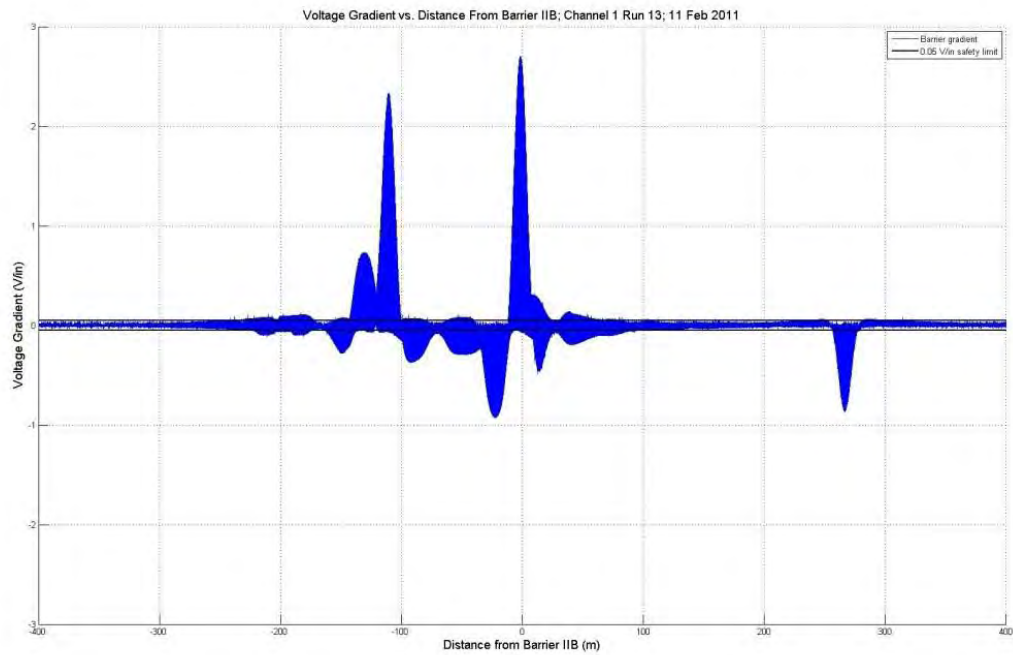


Figure C9. V12 for Run 13 on 11 February 2011 (Configuration B, On, Off, On, East Wall).

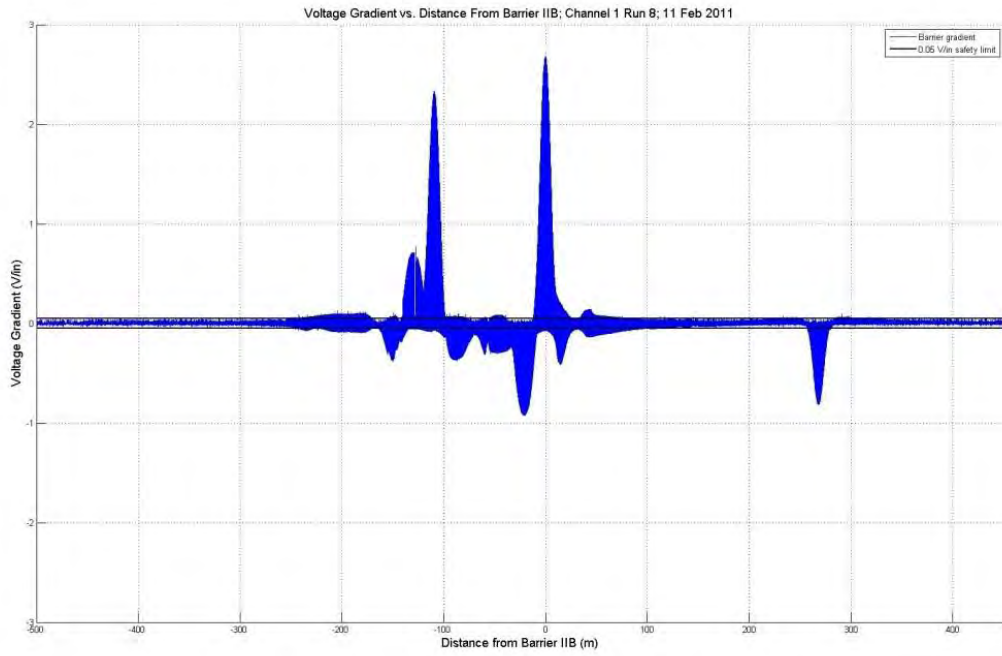


Figure C10. V12 for Run 8 on 11 February 2011 (Configuration B, On, Off, On, Center).

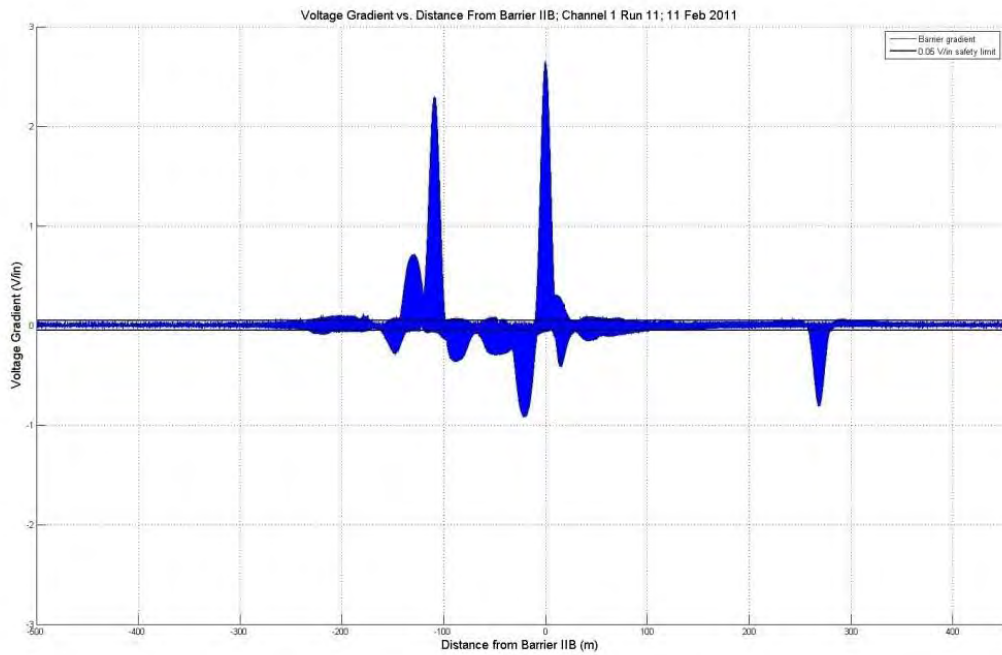


Figure C11. V12 for Run 11 on 11 February 2011 (Configuration B, On, Off, On, Center).

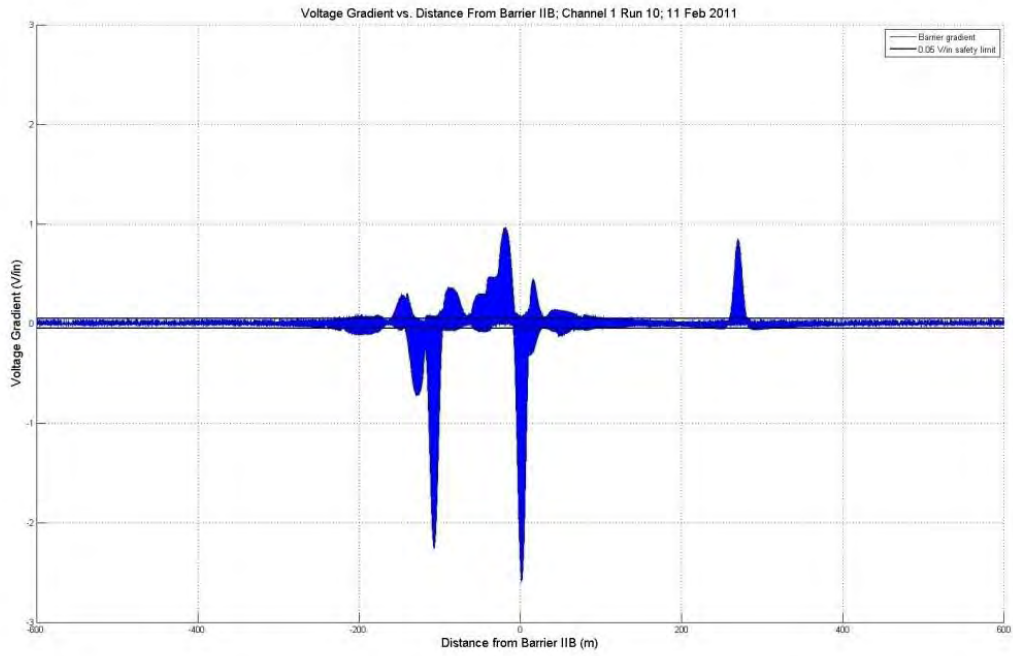


Figure C12. V12 for Run 10 on 11 February 2011 (Configuration B, On, Off, On, West Wall).

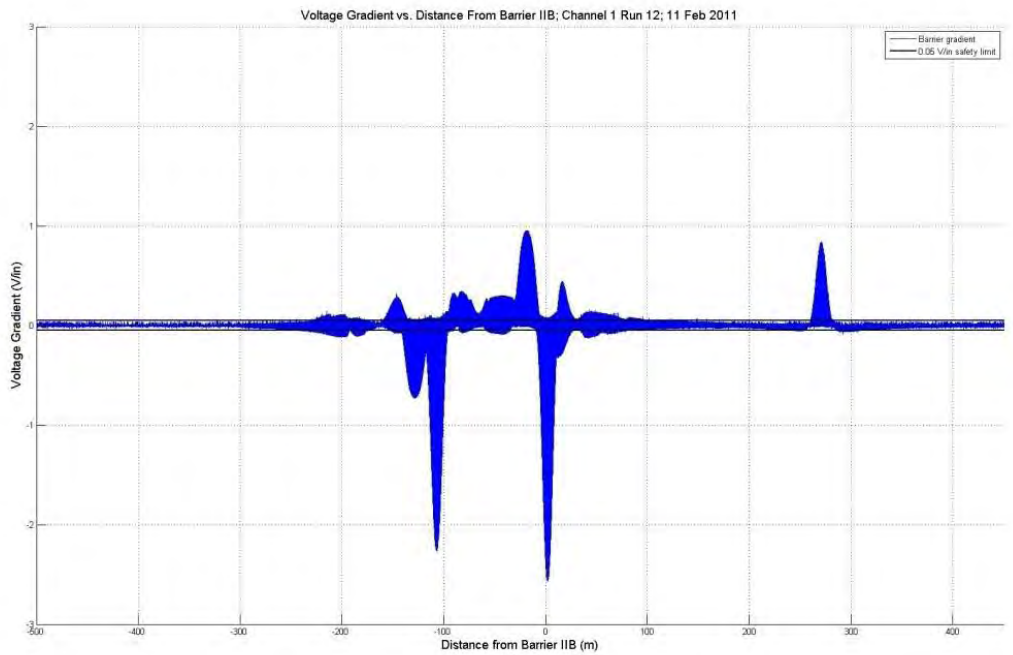


Figure C13. V12 for Run 12 on 11 February 2011 (Configuration B, On, Off, On, West Wall).



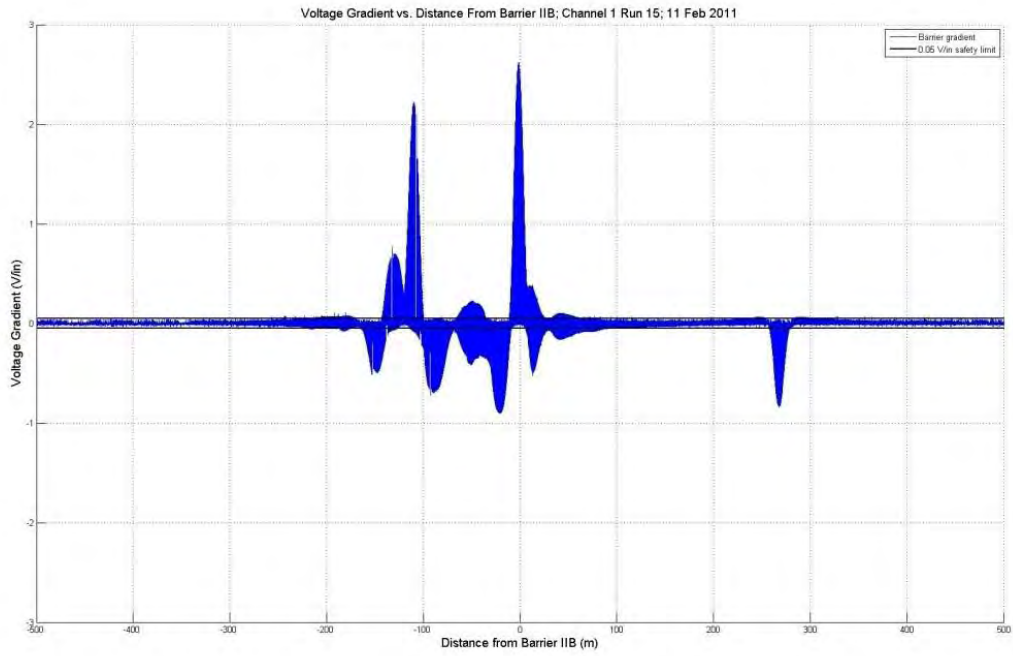


Figure C14. V12 for Run 15 on 11 February 2011 (Configuration B, On, On, On, East Wall).

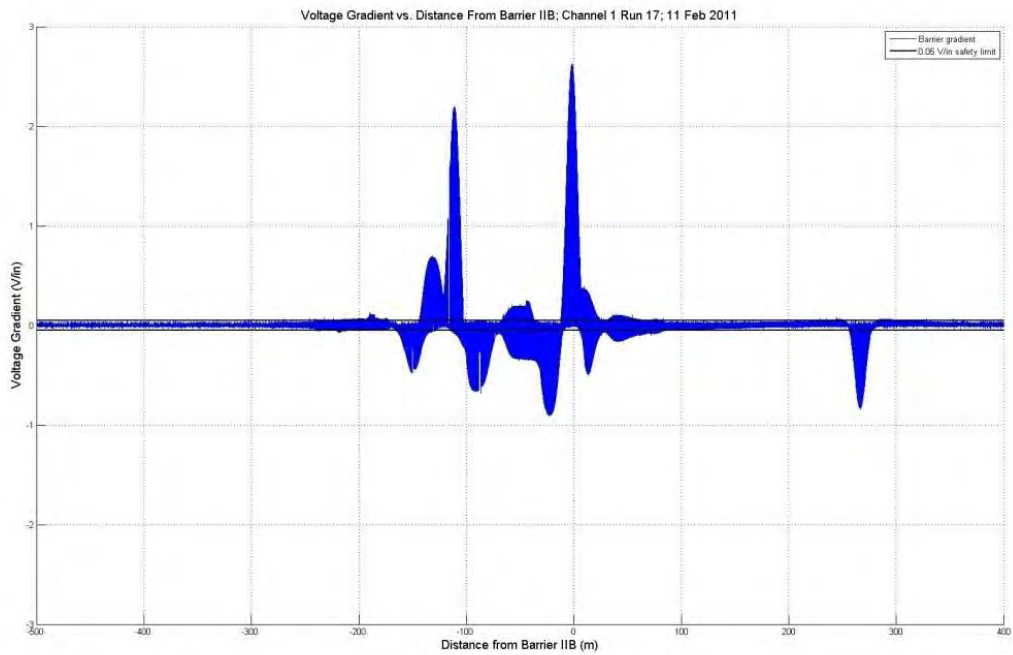


Figure C15. V12 for Run 17 on 11 February 2011 (Configuration B, On, On, On, East Wall).

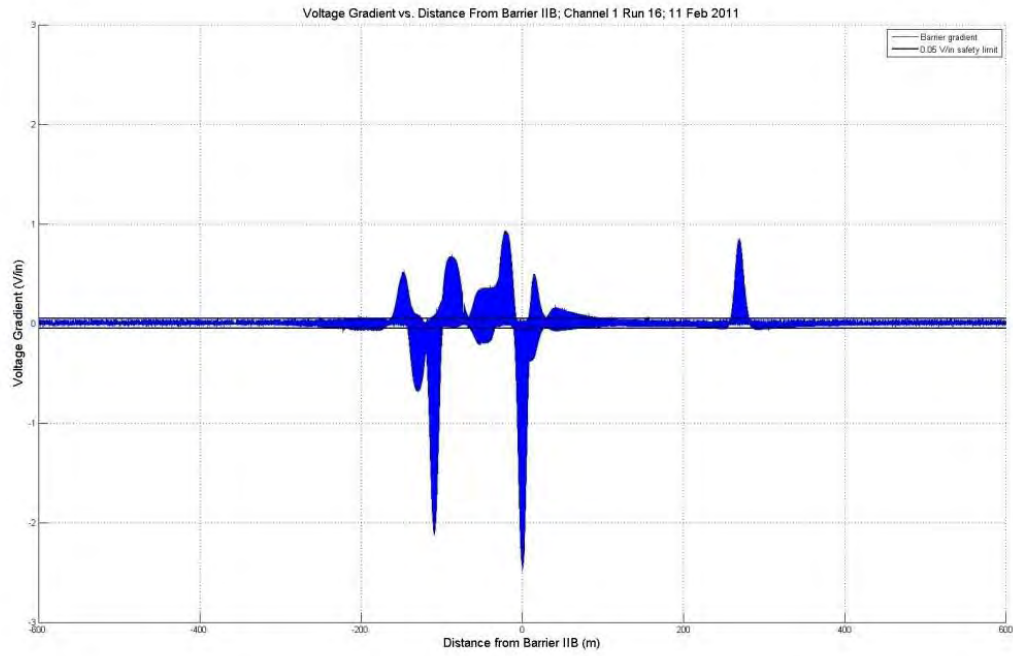


Figure C16. V12 for Run 16 on 11 February 2011 (Configuration B, On, On, On, Center).

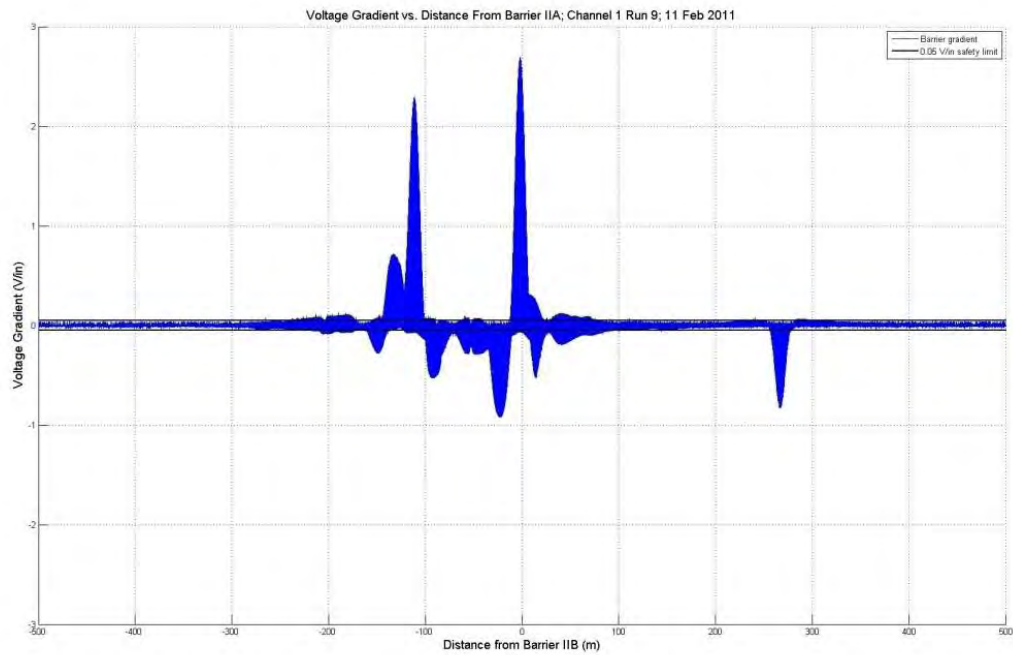


Figure C17. V12 for Run 19 on 11 February 2011 (Configuration B, On, On, On, Center).

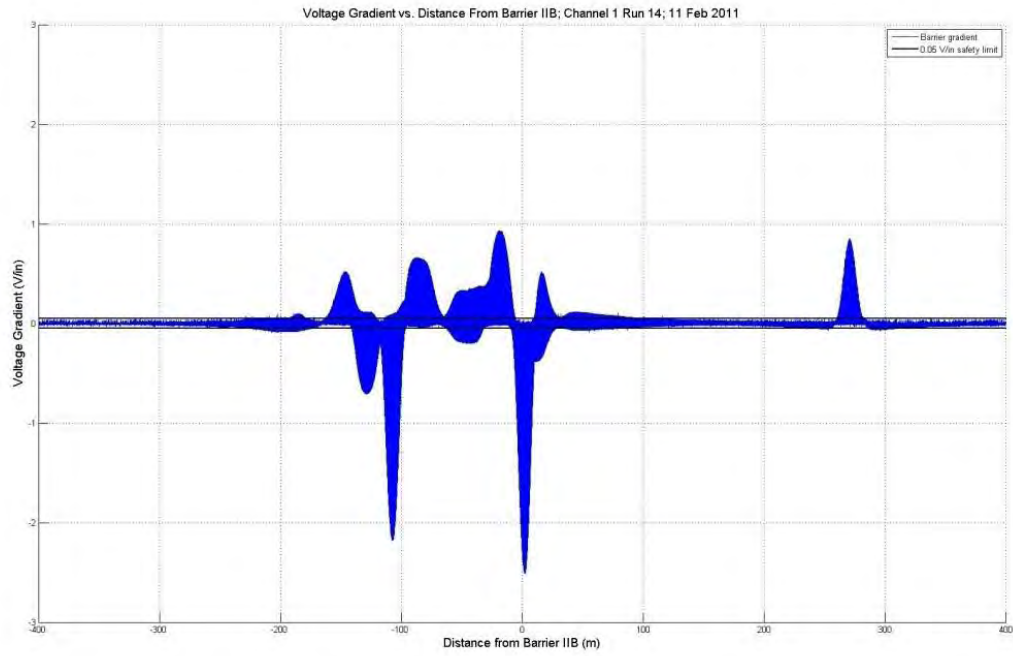


Figure C18. V12 for Run 14 on 11 February 2011 (Configuration B, On, On, On, West Wall).

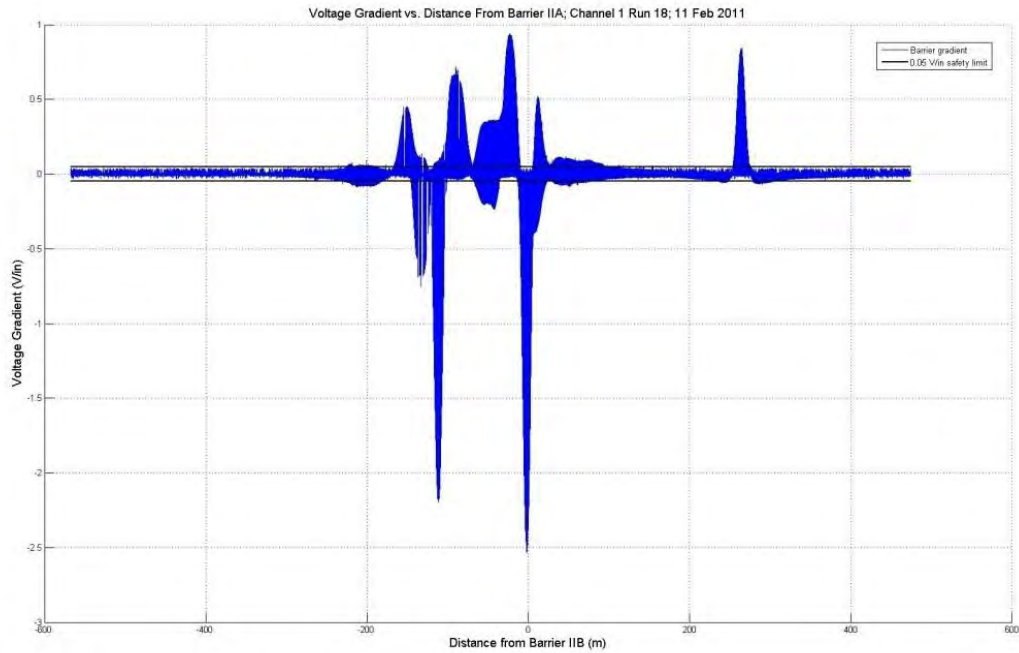


Figure C19. V12 for Run 18 on 11 February 2011 (Configuration B, On, On, On, West Wall).

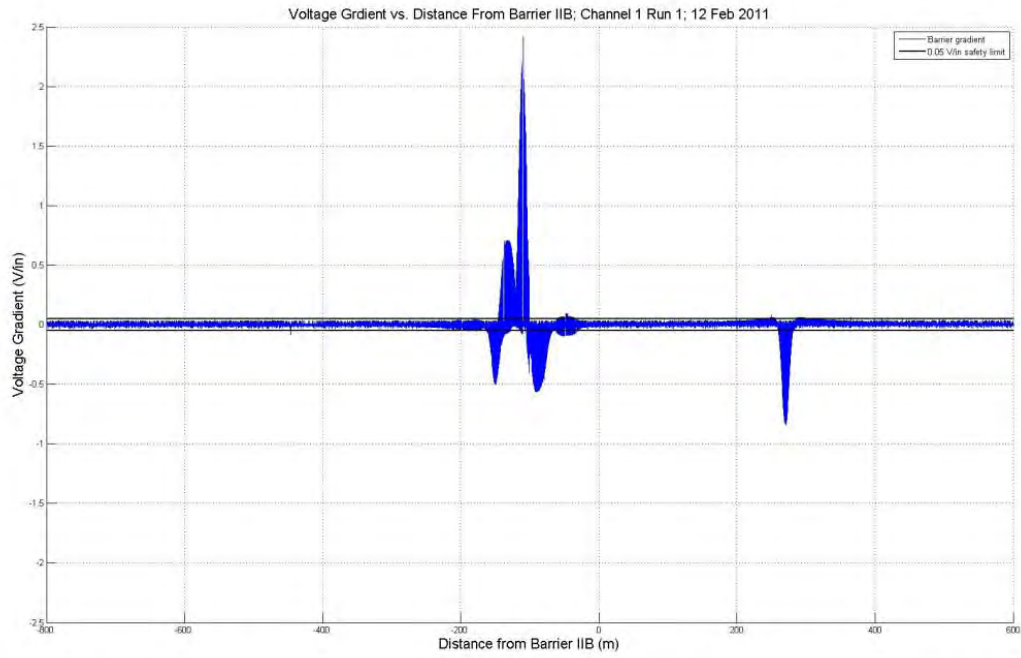


Figure C20. V12 for Run 1 on 12 February 2011. (Configuration D, On, On, Off, East Wall).

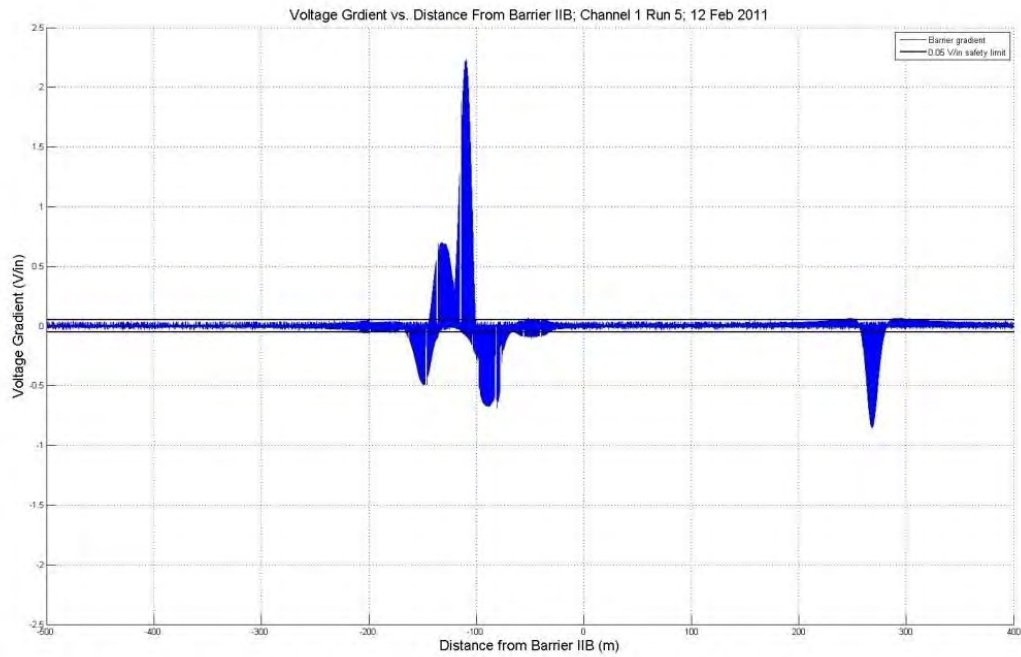


Figure C21. V12 for Run 5 on 12 February 2011 (Configuration D, On, On, Off, East Wall).

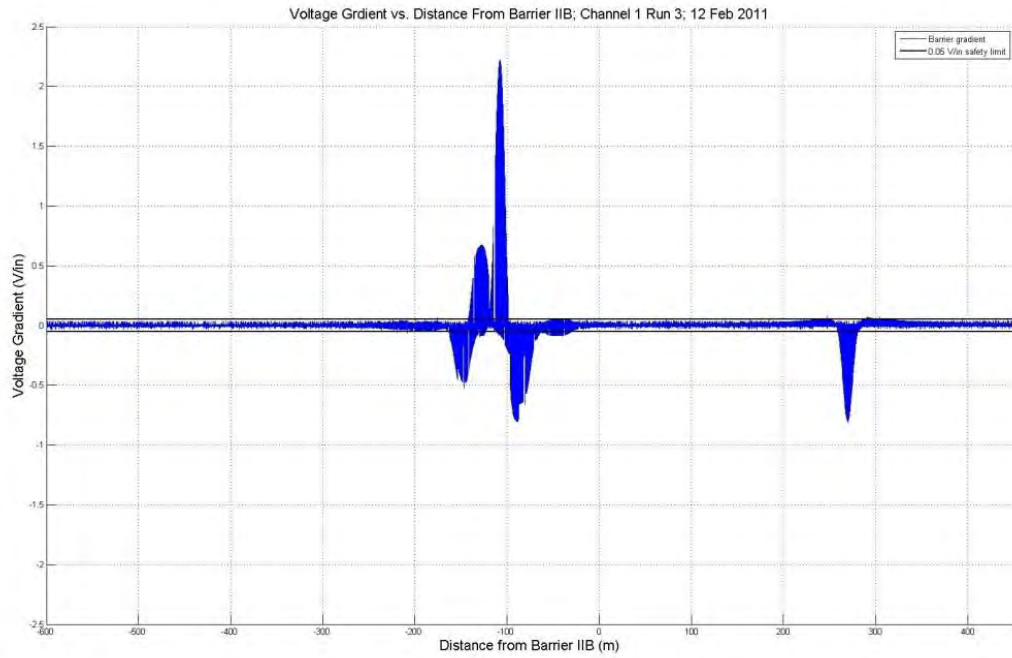


Figure C22. V12 for Run 3 on 12 February 2011 (Configuration D, On, On, Off, Center).

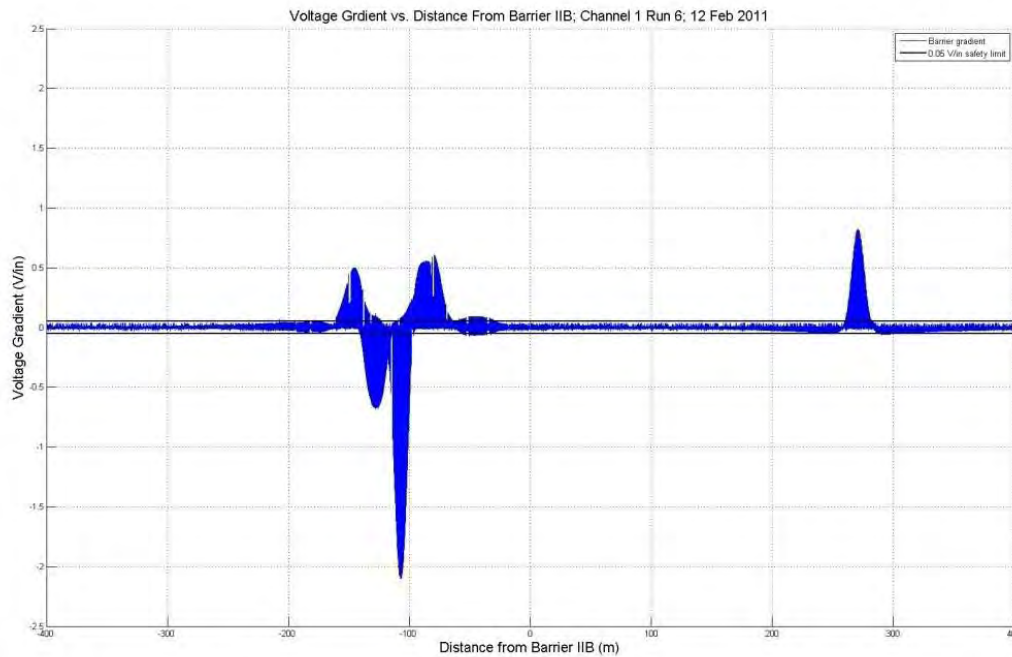


Figure C23. V12 for Run 6 on 12 February 2011 (Configuration D, On, On, Off, Center).



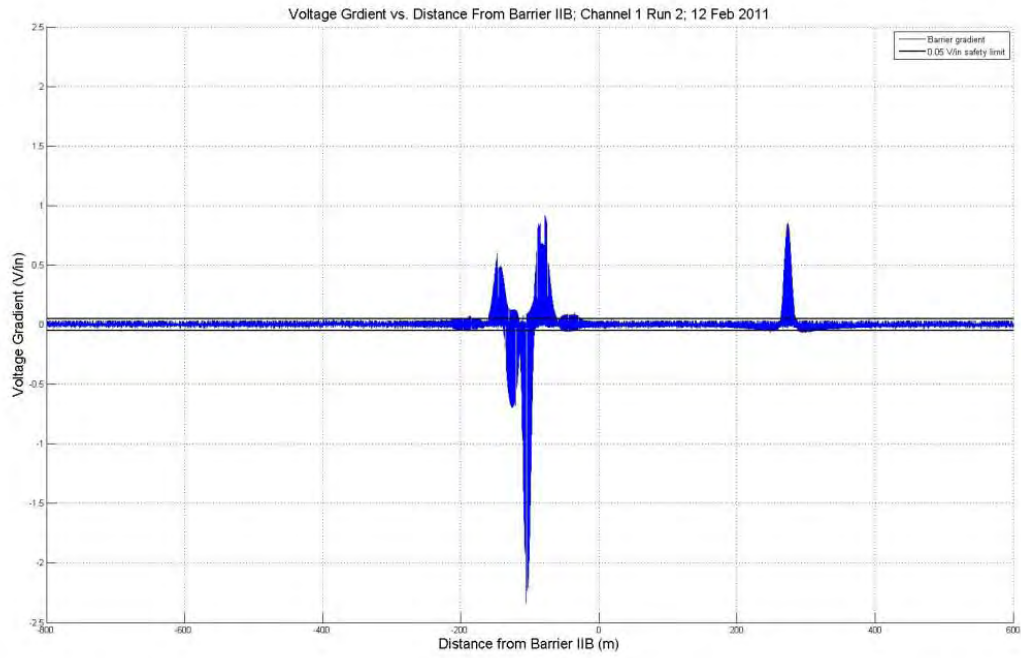


Figure C24. V12 for Run 2 on 12 February 2011 (Configuration D, On, On, Off, West Wall).



Figure C25. V12 for Run 4 on 11 February 2011 (Configuration D, On, On, Off, West Wall).

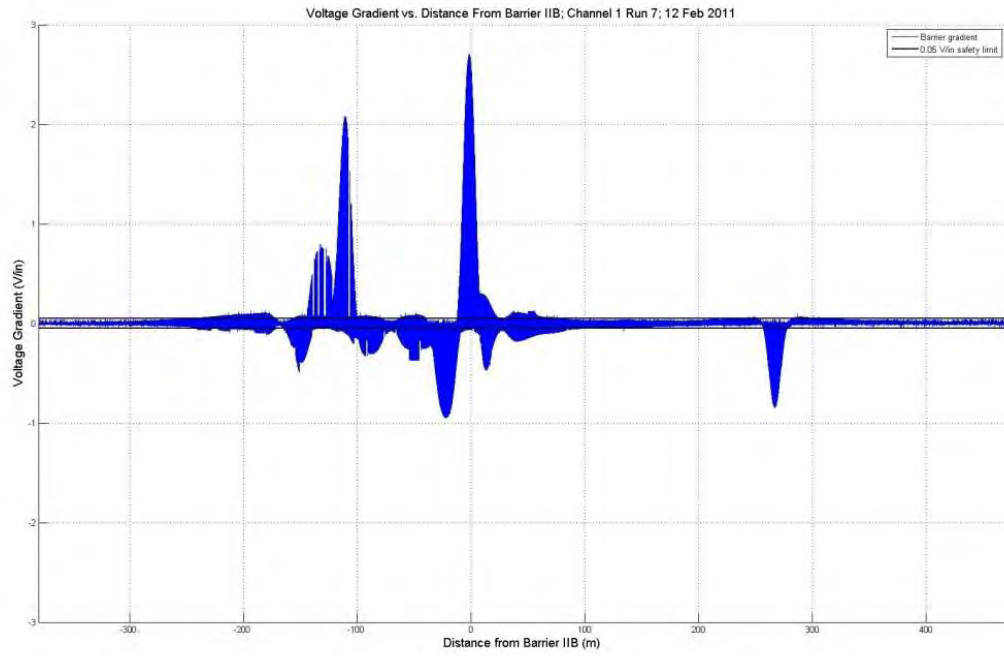


Figure C26. V12 for Run 7 on 12 February 2011 (Configuration A, On, Off, On, East Wall).

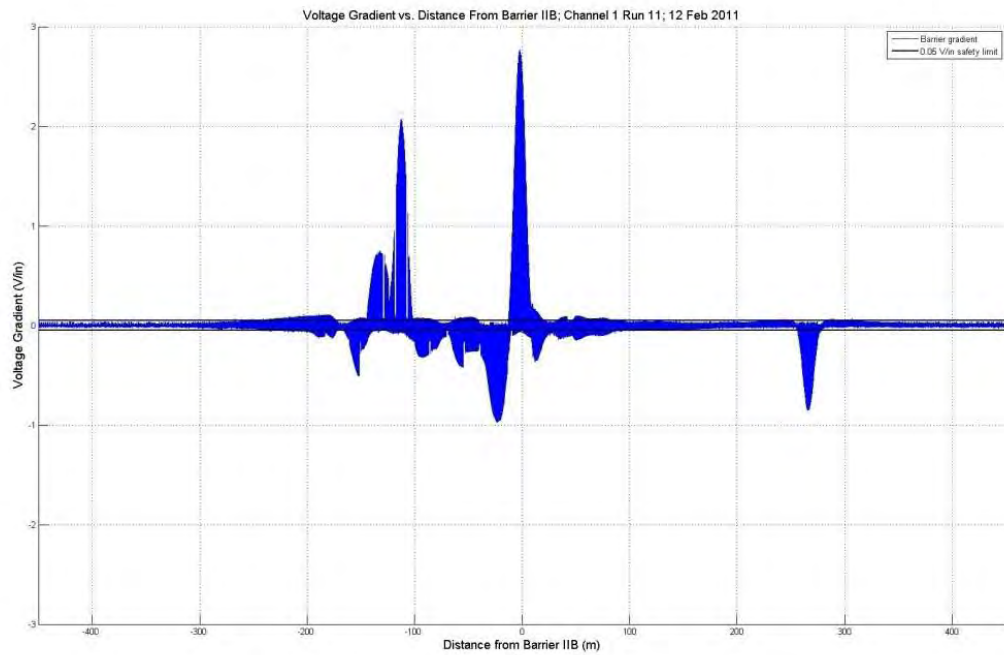


Figure C27. V12 for Run 11 on 12 February 2011 (Configuration A, On, Off, On, East Wall).

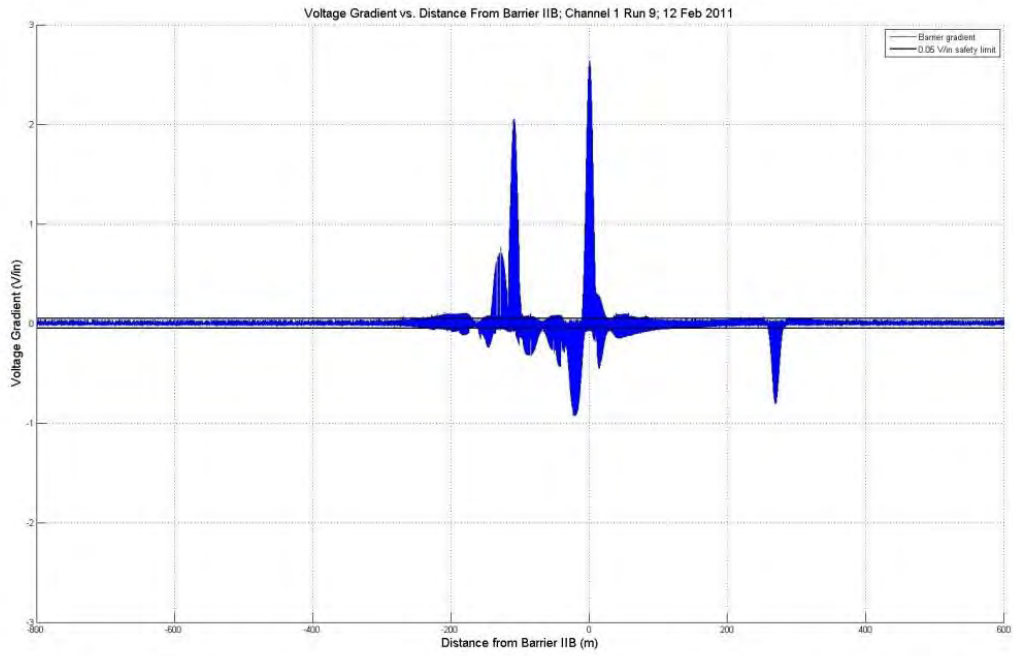


Figure C28. V12 for Run 9 on 12 February 2011 (Configuration A, On, Off, On, Center).

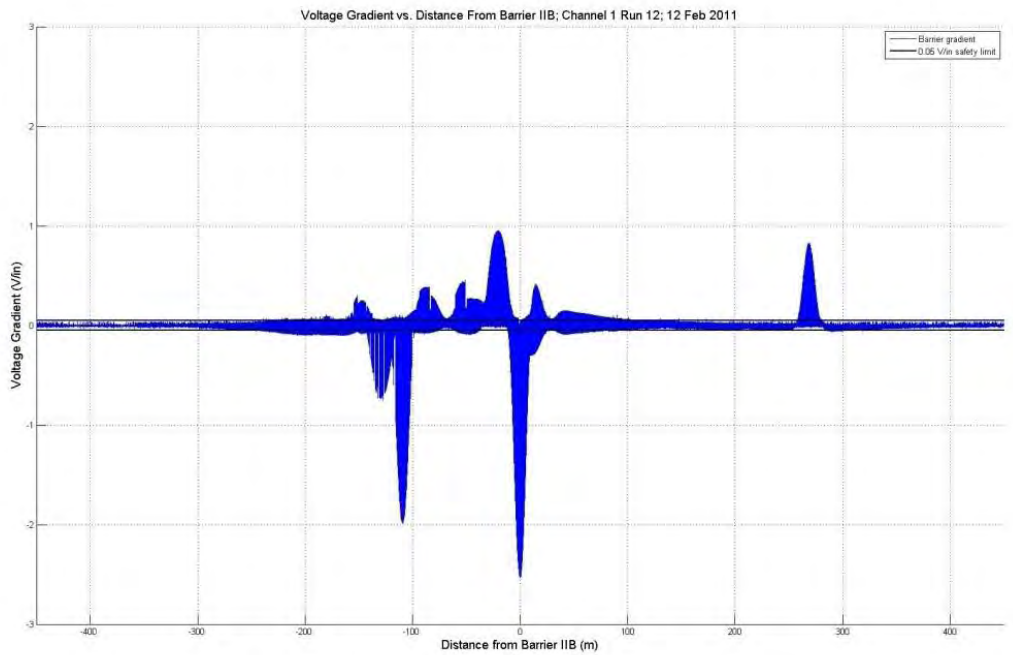


Figure C29. V12 for Run 12 on 12 February 2011 (Configuration A, On, Off, On, Center Wall).



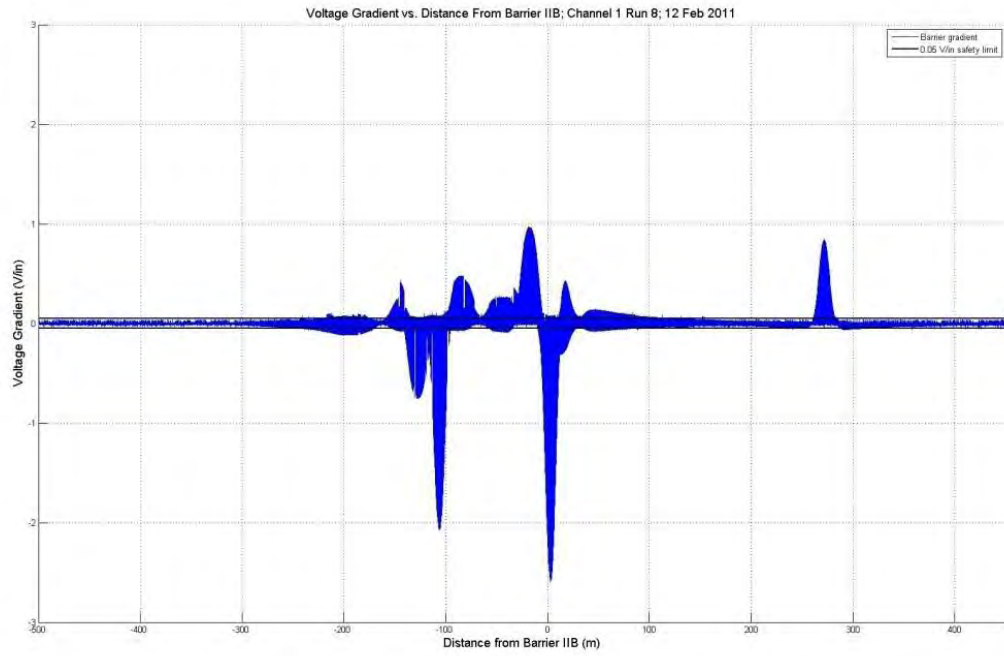


Figure C30. V12 for Run 8 on 12 February 2011 (Configuration A, On, Off, On, West Wall).

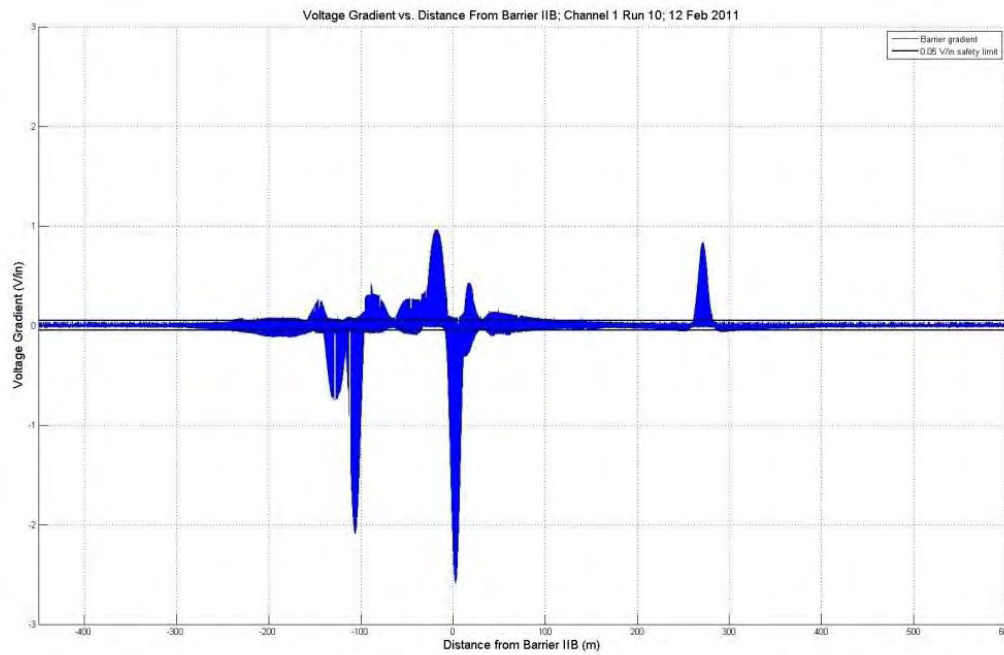


Figure C31. V12 for Run 10 on 12 February 2011 (Configuration A, On, Off, On, West Wall).

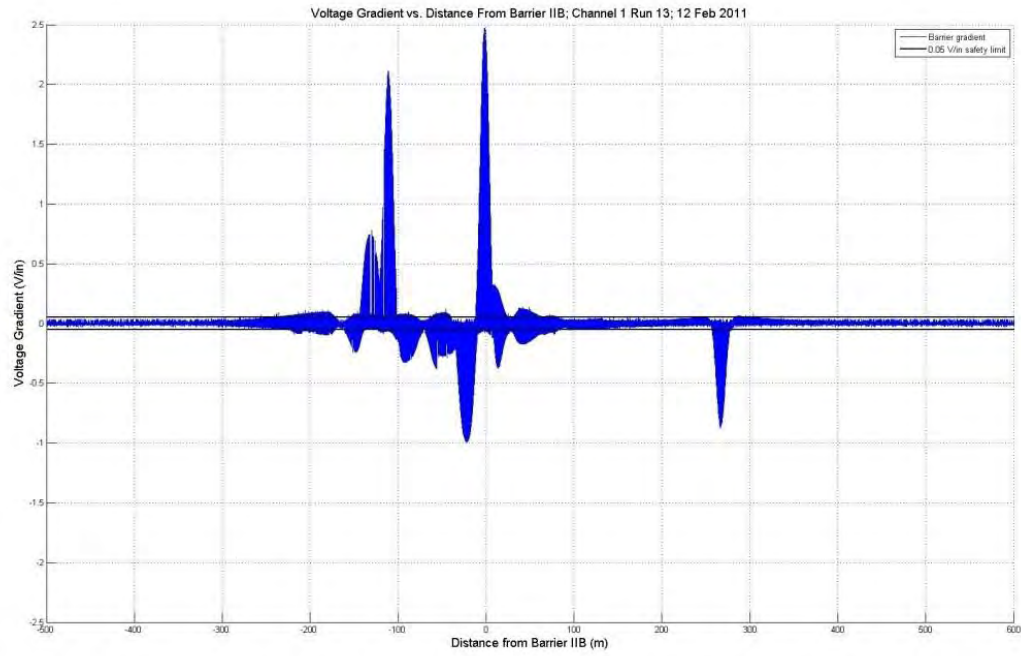


Figure C32. V12 for Run 13 on 12 February 2011 (Configuration C, On, Off, On, East Wall).

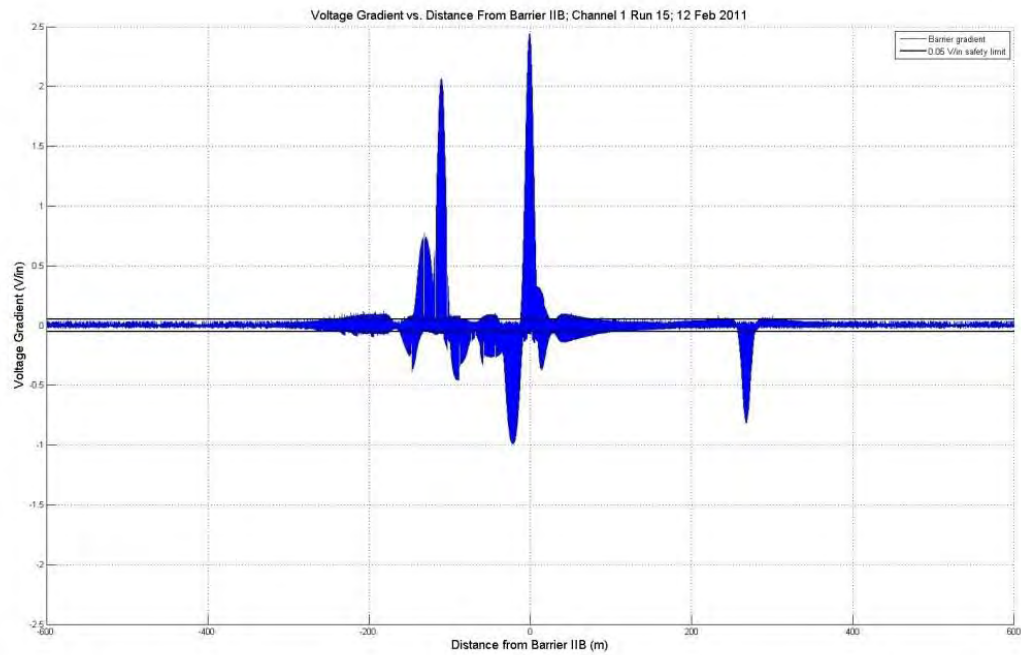


Figure C33. V12 for Run 15 on 12 February 2011 (Configuration C, On, Off, On, Center Wall).

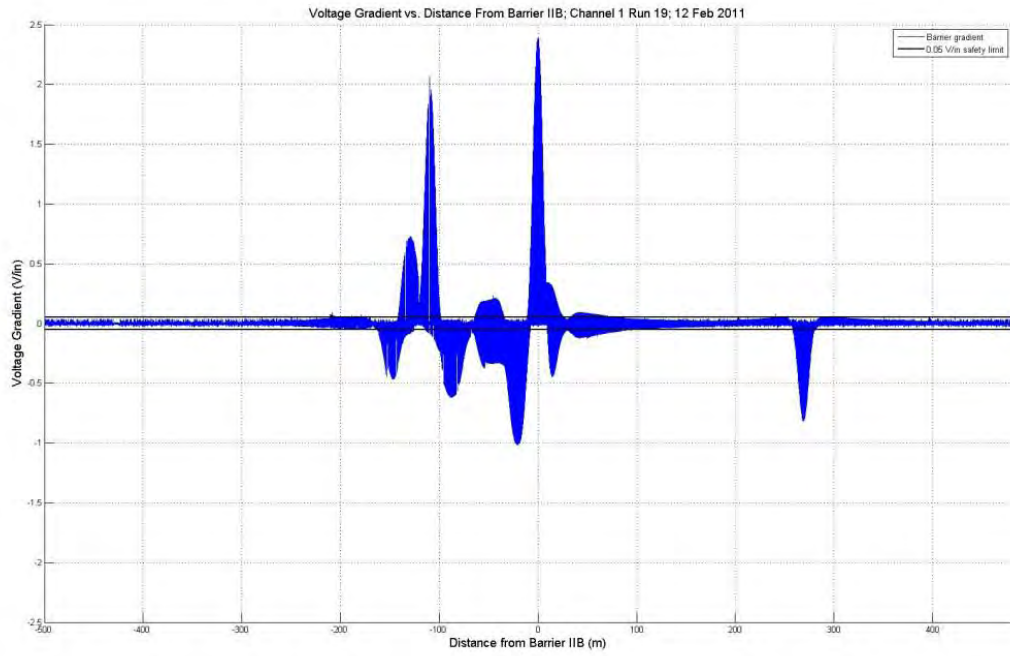


Figure C34. V12 for Run 19 on 12 February 2011 (Configuration C, On, Off, On, Center Wall).

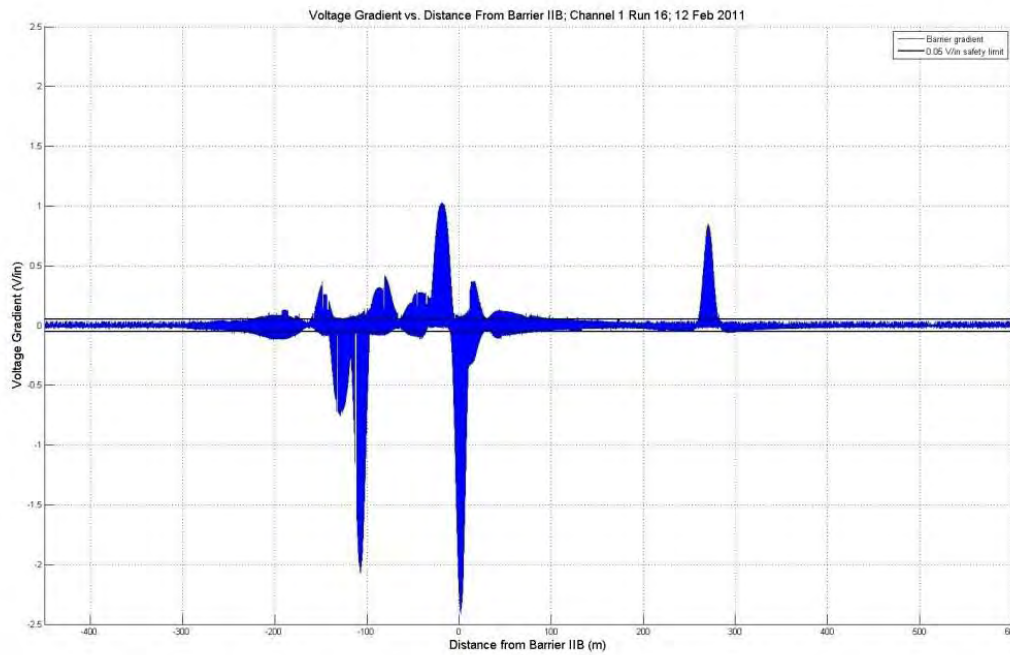


Figure C35. V12 for Run 16 on 12 February 2011 (Configuration C, On, Off, On, West Wall).

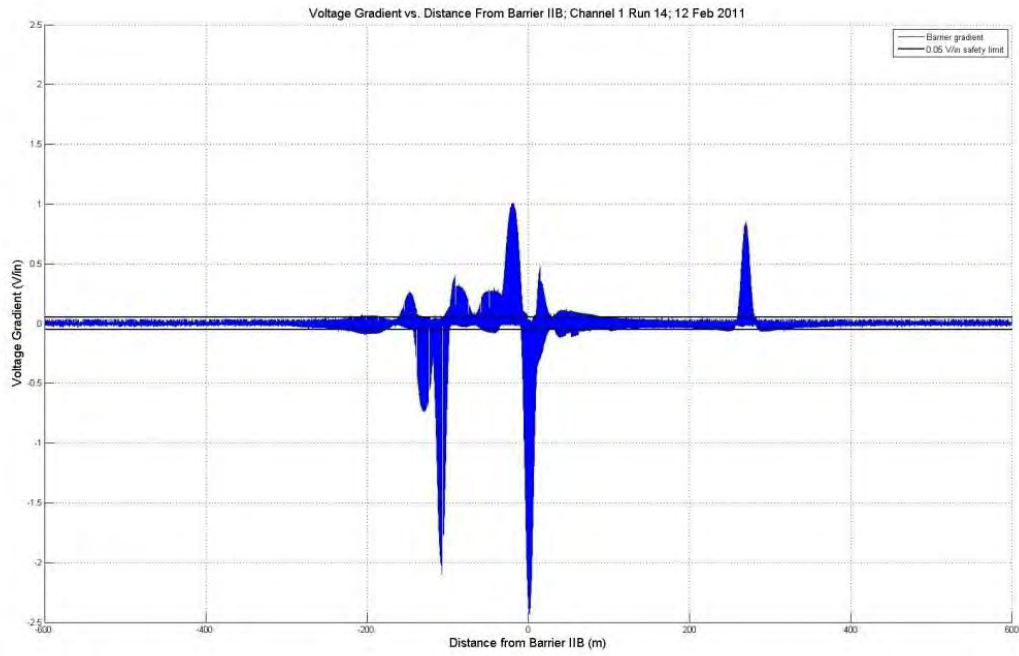


Figure C36. V12 for Run 14 on 12 February 2011 (Configuration C, On, Off, On, West Wall).

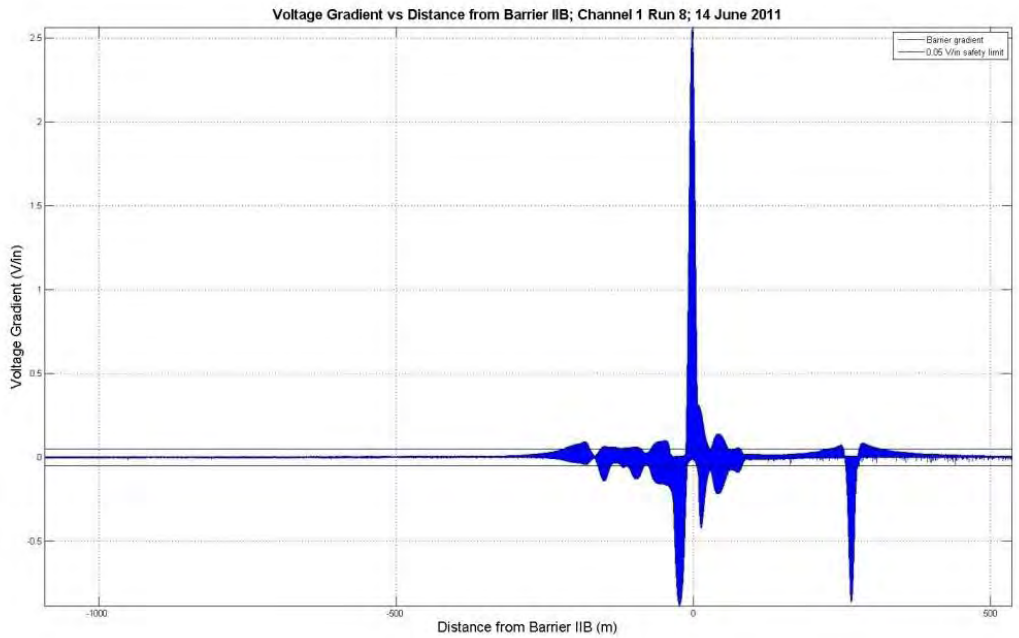


Figure C37. V12 for Run 8 on 14 June 2011 (Configuration E, On Off, On, East Wall).

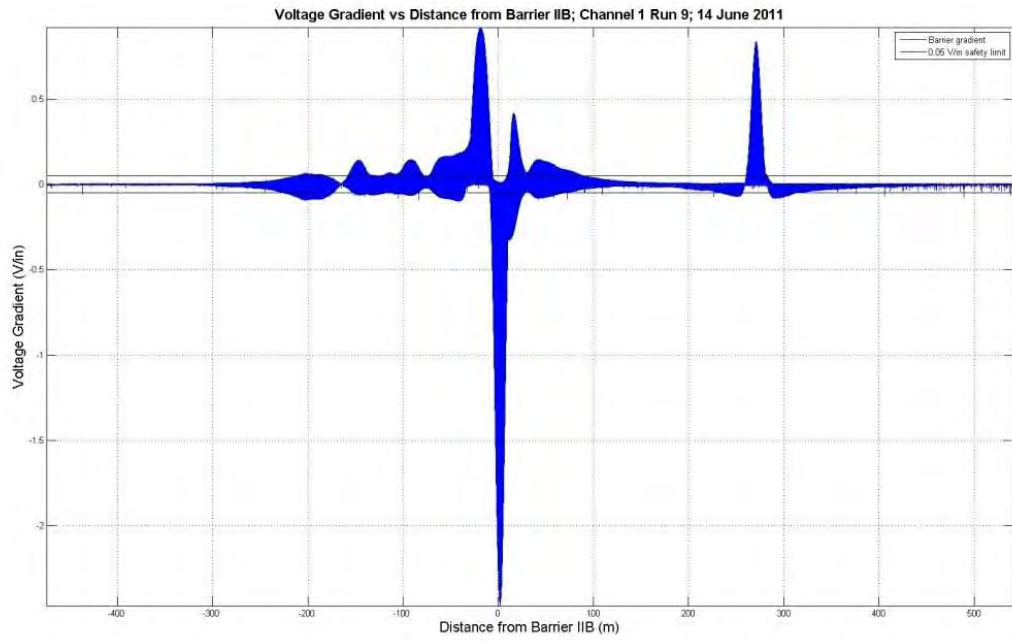


Figure C38. V12 for Run 9 on 14 June 2011 (Configuration E, On Off, On, East Wall).

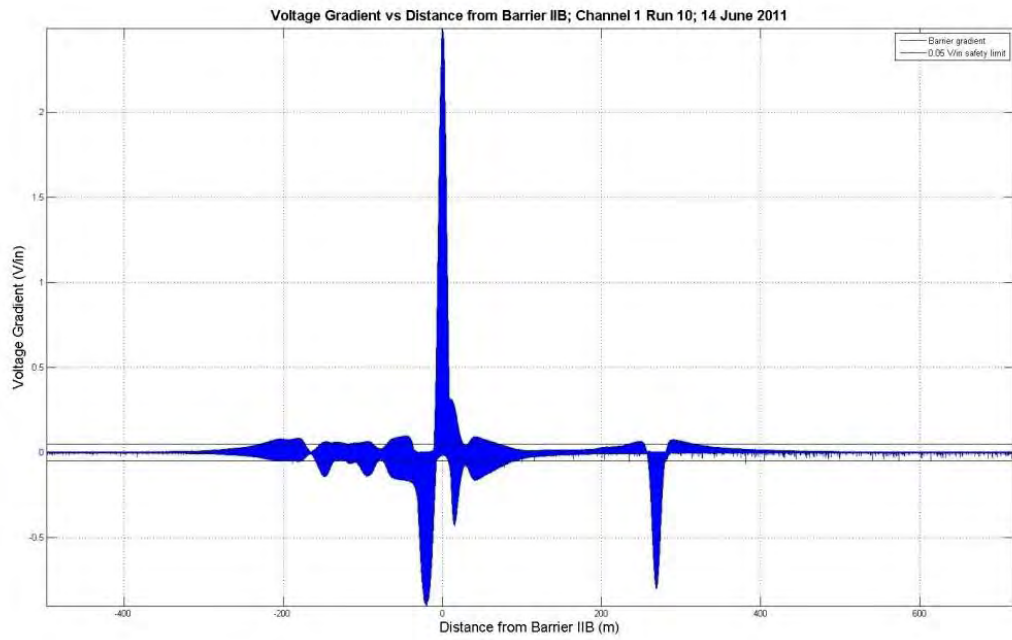


Figure C39. V12 for Run 10 on 14 June 2011 (Configuration E, On Off, On, West Wall).



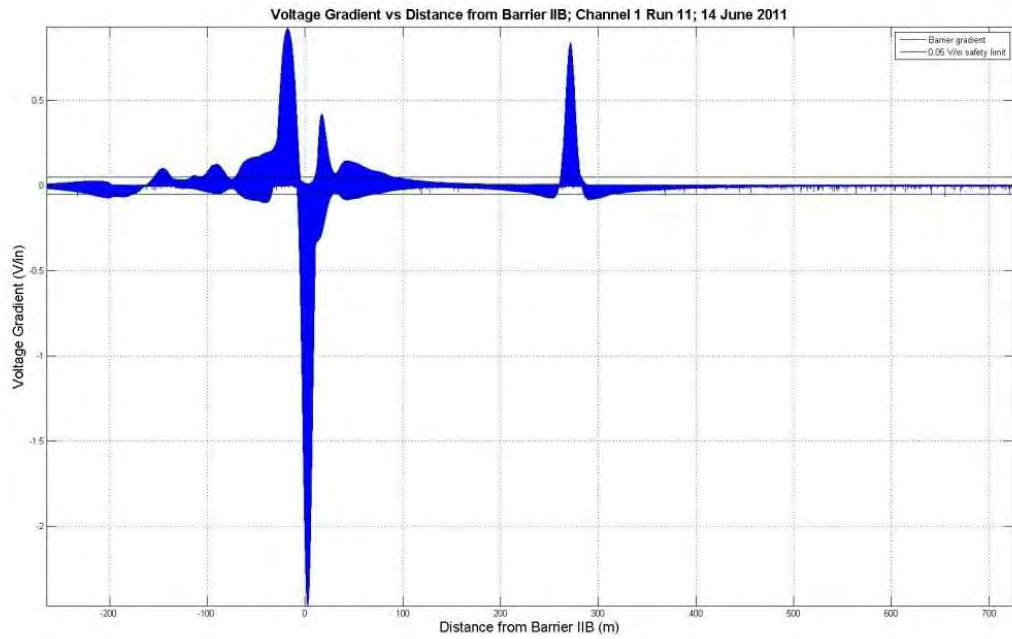


Figure C40. V12 for Run 11 on 14 June 2011 (Configuration E, On Off, On, Center).

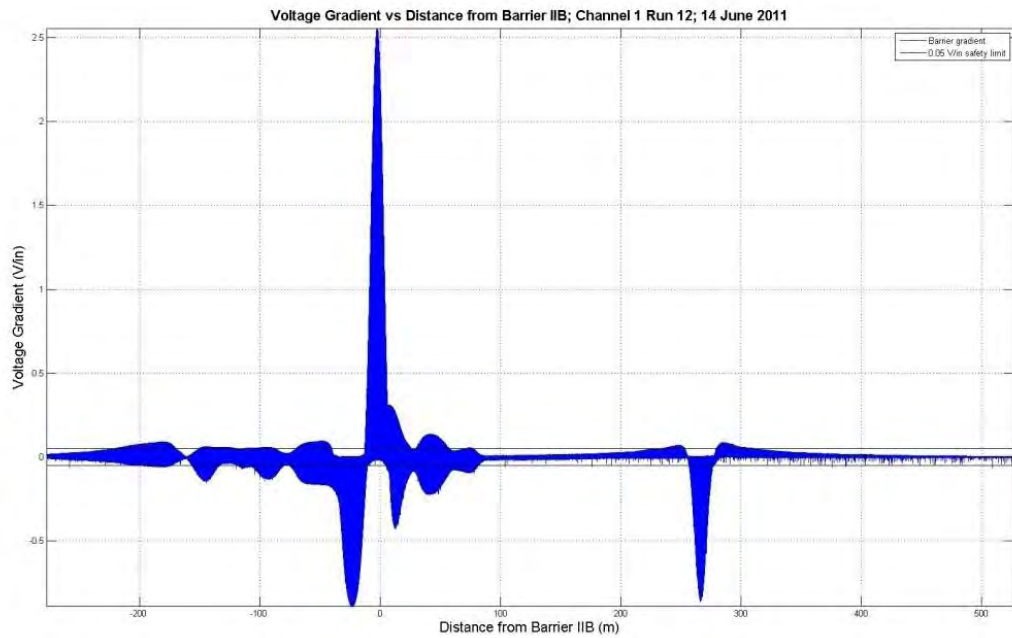


Figure C41. V12 for Run 12 on 14 June 2011 (Configuration E, On Off, On, East Wall).

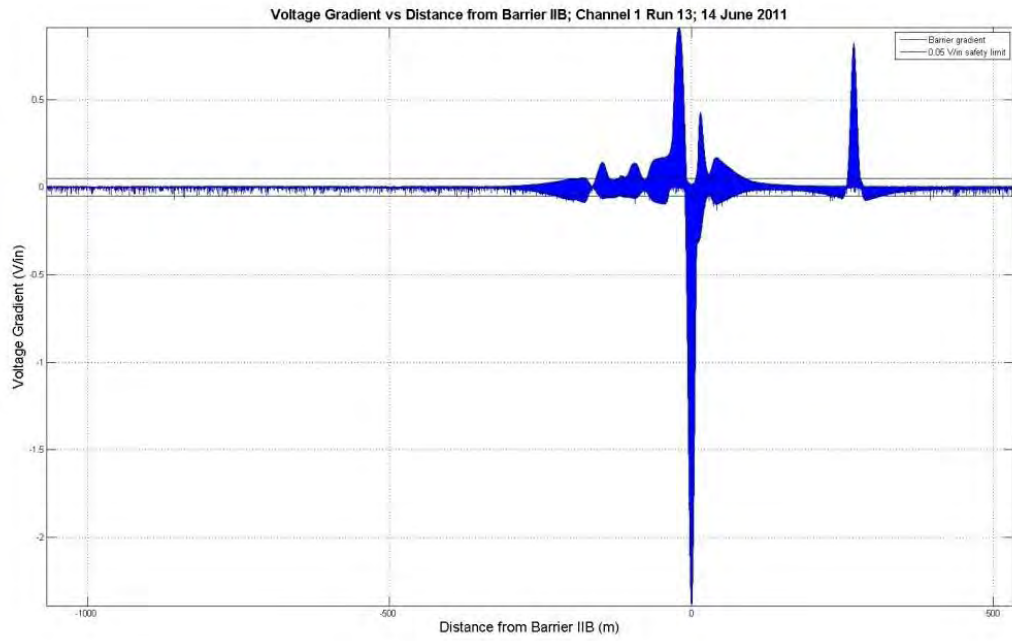


Figure C42. V12 for Run 13 on 14 June 2011 (Configuration E, On Off, On, Center).

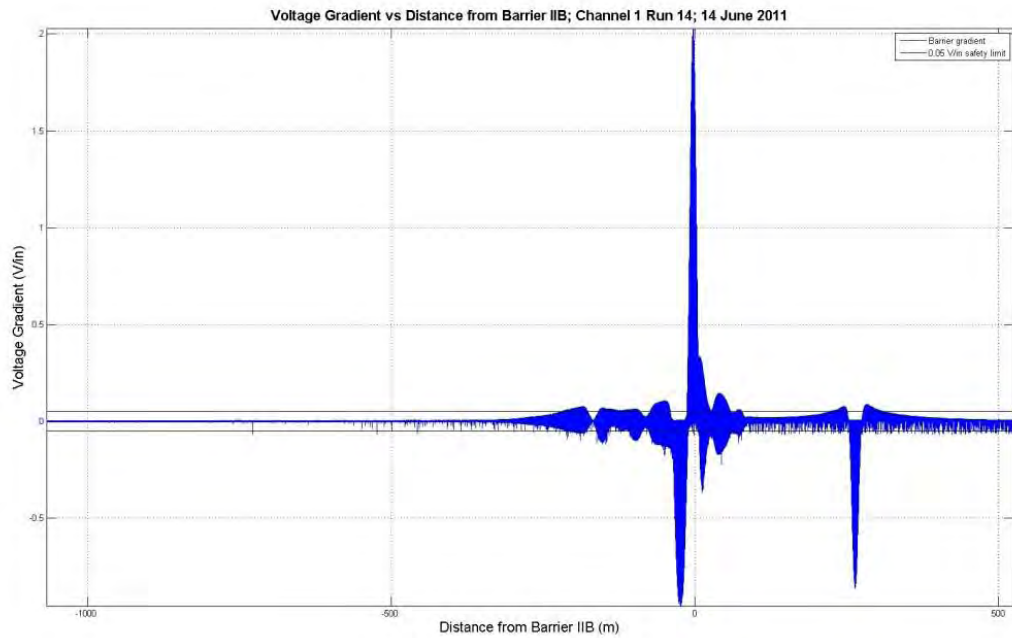


Figure C43. V12 for Run 14 on 14 June 2011 (Configuration F, On Off, On, East Wall).

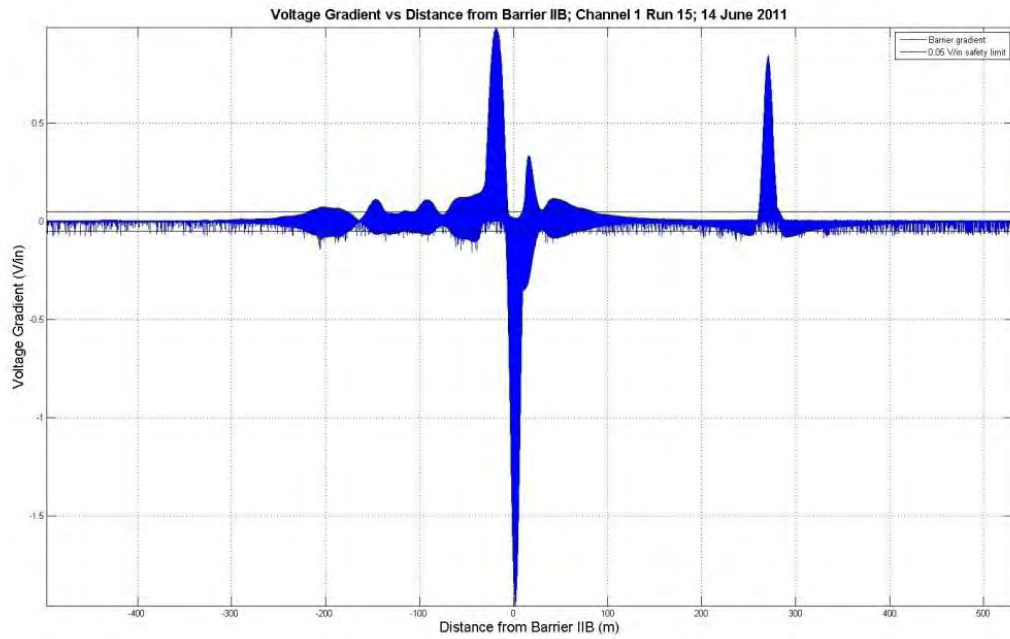


Figure C44. V12 for Run 15 on 14 June 2011 (Configuration F, On Off, On, West Wall).



Figure C45. V12 for Run 17 on 14 June 2011 (Configuration F, On Off, On, West Wall).



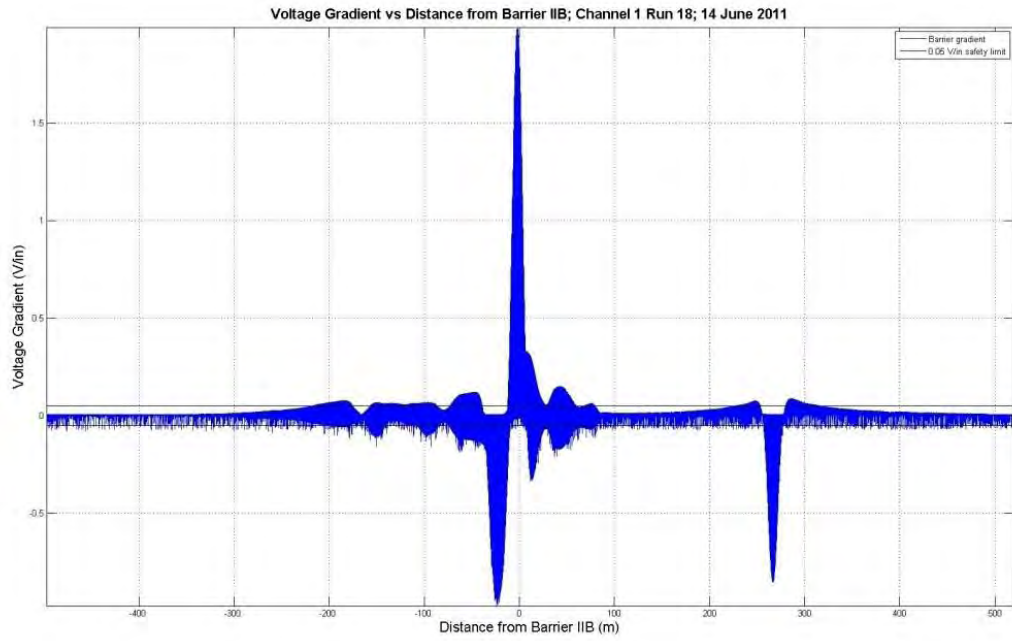


Figure C46. V12 for Run 18 on 14 June 2011 (Configuration F, On Off, On, East Wall).

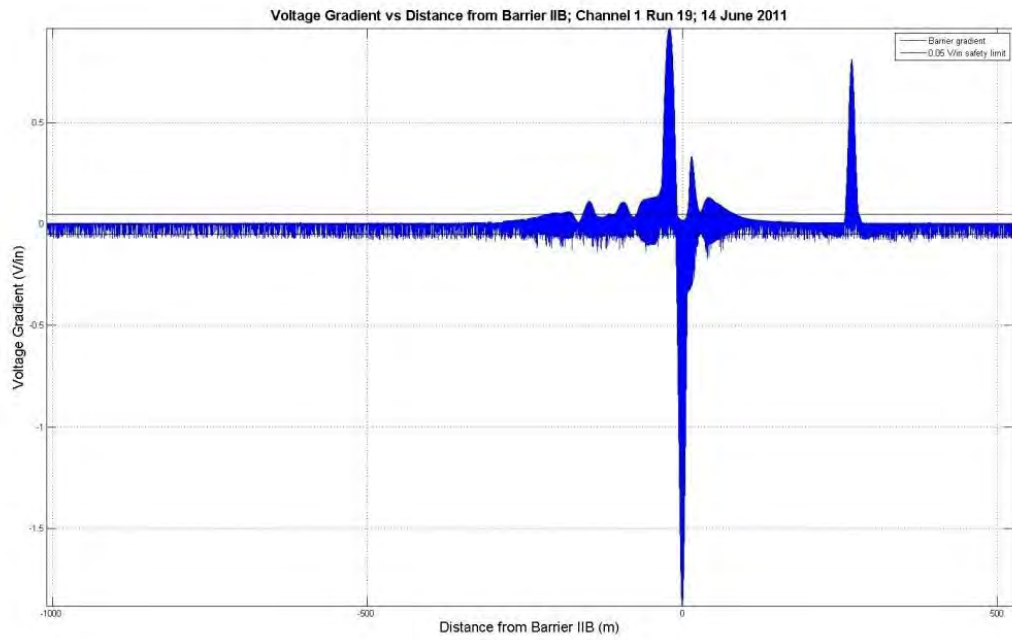


Figure C47. V12 for Run 19 on 14 June 2011 (Configuration F, On Off, On, Center).

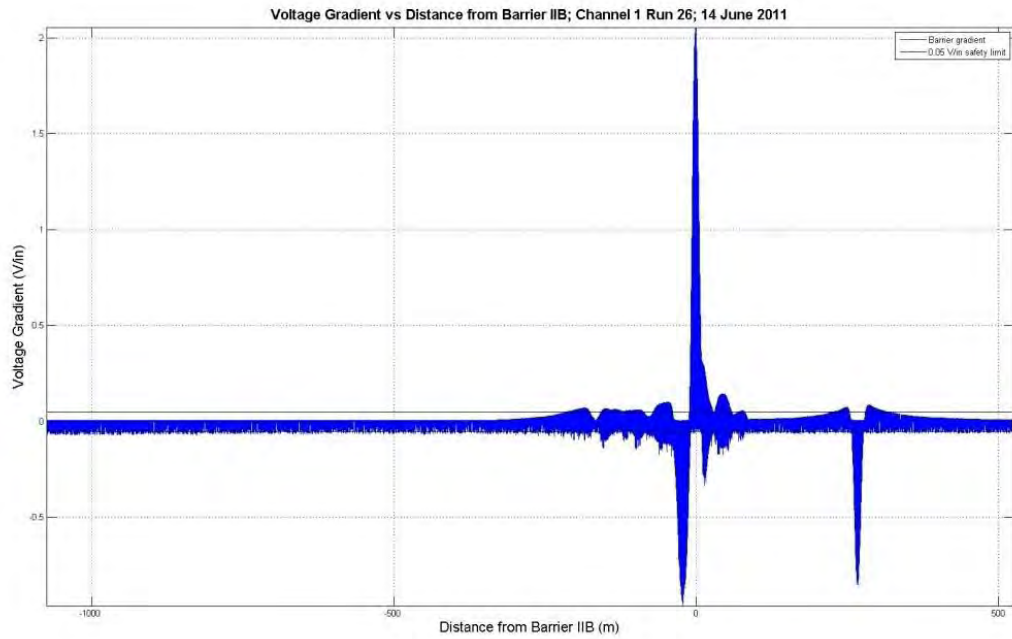


Figure C48. V12 for Run 26 on 14 June 2011 (Configuration F, On Off, On, East Wall).

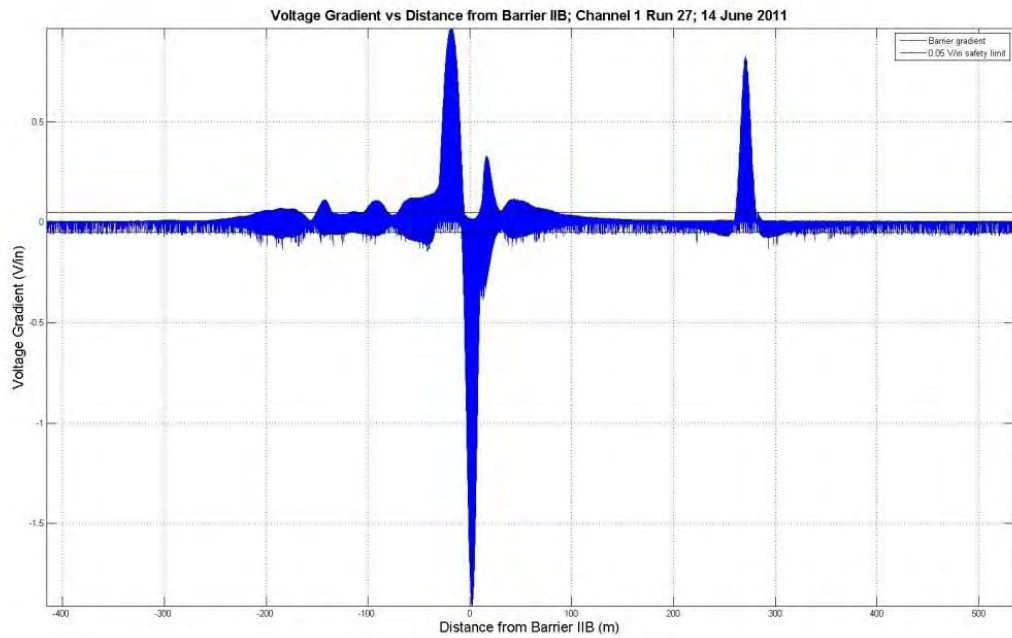


Figure C49. V12 for Run 27 on 14 June 2011 (Configuration F, On Off, On, West Wall).

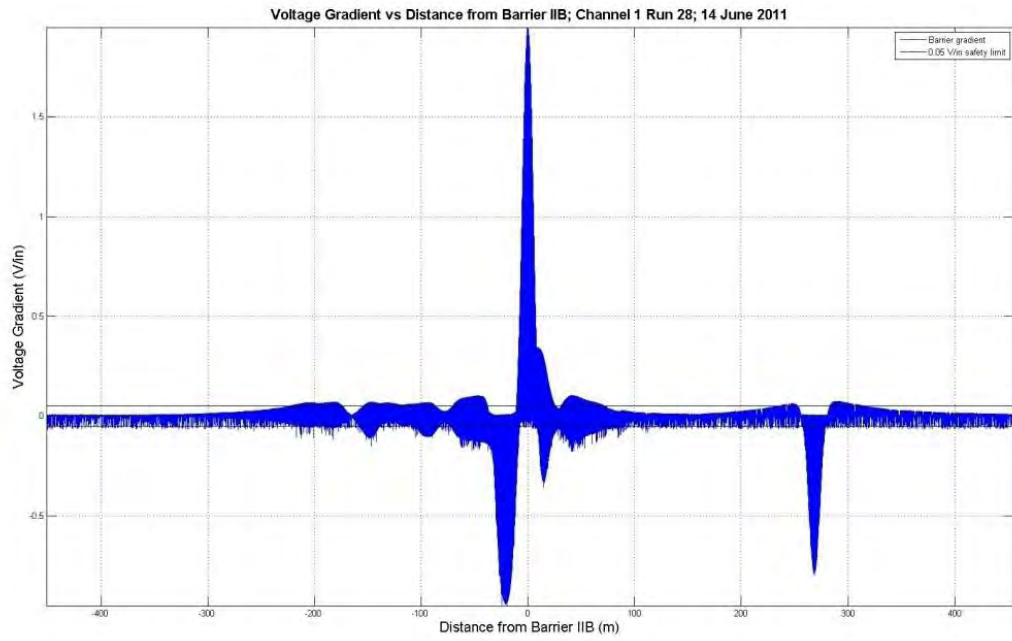


Figure C50. V12 for Run 28 on 14 June 2011 (Configuration F, On Off, On, Center).

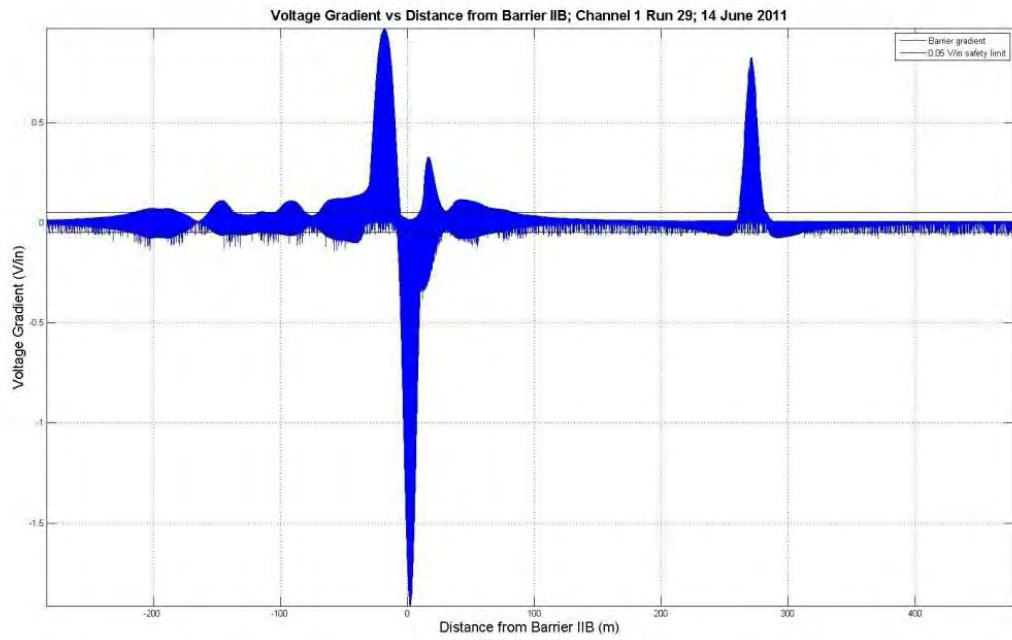


Figure C51. V12 for Run 29 on 14 June 2011 (Configuration F, On Off, On, West Wall).

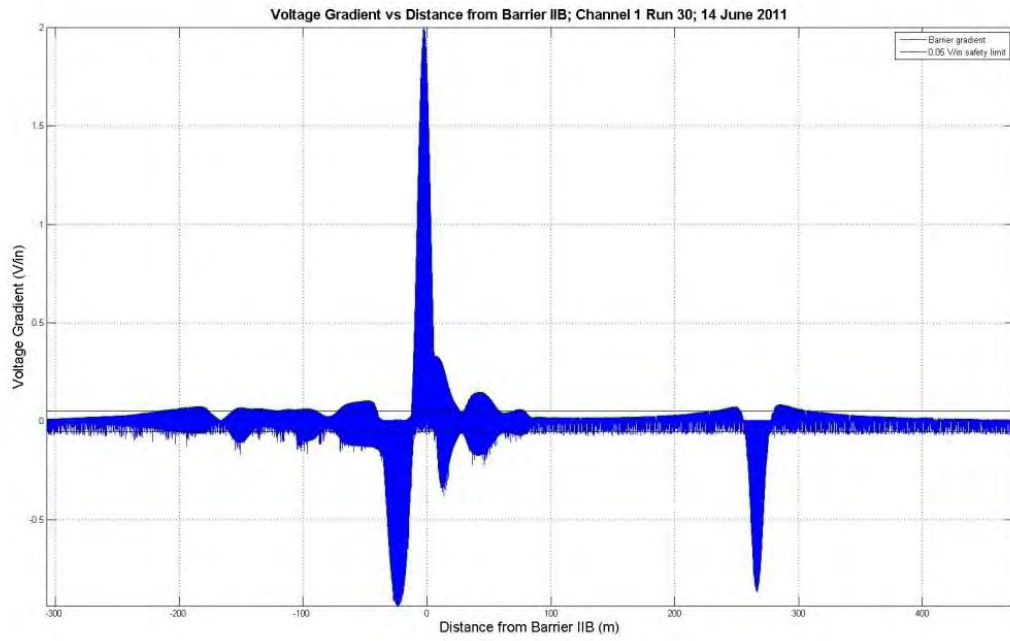


Figure C52. V12 for Run 30 on 14 June 2011 (Configuration F, On Off, On, East Wall).

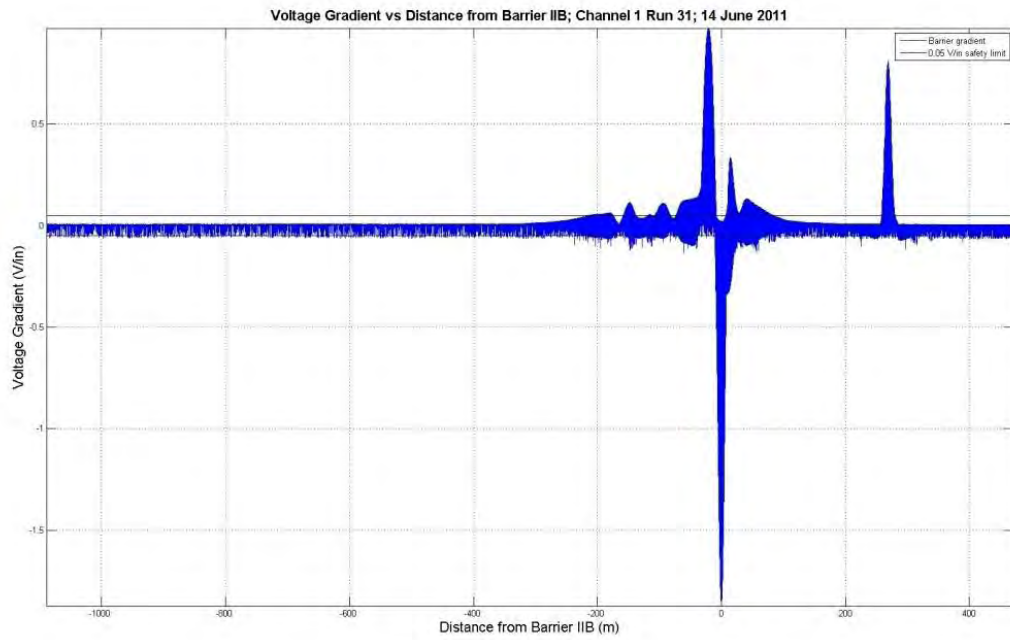


Figure C53. V12 for Run 31 on 14 June 2011 (Configuration F, On Off, On, Center).



## **Appendix D: V12 Electric Field Maps**

This appendix contains maps of the electric field testing results for V12 (channel 1), conducted on 11 and 12 February and 14 June 2011. In these figures, the electric field strength is represented by a progressive color scale and is superimposed on a georeferenced map of the canal with key landmarks included. See Figure 2 in the body of the main report for the location of measurement V12. See Chapter 4, Table 2 in the body of the main report for details of the pulser and parasitic configurations for this data.

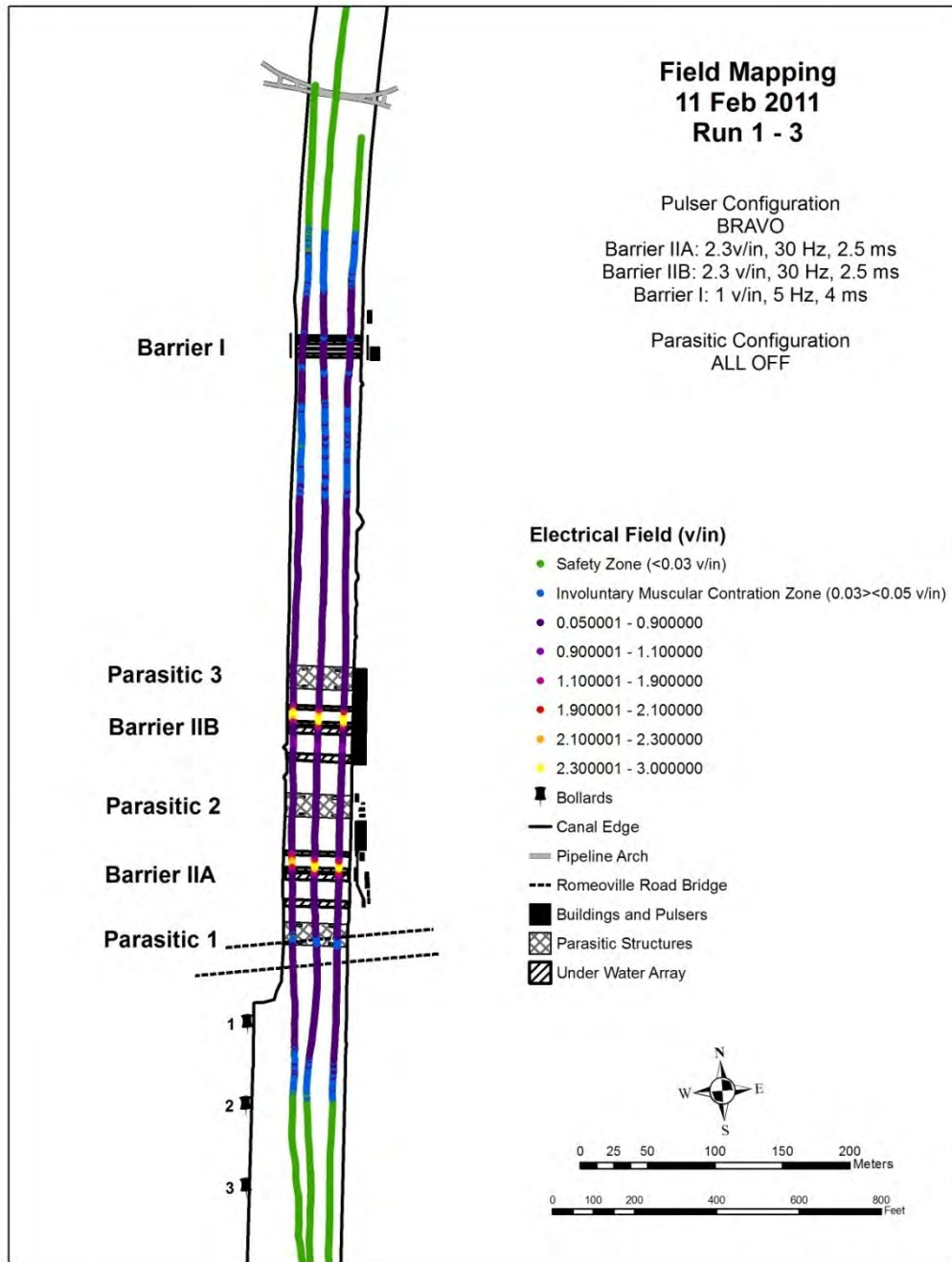


Figure D1. V12 for Runs 1 – 3 on 11 February 2011 (Configuration B, Off, Off, Off).

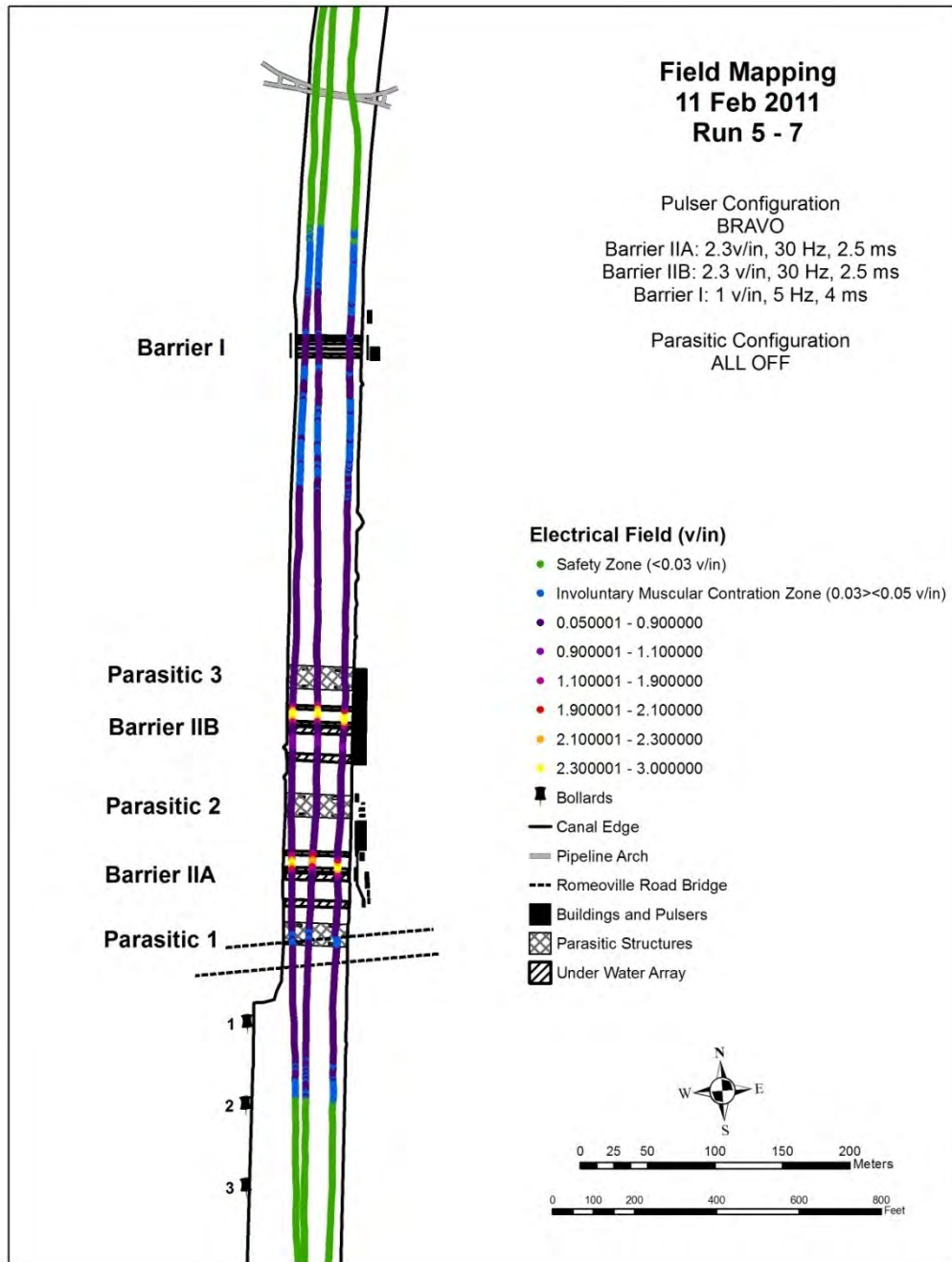


Figure D2. V12 for Runs 5 – 7 on 11 February 2011 (Configuration B, Off, Off, Off).



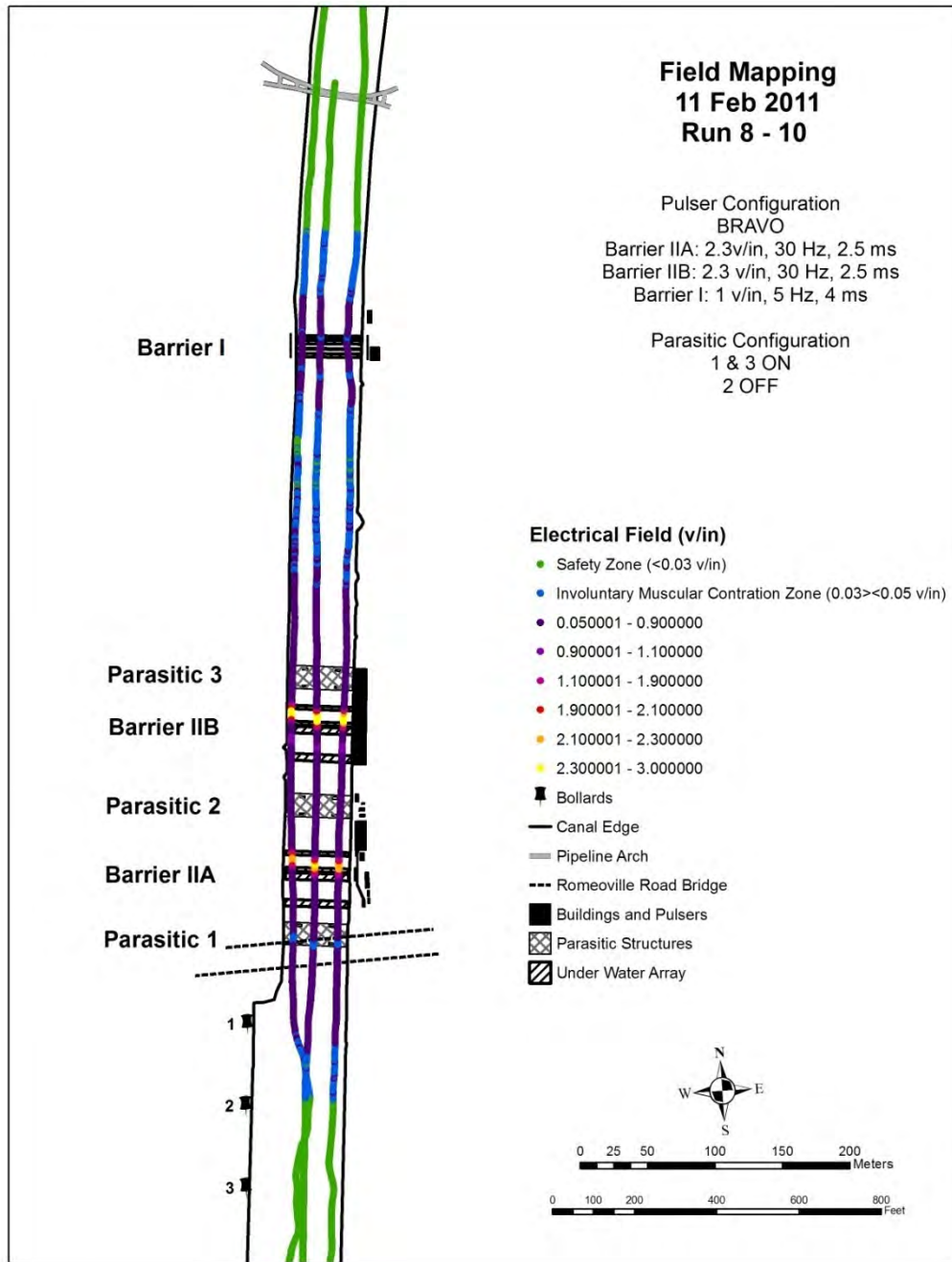


Figure D3. V12 for Runs 8 - 10 on 11 February 2011 (Configuration B, On, Off, On).

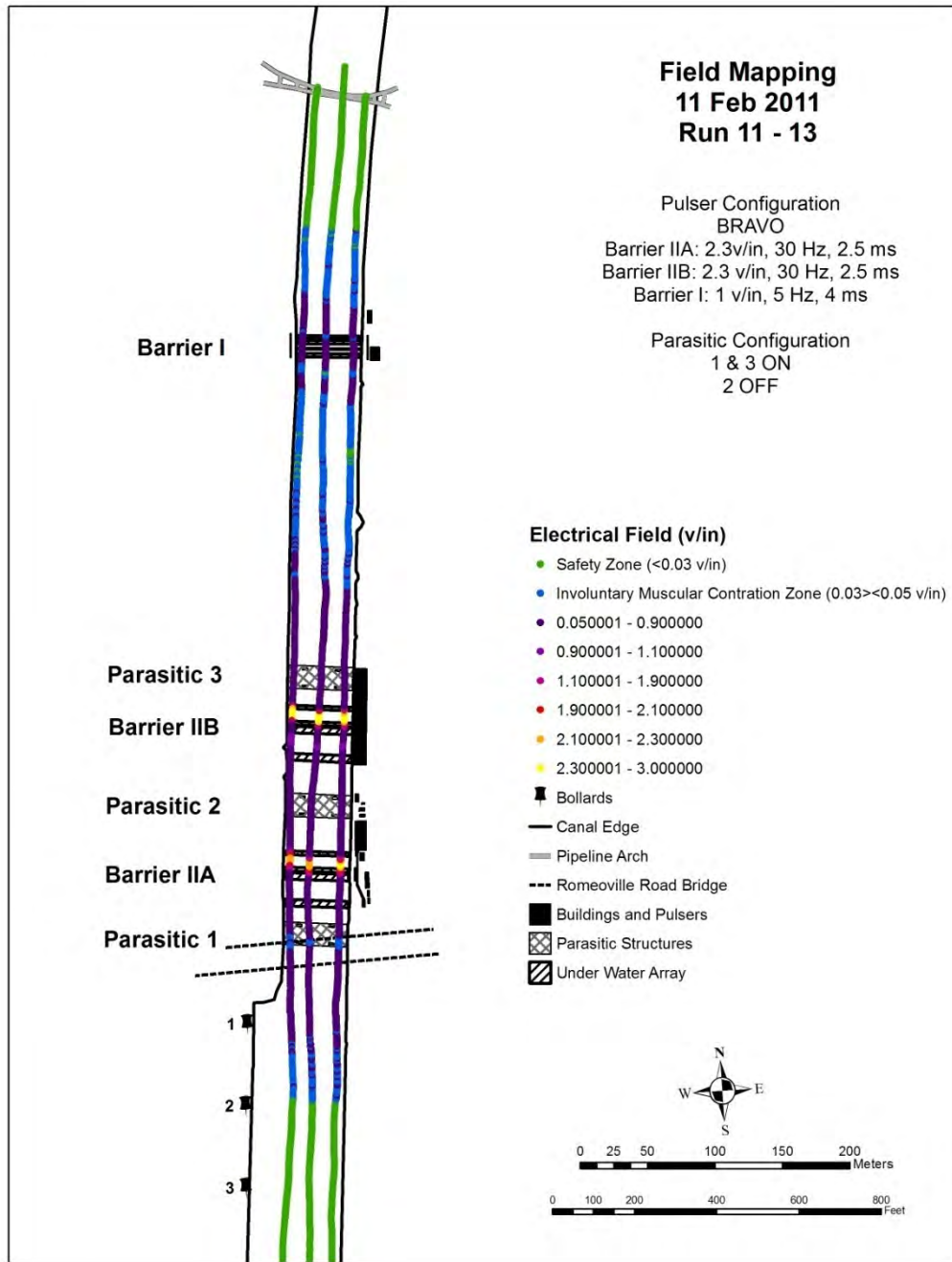


Figure D4. V12 for Runs 11 – 13 on 11 February 2011 (Configuration B, On, Off, On).

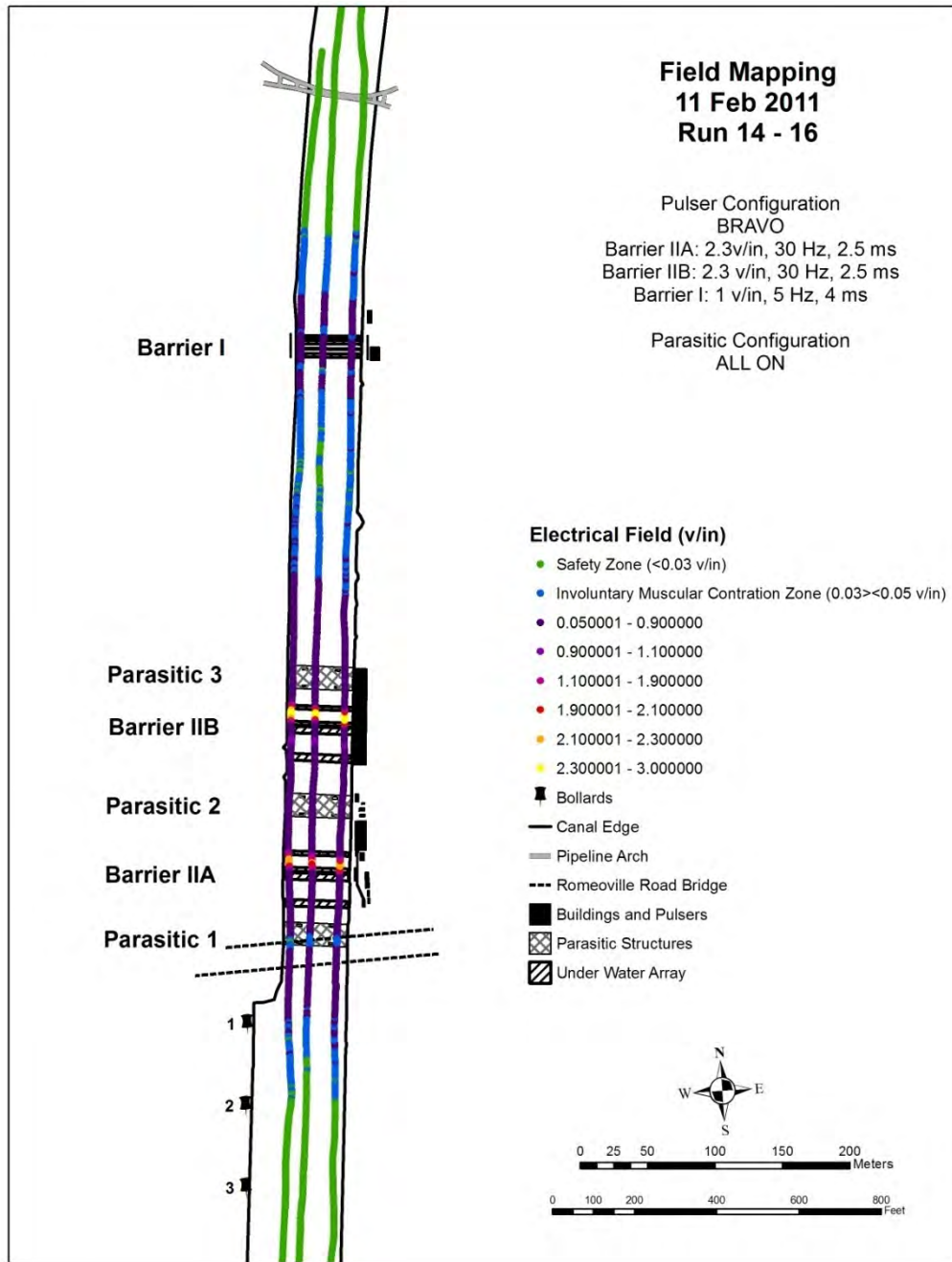


Figure D5. V12 for Runs 14 – 16 on 11 February 2011 (Configuration B, On, On, On).

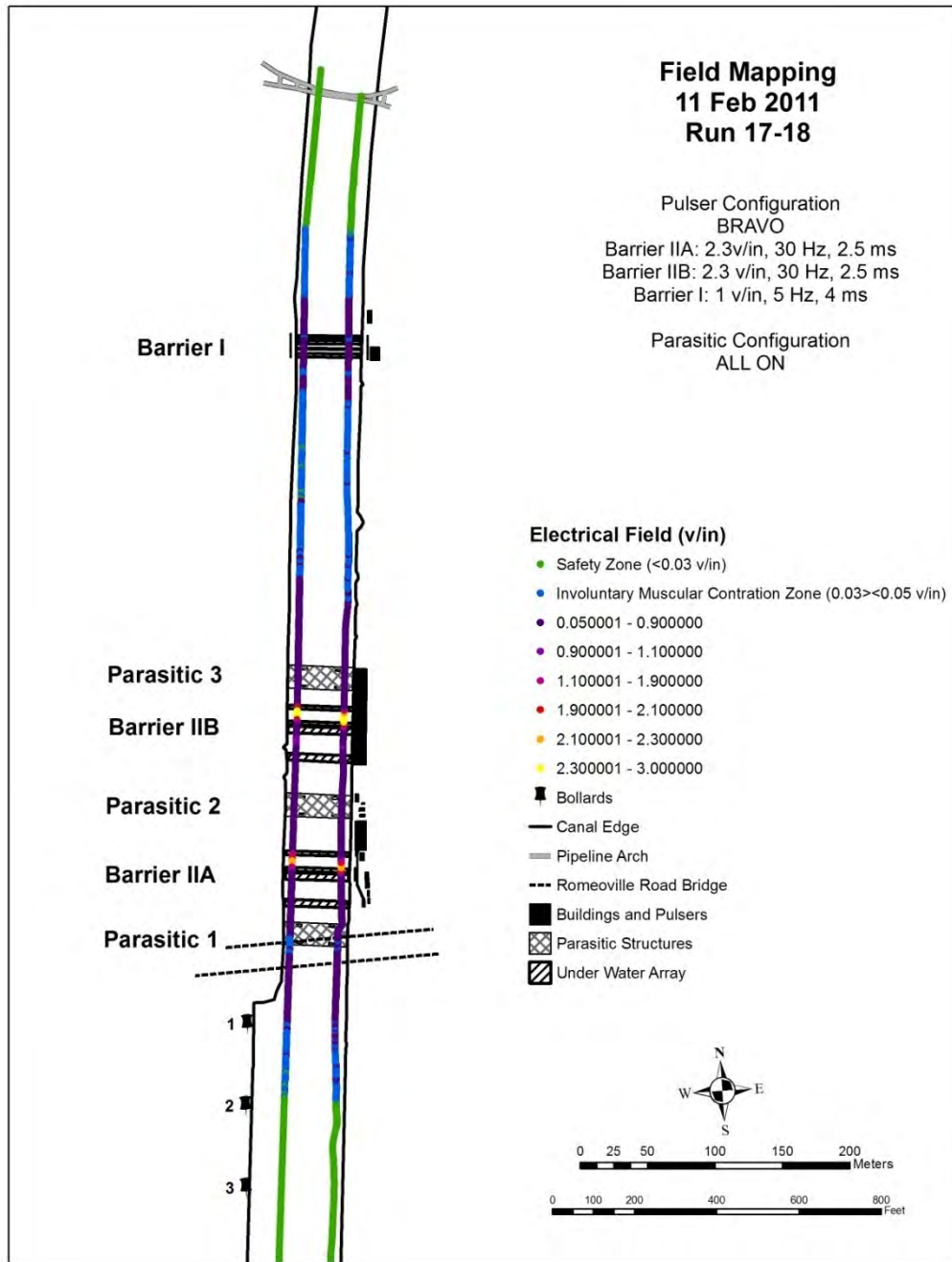


Figure D6. V12 for Runs 17 and 18 on 11 February 2011 (Configuration B, On, On, On).

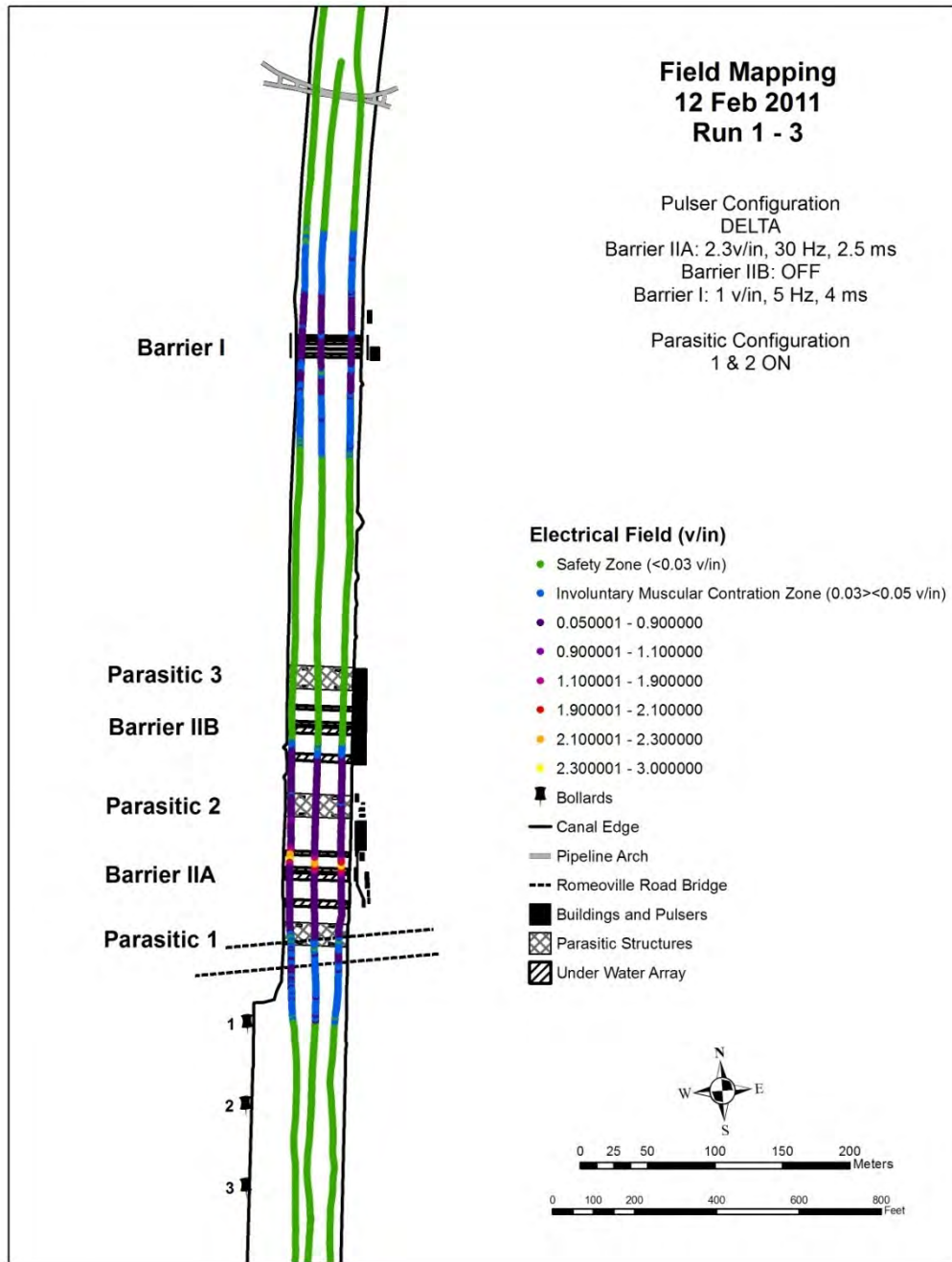


Figure D7. V12 for Runs 1 – 3 on 12 February 2011 (Configuration D, On, On, Off).

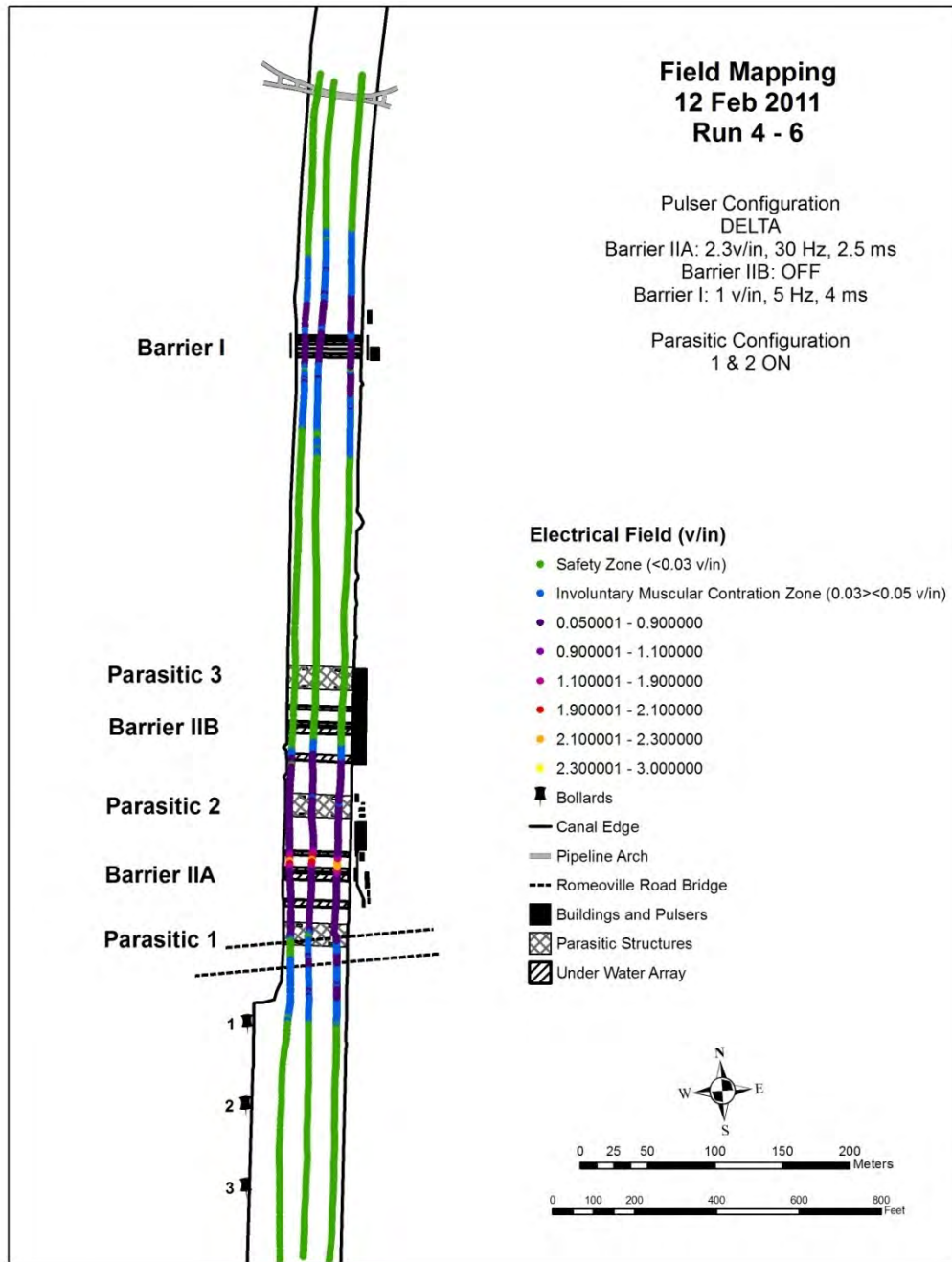


Figure D8. V12 for Runs 4 – 6 on 12 February 2011 (Configuration D, On, On, Off).



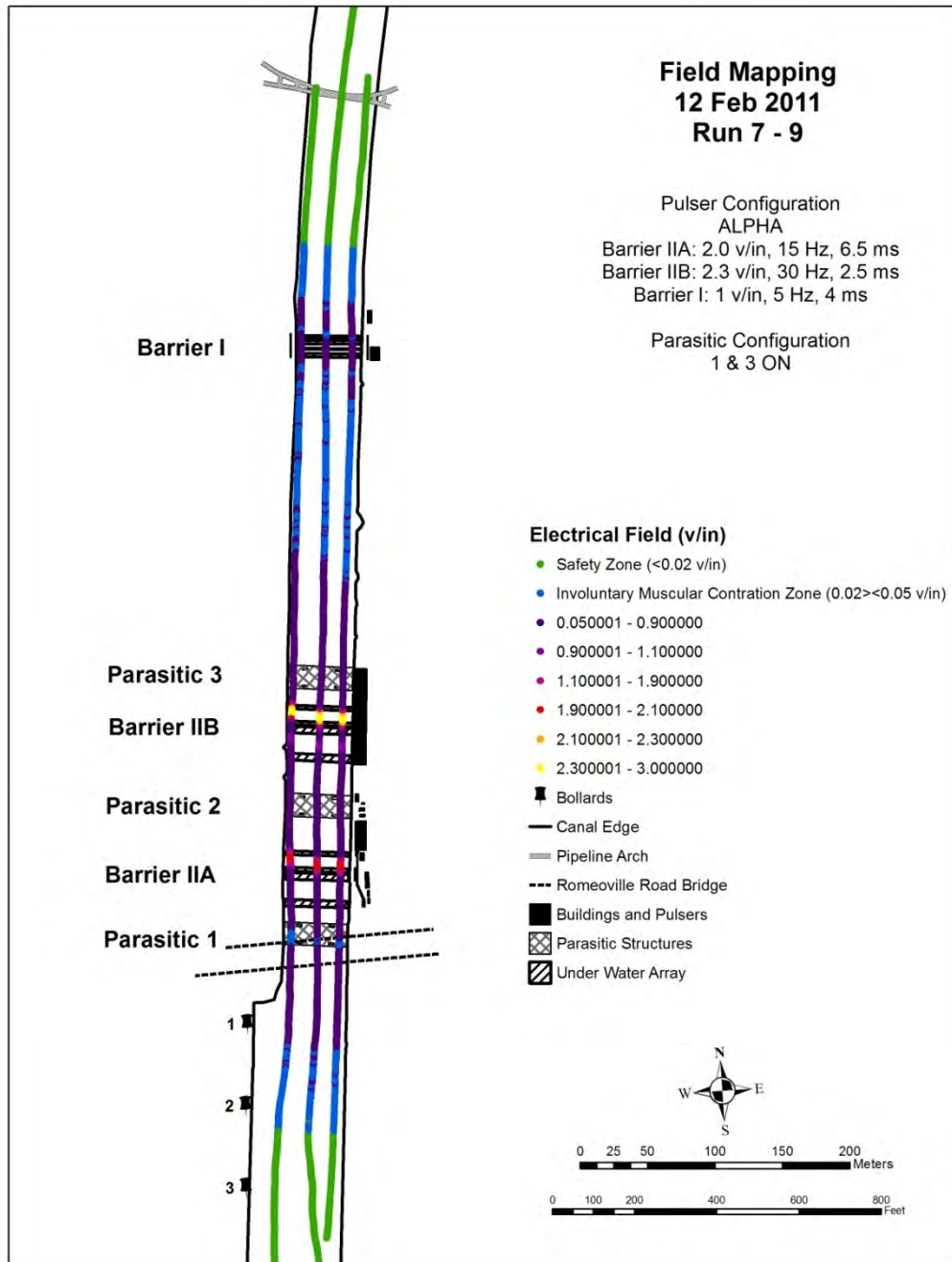


Figure D9. V12 for Runs 7 - 9 on 12 February 2011 (Configuration A, On, Off, On).

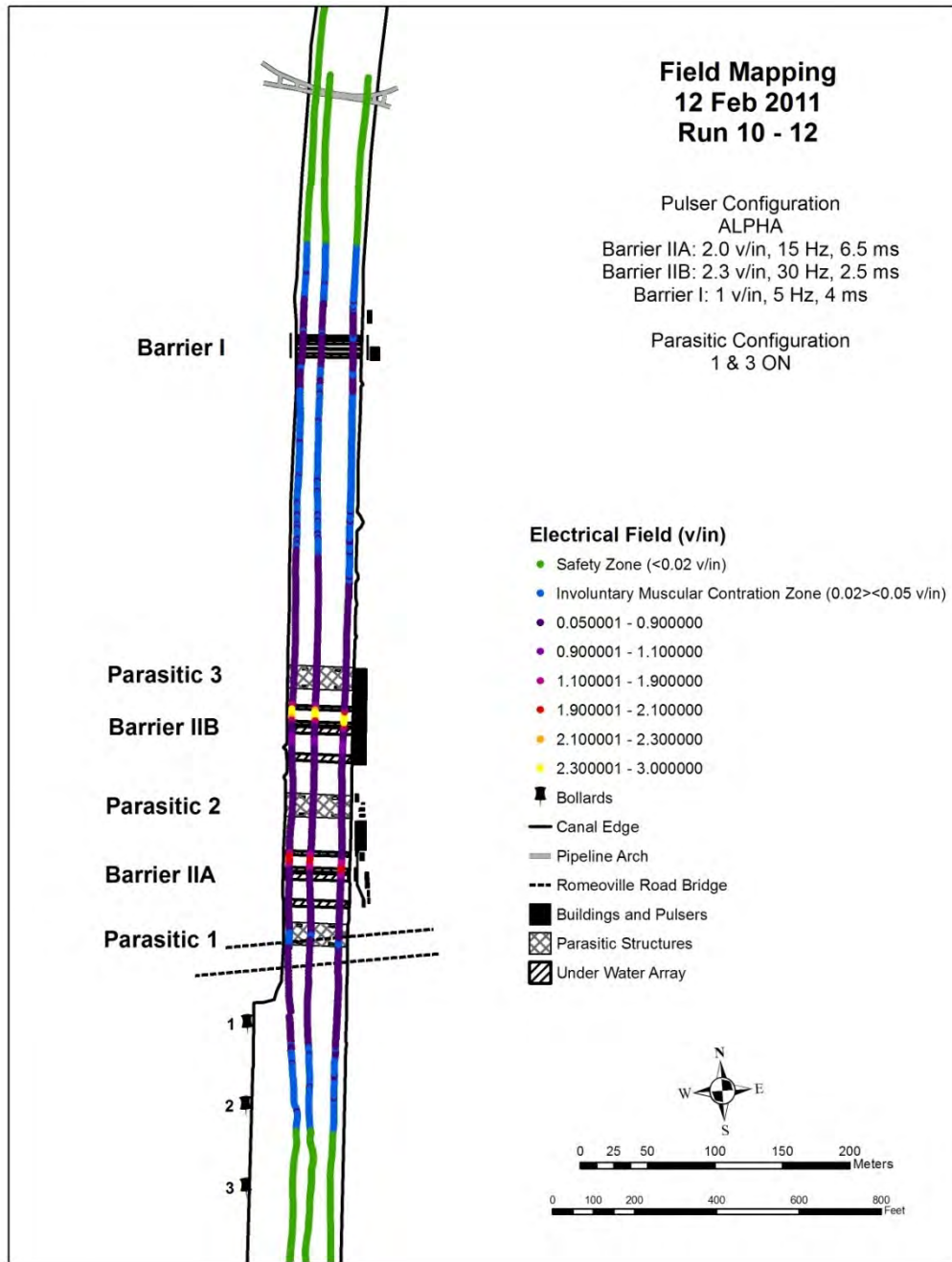


Figure D10. V12 for Runs 10 - 12 on 12 February 2011 (Configuration A, On, Off, On).



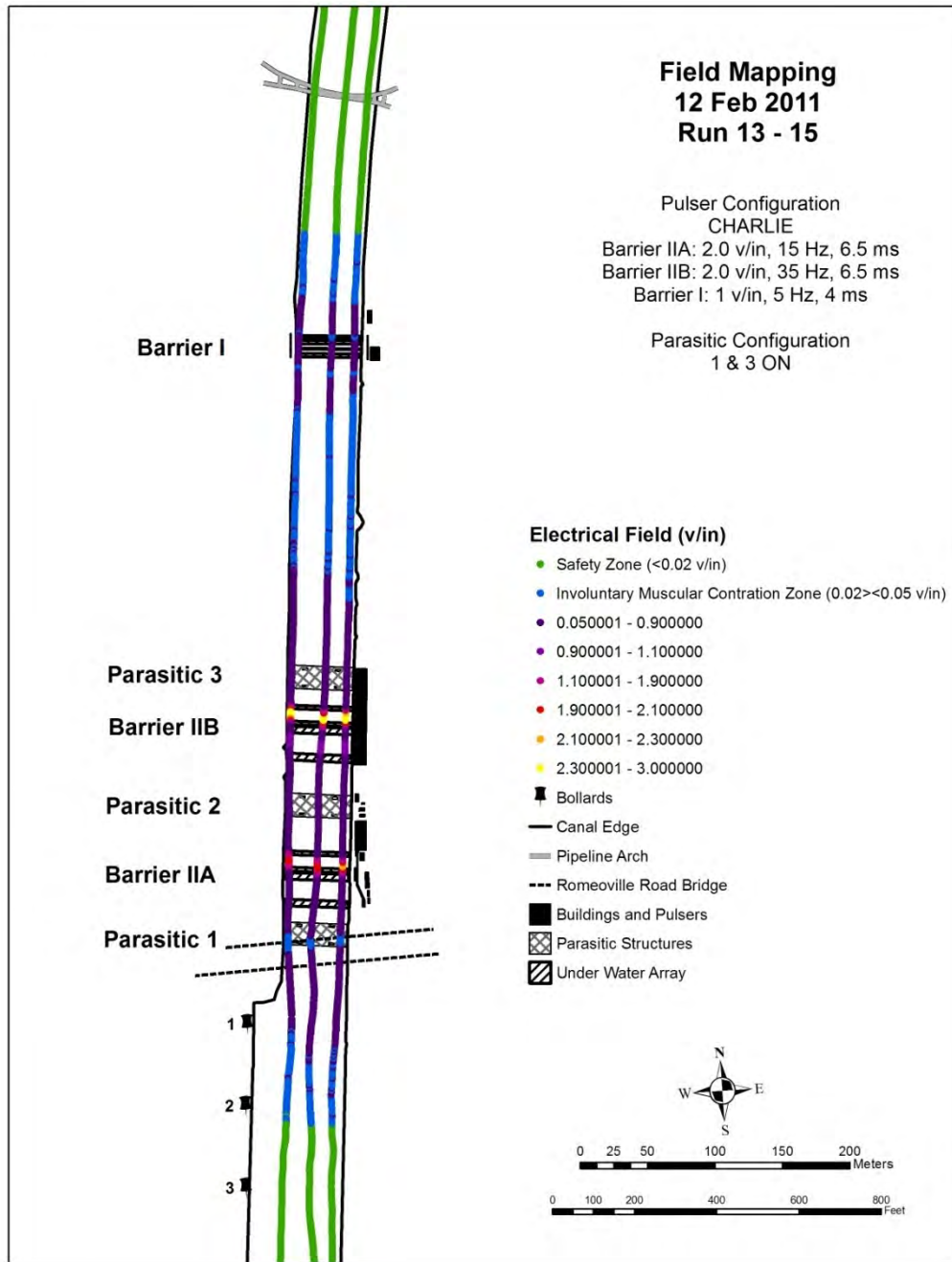


Figure D11. V12 for Runs 13 - 15 on 12 February 2011 (Configuration C, On, Off, On).

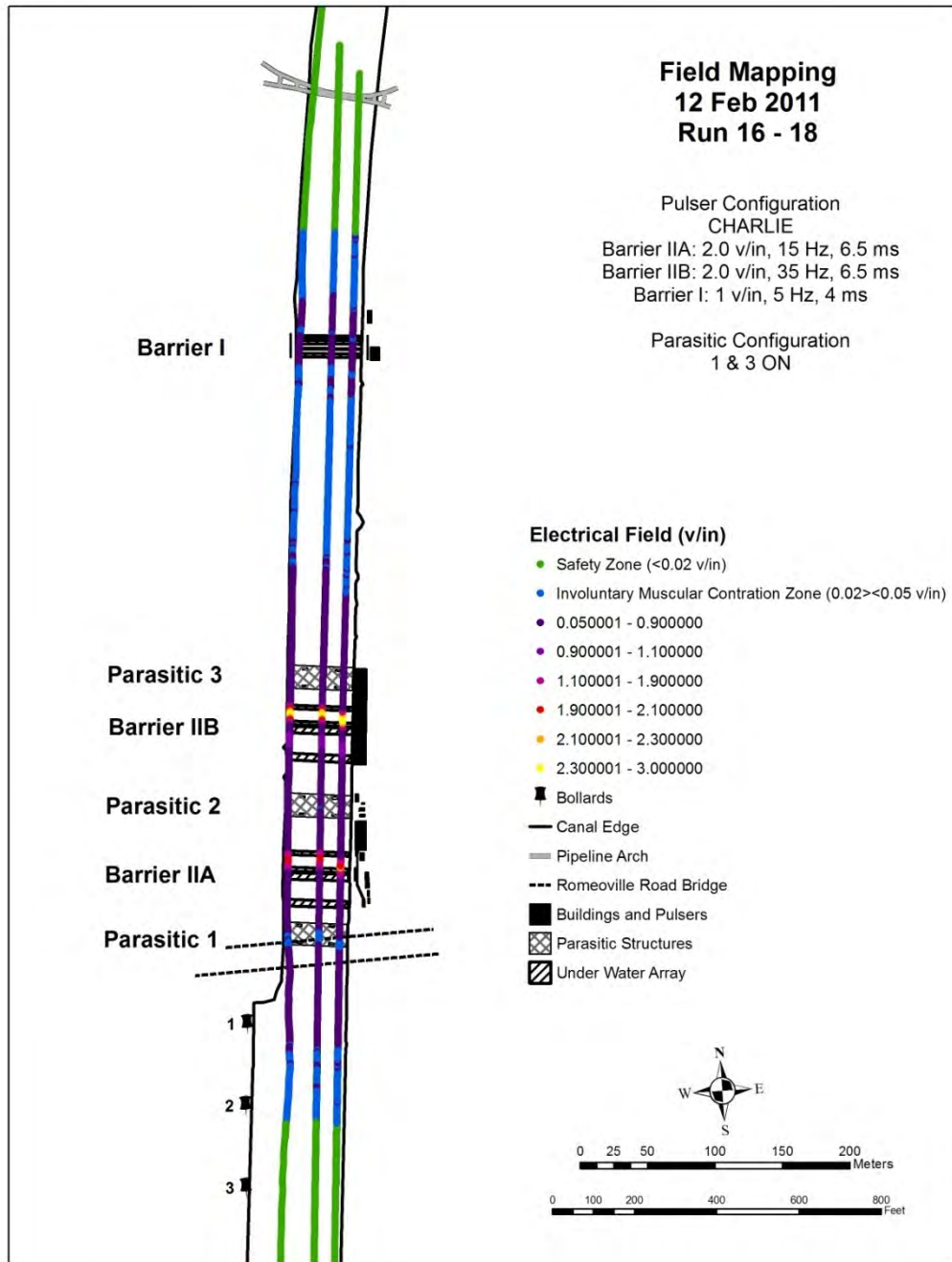


Figure D12. V12 for Runs 16 - 18 on 12 February 2011 (Configuration C, On, Off, On).

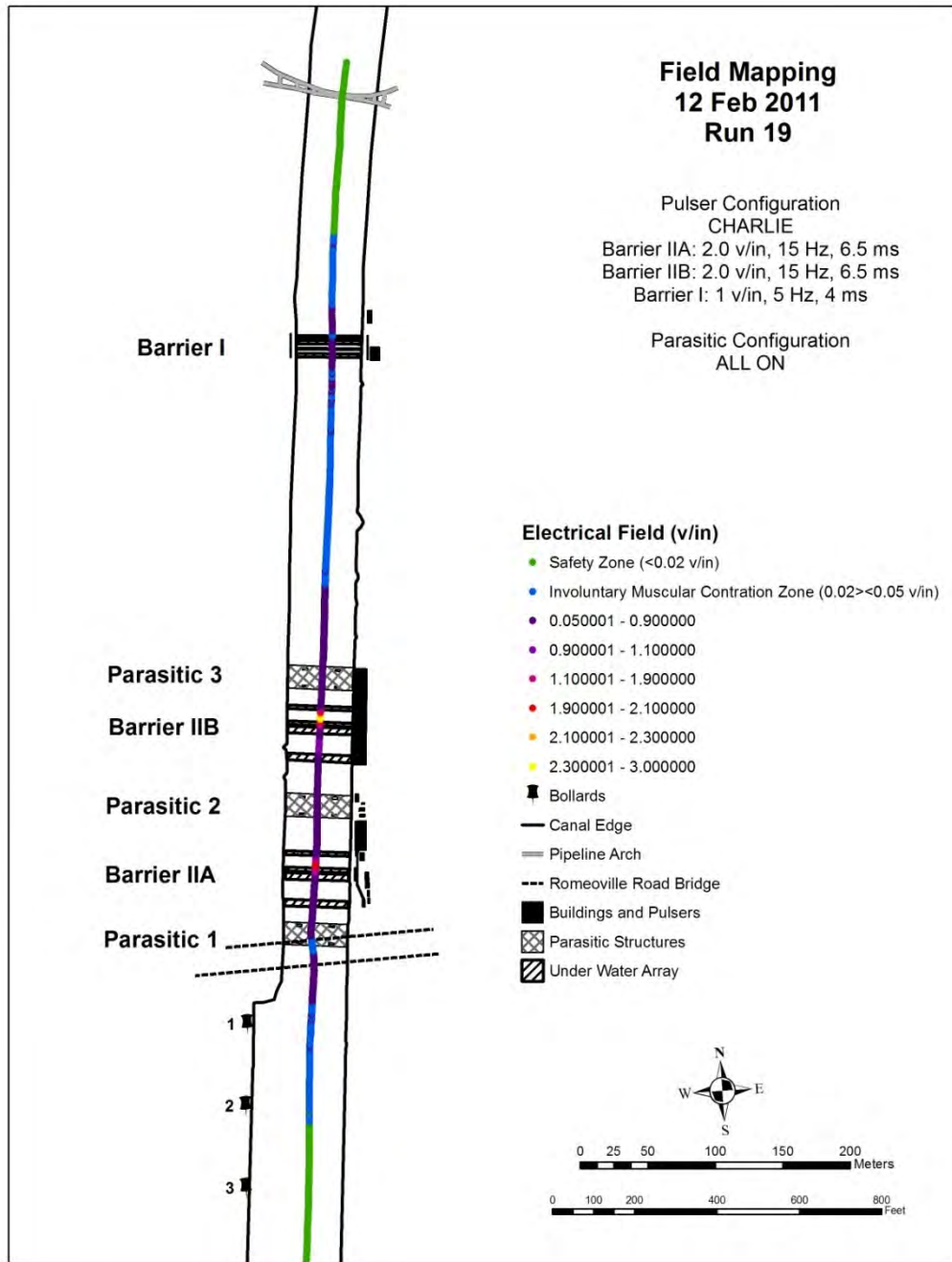


Figure D13. V12 for Run 19 on 12 February 2011 (Configuration C, On, On, On).

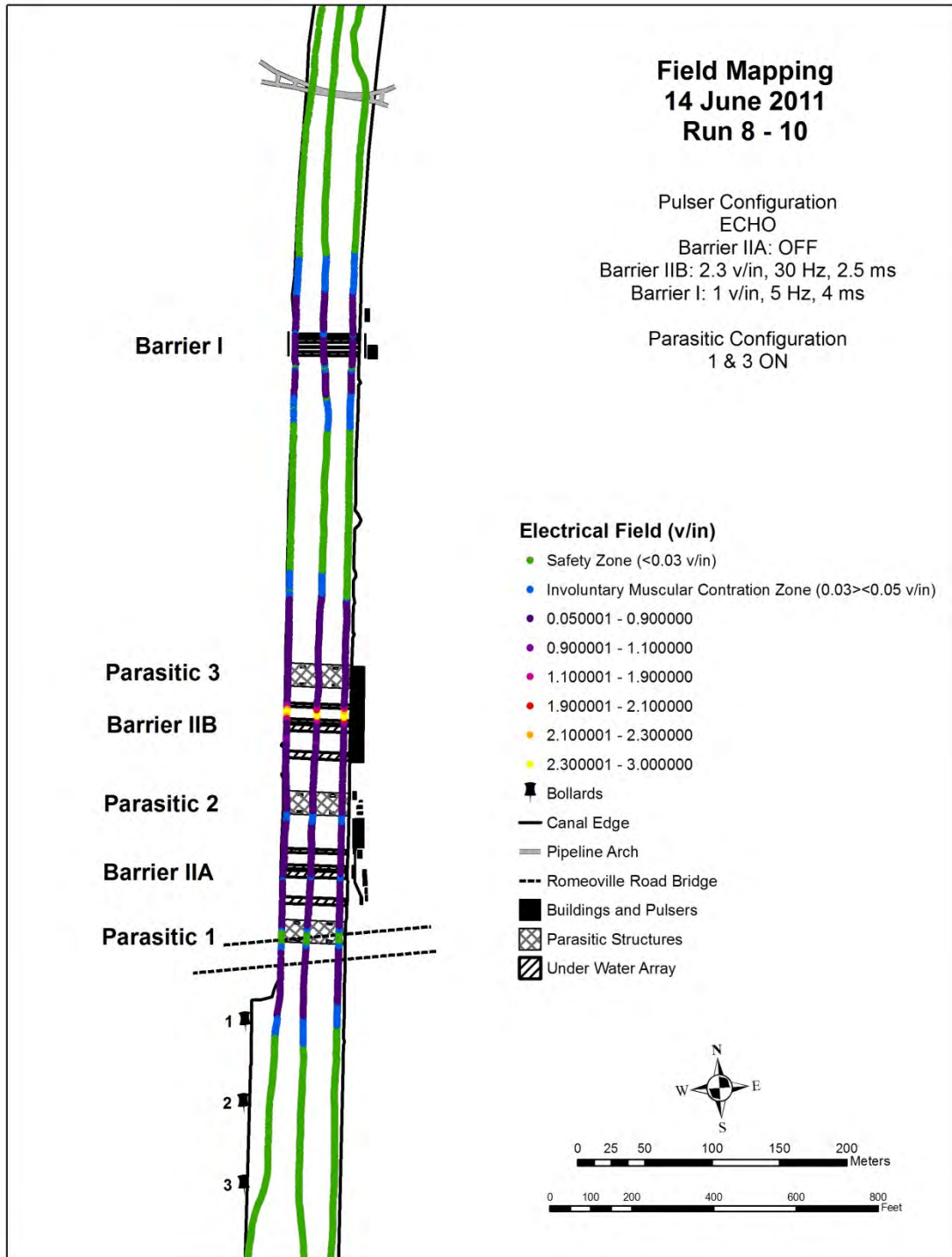


Figure D14. V12 for Runs 8 - 10 on 14 June 2011 (Configuration E, On, Off, On).

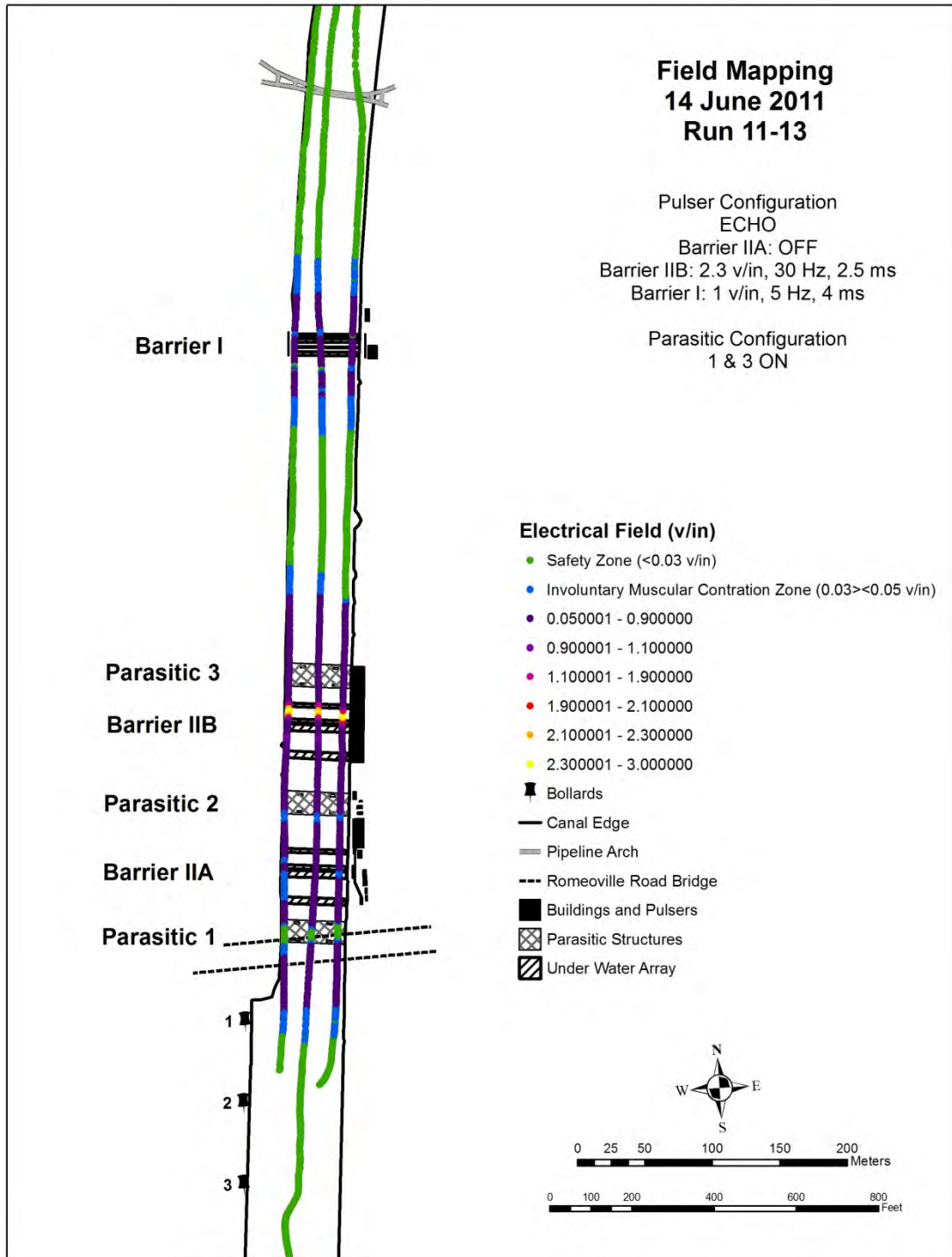


Figure D15. V12 for Runs 11 – 13 on 14 June 2011 (Configuration E, On, Off, On).

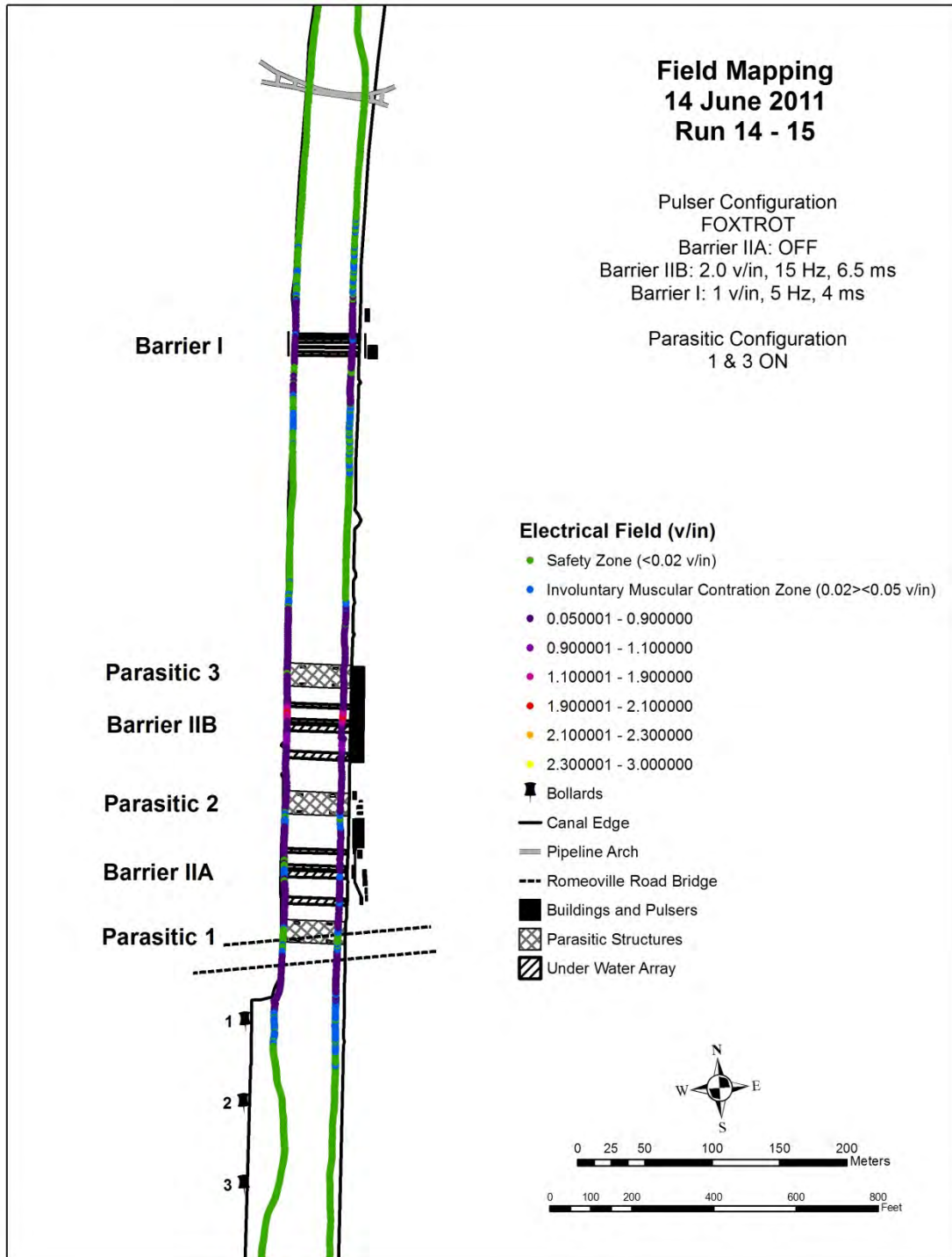


Figure D16. V12 for Runs 14 – 15 on 14 June 2011 (Configuration F, On, Off, On).



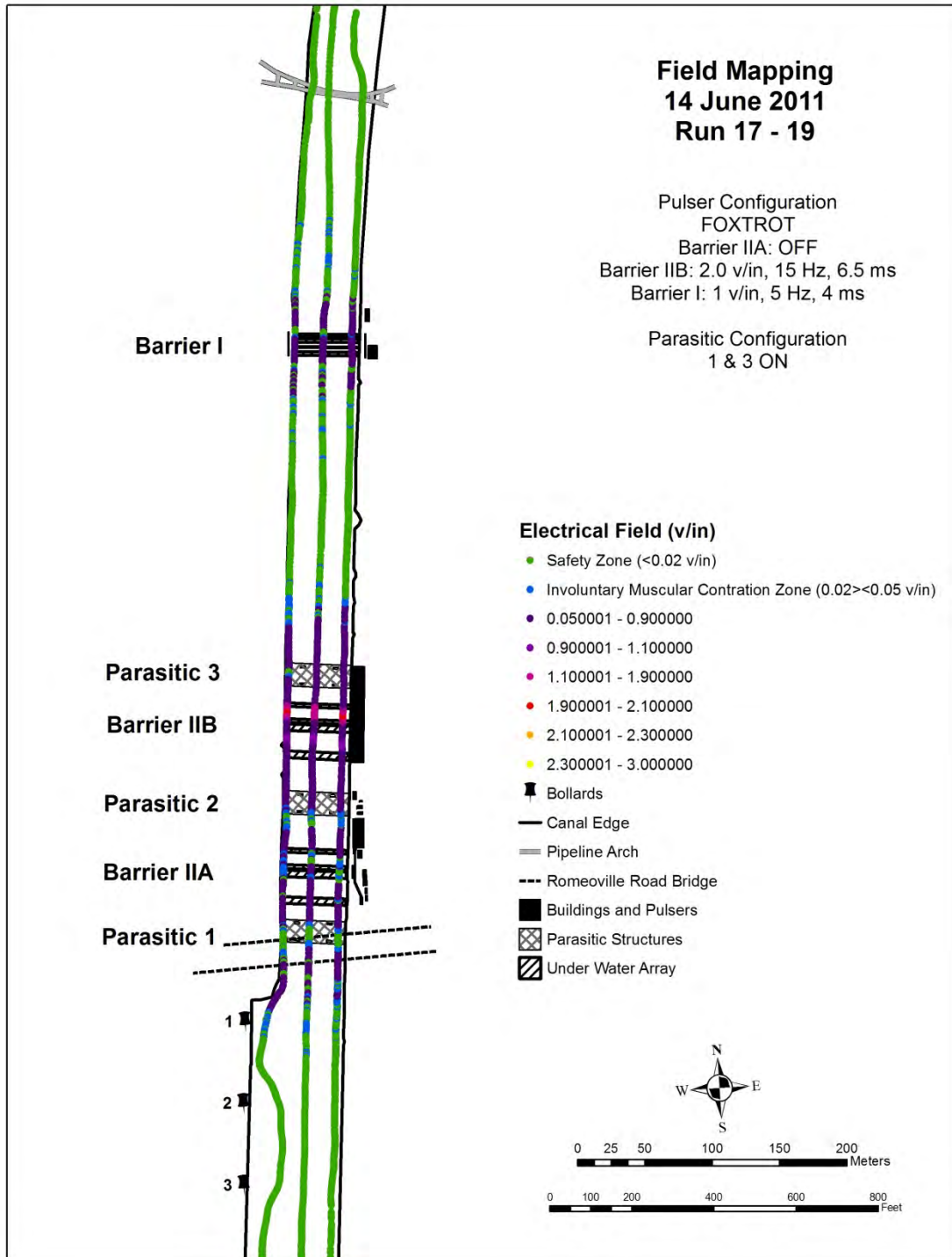


Figure D17. V12 for Runs 17 – 19 on 14 June 2011 (Configuration F, On, Off, On).

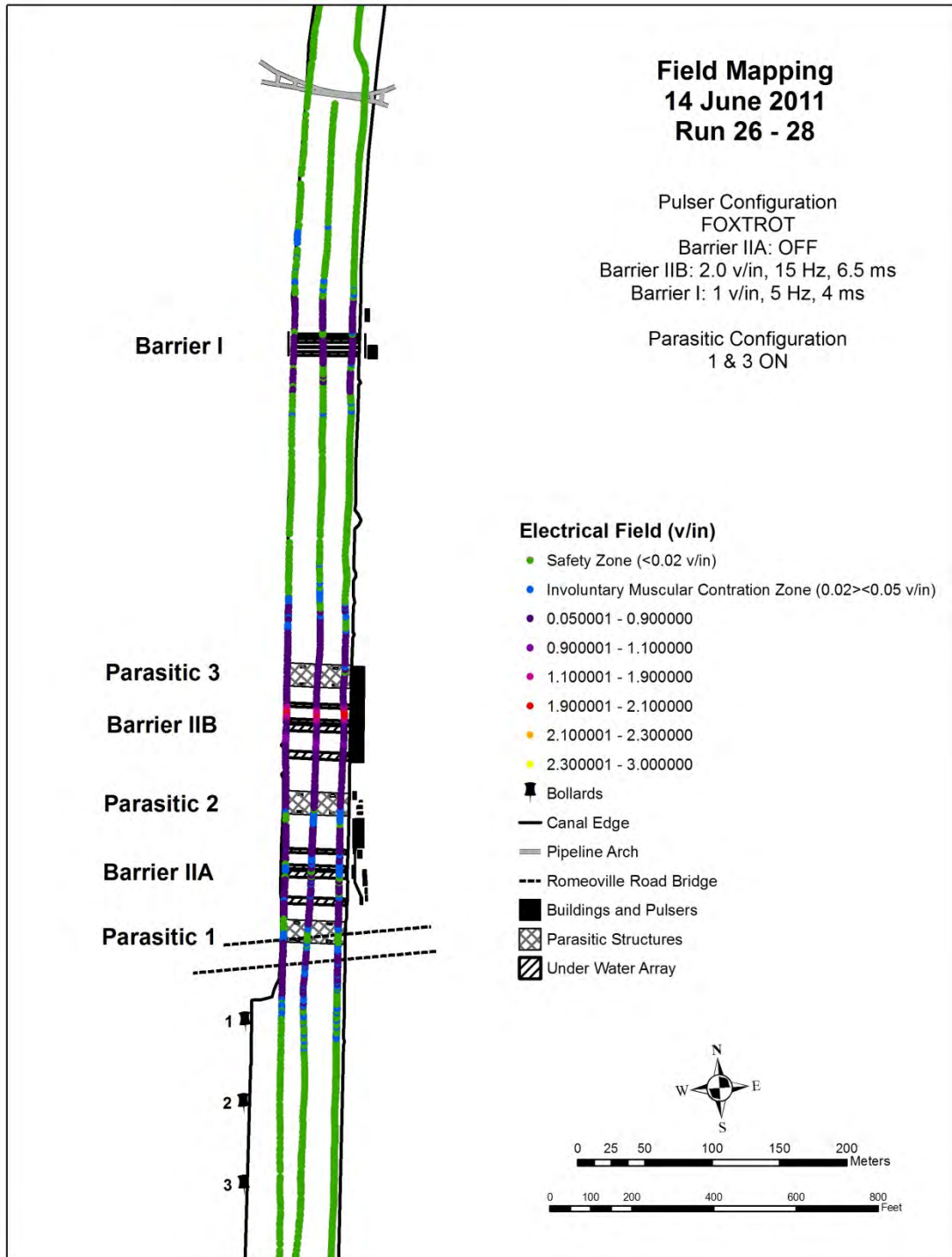


Figure D18. V12 for Runs 26 – 28 on 14 June 2011 (Configuration F, On, Off, On).



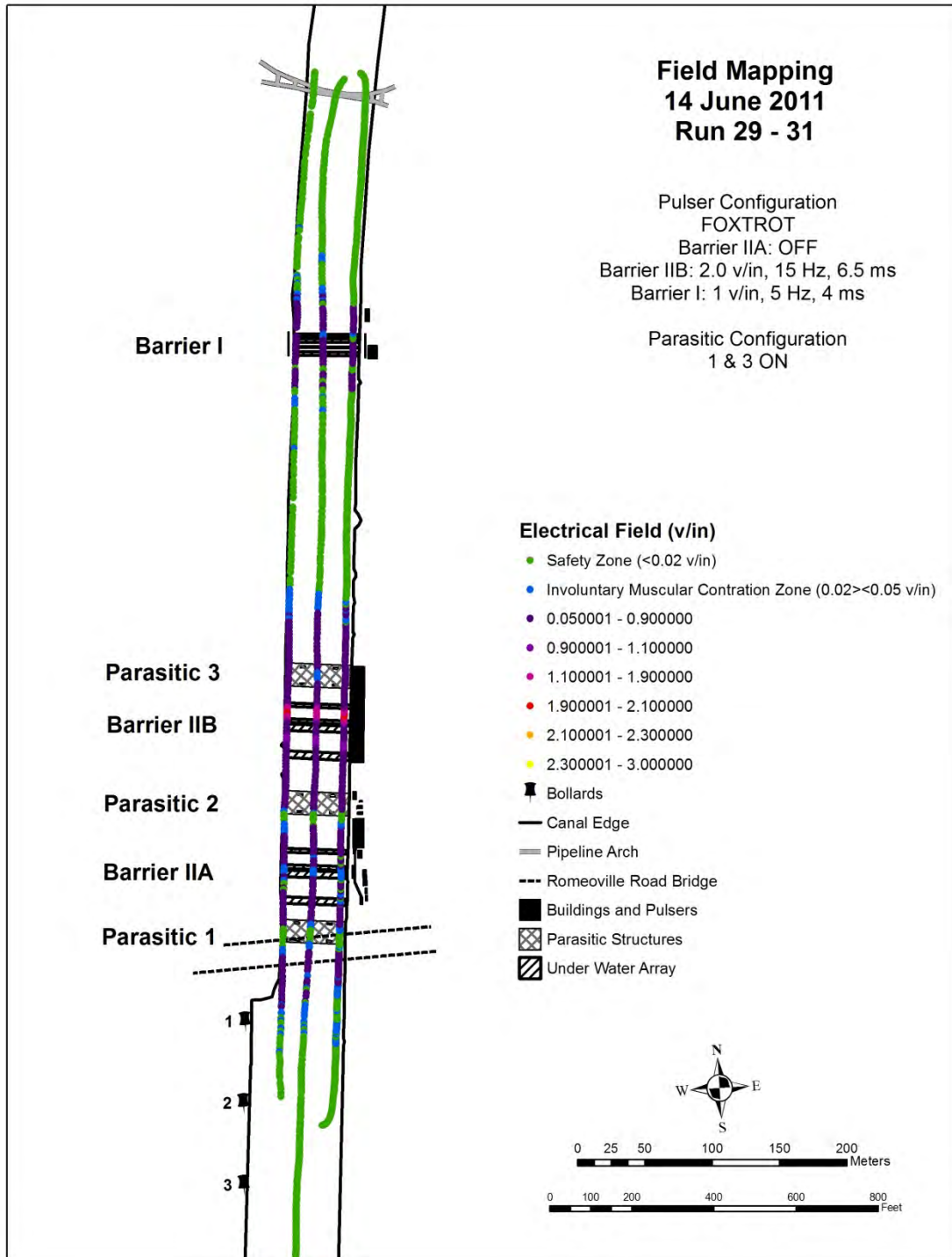


Figure D19. V12 for Runs 29 – 31 on 14 June 2011 (Configuration F, On, Off, On).

# REPORT DOCUMENTATION PAGE

*Form Approved*  
OMB No. 0704-0188

Public reporting burden for this collection of information is estimated to average 1 hour per response, including the time for reviewing instructions, searching existing data sources, gathering and maintaining the data needed, and completing and reviewing this collection of information. Send comments regarding this burden estimate or any other aspect of this collection of information, including suggestions for reducing this burden to Department of Defense, Washington Headquarters Services, Directorate for Information Operations and Reports (0704-0188), 1215 Jefferson Davis Highway, Suite 1204, Arlington, VA 22202-4302. Respondents should be aware that notwithstanding any other provision of law, no person shall be subject to any penalty for failing to comply with a collection of information if it does not display a currently valid OMB control number. **PLEASE DO NOT RETURN YOUR FORM TO THE ABOVE ADDRESS.**

<b>1. REPORT DATE (DD-MM-YYYY)</b> August 2011			<b>2. REPORT TYPE</b> Final			<b>3. DATES COVERED (From - To)</b>			
<b>4. TITLE AND SUBTITLE</b> 2011 In-Water Testing of Aquatic Nuisance Species Dispersal Barriers IIA And IIB with Increased Voltage and Frequency Operating Parameters						<b>5a. CONTRACT NUMBER</b>			
						<b>5b. GRANT NUMBER</b>			
						<b>5c. PROGRAM ELEMENT NUMBER</b>			
<b>6. AUTHOR(S)</b> Michael K. McInerney, Brianna S. Aubin, Jonathan C. Trovillion, Carey L. Baxter, Ethan T. Trovillion, Vincent F. Hock, Jr., and David M. Weir						<b>5d. PROJECT NUMBER</b> 114532			
						<b>5e. TASK NUMBER</b>			
						<b>5f. WORK UNIT NUMBER</b>			
<b>7. PERFORMING ORGANIZATION NAME(S) AND ADDRESS(ES)</b> U.S. Army Engineer Research and Development Center Construction Engineering Research Laboratory P.O. Box 9005 Champaign, IL 61826-9005						<b>8. PERFORMING ORGANIZATION REPORT NUMBER</b> ERDC/CERL TR-11-23			
<b>9. SPONSORING / MONITORING AGENCY NAME(S) AND ADDRESS(ES)</b> US Army Engineer District Chicago 111 North Canal Street Chicago, IL 60606-7206						<b>10. SPONSOR/MONITOR'S ACRONYM(S)</b>			
						<b>11. SPONSOR/MONITOR'S REPORT NUMBER(S)</b>			
<b>12. DISTRIBUTION / AVAILABILITY STATEMENT</b> Approved for public release; distribution is unlimited.									
<b>13. SUPPLEMENTARY NOTES</b>									
<b>14. ABSTRACT</b> US Army Engineer District – Chicago operates an electric field-based aquatic nuisance species dispersal barrier system in the Chicago Sanitary and Ship Canal (CSSC), Romeoville, IL. The barriers were constructed to prevent the movement of invasive species, such as Asian bighead carp ( <i>Hypophthalmichthys nobilis</i> ) and silver carp ( <i>Hypophthalmichthys molitrix</i> ) between the Mississippi River and Great Lakes basins. The objective of this project was to perform a series of in-water tests on the barrier addressing field-strength mapping, sparking potential during barge fleeting and collision, voltage potentials between barges traversing the barriers, personnel in-water shock potential, stray-current corrosion potential, and optimal settings for the parasitic barrier system. Test results and analysis indicate there is no significant risk of personnel shock hazard in the fleeting area during barrier operations for any operating configuration. Also, while some operational scenarios were found to increase sparking risk if barges collide with each other or separate metal objects, analysis indicates that concerns about coal dust explosion hazard from sparking are not supported by the technical literature. A detailed set of data, analysis, conclusions, and recommendations is provided in the report text and four appendices.									
<b>15. SUBJECT TERMS</b> Chicago Sanitary and Ship Canal (CSSC), Asian carp, fish barrier, test and evaluation, sparking potential, shock hazard									
<b>16. SECURITY CLASSIFICATION OF:</b>						<b>17. LIMITATION OF ABSTRACT</b>	<b>18. NUMBER OF PAGES</b>	<b>19a. NAME OF RESPONSIBLE PERSON</b>	
<b>a. REPORT</b> Unclassified		<b>b. ABSTRACT</b> Unclassified		<b>c. THIS PAGE</b> Unclassified			140	<b>19b. TELEPHONE NUMBER (include area code)</b>	